

(NASA-CR-176321) MIDDLE ATMOSPHERE PROGRAM.
HANDBOOK FOR MAP. VOLUME 16: ATMOSPHERIC
STRUCTURE AND ITS VARIATION IN THE REGION 20
TO 120 km. DRAFT OF (International Council
of Scientific Unions) 323 p HC A14/EF A01: G3/46 01714
N86-12814
THRU
N86-12836
Unclass

Middle Atmosphere Program

HANDBOOK FOR MAP VOLUME 16

Edited by
K. Labitzke
J. J. Barnett
B. Edwards



1+23

M I D D L E
A T M O S P H E R E
P R O G R A M

HANDBOOK FOR MAP

Volume 16

Edited by

K. Labitzke
J. J. Barnett
B. Edwards

July 1985

Published for the ICSU Scientific Committee on Solar-
Terrestrial Physics (SCOSTEP) with financial assistance
from the National Aeronautics and Space Administration
under P.O. W-15,897 and Unesco Subvention 1984-1985

Copies available from SCOSTEP Secretariat, University of
Illinois, 1406 W. Green Street, Urbana, Illinois 61801

ATMOSPHERIC STRUCTURE AND ITS VARIATION IN THE REGION 20 TO 120 KM
DRAFT OF A NEW REFERENCE MIDDLE ATMOSPHERE

TABLE OF CONTENTS

TABLE OF CONTENTS.	iii
1. INTRODUCTION, K. Labitzke.	1
2. ATMOSPHERIC STRUCTURE 20 to 80 km.	3
2.1 <u>Discussion on Available Data and on Errors.</u>	3
2.1.1 Temperature data from satellites, J. J. Barnett and M. Corney	3
2.1.2 Temperature and wind data from meteorological rockets, F. J. Schmidlin	12
2.1.3 Observed winds and temperatures in the Southern Hemisphere, Yu. P. Koshelev	15
2.1.4 Mean winds of the mesosphere (60-80 km), as measured by M. F. Radars, A. H. Manson, C. E. Meek, R. A. Vincent, and M. J. Smith	36
2.2 <u>Middle Atmosphere Reference Model Derived from Satellite Data,</u> J. J. Barnett, and M. Corney.	47
2.3 <u>Discussion on Variability in Time and Space</u>	86
2.3.1 Planetary waves	
a) Climatological distribution, J. J. Barnett and M. Corney	86
b) Interannual variability, K. Labitzke and J. J. Barnett.	138
2.3.2 Gravity waves	
a) Seasonal and latitudinal variations, I. Hirota	144
b) Spectral description of mesoscale fluctuations, T. E. VanZandt	149
2.3.3 Atmospheric tides below 80 km, J. M. Forbes and G. V. Groves.	157
2.3.4 Comparison of time-periodic variations in temperature and wind from meteorological rockets and satellites, A. D. Belmont	164
2.3.5 Annual and semiannual cycles based on the middle atmosphere reference model in section 2.2, J. J. Barnett, M. Corney, and K. Labitzke	175
2.3.6 On the quasi-biennial oscillation, QBO, K. Labitzke	181
2.3.7 On the interannual variability and on trends of the temperature in the middle atmosphere, K. Labitzke and B. Naujokat	183
2.4 <u>A Proposed International Tropical Reference Atmosphere</u> <u>up to 80 km</u> , M. R. Ananthasayanam and R. Narasimha.	197
2.5 <u>Interim Reference Ozone Models for the Middle Atmosphere,</u> G. M. Keating and D. F. Young	205

3. ATMOSPHERIC STRUCTURE 80 to 120 km	231
3.1 <u>Discussion on Available Data and Errors</u>	231
3.1.1 Temperature structure of the 80 km to 120 km region, J. M. Forbes.	231
3.1.2 Mean winds of the upper middle atmosphere (60-100 km): A global distribution from radar systems (M. F., meteor, VHF), A. H. Manson, C. E. Meek, M. Massebeuf, J. L. Fellous, W. G. Elford, R. A. Vincent, R. L. Craig, R. G. Roper, S. Avery, B. B. Balsley, G. J. Fraser, M. J. Smith, R. R. Clark, S. Kato, T. Tsuda, and A. Ebel. .	239
3.2 <u>Discussion on Variability in Time and Space</u>	269
3.2.1 Planetary and gravity waves in the mesosphere and lower thermosphere, R. A. Vincent	269
3.2.2 Atmospheric tides between 80 and 120 km, J. M. Forbes . . .	278
3.2.3 Turbulence in the altitude region 80 to 120 km, W. K. Hocking	290
4. NEW TECHNOLOGIES	305
4.1 <u>Contribution to the CIRA Model from Ground-Based Lidar,</u> M. L. Chanin, A. Hauchecorne and M. Smires.	305
4.2 <u>The MST Radar Technique,</u> B. B. Balsley.	315

1. INTRODUCTION

Since the preparation of the last COSPAR Reference Atmosphere (CIRA 1972), there has been a substantial increase in the number of measurements of atmospheric structure by different satellite experiments as well as by meteorological rockets and different ground-based techniques. Therefore, a "COSPAR Task Group for the Preparation of a New CIRA" was formed in Ottawa in 1982, and one part of this group was charged with the task of preparing a "Reference Atmosphere for the Middle Atmosphere".

It is the purpose of this MAP Handbook to present a draft of the new Reference Atmosphere for the region between 20 and 80 km, which depends largely on recent satellite experiments covering the globe from 80° S to 80° N.

A separate "International Tropical Reference Atmosphere" is presented in Section 2.4, as well as "Interim Reference Ozone Models for the Middle Atmosphere" in Section 2.5. Both types of Reference Atmospheres are new for the CIRA, but it was thought to be timely and feasible on the basis of available data to include them.

Section 3 deals with the "Atmospheric Structure between 80 and 120 km" and is based largely on ground-based observation techniques.

"New Technologies" such as lidar and MST radar are discussed only briefly in Section 4. Note, however, that Handbook for MAP, Vol. 13 gives an up-to-date and very complete description of these new methods.

ACKNOWLEDGEMENTS

Members of the "COSPAR Task Group for the Preparation of a New CIRA".

Members of IAMAP's ICMUA (International Commission for the Meteorology of the Upper Atmosphere) were invited to contribute short papers on selected subjects to accompany the new Reference Models. Their enthusiasm and constructive help is very much acknowledged.

K. Labitzke and J. J. Barnett, Chairmen of COSPAR'S Task Group

2.1.1 TEMPERATURE DATA FROM SATELLITES

J. J. Barnett and M. Corney

Department of Atmospheric Physics, Clarendon Laboratory
Oxford OX1 3PU, Great Britain

INTRODUCTION

Middle atmosphere temperature has been measured by a variety of sensors, notably the SIRS, VTPR, ITPR, HIRS/1, HIRS/2, MSU, SSU, SCRs, PMR, LRIR, LIMS, and SAMS. Some of these have been primarily tropospheric sounding instruments, developed to provide forecasting data, but having mid- and lower stratospheric channels to help sharpen tropospheric weighting functions.

Others have been aimed solely at the middle atmosphere. Of these some have been short duration research orientated experiments, e.g., the LRIR and LIMS, while others have been part of a long operational programme, e.g. the SSU. The current US operational sounding system, called the TOVS, is carried by the current NOAA series of satellites and comprises three sensors: the HIRS/2, MSU and SSU. Each makes stratospheric measurements, although the SSU weighting functions reach the greatest altitudes. Each scans across the satellite track to obtain global coverage with a resolution of 200 km or better. Such resolution is considered essential for the troposphere, but for the middle atmosphere where horizontal scales are larger, and particularly for the purposes of climatology, much coarser resolution is adequate. This is fortunate since many of the middle atmosphere sounders, particularly those which reach the highest altitudes, do not scan across the track and have a longitudinal resolution of 2000-3000 km, depending on latitude.

Satellite data from a single sounder are generally reduced by several different algorithms or with different coefficients. Results from experimental sounders are usually processed several times as techniques are improved, giving rise to different generations of results. Operational data are typically processed only once, with improvements in the algorithm being made as necessary and different algorithms used at different analysis centres. In the case of the TOVS, stratospheric values are given in the SATEMS distributed for tropospheric analysis, but the Upper Air Branch of NOAA and the British Meteorological Office separately reduce the data to obtain results which can be expected to be superior.

Satellite data have the advantage of giving uniform global coverage. The last CIRA reference atmosphere (CIRA, 1972) did not use satellite data for the middle atmosphere, but measurements are now sufficiently mature for them to make a valuable contribution.

DATA USED FOR THE PROPOSED SATELLITE-BASED REFERENCE ATMOSPHERE

Table 1 lists the sensors which have been used to produce a proposed revised reference atmosphere, with the time and space domains over which the data were available. As will be described later, only the SCR and PMR were used directly to obtain the climatic means. The SAMS and LIMS, together with, to some extent, the Stratospheric Sounder Units (SSR) on the Tiros-N series satellites and conventional radio/rocketsondes, were used as a check that the means were satisfactory.

The SCR, PMR, SAMS, LIMS, and SSU all measure the infrared emission from the carbon dioxide ν_2 band at about 15 microns in order to determine the temperature profile. The SCR and PMR are essentially vertical sounders which use measurements at wavelengths of differing opacity to measure emissions

Table 1. Data sets and their domains

Experiment	Sounder type	Altitude	Latitude	Time used
Nimbus 5 SelectiveQ Chopper Radiometer (SCR) (ELLIS et al., 1973)	Nadir	100-0.3 mb (15-55 km)	80S-80N	Jan 1973- Dec 1974
Nimbus 6 Pressure Modulator Radiometer (PMR) (CURTIS et al., 1974)	Nadir	10-0.01 mb (30-80 km)	80S-80N	Jun 1975- Jul 1978
Nimbus 7 Stratospheric and Mesospheric Sounder (SAMS) (DRUMMOND et al., 1980)	Limb	50-0.05 mb (20-70 km)	50S-70N	Oct 1978- Dec 1981
Nimbus 7 Limb Infrared Monitor of the Stratosphere (LIMS) (GILLE and RUSSELL, 1984)	Limb	100-0.1 mb (16-66 km)	67S-84N	Oct 1978- May 1979

originating in different layers of the atmosphere. This technique has an inherent limit to the vertical resolution of about 10 km, and the resolution achieved in practice varies from about 12 km in the low stratosphere to about 20 km in the upper mesosphere. The SAMS and LIMS view the atmospheric limb and scan vertically with a narrow field of view. A much better vertical resolution is theoretically possible (the limit is probably about 1-2 km) and the SAMS and LIMS achieve about 8 km and about 3 km, respectively.

RETRIEVAL METHODS

Retrieval is the process of obtaining the temperature profile (or 3-D field) which best fits the measurements of infrared emission. In the case of the SCR and PMR, climatology is used as additional information to give the result that is both consistent with the measurements and statistically most likely. The climatological profile used as an initial estimate was a combination of the CIRA 1972 monthly means for the mesosphere and upper stratosphere, and data by NEWELL (1977) for the lower and mid-stratosphere. These fields were derived from rocketsonde and radiosonde data. A separate field was available for the Northern Hemisphere for each month, and they were used for the Southern Hemisphere displaced by six months. This has the advantage that hemispheric differences apparent in the retrieved temperatures can only be ascribed to differences in the measurements. Values for each individual day were obtained by linear interpolation between the monthly fields in order that the fields varied smoothly with time. The initial estimate was independent of longitude, so that longitudinal structure arises totally from the data and not the initial estimate.

a) The Nimbus 5 SCR

The retrieval method was that due to CRANE (1977, 1979) for the study of a few months of winter SCR data. Its use was extended by VYAS (1984) to the complete years of 1973 and 1974. Channels B12, B34, and A1 of the radiometer were used, these having weighting functions peaking at about 1.5, 8, and 60 mb, respectively. Radiances were Fourier analysed around latitude circles (at 4 deg latitude intervals) into the zonal mean and components of waves 1 to 4. Each component was retrieved separately to obtain the zonal mean and wave components of the temperature profile. This was done with daily analyses and

the resulting retrieved temperature coefficients were averaged over calendar months, with each field containing the mean over the corresponding months in 1973 and 1974.

b) The Nimbus 6 PMR

Channels 1000, 1015, 2100, and 2115 were used, these being radiances obtained from modulators 1 and 2 at 0 deg and 14.5 deg Doppler Scan angles. The highest altitude weighting function obtained from the PMR peaks at about 80 km, after taking into account nonlocal thermodynamic equilibrium effects; it is for a linear combination of channels 1000 and 2100 and is referred to as channel 3000. Thus although channel 3000 radiances are not explicitly used in the retrieval, the information is implicitly available from channels which are used. The radiances were initially available on latitude-longitude grids (at intervals of 4 deg and 10 deg, respectively) for each day, and were averaged to give mean fields on the same grid for each month from July 1975 to June 1978 (36 months). The data were then retrieved at each grid point separately using a maximum probability estimator as described by RODGERS (1976).

The weighting functions of the PMR have a significant temperature dependence, and for levels above about 75 km an allowance must be made in the retrieval process for the ν_2 band of carbon dioxide not being in local thermodynamic equilibrium. These effects were taken into account by HEASEMAN (1981) who obtained mean weighting functions and coefficients of their dependence on the Planck function profile. In the retrieval process two kinds of weighting function are necessary: (1) those used to calculate the radiation emitted by the initial estimate Planck function profile; (2) differential weighting functions which give the changes of emitted radiation which arise from deviations from the initial estimate Planck function profile. The two weighting functions would be equal if there were no temperature dependence. Both are readily calculated from Heaseman's parameterization for any Planck function profile, and since the same initial estimate (hence the same weighting functions) are used at all longitudes for a given latitude, little additional computation is required.

c) The SAMS and LIMS

For limb sounders, temperature retrieval is closely associated with the problem of determining the viewing pressure of each measurement. This renders the process highly nonlinear, so retrieval is performed on individual scans or closely related groupings of data, rather than on gridded radiances. The SAMS and LIMS retrieval methods are described by RODGERS et al. (1984) and GILLE et al. (1984), respectively.

GEOPOTENTIAL HEIGHT DATA

The three-dimensional geopotential height field was obtained by integrating temperature vertically (using the hydrostatic relation) and adding to 30 mb monthly mean geopotential height analyses made by the Berlin Free University, based largely on radiosonde data. In the case of the Northern Hemisphere these had been made by averaging daily analyses to give means for each month for which satellite data were available (STRATOSPHERIC ANALYSIS GROUP). For the Southern Hemisphere, monthly mean fields were made directly from average radiosonde reports (KNITTEL, 1974). These data were available from January 1968 to December 1972, a different period from the satellite data, and therefore they were averaged to give a single mean field for each month.

MERGING OF DATA SETS

Because the data sets cover different time and space domains, averaging over all available data sets for any point was found to lead to discontinuities at data set boundaries. The problem was particularly severe at vertical lines of discontinuity, such as at 70 deg N at the edge of the SAMS data, because the thermal wind equation implied a zonal wind jet. Smoothing out the discontinuity merely broadened and smoothed the jet, without removing it. For this reason only the SCR and PMR data sets were used to give the proposed climatology, since they both measure nearly pole-to-pole. A further reason for not using the LIMS was the lack of data for a complete year, since comparison between corresponding seasons in the two hemispheres would have been misleading.

A smooth transition was made in the vertical between the SCR and PMR data sets by taking a weighted mean of the two where the weight, w , varied linearly between 6 and 8 pressure scale heights, z , (approximately 40 and 56 km, respectively):

$$\begin{aligned} T(z) &= T(\text{SCR}) & z < 6 \\ T(z) &= (1 - w)T(\text{SCR}) + wT(\text{PMR}) & 6 < z < 8 \\ T(z) &= T(\text{PMR}) & z > 8 \end{aligned}$$

where $w = (z-6)/2$ and T is the zonal mean temperature or a sin or cos component of zonal temperature wave. Thus the two temperature fields were smoothly merged over a range of about 16 km. This will inevitably lead to lapse rate errors in this region, but this problem was felt to be acceptable and much less serious than the wind errors produced by a vertical discontinuity.

For both the SCR and PMR the temperature fields were averaged over their respective periods (2 and 3 years, respectively) before combination. For the Northern Hemisphere, 30 mb height fields averaged over the same five years were used for the reference level. For the SCR, retrievals made by A. D. Belmont were also available for the mid- and upper stratosphere. Since they were for the same time period, they were not averaged with the Oxford retrievals but were merely compared.

It was thought important to include tropospheric temperature in the mean climatology because many middle atmosphere applications require data below the tropopause, hence radiosonde data were used for the surface to 30 mb for the zonal mean. The Berlin temperature analyses were used for 30 mb and for 1000, 900, 800, 700, 600, 500, 400, 300, 200, 100, and 50 mb values given in the climatology by OORT (1983). The latter were given for latitudes 80 deg S to 80 deg N and for each calendar month, and are primarily averages over the 1960s and early 1970s. Linear interpolation on a log(pressure) scale was used to obtain values on the grid used for this work. Between 30 mb and 10 mb a smooth transition was made to satellite-only data, so above 10 mb SCR/PMR data were used exclusively. Radiosonde data were not used for the eddy components, apart from the 30 mb geopotential base level, so wave components at all levels were derived from satellite data.

COMPARISON AND VALIDATION

Figure 1 is an example showing the agreement obtained between the SCR retrievals and radiosonde measurements. Temperature around the 60 deg N latitude circle is given as a deviation from the zonal mean as a function of time for a 30-day period in January and February 1973. Agreement is generally excellent both of the longitudinal location and the amplitude of perturbations. However detailed comparisons by VYAS (1984) showed that the SCR zonal mean values at this level were generally about 5 K colder than Berlin radiosonde

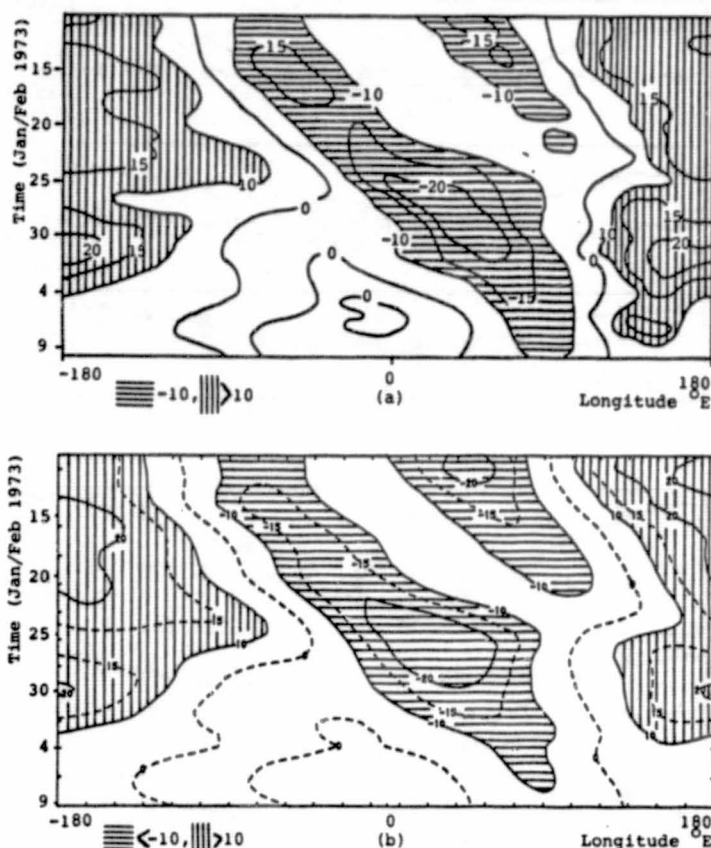


Figure 1. Longitude - time sections of deviations of temperature (K) from the zonal mean for that day at 50 mb 60 deg N; (a) taken from the Berlin Free University radiosonde analyses; (b) from SCR retrievals. Taken from VYAS (1984).

analyses and there is a case for making an empirical adjustment to the SCR zonal mean values to make them agree. BARNETT et al. (1975) have compared the SCR with radiosonde and rocketsonde; the former agree to within 1 K in equivalent temperature whilst the latter are 1-2 K warmer than the SCR at higher levels and approximately 2 K cooler in the lower stratosphere.

Figure 2 shows comparisons between values of height and temperature found over the Volgograd and Fort Churchill rocket stations and the PMR retrievals during the year July 1975 - June 1976. The rocketsonde measurements are direct copies of figures given in NASA (1978), and the PMR monthly mean values for those months of the same years and for the same latitude and longitude have been superimposed. It should be noted that the Volgograd profiles had been corrected in a manner consistent with FINGER et al. (1975) to make them compatible with US rocketsondes. Temperature differences are generally largest at 0.4 mb (about 54 km) being up to about 8 K, while differences were up to about 5 K at lower levels. No consistent bias was apparent at 2 mb but at 5 mb (where the information content of the weighting functions is rather low) the PMR measurements are generally warmer. Geopotential heights generally agreed to within about 200 m, although it should be remembered that the

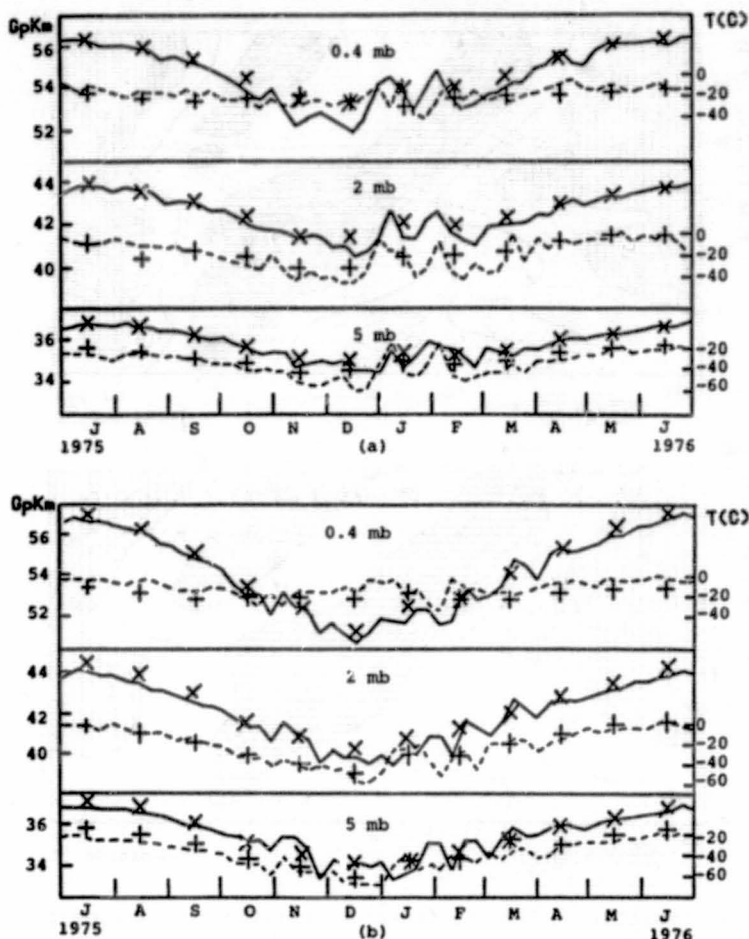


Figure 2. Comparisons between radio/rocketsonde measurements and retrievals for the same locations for (a) Volgograd (49 deg N, 44 deg E) and (b) Fort Churchill (59 deg N, 94 deg W). The rocket geopotential heights are given as solid lines with PMR monthly mean values marked with x. Rocket temperatures are given as dashed lines with PMR values marked by +. The upper, middle and lower boxes are for 0.4, 2, and 5 mb, respectively. The rocket data were extracted from analysed fields made by the Upper Air Branch of NOAA, and the figure is reproduced from NASA (STAFF, UPPER AIR BRANCH NATIONAL WEATHER SERVICE, 1978).

reference level of 30 mb used to determine heights was rather lower than ideal for use with the PMR weighting functions.

Figure 3 shows a comparison between the SAMS means (averaged over the years 1979-1981) and the SCR/PMR mean. For the zonal mean, differences of the SCR/PMR mean for 1973-78 minus SAMS are given. There are large differences, up to 12 K, near the north pole, which is taken to be due to sudden warming-type activity, but at other locations differences are less than about 5 K. The SAMS has been the subject of extensive comparisons. BARNETT and CORNEY (1984) compared the SAMS with the SSU, rocketsondes and radiosondes. The Pre-MAP

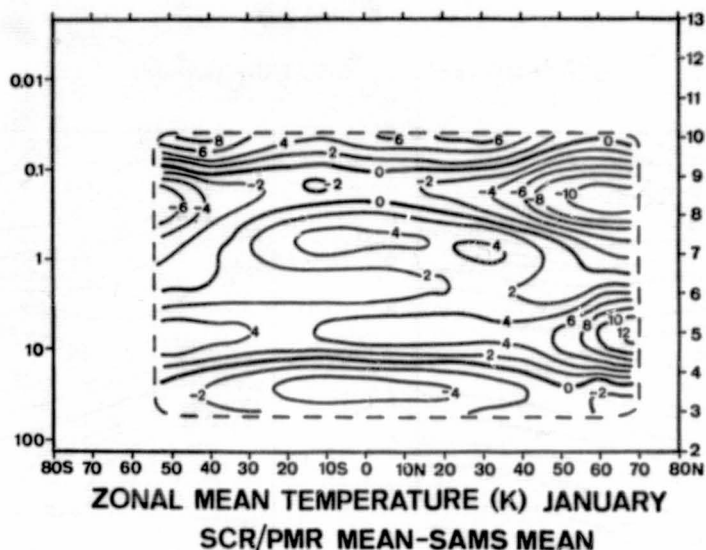


Figure 3. Difference between the SAMS average January zonal mean temperature for 1979, 1980, 1981 and that of the SCR/PMR combined mean, given as SCR/PMR - SAMS (K).

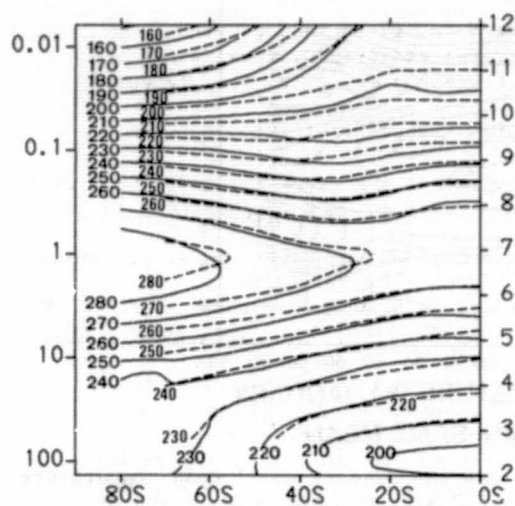
working group PMP-1 has intercompared SAMS, LIMS, SSU and analyses from Berlin Free University, the National Meteorological Center in Washington, and the European Centre for Medium-Range Weather Forecasting for various days and months during the Northern Hemisphere winters of 1979-81. Part of the study has been published as Handbook for MAP, Vol. 12 by RODGERS (1984), and the remainder will be published in a future handbook. The conclusion (for nominally simultaneous measurements) was that agreement was typically within a few K.

Figure 4a-d shows comparisons for January, April, July and October, between the SCR/PMR mean and the Southern Hemisphere Reference Atmosphere proposed by KOSHELKOV (1984) and given in Section 2.1.3) which is based on rocketsondes in the Southern Hemisphere and, to some extent, PMR measurements. In January agreement is excellent with maximum differences of about 5 K, but with values typically within 2 K, and features of the two fields are closely matched. Larger differences occur in April, exceeding 10 K at the top levels, but the general temperature patterns are again very alike. Similar agreement is found in July, and it should be noted that the cold belt around 45 deg S at 1 mb is present in both fields. Agreement in October is comparable with April and July. It is interesting to note that the temperature maximum at the stratopause in July at 80 deg S is very much warmer than that for the Northern Hemisphere 6 months later (see Section 2.2 Figure 1), and that a cold midlatitude belt occurs in the Northern Hemisphere winter, but that it is less marked than in the Southern Hemisphere.

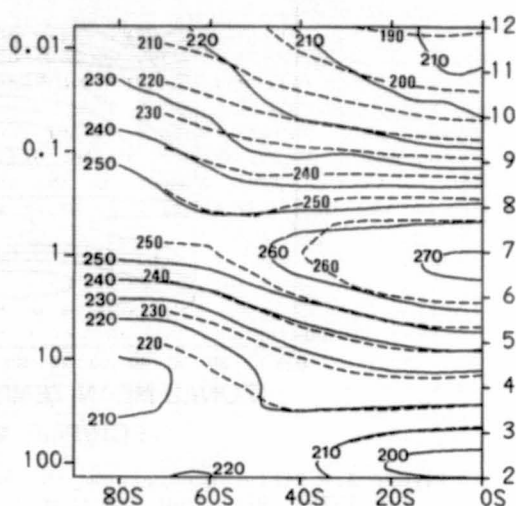
RELATIONSHIP TO LONG-TERM TRENDS

Section 2.3.7 gives an analysis of long-term temperature trends observed in the stratosphere. The satellite data are for only a relatively short period (see Table 1), but Figures 10 and 13 of Section 2.3.7 show that this period, 1973-1978, is representative of the long-term average over the last 20 years.

SCR/PMR (solid); KOSHELKOV(dashed)

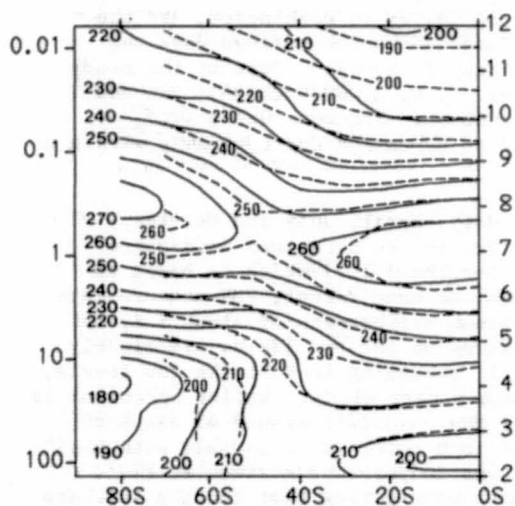


a) JANUARY

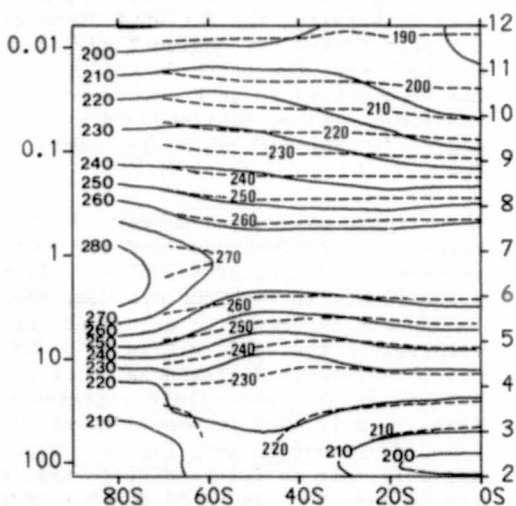


b) APRIL

SCR/PMR (solid); KOSHELKOV(dashed)



c) JULY



d) OCTOBER

Figure 4. Comparison between the SCR/PMR combined temperature means (K) for (a) January, (b) April, (c) July and (d) October and that given by KOSHELKOV (1984) and Section 2.1.3 for the Southern Hemisphere.

REFERENCES

- Barnett, J. J., and M. Corney (1984), Temperature comparisons between the Nimbus 7 SAMS, rocket/radiosondes and the NOAA-6 SSU, J. Geophys. Res., **89**, 5294-5302.
- Barnett, J. J., R. S. Harwood, J. T. Houghton, C. G. Morgan, C. D. Rodgers, and E. J. Williamson (1975), Comparison between radiosonde, rocketsonde and satellite observations of atmospheric temperatures, Q. J. Roy. Meteorol. Soc., **101**, 423-436.
- Crane, A. J. (1977), Uses of satellite data in studies of stratospheric dynamics, Ph.D. Thesis, Oxford University.
- Crane, A. J. (1979), Aspects of the energetics of the upper stratosphere during the January - February 1973 major sudden warming, Q. J. Roy. Meteorol. Soc., **105**, 185-206.
- CIRA (1972), Cospar International Reference Atmosphere, edited by A. C. Strickland, Akademie-Verlag, Berlin.
- Curtis, P. D., J. T. Houghton, G. D. Peskett, C. D. Rodgers (1974), The pressure modulator radiometer for Nimbus F, Proc. Roy. Soc. Lond., **A337**, 135-150.
- Drummond, J. R., J. T. Houghton, G. D. Peskett, C. D. Rodgers, M. J. Wale, J. Whitney, and E. J. Williamson (1980), The stratospheric and mesospheric sounder on Nimbus 7, Phil. Trans. Roy. Soc. Lond., **A296**, 219-241.
- Ellis, P., G. Holah, J. T. Houghton, T. S. Jones, G. Peckham, G. D. Peskett, D. R. Pick, C. D. Rodgers, K. H. Roscoe, R. Sandwell, S. D. Smith, and E. J. Williamson (1973), The selective chopper radiometer for Nimbus 5, Proc. Roy. Soc. Lond., **A334**, 149-170.
- Finger, F. G., M. E. Gelman, F. J. Schmidlin, R. Leviton, and B. Kennedy (1975), Compatibility of meteorological rocketsonde data as indicated by international comparison tests, J. Atmos. Sci., **32**, 1705-1714.
- Gille, J. C., and J. M. Russell III (1984), The limb infrared monitor of the stratosphere (LIMS): an overview of the experiment and its results, J. Geophys. Res., **89**, 5125-5140.
- Gille, J. C., J. M. Russell III, P. L. Bailey, L. L. Gordley, E. E. Remsberg, J. H. Lienesch, W. G. Planet, F. B. House, L. V. Lyjak, and S. A. Beck (1984), Validation of the temperature retrievals obtained by the Limb infrared monitor of the stratosphere (LIMS) experiment on Nimbus 7, J. Geophys. Res., **89**, 5147-5160.
- Heaseman, C. H. (1981), Satellite observations of mesospheric wind structure, Ph.D. Thesis, Oxford University.
- Knittel, J. (1974), Ein Beitrag zur Klimatologie der Stratosphaere der Suedhalbkugel, Meteorol. Abh. Met. Inst., Berlin, **A2**, (No. 1).
- Koshelkov, Y. P. (1984), Reference middle atmosphere for the Southern Hemisphere, Preprint of paper presented at XXV COSPAR, Graz, to be published in Adv. Space Res.
- Newell, R. E. (1977), Private communication.
- Oort, A. H. (1983), Global atmospheric statistics, 1958-1973, NOAA Professional Paper 14.
- Rodgers, C. D. (1976), Retrieval of atmospheric temperature and composition from remote measurements of thermal radiation, Geo. Space Phys., **14**, 609-624.
- Rodgers, C. D. (1984)(Editor), Coordinated Study of the Behaviour of the Middle Atmosphere in Winter (PMP-1), Handbook for MAP, Vol. 12.
- Rodgers, C. D., R. L. Jones, and J. J. Barnett (1984), Retrieval of temperature and composition from Nimbus 7 SAMS measurements, J. Geophys. Res., **89**, 5280-5286.
- Staff, Upper Air Branch National Weather Service, Camp Spring, Maryland (1978), Synoptic analyses, 5-, 2-, and 0.4 millibar surfaces for July 1974 through June 1976, NASA Reference Publication 1023
- Stratospheric Analysis Group, Meteorol. Abh. Met. Inst., Berlin.
- Vyas, N. (1984), Numerical modelling of atmospheric processes, Ph.D. Thesis, Oxford University.

2.1.2 TEMPERATURE AND WIND DATA FROM METEOROLOGICAL ROCKETS

F. J. Schmidlin

NASA Goddard Space Flight Center
Wallops Flight Facility
Wallops Island, VA 23337

Guided by the historical belief that the upper atmosphere is quiescent and steady when compared to the lower atmosphere, meteorologists of the 1950s and early 1960s found it difficult to accept the measurements provided by early rocket measurements. These early measurements were characterized by poor data resolution in every scale: vertical (~8-10 km), horizontal (~5-10000 km), and temporal (~weekly to monthly). Heavy, sophisticated and complex sounding rocket techniques deployed during this early period were costly, and tended to produce oversmooth data.

Development of small, single stage easy to handle meteorological rocket systems led to an increased frequency of launchings; from 1-2 every three months to as many as 3-5 every week from United States rocket ranges. Early efforts saw the development of a coordinated launch schedule from independently scheduled launchings from the different launch ranges. Meteorological rockets also were being developed and in use in other countries, such as the United Kingdom, Japan, France, Australia, and the USSR. The coordinated aspects of rocketsonde launchings in the US led to the formation of the Meteorological Rocket Network. The number of launch sites grew from four in 1950 to 30 in the late 1960s; only about ten sites are still operated by the US today, four by the USSR, and one by Japan. Australia launches an occasional rocketsonde for research studies, as does India.

During the mid-1960s to early 1970s a cooperative effort between Argentina, Brazil, France, and the United States established a schedule of rocketsonde launchings growing from one per month to one per week. The effort of these countries fostered a suggestion that a cooperative series of measurements from two meridional chains of launch sites take place. One chain was established in the Americas (near 70°W) and one in the Eastern Hemisphere (near 70°E). The Eastern Hemisphere network was established and maintained by the USSR. Thus, the Meteorological Rocket Network and the two North-South networks provided a considerable quantity of rocketsonde data between 20 km to 60 km with some launch sites providing data to 90 km.

The number of rocket ranges operated by the United States has diminished critically during the past few years. However, when one considers the frequent requests for data that are received for many reasons and is aware of research planned in the middle atmosphere, it is apparent that the importance of the meteorological rocketsonde continues.

Meteorological rocketsonde data have been published since the autumn of 1959. Initially, reports were published each quarter by the Schellenger Research Laboratory of the University of Texas at El Paso. In 1966, this activity became the responsibility of the World Data Center for Meteorology located in Asheville, North Carolina. In 1969, the archival format was changed by the World Meteorological Organization. This change made it simple to provide a unified format on magnetic tape to any investigator requesting data.

Many tens of thousands of observations are on file in the World Data Center (WDC) in the unified format which began in 1969. For the years of 1959-1968 an almost equal amount of data exists in a somewhat different format. Additionally, thousands of rocketsonde reports in manuscript or different formats, although not easily retrievable, also exist. The quantity of data so

far gathered permits a relatively detailed look at stratospheric and lower mesospheric structure and has led to the partitioning of the Northern Hemisphere atmosphere into climatological seasons as shown in Table 1 (WEBB, 1969). An example of the utility of rocketsonde data also can be noted in the reversal that occurs each spring and autumn. Rocketsonde wind data have shown that each spring the middle atmosphere (between 30-60 km) winds reverse from westerly to easterly beginning in the polar latitudes and progresses equatorward. The upper levels progressing faster than the lower levels. The autumn reversal follows the same pattern, i.e., pole to equator as the wind changes from easterly to westerly.

In recent times the most significant amount of rocket data available in the WDC archives has been obtained from the United States rocketsonde system. Although the problem of data quality may be addressed differently for each rocketsonde system, only the US system is discussed because of the quantity of data archived.

Questions concerning measurement errors and data quality often are asked. Differences have been noted in measurements made within minutes of each other, sometimes looking as if individual measurements were obtained hours, or even days apart. These observed differences generally are considered to be caused by atmospheric small-scale variations, but unless reliable information about the instruments is available, the differences could be instrumental.

Studies of the precision of the US rocketsonde instrument (see BOLLERMAN (1970) for a description of the US Super Loki Datasonde) have been carried out. Accuracy, while not very easy to confirm, can only be judged in relation to measurements from rocketsonde instruments of all countries (FINGER et al., 1975). A comparison of rocketsondes of Great Britain, France, Japan, USSR, and the United States showed that all instruments (except that of the USSR) agreed to within 5°C up to 60 km. Measurements obtained from the USSR rocketsonde became progressively colder than the others above 45 km, the difference in temperature reaching approximately 12°C at 60 km.

Repeatability of the US instrument has been shown by SCHMIDLIN (1981) to be 1°C at 53 km and lower altitudes. This precision decreases to about 4°C at 65 km. This test used paired observations where the second rocketsonde was launched 5 minutes after the first of the pair. Other efforts to understand differences and the quality of high altitude temperature measurements were conducted by HOKIT and HENRY (1973), who evaluated rocketsonde temperatures relative to altitude and solar angle, by KRUMINS and LYONS (1972) and KRUMINS (1978), who developed optimum correction values for the raw temperature measurements.

Validity of rocketsonde temperature measurements also depends on calibration data. Calibrations from a random sample of 18 instruments were checked using laboratory techniques (SCHMIDLIN, 1981); results were positive. The manufacturer supplied calibrations showing no change after 2-3 years.

The quality of wind information obtained from a falling target depends on the quality of the tracking system, sample rate, editing and filtering used with the raw tracking data, the type of sensor, and sensor fall speed. Winds obtained from various targets, whether parachute, chaff, or sphere can be made comparable after suitable corrections. The slower the target falls, the more precise the wind measurements. Thus, the magnitude of the error is a function of the target's fall velocity. At fast fall velocities and large wind shears the magnitude of the measurement difference between the sensor's horizontal velocity and actual wind increases. Additionally, the faster a target falls the more smoothing that must be applied, consequently slow targets have greater wind resolving capability.

Table 1. Climatological periods of the Northern Hemisphere derived from meteorological rocketsonde data.

<u>Period</u>	<u>Date</u>
Winter storm period	16 December - 15 February
Late winter	16 February - 31 March
Spring reversal	1 April - 15 June
Summer	16 June - 15 August
Fall reversal	16 August - 15 October
Early winter	16 October - 15 December

Although it is not possible to establish an exact error for wind measurements based on the previous discussion, unpublished information from studies conducted at White Sands Missile Range and Wallops Island indicate the wind errors may be as large as 7 meters per second near 60-65 km.

REFERENCES

- Bollerman, B. (1970), Space Data Corp., Contractor Report, NASA CR 1529.
- Finger, F. G., M. E. Gelman, F. J. Schmidlin, R. Leviton, and B. W. Kennedy (1975), J. Atmos. Sci., 32, 1705-1714.
- Hoxit, R. and R. H. Henry (1973), J. Atmos. Sci., 30, 922-933.
- Krumins, M. (1978), Ph.D. Thesis, University of Maryland, College Park, MD.
- Krumins, M., and Lyons (1972), NOLTR 72-152, Naval Ordnance Lab., White Oak Silver Spring, MD.
- Schmidlin, F. J. (1981), J. Geophys. Res., 86, 9599-9603.
- Webb, W. L. (1969), World Survey of Climatology, 4, 281-381, Rev. Elsevier Pub. Co, Amsterdam.

2.1.3 OBSERVED WINDS AND TEMPERATURES IN THE SOUTHERN HEMISPHERE

Yu. P. Koshelkov ✓

Central Aerological Observatory of the State Committee of the USSR
for Hydrometeorology and Control of Natural Environment
12 Pavlika Morozova, 123376 Moscow, USSR

(Shortened for this publication by K. Labitzke, Ed.)

(a) TEMPERATURE IN THE SOUTHERN HEMISPHERE BASED ON ROCKET DATA

The presence of hemispheric asymmetry in the structure of the middle atmosphere has been confirmed in a number of papers based on rocketsonde and satellite data (BOROKIKOV et al., 1962; GAIGEROV, 1973; GAIGEROV and KOSHELKOV, 1973; GAIGEROV et al., 1969; ELLIS et al., 1970; KOSHELKOV, 1971a, 1974a; FRITZ and SOULES, 1970; LABITZKE, 1974; 1977a,b; LABITZKE and BARNETT, 1973, 1979; BARNETT, 1974, 1975, 1981; BARNETT et al., 1978; HARWOOD, 1975; NASTROM and BELMONT, 1975; HARTMANN, 1976; LEOVY and WEBSTER, 1976; HOUGHTON, 1978; CRANE, 1979; HIROTA et al., 1983). Therefore the middle atmosphere of the Southern Hemisphere cannot be regarded as identical to that of the Northern Hemisphere, but as a region with its own specific features of circulation and structure. This fact makes it necessary to compile separate reference atmospheres for two hemispheres. However there were not sufficient observational rocket data for this purpose during the time when CIRA 1972 was compiled. Most of the studies on meteorology of the middle atmosphere of the Southern Hemisphere were confined to regional analyses -- for Australia (GROVES, 1965; PEARSON, 1966; ROFE, 1966), South America (BRYNSZTEIN, 1972), Southern Ocean (FINGER and WOOLF, 1967; KOSHELKOV, 1969), and Antarctica (GAIGEROV, 1973; GAIGEROV and KOSHELKOV, 1973; BRIGGS, 1965). Later in the 1970s first attempts were made to generalize the accumulated information for the whole of the Southern Hemisphere. In particular, empirical wind and temperature models for the stratosphere and mesosphere of the Southern Hemisphere were compiled in the Central Aerological Observatory (CAO) based on rocketsonde as well as aerological information (KOSHELKOV, 1983a,b)

These results are analyzed briefly below as a part of the new CIRA. It should be noted also that some attempts are being made in CAO to provide an analytical presentation of the climatic distribution of meteorological parameters.

The available rocketsonde data were collected both at stations and from vessels. The number of temperature measurements conducted by means of the Soviet rocketsondes and published in Bulletins of Results of the Rocket Sounding of the Atmosphere (1960-1982) is presented in Table 1. Besides this, data obtained at Woomera (31°S, 137°E) were used including 28 dropsonde measurements during 1968-1972 (HIND, 1973) and 31 falling sphere observations during 1970-1974 (WEAPONS RESEARCH ESTABLISHMENT, 1962-1974). At other sites, most of the observations were by Arcasondes and Datasondes and the data were obtained from WDC-A (1965-1978); NASA (1968-1970, 1972-1977) and ROCOB exchange. The profiles were corrected according to DREWS (1966); EZEMENARI (1972); and KRUMINS and LYONS (1972). The number of measurements available (at 50 km) are 129 for Mar Chiquita (38°S, 57°W) in 1967-1980, about 1200 profiles for Ascension Is. (8°S, 14°W) in 1965-1980 and about 200 measurements for Natal (6°S, 55°W) in 1966-1980. The results obtained at Chimal (30°S, 60°W) in 1966-1968, at Tartagal (23°S, 64°W) in 1966 and the vessel "Croatan" near the western coast of South America in 1965 (FINGER and WOOLF, 1967; MANNING and CHAMBERLIAN, 1968) were also used. Fort Sherman (9°N, 80°W) data for 1967-1978, Kwajalein Is. (9°N, 168°E) data for 1970-1981 and Thumba (8°N, 77°E)

Table 1. The number of successful temperature measurements by means of Soviet rocketsondes from research vessels and at Molodezhnaya and Kerguelen Is. (up to January 1982). Top - for the 75-km level, bottom - for the 50-km level.

Station	Month												Annual
	J	F	M	A	M	J	J	A	S	O	N	D	
Vessels:													
5°N-15°S	48	76	24	5	19	22	7	11	6	5	20	23	266
	63	85	35	13	33	41	10	17	8	7	35	32	379
15°S-25°S	26	6	11	1	9	8	-	22	6	9	4	11	113
	31	7	13	1	14	10		21	9	14	6	14	140
25°S-35°S	7	15	9	4	8	7	8	0	11	8	6	7	90
	10	16	12	7	9	8	10	2	12	10	9	13	118
35°S-45°S	2	13	11	8	7	3	8	0	4	6	10	9	81
	4	16	13	9	10	3	13	1	4	8	14	10	105
45°S-55°S	1	0	3	-	2	0	2	0	2	-	4	4	18
	5	11	4		6	1	5	2	4		8	5	51
(Kerguelen)	-	9	29	31	23	29	14	6	2	-	-	-	143
49°S		11	32	34	26	32	16	8	2				164
(Molodezhnaya)	42	35	35	33	32	42	51	52	30	42	37	46	477
68°S	47	41	41	41	45	62	72	68	42	52	45	54	610

data for 1970-1981 were of help in the analysis of the equatorial region. Some results of mesospheric measurements by means of grenades and Pitot probes were published (MANNING and CHAMBERLAIN, 1968; NASA, 1966-1972; THEON et al., 1972).

It is known that at altitudes higher than 45 km, temperature readings obtained by means of different rocket systems reveal systematic discrepancies. These were confirmed in the course of direct intercomparison tests (FINGER et al., 1975; IVANOVSKY et al., 1979; SCHMIDLIN et al., 1980) and later were revised (KOSHELKOV, 1983a) by means of indirect comparisons of climatic temperature means at different sites. As a result, adjustments have been worked out to make different sets of data compatible; some of them used in the data analysis for the Southern Hemisphere are presented in Table 2. Before applying such adjustment to the Soviet rocketsonde data, the mean temperatures obtained prior to 1979 had been fitted to the results of 1979-1981 when a modified payload was used: for the equator the bias in the former results proved to be 1.5°C at 50 km, 14°C at 60 km, 13°C at 70 km and 7°C at 75 km and for higher latitudes seasonal variations of the bias were taken into account. Data obtained at Molodezhnaya and Kerguelen Is. were corrected also for the wind effect in temperature readings by approximately -5°C for Molodezhnaya and 3-4°C for Kerguelen data for the lower mesosphere. Arcasonde data accumulated in the Northern Hemisphere and near the equator during 1965-1969 have revealed somewhat higher temperatures at altitudes 30 to 40 km than Datasonde data for

Table 2. Empirical adjustments ($^{\circ}\text{C}$) for obtaining compatibility of different sets of temperature measurements in the mesosphere with grenade measurements.

Alt., km	Technique			
	M 100B (1979-1981)	Datasonde (corrected (44))	Arcasonde (corrected (42,43))	Australian dropsonde (corrected (37))
80	0	-	-	-
70	6	-7	-	-
60	9	-2	-4	-11
50	5	0	-1	-3

1971-1980; to make both sets compatible, Arcsonde data for the Southern Hemisphere sites were lowered by about 2°C and then united with the Datasonde data. It cannot be ruled out however that the discrepancy between the mean temperatures in different years is related to the solar activity cycle (ANGELL and KORSHOVER, 1978; QUIROZ, 1979; KOKIN et al., 1981).

The Australian sphere temperatures for 1970-1974 did not differ significantly from grenade temperatures for corresponding latitudes in the Northern Hemisphere up to the height of 70 km; above this level, the usefulness of the 1970-1974 sphere data was limited since seasonal variations were not in agreement with earlier rocket results (ROFE, 1966) or PMR data (LABITZKE and BARNETT, 1981). The dropsonde temperature data were adjusted (KOSHELKOV, 1977) to the sphere data in the lower mesosphere (Table 2).

Compilation of the reference model from sets of data was achieved by application of both temporal and spatial smoothing. Seasonal variations were approximated for each station by two (for Mar Chiquita and Woomera) or three (for Molodezhnaya and Ascension Is.) harmonics of the annual cycle. In case of the incomplete annual cycle of observations (Kerguelen Is., vessels) smoothing by hand provided better results.

Latitudinal smoothing was based on an application of either third degree polynomials (mainly in the stratosphere where the data amount was greater) or hand smoothing (in the mesosphere); in the latter case, the vertical wind shear and PMR radiance (LABITZKE and BARNETT, 1981) latitudinal variations could be taken into account.

Vertical consistency of the smoothed (in time and space) values was then considered for various latitudes and required usually insignificant ($1-2^{\circ}$) changes to provide smooth vertical variation. The lower part of the rocket-based mean profiles was adjusted to zonal mean temperatures based on aerological observations (KHANEVSKAYA, 1971; ZASTAVENKO, 1975; KOSHELKOV, 1971b, 1980b; VAN LOON et al., 1975; KNITTEL, 1976; MONTHLY CLIMATIC DATA FOR THE WORLD, 1957-1977). The rms error of the monthly mean temperatures in the Southern Hemisphere is estimated to be in the stratosphere about 1°C in summer and $2-2.5^{\circ}\text{C}$ in winter while in the mesosphere appropriate values are about $1.5-2^{\circ}\text{C}$ and 3°C , respectively. Systematic bias of the model data must be small in

the stratosphere and of the order of 5°C in the mesosphere; exact values are difficult to assess since the nature of discrepancies between different rocket measurements has not been finalized (FINGER et al., 1975; IVANOVSKY et al., 1979; SCHMIDLIN et al., 1980; KOKIN and GAIGEROV, 1981). However, the use of the common reference (grenade) in the mesosphere for the Northern and Southern Hemisphere Reference Atmospheres enables one to define hemispheric asymmetry in thermal structure. The accuracy of the analysis applied for the compilation of the Southern Hemisphere Reference Tables is estimated to be about $1\text{--}2^{\circ}\text{C}$ in the stratosphere. The total uncertainty in the reference temperature values amounts to $2\text{--}3^{\circ}\text{C}$ in the stratosphere and $5\text{--}7^{\circ}\text{C}$ in the mesosphere.

The tables for latitudes 40°S to 70°S represent characteristic values for the Indian Ocean sector of the Southern Hemisphere, since the main contributing sites in extratropical latitudes (Molodezhnaya, Kerguelen Is.) are located in this sector and the bulk of vessel sounding data is also for the Indian Ocean area (usually for $65\text{--}70^{\circ}\text{E}$). From satellite information it is found that the upper stratosphere in this sector of the Subantarctic in winter is slightly warmer than mean zonal temperatures (cf. Section 2.3.1). For latitudes lower than 40°S data from various sectors of the Southern Hemisphere have been used and the model should describe conditions close to the zonal mean.

Figure 1 shows a comparison of the model temperatures for 70°S with (a) the Molodezhnaya data for 1982-1983 at the 40-km level, and (b) with the Reference Atmosphere data as presented in Section 2.2. The agreement is generally good.

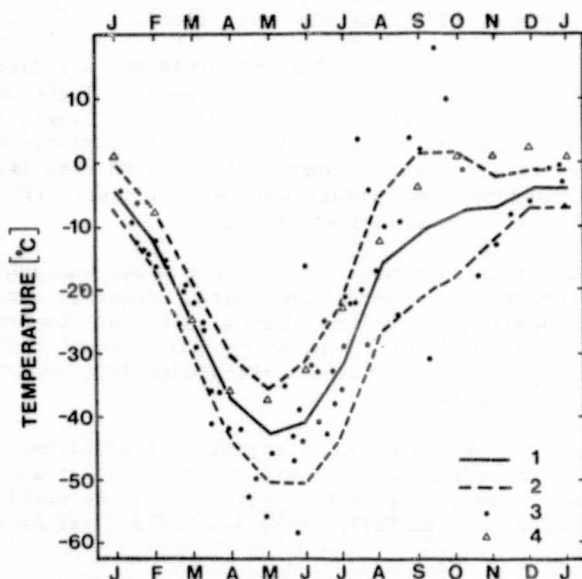


Fig. 1

Figure 1. Comparison of the model temperatures for 70°S with the Molodezhnaya data for 1982-83 at the 40-km level, and with the data given in Section 2.2. 1 - temperature, in the CAO model; 2 - standard deviation of temperature from the model values; 3 - temperature at Molodezhnaya (1982-1983); 4 - temperature data of new Reference Atmosphere, Section 2.2.

(b) WIND IN THE SOUTHERN HEMISPHERE FROM ROCKET DATA

The wind structure of the stratosphere and mesosphere is not identical in the Northern and Southern Hemispheres as it has been revealed in recent years from both rocket (GAIGEROV and KOSHELKOV, 1973; ROFE, 1966; KOSHELKOV, 1969, 1974b, 1975; BUGAEVA and RYAZANOVA, 1969; BELMONT et al., 1974; GAIGEROV et al., 1975; TARASENKO et al., 1976) and satellite (HARTMANN, 1976; HIROTA, et al., 1983; and others) observations. Compilation of reference atmospheres is easier in the case of wind than in the case of temperature due to the absence of systematic discrepancies between wind velocities measured by means of different techniques. However for the Southern Hemisphere the main difficulty arises due to the scanty amount of observations, particularly above 60 km, where diurnal variations are great (e.g. ELFORD, 1974; GROVES, 1974; BOUTKO et al., 1976).

As in the case of temperature models, the information (BOROVIKOV et al., 1962; FINGER and WOOLF, 1967; BRIGGS, 1965; BULLETINS OF RESULTS OF THE ROCKET SOUNDING OF THE ATMOSPHERE, 1960-1982; HIND, 1973; WEAPONS RESEARCH ESTABLISHMENT, 1962-1974; WDC-A, 1965-1978; NASA, 1968, 1969, 1970; NASA, 1972-1977; MANNING and CHAMBERLAIN, 1968; NASA, 1966-1972; THEON et al., 1972) used for compiling reference tables for the Southern Hemisphere has been collected mainly from observations conducted in the southern regions of the Indian Ocean (and partly, of the Pacific), in the Australian and South American sectors of the hemisphere. The number of rocket wind measurements for main sites is clear from Table 3. Additionally, measurements from on board vessels "Ob" in 1958 and "Croatan" in 1965 were used, as well as the results of 28 launchings at McMurdo (78°S, 168°E) in 1962-1973 in Antarctica and a number of firings at Tartagal and Chamental in Argentina in 1966. Most valuable proved to be 24 mesospheric measurements (at the altitude of 80 km) of wind velocity at Natal in 1966-1973.

Table 3. The number of wind measurements for main rocket sites in the Southern Hemisphere up to January 1982, used for compiling the reference atmosphere.

Site	Period of obs.	Altitude, km		
		40	60	80
Vessels: 1961-1981				
5°N - 5°S		359	92	-
5°S - 15°S		92	7	-
15°S - 25°S		173	-	-
25°S - 35°S		128	9	-
35°S - 45°S		99	8	-
45°S - 55°S		121	5	-
Kerguelen Is.	1973-1981	171	158	72
Woomera	1962-1974	111	78	43
Mar Chiquita	1966-1977	164	64	-
Ascension Is.	1964-1978	1684	804	42
Molodezhnaya	1969-1981	688	511	240

Wind measurements at South American sites, Ascension Is. and McMurdo have been conducted mainly by tracking parachutes of the Arcasonde or Datasonde below 60-65 km and chaff measurements in some cases (at Chanical). Falling spheres were applied at Ascension Is. and Woomera for mesospheric heights in addition to rocketsonde parachute measurements in the stratosphere and lower mesosphere over Natal. In the case of Soviet rocketsondes, winds below 60 km were determined by means of parachute and above that height with the help of chaff. A 6-year series (ELFORD, 1974) of radiometeor measurements of wind at Adelaide (35°S, 139°E) was a help for the wind analysis in the meteor layer. Radiosonde data (MONTHLY CLIMATIC DATA FOR THE WORLD, 1957-1977; MONTHLY CLIMATIC DATA - UPPER AIR, 1969-1974; ATLAS OF WIND CHARACTERISTICS OF THE SOUTHERN HEMISPHERE, 1967) provided the basis for the analysis in the middle stratosphere; zonal mean geostrophic winds at 50 and 30 mbar levels (KOSHELKOV, 1971b; KNITTEL, 1976; KOSHELKOV and KOVSHOVA, 1982) were also taken into consideration.

As for the temperature model, the procedure of compiling wind tables involved temporal and latitudinal smoothing of the data. The resulting reference values are of regional character south of 40°S (the Indian Ocean sector) and more closely approach zonal means north of this latitude. Only the zonal component has been considered since for a meaningful analysis of the mean meridional circulation, one should have greater information than has been available. (Some information on the meridional component is given in Section 2.1.4).

An addition of new rocket data to the first version of the model (KOSHELKOV, 1975) did not result in a substantial change of mean values of stratospheric winds (no more than by 5 m/s). However, in the mesosphere certain difficulties were encountered in combining different sets of wind data, e.g., relatively low values of radiometeor winds at Adelaide in winter below 80 km and greater speeds measured by means of the falling spheres at Woomera, or rather weak westerlies above 60-65 km in winter over Kerguelen Is. and greater values over Molodezhnaya (chaff data at both sites). The introduction of the Kerguelen chaff data resulted in a reduction (by 10 m/s of the westerly flow in the present model as compared to the earlier (KOSHELKOV, 1975) version. It seems that values 5 and 10 m/s may reasonably reflect the uncertainty of the present model in the stratosphere and mesosphere, respectively.

Gross features of the latitudinal distribution of zonal wind are common for the two hemispheres, including the dominance of the easterly flow in the strato-mesosphere in summer and westerly flow in winter. A specific feature of the southern atmosphere circulation in summer is an extension of the maximum easterly flow at the heights of 45 to 55 km from 30° latitude into the equatorial region (HIROTA et al., 1983; BARNETT, 1981; KOSHELKOV, 1975) (Figure 2).

Hemispheric differences are insignificant in autumn. However, in winter these are quite pronounced: maximum values of the westerly flow in the Southern Hemisphere are higher than those in the Northern Hemisphere, and the latitude of the core of the flow is lower in the Southern Hemisphere; the subtropical high pressure ridge (determining the division of easterlies and westerlies) in the stratosphere of the Southern Hemisphere is weaker and closer to the equator than its Northern Hemisphere counterpart. In spring, a gradual shift of the core of maximum speeds towards higher latitudes and downward into the stratosphere is typical for the Southern Hemisphere; the easterly flow in the mesosphere of the Southern Hemisphere may appear as early as October, while a delay by 1-1.5 months is observed in the stratosphere.

Seasonal variation of zonal wind in the equatorial atmosphere (Figure 3) revealed that the CAO data deviate from the CIRA 1972 data; first, there is a

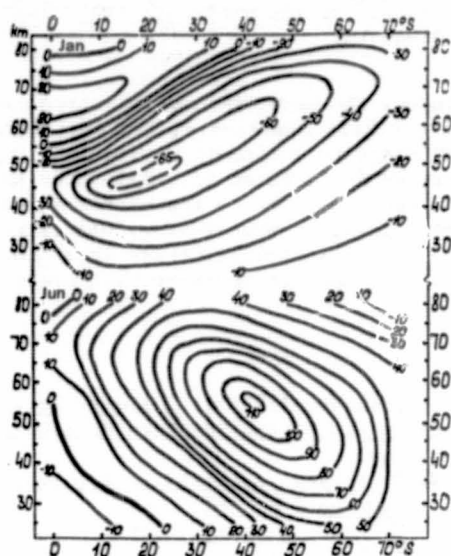


Figure 2. Cross sections of mean zonal wind (m/s) in the middle atmosphere of the Southern Hemisphere; upper part - January; lower part - June.

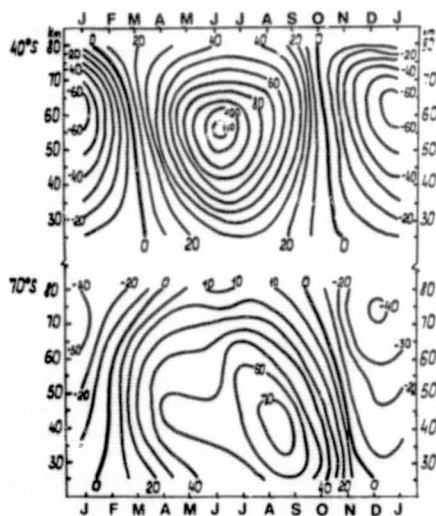


Figure 3. Seasonal variations of mean values of zonal wind at latitudes 40°S and 70°S (CAO model).

variation with a 12-month period (in addition to the predominant 6-month wave); second, the downward spread of the westerly wind arising within the semiannual wave is confined to 35-40 km.

In higher latitudes, the amplitude of the annual wave is greater in the Southern than in the Northern Hemisphere. The amplitude of the semiannual wave is minimum near 40-50°S and no secondary maximum has been found near 50-60°S similar to that described (BELMONT et al., 1974) for the Northern Hemisphere. Maximum speeds of the westerly flow in the middle atmosphere of the Southern Hemisphere are observed in early winter in middle latitudes and in late winter in the polar region. In the Antarctic, there is a time lag of the occurrence of maximum speed values in the stratosphere with decreasing altitude; (cf. also Sections 2.3.4 and 2.3.5).

REFERENCES

- Angell, J. K., and J. Korshover (1978), J. Atmos. Sci., **35**, 1758.
Atlas of Wind Characteristics of the Southern Hemisphere (1967), **1**,
 Gidrometeoizdat, Moscow.
 Barnett, J. J. (1974), Q. J. Roy. Meteorol. Soc., **100**, 505.
 Barnett, J. J. (1975), Nature, **255**, 387.
 Barnett, J. J. (1981), Handbook for MAP, **2**, 45.
 Barnett, J. J., J. T. Houghton, and G. D. Peskett (1978), Preprint to XXI
 COSPAR, Innsbruck.
 Belmont, A. D., D. G. Dartt, and G. D. Nastrom (1974), Q. J. Roy Meteorol.
 Soc., **100**, 203.
 Borovikov, A. M., G. I. Golishev, and G. A. Kokin (1962), Meteorologi i
 gidrologia, **3**, 14.
 Boutko, A. S., E. M. Golubev, I. N. Ivanova, G. A. Kokin, V. V. Mihnevitch, Yu.
 N. Rybin, and K. E. Speransky (1976), in Diurnal and Latitudinal Variations
 of Atmospheric Parameters and Corpuscular Fluxes, Gidrometeoizdat,
 Leningrad.
 Briggs, R. S. (1965), J. Appl. Meteorol., **4**, 238.
 Brynsztejn, S. M. (1972), in EXAMETNET Annual Rep., **163**.
 Bugaeva, I. V., and L. A. Ryazanova (1969), Meteorologia i gidrologia, **1**,
21.
Bulletins of Results of the Rocket Sounding of the Atmosphere (1960-1982),
 Gidrometeoizdat.
 Crane, A. J. (1979), Q. J. Roy. Meteorol. Soc., **105**, 509.
 Drews, W. A. (1966), Atlantic Res. Corp., TR PL-8876.
 Elford, W. G. (1974), in Proc. Int. Conf. on Structure, Composition and
 General Circulation of the Atmosphere, **2**, 708, Toronto
 Ellis, P. J., G. Peckham, S. D. Smith, J. T. Houghton, C. G. Morgan, C. D.
 Rodgers, E. J. Williamson (1970), Nature, **228**, 139.
 Ezemenari, F. (1972), J. Appl. Meteorol., **11**, 704.
 Finger, F. G., M. E. Gelman, F. J. Schmidlin, R. Leviton, and B. Kennedy
 (1975), J. Atmos. Sci., **32**, 1705.
 Finger, F. G., and H. M. Woolf (1967), J. Atmos. Sci., **24**, 387.
 Fritz, S., and S. D. Soules (1970), J. Atmos. Sci., **27**, 1091.
 Gaigerov, S. S. (1973), Investigation of Synoptic Processes in the Upper
 Layers of the Atmosphere, Gidrometeoizdat, Leningrad.
 Gaigerov, S. S., and Yu. P. Koshelkov (1973) Space Res., **XII**, 173.
 Gaigerov, S. S., Yu. P. Koshelkov, D. A. Tarasenko, and E. G. Shvidkovsky
 (1969), in Stratospheric Circulation, Academic Press, New York.
 Gaigerov, S. S., B. P. Zaichikov, M. Ya. Kalikhman, V. V. Federov (1975),
Air Flow in the Mesosphere over the Antarctic, Gidrometeoizdat, Leningrad.
 Groves, G. V. (1965), Depart. Physics, London.
 Groves, G. V. (1974), J. British Interplanet. Soc., **27**, 499.
 Hartmann, D. L. (1976), J. Atmos. Sci., **33**, 1141.

- Harwood, R. S. (1975), Q. J. Roy. Meteorol. Soc., 101, 75.
- Hind, A. D. (1973), Weapons Res. Establ. Tech. Note, 988.
- Hirota, I., T. Hirooka, and M. Shiotani (1983), Q. J. Roy. Meteorol. Soc., 109, 443.
- Houghton, J. T. (1978), Q. J. Roy. Meteorol. Soc., 104, 1.
- Ivanovsky, A. I., L. M. Kolomiitseva, et al., (1979), Space Res., XIX, 127.
- Khanevskaya (1971) (Editor), Atlas of the Mean Air temperature in the Free Atmosphere over the Southern Hemisphere, Gidrometeoizdat, Leningrad.
- Knittel, J. (1976), Meteorol. Abhandl. F. U. Berlin, A2, Berlin.
- Koshelkov, Yu. P. (1969), Meteorologia i gidrologia, 9, 29.
- Koshelkov, Yu. P. (1971a), Space Res., XI, 793.
- Koshelkov, Yu. P. (1971b), CAO Proceedings, 99, 155.
- Koshelkov, Yu. P. (1974a), in Proc. Int. Conf. on Structure, Composition and General Circulation of the Atmosphere, 2, 708, Toronto.
- Koshelkov, Yu. P. (1974b), Space Res., XIV, 49.
- Koshelkov, Yu. P. (1975), Space Res., XV, 167.
- Koshelkov, Yu. P. (1977), Space Res., XVII, 123.
- Koshelkov, Yu. P. (1980a), Space Res., XX, 41.
- Koshelkov, Yu. P. (1980b), Circulation and Structure of the Stratosphere and Mesosphere of the Southern Hemisphere, Gidrometeoizdat, Leningrad.
- Koshelkov, Yu. P. (1983a), Adv. Space Res., 3, 3.
- Koshelkov, Yu. P. (1983b), Preprint to the XVIII Assembly of IUGG, Hamburg.
- Koshelkov, Yu. P., and E. N. Kovshova (1982), Antarctica, 21, 27.
- Kokin, G. A., and S. S. Gaigerov (1981) (Editors), Meteorology of the Upper Atmosphere of the Earth, Gidrometeoizdat, Leningrad.
- Kokin, G. A., L. A. Ryazanova, and G. F. Tulinov (1981), Meteorologia i gidrologia, 6, 105.
- Krumins, M. V., and W. C. Lyons (1972), Naval Ordnance Lab., NOL TR72-152.
- Labitzke, K. (1974), J. Geophys. Res., 79, 2171.
- Labitzke, K. (1977a), Space Res., XVII, 151.
- Labitzke, K. (1977b), Space Res., XVII, 159.
- Labitzke, K., and J. J. Barnett (1973), J. Geophys. Res., 78, 483.
- Labitzke, K., and J. J. Barnett (1979), Space Res., XIX, 97.
- Labitzke, K., and J. J. Barnett (1981), Planet. Space Sci., 29, 673.
- Leovy, C. B., and P. J. Webster (1976), J. Atmos. Sci., 33, 1624.
- Manning, J. S., and L. Chamberlain (1968), NASA TN, D-4429, Washington, D.C.
- Monthly Climatic Data for the World (1957-1977), Asheville, USA.
- Monthly Climatic Data - Upper Air (1969-1974), Bureau Meteorol., Australia.
- NASA (1966-1972), Temperature, Pressure, Density and Wind, NASA TR, R-263, -288, -316, -340, -360, -391.
- NASA (1968, 1969, 1970), EXAMETNET Annual Reports, NASA SP-175, -176, -231, Washington, D. C.
- NASA (1972-1977), Western Meridional Network, Meteorol. Rocketsonde Data, NASA, Washington, D. C.
- Nastrom, G. D., and A. D. Belmont (1975), J. Atmos. Sci., 33, 1715.
- Pearson, P. H. O. (1966), J. Atmos. Terr. Phys., 28, 1057.
- Quiroz, R. S. (1979), J. Geophys. Res., 84, 2415.
- Rofe, B. (1966), Weapons Res. Establ. Tech. Note, PAD 115.
- Schmidlin, F. J., J. R. Duke, A. I. Ivanovsky, Y. M. Chernyshenko (1980), NASA REFER. Publication, 1035.
- Tarasenko, D. A., I. A. Sherba, and R. A. Britvina (1976), Meteorologia i gidrologia, 3, 25.
- Theon, J. S., W. S. Smith, J. F. Casey, and B. R. Kirkwood (1972), NASA TR, R-375.
- van Loon, J. J. Taljaard, T. Sasamori, J. London, D. V. Hoyt, K. Labitzke, and C. W. Newton (1975), Meteorology of the Southern Hemisphere, Meteorol. Mon., 13, American Meteorological Society, Boston.
- WDC-A (1965-1978), WDC-A High Altitude Meteorol. Data, Asheville, USA.
- Weapons Research Establishment Technical Notes (1962-1974), Australia.
- Zastavenko, L. G. (1975), Meteorologia i gidrologia, 7, 46.

(c) MONTHLY MEAN TABULATIONS OF ZONAL MEAN TEMPERATURES ($^{\circ}\text{C}$) AND
GEOPOTENTIAL HEIGHTS (DAM) FOR THE MID-SEASON MONTHS

MEAN TEMPERATURES ($^{\circ}\text{C}$) AT CONSTANT PRESSURES LEVELS
IN THE SOUTHERN HEMISPHERE BASED ON ROCKET DATA

Pressure mbar	Latitude, S							
	0	10	20	30	40	50	60	70
January								
0.01	-76	-76	-77	-81	-88	-96	-102	-107
0.02	-72	-72	-72	-75	-80	-84	-88	-92
0.05	-55	-55	-55	-58	-62	-64	-65	-66
0.1	-39	-39	-41	-45	-48	-48	-46	-44
0.2	-23	-24	-27	-31	-32	-30	-27	-23
0.5	-6	-7	-10	-12	-10	-6	-2	1
1	-4	-4	-3	-1	1	6	9	11
2	-13	-12	-10	-6	-3	1	4	6
5	-32	-30	-27	-24	-20	-17	-14	-12
10	-43	-41	-39	-36	-34	-31	-28	-25
20	-52	-51	-49	-47	-44	-41	-37	-34
30	-58	-57	-55	-53	-50	-46	-42	-38
50	-69	-67	-64	-61	-55	-49	-44	-40
April								
0.01	-81	-81	-80	-78	-74	-69	-65	-62
0.02	-77	-76	-74	-71	-67	-63	-58	-54
0.05	-63	-62	-59	-56	-53	-50	-46	-41
0.1	-46	-45	-44	-42	-41	-39	-36	-32
0.2	-30	-29	-29	-29	-30	-31	-28	-24
0.5	-11	-11	-11	-12	-16	-21	-21	-19
1	-3	-3	-5	-8	-13	-19	-24	-26
2	-7	-8	-10	-14	-20	-26	-32	-35
5	-24	-24	-26	-30	-34	-40	-45	-49
10	-38	-37	-38	-40	-44	-48	-52	-57
20	-49	-48	-48	-49	-50	-53	-56	-60
30	-55	-54	-53	-53	-53	-54	-56	-60
50	-66	-65	-63	-60	-57	-56	-56	-56

Pressure mbar	Latitude, S							
	0	10	20	30	40	50	60	70
July								
0.01	-83	-83	-83	-80	-76	-70	-64	-58
0.02	-77	-76	-75	-72	-68	-61	-54	-49
0.05	-63	-62	-62	-59	-53	-46	-40	-34
0.1	-48	-47	-48	-47	-42	-36	-30	-24
0.2	-31	-31	-33	-34	-31	-28	-22	-17
0.5	-11	-12	-13	-17	-19	-21	-15	-11
1	-6	-6	-6	-12	-19	-25	-24	-22
2	-13	-12	-14	-19	-27	-36	-38	-39
5	-30	-28	-30	-34	-41	-50	-55	-60
10	-41	-39	-41	-43	-48	-57	-66	-73
20	-50	-48	-49	-50	-53	-61	-71	-81
30	-55	-54	-53	-53	-55	-61	-70	-81
50	-64	-63	-61	-59	-57	-60	-70	-81
October								
0.01	-81	-81	-81	-80	-81	-81	-81	-81
0.02	-76	-76	-75	-74	-74	-74	-73	-71
0.05	-63	-62	-60	-59	-59	-58	-57	-54
0.1	-47	-46	-45	-44	-44	-44	-43	-40
0.2	-30	-30	-30	-30	-30	-30	-29	-26
0.5	-11	-11	-11	-12	-12	-13	-11	-8
1	-3	-3	-3	-4	-4	-4	-2	-1
2	-8	-8	-8	-9	-9	-9	-6	-4
5	-25	-25	-27	-28	-27	-25	-21	-18
10	-38	-38	-39	-41	-41	-38	-34	-31
20	-49	-49	-49	-49	-49	-47	-46	-46
30	-56	-55	-54	-53	-52	-50	-51	-55
50	-65	-64	-62	-58	-54	-51	-52	-58

MEAN HEIGHTS (DAM) OF CONSTANT PRESSURE LEVELS
IN THE SOUTHERN HEMISPHERE BASED ON ROCKET DATA

Pressure mbar	Latitude, S							
	0	10	20	30	40	50	60	70
January								
0.01	7931	7941	7944	7950	7960	7995	8044	8087
0.02	7525	7534	7541	7551	7573	7615	7670	7718
0.05	6966	6973	6981	6997	7033	7085	7146	7203
0.1	6510	6517	6527	6550	6592	6648	6707	6762
0.2	6016	6027	6042	6073	6120	6174	6230	6277
0.5	5323	5335	5361	5399	5445	5496	5539	5577
1	4781	4794	4821	4857	4899	4942	4977	5011
2	4247	4254	4279	4310	4347	4383	4412	4436
5	3571	3579	3596	3619	3645	3670	3695	3716
10	3092	3099	3111	3127	3147	3165	3184	3200
20	2633	2640	2648	2660	2673	2684	2695	2705
30	2373	2378	2385	2394	2403	2410	2417	2422
50	2061	2063	2066	2071	2072	2072	2071	2073
April								
0.01	7906	7914	7923	7912	7877	7818	7779	7748
0.02	7512	7518	7523	7508	7465	7400	7352	7314
0.05	6967	6974	6972	6950	6897	6816	6758	6709
0.1	6525	6525	6524	6495	6438	6356	6289	6228
0.2	6048	6049	6042	6015	5959	5872	5799	5731
0.5	5370	5374	5366	5337	5284	5209	5131	5057
1	4831	4838	4828	4805	4759	4697	4624	4547
2	4288	4294	4289	4275	4239	4191	4129	4056
5	3597	3603	3607	3601	3581	3546	3500	3439
10	3105	3112	3118	3118	3108	3082	3046	2992
20	2640	2647	2653	2656	2650	2631	2601	2560
30	2377	2382	2388	2391	2388	2375	2344	2306
50	2061	2064	2068	2069	2062	2048	2019	1988

Pressure mbar	Latitude, S							
	0	10	20	30	40	50	60	70
July								
0.01	7859	7863	7864	7828	7783	7707	7646	7586
0.02	7468	7472	7469	7430	7378	7287	7211	7139
0.05	6927	6929	6924	6876	6807	6698	6608	6520
0.1	6485	6485	6482	6431	6352	6228	6125	6023
0.2	6012	6012	6009	5960	5873	5740	5626	5514
0.5	5337	5341	5340	5292	5209	5072	4942	4816
1	4802	4807	4808	4769	4694	4566	4429	4296
2	4267	4270	4276	4248	4187	4076	3938	3806
5	3592	3595	3600	3586	3546	3458	3335	3207
10	3109	3114	3120	3111	3085	3018	2905	2789
20	2649	2653	2658	2653	2635	2584	2490	2391
30	2388	2390	2392	2389	2375	2334	2253	2164
50	2067	2070	2071	2066	2051	2014	1948	1876
October								
0.01	7901	7908	7917	7924	7926	7927	7917	7875
0.02	7507	7513	7520	7522	7524	7526	7518	7477
0.05	6964	6968	6970	6968	6972	6974	6961	6913
0.1	6524	6526	6524	6524	6522	6523	6510	6454
0.2	6048	6049	6046	6042	6045	6045	6028	5968
0.5	5370	5371	5371	5368	5369	5371	5350	5284
1	4831	4833	4832	4830	4831	4834	4810	4739
2	4289	4290	4290	4288	4290	4293	4264	4191
5	3600	3602	3604	3605	3608	3605	3567	3489
10	3111	3113	3117	3119	3122	3115	3070	2986
20	2646	2649	2655	2658	2660	2648	2599	2512
30	2382	2386	2390	2395	2396	2382	2330	2250
50	2064	2066	2070	2072	2068	2050	1999	1924

(d) MEAN TEMPERATURES ($^{\circ}\text{C}$) IN THE SOUTHERN HEMISPHEREMEAN TEMPERATURE IN THE SOUTHERN HEMISPHERE ($^{\circ}\text{C}$)

Height km	J	F	M	A	M	J	J	A	S	O	N	D
Equator												
80	-76	-77	-80	-81	-82	-83	-83	-84	-83	-81	-78	-76
75	-69	-71	-73	-75	-77	-76	-76	-76	-76	-74	-73	-70
70	-53	-55	-58	-60	-62	-63	-63	-63	-64	-61	-60	-56
65	-35	-38	-40	-42	-44	-45	-45	-44	-45	-43	-42	-38
60	-20	-23	-24	-26	-28	-28	-28	-27	-27	-26	-26	-23
55	-8	-9	-10	-12	-14	-14	-14	-13	-13	-13	-13	-11
50	-4	-2	-2	-4	-5	-6	-6	-6	-4	-4	-5	-6
45	-8	-4	-3	-5	-7	-9	-9	-7	-6	-5	-5	-7
40	-20	-17	-13	-13	-15	-18	-20	-19	-16	-15	-15	-19
35	-34	-33	-30	-28	-28	-30	-33	-33	-30	-29	-29	-32
30	-45	-44	-42	-41	-41	-43	-44	-44	-43	-41	-41	-43
25	-55	-54	-54	-52	-52	-53	-53	-53	-53	-53	-53	-54
20	-70	-71	-71	-69	-67	-66	-66	-66	-66	-67	-68	-69
10°S												
80	-76	-77	-80	-81	-82	-83	-83	-84	-82	-81	-78	-76
75	-69	-70	-72	-74	-76	-75	-75	-75	-75	-73	-72	-70
70	-52	-54	-57	-59	-61	-62	-62	-62	-63	-60	-59	-56
65	-35	-38	-39	-41	-43	-45	-45	-44	-45	-42	-42	-39
60	-21	-23	-24	-26	-28	-29	-29	-28	-28	-26	-26	-23
55	-9	-10	-11	-13	-14	-14	-14	-13	-13	-13	-13	-11
50	-4	-3	-3	-4	-6	-6	-6	-6	-4	-4	-5	-6
45	-7	-5	-4	-5	-7	-9	-9	-7	-6	-5	-5	-6
40	-19	-17	-15	-14	-15	-18	-19	-19	-16	-15	-15	-18
35	-33	-32	-30	-28	-28	-30	-33	-33	-31	-29	-29	-31
30	-44	-43	-42	-41	-41	-43	-44	-44	-43	-41	-41	-42
25	-55	-54	-53	-52	-52	-52	-52	-53	-53	-53	-53	-53
20	-69	-70	-70	-68	-66	-65	-65	-65	-65	-66	-67	-68

Height km	J	F	M	A	M	J	J	A	S	O	N	D
20°S												
80	-77	-78	-79	-79	-81	-82	-83	-83	-81	-81	-79	-77
75	-69	-69	-70	-72	-74	-74	-74	-74	-73	-72	-72	-71
70	-53	-54	-56	-57	-60	-61	-61	-61	-61	-58	-58	-57
65	-38	-39	-40	-40	-43	-45	-46	-45	-45	-42	-42	-41
60	-24	-25	-25	-26	-28	-30	-31	-29	-28	-26	-26	-25
55	-12	-12	-12	-13	-15	-16	-16	-15	-14	-13	-12	-12
50	-4	-4	-5	-5	-6	-7	-7	-7	-5	-4	-4	-4
45	-5	-6	-6	-7	-8	-10	-10	-9	-7	-5	-4	-4
40	-17	-16	-16	-17	-17	-19	-20	-20	-18	-15	-15	-16
35	-31	-31	-31	-30	-30	-31	-33	-33	-32	-30	-29	-30
30	-42	-42	-41	-41	-42	-43	-44	-44	-43	-42	-42	-42
25	-53	-53	-52	-52	-52	-52	-52	-53	-53	-53	-53	-53
20	-66	-67	-66	-65	-64	-63	-63	-63	-63	-64	-65	-66
30°S												
80	-80	-80	-79	-78	-79	-80	-81	-81	-79	-80	-81	-81
75	-71	-70	-69	-69	-70	-71	-72	-71	-70	-71	-72	-72
70	-56	-56	-56	-55	-57	-58	-60	-59	-59	-57	-59	-59
65	-41	-41	-41	-40	-42	-44	-47	-46	-44	-41	-42	-42
60	-27	-27	-27	-27	-29	-31	-33	-32	-29	-27	-25	-25
55	-13	-13	-13	-14	-17	-18	-20	-19	-16	-14	-11	-11
50	-2	-5	-7	-8	-10	-11	-12	-11	-9	-5	-2	-1
45	-3	-6	-9	-11	-13	-14	-15	-13	-9	-5	-3	-2
40	-14	-15	-18	-21	-23	-24	-24	-22	-20	-17	-14	-13
35	-28	-29	-31	-33	-35	-36	-36	-35	-34	-31	-29	-27
30	-40	-41	-41	-43	-44	-46	-46	-45	-44	-44	-43	-41
25	-51	-51	-51	-52	-52	-53	-53	-53	-53	-53	-52	-52
20	-62	-63	-62	-61	-61	-60	-60	-59	-59	-60	-61	-62

Height km	J	F	M	A	M	J	J	A	S	O	N	D
40°S												
80	-87	-85	-79	-74	-74	-75	-77	-78	-78	-80	-85	-88
75	-75	-73	-69	-66	-65	-66	-69	-69	-68	-71	-74	-77
70	-58	-59	-58	-54	-53	-53	-56	-58	-57	-57	-60	-60
65	-42	-44	-44	-41	-40	-40	-44	-46	-43	-41	-41	-42
60	-26	-28	-30	-29	-29	-30	-33	-34	-30	-27	-24	-24
55	-10	-12	-16	-18	-20	-22	-23	-23	-18	-14	-9	-9
50	1	-4	-9	-13	-16	-18	-17	-15	-11	-5	-1	2
45	-1	-5	-10	-16	-19	-22	-22	-17	-11	-6	-2	0
40	-11	-14	-19	-25	-29	-32	-31	-27	-21	-17	-13	-11
35	-25	-28	-32	-37	-41	-44	-43	-39	-35	-31	-27	-25
30	-38	-39	-42	-46	-49	-51	-50	-48	-46	-44	-41	-39
25	-48	-49	-50	-52	-54	-55	-55	-53	-52	-51	-50	-49
20	-56	-57	-58	-58	-58	-57	-57	-56	-55	-55	-56	-56

50°S												
80	-94	-90	-79	-70	-67	-69	-72	-74	-77	-81	-89	-95
75	-77	-76	-69	-63	-59	-60	-64	-66	-67	-71	-77	-79
70	-59	-60	-58	-53	-48	-47	-52	-56	-56	-57	-60	-60
65	-40	-44	-46	-41	-36	-35	-40	-45	-43	-41	-40	-40
60	-22	-27	-32	-32	-29	-28	-31	-34	-31	-27	-22	-21
55	-5	-10	-18	-24	-25	-24	-24	-24	-21	-15	-7	-5
50	6	-1	-10	-19	-23	-23	-21	-18	-12	-5	1	6
45	3	-3	-11	-22	-28	-31	-27	-20	-11	-6	0	3
40	-8	-13	-21	-30	-39	-42	-39	-28	-21	-15	-10	-8
35	-23	-27	-33	-41	-49	-54	-50	-41	-34	-28	-24	-22
30	-35	-38	-43	-49	-55	-60	-58	-52	-46	-41	-38	-35
25	-44	-46	-49	-54	-57	-61	-61	-59	-54	-49	-47	-45
20	-50	-52	-54	-56	-57	-59	-60	-58	-56	-52	-51	-50

Height km	J	F	M	A	M	J	J	A	S	O	N	D
60°S												
80	-98	-95	-80	-66	-61	-64	-68	-71	-76	-81	-93	-100
75	-78	-77	-69	-60	-53	-53	-59	-63	-66	-70	-78	-80
70	-56	-58	-56	-50	-43	-42	-48	-53	-54	-56	-59	-58
65	-35	-40	-43	-39	-32	-30	-36	-41	-41	-41	-38	-36
60	-17	-24	-30	-30	-26	-24	-27	-30	-29	-27	-20	-16
55	0	-8	-19	-23	-24	-21	-20	-21	-18	-14	-5	0
50	9	1	-10	-21	-23	-20	-15	-13	-9	-4	3	9
45	5	-2	-13	-27	-30	-30	-23	-14	-8	-3	1	6
40	-6	-12	-23	-35	-43	-44	-37	-24	-17	-11	-8	-6
35	-20	-26	-35	-45	-55	-57	-51	-39	-30	-23	-21	-20
30	-32	-37	-44	-53	-62	-67	-65	-55	-46	-36	-33	-32
25	-40	-44	-49	-56	-64	-70	-71	-67	-58	-48	-41	-40
20	-44	-47	-51	-56	-61	-66	-70	-68	-63	-53	-45	-44
70°S												
80	-101	-98	-81	-64	-56	-59	-64	-70	-75	-82	-96	-103
75	-78	-77	-68	-57	-47	-48	-55	-61	-64	-70	-78	-80
70	-52	-55	-54	-46	-37	-37	-44	-50	-52	-55	-56	-52
65	-30	-36	-40	-36	-27	-26	-32	-38	-40	-40	-35	-29
60	-10	-21	-28	-27	-22	-21	-23	-26	-28	-26	-18	-10
55	4	-7	-17	-21	-20	-18	-16	-16	-17	-13	-3	5
50	12	3	-10	-19	-21	-17	-10	-6	-6	-2	6	12
45	7	-2	-15	-27	-28	-25	-16	-6	-5	-2	2	8
40	-4	-12	-25	-37	-43	-41	-32	-16	-11	-8	-7	-4
35	-18	-26	-36	-48	-58	-57	-50	-35	-25	-18	-19	-18
30	-29	-36	-44	-57	-69	-73	-68	-57	-42	-31	-28	-28
25	-37	-41	-50	-60	-71	-80	-80	-75	-60	-47	-35	-35
20	-40	-43	-49	-58	-67	-76	-81	-80	-73	-58	-41	-39

(e) MEAN ZONAL WIND (m/s) IN THE SOUTHERN HEMISPHERE

MEAN ZONAL WIND IN THE SOUTHERN HEMISPHERE (m/s)

Height km	J	F	M	A	M	J	J	A	S	O	N	D
Equator												
80	-2	-43	-42	-34	-20	-9	9	-6	-31	-35	-17	3
75	8	-13	-16	-17	-10	1	10	2	-16	-20	-15	11
70	22	23	18	7	4	11	10	12	3	8	3	15
65	23	27	27	22	12	12	8	13	15	23	21	11
60	12	22	26	32	13	6	-1	7	15	27	15	0
55	-5	15	25	29	13	0	-11	-2	10	22	7	-15
50	-34	0	18	23	14	-3	-22	-11	4	17	5	-26
45	-38	-22	6	16	12	-3	-24	-18	-3	12	5	-21
40	-26	-32	-16	-1	4	-7	-20	-21	-11	2	2	-15
35	-16	-22	-22	-13	-10	-11	-17	-18	-14	-7	-5	-14
30	-9	-12	-12	-12	-15	-15	-15	-15	-15	-12	-11	-11
25	-6	-7	-7	-8	-12	-17	-15	-15	-15	-15	-13	-8
20	-2	-1	0	1	1	1	0	-1	-3	-3	-3	-3
10°S												
80	-4	-48	-38	-14	9	17	29	3	-15	-27	-13	10
75	10	-10	-13	-4	18	26	30	22	5	-18	-13	13
70	23	20	14	19	26	32	28	31	25	2	-7	7
65	16	22	24	37	34	35	24	23	31	16	-2	-4
60	1	14	25	40	32	29	16	4	20	19	-11	-21
55	-22	2	21	34	27	18	-1	5	12	15	-12	-42
50	-56	-20	10	28	19	11	-12	-4	5	14	-8	-49
45	-63	-43	-9	20	16	7	-12	-7	-1	10	-3	-36
40	-49	-44	-28	7	12	4	-8	-8	-4	3	-4	-21
35	-35	-36	-31	-10	-1	0	-6	-8	-7	-3	-8	-18
30	-27	-25	-21	-15	-11	-8	-8	-9	-9	-9	-12	-17
25	-18	-17	-15	-14	-12	-12	-10	-11	-12	-13	-14	-16
20	-12	-12	-10	-5	-1	0	-1	-2	-4	-6	-8	-10

Height km	J	F	M	A	M	J	J	A	S	O	N	D
20°S												
80	13	-5	12	16	34	37	40	29	10	-15	-10	12
75	18	13	21	28	45	47	44	40	27	-10	-15	3
70	10	14	23	40	53	56	43	43	40	2	-19	-14
65	-13	5	18	45	57	59	40	36	40	10	-21	-32
60	-40	-13	11	42	53	53	31	26	36	14	-21	-47
55	-56	-31	-2	36	46	47	22	16	23	14	-19	-53
50	-65	-42	-14	30	37	38	14	9	13	13	-12	-50
45	-62	-48	-24	20	28	31	10	4	5	9	-7	-39
40	-50	-43	-30	10	18	22	9	0	-1	4	-5	-30
35	-38	-36	-30	-3	5	11	7	0	-3	0	-5	-20
30	-27	-28	-25	-9	-3	3	4	-1	-4	-5	-7	-17
25	-19	-20	-18	-11	-5	-2	0	-3	-5	-8	-10	-14
20	-14	-14	-12	-6	-1	1	1	0	-2	-4	-6	-9
30°S												
80	15	16	21	32	43	47	50	46	24	-1	-4	7
75	0	12	21	37	55	60	58	54	36	-2	-20	-18
70	-29	1	18	44	70	73	68	63	47	-1	-26	-36
65	-47	-23	12	50	78	86	72	65	47	4	-28	-51
60	-58	-35	5	45	74	88	68	52	44	11	-27	-54
55	-63	-41	-1	39	67	84	60	48	38	14	-20	-52
50	-59	-42	-8	32	57	73	51	38	30	13	-15	-46
45	-53	-39	-11	24	43	58	39	28	20	9	-11	-37
40	-45	-32	-13	15	30	36	28	19	12	4	-9	-29
35	-35	-27	-13	7	20	24	18	14	8	1	-8	-21
30	-24	-22	-12	1	9	16	13	11	6	-1	-7	-15
25	-14	-18	-11	-2	4	9	9	8	3	-2	-5	-10
20	-5	-6	-4	2	6	9	9	8	4	1	-1	-2

Height km	J	F	M	A	M	J	J	A	S	O	N	D
40°S												
80	-4	11	17	26	32	40	43	36	25	-2	-7	-10
75	-32	-4	20	35	46	53	54	48	36	-2	-10	-35
70	-50	-22	17	41	59	66	66	63	45	-1	-32	-50
65	-63	-32	12	47	74	87	82	72	52	2	-31	-55
60	-63	-36	7	48	83	105	92	78	52	6	-29	-54
55	-59	-35	2	44	84	110	97	76	48	7	-25	-49
50	-52	-32	0	39	73	101	91	70	43	7	-19	-43
45	-43	-27	-1	32	64	89	83	61	39	6	-17	-35
40	-36	-21	-2	24	50	74	72	51	30	5	-14	-28
35	-29	-17	-2	17	36	56	59	41	22	5	-11	-20
30	-19	-12	-3	12	25	37	42	33	18	6	-7	-14
25	-10	-7	-2	8	18	23	30	25	15	6	-3	-8
20	1	2	5	9	13	18	20	18	15	10	5	3
50°S												
80	-26	-9	13	18	25	28	30	25	19	-5	-19	-31
75	-46	-21	15	26	35	42	44	37	28	-3	-31	-47
70	-57	-27	17	34	46	54	55	50	37	-1	-37	-52
65	-57	-27	17	41	58	66	67	62	46	0	-33	-53
60	-52	-25	17	46	70	82	81	72	54	3	-28	-51
55	-46	-22	16	48	77	93	93	81	56	5	-24	-44
50	-38	-18	13	48	77	100	101	84	56	8	-20	-37
45	-31	-15	11	42	71	98	101	82	54	10	-16	-31
40	-25	-12	10	34	60	87	93	76	51	13	-13	-25
35	-20	-8	9	27	49	76	84	71	49	17	-9	-19
30	-14	-5	7	20	38	63	72	64	48	22	-4	-13
25	-7	-2	7	17	30	43	56	53	46	26	1	-7
20	3	7	11	16	22	30	36	37	32	24	9	4

Height km	J	F	M	A	M	J	J	A	S	O	N	D
60°S												
80	-32	-20	-4	8	19	18	20	18	12	-8	-26	-38
75	-43	-27	5	21	27	30	34	26	19	-5	-37	-46
70	-48	-27	12	30	37	44	47	39	29	-1	-36	-50
65	-45	-21	20	38	47	53	58	53	38	4	-30	-47
60	-39	-16	26	46	56	62	68	63	48	8	-24	-42
55	-33	-12	30	52	62	71	78	73	57	12	-20	-36
50	-28	-10	29	54	66	79	86	82	64	18	-15	-30
45	-22	-8	25	52	68	80	92	90	70	24	-11	-25
40	-18	-6	21	46	64	79	88	89	73	30	-8	-20
35	-14	-4	17	38	58	75	82	83	74	38	-3	15
30	-9	-2	14	30	50	65	74	76	71	45	1	-11
25	-4	2	12	25	42	54	64	69	67	44	6	-5
20	1	6	13	19	28	37	47	52	49	41	13	2

70°S												
80	-29	-26	-17	0	12	4	14	13	5	-9	-30	-36
75	-34	-24	-9	10	20	16	23	18	9	-5	-34	-41
70	-35	-17	1	24	29	31	35	28	17	0	-30	-40
65	-32	-10	14	33	37	40	50	38	26	7	-27	-36
60	-27	-5	22	39	42	45	57	49	36	13	-21	-32
55	-23	-3	26	44	45	46	62	60	44	19	-15	-28
50	-19	-2	27	51	47	48	64	67	52	24	-10	-23
45	-15	-2	26	52	49	50	64	75	61	30	-6	-19
40	-13	-1	24	47	52	51	61	76	67	37	-3	-16
35	-9	0	20	41	49	50	56	71	69	43	0	-13
30	-6	1	16	32	44	47	50	65	66	48	5	-8
25	-3	3	12	27	37	43	45	55	58	43	10	-3
20	-1	4	9	17	24	29	33	36	37	28	13	0

2.1.4 MEAN WINDS OF THE MESOSPHERE (60-80 KM), AS MEASURED BY MF RADARS

J A. H. Manson¹, C. E. Meek¹, R. A. Vincent², and M. J. Smith³¹Institute of Space and Atmospheric Studies
University of Saskatchewan
Saskatoon, Canada²Physics Department, University of Adelaide
South Australia³Department of Scientific and Industrial Research
Physics and Engineering Laboratory
Lower Hutt, New Zealand

ABSTRACT

Winds data obtained from medium frequency (MF) radars for heights of 60-80 km are discussed: locations are Saskatoon (52°N, 107°W), Christchurch (44°S, 173°W), Adelaide (35°S, 183°E) and Townsville (20°S, 147°E). Whereas well-defined summer easterly jets centred near 70 km develop in summer, no regular buildups and decays are observed in winter at midlatitudes. Part of this variability can be associated with stratospheric warmings, which develop into breakdowns of the polar vortex in the Northern Hemisphere. Amplitude and phase profiles of the annual and semiannual oscillations are also presented.

The radar winds from Saskatoon are compared and combined with rocket-derived winds up to 60 km from Primrose Lake (54°N, 110°W) to give consistent cross sections from 20-110 km. The SH radar winds are compared with a model based on rocket winds (Koshelkov, Section 2.1.3) which extends up to 80 km. The latter evidence considerable smoothing, as no winter variability is evident. The other consistent difference is that heights of the summer easterly maxima for the model are 5-10 km lower than the radar winds at all latitudes.

INTRODUCTION

Very little winds data have been gathered in the last decade in the height range from 60-80 km. Small rocket systems (e.g. datasondes used within the Meteorological Rocket Network, MRN) provide data to 60 km regularly, but above that height with less regularity and probably more error. Few stations are now operational. These data are discussed in Section 2.1.2. The best source of tidally corrected winds at and above 80 km are radars: these include medium frequency (MF) or partial reflection systems, meteor radars with height ranging (unfortunately a minority); and VHF radars or MST systems. Until now the latter have provided little data of this type due to limitations in the heights and hours of the day for which suitable echoes are available. A new data set from the MST at Poker Flat including winds from meteor and turbulence echoes (BALSLEY and RIDDLE, 1984) is discussed in Section 3.1.2.

As well as giving excellent almost continuous winds data in height and time above 80 km, MF radars provide winds almost continuously with height from 55/70 - 80 km (the lowest height depending on latitude and season), and for at least the daylight hours. An example of data yield for summer and winter months has been shown for Saskatoon (GREGORY et al., 1982) depending on season, 8-12 hours may be represented near 60 km, and approaching ~ 20 hours near 80 km. Thus daily means of the winds, obtained from simple means of all measured values or from harmonic analysis should have negligible contributions from the 12-hour tide, and small (although often not estimated) contributions from the 24-hour tide. At present there are MF radars producing winds by the spaced antenna drifts method at Adelaide (35°S), Christchurch (44°S) and Saskatoon (52°N), with new systems at Scott Base (78°S) and Mawson (68°S). Data from the first three systems and one which operated for several years at

Townsville (20°S), are presented here.

The winds for 60–80 km are discussed from several viewpoints. Firstly, comparisons are made between MF radar and rocket winds. A detailed comparison between Saskatoon radar and Primrose rocket (54°N, 110°W) winds has been completed (MEEK and MANSON, 1984) and is summarized here. Also a comparison is made between radar winds from Christchurch, Adelaide, and Townsville, and rocket winds in a Southern Hemisphere data model obtained by Russian workers (KOSHELKOV, 1983 and Section 2.1.3). It is vital to estimate the difference between zonal mean winds and those for the Oceanian region (~140°E); and to check for the presence of tidal contamination in a data set derived from rocket systems. Secondly, and within each of these presentations the nature of the variability in the wind cross sections, especially during the winter seasons, will be discussed. Although in many cases the summer winds at 60 km could be interpolated to those at 80 km, due to the regularity and smoothness of the contours, that would seldom be possible in winter, even in the Southern Hemisphere (SH). The planetary waves, especially those associated with the stratwinds of the NH, lead to significant winter variability, much of which is not evident above 80 km in the meteor winds data. There is also strong evidence for 12-, 6-month oscillations (annual, semiannual) in these radar winds and these profiles may be compared with, and added to, rocket-derived profiles for 20–60 km shown in Section 2.3.4.

WIND CROSS SECTIONS (20–110 km) FROM SASKATOON AND PRIMROSE LAKE (~53°N, ~109°W), 1979–1982

Winds for Primrose Lake, obtained by radar tracking of starutes released from Loki Darts have provided coverage from 20–65 km, with 8–12 firings per month in 1978/9 reducing to 4–5 per month by 1983. The firings are near 1000 h local time (LT). The radar winds for Saskatoon are obtained continuously, as described in the Introduction: below 75 km the daylight means (8–19h) are calculated, and then tidal corrections made; while above 74 km harmonic analysis is applied to 1 or 4d sets to obtain tidal amplitudes and phases and the mean wind (GREGORY et al., 1981; MANSON et al., 1981a,b, 1982; MANSON and MEEK, 1984). Careful selection of harmonic analysis data from 60–75 km has shown that the diurnal tide dominates there (~7 m/s amplitudes, northward/eastward maxima at ~12 h/18 h local solar time). These parameters are very consistent with the rocket-derived tides for 60 km shown in Section 2.3.3. Detailed corrections, also allowing for seasonal and height variations, and 12-h tides, have been applied to the Saskatoon radar winds and Primrose Lake rocket winds, so that a true daily mean may be obtained (MEEK and MANSON, 1984). The corrections are up to 5 m/s in magnitude, and are vital for the small meridional flow.

There was also evidence for noise in both data sets. Correlations of the 65 km rocket data with lower heights, and with the radar winds, demonstrated that a strong ballistic effect was still present above 60 km, despite smoothing and analysis corrections. The upper heights of all MRN data sets should thus be treated with caution. Finally, the radar winds (<70 km) for the same hour as the rocket firing were smaller by 20–30% in summer months only. Careful study and modelling showed that reduced radar-echo signal-to-noise ratios in summer were the cause of this reduction. Empirical corrections were applied to the radar data from 60–70 km mainly for summer months (MEEK and MANSON, 1984). With these corrections and tidal adjustments the two data sets could be combined.

We show winds for a combination of 4 years (1979–1982) in Figure 1 and for CIRA-72 and a compilation by GROVES (1969) in Figure 2. Ten-day means have been used for the radar winds and monthly means for the rocket winds. The adjustments have led to an extremely good match of radar and rocket data.

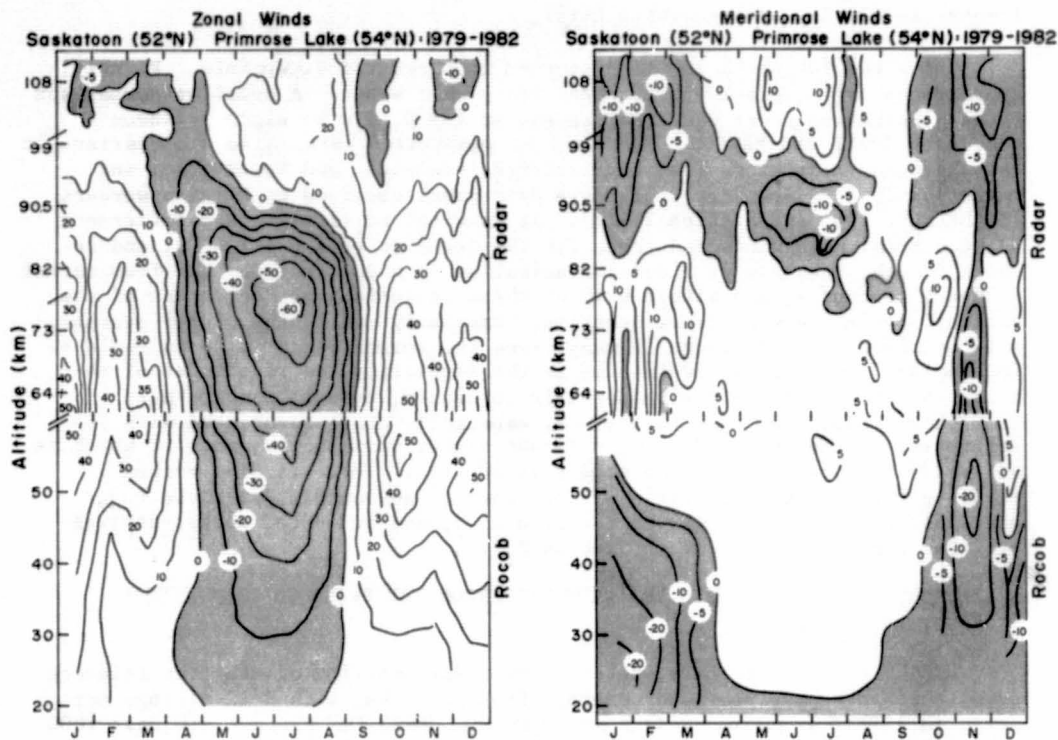


Figure 1. Zonal and meridional winds: 10d means above 60 km. Above 100 km the data apply to a ~ 5 km layer. The s.d. are typically 6 m/s near 90 km.

Temporal features of periods less than 30-d clearly emerge in the radar winds. There are also small differences in the relative positions of contours during the equinoxes and in magnitudes during the solstices, consistent with the latitudinal separation of 340 km. Individual years are available elsewhere (MEEK and MANSON, 1984). Consider first the zonal winds. For the composite the summer-centred months are dominated by a strong and smoothly contoured easterly flow 20-95 km. The 50° contour from CIRA-72 is very similar, although its easterly maximum and zero line are ~ 5 km lower. Also its westerly flow near 100 km is stronger probably due to tidal contamination (MANSON et al., 1981b). The equinoctial transitions are very regular and rapid. Hence, unlike CIRA, May is more summer-like and September more winter-like. For the winter-centred Canadian months the westerly maxima are somewhat weaker than the December/January maximum of CIRA. However, there is much more structured variability in these months than in CIRA: causes are planetary waves and stratwarms (MANSON et al., 1981a; MANSON and MEEK, 1984), but also long period oscillations (12-, 6-month) (MANSON et al., 1981b) e.g. the maxima of December and October, respectively. These latter are discussed below in more detail. Because of the regularity of the stratwarm dates, (4 years and temperature perturbations near January 31 and/or February 28) the composite (Figure 1) shows westerly minima near those times, and also small northerly cells. In CIRA-72 the 60 km transition between mainly MRN rocket data and rocket/radar data is almost discontinuous in December-March, indicating strong longitudinal differences and stratwarm effects. The CIRA-72 February winds above 60 km are

quite unrealistic when compared to those from Canada. Also note that there is a considerable bias toward North America in CIRA-72, so even there a zonal mean is probably not available.

The meridional cross sections are also very consistent from year to year, so that each closely resembles the composite of Figure 1. In summer there is poleward flow 20–80 km and above 95 km, with equatorward flow between. This cell is quite strong (10 m/s) and maximizes in June/July; this has been detected at all longitudes near 50/60°N (NASTROM et al., 1982; DARTT et al., 1983). Here is an appropriate place to explain the westerly vertical gradient (thermal wind) of the zonal flows above ~75 km. For December–March there is poleward flow from ~50 to ~87 with reverse flow above and below. One explanation is for similar flow to summer, with upward motion at high latitudes from ~75–95 km, although this is inconsistent with the thermal wind associated with the zonal flow. A second is for two cells, one in the thermosphere and one in the mesosphere, giving downward motions throughout the upper middle atmosphere (60–110 km) (GROVES, 1980). The rocket data show an appropriate stratospheric equatorward flow. The Canadian meridional cross sections differ significantly from the data model of GROVES (1969) shown in Figure 2. His contour is dominated by the summer-centred equatorward flow. The transition between ROCOB and radar meridional winds is definitely made more continuous by the tidal and noise corrections. This is especially evident in the fall months, when a narrow equatorward tongue is established.

WIND CROSS SECTIONS FOR CHRISTCHURCH (44°S, 173°E), ADELAIDE (35°S, 138°E) AND TOWNSVILLE (20°S, 147°E) for ~1978–1983

The zonal cross sections for these locations (Figures 3, 4, 5) are quite similar to Saskatoon's, and may best be described as midlatitude in their characteristics. There are some tropical features in the Townsville data, but overall they differ considerably from CIRA-72 at 20°. There is a more detailed

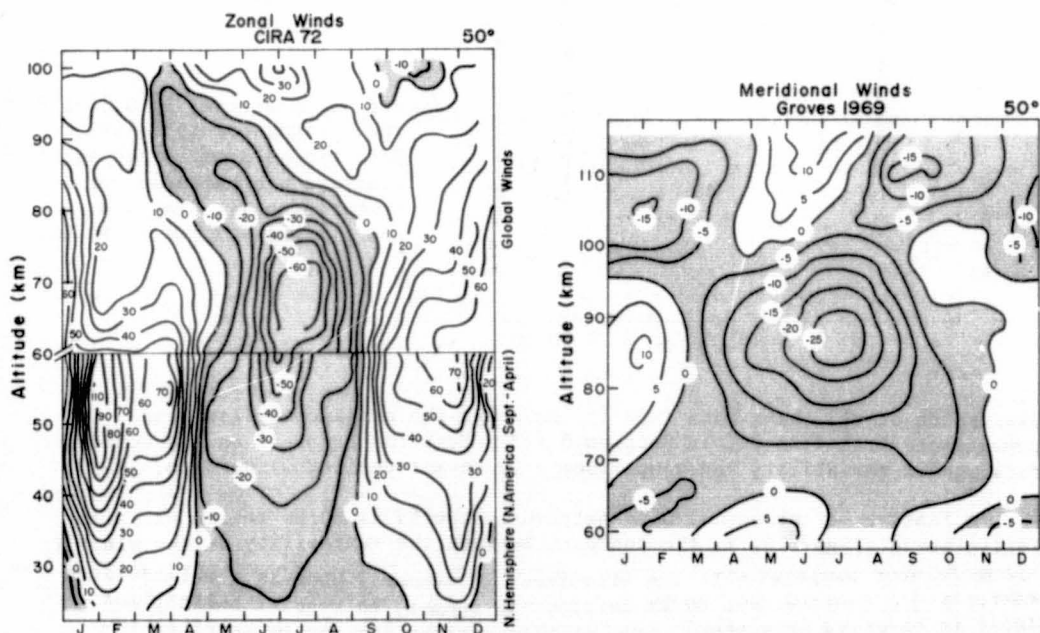


Figure 2. CIRA (1972); Groves (1969)

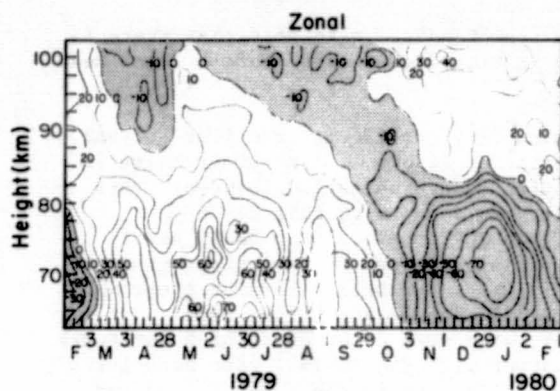


Figure 3. Christchurch, 44°S, 173°E:
7 d means; s.d. typically 7 m/s
at 90 km, increasing to 10 m/s
at 80 km.

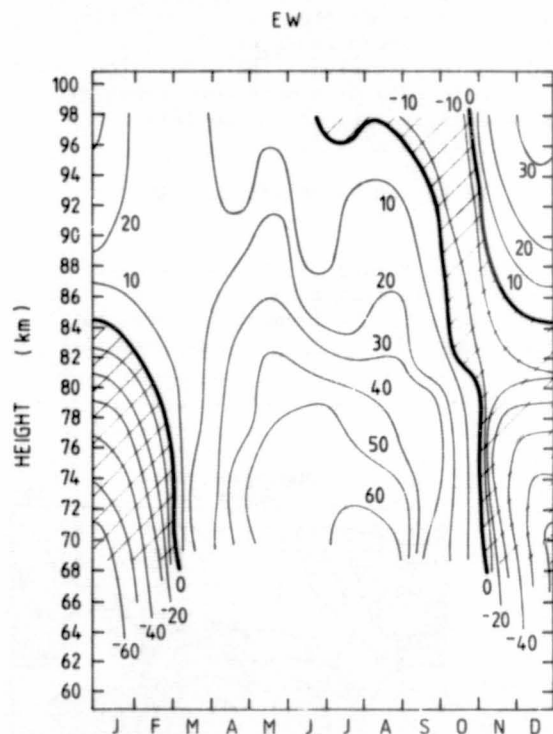


Figure 4. Adelaide, 35°S, 138°E:
zonal winds for 1978-1983.
Data extend down to ~70 km;
contours are extended for
numbering only. The s.d.
are typically 7 m/s at 90 km.

discussion of all these data (~60-110 km) plus the meridional flow, and comparisons with CIRA-72, in Section 3.1.2. Here the focus is on the 60-80 km data; their variability and comparison with rocket-derived winds data.

A feature of the annual wind pattern in the 65 to 80 km region at Christchurch (Figure 3) is the contrast between the variability of the winds in autumn/winter compared with the steadiness in summer. Whereas a well-defined easterly jet centred near 80 km develops in summer, no regular buildup and decay is observed in winter. Some of this variability can be ascribed to regular wave motion: the 2-day wave has been detected in a coherent form throughout the 67 to 100 km range. Transitory responses, however, are more

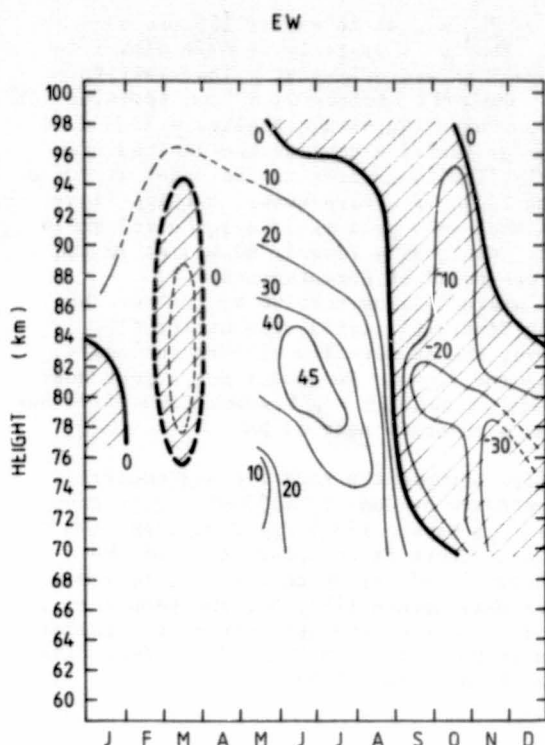


Figure 5. Townsville, 20°S, 147°E. Zonal winds for 1978-1980.

important in winter. For the 1979 data shown, a particular example of this is in early August, when winds were reversed from their usual westerly values for a period of 5 days over most of the 65-100 km range; the thermal wind at this time also suggested a high latitude cooling in the mesosphere. Stratospheric radiance charts from TIROS-N indicated a wave number 2 thermal centre moving eastward across New Zealand. As is usual for the Southern Hemisphere warmings, this did not lead to a strong polar heating. So while Southern Hemisphere warmings do not result in a breakdown of the polar vortex, very strong disturbances of the local mean flow can occur. The effects of this are most evident at heights below 75 km.

At Adelaide (Figure 4) also there is considerable variability in the prevailing winds in winter compared with the situation in summer. Both the EW and NS winds vary in a quasi-periodic manner with the maximum variability occurring in the period May-August and peaking in June-July. Amplitudes can be up to 20-30 m/s in each component with the amplitudes appearing to maximize at or below 75 km altitude. The variations have time scales of between one week and a month and are presumably associated with the passage of large-scale planetary waves.

These zonal winds are now compared with a detailed empirical model for the Southern Hemisphere, based on rocketsonde data from the USSR (KOSHELKOV, 1983). A summary of these data due to Koshelev appears in Section 2.1.3. We consider Christchurch (44°S) first, and compare with Koshelev's 40 and 50° data. Contours based on the latter are very smooth and symmetrical, and show none of the winter variability visible in Figure 3. There is evidently much smoothing in the model. The model gives a westerly winter flow of ~80 m/s at 65 km compared with ~60 m/s in Figure 3. Values are similar at 80 km (~30 m/s), meaning that the thermal wind in the model is stronger. In summer, Koshelev's

peak is at a lower altitude (60/65 km vs 70 km), it is weaker (60 m/s vs 75 m/s), and the thermal wind is less. The 80 km easterly flow is weaker in the rocket-based model, inferring reversal to westerlies at a lower altitude. The spring and autumn transitions are similarly placed. Data from Adelaide (35° S) are available from 69 km (Figure 4). Comparing with Koshelkov's 30 and 40° data, the winter variability is greater at Adelaide despite the limited time resolution there (10-30d). The westerly flow is greater in the model at 70 km (70 m/s vs 60 m/s), the peak is earlier (June vs July/August), but the flows are comparable at 80 km. In summer, Koshelkov's peak is at a low 55/60 km (60 m/s) giving a flow of ~40 m/s at 70 km. Adelaide's flow is 60 m/s at 70 km, suggesting a higher altitude peak, as was found at Christchurch. The rocket-based model has a transition to westerly flow near 80 km, rather than Adelaide's 85 km. Finally, considering Townsville (20°), the winter flow is similar to the model (Figure 5). However the summer flow differs seriously, following the trend at 44° and 35° (Figures 3, 4). The model has a peak near 50 km, and the reversal to westerly flow is near 68 km. However Townsville has easterly flow from 70 km (~30 m/s), and a reversal near 83 km.

These differences in the summer flow between the rocket-based empirical model and the radar data are also illustrated by January (1980-82) data from the same three stations, plus new data from Mawson (68°) and Scott Base (78°S) (VINCENT, 1984; FRASER, 1984) (Figure 6). There is an upward tilt of the easterly peak with latitude, varying from 75 m/s at 70 km and 40°, to ~30 m/s at 80 km and 80°. The model also shows this upward tilt, but the peak is 5-10 km lower in height. The new summer data from the Antarctic are quite similar to those from Poker Flat (65°N), shown in Section 3.1.2, and differ from CIRA which shows a peak below 70 km (Figure 14, Section 3.1.2).

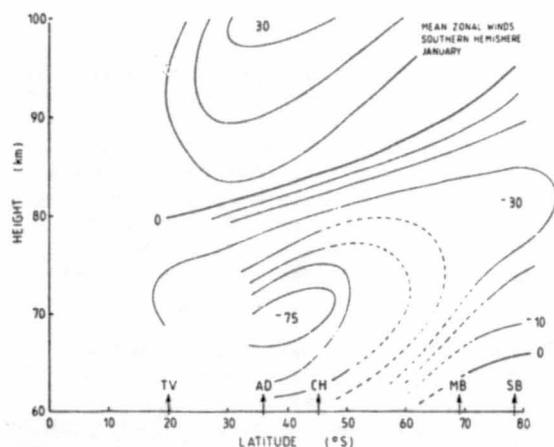


Figure 6. Contours of the zonal winds for January, Southern Hemisphere. New stations are Mawson and Scott Base.

In conclusion, the radar and rocket-based model show quite serious differences, and the major source of these is not clear. There will be differences due to comparing one longitude (Oceania) with a zonal average of some type; but until the amplitude of standing waves at these heights is known, this effect cannot be estimated. Other differences will be due to the years involved in the data sets, and comparatively small quantities of rocket data above 60 km.

ANNUAL AND SEMIANNUAL OSCILLATIONS

The presence of strong annual and semiannual oscillations in the midlatitude mesosphere and lower thermosphere are already evident from careful study of the high resolution cross sections from Saskatoon, Christchurch and

Adelaide. Harmonic analysis of the daily (Saskatoon) or approximately weekly values gives the profiles for these harmonics, for EW and NS components, (MANSON et al., 1981b; SMITH, 1981) (Figures 7, 8, and 9). Considering first Saskatoon: below 80 km the annual zonal oscillation is dominant (45 m/s), and the December maximum (westerly) is clearly evident in the zonal cross section of Figure 1. For the semiannual oscillation (20 m/s at 70 km) the maximum in mid-October and minimum in January are also evident in Figure 1. Above 90 km the oscillations are shifted by $\sim 180^\circ$ and the small easterly cells of April and October are clearly associated with the 6-month oscillation. Near 90 km, the semiannual oscillation dominates the annual oscillation (Figures 1, 7). Harmonics for individual years from 1979-1981 show excellent agreement with Figure 7; interannual fluctuations are typically less than 15 days.

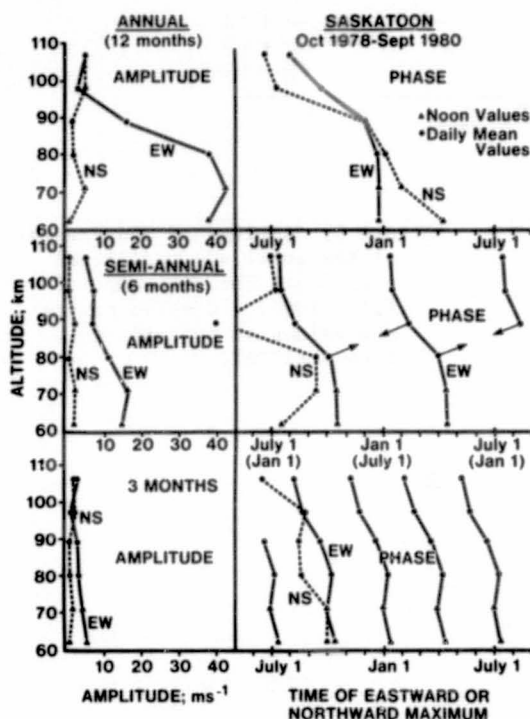


Figure 7. Amplitudes and phases of the zonal (EW) and meridional (NS) components for Saskatoon.

For Christchurch: spectral analysis of weekly wind data covering more than a year indicate that the principal long-term seasonal components are harmonics of an annual oscillation (Figure 8). The annual variation dominates below 80 km with a zonal amplitude of 60 m/s maximising at the end of June. Its strength decreases with increasing height, with minimum values in the 88-95 km region. The circulation above 95 km is 180° out of phase with that of the mesosphere. The annual variation of the zonal wind at Adelaide was very similar for early data also shown in Figure 8, but the meridional component there did not show such a large phase variation as at Christchurch (ELFORD, 1976). The semiannual oscillation achieves largest amplitude near 70 km (23 m/s). It assumes an additional importance in the 86-95 km region where it exceeds the annual variation; in this region easterly winds are observed at two intervals each year (Figure 3). A 3-monthly zonal component, with amplitudes less than 10 m/s, is also evident with a constant phase slope with height.

ORIGINAL PAGE IS
OF POOR QUALITY

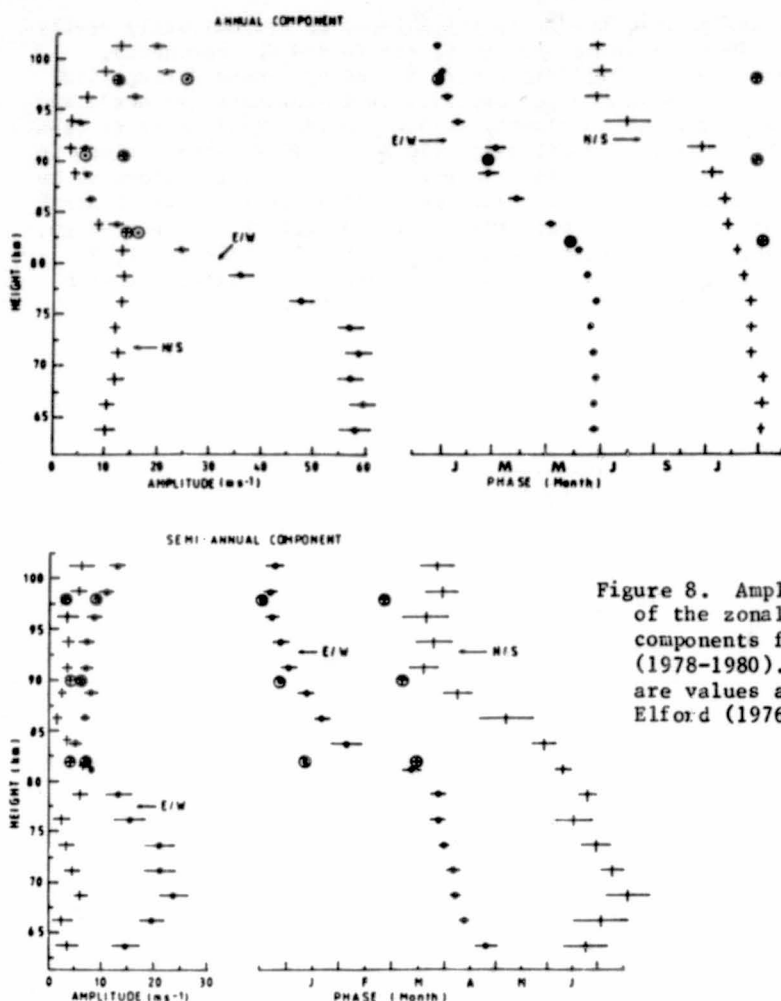


Figure 8. Amplitudes and phases of the zonal and meridional components for Christchurch (1978-1980). Circled points are values at Adelaide from Elford (1976).

The recent data from Adelaide, used in the cross section of Figure 4, provide profiles of annual and semiannual oscillations (Figure 9) which are remarkably similar to those from Christchurch, and also Elford's earlier analysis. The main differences are that the meridional annual oscillation is smaller in amplitude, and has a smaller phase variation near 95 km; amplitudes of both components of the semiannual oscillation are smaller, and the phase variation of the NS is again small. These oscillations appear to be very regular over time and geographical location.

Overall, the profiles of Figures 7 and 8 are similar to those shown by GROVES (1972), although the resolution here is improved. However, the comparison with Adelaide is not good, as Groves shows major differences in the positions of maxima and phase gradients below 40° , whereas the data of Figure 9 are quite midlatitude in character. Also, differences above 90 km at the three locations are likely due to tidal contamination in the earlier data analysis.

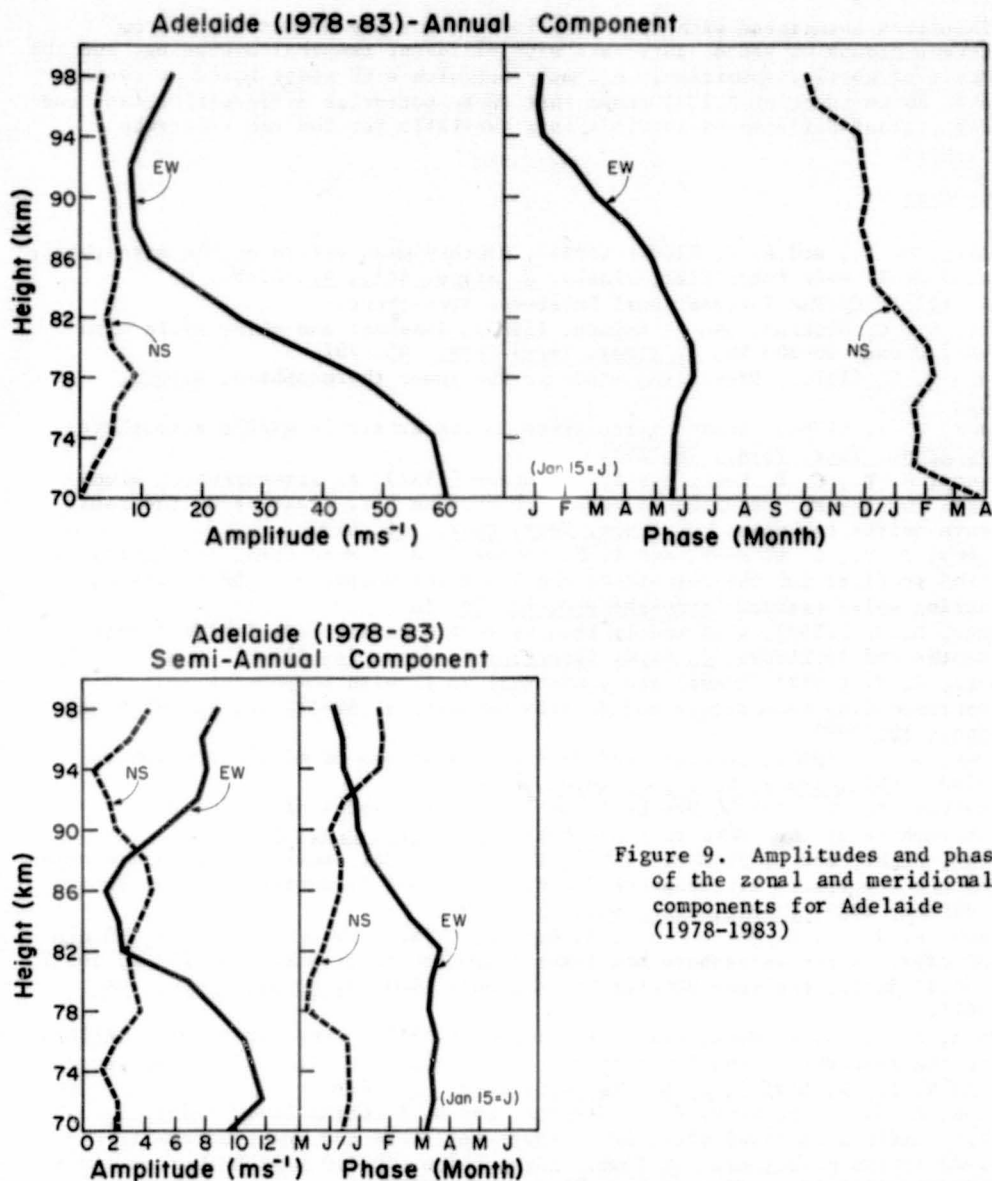


Figure 9. Amplitudes and phases of the zonal and meridional components for Adelaide (1978-1983)

CONCLUSION

The heights of 60-80 km are of considerable interest in the middle atmosphere, as they include the maxima of the summer and winter zonal cells at midlatitudes. MF radar winds data (60-80 km) usefully extend the small-rocket (MNR) winds data so that, supplemented by radar data for above 80 km (MF, meteor, VHF/MST), winds data continuity from 20-110 km is available.

Differences between Southern and Northern Hemisphere winds, and with CIRA-72, highlight the need for a global reference atmosphere. The

difficulties associated with this task include the use of data sets from different groups of years, data sets with different temporal averaging, and the presence of zonal asymmetries. A comparison with a SH model based on rocket data to 80 km (Section 2.1.3) shows that these potential difficulties can lead to significant differences in winds data available for the new reference atmosphere.

REFERENCES

- Balsley, B. B., and A. C. Riddle (1984), Monthly mean values of the mesospheric wind field over Poker Flat, Alaska, J. Atmos. Sci., **41**, 2368.
- CIRA (1972), COSPAR International Reference Atmosphere.
- Dartt, D., G. Nastrom, and A. Belmont (1983), Seasonal and solar cycle wind variations, 80-100 km, J. Atmos. Terr. Phys., **45**, 707.
- Elford W. G. (1976), Prevailing winds in the lower thermosphere, Nature, **261**, 123.
- Fraser, G. J. (1984), Summer circulation in the Antarctic middle atmosphere, J. Atmos. Terr. Phys., **46**, 143.
- Gregory, J. B., C. E. Meek, and A. H. Manson (1982), An assessment of winds data (60-110 km) obtained in real-time from an M.F. radar using the radio wave drifts technique, J. Atmos. Terr. Phys., **44**, 649.
- Gregory, J. B., C. E. Meek, and A. H. Manson (1981), Mean zonal and meridional wind profiles for the mesosphere and lower thermosphere at 52°N, L=4.4, during solar maximum, Atmosphere-Ocean, **19**, 24.
- Groves, G. V. (1969), Wind models from 60 to 130 km altitude for different months and latitudes, J. Brit. Interplanet. Soc., **22**, 285.
- Groves, G. V. (1972), Annual and semiannual zonal wind components and corresponding temperature and density variations, 60-130 km, Planet Space Sci., **20**, 2099.
- Groves, G. V. (1980), Seasonal and diurnal variations of middle atmosphere winds, Phil. Trans. Roy. Soc. Lond., **A296**, 19.
- Koshelkov, Yu. P. (1983), Proposal for a reference model of the middle atmosphere of the southern hemisphere, Adv. Space Res., **3**, 3.
- Manson, A. H., and C. E. Meek (1984), Winds and tidal oscillations in the upper middle atmosphere at Saskatoon (52°N, 107°W, L=4.3) during the year June 1982-May 1983, Planet. Space Sci., **31**, 1087.
- Manson, A. H., C. E. Meek, and J. B. Gregory (1981a), Winds and waves (10 min - 30 days) in the mesosphere and lower thermosphere at Saskatoon (52°N, 107°W, L=4.3) during the year October 1979 to July 1980, J. Geophys. Res., **86**, 9615.
- Manson, A. H., C. E. Meek, and J. B. Gregory (1981b), Long period oscillations in the mesospheric and lower thermospheric winds (60-110 km) at Saskatoon (52°N, 107°W, L=4.3), J. Geomag. Geoelectr., **33**, 613.
- Manson, A. H., C. E. Meek, J. B. Gregory, and D. K. Chakrabarty (1982), Fluctuations in tidal (24-, 12-h) characteristics and oscillations (8-h - 5-d) in the mesosphere and lower thermosphere (70-110 km): Saskatoon (52°N, 107°W), 1979-1981, Planet. Space Sci., **30**, 1283.
- Meek, C. E., and A. H. Manson, (1984), Comparisons between Primrose Lake (54°N, 110°W) Rocob winds (20-60 km) and Saskatoon (52°N, 107°W) MF radar winds (60-110 km): 1978-1983, Report #1, Dynamics Group, ISAS, University of Saskatchewan, Saskatoon, Canada.
- Nastrom, G. D., B. B. Balsley, and D. A. Carter (1982), Mean meridional winds in the mid and high latitude summer mesosphere, Geophys. Res., **9**, 139.
- Smith, M. J. (1981), Upper atmosphere circulation and wave motion, Ph.D. Thesis, Physics Department, University of Canterbury, Christchurch, New Zealand.
- Vincent, R. A. (1984), MF/HF radar measurements of the dynamics of the mesopause region -- a review, J. Atmos. Terr. Phys., **46**, 961.

2.2 MIDDLE ATMOSPHERE REFERENCE MODEL DERIVED FROM SATELLITE DATA

J. J. Barnett and M. Corney

Department of Atmospheric Physics, Clarendon Laboratory
Oxford OX1 3PU, Great Britain

Table I and Figures 1.1 - 1.12 give zonally averaged temperature and geostrophic zonal wind for each month and for latitudes from 80°S to 80°N with pressure scale height as a vertical coordinate. The pressure scale height is defined as $-\ln(p/p_0)$ where p is pressure and p_0 is surface pressure. The height interval corresponding to one pressure scale height is proportional to absolute temperature, and is 7 km at 240 K. Values in Table I are given at intervals of 0.5 pressure scale heights, i.e., approximately 3.5 km. Figure 2 gives the geopotential height fields for the principal seasons.

Table II gives temperature, pressure and density with geometric height as the vertical coordinate at intervals of 5 km.

The temperature values have been obtained from a combination of satellite data above 30 mb with values supplied by the Berlin Free University at 30 mb and the climatology derived by OORT (1983) for 50 mb and below. The geopotential height fields were obtained from these temperature fields by integrating up and down from the 30 mb geopotential height supplied by Berlin Free University. The geostrophic winds were obtained by differentiating these geopotential height fields.

In order to derive Table II it was necessary to obtain the geometric height from the geopotential height. This was done using the scaling factors given in the Smithsonian Meteorological Tables (LIST, 1958). For some applications users may wish to use geometric and geopotential heights interchangeably. The following table which gives the geopotential height for different geometric heights and latitudes will show whether such an approximation is satisfactory for their purposes:

Geomagnetic Height (m)	0°	40°	80° latitude
Geopotential Height			
20000	19897	19941	20000
40000	39669	39756	39874
60000	59318	59449	59626
80000	78844	79018	79255

The basic grid used for the calculations, interpolation and plotting had intervals of 0.2 in $\ln(\text{pressure})$ and 4 deg in latitude. Values were interpolated to a coarser resolution of 10 deg latitude and 0.5 intervals in $\ln(\text{pressure})$ and 5 km for tabulation.

It must be emphasised that the zonal wind values given are geostrophic. Below about 60 km they can be expected to be within a few m/s of the true zonal wind, but above that level increasing departures can be expected because of forcing by tides and gravity waves.

Values are tabulated to at least one significant figure more than their accuracy justifies. This is to avoid truncation problems where the data are to be used in calculations which demand particularly smooth fields.

Temperature values in Table I for 70°S and 80°S at 1013 mb and 0 km are left blank because these levels are within the Antarctic land mass. Wind values for 80°S and 80°N have been left blank because the geopotential height was not available nearer to the pole for a gradient to be found. Between 16°S and 16°N wind values were omitted because the large values of Coriolis parameter near the equator causes the wind calculation to be very sensitive to errors in the geopotential height gradient.

REFERENCES

- List, R. J. (1958), Smithsonian Meteorological Tables, Smithsonian Misc. Collections, Vol. 114.
OORT, A. H. (1983), Global atmospheric statistics, 1958-1973, NOAA Professional Paper 14.

ORIGINAL PAGE IS
OF POOR QUALITY

Table I.

TABLE I		PRESSURE COORDINATES																
JANUARY ZONAL MEAN TEMPERATURE (K)		LATITUDE																
SCALE	PRESSURE	-80	-70	-60	-50	-40	-30	-20	-10	0	10	20	30	40	50	60	70	80
HEIGHT	(mb)																	
12.0	0.0062	148.8	152.2	157.6	170.1	184.9	197.7	203.9	204.5	204.2	204.4	204.5	209.1	214.4	220.7	224.1	224.1	225.1
11.5	0.0103	160.1	163.1	167.8	178.7	191.5	201.9	206.4	205.9	206.0	206.7	207.8	211.7	216.6	222.7	225.4	224.7	225.5
11.0	0.0169	174.1	176.7	180.4	188.9	198.5	205.7	208.6	207.3	207.7	208.7	210.4	214.2	219.0	223.9	226.1	225.3	226.4
10.5	0.0279	189.9	191.9	194.5	199.8	205.1	208.8	210.8	210.1	210.4	211.3	212.7	216.5	220.4	224.6	227.1	226.4	228.1
10.0	0.0460	206.2	207.5	208.9	210.7	211.2	212.2	214.0	215.1	215.3	215.5	215.9	219.1	221.3	225.2	228.1	228.6	231.4
9.5	0.0758	222.5	222.9	222.8	221.4	218.9	218.4	221.2	223.8	225.0	223.8	223.3	224.0	224.7	226.0	229.5	232.8	237.4
9.0	0.1250	236.5	237.5	236.0	232.5	229.1	228.5	232.4	236.1	237.9	235.5	233.3	230.5	228.5	228.0	232.6	239.1	245.3
8.5	0.2061	253.4	251.5	248.8	245.1	241.7	241.0	244.9	250.0	250.7	248.0	243.0	238.3	233.4	232.8	237.9	246.3	252.7
8.0	0.3398	267.3	264.6	261.4	257.0	253.3	252.4	255.0	260.0	261.7	258.9	253.5	247.6	242.0	240.9	244.8	251.8	256.0
7.5	0.5603	279.1	275.6	271.8	267.1	263.1	261.9	262.7	265.7	267.4	266.0	262.8	258.0	253.6	250.7	252.4	254.9	255.1
7.0	0.9237	287.2	283.2	278.7	274.8	271.2	269.1	268.2	267.8	267.3	268.0	267.7	264.9	261.3	255.4	253.8	253.4	251.7
6.5	1.52	288.3	284.9	280.9	276.8	273.3	269.9	267.4	264.1	263.6	264.5	265.9	264.3	260.0	253.4	250.8	249.9	248.7
6.0	2.51	283.0	280.4	277.0	272.7	268.8	264.3	260.1	257.6	257.6	257.9	258.8	256.9	252.0	247.1	246.2	245.4	244.9
5.5	4.14	273.3	271.1	268.1	263.9	259.4	254.7	250.6	248.8	249.5	248.7	248.5	245.9	242.5	239.2	238.5	237.6	236.4
5.0	6.83	261.7	260.3	257.6	253.6	248.8	244.3	241.1	238.9	239.1	238.7	238.2	236.1	234.3	232.0	230.8	228.1	225.2
4.5	11.25	249.1	248.4	246.9	243.5	238.2	233.6	230.2	228.7	227.5	228.8	228.9	226.0	222.8	220.4	219.6	218.0	212.3
4.0	18.55	238.1	237.2	235.7	233.9	230.0	226.4	223.0	221.6	220.8	221.7	221.9	222.8	222.2	220.4	219.6	218.0	202.3
3.5	30.59	235.4	233.5	231.5	227.5	223.3	219.9	216.9	215.5	214.8	215.2	215.8	217.0	217.9	217.0	213.2	207.2	201.6
3.0	50.43	234.8	233.3	229.9	223.5	216.7	212.0	209.3	207.2	205.9	206.4	208.2	210.9	214.7	216.8	215.6	212.5	207.8
2.5	83.15	233.6	232.5	228.3	220.9	212.1	204.9	200.4	197.8	196.7	197.3	200.7	206.9	214.0	217.4	216.7	214.1	210.7
2.0	137.09	231.8	230.5	226.8	220.4	213.0	207.0	203.0	200.9	200.4	200.8	203.6	209.4	215.1	217.9	217.0	214.4	212.3
1.5	226.05	228.0	226.6	225.1	223.5	222.9	224.7	226.2	226.0	226.2	225.7	224.7	222.1	219.0	218.2	216.9	215.2	214.1
1.0	372.66	222.2	220.8	219.2	217.5	216.0	214.9	213.2	211.6	210.9	210.8	209.4	206.9	204.0	202.6	201.4	200.0	197.9
0.5	614.42	248.9	251.5	255.6	262.1	267.2	271.3	275.0	278.7	279.9	277.0	274.5	267.2	258.7	252.0	247.5	243.8	241.1
0.0	1013.0			275.8	281.6	289.5	296.0	299.2	300.7	300.8	300.3	297.4	291.7	284.4	278.1	267.0	254.2	248.5

JANUARY ZONAL MEAN GEOPOTENTIAL HEIGHT (m)		LATITUDE																
SCALE	PRESSURE	-80	-70	-60	-50	-40	-30	-20	-10	0	10	20	30	40	50	60	70	80
HEIGHT	(mb)																	
12.0	0.0062	83647	83407	83128	82857	82593	82441	82424	82409	82434	82387	82245	82076	81749	81417	81299	80990	80752
11.5	0.0103	81385	81098	80746	80302	79836	79513	79418	79403	79426	79375	79224	78993	78592	78168	78006	77703	77453
11.0	0.0169	78945	78617	78202	77615	76982	76529	76379	76378	76395	76334	76162	75875	75404	74898	74699	74409	74145
10.5	0.0279	76277	75915	75454	74766	74024	73492	73308	73322	73332	73259	73064	72720	72184	71614	71380	71101	70818
10.0	0.0460	73381	72995	72504	71763	70978	70411	70200	70212	70216	70138	69929	69534	68951	68321	68047	67771	67455
9.5	0.0758	70236	69838	69338	68595	67828	67261	67015	66999	66994	66924	66714	66290	65686	65017	64697	64393	64023
9.0	0.1250	66864	66470	65981	65275	64553	63995	63700	63639	63615	63565	63374	62965	62368	61696	61316	60942	60491
8.5	0.2061	63257	62884	62428	61776	61103	60555	60200	60074	60037	60020	59883	59531	58987	58324	57872	57385	56840
8.0	0.3398	59446	59108	58694	58100	57479	56942	56538	56336	56290	56309	56251	55976	55513	54860	54342	53736	53108
7.5	0.5603	55439	55146	54783	54257	53693	53172	52744	52481	52414	52459	52465	52269	51879	51254	50695	50020	49362
7.0	0.9237	51289	51051	50750	50288	49779	49281	48855	48570	48495	48544	48575	48436	48104	47543	46981	46294	45650
6.5	1.52	47067	46884	46646	46241	45783	45326	44926	44671	44602	44642	44662	44553	44277	43811	43285	42610	41988
6.0	2.51	42876	42736	42551	42211	41806	41407	41055	40845	40780	40811	40814	40728	40520	40141	39642	38979	38369
5.5	4.14	38802	38698	38560	38281	37938	37608	37320	37139	37071	37103	37102	37048	36903	36581	36094	35442	34845
5.0	6.83	34880	34802	34706	34488	34213	33950	33714	33563	33495	33531	33535	33519	33411	33130	32656	32028	31459
4.5	11.25	31139	31077	31015	30851	30651	30455	30267	30142	30082	30113	30120	30117	30031	29778	29332	28763	28260
4.0	18.55	27577	27526	27469	27354	27223	27087	26950	26846	26797	26815	26819	26807	26734	26507	26118	25639	25227
3.5	30.59	24116	24082	24043	23980	23905	23820	23730	23644	23605	23616	23616	23590	23514	23309	22986	22602	22280
3.0	50.43	20673	20671	20668	20679	20681	20655	20605	20545	20518	20525	20507	20454	20346	20136	19851	19536	19290
2.5	83.15	17242	17259	17312	17427	17545	17605	17607	17568	17568	17571	17515	17399	17210	16957	16684	16408	16221
2.0	137.09	13833	13866	13979	14198	14442	14609	14682	14693	14690	14687	14581	14365	14069	13768	13507	13271	13125

JANUARY MEAN ZONAL MEAN GEOSTROPHIC WIND (m s ⁻¹)		LATITUDE																
SCALE	PRESSURE	-80	-70	-60	-50	-40	-30	-20	-10	0	10	20	30	40	50	60	70	80
HEIGHT	(mb)																	
12.0	0.0062		-9.8	-21.7	-20.3	-20.9	-12.3	3.4				21.2	31.4	31.3	20.5	9.3	19.4	
11.5	0.0103		-13.6	-30.2	-35.4	-39.4	-27.1	-3.2				27.4	40.3	42.0	24.6	10.8	18.8	
11.0	0.0169		-16.9	-37.3	-47.9	-54.1	-37.8	-6.4				34.2	48.5	51.9	28.2	11.7	18.0	
10.5	0.0279		-19.4	-42.5	-56.3	-63.4	-44.5	-8.1				41.4	56.5	60.0	31.2	12.6	17.6	
10.0	0.0460		-21.1	-45.3	-60.3	-67.1	-48.1	-11.2				47.4	63.0	66.1	34.5	14.0	18.1	
9.5	0.0758		-21.9	-45.8	-59.7	-66.0	-50.2	-17.9				50.6	66.5	68.7	37.7	16.8	20.5	
9.0	0.1250		-21.4	-44.1	-56.4	-62.9	-52.8	-27.8				48.5	65.3	67.1	40.4	21.7	25.5	
8.5	0.2061		-19.6	-41.0	-52.3	-59.5	-56.0	-40.5				39.4	58.4	62.0	33.5	28.5	32.7	
8.0	0.3398		-17.0	-37.5	-47.8	-55.9	-58.6	-53.4				25.8	48.0	55.7	46.5	35.3	40.1	
7.5	0.5603		-13.7	-33.9	-42.7	-52.2	-59.4	-62.0				13.0	37.8	49.7	47.8	39.3	44.3	
7.0	0.9237		-9.7	-29.2	-37.9	-48.4	-58.0	-64.4				5.9	30.1	43.2	45.7	40.0	45.2	
6.5	1.52		-5.6	-25.1	-33.6	-44.1	-53.8	-59.5				4.6	24.4	35.3	40.6	38.9	44.6	
6.0	2.51		-2.3	-21.0	-29.0	-38.8	-47.1	-50.6				5.3	18.4	27.3	36.0	38.5	43.8	
5.5	4.14		0.5	-17.1	-24.2	-32.6	-38.7	-41.9				3.9	12.1	21.1	32.8	38.8	42.7	
5.0	6.83		2.7	-13.4	-19.3	-26.0	-31.1	-34.0				0.5	7.1	17.3	30.3	38.6	40.4	
4.5	11.25																	

FEBRUARY ZONAL MEAN TEMPERATURE (K)

SCALE PRESSURE			LATITUDE																
HEIGHT	(mb)		-80	-70	-60	-50	-40	-30	-20	-10	0	10	20	30	40	50	60	70	80
12.0	0.0062	165.6	167.7	171.2	181.1	192.0	199.5	202.7	204.0	204.9	204.9	205.1	207.0	211.5	216.8	220.2	220.5	220.1	
11.5	0.0103	174.5	176.1	178.6	187.6	197.2	203.5	204.7	204.8	205.4	206.5	208.8	210.6	214.6	220.2	224.0	225.4	225.3	
11.0	0.0169	185.5	186.7	188.5	195.6	202.8	207.0	207.2	206.4	206.9	208.8	211.7	214.1	218.2	223.2	226.7	228.8	225.9	
10.5	0.0279	198.0	198.0	200.0	204.2	208.2	210.3	210.6	209.9	209.9	211.6	214.5	217.0	220.9	225.3	229.0	228.6	229.8	
10.0	0.0460	211.2	211.3	212.0	212.6	213.4	214.3	215.3	215.2	214.7	215.1	217.0	219.5	222.6	226.6	231.4	233.1	236.4	
9.5	0.0758	225.5	224.5	223.5	221.1	217.9	220.7	222.8	223.0	222.4	221.7	222.5	223.5	225.8	228.8	233.9	239.1	245.4	
9.0	0.1250	240.5	237.6	234.4	230.2	227.9	229.7	232.7	233.0	232.6	232.1	229.6	228.7	229.1	231.5	237.5	246.1	254.9	
8.5	0.2061	253.0	249.4	245.4	240.9	238.6	240.1	243.5	245.1	244.4	243.0	239.0	236.8	234.1	236.0	243.5	253.3	262.8	
8.0	0.3398	263.6	260.0	256.4	252.1	249.4	249.7	252.7	256.5	257.7	256.0	251.2	247.7	243.5	243.7	249.2	257.6	265.2	
7.5	0.5603	272.4	265.4	266.4	263.0	259.8	259.5	261.0	265.8	268.1	266.9	263.5	259.2	254.8	252.4	253.0	255.5	267.3	
7.0	0.9237	278.6	275.9	273.1	271.3	268.7	267.7	268.2	270.5	271.9	271.9	270.4	269.2	264.4	256.8	253.5	249.5	247.8	
6.5	1.52	278.2	276.2	274.4	272.7	270.4	268.3	268.7	268.6	269.9	270.5	270.2	266.9	261.8	254.1	248.0	243.4	240.2	
6.0	2.51	272.1	270.5	268.9	267.2	266.0	262.8	261.9	262.2	263.3	263.6	263.1	259.8	254.2	246.1	241.6	238.4	235.6	
5.5	4.14	262.6	261.4	259.9	258.3	256.3	253.6	252.5	252.2	252.9	252.7	252.4	249.1	243.9	236.7	234.5	233.7	231.8	
5.0	6.83	252.3	251.6	250.5	248.6	245.5	243.5	242.5	240.9	240.8	240.4	242.1	238.6	233.7	228.1	227.6	228.6	227.0	
4.5	11.25	241.9	241.6	240.9	239.0	235.7	233.6	231.3	229.8	228.8	229.7	229.9	229.4	225.3	221.8	221.5	222.2	219.9	
4.0	18.55	234.0	233.4	232.7	230.6	226.2	226.2	223.4	222.3	221.9	222.2	222.1	222.2	220.6	219.0	217.1	215.0	211.4	
3.5	30.59	232.8	230.9	228.4	225.2	226.6	219.8	217.2	215.9	215.2	215.0	215.3	216.1	214.7	217.6	215.9	212.2	208.3	
3.0	50.43	232.3	230.8	227.8	222.2	216.4	212.0	209.3	207.1	205.6	206.4	208.4	211.1	214.9	217.6	217.1	214.1	209.6	
2.5	83.15	231.4	230.2	226.7	219.7	211.8	205.1	200.3	197.8	196.9	197.6	200.8	207.6	214.5	218.3	217.8	214.8	210.2	
2.0	137.09	230.2	229.4	225.9	219.4	212.7	207.1	203.1	201.2	201.1	201.3	203.9	209.6	215.7	218.6	217.8	214.8	211.2	
1.5	226.03	226.9	227.0	225.5	223.4	223.3	225.1	226.4	226.3	226.4	226.2	225.5	222.7	219.3	218.5	217.4	215.5	213.6	
1.0	372.66	226.1	228.1	232.1	238.6	244.9	249.7	252.9	255.6	255.8	253.5	250.3	242.3	233.7	228.3	225.2	222.9	220.8	
0.5	614.42	248.0	249.9	254.9	262.7	270.0	274.6	276.7	276.9	277.0	277.2	274.5	267.2	258.5	251.7	247.5	244.1	241.5	
0.0	1013.0			277.0	282.3	289.9	296.4	299.8	301.2	301.1	300.2	297.1	291.2	284.0	277.9	266.9	254.1	247.4	

FEBRUARY ZONAL MEAN GEOPOTENTIAL HEIGHT (m)

SLANT HEIGHT	LOCAL PRESSURE (mb)	MEAN GEOPOTENTIAL HEIGHT (m)																	
		-80	-70	-60	-50	-40	-30	-20	-10	0	10	20	30	40	50	60	70	80	
12.0	0.0062	83051	82813	82601	82530	82466	82443	82454	82446	82489	82529	82443	82190	81810	81475	81519	81478	81461	
11.5	0.0103	80562	80296	80040	79831	79616	79491	79470	79452	79485	79517	79410	79131	78690	78273	78264	78226	78214	
11.0	0.0169	77930	77645	77357	77029	76686	76465	76455	76443	76464	76477	76331	76023	75522	75026	74964	74936	74928	
10.5	0.0279	75118	74819	74510	74099	73677	73428	73396	73395	73408	73398	73210	72864	72305	71740	71627	71610	71592	
10.0	0.0460	72126	71820	71497	71048	70592	70322	70280	70285	70297	70277	70055	69668	69059	68432	68255	68232	68182	
9.5	0.0758	68925	68626	68304	67869	67420	67138	67073	67075	67094	67080	66804	66427	65777	65097	64848	64774	64652	
9.0	0.1250	65516	65265	64953	64568	64147	63846	63744	63741	63765	63767	63534	63120	62449	61728	61398	61224	60991	
8.5	0.2061	61896	61673	61436	61116	60729	60403	60250	60237	60268	60261	60102	59711	59059	58308	57880	57665	57194	
8.0	0.3398	58114	57944	57746	57509	57157	56818	56615	56635	56595	56591	56519	56168	55569	54800	54277	53820	53319	
7.5	0.5603	54185	54064	53931	53734	53425	53088	52853	52734	52742	52804	52745	52450	51826	51162	50595	50065	49492	
7.0	0.9237	50146	50068	49977	49819	49552	49224	48976	48801	48786	48853	48853	48597	48125	47428	46888	46465	45951	
6.5	1.52	46065	46017	45961	45830	45597	45291	45036	44848	44814	44875	44867	44683	44277	43680	43222	42757	42223	
6.0	2.51	42026	42006	41974	41871	41661	41394	41143	40955	40904	40957	40955	40818	40490	40011	39633	39228	38741	
5.5	4.14	38112	38113	38104	38024	37837	37615	37380	37190	37129	37178	37181	37094	36845	36477	36149	35773	35320	
5.0	6.83	34358	34353	34363	34204	34159	33968	33751	33576	33512	33560	33563	33520	33345	33072	32763	32385	31958	
4.5	11.25	30722	30744	30768	30741	30640	30479	30285	30133	30077	30120	30119	30089	29991	29784	29478	29085	28665	
4.0	18.55	27243	27269	27300	27303	27243	27112	26957	26824	26778	26811	26810	26798	26725	26555	26267	25883	25527	
3.5	30.59	23820	23875	23931	23967	23943	23848	23732	23616	23580	23612	23611	23585	23522	23360	23099	22762	22462	
3.0	50.43	20435	20452	20493	20589	20526	20682	20605	20513	20493	20523	20506	20484	20358	20194	19939	19645	19407	
2.5	83.15	17026	17119	17264	17455	17593	17630	17607	17570	17545	17567	17510	17396	17216	16983	16745	16503	16332	
2.0	137.09	13645	13753	13950	14242	14496	14636	14682	14660	14660	14678	14574	14360	14068	13782	13535	13299	13244	

FEBRUARY MEAN ZONAL MEAN GEOSTROPHIC WIND (m s^{-1})

SCALE	PRESSURE	-80	-70	-60	-50	-40	-30	-20	-10	0	10	20	30	40	50	60	70	80
HEIGHT	(mb)																	
12.0	0.0062	-14.2	-9.3	-5.4	-5.2	1.2	0.6					28.6	36.0	45.0	10.8	-1.6	7.2	
11.5	0.0103	-16.7	-15.4	-17.2	-17.7	-6.8	-1.4					32.6	42.2	51.5	16.7	-0.1	6.8	
11.0	0.0169	-18.7	-20.5	-27.1	-27.8	-12.1	0.2					38.5	48.4	57.2	22.5	1.0	6.1	
10.5	0.0279	-20.0	-24.0	-33.9	-34.0	-15.1	2.3					45.7	54.9	62.7	27.5	2.1	5.4	
10.0	0.0460	-20.7	-25.7	-36.9	-36.5	-17.2	2.4					52.6	60.8	67.6	32.6	4.3	5.8	
9.5	0.0758	-20.4	-25.2	-36.1	-36.4	-19.9	-0.3					56.5	65.1	71.6	37.6	8.3	8.6	
9.0	0.1250	-18.2	-22.5	-32.9	-35.7	-24.1	-4.7					56.6	66.3	74.3	42.3	14.4	14.0	
8.5	0.2061	-14.3	-18.4	-28.8	-35.0	-29.3	-11.3					48.8	63.5	74.4	47.2	22.8	21.6	
8.0	0.3398	-10.4	-14.3	-24.7	-33.8	-33.6	-20.4					38.6	57.3	72.0	51.6	31.3	29.4	
7.5	0.5603	-7.0	-10.7	-20.6	-31.7	-35.5	-30.5					27.1	49.7	67.5	52.7	35.9	33.7	
7.0	0.9237	-4.2	-8.0	-17.2	-29.2	-35.8	-37.3					18.1	42.1	61.4	49.3	35.0	33.6	
6.5	1.52	-2.0	-6.0	-14.8	-26.5	-34.7	-39.5					12.5	34.8	53.0	42.1	30.4	30.7	
6.0	2.51	-0.3	-4.2	-12.7	-23.4	-32.1	-39.5					8.6	27.2	42.7	34.2	25.8	27.5	
5.5	4.14	1.2	-2.8	-10.8	-20.1	-28.2	-38.1					4.8	19.5	32.3	27.6	23.7	25.8	
5.0	6.83	2.2	-1.4	-8.2	-16.5	-25.1	-35.4					2.1	12.4	22.8	23.0	23.8	25.5	
4.5	11.25	2.8	-0.1	-5.1	-12.6	-21.8	-31.1					1.4	7.3	15.4	20.1	24.9	25.4	
4.0	18.55	2.0	1.4	-2.3	-9.2	-17.5	-25.8					1.7	5.0	10.8	18.0	24.2	23.9	
3.5	30.39	3.3	3.5	0.5	-5.9	-12.9	-20.9					2.3	5.3	10.3	16.7	21.5	20.7	
3.0	50.43	6.0	7.3	5.1	-0.5	-7.7	-15.2					5.6	8.9	13.5	16.8	19.0	16.8	
2.5	83.15	8.0	13.2	12.5	8.6	0.2	-7.1					14.6	18.3	20.6	18.4	17.2	13.1	
2.0	137.09	9.9	19.0	21.3	19.1	10.7	2.9					27.8	32.3	28.9	17.9	14.9	9.5	

PRESSURE COORDINATES

MARCH		MEAN GEOSTROPHIC WIND ($m\ s^{-1}$)																
SCALE	PRESSURE	-80	-70	-60	-50	-40	-30	-20	-10	0	10	20	30	40	50	60	70	80
HEIGHT	(mb)																	
12.0	0.0062		9.1	11.7	9.9	13.8	12.6	13.3				3.2	17.6	10.0	25.5	22.3	22.9	
11.5	0.0103		9.8	11.2	7.8	12.2	12.0	10.2				4.1	17.3	11.2	28.1	24.1	21.9	
11.0	0.0169		10.8	11.5	6.7	11.3	13.1	11.1				9.5	19.6	16.5	31.3	24.9	19.6	
10.5	0.0279		11.9	12.6	7.1	11.1	14.2	13.5				18.7	24.6	19.8	33.9	24.2	16.8	
10.0	0.0460		13.2	14.6	9.2	11.0	14.0	16.0				29.3	30.0	25.4	35.8	23.3	14.4	
9.5	0.0758		15.6	18.0	12.4	9.7	12.0	18.5				38.2	34.2	30.5	36.9	22.5	13.1	
9.0	0.1250		19.3	22.3	15.3	7.0	8.5	20.4				42.8	36.6	35.0	37.2	22.2	13.2	
8.5	0.2061		23.1	26.3	18.1	4.7	5.8	19.1				42.3	37.1	38.1	37.2	23.4	15.5	
8.0	0.3398		26.4	29.1	20.0	3.6	-0.1	13.9				37.9	35.9	39.4	38.0	26.4	19.4	
7.5	0.5603		28.6	30.3	20.5	2.9	-1.5	6.1				31.2	34.4	39.0	38.0	28.8	22.5	
7.0	0.9237		28.7	29.9	19.9	2.5	-1.8	0.6				24.7	30.5	37.5	36.8	28.7	22.3	
6.5	1.52		26.8	27.2	18.3	2.6	-3.0	-4.4				19.0	27.1	34.6	33.3	25.3	18.9	
6.0	2.51		24.1	23.2	15.6	2.7	-5.2	-10.7				13.2	22.6	30.7	28.2	19.8	14.2	
5.5	4.14		21.5	18.6	12.3	2.1	-7.4	-15.8				7.3	17.9	25.7	22.1	15.1	10.7	
5.0	6.83		18.8	14.8	10.0	1.0	-9.3	-18.2				2.6	13.0	19.6	16.5	12.4	9.7	
4.5	11.25		16.5	12.7	8.6	-0.1	-10.4	-18.2				1.2	8.2	12.9	12.5	11.8	10.6	
4.0	18.55		13.2	11.6	7.7	-0.7	-10.1	-17.2				1.1	4.7	7.8	10.1	12.1	12.2	
3.5	30.59		11.2	11.1	8.0	0.1	-8.5	-15.4				1.2	3.8	6.9	9.9	12.3	12.8	
3.0	50.43		11.7	11.8	10.1	3.8	-4.1	-11.1				4.1	7.0	10.0	11.3	12.3	11.5	
2.5	83.15		12.9	14.2	15.1	11.3	4.6	-2.2				13.3	16.4	16.8	13.3	11.8	8.6	
2.0	137.09		13.8	17.8	21.6	20.9	16.0	9.1				27.2	29.9	24.7	16.0	11.2	6.1	

TABLE 1 (continued)

PRESSURE COORDINATES

APRIL ZONAL MEAN TEMPERATURE (K)

SCALE HEIGHT	PRESSURE (mb)	-80	-70	-60	-50	-40	-30	-20	-10	0	10	20	30	40	50	60	70	80
12.0	0.0062	226.6	223.0	216.5	212.5	209.4	206.1	207.0	212.3	214.2	209.9	207.8	203.8	196.6	191.3	190.0	189.8	189.9
11.5	0.0103	229.1	225.7	219.5	215.3	211.5	208.0	207.2	211.0	212.1	209.5	208.4	206.9	202.7	199.8	200.3	199.5	199.1
11.0	0.0169	229.7	227.2	223.2	217.6	213.7	210.5	208.1	209.6	209.4	208.3	209.0	210.5	209.3	209.0	210.3	209.2	208.6
10.5	0.0279	231.4	229.3	226.5	220.1	216.1	213.5	210.5	209.7	208.4	208.5	211.8	215.1	215.8	217.7	219.0	218.2	217.5
10.0	0.0460	236.0	233.0	229.7	223.0	219.4	217.2	214.2	211.7	210.1	211.9	217.1	220.3	221.8	224.1	225.7	225.7	225.4
9.5	0.0758	242.6	238.4	233.7	226.9	224.6	224.4	221.1	217.9	216.6	219.0	224.0	226.6	228.2	230.2	231.1	230.9	230.1
9.0	0.1250	249.1	244.0	238.4	232.8	231.3	232.5	230.4	227.5	226.9	228.4	230.9	233.2	235.0	236.4	236.9	235.9	234.8
8.5	0.2061	253.0	248.5	243.6	240.4	239.2	239.4	239.7	239.0	239.5	239.0	238.2	239.6	241.6	243.1	243.9	244.3	243.9
8.0	0.3398	256.2	252.3	247.9	247.7	248.4	248.6	250.3	251.4	252.5	250.7	247.9	248.8	251.1	252.8	252.9	254.4	255.0
7.5	0.5603	258.9	257.2	254.4	255.3	258.8	260.2	261.3	263.0	263.9	262.3	260.1	260.5	262.7	263.5	263.8	264.8	265.1
7.0	0.9237	254.4	255.0	255.5	258.8	264.3	266.8	267.8	269.7	270.2	269.8	269.1	269.3	270.7	270.8	270.6	269.7	268.8
6.5	1.52	243.1	244.6	248.0	254.4	260.4	264.0	267.4	269.8	270.6	270.1	269.4	269.6	270.6	271.0	268.5	264.9	262.5
6.0	2.51	231.3	231.9	236.6	244.9	251.3	255.7	260.7	264.1	265.2	264.5	263.0	262.6	264.1	263.5	259.3	254.7	251.8
5.5	4.14	220.2	220.9	226.6	234.6	241.2	245.9	250.5	254.4	255.9	255.3	253.3	252.5	253.3	251.4	247.1	242.6	240.2
5.0	6.83	212.7	214.2	219.2	225.9	232.4	236.9	240.4	243.5	244.5	244.1	243.0	241.9	240.7	238.7	235.6	232.0	230.2
4.5	11.25	207.5	210.5	214.8	220.7	225.7	229.3	231.8	232.9	232.4	231.6	232.8	231.7	229.7	227.2	226.3	225.5	225.2
4.0	18.55	202.8	208.1	215.1	219.5	222.5	224.5	225.5	225.2	225.0	224.3	224.8	224.3	222.4	221.6	222.2	223.9	225.5
3.5	30.59	208.0	211.7	217.4	219.6	220.2	219.7	219.1	218.3	217.9	217.3	218.0	218.2	218.0	219.2	221.5	224.5	227.3
3.0	50.43	212.6	214.7	216.9	217.5	215.5	216.2	216.0	208.7	207.9	208.4	210.1	212.4	215.3	218.6	221.1	223.0	224.3
2.5	83.15	215.9	217.6	218.4	217.3	212.9	206.9	201.2	198.0	197.1	198.3	202.1	208.2	214.8	218.7	221.2	222.7	223.5
2.0	137.09	218.2	219.9	220.1	217.7	213.5	208.3	203.6	200.6	200.2	201.0	204.4	209.6	214.8	218.7	221.3	222.8	223.3
1.5	226.03	218.4	220.0	220.1	219.8	220.1	222.5	225.1	226.3	226.9	226.3	224.8	221.5	219.0	219.6	221.0	221.9	222.1
1.0	372.66	221.9	224.5	228.9	234.8	240.7	246.4	251.3	253.6	254.2	253.3	250.3	244.8	238.1	235.0	229.0	226.1	224.2
0.5	614.42	243.0	246.4	252.2	259.6	266.6	271.9	275.7	276.9	277.1	277.2	275.6	270.7	264.0	257.7	252.4	247.7	244.2
0.0	1013.0			275.4	281.1	288.9	295.0	299.0	301.3	301.6	301.0	298.3	293.0	286.1	280.4	273.0	261.9	253.2

APRIL ZONAL MEAN GEOPOTENTIAL HEIGHT (m)

SCALE HEIGHT	PRESSURE (mb)	-80	-70	-60	-50	-40	-30	-20	-10	0	10	20	30	40	50	60	70	80
12.0	0.0062	80914	80974	81170	81501	81984	82221	82332	82497	82503	82404	82488	82606	82610	82572	82498	82328	82227
11.5	0.0103	77573	77686	77977	78367	78902	79188	79298	79395	79388	79331	79438	79598	79684	79706	79637	79475	79377
11.0	0.0169	74213	74370	74736	75196	75790	76125	76260	76316	76303	76272	76382	76543	76669	76716	76632	76484	76394
10.5	0.0279	70839	71028	71442	71960	72643	73022	73195	73247	73242	73223	73303	73425	73553	73586	73483	73351	73271
10.0	0.0460	67421	67646	68103	68746	69456	69872	70089	70164	70172	70150	70166	70240	70351	70352	70227	70100	70027
9.5	0.0758	63914	64193	64709	65451	66205	66639	66903	67021	67039	66996	66934	66967	67054	67024	66880	66753	66687
9.0	0.1250	60313	60661	61254	62089	62868	63293	63600	63764	63789	63726	63605	63602	63664	63610	63455	63338	63286
8.5	0.2061	56635	57052	57722	58623	59422	59836	60155	60346	60371	60301	60169	60140	60174	60100	59935	59822	59782
8.0	0.3398	52905	53386	54124	55050	55854	56269	56571	56798	56778	56719	56616	56569	56572	56475	56302	56174	56131
7.5	0.5603	49130	49650	50443	51364	52136	52537	52818	52984	52956	52891	52637	52806	52956	52814	52366	52316	52266
7.0	0.9237	45359	45887	46700	47593	48299	48672	48940	49079	49084	49055	49012	48955	48896	48774	48596	48444	48397
6.5	1.52	41718	42228	43010	43830	44450	44779	45014	45123	45118	45094	45061	45000	44924	44798	44640	44522	44500
6.0	2.51	38241	38734	39435	40168	40697	40966	41140	41206	41190	41173	41154	41096	41001	40876	40765	40710	40729
5.5	4.14	34941	35425	36069	36661	37094	37297	37398	37411	37378	37368	37375	37327	37213	37110	37061	37071	37129
5.0	6.83	31775	32242	32805	33289	33626	33761	33801	33761	33711	33705	33737	33703	33591	33516	33524	33596	33685
4.5	11.25	28695	29132	29633	30025	30276	30353	30348	30278	30225	30228	30258	30240	30158	30112	30149	30253	30359
4.0	18.55	25703	26075	26490	26805	26996	27031	26999	26925	26882	26891	26907	26900	26853	26829	26868	26965	27061
3.5	30.59	22697	23003	23321	23588	23753	23778	23744	23678	23646	23658	23666	23663	23632	23606	23622	23681	23742
3.0	50.43	19617	19880	20139	20385	20559	20608	20597	20546	20526	20537	20529	20510	20461	20402	20382	20403	20430
2.5	83.15	16477	16714	16954	17203	17425	17539	17589	17570	17558	17560	17513	17433	17317	17201	17145	17141	17154
2.0	137.09	13298	13509	13740	14017	14307	14514	14652	14685	14680	14670	14562	14386	14175	13997	13903	13878	13881

APRIL MEAN ZONAL MEAN GEOSTROPHIC WIND ($m s^{-1}$)

SCALE HEIGHT	PRESSURE (mb)	-80	-70	-60	-50	-40	-30	-20	-10	0	10	20	30	40	50	60	70	80
12.0	0.0062		9.8	16.8	34.4	35.5	18.6	20.6				-22.2	-10.9	0.1	6.7	7.2	10.4	
11.5	0.0103		14.5	22.2	39.0	40.5	22.0	14.6				-26.2	-18.5	-6.9	3.9	6.9	10.6	
11.0	0.0169		18.3	27.5	44.3	45.5	27.1	13.4				-25.0	-21.0	-10.1	3.3	7.1	10.3	
10.5	0.0279		20.9	32.4	50.1	50.2	32.8	17.1				-17.2	-18.8	-9.5	4.4	7.3	9.9	
10.0	0.0460		23.7	37.5	56.0	54.4	38.2	24.1				-5.8	-14.8	-6.8	6.4	7.8	9.8	
9.5	0.0758		27.8	43.4	61.3	56.9	42.5	33.3				5.9	-10.8	-4.0	8.2	8.7	9.8	
9.0	0.1250		33.1	50.0	65.5	57.0	44.7	42.7				14.9	-6.8	-1.5	9.4	8.8	9.0	
8.5	0.2061		38.6	55.4	68.3	57.2	44.7	47.0				17.9	-3.2	0.7	10.5	9.2	8.3	
8.0	0.3398		43.5	58.8	69.0	57.6	43.5	45.1				16.2	0.1	3.3	11.7	10.2	8.5	
7.5	0.5603		47.1	60.6	67.4	55.3	41.0	40.7				12.4	3.0	5.8	12.6	11.1	9.0	
7.0	0.9237		48.2	60.6	63.7	50.3	38.5	36.9				9.9	5.1	7.4	12.9	11.3	8.7	
6.5	1.52		46.8	56.9	57.4	43.8	33.9	31.0				8.9	6.7	8.8	12.2	9.3	6.4	
6.0	2.51		44.6	50.6	49.4	36.8	26.6	21.5				7.1	8.0	10.3	10.1	5.4	2.6	
5.5	4.14		42.1	43.0	40.7	29.4	18.1	10.0				3.3	8.8	10.7	6.6	0.8	-1.3	
5.0	6.83		39.1	35.9	32.4	21.9	10.4	-0.2				-0.5	8.3	9.6	3.0	-3.4	-4.7	
4.5	11.25		35.7	30.3	25.3	15.1	4.1	-7.1				-1.5	5.8	6.9	0.5	-5.4	-6.6	
4.0	18.55		28.3	25.3	19.9	10.4	0.0	-9.9				-1.0	3.2	3.9	-0.5	-5.0	-6.2	
3.5	30.59		20.2	21.0	17.1	8.8	-0.7	-9.4				-0.8	2.1	3.2	0.4	-2.8	-3.9	

TABLE I (continued)

PRESSURE COORDINATES

MAY		ZONAL MEAN TEMPERATURE (K)																
SCALE	PRESSURE	-80	-70	-60	-50	-40	-30	-20	-10	0	10	20	30	40	50	60	70	80
HEIGHT	(mb)																	
12.0	0.0062	233.9	228.5	222.1	217.9	212.8	207.1	205.6	208.3	209.5	206.6	203.5	197.2	186.3	175.7	169.0	165.2	162.1
11.5	0.0103	234.2	230.0	225.2	221.3	214.7	208.0	205.2	207.4	208.7	206.6	203.8	200.2	192.4	185.2	180.4	176.6	174.0
11.0	0.0169	233.5	231.4	230.2	224.4	217.1	209.9	205.5	205.3	205.7	205.8	205.1	203.5	199.3	195.9	193.5	189.9	187.4
10.5	0.0279	234.9	234.3	234.8	228.2	220.4	212.7	206.8	204.1	203.5	206.0	208.2	208.2	206.6	206.4	206.6	203.9	201.8
10.0	0.0460	238.5	238.6	239.5	232.7	224.4	216.4	209.4	205.6	205.0	209.1	213.2	214.6	214.2	215.5	217.5	217.1	216.4
9.5	0.0758	243.9	244.2	244.7	237.2	229.3	223.7	216.9	212.7	212.6	216.8	220.9	222.1	222.7	224.4	226.8	227.8	227.9
9.0	0.1250	251.2	250.5	248.8	241.6	234.5	232.4	228.3	224.7	225.2	227.9	230.3	231.1	231.7	234.0	236.1	237.0	237.3
8.5	0.2061	257.0	255.8	251.9	246.2	240.1	240.0	239.6	239.3	239.9	240.3	239.8	240.1	240.4	243.8	246.1	248.4	250.1
8.0	0.3398	260.1	258.8	254.2	249.8	247.2	248.4	250.6	252.3	253.0	251.0	248.9	249.6	251.2	254.6	257.3	260.4	263.0
7.5	0.5603	259.4	258.8	254.3	252.1	253.8	257.3	260.2	262.1	262.6	260.6	259.7	260.8	263.5	265.9	268.1	270.9	273.9
7.0	0.9237	250.4	250.8	248.4	249.8	257.0	262.4	265.6	267.1	267.1	267.1	268.7	269.9	271.6	273.7	275.4	277.9	280.6
6.5	1.52	238.0	238.6	238.1	242.6	253.6	260.8	265.6	266.2	266.3	266.8	267.9	270.2	273.2	275.0	276.2	277.1	278.4
6.0	2.51	227.0	226.8	226.8	232.1	242.9	252.7	259.0	261.0	261.3	261.6	261.5	263.5	267.2	268.5	269.0	270.5	270.9
5.5	4.14	216.4	215.7	215.8	221.4	232.8	242.3	249.4	253.0	254.2	253.8	252.7	253.5	256.2	257.1	257.3	258.3	258.0
5.0	6.83	206.2	206.3	207.7	214.6	225.6	233.6	239.7	243.5	244.7	243.9	242.9	243.1	243.7	244.3	245.2	245.7	245.2
4.5	11.25	194.8	198.6	204.1	212.7	221.1	227.5	230.9	233.2	233.1	232.2	233.2	233.3	232.3	232.3	233.7	235.6	236.4
4.0	18.55	187.4	195.9	205.4	213.6	219.7	223.5	225.2	225.6	225.3	225.0	226.2	226.2	225.2	225.6	226.7	228.3	230.0
3.5	30.59	194.3	201.1	209.1	215.2	218.7	219.5	219.2	218.6	218.1	218.2	219.6	219.7	219.8	221.4	223.8	226.5	229.1
3.0	50.43	200.1	204.9	210.4	214.9	215.4	213.3	211.1	209.6	208.8	209.6	211.4	213.8	216.7	220.4	224.1	227.5	230.0
2.5	83.15	204.9	208.5	212.8	215.7	214.0	208.5	202.4	198.9	198.0	199.0	202.4	208.2	214.6	219.7	223.8	227.0	229.4
2.0	137.09	208.9	211.8	214.8	216.1	214.2	209.5	204.2	201.0	200.7	201.3	204.1	209.1	214.4	219.3	223.3	226.2	228.5
1.5	226.03	211.7	214.2	216.1	217.3	218.5	221.4	224.4	225.8	226.7	226.4	225.3	222.6	219.9	220.8	223.3	225.3	227.1
1.0	372.66	219.4	222.2	227.0	232.7	238.2	244.3	250.1	253.3	254.1	253.7	251.8	247.4	241.7	236.7	232.8	230.2	228.6
0.5	614.42	241.2	245.2	251.0	257.7	264.2	269.9	274.7	276.7	277.1	277.3	276.6	273.2	267.9	262.0	257.2	253.4	250.4
0.0	1013.0			276.9	280.9	287.6	293.5	298.0	300.8	301.4	301.3	299.2	294.6	288.0	281.7	277.5	269.3	263.6

MAY ZONAL MEAN GEOPOTENTIAL HEIGHT (m)

SCALE	PRESSURE	-80	-70	-60	-50	-40	-30	-20	-10	0	10	20	30	40	50	60	70	80
HEIGHT	(mb)																	
12.0	0.0062	79802	80323	80770	81064	81497	81790	81886	81949	82020	82116	82262	82359	82317	82438	82658	82857	83012
11.5	0.0103	76372	76965	77496	77847	78366	78750	78878	78901	78962	79088	79278	79448	79543	79793	80098	80353	80546
11.0	0.0169	72948	73587	74164	74585	75206	75691	75872	75878	75929	76067	76286	76493	76678	77006	77365	77674	77904
10.5	0.0279	69519	70177	70757	71270	72002	72596	72853	72863	72930	73055	73261	73478	73703	74056	74430	74866	75051
10.0	0.0460	66056	66717	67286	67897	68746	69458	69809	69886	69932	70020	70180	70385	70625	70968	71324	71705	71991
9.5	0.0758	62524	63181	63739	64454	65423	66237	66691	66827	66867	66904	67001	67183	67424	67746	68068	68441	68731
9.0	0.1250	58901	59561	60125	60947	62028	62899	63435	63631	63660	63653	63701	63865	64099	64392	64682	65041	65327
8.5	0.2061	55173	55849	56457	57373	58553	59437	60006	60229	60247	60220	60256	60413	60640	60891	61149	61486	61757
8.0	0.3398	51385	52078	52750	53740	54987	55864	56419	56630	56642	56622	56680	56830	57048	57247	57467	57763	58001
7.5	0.5603	47576	48282	49021	50060	51313	52157	52672	52856	52866	52871	52955	53091	53273	53631	53615	53869	54064
7.0	0.9237	43830	44539	45331	46378	47570	48347	48820	48977	48985	49003	49081	49202	49352	49477	49632	49846	49997
6.5	1.52	40259	40959	41771	42770	43823	44509	44923	45066	45073	45087	45144	45238	45354	45452	45585	45775	45897
6.0	2.51	36852	37548	38362	39289	40181	40742	41073	41202	41203	41212	41262	41322	41387	41462	41583	41758	41868
5.5	4.14	33609	34313	35127	35974	36705	37121	37353	37438	37430	37439	37498	37539	37555	37615	37731	37887	37996
5.0	6.83	30512	31222	32028	32785	33449	33636	33768	33798	33774	33789	33866	33900	33890	33939	34048	34195	34310
4.5	11.25	27573	28260	29018	29662	30082	30263	30327	30311	30283	30308	30384	30417	30413	30457	30548	30676	30790
4.0	18.55	24792	25382	26024	26542	26856	26962	26988	26953	26931	26962	27019	27051	27064	27106	27180	27280	27374
3.5	30.59	22000	22472	22988	23401	23645	23718	23734	23702	23689	23717	23755	23789	23809	23837	23887	23956	24018
3.0	50.43	19111	19502	19914	20250	20463	20545	20578	20562	20560	20582	20596	20613	20614	20605	20610	20635	20658
2.5	83.15	16144	16475	16816	17098	17321	17459	17552	17572	17578	17592	17568	17525	17458	17383	17330	17306	17293
2.0	137.09	13114	13397	13683	13934	14188	14411	14600	14677	14690	14694	14618	14485	14320	14168	14056	13988	13941

MAY MEAN ZONAL MEAN GEOSTROPHIC WIND ($m s^{-1}$)

SCALE	PRESSURE	-80	-70	-60	-50	-40	-30	-20	-10	0	10	20	30	40	50	60	70	80
HEIGHT	(mb)																	
12.0	0.0062		32.2	23.8	27.5	41.0	20.8	13.1										
11.5	0.0103		37.4	28.5	33.1	49.9	28.0	11.4										
11.0	0.0169		40.5	32.2	39.9	59.9	38.9	13.6										
10.5	0.0279		41.3	35.2	48.0	70.4	50.7	22.1										
10.0	0.0460		41.1	37.7	57.0	81.5	64.1	34.3										
9.5	0.0758		40.5	40.4	66.5	91.8	77.2	48.6										
9.0	0.1250		40.8	43.9	75.9	99.1	86.2	61.5										
8.5	0.2061		42.6	48.4	84.3	103.9	89.3	66.9										
8.0	0.3398		45.2	53.4	90.4	106.2	88.1	64.3										
7.5	0.5603		47.7	58.2	92.9	104.1	83.4	58.7										
7.0	0.9237		49.5	61.3	90.7	97.1	76.7	52.8										
6.5	1.52		50.1	61.4	83.0	85.1	67.2	46.9										
6.0	2.51		50.8	59.8	73.3	70.4	54.5	38.7										
5.5	4.14		51.9	57.6	63.2	54.6	39.4	26.7										
5.0	6.83		52.6	54.7	52.5	39.8	25.3	13.3										
4.5	11.25		50.3	49.2	42.1	27.6	14.7	3.5										
4.0	18.55		41.7	41.2	32.8	18.9	7.9	-1.4										
3.5	30.59		31.9	33.4	25.9	14.2	5.3	-2.1										
3.0	50.43		25.3	27.0	21.7	13.5	6.9	1.1										
2.5	83.15		21.0	22.0	19.9	17.3	14.3	10.5										
2.0	137.09		17.4	18.5	19.8	23.1	26.1	25.4										

TABLE 1 (continued)

PRESSURE COORDINATES

JUNE		ZONAL MEAN TEMPERATURE (K)																	LATITUDE							
SCALE	PRESSURE	-80	-70	-60	-50	-40	-30	-20	-10	0	10	20	30	40	50	60	70	80								
HEIGHT	(mb)																									
12.0	0.0062	227.3	222.5	217.8	214.6	209.6	204.2	201.6	202.7	203.9	202.4	199.7	193.4	178.5	166.4	155.7	150.9	147.9								
11.5	0.0103	228.6	224.8	221.4	218.5	212.4	205.3	201.9	203.1	204.7	202.7	201.0	196.7	184.6	175.8	166.7	162.3	159.5								
11.0	0.0169	230.6	228.4	227.3	223.3	216.4	207.3	202.9	202.3	203.4	202.5	202.8	200.1	191.9	186.5	180.2	176.4	174.0								
10.5	0.0279	235.3	233.9	234.0	229.3	220.8	210.5	204.5	202.1	202.3	203.6	205.4	204.1	199.8	197.5	194.6	191.9	189.9								
10.0	0.0461	241.1	240.4	241.0	235.7	225.7	215.3	207.2	204.7	204.6	206.6	208.8	209.1	208.1	208.2	208.6	207.4	206.4								
9.5	0.0758	248.4	247.9	248.0	241.7	232.4	223.6	215.7	212.6	212.8	214.6	215.9	216.4	217.9	219.4	221.9	222.3	222.2								
9.0	0.1250	257.7	256.3	253.9	247.0	238.5	233.2	228.0	225.2	226.0	226.9	226.8	226.4	229.1	231.5	235.0	235.9	236.3								
8.5	0.2061	265.4	263.1	257.9	251.4	243.3	241.4	239.5	239.7	240.3	240.7	239.3	238.6	240.5	244.0	247.7	249.7	251.0								
8.0	0.3398	267.9	266.0	259.8	253.8	248.7	248.9	249.9	252.0	252.4	251.5	250.0	250.2	251.8	256.2	259.7	263.3	265.8								
7.5	0.5603	262.3	262.2	258.4	254.4	253.7	256.9	259.6	261.2	261.3	260.4	259.8	260.7	262.4	267.0	270.1	274.1	277.4								
7.0	0.9237	250.3	252.0	250.6	249.8	255.3	261.5	265.2	265.1	264.5	265.2	266.9	268.1	269.8	273.6	277.0	281.3	285.0								
6.5	1.52	238.2	240.6	239.4	239.9	249.9	258.8	264.0	262.9	262.6	263.4	265.7	268.6	272.2	275.1	278.9	282.6	285.7								
6.0	2.51	227.1	229.7	227.6	227.2	237.1	249.8	256.8	257.3	257.5	257.5	258.9	262.0	266.0	270.0	274.0	277.6	279.8								
5.5	4.14	213.7	216.5	214.4	214.7	225.6	238.5	247.3	250.2	251.0	250.0	250.0	252.5	255.5	259.7	263.4	267.0	268.6								
5.0	6.83	198.0	202.4	204.0	207.6	219.1	230.2	237.9	241.7	242.5	241.3	241.0	242.9	245.1	248.1	251.5	254.7	255.8								
4.5	11.25	182.7	189.9	198.5	206.8	217.2	226.1	229.7	232.1	231.8	231.8	232.8	233.7	235.6	237.5	240.5	243.0	244.4								
4.0	18.55	181.4	189.0	199.2	209.5	217.7	223.0	224.6	224.7	224.3	225.0	226.2	227.1	228.1	229.3	231.7	233.9	236.0								
3.5	30.59	189.4	196.5	204.8	212.9	218.0	219.3	219.3	218.3	217.7	218.6	219.7	220.5	221.9	224.1	227.1	229.9	232.6								
3.0	50.43	192.8	199.8	206.8	213.2	215.4	213.9	212.0	211.1	210.1	210.8	212.3	214.4	217.7	222.0	226.1	229.8	232.4								
2.5	83.15	196.7	202.7	209.5	214.9	215.0	209.6	203.5	200.6	200.0	200.5	202.8	207.3	214.0	220.6	225.2	228.8	231.4								
2.0	137.09	201.5	206.1	211.5	215.7	215.7	210.6	204.9	201.8	201.8	202.2	204.3	208.4	214.2	220.0	224.3	227.8	230.7								
1.5	226.03	207.3	210.1	213.2	216.2	218.7	221.7	224.4	225.2	225.9	226.1	226.4	225.2	222.9	222.7	224.6	227.3	229.8								
1.0	372.66	218.5	221.2	225.7	231.0	236.1	243.1	249.8	252.8	253.4	253.5	253.2	250.8	245.4	240.6	237.3	234.9	233.1								
0.5	614.42	241.1	244.1	250.0	256.4	262.0	268.2	274.0	276.3	276.7	277.1	277.5	275.7	271.4	266.2	262.4	259.5	256.7								
0.0	1013.0				274.9	280.2	286.3	292.0	296.9	300.1	301.0	301.2	300.0	296.7	290.2	283.2	281.5	276.4	271.3							

JUNE		ZONAL MEAN GEOPOTENTIAL HEIGHT (m)																	
SCALE	PRESSURE	-80	-70	-60	-50	-40	-30	-20	-10	0	10	20	30	40	50	60	70	80	
HEIGHT	(mb)																		
12.0	0.0062	79139	79892	80474	80746	81144	81468	81557	81582	81624	81680	81842	81969	81970	82288	82650	83049	83341	
11.5	0.0103	75799	76616	77260	77574	78055	78469	78602	78608	78637	78711	78906	79112	79309	79781	80288	80756	81091	
11.0	0.0169	72439	73300	73977	74341	74917	75449	75640	75639	75656	75743	75951	76208	76586	77131	77753	78281	78656	
10.5	0.0279	69028	69915	70597	71026	71713	72389	72656	72680	72688	72770	72962	73247	73685	74317	75004	75580	75987	
10.0	0.0460	65542	66443	67121	67623	68447	69276	69645	69706	69710	69771	69932	70224	70701	71349	72055	72660	73089	
9.5	0.0758	61957	62866	63537	64125	65091	66063	66554	66554	66653	66690	66825	67108	67580	68217	68898	69508	69943	
9.0	0.1250	58254	59176	59862	60548	61643	62719	63309	63456	63445	63464	63590	63872	64310	64919	65596	66156	66589	
8.5	0.2061	54416	55367	56110	56895	58113	59240	59880	60046	60026	60034	60172	60464	60868	61434	62018	62597	63017	
8.0	0.3398	50504	51488	52317	53194	54512	55651	56298	56445	56419	56428	56589	56886	57266	57774	58305	58842	59255	
7.5	0.5603	46615	47614	48517	49468	50829	51944	52561	52680	52652	52673	52853	53141	53496	53936	54420	54901	55251	
7.0	0.9237	42854	43842	44780	45768	47098	48144	48714	48821	48797	48820	48992	49265	49598	49975	50412	50832	51130	
6.5	1.52	39283	40240	41195	42182	43391	44328	44833	44949	44930	44944	45085	45327	45621	45951	46335	46695	46944	
6.0	2.51	35871	36793	37769	38755	39816	40595	41013	41136	41116	41125	41237	41433	41670	41950	42278	42586	42795	
5.5	4.14	32645	33528	34538	35526	36437	37024	37325	37420	37395	37410	37513	37668	37854	38072	38344	38598	38780	
5.0	6.83	29624	30457	31476	32439	33184	33594	33769	33814	33781	33809	33915	34038	34186	34349	34569	34774	34936	
4.5	11.25	26848	27595	28535	29410	29993	30296	30350	30348	30314	30349	30449	30553	30671	30799	30971	31135	31280	
4.0	18.55	24199	24834	25631	26366	26811	26967	27024	27004	26974	27005	27087	27179	27275	27381	27513	27643	27761	
3.5	30.59	21481	22009	22671	23270	23618	23728	23773	23762	23736	23757	23822	23904	23984	24066	24160	24254	24355	
3.0	50.43	18682	19107	19655	20149	20444	20553	20612	20615	20598	20610	20656	20718	20786	20863	20945	20982	20933	
2.5	83.15	15830	16160	16608	17015	17291	17454	17569	17601	17593	17600	17617	17631	17606	17563	17540	17533	17536	
2.0	137.09	12916	13168	13523	13859	14137	14389	14604	14686	14682	14683	14665	14609	14479	14338	14249	14191	14154	

JUNE		MEAN ZONAL MEAN GEOSTROPHIC WIND (m s ⁻¹)																
SCALE	PRESSURE	-80	-70	-60	-50	-40	-30	-20	-10	0	10	20	30	40	50	60	70	80
HEIGHT	(mb)																	
12.0	0.0062		41.4	27.8	22.9	41.8	24.8	5.3				-25.0	-12.4	-19.8	-21.2	-28.5	-24.6	
11.5	0.0103		45.6	30.8	27.6	50.7	33.7	6.9				-33.5	-28.1	-35.4	-34.2	-36.4	-28.1	
11.0	0.0169		48.3	33.0	33.1	61.7	45.1	10.9				-38.1	-39.3	-46.5	-44.1	-42.9	-30.9	
10.5	0.0279		49.6	34.6	40.1	74.5	59.3	19.1				-38.7	-45.8	-52.5	-49.8	-47.2	-33.0	
10.0	0.0460		50.2	36.1	48.5	88.8	75.6	31.0				-36.5	-48.1	-54.8	-51.7	-49.0	-34.3	
9.5	0.0758		50.6	37.9	57.9	102.6	92.5	44.9				-34.2	-47.1	-54.1	-50.5	-48.1	-34.2	
9.0	0.1250		51.8	41.0	67.4	113.7	105.7	57.1				-34.3	-44.9	-51.6	-47.7	-45.7	-33.3	
8.5	0.2061		54.9	46.1	76.7	121.9	112.2	62.6				-37.4	-43.5	-48.3	-43.9	-42.7	-31.7	
8.0	0.3398		59.0	52.3	84.8	127.1	113.3	60.7				-40.7	-42.5	-44.4	-39.7	-39.0	-29.2	
7.5	0.5603		61.9	58.0	89.8	127.5	109.4	55.6				-41.7	-40.4	-39.2	-35.6	-35.4	-25.7	
7.0	0.9237		62.7	61.4	90.2	121.8	101.6	51.0				-39.8	-38.2	-34.1	-31.9	-32.0	-21.5	
6.5	1.52		62.3	63.2	85.6	109.4	90.1	47.2				-34.4	-33.7	-29.5	-28.3	-28.2	-17.8	
6.0	2.51		62.0	65.6	80.0	92.8	74.2	41.7				-27.9	-27.0	-24.4	-24.2	-24.2	-15.0	
5.5	4.14		61.8	68.9	74.4	74.0	54.6	30.7				-23.1	-21.1	-19.0	-19.3	-19.9	-13.0	
5.0	6.83		60.3	70.2	67.1	55.7	35.3	16.4				-20.1	-16.6	-14.6	-15.0	-15.8	-11.4	
4.5	11.25		54.4	65.5	57.4	39.6	21.3	6.1				-17.9	-13.5	-11.4	-11.7	-12.3	-10.0	
4.0	18.55		45.9	55.7	46.5	27.3	12.8	2.1				-15.4	-11.4	-9.3	-9.4	-9.4	-8.1	
3.5	30.59		38.5	45.9	37.4	20.5	9.3	2.3				-13.0	-9.9	-7.5	-7.0	-6.7	-5.7	
3.0	50.43		31.8	37.7	30.9	18.3	10.5	5.1				-9.6	-6.9	-3.8	-3.2	-3.2	-2.8	
2.5	83.15		25.2	30.8	26.5	20.6	18.1	12.7				-3.0	0.3	4.0	2.7	0.9	0.4	
2.0	137.09		19.5	24.4	23.3	25.3	31.0	26.6				6.6	10.6	14.4	9.1	4.8	3.4	

TABLE 1 (continued)

PRESSURE COORDINATES

JULY		ZONAL MEAN TEMPERATURE (K)															
SCALE HEIGHT	PRESSURE (mb)	LATITUDE															
		-80	-70	-60	-50	-40	-30	-20	-10	0	10	20	30	40	50	60	80
12.0	0.0062	219.9	217.3	215.5	213.0	207.9	202.9	199.2	199.9	200.6	201.8	200.5	194.7	182.6	167.7	155.6	150.2
11.5	0.0103	222.2	219.9	218.8	216.4	210.5	205.4	202.1	201.7	201.9	202.7	202.7	198.7	188.9	175.9	165.3	160.6
11.0	0.0169	226.3	224.0	223.0	220.1	214.1	208.0	204.5	203.3	203.0	203.6	204.7	202.4	195.8	185.9	177.7	174.0
10.5	0.0279	231.9	229.6	228.7	224.6	217.2	210.8	206.6	205.3	204.9	205.8	206.7	205.7	202.2	196.6	191.5	189.2
10.0	0.0460	239.8	237.0	235.2	229.6	220.5	214.2	209.8	208.8	208.9	209.9	209.7	209.0	202.2	207.4	205.9	204.9
9.5	0.0758	250.4	246.3	242.2	235.1	226.3	220.1	217.2	216.5	217.4	217.6	216.6	215.4	215.8	218.2	220.0	220.7
9.0	0.1250	261.8	256.7	249.8	240.9	232.5	227.9	227.4	227.8	229.5	228.9	227.5	225.4	225.8	229.4	233.3	236.0
8.5	0.2061	270.8	265.5	256.8	247.1	238.4	236.9	237.9	240.5	242.2	242.6	239.9	237.8	238.3	242.0	246.4	250.2
8.0	0.3398	273.1	269.7	262.1	253.3	246.3	247.0	249.3	252.5	254.0	253.1	250.2	248.9	249.8	253.8	258.7	263.1
7.5	0.5603	266.0	266.6	263.7	257.8	255.6	257.6	260.4	262.1	262.4	261.0	258.9	258.6	259.9	263.7	268.7	273.1
7.0	0.9237	256.0	258.9	258.8	256.9	259.9	263.2	265.7	265.4	264.1	264.4	264.7	265.2	267.4	270.8	274.8	279.7
6.5	1.52	246.6	249.9	250.3	249.7	254.9	260.4	263.1	262.3	261.1	261.1	263.5	265.0	268.4	271.8	276.5	280.5
6.0	2.51	236.9	239.9	239.8	238.0	243.0	251.0	254.9	255.3	255.3	254.3	255.2	258.3	262.4	266.7	271.6	275.4
5.5	4.14	222.3	225.2	225.3	225.0	231.4	239.7	245.2	247.0	248.1	246.4	246.5	249.0	252.8	257.5	262.1	265.6
5.0	6.83	204.4	208.5	211.5	215.0	223.7	231.5	236.5	238.5	239.3	238.2	238.7	240.2	243.1	247.5	251.3	254.3
4.5	11.25	185.1	192.3	200.7	210.0	220.4	227.3	229.5	230.3	229.4	230.0	230.4	232.0	234.6	238.4	241.0	243.5
4.0	18.55	178.0	186.7	197.1	210.2	219.7	223.8	224.4	223.8	223.1	223.8	224.6	226.4	228.0	230.2	232.5	234.9
3.5	30.59	185.0	192.5	201.3	212.3	218.6	219.5	219.3	218.0	217.3	217.9	219.0	220.5	222.4	224.9	227.8	230.5
3.0	50.43	197.9	195.0	203.1	211.3	215.3	214.5	212.7	211.4	210.3	211.1	212.6	214.6	217.8	222.3	226.6	230.0
2.5	83.15	191.5	197.2	205.3	212.8	214.7	210.0	204.2	201.9	201.3	201.8	203.7	206.9	212.8	220.2	225.5	229.1
2.0	137.09	196.3	200.3	207.3	214.2	215.8	211.0	205.3	203.0	203.0	203.4	205.1	208.2	213.5	219.9	224.4	227.9
1.5	226.03	203.4	205.8	210.0	215.1	219.3	222.4	224.5	224.9	225.3	225.7	226.6	227.1	225.9	224.5	220.3	227.4
1.0	372.66	218.5	220.4	224.3	229.3	235.1	242.8	249.7	252.5	252.9	253.1	253.5	252.9	249.0	244.0	240.4	237.6
0.5	614.42	240.5	243.0	249.0	255.3	261.5	267.8	273.7	276.1	276.3	276.6	277.3	277.1	274.1	269.3	265.8	260.4
0.0	1013.0			274.8	279.6	286.1	291.2	295.9	299.4	300.3	301.1	300.4	298.5	293.3	285.5	283.8	279.8

JULY ZONAL MEAN GEOPOTENTIAL HEIGHT (m)

JULY		ZONAL MEAN GEOPOTENTIAL HEIGHT (m)															
SCALE HEIGHT	PRESSURE (mb)	-80	-70	-60	-50	-40	-30	-20	-10	0	10	20	30	40	50	60	80
12.0	0.0062	79226	79809	80533	80877	81139	81403	81572	81647	81664	81687	81730	81778	81865	82084	82433	82915
11.5	0.0103	75990	76608	77352	77732	78075	78411	78632	78705	78712	78724	78776	78895	79143	79567	80084	80639
11.0	0.0169	72709	73360	74119	74537	74967	75385	75654	75740	75744	75750	75793	75958	76328	76922	77577	78195
10.5	0.0279	69354	70039	70811	71280	71807	72317	72643	72749	72754	72753	72781	72967	73411	74117	74870	75532
10.0	0.0460	65903	66626	67417	67957	68604	69207	69596	69720	69724	69713	69734	69932	70407	71161	71965	72651
9.5	0.0758	62313	63086	63920	64552	65332	66027	66471	66607	66603	66584	66615	66826	67302	68041	68841	69529
9.0	0.1250	58565	59406	60319	61069	61973	62750	63218	63360	63340	63321	63370	63605	64074	64768	65524	66188
8.5	0.2061	54657	55576	56606	57494	58525	59345	59809	59927	59885	59863	59943	60210	60672	61314	62007	62623
8.0	0.3398	50665	51651	52805	53830	54980	55806	56246	56319	56255	56231	56353	56645	57099	57685	58311	58867
7.5	0.5603	46714	47718	48948	50081	51299	52105	52506	52544	52469	52461	52619	52924	53362	53891	54443	54936
7.0	0.9237	42889	43864	45114	46304	47517	48286	48648	48675	48607	48608	48781	49085	49498	49975	50461	50886
6.5	1.52	39212	40142	41388	42592	43739	44445	44769	44806	44754	44756	44906	45195	45567	45995	46419	46779
6.0	2.51	35667	36550	37793	39013	40084	40692	40968	41010	40969	40978	41100	41356	41672	42044	42397	42893
5.5	4.14	32305	33146	34390	35627	36617	37103	37309	37333	37290	37314	37432	37644	37901	38206	38490	38739
5.0	6.83	29173	29964	31189	32407	33287	33656	33781	33776	33724	33763	33875	34060	34268	34506	34727	34927
4.5	11.25	26330	27040	28178	29303	30039	30301	30373	30347	30297	30338	30444	30607	30773	30951	31126	31288
4.0	18.55	23689	24278	25275	26230	26817	26995	27049	27022	26982	27016	27112	27249	27386	27520	27660	27785
3.5	30.59	21031	21503	22359	23134	23607	23750	23800	23789	23758	23783	23865	23979	24192	24429	24854	24459
3.0	50.43	18299	18665	19398	20030	20427	20569	20633	20641	20622	20639	20702	20792	20868	20920	20970	21016
2.5	83.15	15521	15793	16407	16927	17280	17461	17580	17615	17605	17616	17653	17706	17762	17860	17954	17655
2.0	137.09	12684	12886	13385	13797	14128	14391	14606	14680	14673	14678	14688	14690	14609	14463	14366	14308

JULY MEAN ZONAL MEAN GEOSTROPHIC WIND (m s⁻¹)

SCALE		MEAN ZONAL MEAN GEOSTROPHIC WIND (m s ⁻¹)																
HEIGHT	PRESSURE (mb)	-80	-70	-60	-50	-40	-30	-20	-10	0	10	20	30	40	50	60	70	80
12.0	0.0062		38.7	38.8	19.9	28.3	28.3	21.3				-7.7	-6.3	-13.6	-23.2	-30.3	-28.0	
11.5	0.0103		40.6	40.2	24.2	36.3	36.3	29.7				-13.5	-20.3	-31.9	-38.1	-38.3	-31.9	
11.0	0.0169		42.4	41.5	29.0	44.5	44.5	31.0				-15.3	-30.3	-41.7	-50.5	-45.0	-35.3	
10.5	0.0279		44.2	43.1	34.8	54.8	53.7	37.6				-14.8	-36.2	-56.1	-68.8	-51.9	-37.7	
10.0	0.0460		46.4	45.5	42.4	65.6	63.3	44.4				-14.7	-39.1	-59.9	-62.7	-49.9	-39.3	
9.5	0.0758		49.8	49.5	51.5	76.9	72.1	49.9				-16.9	-40.4	-59.1	-61.9	-51.6	-39.5	
9.0	0.1250		55.1	59.7	61.5	87.2	78.3	51.8				-21.2	-42.2	-56.4	-58.3	-49.0	-38.1	
8.5	0.2061		61.9	64.4	72.6	95.4	80.3	48.2				-27.8	-44.4	-53.2	-53.5	-45.1	-35.3	
8.0	0.3398		68.4	73.7	83.4	101.2	78.9	40.7				-34.8	-46.0	-50.0	-48.3	-40.8	-31.8	
7.5	0.5603		71.5	80.6	90.9	103.0	74.9	32.7				-40.0	-45.9	-46.7	-42.9	-36.2	-27.7	
7.0	0.9237		71.1	84.0	93.5	100.1	69.9	28.0				-42.0	-44.4	-43.0	-38.2	-31.8	-23.3	
6.5	1.52		69.3	85.3	92.1	92.7	63.1	25.9				-39.2	-40.8	-38.7	-33.8	-27.5	-19.1	
6.0	2.51		67.5	86.9	90.3	82.8	53.6	23.1				-33.9	-35.2	-33.2	-28.9	-23.1	-15.9	
5.5	4.14		65.7	89.0	88.1	71.3	41.3	16.5				-29.5	-28.8	-27.1	-23.4	-18.7	-13.3	
5.0	6.83		62.9	89.1	83.2	59.1	26.8	7.6				-26.3	-23.8	-21.6	-18.2	-14.7	-11.2	
4.5	11.25		56.9	83.7	73.6	46.2	19.3	1.9				-24.0	-19.9	-16.6	-14.0	-11.7	-9.6	
4.0	18.55		49.1	72.5	60.9	34.7	13.7	0.9				-20.9	-16.5	-12.9	-10.8	-9.3	-7.6	
3.5	30.59		43.1	60.1	49.3	27.9	11.6	2.3				-17.6	-13.7	-10.1	-8.1	-6.8	-5.3	
3.0	50.43		36.9	49.9	40.4	24.7	12.8	5.7				-13.9	-10.1	-5.9	-4.0	-3.4	-2.7	
2.5	83.15		29.5	41.3	33.7	25.1	19.4	13.4				-8.4	-4.3	2.0	2.4	0.9	0.2	
2.0	137.09		23.3	32.5	28.1	28.5	31.7	26.3				-1.0	3.5	12.8	9.8	5.1	3.1	

TABLE 1 (continued)

PRESSURE COORDINATES

AUGUST	ZONAL MEAN TEMPERATURE (K)																		
SCALE	PRESSURE	-80	-70	-60	-50	-40	-30	-20	-10	LATITUDE	0	10	20	30	40	50	60	70	80
HEIGHT	(mb)																		
12.0	0.0062	217.3	216.6	216.1	213.1	208.8	204.7	201.8	201.1	202.3	203.6	203.1	199.4	191.1	180.3	170.3	165.7	165.3	
11.5	0.0103	219.8	219.3	219.7	216.6	211.9	208.2	205.3	202.7	202.9	204.4	205.1	203.6	196.4	186.8	177.8	174.0	174.3	
11.0	0.0169	222.5	221.4	222.3	220.0	215.7	211.7	208.4	205.1	204.5	206.0	207.6	207.3	202.3	194.9	187.6	184.9	185.6	
10.5	0.0279	226.4	224.2	224.9	222.8	218.8	214.7	211.1	208.1	207.7	209.4	211.0	210.9	208.0	203.7	199.3	197.5	198.4	
10.0	0.0460	233.2	229.0	229.7	225.2	220.9	217.1	214.1	211.9	212.7	214.7	215.6	215.1	213.8	212.2	211.8	210.9	212.1	
9.5	0.0758	243.4	236.3	231.4	228.5	224.2	220.9	219.6	218.8	220.5	222.1	222.7	221.6	220.3	220.9	223.5	224.9	226.7	
9.0	0.1250	255.4	245.8	237.1	232.3	228.1	226.3	227.2	228.6	230.5	231.5	232.1	230.3	228.4	229.7	234.3	238.4	241.5	
8.5	0.2061	265.7	257.8	249.5	237.6	233.0	234.3	236.5	239.4	241.9	242.7	242.3	239.8	238.3	239.6	244.4	249.7	253.2	
8.0	0.3398	275.5	267.6	255.7	245.6	241.7	245.1	248.5	252.5	254.1	253.0	252.0	248.0	247.6	249.6	254.1	258.7	262.2	
7.5	0.5603	273.6	270.5	262.7	253.8	252.1	256.3	260.5	261.3	264.0	262.2	258.2	256.8	256.8	259.5	262.8	266.3	269.7	
7.0	0.9237	267.1	268.0	264.2	257.9	258.1	262.5	266.9	267.9	267.4	266.5	264.8	263.9	264.5	267.3	269.1	272.2	275.3	
6.5	1.52	259.0	262.2	260.4	255.4	256.3	261.0	265.5	266.0	265.3	264.0	263.9	263.3	265.3	267.7	270.3	272.8	274.7	
6.0	2.51	249.8	254.7	253.7	248.0	247.8	252.2	257.1	258.7	258.3	256.7	255.6	256.3	259.7	261.8	264.6	266.9	267.9	
5.5	4.14	234.9	241.3	241.8	237.8	238.3	242.2	246.9	248.6	248.8	247.3	246.4	247.0	250.1	252.8	255.4	257.5	258.1	
5.0	6.83	215.7	223.9	227.9	227.6	230.3	234.2	237.5	238.6	238.6	237.9	238.2	238.3	240.2	243.5	246.3	247.7	247.9	
4.5	11.25	192.7	203.7	212.6	216.2	222.1	228.7	229.4	229.7	228.9	229.4	229.4	229.8	230.9	232.5	235.6	237.2	238.3	238.8
4.0	18.55	179.9	191.5	204.5	216.2	222.8	224.9	224.3	223.3	222.4	222.7	223.4	225.2	226.3	228.3	229.8	230.9	232.0	
3.5	30.59	186.2	194.2	204.9	214.7	220.1	220.3	219.0	211.9	216.4	216.8	217.8	219.6	221.5	223.7	225.8	227.6	229.3	
3.0	50.43	188.3	194.7	204.3	213.4	217.3	215.7	213.1	211.9	211.2	211.3	212.4	214.5	217.5	221.6	225.1	227.8	229.8	
2.5	83.15	190.9	196.0	205.1	213.8	215.9	210.7	204.6	203.3	202.0	202.1	203.7	206.8	212.4	219.4	224.2	227.4	229.6	
2.0	137.09	195.0	198.9	206.4	214.3	216.2	211.4	205.4	203.0	203.0	203.3	205.0	207.9	213.0	219.4	223.7	226.7	229.2	
1.5	226.03	202.0	204.7	209.4	215.5	220.1	222.9	224.4	224.7	225.1	225.6	226.6	227.0	225.8	224.4	224.5	225.9	227.9	
1.0	372.66	217.2	220.8	224.8	229.8	235.4	242.8	249.6	252.3	252.8	253.2	253.5	252.8	249.1	243.6	239.4	234.6	234.0	
0.5	614.42	239.8	243.8	249.1	255.2	261.0	267.6	273.8	276.0	276.1	276.6	277.4	277.7	274.3	268.9	264.7	261.5	258.7	
0.0	1013.0			273.1	278.1	285.1	290.9	295.7	299.0	300.1	301.3	300.7	299.3	295.1	287.2	284.0	279.5	273.3	

[illegible]

AUGUST	MEAN ZONAL GEOSTROPHIC WIND (m s ⁻¹)																	
SCALE HEIGHT	PRESSURE (mb)	-80	-70	-60	-50	-40	-30	-20	-10	0	10	20	30	40	50	60	70	80
12.0	0.0062		39.6	23.6	8.3	26.0	38.4	21.1				-0.8	6.9	-1.8	-11.5	-15.7	-26.4	
11.5	0.0105		39.8	25.1	12.5	32.0	44.4	28.9				-1.3	-1.6	-14.9	-22.9	-22.4	-29.6	
11.0	0.0169		40.0	25.8	16.4	36.0	50.5	38.4				-3.8	-7.0	-25.8	-32.5	-28.0	-32.5	
10.5	0.0279		40.6	26.9	19.8	43.7	57.2	48.0				1.3	-10.1	-52.7	-39.0	-32.0	-34.2	
10.0	0.0460		42.6	26.3	23.4	49.3	63.7	56.6				3.3	-12.1	-36.2	-42.0	-34.1	-34.9	
9.5	0.0758		47.6	28.2	27.5	54.7	69.0	61.4				3.6	-14.3	-37.0	-41.3	-33.8	-33.8	
9.0	0.1250		55.8	32.6	32.3	59.4	71.7	60.8				3.3	-17.7	-37.1	-38.6	-31.1	-30.5	
8.5	0.2061		66.4	40.9	39.0	62.2	70.3	54.3				1.0	-22.2	-37.1	-35.1	-26.8	-25.2	
8.0	0.3398		77.3	52.0	47.2	63.0	65.6	44.7				-3.4	-26.2	-36.2	-31.5	-22.4	-20.0	
7.5	0.5603		84.9	62.9	54.9	61.4	58.3	34.8				-12.3	-28.6	-34.4	-27.8	-18.6	-15.8	
7.0	0.9237		88.3	71.0	60.3	58.0	49.8	26.8				-18.8	-29.7	-52.1	-24.6	-15.9	-12.6	
6.5	1.52		88.6	76.3	63.6	53.3	40.8	20.5				-21.6	-29.4	-29.2	-21.7	-13.5	-10.1	
6.0	2.51		87.3	80.9	67.0	48.8	31.4	13.4				-22.9	-27.0	-25.5	-18.7	-11.1	-8.1	
5.5	4.14		84.5	85.1	70.5	45.1	22.4	5.0				-24.1	-23.2	-21.1	-15.7	-8.8	-6.4	
5.0	6.83		79.6	86.6	71.3	40.9	14.6	-2.1				-24.4	-20.7	-16.8	-12.3	-6.8	-5.1	
4.5	11.25		71.2	82.6	67.0	35.1	9.4	-5.1				-23.3	-18.5	-12.8	-9.0	-5.5	-4.2	
4.0	18.55		58.8	72.2	57.9	28.9	7.4	-4.3				-20.7	-15.9	-10.1	-6.7	-4.4	-3.2	
3.5	30.59		47.7	60.1	48.3	24.2	7.6	-1.1				-17.4	-13.0	-7.8	-4.6	-2.9	-1.8	
3.0	50.43		39.4	49.4	39.8	22.1	10.2	3.5				-13.6	-9.3	-3.9	-1.2	-0.3	0.0	
2.5	83.15		31.7	39.1	32.3	23.2	18.0	11.8				-8.2	-3.8	3.7	4.7	3.3	2.3	
2.0	137.09		25.1	29.5	25.8	26.7	30.7	25.1				-1.4	3.8	14.2	12.2	7.1	4.6	

TABLE 1 (continued)

PRESSURE COORDINATES

SEPTEMBER ZONAL MEAN TEMPERATURE (K)

		LATITUDE																	
SCALE	PRESSURE	-80	-70	-60	-50	-40	-30	-20	-10	0	10	20	30	40	50	60	70	80	
HEIGHT	(mb)																		
12.0	0.0062	209.1	210.4	208.8	206.5	205.0	204.3	204.4	205.4	207.0	206.9	205.0	203.7	201.8	198.0	195.0	195.6	194.1	
11.5	0.0103	214.1	214.9	215.8	212.4	209.9	207.8	206.4	205.5	205.9	206.3	205.9	206.6	205.2	202.0	199.7	201.1	199.9	
11.0	0.0169	217.7	219.0	221.6	219.1	215.3	211.7	208.4	206.1	205.9	207.1	207.8	209.4	208.7	206.6	205.3	206.7	205.9	
10.5	0.0279	222.2	222.9	225.5	224.3	220.2	215.7	211.4	208.2	207.8	210.0	211.4	212.6	212.0	211.2	211.7	212.9	212.8	
10.0	0.0460	227.8	227.1	228.6	227.3	224.0	219.4	215.7	212.0	211.9	214.3	216.4	217.6	216.0	216.0	218.5	220.0	220.9	
9.5	0.0758	234.8	232.0	231.6	230.6	227.7	224.1	221.4	219.1	218.9	221.2	223.5	224.0	221.9	221.6	225.3	226.2	230.9	
9.0	0.1250	244.9	239.2	235.8	234.1	231.6	229.6	228.1	228.1	228.2	230.3	232.1	231.9	229.2	229.0	232.5	236.5	240.5	
8.5	0.2061	258.7	249.9	242.0	238.2	236.6	236.4	236.3	238.3	239.6	239.9	241.1	239.1	237.3	237.8	240.7	243.9	247.7	
8.0	0.3398	272.6	261.7	250.4	245.4	244.8	246.7	248.2	250.9	252.2	251.1	249.4	247.7	246.7	246.9	248.2	251.1	254.5	
7.5	0.5603	277.8	268.3	256.1	253.5	254.5	257.8	260.3	262.5	263.3	262.2	259.1	258.8	257.7	257.3	257.6	259.0	260.2	
7.0	0.9237	277.9	271.1	263.4	258.6	260.4	264.3	267.5	268.7	269.2	268.1	267.0	266.3	265.4	264.6	263.5	262.4	261.3	
6.5	1.52	275.3	270.2	262.8	257.5	258.8	263.4	267.5	268.6	268.9	267.5	266.0	264.0	263.6	263.0	260.9	257.6	255.3	
6.0	2.51	271.5	267.2	258.3	250.6	250.6	255.2	260.5	262.2	262.3	260.8	258.7	256.3	256.7	255.7	252.5	248.4	246.1	
5.5	4.14	259.5	257.4	249.1	241.4	241.2	245.2	250.5	252.3	251.9	250.6	248.8	247.2	246.9	246.3	243.8	239.6	237.4	
5.0	6.83	240.6	242.2	237.7	232.3	232.5	236.5	240.3	241.6	240.9	240.1	239.2	238.1	237.3	237.3	236.3	232.7	230.6	
4.5	11.25	215.9	222.7	225.5	225.1	226.1	229.2	230.9	231.1	230.8	230.9	230.9	230.0	229.7	229.1	227.4	226.0		
4.0	18.55	198.5	207.1	215.7	222.1	224.2	224.7	224.1	223.9	223.4	223.0	223.5	223.7	224.0	224.1	223.6	222.9	222.1	
3.5	30.59	197.7	202.3	210.5	219.7	222.1	220.4	218.4	217.0	216.2	216.1	217.2	218.7	220.0	220.9	221.7	221.8	221.6	
3.0	50.43	194.4	199.7	208.1	216.9	218.7	215.7	212.6	211.1	210.4	210.7	212.1	214.5	217.0	219.9	222.0	222.8	223.1	
2.5	83.15	193.6	198.6	207.2	215.9	216.9	210.7	204.4	201.5	201.0	201.3	203.0	206.7	212.5	218.6	222.3	223.8	224.5	
2.0	137.09	196.1	199.9	207.4	215.6	217.0	211.4	205.4	202.6	202.5	202.8	204.2	207.2	212.2	218.4	222.1	224.0	225.3	
1.5	226.03	202.8	205.1	210.3	216.8	220.8	223.0	224.4	225.1	225.6	225.8	226.2	225.6	225.2	222.2	222.6	223.4	224.4	
1.0	372.66	218.4	220.7	225.0	230.5	236.4	243.5	249.9	252.5	253.2	253.4	253.2	251.3	246.0	240.3	235.8	232.5	230.2	
0.5	614.42	240.2	243.6	249.3	255.6	262.1	268.7	274.2	276.1	276.4	277.0	277.2	276.0	271.6	265.4	260.5	256.8	254.0	
0.0	1013.0			274.5	279.0	285.4	290.9	295.8	299.1	300.2	301.2	300.8	299.0	293.8	286.3	281.7	275.8	268.8	

SEPTEMBER ZONAL MEAN GEOPOTENTIAL HEIGHT (m)

		LATITUDE																	
		PRESSURE (mb)																	
SCALE	PRESSURE	-80	-70	-60	-50	-40	-30	-20	-10	0	10	20	30	40	50	60	70	80	
HEIGHT	(mb)																		
12.0	0.0062	81399	81489	81659	81756	81940	82123	82236	82219	82216	82258	82285	82247	82081	81897	81837	81795	81747	
11.5	0.0103	78295	78379	78547	78688	78900	79103	79228	79211	79194	79232	79275	79242	79100	78967	78947	78889	78860	
11.0	0.0169	75135	75202	75344	75531	75788	76032	76191	76198	76179	76208	76249	76197	76070	75977	75984	75905	75890	
10.5	0.0279	71914	71965	72067	72279	72596	72901	73116	73164	73145	73155	73180	73107	72988	72916	72929	72832	72822	
10.0	0.0460	68621	68671	68741	68972	69343	69716	69992	70091	70067	70052	70051	69963	69856	69789	69781	69665	69650	
9.5	0.0758	65233	65310	65370	65619	66035	66469	66790	66935	66905	66864	66830	66734	66650	66585	66529	66382	66340	
9.0	0.1250	61728	61863	61951	62216	62673	63148	63501	63664	63628	63561	63498	63397	63349	63290	63181	62982	62888	
8.5	0.2061	58038	58281	58453	58758	59246	59737	60101	60248	60198	60117	60029	59946	59931	59870	59714	59462	59310	
8.0	0.3398	54150	54537	54850	55222	55727	56205	56560	56672	56605	56526	56439	56366	56300	56234	56135	55839	55634	
7.5	0.5603	50113	50651	51124	51565	52066	52503	52829	52905	52827	52759	52714	52675	52630	52429	52101	51862		
7.0	0.9237	46038	46697	47300	47811	48291	48676	48961	49011	48926	48871	48857	48823	48858	48803	48607	48276	48036	
6.5	1.52	41987	42731	43442	44024	44481	44804	45036	45070	44982	44942	44946	44933	44977	44932	44760	44463	44250	
6.0	2.51	37980	38791	39620	40295	40745	40998	41161	41176	41089	41066	41097	41116	41161	41126	40993	40752	40574	
5.5	4.14	34089	34947	35904	36694	37147	37338	37422	37411	37328	37323	37382	37432	37475	37452	37363	37183	37037	
5.0	6.83	30414	31278	32334	33223	33676	33810	33826	33791	33718	33727	33807	33876	33928	33909	33845	33724	33611	
4.5	11.25	27077	27878	28946	29879	30326	30405	30380	30356	30268	30282	30367	30452	30510	30493	30439	30357	30270	
4.0	18.55	24053	24736	25716	26607	27030	27082	27049	27005	26944	26958	27039	27129	27186	27172	27126	27060	26990	
3.5	30.59	21162	21748	22601	23373	23763	23825	23812	23780	23733	23747	23815	23893	23938	23917	23869	23808	23745	
3.0	50.43	18289	18806	19537	20175	20532	20629	20654	20643	20609	20621	20671	20721	20758	20691	20623	20555	20492	
2.5	83.15	15452	15891	16498	17009	17345	17507	17600	17620	17593	17603	17630	17636	17593	17481	17370	17285	17213	
2.0	137.09	12602	12977	13463	13848	14170	14429	14624	14691	14668	14675	14678	14630	14492	14284	14115	14004	13918	

SEPTEMBER MEAN ZONAL MEAN GEOSTROPHIC WIND ($m s^{-1}$)

SEPTEMBER MEAN ZONAL MEAN GEOSTROPHIC WIND (K S)																		
SCALE HEIGHT	PRESSURE (mb)	-80	-70	-60	-50	-40	-30	-20	-10	0	10	20	30	40	50	60	70	80
12.0	0.0062		4.3	8.3	10.8	22.3	20.9	4.0				-1.7	14.1	19.8	6.5	2.4	3.9	
11.5	0.0103		3.5	10.0	13.8	24.6	23.3	4.7				-3.0	12.4	16.0	3.2	1.6	4.1	
11.0	0.0169		1.7	10.8	17.5	28.5	28.5	9.7				-0.2	12.7	13.1	0.9	1.4	4.8	
10.5	0.0279		-0.5	10.0	21.0	34.4	36.2	18.3				3.9	13.6	11.2	0.1	1.8	5.6	
10.0	0.0460		-1.9	9.2	23.9	40.3	44.4	28.1				8.0	13.8	9.6	1.1	3.3	6.7	
9.5	0.0758		-1.5	9.1	26.4	45.5	51.0	36.4				12.0	13.0	7.3	3.3	6.0	9.0	
9.0	0.1250		1.4	10.0	28.7	49.5	55.5	40.8				15.6	11.2	3.9	5.5	9.8	12.8	
8.5	0.2061		8.1	13.9	31.4	51.6	56.9	40.3				16.3	7.9	1.5	7.7	13.3	16.8	
8.0	0.3398		18.1	20.9	34.5	51.2	55.4	36.7				13.4	4.6	0.5	9.2	15.9	20.4	
7.5	0.5603		29.1	28.9	36.9	48.3	50.9	31.2				7.7	2.5	-0.3	9.6	17.6	22.9	
7.0	0.9237		38.5	36.0	38.6	43.8	44.8	25.7				4.3	1.0	-1.3	8.9	17.5	23.2	
6.5	1.52		45.7	42.9	40.4	38.6	37.0	20.5				0.8	-1.1	-1.9	7.7	15.5	21.1	
6.0	2.51		52.6	51.3	43.7	33.7	27.7	13.5				-4.8	-3.4	-2.0	6.0	12.3	17.5	
5.5	4.14		58.9	61.3	48.3	29.7	17.9	4.9				-9.9	-5.4	-1.9	4.1	8.8	13.5	
5.0	6.83		62.5	69.8	52.3	26.0	9.3	-2.7				-13.2	-7.3	-2.1	3.3	6.1	9.1	
4.5	11.25		60.5	73.1	54.0	22.5	3.2	-6.8				-15.1	-8.7	-2.2	3.0	4.6	6.1	
4.0	18.55		53.1	69.1	51.7	20.1	1.0	-7.5				-15.4	-9.1	-2.0	2.5	3.9	4.5	
3.5	30.59		46.6	59.8	45.9	19.5	2.8	-4.9				-13.3	-7.6	-1.1	2.7	4.0	4.0	
3.0	50.43		41.4	49.5	39.1	20.5	7.4	0.5				-9.1	-4.1	1.5	4.6	5.0	4.1	
2.5	83.15		34.5	39.5	32.6	23.8	16.5	9.5				-2.7	2.1	7.9	9.0	7.1	4.7	
2.0	137.09		28.2	29.7	26.6	28.7	30.1	23.3				4.3	11.0	17.9	15.2	9.8	5.8	

TABLE 1 (continued)

PRESSURE COORDINATES

OCTOBER ZONAL MEAN TEMPERATURE (K)

		LATITUDE																
SCALE HEIGHT	PRESSURE (mb)	-80	-70	-60	-50	-40	-30	-20	-10	0	10	20	30	40	50	60	70	80
12.0	0.0062	189.1	190.1	191.1	192.6	197.2	202.2	205.8	208.9	214.2	212.5	208.3	206.8	208.8	211.2	213.2	219.2	222.2
11.5	0.0103	198.4	199.9	201.6	201.3	203.6	205.3	206.3	208.4	212.1	211.3	208.4	208.7	210.9	213.9	216.1	221.7	224.9
11.0	0.0169	208.2	209.8	211.9	210.7	210.3	209.0	207.0	207.2	209.2	209.8	209.1	210.9	213.1	216.1	219.8	223.4	225.9
10.5	0.0279	217.6	219.1	220.8	219.5	216.9	213.8	209.8	207.5	208.0	209.7	211.3	213.4	215.5	218.5	223.1	225.9	228.5
10.0	0.0460	226.2	227.0	227.6	226.1	223.0	219.4	215.6	210.9	209.5	211.5	214.5	217.0	218.7	221.4	226.6	230.2	233.9
9.5	0.0758	232.2	232.6	232.9	232.0	229.2	226.1	222.7	218.1	215.7	217.5	221.2	224.0	223.9	225.4	231.0	236.0	241.3
9.0	0.1250	238.4	238.1	238.2	237.4	235.5	233.0	230.1	227.6	225.9	227.0	230.1	231.9	230.9	231.5	236.3	242.0	248.0
8.5	0.2061	249.8	247.1	244.5	242.8	241.0	239.6	237.8	238.4	238.4	238.3	239.1	238.8	239.0	239.8	242.4	246.6	251.9
8.0	0.3398	263.5	258.1	252.7	250.7	249.1	248.6	248.0	250.2	251.5	250.7	249.8	248.6	248.5	248.1	247.9	250.6	254.3
7.5	0.5603	273.3	267.2	261.8	259.7	260.1	260.2	260.1	261.5	262.8	262.2	260.8	260.4	258.9	256.3	255.0	255.4	256.3
7.0	0.9237	281.6	275.1	269.2	266.2	267.4	268.5	268.9	268.7	269.1	268.6	267.2	266.9	264.6	259.9	256.4	253.1	250.6
6.5	1.52	284.2	277.2	269.7	266.1	266.3	267.9	268.8	268.8	269.2	268.5	266.7	264.1	260.8	255.8	249.5	242.8	237.9
6.0	2.51	283.8	275.2	263.9	258.1	258.2	259.7	262.0	263.4	263.8	262.7	260.0	255.6	251.7	246.9	239.3	230.5	224.2
5.5	4.14	272.8	265.4	253.7	247.1	247.2	249.2	252.4	254.7	254.9	253.3	250.1	245.8	241.8	237.0	230.3	221.3	214.3
5.0	6.83	259.0	251.0	242.6	236.2	235.6	239.0	242.4	244.0	244.3	243.0	240.3	236.7	232.8	228.2	223.4	216.7	210.6
4.5	11.25	233.6	234.4	231.8	227.2	226.7	230.0	232.6	232.2	232.8	232.9	231.8	228.9	225.7	222.4	216.4	215.3	211.1
4.0	18.55	217.0	221.8	226.9	225.1	224.0	224.5	224.7	224.3	224.0	224.1	224.4	223.3	221.4	219.2	216.3	213.6	210.2
3.5	30.59	212.7	217.1	224.1	223.9	222.2	220.1	218.2	217.1	216.4	216.7	217.7	218.6	218.5	217.8	216.9	214.6	212.1
3.0	50.43	207.2	210.8	226.3	219.9	218.9	215.1	211.9	210.5	210.0	210.2	211.4	213.2	215.2	217.3	218.3	217.0	215.1
2.5	83.15	203.7	208.0	214.0	218.7	216.9	210.2	203.5	200.2	199.6	199.9	202.0	206.4	212.1	216.9	219.5	219.4	218.5
2.0	137.09	207.7	207.1	213.3	218.2	217.0	211.0	204.9	201.6	201.2	201.4	203.2	207.4	212.6	217.1	220.0	220.7	220.9
1.5	226.03	205.7	208.5	213.3	218.6	221.2	222.9	224.6	225.4	225.9	225.7	225.4	223.6	220.8	220.2	220.7	220.9	220.9
1.0	372.66	220.2	224.0	226.3	232.1	238.0	244.3	250.1	252.7	253.4	253.3	252.1	248.2	242.0	236.6	232.0	226.0	224.9
0.5	614.42	242.6	244.5	250.1	256.6	263.5	269.8	274.3	276.2	276.5	276.9	276.5	273.4	267.7	261.3	255.8	251.0	246.6
0.0	1013.0			276.0	280.5	286.4	292.1	296.5	299.4	300.5	301.3	300.5	297.3	291.1	283.7	277.5	268.5	261.6

OCTOBER ZONAL MEAN GEOPOTENTIAL HEIGHT (m)

SCALE HEIGHT	PRESSURE (mb)	-80	-70	-60	-50	-40	-30	-20	-10	0	10	20	30	40	50	60	70	80
12.0	0.0062	82605	82653	82623	82439	82482	82494	82385	82301	82367	82384	82321	82192	81933	81574	81317	81078	80891
11.5	0.0103	79766	79795	79745	79554	79546	79509	79367	79244	79256	79278	79267	79150	78860	78461	78174	77847	77614
11.0	0.0169	76791	76798	76718	76541	76518	76477	76342	76200	76175	76195	76212	76079	75796	75313	74984	74588	74314
10.5	0.0279	73670	73653	73544	73385	73387	73380	73293	73167	73119	73125	73134	72972	72617	72131	71739	71298	70988
10.0	0.0460	70420	70387	70260	70121	70168	70211	70181	70107	70058	70045	70020	69823	69441	68911	68448	67962	67608
9.5	0.0758	67059	67018	66886	66764	66855	66947	66970	66967	66936	66907	66832	66596	66200	65641	65097	64548	64127
9.0	0.1250	63618	63575	63438	63327	63453	63586	63657	63707	63698	63657	63531	63298	62872	62300	61679	61049	60544
8.5	0.2061	60044	60022	59903	59810	59963	60124	60230	60293	60292	60248	60093	59809	59431	58847	58172	57468	56879
8.0	0.3398	56290	56326	56266	56201	56380	56555	56679	56719	56711	56672	56517	56246	55865	55276	54582	53829	53172
7.5	0.5603	52358	52478	52497	52460	52647	52826	52954	52966	52943	52908	52772	52513	52145	51578	50897	50121	49430
7.0	0.9237	48291	48504	48605	48606	48780	48951	49076	49080	49046	49017	48901	48645	48304	47791	47142	46384	45705
6.5	1.52	44143	44454	44651	44698	44864	45014	45131	45137	45099	45077	44984	44750	44449	44009	43435	42751	42129
6.0	2.51	39980	40404	40736	40849	41015	41142	41237	41233	41190	41179	41119	40938	40689	40321	39850	39280	38742
5.5	4.14	35899	36442	36947	37152	37316	37419	37472	37441	37396	37401	37385	37271	37079	36782	36416	35979	35539
5.0	6.83	32024	32652	33309	33610	33776	33842	33845	33783	33738	33763	33792	33736	33602	33375	33093	32775	32434
4.5	11.25	28452	29102	29842	30250	30398	30413	30371	30302	30251	30281	30338	30330	30249	30080	29861	29611	29346
4.0	18.55	25157	25766	26488	26917	27101	27086	27023	26959	26907	26954	26995	27018	26977	26848	26680	26472	26263
3.5	30.59	22020	22598	23184	23628	23834	23831	23783	23729	23688	23710	23761	23784	23757	23649	23510	23339	23173
3.0	50.43	18943	19421	19994	20375	20601	20642	20632	20597	20565	20584	20618	20621	20580	20464	20324	20180	20047
2.5	83.15	15938	16359	16810	17167	17412	17530	17590	17563	17581	17581	17569	17549	17452	17285	17118	16983	16871
2.0	137.09	12966	13319	13678	13966	14237	14459	14625	14680	14661	14675	14653	14541	14350	14108	13898	13757	13652

OCTOBER MEAN ZONAL MEAN GEOSTROPHIC WIND ($m s^{-1}$)

SCALE HEIGHT	PRESSURE (mb)	-80	-70	-60	-50	-40	-30	-20	-10	0	10	20	30	40	50	60	70	80
12.0	0.0062		3.8	-13.3	-3.1	7.9	-6.6	-25.1				14.9	22.3	31.1	25.4	15.2	14.5	
11.5	0.0103		2.2	-13.9	-5.3	2.6	-11.2	-30.7				8.6	23.7	34.7	28.3	18.8	18.9	
11.0	0.0169		0.2	-14.2	-5.3	1.2	-10.7	-30.9				7.1	26.9	38.5	31.7	22.1	22.7	
10.5	0.0279		-1.9	-14.4	-3.5	3.8	-5.3	-24.5				10.5	30.8	41.8	36.0	25.4	25.5	
10.0	0.0460		-3.3	-14.2	-0.9	8.3	1.7	-13.9				17.0	34.9	44.7	40.4	29.3	28.7	
9.5	0.0758		-4.0	-13.6	1.4	12.9	8.1	-2.3				25.9	38.1	46.1	44.6	34.4	33.3	
9.0	0.1250		-4.4	-13.2	3.0	16.6	13.7	7.3				35.0	39.6	45.4	48.1	40.3	39.0	
8.5	0.2061		-3.2	-12.0	4.6	19.5	17.7	11.6				39.3	39.8	45.1	50.5	45.3	44.3	
8.0	0.3398		0.8	-8.9	6.4	21.4	19.8	11.4				38.2	39.2	45.3	51.2	48.3	48.3	
7.5	0.5603		6.4	-5.2	7.5	22.0	20.2	9.4				35.3	38.0	43.5	49.7	49.6	50.0	
7.0	0.9237		12.6	-1.0	8.3	20.4	19.6	8.7				32.9	36.6	39.2	46.2	48.5	48.7	
6.5	1.52		19.7	4.1	9.4	18.3	17.7	8.8				28.8	33.0	33.7	40.4	43.7	44.1	
6.0	2.51		29.0	11.4	11.6	16.3	14.7	6.6				21.1	26.5	28.0	33.4	36.1	37.3	
5.5	4.14		39.9	21.4	14.7	14.0	10.3	1.0				11.3	18.8	22.4	26.3	27.8	29.4	
5.0	6.83		48.7	30.9	18.2	11.2	4.6	-5.8				2.1	11.6	16.7	20.1	20.8	21.9	
4.5	11.25		52.4	37.7	21.7	8.2	-1.4	-10.3				-4.6	5.3	11.6	15.3	16.4	17.0	
4.0	18.55		47.8	40.2	24.1	6.9	-4.8	-11.6				-7.9	0.9	8.1	11.7	13.3	13.5	
3.5	30.59		37.6	39.0	25.6	8.5	-3.2	-9.5				-7.2	0.2	6.4	9.8	11.0	10.9	
3.0	50.43		30.0	35.3	25.5	11.9	2.1	-4.4				-3.5	2.2	7.5	10.2	10.1	8.8	
2.5	83.15		25.8	29.1	23.7	17.2	11.9	5.0				3.1	8.3	13.0	13.4	10.8	7.5	
2.0	137.09		20.6	22.5	21.9	24.2	25.8	19.9				12.5	18.7	21.2	18.1	12.5	7.5	

TABLE I (continued)

PRESSURE COORDINATES

NOVEMBER ZONAL MEAN TEMPERATURE (K)

SCALE HEIGHT	PRESSURE (mb)	-80	-70	-60	-50	-40	-30	-20	-10	0	10	20	30	40	50	60	70	80
12.0	0.0062	162.9	165.8	169.9	177.1	188.0	198.0	204.7	208.6	213.5	212.7	210.2	210.5	214.0	218.1	221.4	225.6	228.4
11.5	0.0103	174.1	177.1	181.4	186.8	194.3	201.1	205.1	208.7	212.9	212.0	209.9	211.2	215.7	220.7	223.6	226.5	228.5
11.0	0.0169	187.3	190.2	194.3	197.4	201.2	204.3	206.2	207.8	209.7	209.8	209.9	212.7	217.6	222.6	227.1	229.4	229.9
10.5	0.0279	201.6	204.0	207.1	207.8	208.6	208.8	209.1	208.1	207.3	208.5	210.8	214.8	220.1	225.1	230.1	232.4	232.9
10.0	0.0460	216.0	216.9	217.6	216.8	216.1	215.2	214.0	211.3	208.5	209.7	212.8	217.7	223.3	228.2	233.3	236.9	235.1
9.5	0.0758	227.4	227.1	226.3	225.3	224.3	223.0	221.6	219.0	215.6	216.4	219.5	224.2	227.8	231.9	237.4	238.1	238.9
9.0	0.1250	236.8	236.1	235.3	234.6	233.4	231.7	230.9	230.0	227.8	227.6	229.8	234.2	235.1	236.5	241.5	244.7	246.8
8.5	0.2061	250.0	247.9	245.2	244.1	241.7	241.1	240.5	242.1	241.6	241.1	240.5	240.0	239.9	243.1	246.5	251.2	254.1
8.0	0.3398	263.9	260.6	256.8	254.8	252.6	251.0	250.0	252.4	253.5	252.7	250.7	249.1	248.7	250.4	252.1	256.7	259.1
7.5	0.5603	274.5	271.2	267.8	265.9	264.7	262.9	261.1	261.2	262.4	261.8	260.1	258.7	256.8	256.2	256.6	260.0	261.6
7.0	0.9237	283.2	279.8	276.3	274.1	273.2	272.5	270.5	267.6	267.0	267.0	266.2	264.6	260.9	255.8	252.9	253.5	252.8
6.5	1.52	284.9	281.9	278.9	276.8	275.4	273.1	270.3	267.9	266.9	266.9	267.1	263.3	257.5	248.9	243.2	240.0	237.3
6.0	2.51	282.1	278.8	274.5	271.9	270.0	266.6	264.6	263.2	262.7	262.5	261.2	255.4	246.9	238.2	231.8	225.9	221.3
5.5	4.14	272.5	269.3	264.4	260.9	258.2	255.6	255.0	255.0	255.1	254.0	251.2	244.7	236.3	227.5	221.6	215.6	210.4
5.0	6.83	260.5	257.6	252.8	247.6	244.3	243.4	243.7	244.3	244.8	243.6	240.4	234.6	227.5	219.3	213.7	208.4	203.4
4.5	11.25	248.1	245.6	240.4	234.3	231.0	231.4	232.0	231.3	232.1	232.2	229.9	228.4	220.5	215.0	209.4	204.8	199.6
4.0	18.55	236.6	235.9	232.8	228.5	224.8	224.2	223.7	223.2	223.2	223.5	223.0	221.0	217.4	215.9	209.4	204.8	200.2
3.5	30.59	235.8	234.4	229.7	226.2	221.8	219.3	217.8	216.8	216.2	216.6	217.2	217.1	216.5	215.2	212.8	209.4	206.5
3.0	50.43	233.7	232.0	228.2	222.4	217.2	215.0	210.5	209.4	208.6	208.8	210.2	211.8	214.1	215.5	215.2	212.5	208.9
2.5	83.15	228.9	228.0	225.0	220.9	215.0	208.0	202.0	198.6	197.9	198.3	201.2	206.3	212.4	216.1	217.0	215.2	212.5
2.0	137.09	221.8	222.4	221.8	220.0	215.5	209.4	203.8	200.4	200.0	200.5	202.8	207.7	213.0	216.7	218.2	217.3	215.7
1.5	226.03	214.8	216.5	218.7	220.5	221.0	222.5	224.6	225.5	226.0	225.7	224.3	222.0	219.2	218.7	218.9	218.1	217.0
1.0	372.66	223.4	225.1	228.8	234.4	240.0	245.7	250.5	252.8	253.6	253.2	250.9	245.2	238.1	236.6	228.2	225.0	222.9
0.5	614.42	246.4	247.7	252.2	258.9	265.6	271.4	275.2	276.3	277.0	275.7	275.0	267.6	263.5	256.8	251.1	246.6	243.8
0.0	1013.0			275.0	280.4	287.2	292.9	297.2	299.9	300.5	301.0	299.7	295.2	288.3	281.4	272.3	261.3	255.7

NOVEMBER ZONAL MEAN GEOPOTENTIAL HEIGHT (m)

SCALE HEIGHT	PRESSURE (mb)	-80	-70	-60	-50	-40	-30	-20	-10	0	10	20	30	40	50	60	70	80
12.0	0.0062	83529	83579	83063	82834	82708	82594	82478	82346	82311	82298	82207	82015	81661	81265	81009	80609	80182
11.5	0.0103	80860	80767	80489	80167	79906	79671	79477	79288	79199	79184	79130	78927	78514	78052	77752	77298	76834
11.0	0.0169	78219	78082	77744	77358	77013	76704	76467	76237	76110	76095	76058	75824	75343	74806	74454	73976	73494
10.5	0.0279	75368	75192	74799	74387	74009	73680	73427	73194	73057	73035	72977	72893	72137	71528	71104	70633	70148
10.0	0.0460	72313	72112	71689	71278	70902	70579	70332	70127	70008	69977	69879	69529	68892	68211	67713	67250	66765
9.5	0.0758	69058	68855	68436	68039	67674	67369	67143	66978	66893	66862	66717	66295	65589	64841	64266	63801	63309
9.0	0.1250	65661	65465	65059	64674	64323	64042	63833	63695	63642	63618	63432	62955	62216	61414	60762	60269	59754
8.5	0.2061	62096	61920	61539	61167	60842	60579	60378	60233	60196	60181	59987	59496	58753	57903	57188	56635	56082
8.0	0.3398	58336	58200	57868	57519	57229	56978	56789	56612	56571	56565	56394	55919	55179	54292	53538	52916	52322
7.5	0.5603	54391	54302	54022	53701	53435	53212	53045	52848	52792	52790	52648	52195	51471	50576	49805	49124	48501
7.0	0.9237	50303	50265	50036	49744	49493	49289	49149	48972	48914	48914	48791	48358	47675	46819	46064	45352	44718
6.5	1.52	46136	46145	45962	45702	45468	45284	45180	45044	44999	45000	44879	44485	43870	43119	42431	41742	41132
6.0	2.51	41979	42032	41901	41675	41465	41323	41257	41150	41115	41119	41002	40678	40168	39546	38947	38326	37769
5.5	4.14	37915	38016	37956	37773	37597	37501	37452	37355	37325	37337	37252	37018	36636	36140	35632	35099	34615
5.0	6.83	34010	34153	34163	34043	33911	33843	33795	33692	33662	33668	33646	33507	33236	32870	32445	31995	31587
4.5	11.25	30284	30470	30557	30522	30440	30372	30317	30215	30177	30207	30208	30136	29962	29695	29351	28976	28640
4.0	18.55	26742	26951	27094	27159	27107	27036	26981	26887	26847	26872	26693	26683	26758	26557	26289	25986	25719
3.5	30.59	23289	23512	23713	23810	23837	23792	23749	23669	23630	23651	23671	23654	23582	23414	23197	22952	22736
3.0	50.43	19846	20094	20360	20523	20619	20623	20546	20546	20516	20533	20530	20510	20426	20260	20063	19864	19697
2.5	83.15	16458	16726	17037	17279	17458	17542	17591	17599	17557	17553	17526	17451	17305	17100	16897	16733	16611
2.0	137.09	13153	13424	13759	14048	14309	14499	14646	14670	14657	14667	14596	14436	14195	13931	13708	13564	13474

NOVEMBER MEAN ZONAL MEAN GEOSTROPHIC WIND ($m s^{-1}$)

SCALE HEIGHT	PRESSURE (mb)	-80	-70	-60	-50	-40	-30	-20	-10	0	10	20	30	40	50	60	70	80
12.0	0.0062		-5.5	-18.1	-12.7	-9.7	-15.2	-29.1				20.7	31.9	39.4	25.4	18.9	28.2	
11.5	0.0103		-9.1	-23.2	-21.8	-22.4	-27.2	-39.8				17.2	36.9	45.7	30.0	22.5	30.9	
11.0	0.0169		-12.6	-27.4	-27.6	-30.2	-34.1	-46.6				17.4	43.7	52.6	35.1	25.5	31.9	
10.5	0.0279		-15.9	-30.2	-29.9	-32.8	-36.3	-47.9				23.4	52.0	59.5	40.9	28.0	31.5	
10.0	0.0460		-17.8	-31.1	-29.7	-32.6	-35.4	-44.6				33.0	61.5	66.6	46.7	30.5	31.0	
9.5	0.0758		-17.8	-30.4	-28.7	-31.4	-32.9	-39.1				44.2	70.7	72.6	52.2	33.5	31.1	
9.0	0.1250		-17.1	-29.5	-27.7	-29.6	-30.4	-35.5				53.7	76.2	76.1	57.4	37.6	32.7	
8.5	0.2061		-15.5	-28.3	-26.2	-27.6	-28.7	-35.7				56.2	77.2	78.1	61.7	42.2	36.0	
8.0	0.3398		-12.3	-25.9	-24.0	-25.2	-27.2	-37.7				52.7	75.8	79.7	64.6	46.2	39.9	
7.5	0.5603		-8.7	-23.2	-22.2	-22.7	-24.1	-37.7				48.3	73.2	79.4	65.4	48.9	43.1	
7.0	0.9237		-5.0	-20.6	-20.8	-21.2	-21.0	-33.2				45.0	69.2	75.6	63.1	49.5	44.8	
6.5	1.52		-1.5	-18.1	-19.1	-19.6	-17.2	-25.8				41.7	62.4	66.9	56.2	46.5	43.5	
6.0	2.51		2.1	-15.0	-17.1	-16.7	-12.0	-18.9				36.0	51.5	55.3	47.6	41.4	39.5	
5.5	4.14		6.5	-11.0	-14.3	-12.9	-8.1	-15.2				26.2	37.9	42.6	39.1	35.7	34.1	
5.0	6.83		10.8	-6.2	-10.3	-9.6	-6.5	-14.5				14.8	25.1	30.6	30.8	30.5	28.6	
4.5	11.25		14.9	-0.2	-5.0	-7.3	-7.1	-14.2				5.6	15.0	21.0	23.7	25.5	23.5	
4.0	18.55		16.6	5.7	0.3	-5.2	-7.5	-13.0				0.5	8.1	14.4	18.4	20.4	18.5	
3.5	30.59		13.7	10.7	4.9	-1.3	-5.3	-10.9				-0.8	5.3	11.4	15.2	16.6	14.8	
3.0	50.43		15.3	15.9	10.4	4.4	-0.7	-6.9				1.6	6.5	12.2	14.4	14.2	11.6	
2.5	83.15		17.6	20.6	16.8	12.3	8.2	1.5				8.8	13.3	17.5	16.1	13.3	8.6	
2.0	137.09		18.6	23.1	22.0	21.5	21.1	15.9				20.5	24.8	25.2	19.2	13.3	6.6	

TABLE 1 (continued)

PRESSURE COORDINATES

DECEMBER ZONAL MEAN TEMPERATURE (K)

SCALE HEIGHT	PRESSURE (mb)	-80	-70	-60	-50	-40	-30	-20	-10	0	10	20	30	40	50	60	70	80
12.0	0.0062	148.0	151.4	157.0	167.9	182.0	194.6	202.1	205.5	207.5	207.0	205.9	209.0	214.4	219.3	222.1	225.7	229.2
11.5	0.0103	159.6	163.0	168.2	177.5	188.5	198.1	203.7	206.2	209.0	207.9	206.6	209.9	216.2	221.5	224.2	226.9	229.6
11.0	0.0169	174.0	177.0	181.6	188.3	195.4	201.7	205.6	208.6	208.3	207.6	207.6	211.3	218.5	223.7	227.7	228.7	230.2
10.5	0.0279	189.9	192.4	195.9	199.4	202.8	205.9	208.3	208.2	208.1	208.1	209.2	213.3	220.4	226.2	231.4	232.2	233.2
10.0	0.0460	206.2	207.8	209.6	210.1	210.5	211.2	212.0	212.1	211.4	211.5	212.0	216.7	222.1	228.8	235.0	236.3	237.0
9.5	0.0758	221.8	222.3	222.3	221.2	219.9	218.9	219.5	220.9	220.6	219.9	220.3	223.4	225.9	231.3	235.2	241.5	242.4
9.0	0.1250	236.1	235.9	235.0	233.4	231.1	229.3	230.8	233.9	234.5	232.8	232.3	231.6	230.0	234.8	243.2	248.2	250.2
8.5	0.2061	251.3	250.0	247.9	245.9	242.8	241.9	243.4	247.5	248.2	246.5	243.1	239.4	235.5	240.1	247.6	254.5	257.2
8.0	0.3398	267.1	264.3	260.8	258.2	254.9	253.7	254.0	257.2	258.5	257.0	252.6	247.8	244.3	246.7	251.9	258.3	260.5
7.5	0.5603	279.3	275.6	271.5	268.7	265.5	263.6	262.6	263.4	264.1	263.5	260.8	257.5	254.2	252.8	254.1	257.5	258.0
7.0	0.9237	287.5	283.6	279.5	276.0	273.5	271.3	269.5	266.8	265.6	266.1	266.6	264.6	260.5	252.5	245.0	247.2	248.7
6.5	1.52	288.9	285.7	282.4	278.8	276.7	272.9	269.1	265.2	263.8	264.3	266.9	264.6	258.2	245.6	239.6	238.1	237.9
6.0	2.51	284.4	281.9	278.7	275.1	271.9	267.9	263.5	260.1	259.3	259.7	261.6	258.0	248.5	235.8	229.7	226.9	227.2
5.5	4.14	274.8	272.7	269.1	265.3	261.5	257.9	254.0	251.7	252.0	251.8	251.8	247.0	238.4	226.7	220.7	216.7	216.4
5.0	6.83	265.1	261.3	257.4	252.9	249.3	246.0	242.9	241.4	242.0	241.8	240.5	236.5	223.0	220.7	214.1	207.6	204.9
4.5	11.25	249.9	248.9	245.6	240.6	236.9	233.5	231.6	229.9	229.6	230.2	229.2	228.1	223.1	216.8	210.4	201.0	194.7
4.0	18.55	237.7	238.0	236.5	231.9	228.5	225.7	223.8	222.7	222.2	222.3	222.1	221.5	218.5	214.6	208.6	200.3	193.5
3.5	30.59	236.4	235.1	231.8	227.1	222.9	220.2	218.2	217.2	216.5	216.3	217.0	217.0	216.7	214.9	210.9	205.0	199.7
3.0	50.43	236.3	234.3	229.6	222.7	216.7	212.5	210.0	208.6	207.4	208.0	209.4	211.3	214.4	215.9	214.2	209.8	205.7
2.5	83.15	234.2	232.1	228.0	221.2	213.5	206.2	201.0	198.2	197.0	197.9	200.9	206.7	213.2	216.6	216.0	212.7	209.3
2.0	137.09	230.1	228.5	225.8	220.7	213.9	207.8	203.5	200.5	200.0	200.4	203.0	208.4	214.0	217.1	216.9	214.5	212.1
1.5	226.03	223.9	223.3	222.7	221.7	221.3	223.2	222.7	222.7	226.0	225.5	224.2	221.4	218.8	218.5	217.6	215.9	214.8
1.0	372.66	226.5	228.0	231.0	236.0	242.0	247.5	251.8	253.1	253.5	253.0	250.2	243.5	235.5	230.0	226.5	223.8	221.9
0.5	614.42	249.2	251.1	254.8	260.4	267.2	272.8	275.9	276.5	276.8	277.1	275.0	268.6	260.4	253.6	249.1	245.4	242.5
0.0	1013.0			275.7	281.5	288.5	294.6	298.4	300.4	300.6	300.7	298.5	293.1	285.9	279.6	268.7	257.2	251.7

DECEMBER ZONAL MEAN GEOPOTENTIAL HEIGHT (m)

SCALE HEIGHT	PRESSURE (mb)	-80	-70	-60	-50	-40	-30	-20	-10	0	10	20	30	40	50	60	70	80
12.0	0.0062	83947	83363	83072	82805	82630	82491	82388	82337	82325	82244	82133	81948	81505	80944	80764	80322	79924
11.5	0.0103	81295	81061	80690	80275	79915	79614	79416	79321	79280	79202	79111	78879	78351	77716	77498	77008	76563
11.0	0.0169	78858	78577	78134	77601	77107	76537	76421	76299	76232	76159	76080	75797	75169	74456	74191	73674	73198
10.5	0.0279	76190	75869	75366	74759	74188	73702	73390	73263	73187	73116	73027	72688	71954	71161	70829	70299	69806
10.0	0.0460	73295	72943	72400	71764	71165	70651	70315	70191	70117	70049	69947	69544	68715	67830	67415	66870	66364
9.5	0.0758	70153	69788	69233	68602	67903	67158	67023	66953	66894	66786	66323	65435	64461	63942	63372	62855	
9.0	0.1250	66803	66436	65888	65277	64714	64226	63867	63699	63627	63586	63476	62994	62097	61052	60410	59789	59251
8.5	0.2061	63231	62875	62349	61764	61240	60773	60390	60168	60088	60070	59990	59542	58690	57574	56815	56105	55531
8.0	0.3398	59438	59113	58627	58076	57600	57145	56747	56470	56379	56381	56362	55978	55182	54013	53159	52348	51735
7.5	0.5603	55431	55154	54724	54212	53783	53353	52963	52654	52551	52565	52598	52274	51526	50349	49447	48563	47932
7.0	0.9237	51278	51057	50687	50223	49835	49435	49063	48768	48668	48685	48733	48448	47753	46641	45754	44844	44214
6.5	1.52	47049	46800	46566	46154	45798	45442	45112	44868	44786	44798	44821	44566	43946	42991	42177	41278	40655
6.0	2.51	42844	42716	42448	42089	41771	41474	41206	41017	40949	40958	40944	40731	40228	39460	38736	37869	37244
5.5	4.14	38749	38654	38436	38131	37867	37625	37417	37270	37208	37212	37186	37034	36667	36078	35443	34625	33999
5.0	6.83	34805	34740	34575	34330	34124	33930	33774	33653	33588	33592	33576	33492	33235	32807	32260	31516	30909
4.5	11.25	31047	31005	30896	30722	30569	30424	30304	30206	30141	30140	30142	30093	29921	29610	29154	28530	27993
4.0	18.55	27485	27445	27369	27264	27163	27063	26971	26896	26837	26830	26840	26801	26688	26452	26088	25598	25161
3.5	30.59	24019	23988	23946	23906	23860	23798	23734	23674	23627	23619	23625	23592	23503	23309	23019	22631	22282
3.0	50.43	20556	20551	20506	20462	20416	20366	20316	20266	20216	20208	20208	20155	20045	19859	19595	19259	18936
2.5	83.15	17109	17134	17219	17364	17494	17562	17586	17574	17554	17538	17496	17395	17215	16988	16756	16499	16273
2.0	137.09	13706	13758	13892	14126	14371	14547	14653	14687	14678	14655	14565	14370	14090	13812	13585	13370	13189

DECEMBER MEAN ZONAL MEAN GEOSTROPHIC WIND ($m s^{-1}$)

SCALE HEIGHT	PRESSURE (mb)	-80	-70	-60	-50	-40	-30	-20	-10	0	10	20	30	40	50	60	70	80
12.0	0.0062	-8.3	-24.0	-18.9	-12.9	-15.4	-19.6					24.9	33.1	57.4	27.4	16.1	31.2	
11.5	0.0103	-12.6	-31.8	-31.9	-30.3	-30.7	-30.4					25.9	42.6	64.9	31.9	18.4	34.5	
11.0	0.0169	-16.5	-38.4	-41.9	-43.0	-41.8	-37.5					27.6	53.2	73.3	36.9	20.4	36.6	
10.5	0.0279	-19.8	-43.0	-47.6	-50.3	-48.6	-40.9					32.0	64.2	82.2	42.8	23.0	37.7	
10.0	0.0460	-22.1	-45.4	-49.7	-53.1	-51.8	-42.1					37.7	74.8	91.0	49.7	26.4	38.8	
9.5	0.0758	-22.9	-45.4	-49.1	-52.6	-52.3	-43.7					42.7	82.5	97.9	57.4	31.2	40.1	
9.0	0.1250	-22.7	-44.5	-47.2	-50.0	-52.1	-48.5					44.0	84.2	101.4	65.2	38.0	42.6	
8.5	0.2061	-21.6	-42.8	-44.5	-46.7	-52.5	-56.4					37.9	79.0	102.4	73.0	46.0	46.7	
8.0	0.3398	-19.1	-40.2	-41.4	-43.4	-52.8	-64.0					26.0	71.0	102.0	79.5	53.7	51.2	
7.5	0.5603	-15.4	-37.1	-38.2	-39.6	-50.9	-67.0					15.7	63.8	99.6	82.1	58.7	54.0	
7.0	0.9237	-11.1	-33.6	-34.9	-36.2	-47.7	-64.7					11.1	57.9	93.0	79.1	59.7	54.7	
6.5	1.52	-7.3	-29.9	-31.6	-32.8	-42.2	-56.3					11.6	51.6	80.6	69.9	57.4	54.1	
6.0	2.51	-4.8	-26.3	-27.8	-28.5	-34.7	-44.9					13.0	42.2	64.4	58.6	54.0	52.8	
5.5	4.14	-2.9	-22.2	-23.0	-23.4	-27.6	-34.1					11.2	30.5	47.7	47.8	50.0	50.4	
5.0	6.83	-1.2	-17.6	-18.0	-18.5	-21.5	-25.5					6.1	19.8	33.5	38.0	45.3	46.2	
4.5	11.25	0.4	-12.4	-12.9	-13.8	-16.2	-19.2					2.6	12.9	23.1	29.9	38.4	38.7	
4.0	18.55	-1.5	-7.3	-8.1	-9.3	-11.8	-14.6					1.6	8.9	16.3	23.6	30.7	30.3	
3.5	30.59	-2.4	-2.8	-3.4	-5.1	-7.7	-10.9					1.9	7.3	13.1	19.1	24.4	23.9	
3.0	50.43	0.0	2.6	2.9	0.6	-2.8	-6.7					4.7	9.1	14.2	17.2	0.0	19.0	
2.5	83.15	3.1	8.8	11.3	9.7	5.3	1.2					12.3	17.1	20.3	18.1	17.2	15.0	
2.0	137.09	5.6	13.7	19.6	20.8	16.8	13.3					25.0	29.8	28.1	19.7	15.3	11.9	

ORIGINAL PAGE IS
OF POOR QUALITY

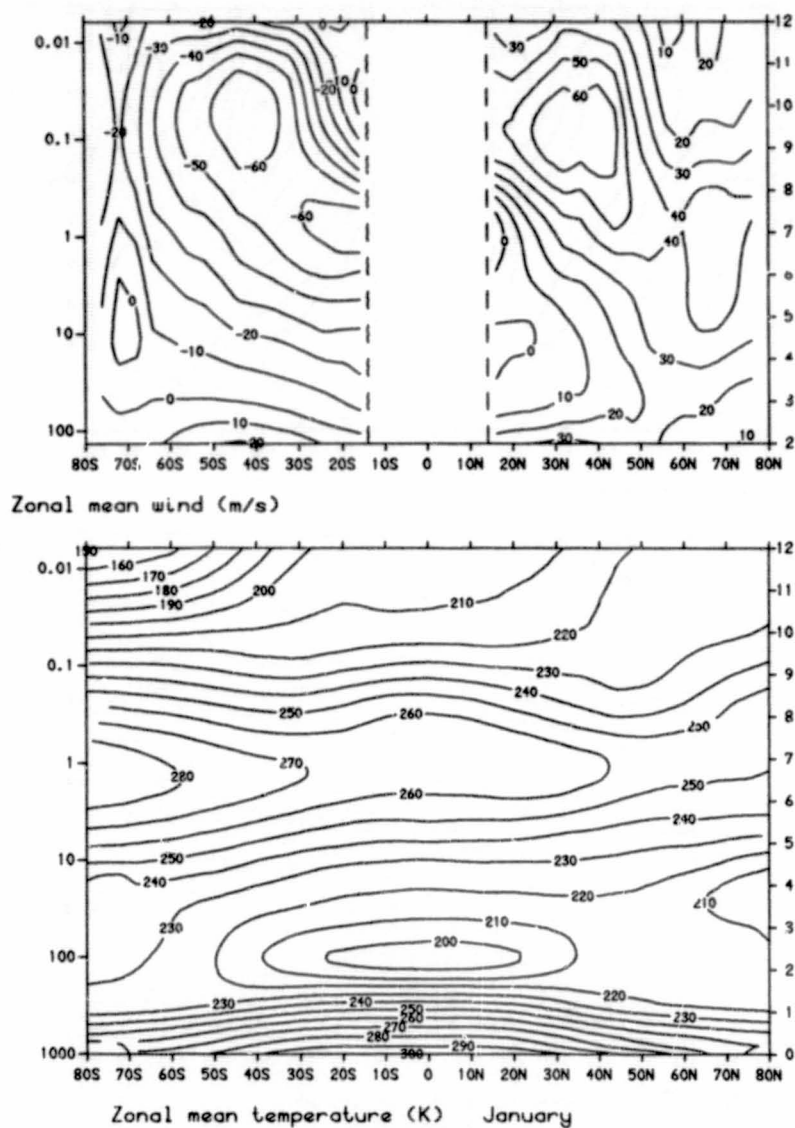


Figure 1.1.

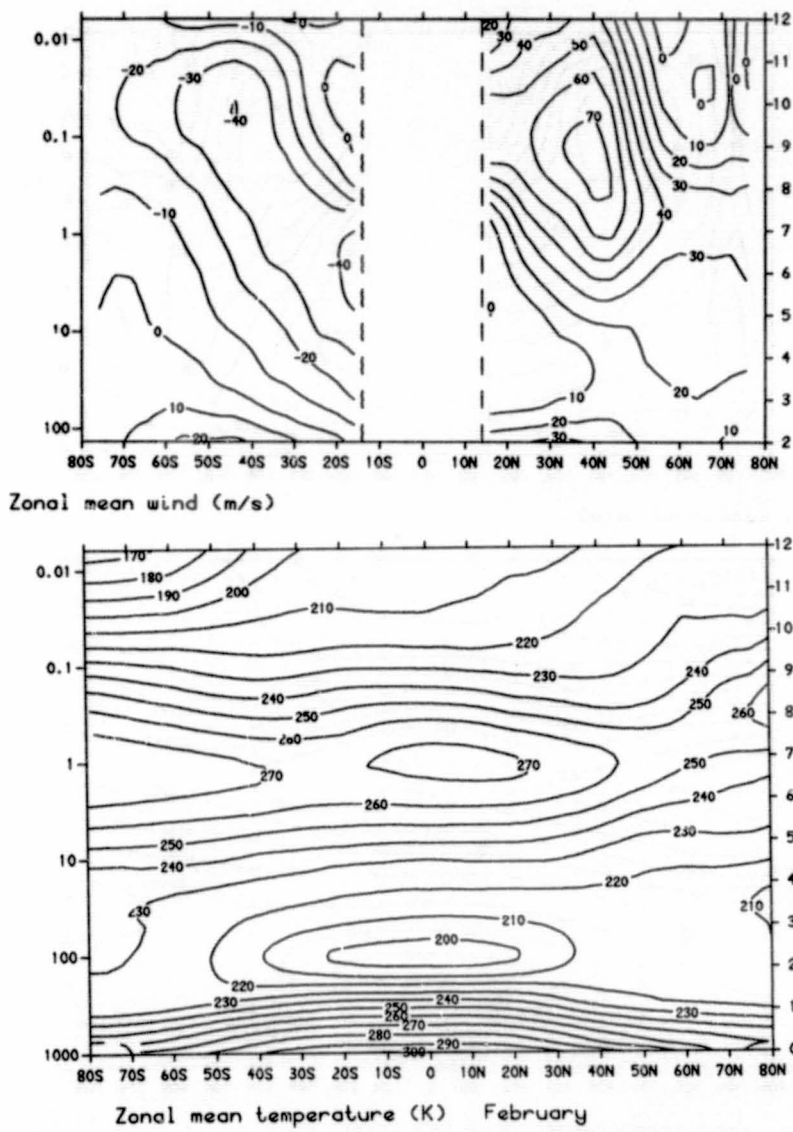
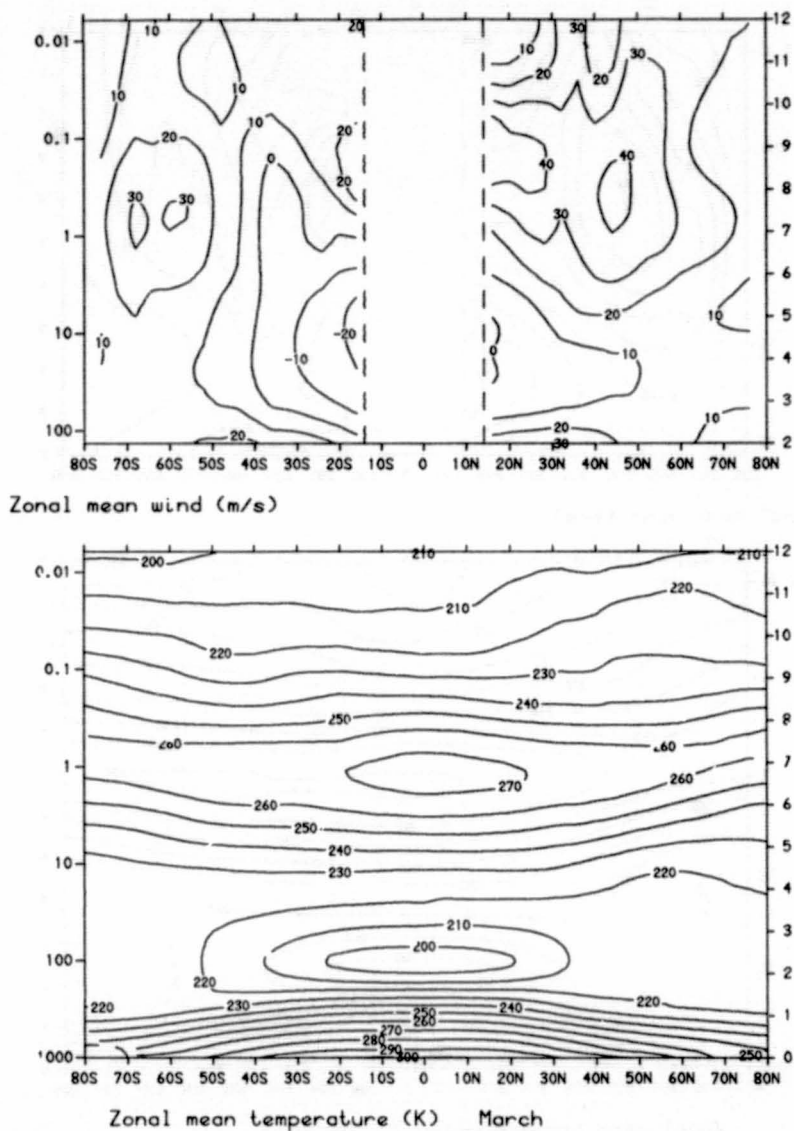


Figure 1.2.



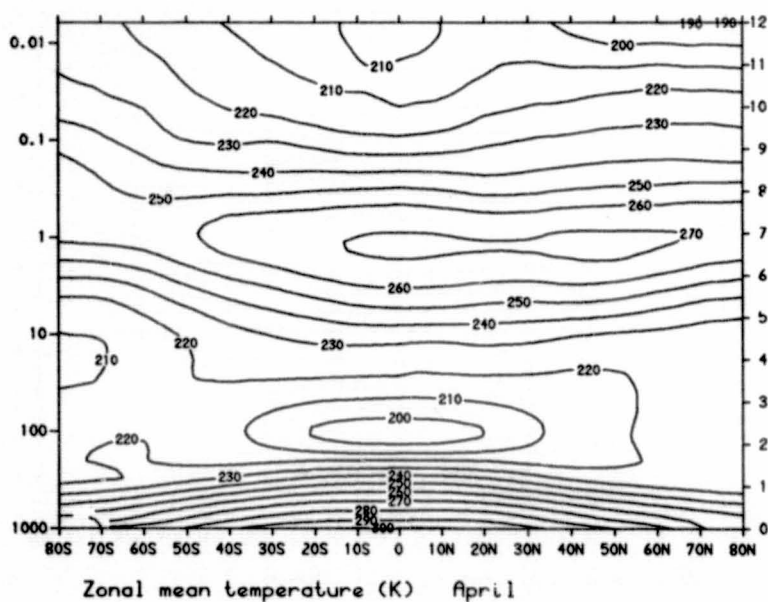
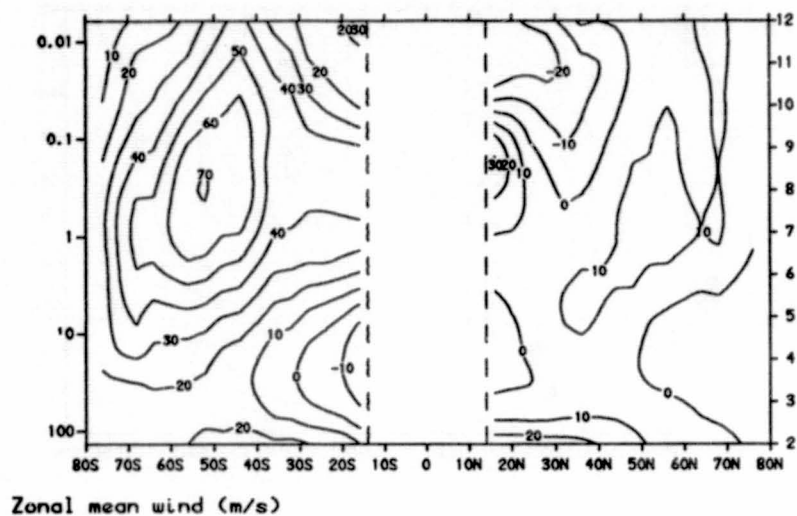


Figure 1.4.

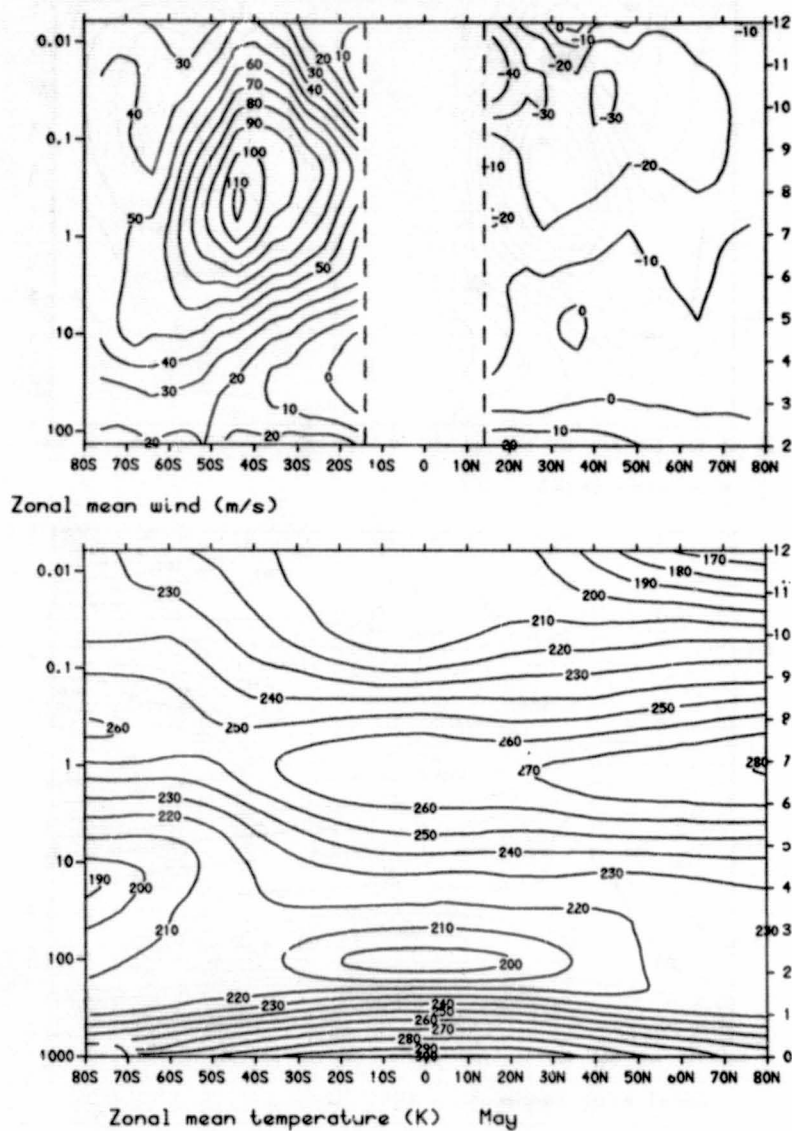


Figure 1.5.

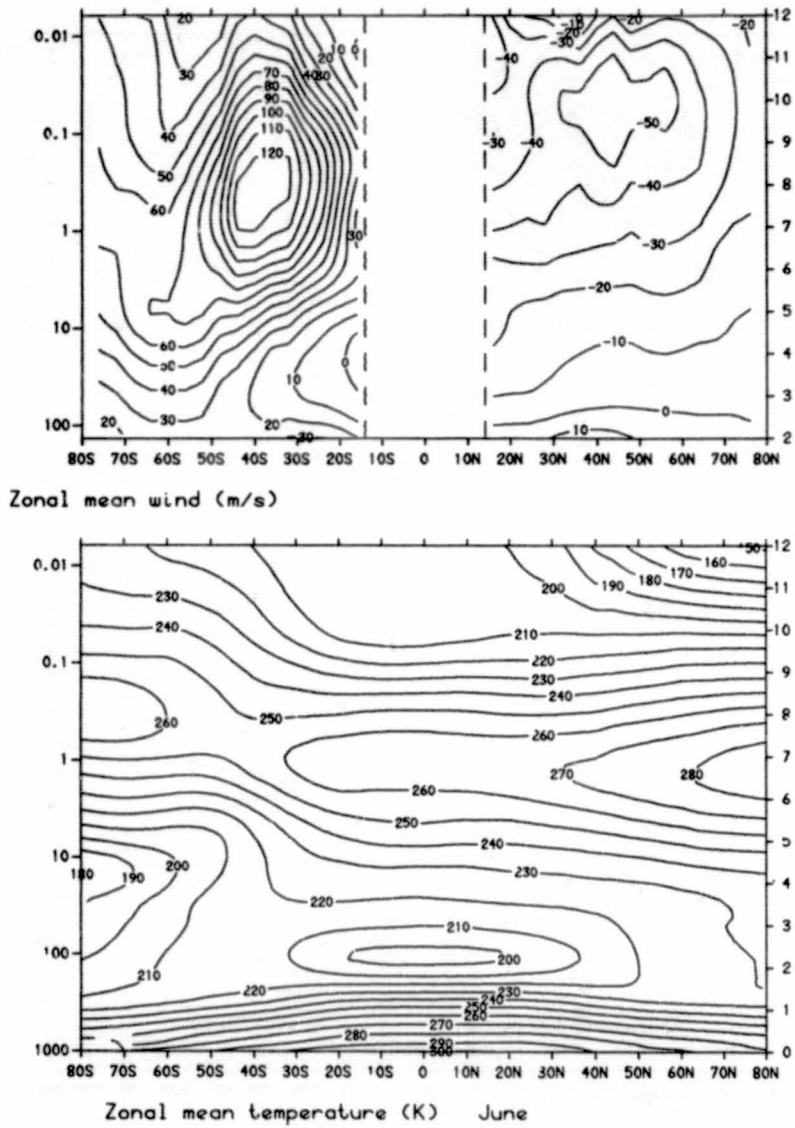
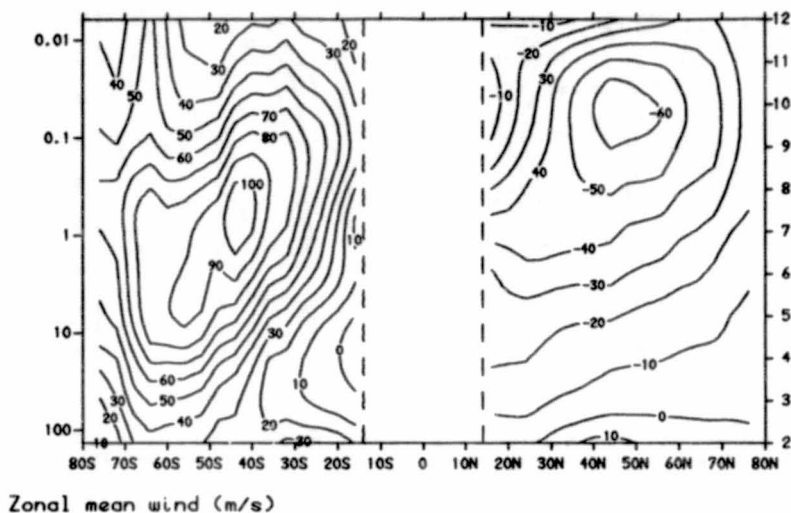


Figure 1.6.



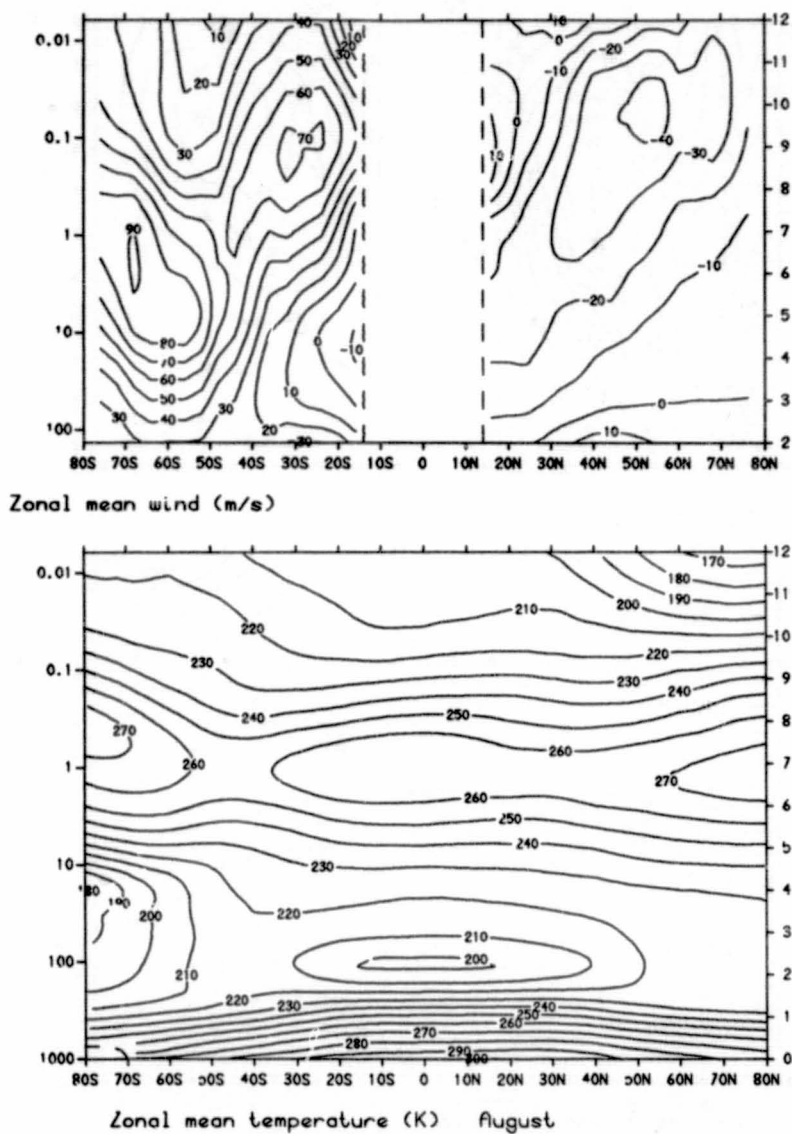


Figure 1.8.

ORIGINAL PAGE IS
OF POOR QUALITY

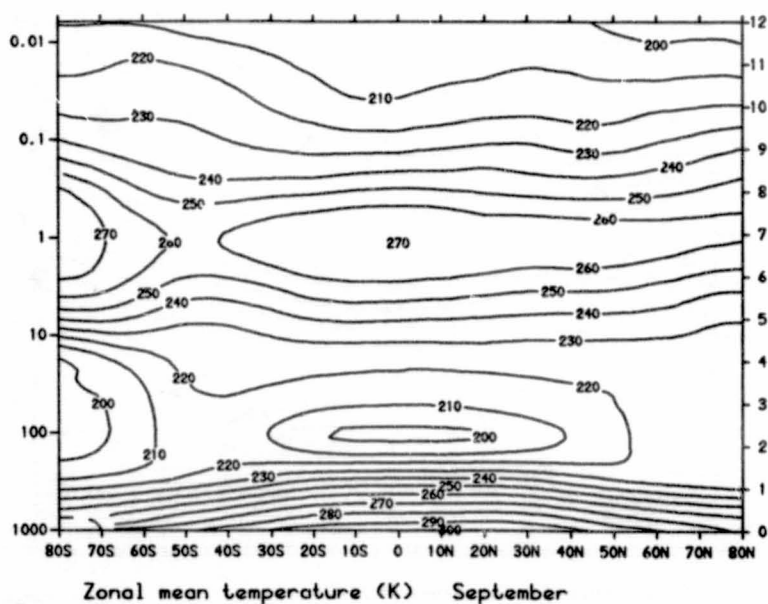
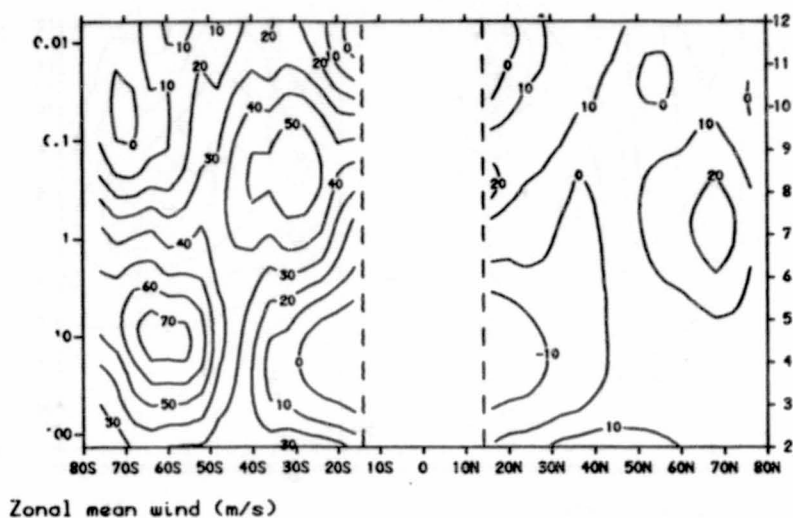
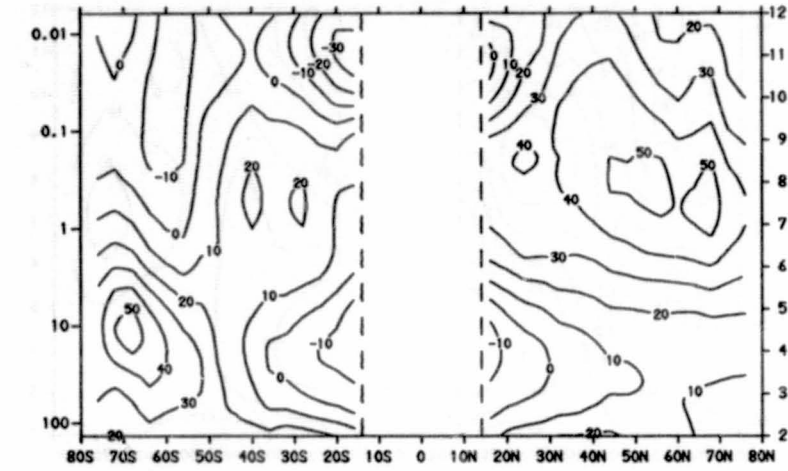
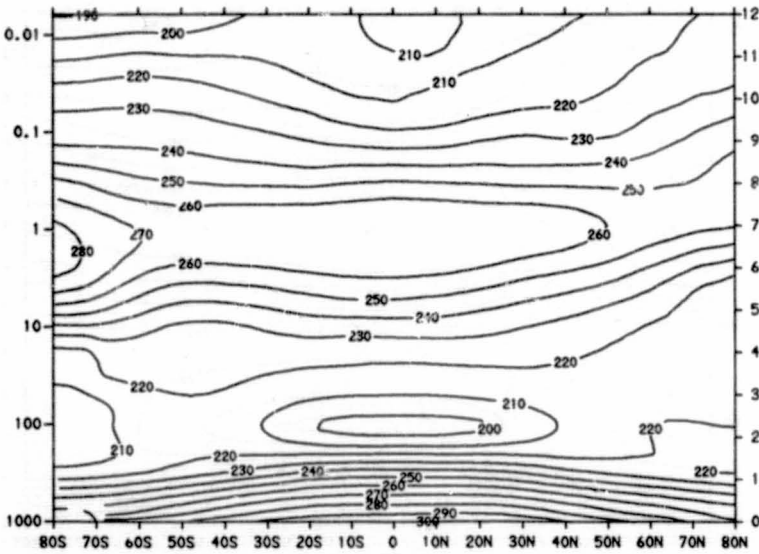


Figure 1.9.



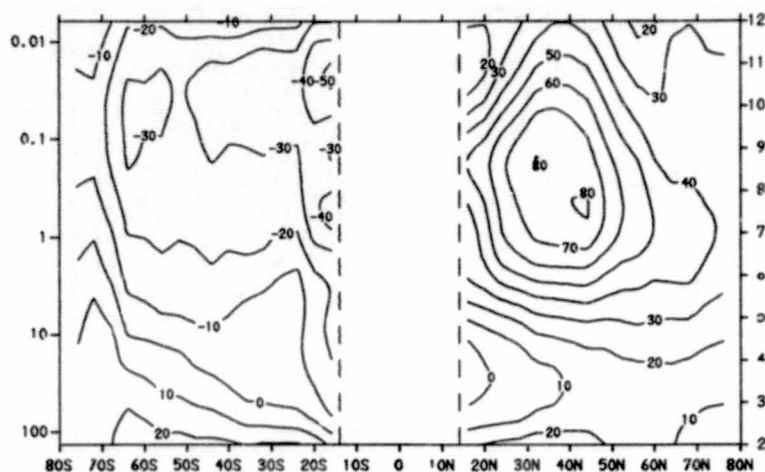
Zonal mean wind (m/s)



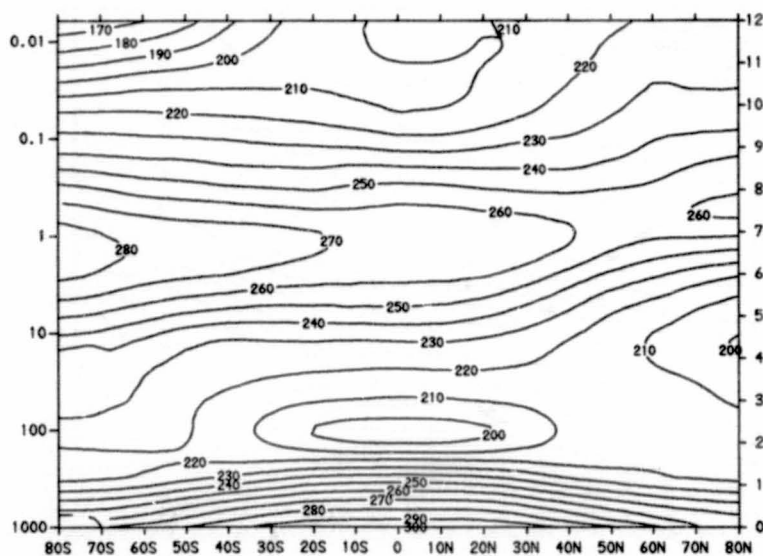
Zonal mean temperature (K) October

Figure 1.10.

ORIGINAL PAGE IS
OF POOR QUALITY



Zonal mean wind (m/s)



Zonal mean temperature (K) November

Figure 1.11.

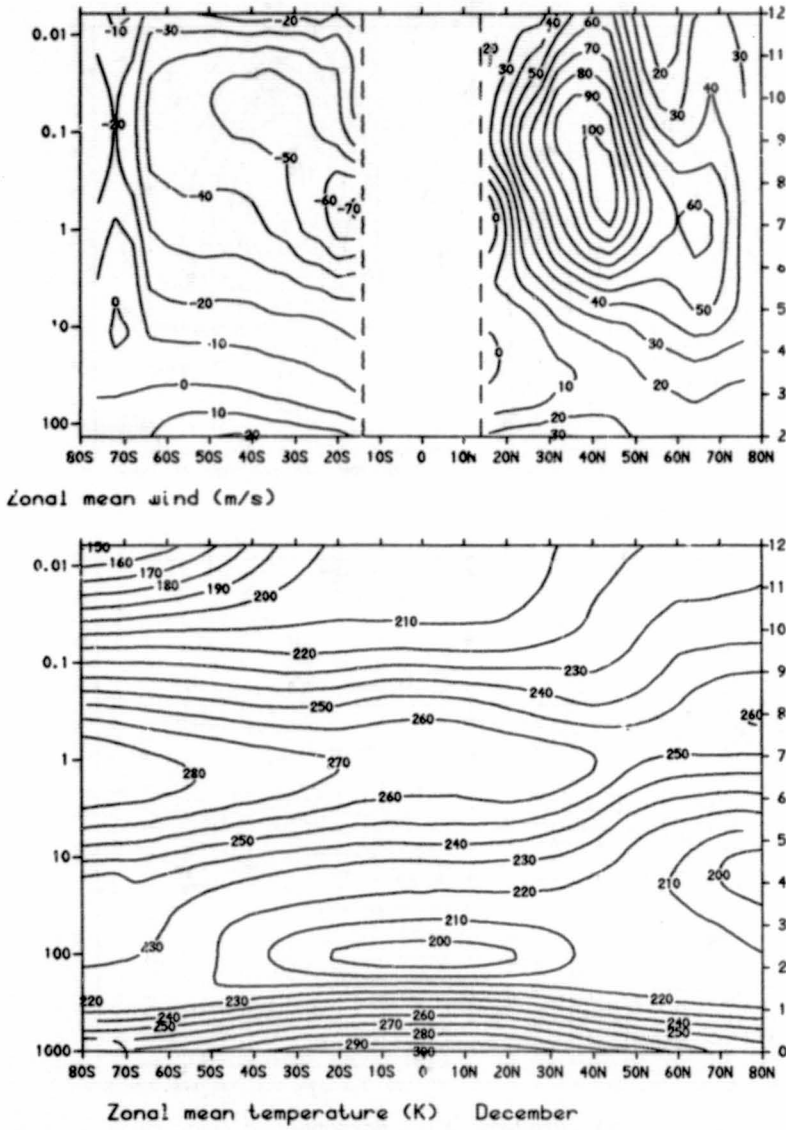


Figure 1.12.

ORIGINAL PAGE IS
OF POOR QUALITY

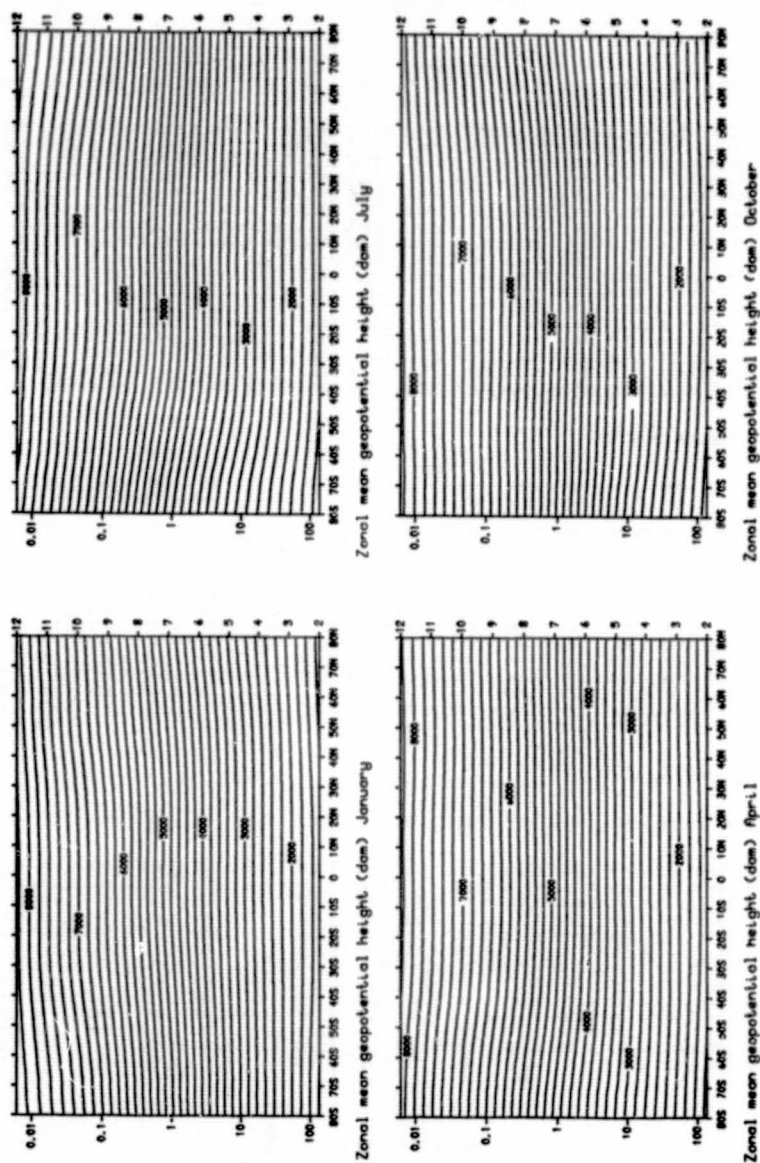


Figure 2.

Table II.

TABLE II

HEIGHT COORDINATES

JANUARY ZONAL MEAN TEMPERATURE (K)

HEIGHT (Km)	LATITUDE																
	-80	-70	-60	-50	-40	-30	-20	-10	0	10	20	30	40	50	60	70	80
80	172.2	173.3	175.5	185.2	193.5	202.7	206.8	206.1	206.5	207.1	208.0	211.8	216.2	222.3	225.0	224.4	225.2
75	200.9	200.5	200.4	202.0	204.8	208.3	210.3	209.3	209.9	210.5	211.9	215.5	219.8	224.0	226.2	225.3	226.3
70	226.4	224.8	222.7	219.0	215.2	214.1	215.9	217.8	218.3	217.7	217.5	219.5	221.2	225.0	227.7	227.3	229.3
65	248.3	245.3	241.5	235.5	229.8	227.5	230.4	233.8	235.1	233.1	230.7	227.8	226.3	226.2	229.6	232.6	236.4
60	266.7	262.9	258.7	252.8	247.4	245.0	247.7	252.6	252.9	250.2	244.5	238.7	232.5	230.7	235.0	241.9	247.2
55	281.1	276.8	272.1	266.3	261.1	258.7	259.4	263.3	264.6	262.9	258.3	251.9	245.2	241.7	244.2	250.7	255.5
50	288.5	284.4	279.7	275.4	271.4	268.7	267.4	267.8	267.8	267.9	267.0	263.4	259.2	253.5	253.5	255.0	255.4
45	286.1	283.4	280.0	275.8	272.8	269.5	267.1	264.0	263.8	264.5	265.8	264.4	260.6	254.4	252.3	252.0	251.0
40	276.2	274.1	271.2	267.6	264.1	260.2	256.5	254.9	255.2	255.2	255.8	254.0	250.0	246.4	246.5	246.7	246.9
35	261.8	260.5	258.1	254.6	250.6	246.8	244.1	242.3	242.5	242.1	241.7	239.2	237.4	235.4	235.7	236.3	236.6
30	244.5	244.1	243.7	240.7	236.1	232.0	228.9	227.8	227.2	228.0	228.1	228.5	227.5	226.2	224.7	221.7	219.1
25	235.6	233.8	232.6	229.0	225.4	222.1	219.2	218.1	217.5	218.0	218.3	219.3	219.6	218.2	213.8	207.8	202.0
20	234.6	233.2	229.6	222.8	215.5	210.2	207.4	205.3	204.3	204.6	206.7	210.0	214.5	216.8	215.5	211.4	205.9
15	232.5	231.3	227.3	220.3	212.3	206.0	202.0	199.8	199.3	199.7	202.2	208.1	214.7	217.9	217.0	214.1	211.2
10	226.9	225.5	224.8	225.9	229.8	235.0	238.3	239.0	239.2	238.6	235.4	228.6	221.6	218.8	217.1	215.2	214.0
5	240.8	243.7	248.3	255.8	263.8	269.4	271.9	272.3	272.4	272.4	269.6	261.8	252.5	244.5	239.1	234.8	231.9
0			275.2	281.4	289.5	295.9	298.9	300.5	300.6	300.0	297.1	291.7	284.7	277.7	266.4	254.1	248.6

JANUARY ZONAL MEAN PRESSURE (N m⁻²)

HEIGHT (Km)	LATITUDE																	EXPONENT
	-80	-70	-60	-50	-40	-30	-20	-10	0	10	20	30	40	50	60	70	80	
80	1.590	1.504	1.408	1.290	1.186	1.129	1.119	1.123	1.130	1.118	1.083	1.033	0.960	0.890	0.851	0.815	0.781	E+0
75	3.903	3.680	3.421	3.069	2.737	2.537	2.486	2.503	2.514	2.480	2.391	2.253	2.060	1.880	1.806	1.714	1.639	E+0
70	8.541	8.080	7.545	6.786	6.067	5.592	5.440	5.473	5.484	5.408	5.206	4.854	4.392	3.956	3.769	3.591	3.417	E+0
65	1.730	1.647	1.552	1.417	1.288	1.195	1.152	1.148	1.146	1.136	1.099	1.025	0.928	0.831	0.784	0.745	0.703	E+1
60	3.321	3.189	3.032	2.814	2.597	2.426	2.319	2.282	2.273	2.267	2.219	2.101	1.926	1.733	1.616	1.513	1.410	E+1
55	6.130	5.940	5.710	5.372	5.019	4.713	4.483	4.359	4.333	4.346	4.320	4.163	3.893	3.532	3.262	2.993	2.749	E+1
50	1.107	1.081	1.049	0.998	0.942	0.890	0.847	0.818	0.812	0.816	0.817	0.797	0.757	0.695	0.640	0.582	0.531	E+2
45	1.989	1.956	1.913	1.835	1.747	1.658	1.584	1.537	1.525	1.531	1.531	1.503	1.443	1.345	1.244	1.130	1.033	E+2
40	3.624	3.579	3.524	3.410	3.266	3.127	3.006	2.935	2.912	2.922	2.914	2.872	2.786	2.636	2.447	2.224	2.037	E+2
35	6.791	6.737	6.677	6.509	6.288	6.081	5.892	5.776	5.724	5.747	5.735	5.690	5.572	5.313	4.932	4.473	4.099	E+2
30	1.326	1.318	1.311	1.288	1.260	1.231	1.203	1.184	1.174	1.178	1.177	1.173	1.154	1.106	1.030	0.937	0.861	E+3
25	2.700	2.690	2.675	2.654	2.628	2.595	2.560	2.528	2.512	2.516	2.512	2.497	2.462	2.372	2.235	2.071	1.935	E+3
20	5.363	5.371	5.391	5.633	5.669	5.678	5.652	5.613	5.593	5.596	5.568	5.499	5.382	5.187	4.944	4.686	4.487	E+3

JANUARY ZONAL MEAN DENSITY (Kg m⁻³)

HEIGHT (Km)	LATITUDE																	EXPONENT
	-80	-70	-60	-50	-40	-30	-20	-10	0	10	20	30	40	50	60	70	80	
80	3.217	3.022	2.794	2.452	2.136	1.941	1.886	1.898	1.906	1.880	1.814	1.700	1.546	1.396	1.334	1.265	1.208	E-5
75	6.768	6.393	5.946	5.294	4.656	4.242	4.119	4.164	4.173	4.105	3.931	3.642	3.265	2.924	2.781	2.650	2.522	E-5
70	1.314	1.252	1.180	1.079	0.982	0.910	0.878	0.876	0.875	0.865	0.834	0.770	0.692	0.613	0.577	0.550	0.519	E-4
65	2.428	2.339	2.238	2.096	1.953	1.830	1.741	1.711	1.698	1.697	1.659	1.567	1.429	1.280	1.190	1.116	1.037	E-4
60	4.338	4.225	4.083	3.878	3.656	3.450	3.262	3.148	3.131	3.156	3.162	3.066	2.885	2.617	2.396	2.180	1.986	E-4
55	7.597	7.476	7.311	7.028	6.697	6.346	6.020	5.768	5.704	5.758	5.826	5.756	5.531	5.090	4.653	4.160	3.748	E-4
50	1.337	1.324	1.306	1.262	1.210	1.153	1.103	1.065	1.056	1.061	1.066	1.054	1.017	0.955	0.879	0.795	0.724	E-3
45	2.422	2.404	2.380	2.318	2.230	2.143	2.065	2.027	2.014	2.017	2.006	1.980	1.929	1.842	1.718	1.562	1.434	E-3
40	4.571	4.549	4.527	4.439	4.308	4.186	4.083	4.010	3.974	3.988	3.969	3.939	3.882	3.726	3.458	3.140	2.875	E-3
35	9.037	9.008	9.012	8.906	8.741	8.584	8.409	8.302	8.221	8.269	8.267	8.285	8.176	7.861	7.289	6.596	6.035	E-3
30	1.889	1.881	1.875	1.864	1.859	1.849	1.831	1.810	1.800	1.800	1.798	1.788	1.767	1.703	1.596	1.472	1.369	E-2
25	3.992	4.008	4.007	4.037	4.061	4.069	4.069	4.039	4.023	4.021	4.009	3.967	3.906	3.786	3.641	3.472	3.337	E-2
20	8.260	8.322	8.482	8.805	9.165	9.408	9.494	9.524	9.538	9.531	9.385	9.122	8.741	8.336	7.991	7.722	7.591	E-2

(note that 1 N m⁻² = 1 Pa = 0.01 mb = 10 dynes cm⁻²; 1000 Kg m⁻³ = 1 g cm⁻³)

ORIGINAL PAGE IS
OF POOR QUALITY

TABLE II (continued)

HEIGHT COORDINATES

FEBRUARY ZONAL MEAN TEMPERATURE (K)

HEIGHT (Km)	LATITUDE																	
	-80	-70	-60	-50	-40	-30	-20	-10	0	10	20	30	40	50	60	70	80	
80	179.9	180.3	181.7	189.6	198.3	204.3	205.2	205.0	205.8	206.9	209.3	210.8	214.2	219.5	223.1	222.6	222.2	
75	201.4	200.9	200.9	203.9	207.4	209.6	209.8	209.0	209.6	211.1	213.7	216.0	219.6	223.9	227.2	226.2	226.4	
70	223.1	221.2	219.8	217.3	216.0	216.2	217.6	217.9	217.6	217.1	218.2	220.0	222.5	226.2	230.7	231.3	233.7	
65	244.1	240.2	235.9	230.7	227.3	228.4	231.1	231.5	231.3	230.0	228.0	226.7	227.1	229.4	234.2	239.6	245.7	
60	259.7	255.5	251.2	245.9	242.7	243.0	246.3	248.2	248.0	246.4	241.3	237.7	233.3	234.0	240.2	249.3	258.1	
55	271.4	268.1	264.8	260.6	256.8	255.8	257.3	262.2	263.9	262.9	258.2	253.3	246.7	244.3	248.6	257.1	265.4	
50	278.8	276.1	273.3	271.5	268.6	267.1	267.4	270.0	271.4	271.4	269.5	265.1	260.3	254.9	253.3	254.7	257.9	
45	276.9	275.1	273.5	271.5	270.0	267.9	268.3	268.4	269.7	270.2	270.0	266.8	262.3	255.6	250.2	246.8	245.5	
40	267.1	265.6	264.0	262.5	261.6	259.0	258.2	259.0	259.9	260.1	259.6	256.7	252.2	245.5	242.0	239.2	236.7	
35	253.9	253.0	251.8	250.0	247.4	245.8	245.5	244.6	244.9	244.9	245.0	242.3	238.0	232.4	231.9	232.5	231.3	
30	239.4	239.1	238.6	236.7	233.8	231.9	229.9	228.9	228.2	228.8	229.0	228.8	225.1	221.9	222.2	224.0	222.9	
25	232.8	231.2	229.2	226.7	224.3	221.9	219.5	218.5	217.9	217.9	217.8	218.3	218.4	218.1	216.2	213.6	210.4	
20	232.2	230.7	227.7	221.5	215.1	210.3	207.3	205.3	204.1	204.6	207.0	210.3	214.8	217.6	217.1	213.8	209.1	
15	230.7	229.7	226.1	219.2	212.1	206.2	202.0	199.9	199.8	200.1	202.5	208.3	215.2	218.8	217.9	214.6	210.4	
10	226.1	226.1	225.3	226.5	230.7	235.5	238.7	239.1	239.1	238.9	236.0	228.9	221.6	219.0	217.5	215.6	213.7	
5	239.2	241.6	247.4	256.5	264.8	269.8	272.0	272.3	272.5	269.4	261.7	252.2	244.3	239.3	235.6	233.0		
0				276.2	282.2	290.0	296.3	299.5	300.7	300.6	299.8	296.7	291.2	284.3	277.6	266.5	254.0	247.4

FEBRUARY ZONAL MEAN PRESSURE (N m⁻²)

HEIGHT (Km)	LATITUDE																EXPONENT	
	-80	-70	-60	-50	-40	-30	-20	-10	0	10	20	30	40	50	60	70		80
80	1.320	1.262	1.213	1.173	1.138	1.124	1.130	1.134	1.141	1.144	1.117	1.057	0.974	0.904	0.895	0.881	0.875	E+0
75	3.177	3.037	2.906	2.740	2.585	2.513	2.521	2.534	2.544	2.538	2.452	2.306	2.100	1.917	1.877	1.856	1.844	E+0
70	7.000	6.715	6.429	6.055	5.691	5.503	5.506	5.536	5.556	5.534	5.306	4.955	4.468	4.028	3.899	3.861	3.822	E+0
65	1.432	1.387	1.341	1.279	1.212	1.169	1.160	1.164	1.170	1.169	1.123	1.048	0.940	0.840	0.801	0.787	0.770	E+1
60	2.791	2.729	2.670	2.584	2.473	2.377	2.336	2.338	2.351	2.358	2.294	2.157	1.947	1.733	1.626	1.564	1.500	E+1
55	5.255	5.185	5.121	5.014	4.837	4.652	4.537	4.503	4.517	4.546	4.483	4.268	3.921	3.500	3.236	3.035	2.844	E+1
50	9.682	9.614	9.557	9.419	9.164	8.831	8.596	8.438	8.434	8.497	8.442	8.144	7.601	6.857	6.317	5.849	5.405	E+1
45	1.773	1.769	1.766	1.748	1.707	1.651	1.606	1.572	1.565	1.577	1.571	1.529	1.443	1.322	1.232	1.145	1.056	E+2
40	3.299	3.302	3.306	3.284	3.214	3.126	3.036	2.969	2.951	2.967	2.961	2.903	2.772	2.589	2.444	2.296	2.131	E+2
35	6.313	6.342	6.370	6.345	6.238	6.096	5.928	5.793	5.744	5.782	5.770	5.704	5.516	5.247	4.986	4.703	4.392	E+2
30	1.255	1.261	1.270	1.271	1.259	1.236	1.206	1.162	1.173	1.179	1.177	1.170	1.147	1.107	1.051	0.987	0.926	E+3
25	2.583	2.603	2.628	2.645	2.641	2.607	2.560	2.518	2.502	2.515	2.510	2.494	2.462	2.393	2.282	2.147	2.028	E+3
20	5.366	5.434	5.535	5.644	5.715	5.704	5.652	5.565	5.574	5.596	5.563	5.499	5.388	5.218	5.008	4.774	4.577	E+3

FEBRUARY ZONAL MEAN DENSITY (Kg m⁻³)

HEIGHT (Km)	LATITUDE																EXPONENT	
	-80	-70	-60	-50	-40	-30	-20	-10	0	10	20	30	40	50	60	70		80
80	2.557	2.439	2.325	2.156	1.998	1.917	1.918	1.926	1.932	1.927	1.860	1.747	1.584	1.435	1.397	1.379	1.372	E-5
75	5.495	5.267	5.039	4.681	4.342	4.176	4.187	4.224	4.229	4.189	3.997	3.718	3.331	2.984	2.878	2.858	2.837	E-5
70	1.093	1.058	1.019	0.970	0.918	0.887	0.881	0.885	0.890	0.888	0.847	0.785	0.699	0.620	0.589	0.581	0.570	E-4
65	2.044	2.012	1.980	1.932	1.857	1.783	1.748	1.752	1.762	1.770	1.716	1.610	1.442	1.276	1.192	1.144	1.091	E-4
60	3.743	3.720	3.703	3.660	3.549	3.407	3.303	3.281	3.302	3.334	3.312	3.161	2.907	2.580	2.359	2.186	2.024	E-4
55	6.746	6.737	6.736	6.701	6.561	6.336	6.143	5.984	5.962	6.023	6.048	5.869	5.536	4.991	4.534	4.113	3.733	E-4
50	1.210	1.213	1.218	1.209	1.189	1.152	1.120	1.089	1.083	1.091	1.091	1.070	1.017	0.937	0.869	0.800	0.730	E-3
45	2.231	2.241	2.249	2.243	2.202	2.147	2.085	2.040	2.022	2.033	2.027	1.996	1.916	1.802	1.715	1.616	1.499	E-3
40	4.303	4.331	4.362	4.358	4.281	4.203	4.097	3.994	3.956	3.974	3.974	3.939	3.829	3.673	3.518	3.343	3.137	E-3
35	8.662	8.731	8.813	8.840	8.784	8.638	8.412	8.249	8.171	8.226	8.204	8.201	8.074	7.864	7.490	7.046	6.614	E-3
30	1.825	1.838	1.854	1.870	1.875	1.856	1.827	1.799	1.791	1.796	1.791	1.781	1.775	1.737	1.648	1.535	1.447	E-2
25	3.866	3.922	3.994	4.064	4.101	4.091	4.063	4.014	4.000	4.021	4.014	3.982	3.927	3.822	3.677	3.502	3.358	E-2
20	8.051	8.203	8.468	8.875	9.256	9.448	9.499	9.477	9.511	9.531	9.362	9.109	8.737	8.353	8.036	7.778	7.626	E-2

(note that 1 N m⁻² = 1 Pa = 0.01mb = 10 dynes cm⁻²; 1000 Kg m⁻³ = 1 g cm⁻³)

TABLE II (continued)

HEIGHT COORDINATES

MARCH ZONAL MEAN TEMPERATURE (K)

HEIGHT (Km)	LATITUDE																
	-80	-70	-60	-50	-40	-30	-20	-10	0	10	20	30	40	50	60	70	80
80	203.1	202.9	201.9	203.7	205.8	205.9	205.3	206.9	208.6	208.6	209.5	211.1	210.2	212.2	214.9	213.8	212.0
75	212.6	211.9	211.0	210.6	210.8	210.8	210.2	210.2	210.4	210.5	213.4	217.2	218.4	221.9	222.9	219.7	216.7
70	223.3	221.8	220.9	217.4	216.6	218.5	219.1	217.7	217.2	216.8	219.8	222.8	224.1	226.9	227.2	224.6	222.1
65	236.8	233.3	230.3	226.5	226.6	230.3	231.7	230.6	229.8	229.1	229.0	229.9	229.9	232.0	231.0	229.9	228.6
60	247.1	243.8	241.5	239.3	238.9	241.1	244.4	244.9	245.4	243.6	240.5	239.2	237.9	238.4	238.2	239.9	240.8
55	256.3	254.2	252.9	253.5	254.2	254.9	256.0	260.6	261.9	260.8	257.2	254.2	252.1	250.5	250.1	253.6	256.5
50	263.6	263.8	264.5	266.3	267.3	267.3	267.8	270.2	271.5	270.7	268.8	265.9	264.7	262.4	261.1	261.2	261.9
45	259.7	261.0	263.4	265.7	266.3	266.1	268.3	270.3	271.6	271.3	270.0	267.5	266.0	263.5	260.2	256.6	254.4
40	247.9	248.8	251.4	255.1	256.5	256.4	258.7	260.9	261.9	261.6	260.1	257.2	255.7	252.4	247.9	243.1	240.2
35	235.0	236.7	239.4	241.5	242.1	243.4	244.4	245.5	246.2	246.4	245.4	243.1	240.6	236.4	233.0	231.8	232.0
30	225.7	227.1	228.3	229.1	229.8	230.2	230.5	230.0	229.7	229.8	230.1	229.3	225.5	221.9	221.0	222.4	224.4
25	221.6	221.7	223.3	223.2	222.6	221.6	220.7	220.3	219.3	218.9	218.9	218.9	218.4	218.1	218.2	218.8	219.7
20	224.2	223.8	222.3	219.7	215.3	210.9	207.4	205.6	205.3	205.4	207.3	210.8	215.2	218.2	218.8	217.2	214.6
15	225.4	225.5	223.4	218.5	212.5	206.4	202.0	199.6	199.3	199.9	202.8	208.6	215.2	218.9	219.4	217.6	214.6
10	224.2	223.9	223.3	224.8	229.0	234.3	238.1	239.2	239.3	238.9	235.7	228.7	222.1	219.6	218.9	217.6	215.8
5	235.9	239.8	246.8	255.7	263.5	268.8	271.8	272.3	272.4	272.4	269.8	262.6	254.2	246.8	241.4	237.2	234.0
0			275.0	281.3	289.7	296.0	299.4	301.0	300.9	300.1	297.0	291.4	284.8	279.0	268.5	256.4	248.2

MARCH ZONAL MEAN PRESSURE (N m⁻²)

HEIGHT (Km)	LATITUDE																	EXPONENT
	-80	-70	-60	-50	-40	-30	-20	-10	0	10	20	30	40	50	60	70	80	
80	0.953	0.968	1.006	1.040	1.074	1.107	1.135	1.152	1.159	1.145	1.131	1.107	1.051	1.007	0.943	0.880	0.832	E+0
75	2.132	2.167	2.259	2.326	2.391	2.463	2.532	2.562	2.569	2.535	2.484	2.408	2.288	2.170	2.019	1.900	1.813	E+0
70	4.604	4.692	4.903	5.078	5.227	5.359	5.506	5.586	5.606	5.539	5.365	5.141	4.864	4.565	4.241	4.034	3.888	E+0
65	0.954	0.980	1.031	1.080	1.112	1.129	1.155	1.177	1.184	1.171	1.129	1.075	1.015	0.947	0.881	0.844	0.819	E+1
60	1.908	1.979	2.099	2.219	2.287	2.297	2.331	2.378	2.393	2.377	2.305	2.198	2.080	1.932	1.804	1.727	1.677	E+1
55	3.722	3.889	4.146	4.390	4.514	4.517	4.555	4.610	4.629	4.612	4.519	4.339	4.130	3.843	3.594	3.414	3.301	E+1
50	7.108	7.443	7.927	8.363	8.578	8.574	8.630	8.656	8.665	8.652	8.536	8.259	7.903	7.395	6.933	6.552	6.304	E+1
45	1.351	1.412	1.497	1.572	1.609	1.607	1.611	1.607	1.605	1.604	1.588	1.548	1.485	1.400	1.319	1.254	1.210	E+2
40	2.629	2.736	2.883	2.999	3.061	3.056	3.046	3.023	3.008	3.011	2.991	2.935	2.831	2.688	2.559	2.462	2.396	E+2
35	5.300	5.500	5.741	5.922	6.024	6.002	5.952	5.878	5.834	5.840	5.828	5.756	5.583	5.361	5.174	5.024	4.912	E+2
30	1.107	1.142	1.185	1.217	1.234	1.226	1.212	1.196	1.187	1.188	1.185	1.178	1.155	1.124	1.092	1.060	1.032	E+3
25	2.373	2.441	2.517	2.577	2.609	2.594	2.565	2.535	2.520	2.522	2.520	2.506	2.480	2.432	2.368	2.290	2.219	E+3
20	5.084	5.236	5.393	5.546	5.658	5.669	5.647	5.599	5.579	5.593	5.568	5.513	5.420	5.294	5.150	4.993	4.851	E+3

MARCH ZONAL MEAN DENSITY (Kg m⁻³)

HEIGHT (Km)	LATITUDE																	EXPONENT
	-80	-70	-60	-50	-40	-30	-20	-10	0	10	20	30	40	50	60	70	80	
80	1.635	1.662	1.735	1.778	1.819	1.873	1.926	1.940	1.937	1.912	1.880	1.827	1.742	1.653	1.528	1.433	1.367	E-5
75	3.493	3.562	3.729	3.848	3.952	4.069	4.196	4.247	4.254	4.197	4.055	3.863	3.650	3.408	3.156	3.013	2.914	E-5
70	7.182	7.368	7.732	8.135	8.407	8.547	8.754	8.939	8.993	8.903	8.503	8.041	7.561	7.008	6.503	6.256	6.098	E-5
65	1.404	1.463	1.559	1.662	1.710	1.709	1.737	1.778	1.795	1.781	1.717	1.630	1.539	1.422	1.329	1.279	1.248	E-4
60	2.690	2.828	3.027	3.231	3.335	3.319	3.322	3.383	3.398	3.398	3.339	3.202	3.045	2.823	2.639	2.508	2.427	E-4
55	5.059	5.330	5.712	6.032	6.187	6.174	6.199	6.164	6.158	6.161	6.121	5.946	5.707	5.343	5.006	4.690	4.483	E-4
50	0.939	0.983	1.044	1.094	1.118	1.118	1.123	1.116	1.112	1.113	1.106	1.082	1.040	0.982	0.925	0.874	0.839	E-3
45	1.812	1.884	1.980	2.061	2.105	2.104	2.091	2.071	2.058	2.060	2.049	2.015	1.945	1.850	1.766	1.703	1.657	E-3
40	3.695	3.832	3.994	4.095	4.157	4.152	4.101	4.037	4.001	4.009	4.006	3.974	3.857	3.709	3.596	3.528	3.474	E-3
35	7.856	8.096	8.354	8.542	8.667	8.593	8.483	8.340	8.255	8.255	8.273	8.246	8.083	7.900	7.736	7.548	7.376	E-3
30	1.709	1.752	1.809	1.850	1.870	1.855	1.831	1.811	1.800	1.801	1.795	1.789	1.784	1.764	1.721	1.660	1.601	E-2
25	3.730	3.837	3.927	4.022	4.084	4.077	4.049	4.009	4.001	4.015	4.010	3.987	3.955	3.884	3.781	3.647	3.519	E-2
20	7.899	8.149	8.451	8.792	9.155	9.363	9.405	9.487	9.467	9.489	9.357	9.113	8.774	8.452	8.200	8.009	7.874	E-2

(note that 1 N m⁻² = 1 Pa = 0.01 mb = 10 dynes cm⁻²; 1000 Kg m⁻³ = 1 g cm⁻³)

ORIGINAL PAGE IS
OF POOR QUALITY

TABLE 11 (continued)

HEIGHT COORDINATES

APRIL ZONAL MEAN TEMPERATURE (K)

HEIGHT (Km)	LATITUDE																
	-80	-70	-60	-50	-40	-30	-20	-10	0	10	20	30	40	50	60	70	80
80	228.2	224.6	218.3	214.7	211.4	208.2	207.2	210.7	211.3	209.3	208.5	207.5	204.2	201.6	202.0	200.4	199.5
75	229.7	227.2	223.7	218.4	214.8	212.2	209.7	209.6	208.7	208.1	210.9	214.1	214.7	216.3	217.2	215.6	214.5
70	232.9	230.8	228.5	222.5	219.7	218.5	215.9	213.3	212.6	213.9	219.3	222.2	223.9	226.0	227.1	226.9	226.4
65	241.4	237.9	234.0	228.5	228.3	230.4	228.6	226.1	225.9	226.9	229.6	231.9	233.7	234.9	235.1	234.0	232.8
60	249.9	245.5	241.0	238.5	235.2	240.3	242.0	242.6	243.1	242.1	240.1	241.2	243.1	244.4	244.7	244.9	244.4
55	254.7	250.9	247.3	248.7	252.2	254.5	257.0	259.2	259.7	258.2	255.2	255.4	257.5	258.4	257.8	258.8	259.2
50	258.9	257.2	255.5	257.7	263.4	265.9	267.1	269.2	269.7	269.2	268.2	268.2	269.6	269.5	269.3	269.1	268.7
45	252.8	252.3	252.2	256.1	260.9	263.8	267.0	269.5	270.2	269.7	269.0	269.2	270.4	270.9	268.7	265.5	263.2
40	237.0	236.2	237.9	243.8	248.6	252.3	257.0	260.4	261.6	261.1	259.5	259.0	260.9	260.0	256.2	252.0	249.2
35	220.0	219.5	223.6	229.6	235.3	239.4	243.0	246.5	247.8	247.5	246.0	245.1	245.2	243.5	239.9	235.5	233.3
30	210.3	211.9	215.0	220.6	225.1	228.4	230.6	231.5	231.0	230.4	231.6	230.7	228.4	226.6	225.8	225.2	225.1
25	203.6	209.0	216.3	219.7	221.2	221.6	221.5	221.1	220.5	220.1	220.6	220.4	219.4	219.8	221.5	224.3	227.0
20	212.1	214.6	216.9	217.4	214.9	211.3	208.0	206.4	206.0	206.4	208.5	211.6	215.1	218.6	221.1	222.9	224.1
15	217.1	219.1	219.8	217.6	213.1	207.4	202.5	199.5	199.1	199.8	203.0	208.6	214.6	218.8	221.4	222.9	223.5
10	218.3	219.7	220.6	222.0	226.0	231.6	237.0	239.3	239.7	238.9	235.5	229.4	223.5	221.2	221.1	221.5	221.4
5	233.7	237.8	244.1	252.5	260.7	266.9	271.2	272.4	272.5	272.4	270.2	264.9	257.6	250.8	245.2	240.9	237.9
0			274.5	280.8	288.9	295.0	298.8	301.0	301.1	300.5	297.8	292.6	286.0	280.3	273.1	262.2	253.2

APRIL ZONAL MEAN PRESSURE (N m⁻²)

HEIGHT (Km)	LATITUDE																	EXPONENT
	-80	-70	-60	-50	-40	-30	-20	-10	0	10	20	30	40	50	60	70	80	
80	0.798	0.814	0.853	0.915	1.007	1.067	1.097	1.119	1.120	1.109	1.122	1.141	1.148	1.139	1.113	1.072	1.048	E+0
75	1.655	1.704	1.816	1.976	2.201	2.357	2.440	2.473	2.474	2.462	2.484	2.516	2.544	2.532	2.467	2.393	2.349	E+0
70	3.417	3.539	3.807	4.216	4.749	5.118	5.349	5.451	5.470	5.435	5.397	5.411	5.446	5.384	5.227	5.093	5.012	E+0
65	6.694	6.724	6.785	6.886	7.002	7.078	7.135	7.167	7.173	7.160	7.136	7.128	7.130	7.113	7.079	7.054	7.040	E+1
60	1.373	1.450	1.592	1.818	2.053	2.194	2.310	2.382	2.392	2.367	2.315	2.290	2.282	2.241	2.173	2.127	2.107	E+1
55	2.673	2.854	3.165	3.621	4.064	4.324	4.519	4.640	4.654	4.619	4.555	4.501	4.465	4.372	4.247	4.149	4.109	E+1
50	5.151	5.533	6.186	7.027	7.785	8.226	8.553	8.739	8.752	8.712	8.639	8.536	8.434	8.254	8.023	7.836	7.762	E+1
45	0.993	1.069	1.198	1.349	1.475	1.548	1.601	1.627	1.628	1.621	1.611	1.591	1.568	1.535	1.497	1.469	1.460	E+2
40	1.979	2.133	2.381	2.646	2.857	2.967	3.039	3.064	3.058	3.050	3.039	3.006	2.953	2.894	2.845	2.820	2.823	E+2
35	4.157	4.489	4.961	5.404	5.741	5.895	5.964	5.955	5.922	5.910	5.922	5.866	5.747	5.653	5.622	5.642	5.695	E+2
30	0.916	0.987	1.076	1.149	1.197	1.215	1.217	1.207	1.198	1.198	1.201	1.194	1.176	1.163	1.165	1.180	1.197	E+3
25	2.094	2.222	2.368	2.483	2.560	2.577	2.570	2.547	2.533	2.537	2.537	2.530	2.507	2.491	2.492	2.515	2.540	E+3
20	4.740	4.956	5.176	5.393	5.563	5.633	5.647	5.610	5.596	5.605	5.579	5.546	5.480	5.404	5.371	5.374	5.388	E+3

APRIL ZONAL MEAN DENSITY (Kg m⁻³)

HEIGHT (Km)	LATITUDE																	EXPONENT
	-80	-70	-60	-50	-40	-30	-20	-10	0	10	20	30	40	50	60	70	80	
80	1,219	1,262	1,361	1,484	1,659	1,785	1,845	1,851	1,846	1,845	1,874	1,916	1,958	1,968	1,919	1,865	1,830	E-5
75	2,510	2,612	2,829	3,151	3,569	3,868	4,053	4,110	4,129	4,121	4,103	4,095	4,128	4,078	3,956	3,866	3,814	E-5
70	5,111	5,342	5,604	6,599	7,529	8,161	8,630	8,903	8,964	8,851	8,573	8,483	8,473	8,300	8,018	7,821	7,712	E-5
65	1,001	1,060	1,169	1,351	1,529	1,630	1,729	1,798	1,808	1,782	1,723	1,695	1,684	1,650	1,599	1,566	1,556	E-4
60	1,914	2,057	2,302	2,656	2,990	3,181	3,325	3,421	3,429	3,406	3,358	3,308	3,271	3,194	3,094	3,026	3,003	E-4
55	3,656	3,962	4,459	5,073	5,614	5,920	6,125	6,238	6,244	6,232	6,218	6,139	6,040	5,894	5,739	5,584	5,523	E-4
50	0,693	0,749	0,843	0,950	1,030	1,078	1,115	1,131	1,130	1,127	1,122	1,109	1,090	1,067	1,038	1,014	1,006	E-3
45	1,368	1,476	1,655	1,836	1,970	2,044	2,089	2,103	2,099	2,094	2,086	2,059	2,020	1,974	1,941	1,927	1,933	E-3
40	2,909	3,146	3,487	3,782	4,003	4,097	4,120	4,099	4,072	4,069	4,080	4,043	3,942	3,877	3,869	3,898	3,946	E-3
35	6,582	7,126	7,730	8,200	8,500	8,579	8,549	8,415	8,327	8,319	8,386	8,336	8,165	8,086	8,164	8,344	8,504	E-3
30	1,517	1,623	1,743	1,814	1,853	1,853	1,838	1,817	1,807	1,812	1,806	1,805	1,794	1,788	1,798	1,825	1,853	E-2
25	3,583	3,706	3,814	3,938	4,032	4,052	4,043	4,014	4,005	4,016	4,007	3,998	3,981	3,948	3,919	3,905	3,898	E-2
20	7,786	8,045	8,314	8,642	9,017	9,286	9,457	9,467	9,464	9,462	9,322	9,133	8,875	8,611	8,463	8,401	8,375	E-2

(note that 1 N m⁻² = 1 Pa = 0.01 mb = 10 dynes cm⁻²; 1000 Kg m⁻³ = 1 g cm⁻³)

TABLE 11 (continued)

HEIGHT COORDINATES

MAY ZONAL MEAN TEMPERATURE (K)

HEIGHT (Km)	LATITUDE															
	-80	-70	-60	-50	-40	-30	-20	-10	0	10	20	30	40	50	60	80
80	234.1	229.0	223.3	220.0	214.3	208.0	205.2	207.4	208.2	206.6	203.9	200.7	193.5	187.8	184.9	182.2
75	233.6	231.1	230.0	224.8	218.1	211.3	206.3	204.3	204.5	205.6	207.2	207.1	205.5	206.0	207.3	206.1
70	235.0	235.2	236.6	230.8	223.7	216.9	210.6	206.9	207.4	211.0	215.5	217.5	217.7	220.0	225.1	224.9
65	240.6	241.9	243.7	237.3	231.0	228.9	225.4	222.3	223.4	225.9	228.7	229.9	231.0	233.9	236.7	238.6
60	249.8	250.5	249.3	243.5	238.5	240.1	241.6	243.0	243.5	243.2	242.1	242.8	243.6	247.8	250.9	254.7
55	257.6	257.0	253.2	249.2	248.1	252.0	256.1	258.5	258.7	256.8	255.2	256.6	259.7	262.8	265.5	268.9
50	260.4	259.5	254.8	252.3	255.7	261.3	264.8	266.7	266.7	266.5	267.9	269.2	271.2	273.4	275.3	277.9
45	253.6	251.5	246.8	247.1	255.2	261.0	265.3	265.8	266.0	265.4	267.3	269.7	272.9	274.6	275.6	276.9
40	236.7	234.8	231.8	233.7	241.5	249.8	255.5	258.0	258.7	258.6	258.0	259.4	262.9	263.9	263.9	264.9
35	220.6	217.6	215.0	218.5	228.5	236.2	242.4	246.1	247.3	246.7	245.4	245.7	247.0	247.6	248.0	247.2
30	204.2	202.9	204.7	212.6	220.9	226.9	229.8	231.7	231.4	230.8	231.9	231.9	230.8	230.8	232.0	233.8
25	187.5	196.5	206.6	214.6	219.2	221.1	221.5	221.5	220.6	220.8	222.0	221.8	221.3	222.5	224.2	226.6
20	198.5	204.3	210.4	215.0	215.1	212.3	209.2	207.4	206.8	207.3	209.4	212.5	216.2	220.2	224.1	227.5
15	206.5	210.2	214.5	216.2	214.0	208.6	203.0	199.9	199.7	200.2	203.0	208.2	214.2	219.4	223.4	226.4
10	211.7	214.3	216.8	219.5	223.3	229.4	235.6	238.8	239.5	239.4	237.0	232.1	226.3	223.7	224.8	226.2
5	231.8	236.6	243.4	250.7	258.1	264.6	270.0	272.3	272.5	272.5	271.3	267.5	261.9	255.5	250.3	246.0
0		276.7	280.7	287.5	293.4	297.8	300.5	301.0	300.9	298.7	294.2	287.9	281.6	277.3	269.2	263.6

MAY ZONAL MEAN PRESSURE (N m⁻²)

HEIGHT (Km)	LATITUDE																EXPONENT
	-80	-70	-60	-50	-40	-30	-20	-10	0	10	20	30	40	50	60	70	80
80	0.674	0.734	0.797	0.846	0.925	0.993	1.023	1.034	1.046	1.066	1.095	1.117	1.126	1.167	1.222	1.274	1.316
75	1.377	1.518	1.665	1.792	2.001	2.200	2.300	2.319	2.343	2.390	2.462	2.530	2.596	2.722	2.863	3.014	3.136
70	2.815	3.114	3.407	3.733	4.258	4.796	5.129	5.230	5.280	5.333	5.429	5.556	5.714	5.959	6.220	6.539	6.799
65	0.570	0.629	0.685	0.763	0.889	1.016	1.105	1.141	1.149	1.147	1.152	1.172	1.204	1.246	1.290	1.348	1.397
60	1.132	1.244	1.352	1.532	1.814	2.073	2.262	2.343	2.350	2.339	2.343	2.380	2.438	2.500	2.566	2.664	2.746
55	2.195	2.410	2.636	3.026	3.616	4.097	4.429	4.560	4.571	4.562	4.596	4.656	4.751	4.825	4.920	5.062	5.177
50	4.201	4.622	5.110	5.911	7.031	7.868	8.417	8.617	8.634	8.647	8.708	8.809	8.929	9.023	9.155	9.358	9.500
45	0.808	0.892	0.999	1.158	1.355	1.494	1.584	1.616	1.620	1.620	1.629	1.640	1.655	1.665	1.685	1.717	1.738
40	1.609	1.786	2.019	2.332	2.666	2.885	3.015	3.070	3.070	3.072	3.085	3.095	3.098	3.110	3.145	3.202	3.237
35	3.376	3.774	4.309	4.932	5.478	5.776	5.934	5.984	5.970	5.979	6.024	6.036	6.005	6.021	6.090	6.195	6.276
30	0.750	0.845	0.969	1.084	1.164	1.200	1.213	1.212	1.208	1.212	1.223	1.225	1.220	1.223	1.234	1.252	1.270
25	1.793	1.993	2.217	2.399	2.512	2.553	2.565	2.558	2.551	2.563	2.576	2.582	2.581	2.586	2.601	2.626	2.651
20	4.332	4.649	4.993	5.281	5.480	5.574	5.624	5.624	5.627	5.641	5.641	5.633	5.607	5.574	5.557	5.557	5.563

MAY ZONAL MEAN DENSITY (Kg m⁻³)

HEIGHT (Km)	LATITUDE																EXPONENT
	-80	-70	-60	-50	-40	-30	-20	-10	0	10	20	30	40	50	60	70	80
80	1.003	1.117	1.243	1.340	1.503	1.664	1.737	1.737	1.750	1.797	1.871	1.939	2.028	2.164	2.303	2.435	2.539
75	2.053	2.288	2.522	2.777	3.197	3.626	3.884	3.955	3.992	4.050	4.139	4.255	4.400	4.604	4.811	5.095	5.321
70	0.417	0.461	0.502	0.564	0.663	0.770	0.848	0.881	0.887	0.881	0.878	0.890	0.914	0.944	0.971	1.013	1.049
65	0.826	0.906	0.979	1.120	1.341	1.547	1.709	1.788	1.792	1.769	1.754	1.776	1.815	1.857	1.898	1.957	2.028
60	1.579	1.730	1.889	2.191	2.649	3.007	3.262	3.359	3.362	3.350	3.371	3.416	3.487	3.515	3.562	3.643	3.711
55	2.969	3.267	3.627	4.230	5.077	5.665	6.025	6.145	6.154	6.187	6.274	6.323	6.372	6.397	6.455	6.558	6.621
50	0.562	0.620	0.699	0.816	0.958	1.049	1.107	1.126	1.128	1.131	1.132	1.140	1.147	1.150	1.158	1.173	1.179
45	1.110	1.235	1.410	1.633	1.849	1.995	2.079	2.118	2.121	2.119	2.122	2.119	2.112	2.112	2.130	2.167	2.186
40	2.368	2.650	3.035	3.476	3.846	4.025	4.111	4.145	4.135	4.138	4.166	4.156	4.105	4.106	4.151	4.211	4.260
35	5.331	6.042	6.982	7.863	8.351	8.519	8.528	8.471	8.411	8.441	8.551	8.559	8.470	8.471	8.555	8.701	8.844
30	1.279	1.452	1.648	1.777	1.836	1.842	1.839	1.823	1.818	1.830	1.837	1.840	1.842	1.846	1.853	1.867	1.884
25	3.332	3.534	3.738	3.895	3.992	4.023	4.035	4.027	4.028	4.043	4.042	4.055	4.063	4.049	4.042	4.038	4.033
20	7.603	7.929	8.267	8.559	8.875	9.146	9.366	9.447	9.479	9.480	9.385	9.234	9.035	8.818	8.639	8.511	8.425

(note that 1 N m⁻² = 1 Pa = 0.01 mb = 10 dynes cm⁻²; 1000 Kg m⁻³ = 1 g cm⁻³)

ORIGINAL PAGE IS
OF POOR QUALITY

TABLE II (continued)

HEIGHT COORDINATES

JUNE ZONAL MEAN TEMPERATURE (K)

HEIGHT (Km)	LATITUDE																
	-80	-70	-60	-50	-40	-30	-20	-10	0	10	20	30	40	50	60	70	80
80	227.2	223.0	218.9	216.6	211.4	205.1	201.8	203.2	204.1	202.7	201.0	196.8	185.3	178.6	172.6	170.9	170.4
75	229.2	227.1	226.7	223.5	217.6	208.6	203.8	202.0	202.5	203.1	204.4	202.9	198.7	197.9	198.3	198.8	199.4
70	234.6	234.9	236.5	232.5	224.4	215.5	208.2	205.8	206.2	208.0	210.3	211.3	212.6	215.4	220.0	222.7	224.5
65	243.0	244.3	246.3	241.2	233.9	228.8	224.4	222.0	222.7	223.9	224.4	225.0	229.0	233.4	239.0	242.3	244.7
60	254.3	255.4	254.3	248.4	241.5	241.1	241.2	242.6	243.1	243.3	242.1	242.3	245.0	250.6	255.8	260.7	264.4
55	265.0	264.0	258.9	253.2	248.7	251.6	255.1	257.5	257.5	256.6	255.6	257.2	259.7	265.5	269.5	274.7	278.8
50	267.3	265.1	259.5	254.5	254.7	260.5	264.3	264.8	264.4	264.6	266.2	267.7	269.8	273.9	277.7	282.2	285.9
45	257.1	254.9	250.6	247.3	252.8	259.3	263.7	262.5	262.5	263.1	265.2	268.0	271.6	274.3	277.8	281.1	283.4
40	240.1	239.4	235.0	231.4	236.9	247.1	253.4	254.7	255.0	254.7	255.3	257.8	260.8	264.6	267.7	270.7	271.9
35	223.4	222.3	215.7	212.6	221.8	232.5	240.5	244.1	244.7	243.7	243.1	244.9	246.9	249.7	252.5	255.1	255.7
30	199.8	199.9	200.5	206.6	217.1	225.7	228.7	230.7	230.4	230.4	231.5	232.1	233.6	235.1	237.6	239.7	241.1
25	180.2	188.8	200.4	211.2	218.1	220.7	221.3	220.3	220.3	221.0	221.9	222.5	223.4	225.1	227.8	230.3	232.9
20	191.5	198.9	206.6	213.3	215.2	212.9	210.2	208.8	208.1	208.6	210.2	212.7	216.7	221.6	225.9	229.6	232.2
15	198.0	204.0	210.8	215.9	215.6	209.7	203.8	200.8	200.8	201.2	203.3	207.5	213.7	220.1	224.5	227.9	230.7
10	207.1	210.4	213.9	218.0	222.4	228.8	235.5	238.3	238.9	239.1	238.6	236.0	230.6	226.8	226.1	227.2	228.8
5	231.1	235.0	241.7	248.9	255.5	262.7	269.3	272.0	272.2	272.3	272.1	270.2	265.6	260.2	255.9	252.5	249.5
0			274.2	279.9	286.3	292.0	296.9	300.0	300.7	300.8	299.5	296.2	290.1	283.1	281.3	276.2	271.2

JUNE ZONAL MEAN PRESSURE (N m⁻²)

HEIGHT (Km)	LATITUDE																EXPONENT
	-80	-70	-60	-50	-40	-30	-20	-10	0	10	20	30	40	50	60	70	
80	0.612	0.690	0.764	0.809	0.879	0.948	0.977	0.984	0.991	1.001	1.028	1.056	1.083	1.172	1.288	1.407	E+0
75	1.272	1.451	1.619	1.727	1.911	2.120	2.221	2.236	2.245	2.274	2.339	2.429	2.583	2.843	3.170	3.474	E+0
70	2.622	2.998	3.333	3.594	4.071	4.664	4.997	5.080	5.090	5.129	5.232	5.440	5.817	6.384	7.049	7.682	E+0
65	0.529	0.603	0.666	0.728	0.845	0.990	1.084	1.112	1.112	1.114	1.130	1.171	1.243	1.346	1.461	1.580	E+1
60	1.041	1.181	1.302	1.444	1.708	2.016	2.222	2.282	2.278	2.278	2.315	2.398	2.517	2.691	2.878	3.229	E+1
55	1.988	2.255	2.505	2.817	3.388	3.980	4.359	4.452	4.440	4.445	4.532	4.689	4.890	5.154	5.454	5.762	E+1
50	0.373	0.425	0.479	0.546	0.659	0.766	0.830	0.844	0.843	0.844	0.861	0.888	0.922	0.960	1.008	1.054	E+2
45	0.709	0.812	0.925	1.065	1.276	1.459	1.565	1.594	1.591	1.592	1.617	1.660	1.712	1.772	1.845	1.916	E+2
40	1.399	1.608	1.855	2.152	2.534	2.833	2.997	3.050	3.046	3.046	3.082	3.145	3.218	3.307	3.420	3.530	E+2
35	2.903	3.344	3.922	4.612	5.305	5.727	5.928	5.990	5.970	5.987	6.060	6.151	6.257	6.377	6.551	6.710	E+2
30	0.645	0.746	0.888	1.039	1.148	1.199	1.218	1.219	1.214	1.220	1.235	1.249	1.265	1.283	1.307	1.333	E+3
25	1.600	1.810	2.084	2.342	2.499	2.556	2.581	2.579	2.570	2.578	2.601	2.630	2.654	2.682	2.716	2.750	E+3
20	3.991	4.334	4.783	5.197	5.458	5.579	5.652	5.667	5.658	5.664	5.692	5.726	5.744	5.744	5.749	5.764	E+3

JUNE ZONAL MEAN DENSITY (Kg m⁻³)

HEIGHT (Km)	LATITUDE																EXPONENT
	-80	-70	-60	-50	-40	-30	-20	-10	0	10	20	30	40	50	60	70	
80	0.938	1.078	1.216	1.301	1.448	1.609	1.687	1.687	1.691	1.721	1.782	1.869	2.036	2.286	2.599	2.867	E-5
75	1.934	2.226	2.488	2.691	3.060	3.540	3.796	3.857	3.863	3.901	3.987	4.169	4.528	5.003	5.570	6.089	E-5
70	0.389	0.445	0.491	0.538	0.632	0.754	0.836	0.860	0.860	0.859	0.867	0.897	0.953	1.033	1.116	1.202	E-4
65	0.758	0.860	0.943	1.052	1.258	1.507	1.682	1.744	1.740	1.734	1.754	1.814	1.890	2.010	2.130	2.271	E-4
60	1.426	1.612	1.784	2.025	2.464	2.914	3.209	3.278	3.265	3.261	3.331	3.448	3.580	3.740	3.920	4.113	E-4
55	2.614	2.976	3.371	3.876	4.746	5.512	5.953	6.024	6.006	6.033	6.177	6.352	6.560	6.763	7.049	7.308	E-4
50	0.487	0.559	0.643	0.747	0.902	1.024	1.094	1.111	1.110	1.111	1.127	1.156	1.190	1.222	1.264	1.301	E-3
45	0.960	1.109	1.285	1.501	1.758	1.960	2.067	2.115	2.112	2.109	2.124	2.157	2.196	2.251	2.314	2.375	E-3
40	2.030	2.340	2.749	3.240	3.726	3.993	4.120	4.172	4.161	4.166	4.206	4.250	4.298	4.354	4.451	4.543	E-3
35	4.527	5.240	6.335	7.557	8.332	8.581	8.587	8.551	8.498	8.559	8.684	8.752	8.828	8.897	9.039	9.166	E-3
30	1.125	1.300	1.543	1.752	1.842	1.850	1.855	1.841	1.835	1.844	1.858	1.875	1.887	1.901	1.917	1.937	E-2
25	3.093	3.341	3.622	3.863	3.992	4.035	4.063	4.074	4.066	4.064	4.084	4.119	4.139	4.151	4.153	4.161	E-2
20	7.268	7.594	8.065	8.490	8.835	9.127	9.368	9.454	9.469	9.461	9.434	9.381	9.233	9.029	8.866	8.745	E-2

(note that 1 N m⁻² = 1 Pa = 0.01 mb = 10 dynes cm⁻²; 1000 Kg m⁻³ = 1 g cm⁻³)

TABLE 11 (continued)

HEIGHT COORDINATES

JULY ZONAL MEAN TEMPERATURE (K)

HEIGHT (km)	LATITUDE																
	-80	-70	-60	-50	-40	-30	-20	-10	0	10	20	30	40	50	60	70	80
80	219.9	217.7	216.8	214.9	209.6	204.9	201.9	201.6	202.1	202.7	202.6	198.6	189.3	177.7	169.8	168.3	169.1
75	224.0	222.6	222.8	220.5	215.0	209.2	205.7	204.3	204.3	204.8	205.8	204.6	200.7	196.3	194.6	195.9	197.9
70	231.7	230.8	231.4	227.4	219.7	214.2	210.7	210.1	210.6	211.2	210.8	210.3	210.9	213.9	217.7	221.3	224.0
65	243.6	242.4	241.1	235.3	228.3	224.1	224.2	224.7	225.8	225.5	224.3	223.1	224.9	230.6	237.3	242.9	246.3
60	258.7	256.1	251.3	243.5	236.6	236.8	239.3	242.7	244.2	244.5	242.0	240.8	242.5	248.3	254.8	260.7	264.6
55	270.8	267.1	259.9	252.2	247.5	251.1	255.2	257.9	258.5	257.2	255.0	254.8	256.9	262.2	268.2	273.6	278.2
50	271.9	269.0	264.0	258.1	258.5	262.1	265.1	265.1	264.4	264.1	263.9	264.7	267.2	271.1	275.4	280.4	284.5
45	261.1	261.0	258.1	254.5	257.0	260.8	262.9	262.0	261.0	260.8	263.1	264.5	267.7	270.9	275.3	278.8	281.1
40	248.2	249.1	246.1	240.9	241.8	248.0	251.5	252.4	252.5	251.5	251.5	254.2	257.6	261.5	265.6	268.7	269.9
35	234.0	233.2	227.5	222.3	226.7	233.6	238.7	240.8	241.5	240.5	240.8	242.0	244.5	248.4	251.7	254.2	254.9
30	209.2	208.3	206.5	210.4	220.3	227.0	228.5	229.1	228.5	228.8	229.1	230.6	232.6	235.7	237.7	240.0	241.2
25	179.2	186.9	197.4	211.2	219.2	221.0	221.2	220.0	219.4	220.0	220.8	222.1	223.7	225.8	228.3	230.8	233.3
20	186.5	194.0	202.8	211.3	215.1	213.6	210.9	209.3	208.6	209.0	210.5	212.6	216.3	221.6	226.3	229.8	232.3
15	192.2	197.8	206.4	214.2	215.5	210.1	204.3	202.1	202.1	202.5	204.2	207.5	212.9	219.8	224.6	228.1	230.9
10	202.5	205.5	210.8	216.6	222.3	229.1	235.4	237.8	238.1	238.6	239.0	238.6	234.8	230.0	227.9	227.9	228.8
5	229.9	233.0	240.4	247.7	254.7	262.3	269.2	271.9	271.8	271.9	272.1	271.8	268.6	263.6	259.7	256.5	253.6
0			273.9	279.4	286.2	291.3	295.9	299.3	300.1	300.8	299.9	298.0	293.1	285.4	283.6	279.6	274.2

JULY ZONAL MEAN PRESSURE (N m⁻²)

HEIGHT (Km)	LATITUDE																	EXPONENT
	-80	-70	-60	-50	-40	-30	-20	-10	0	10	20	30	40	50	60	70	80	
80	0.620	0.683	0.773	0.828	0.881	0.938	0.982	1.000	1.003	1.003	1.006	1.016	1.050	1.126	1.238	1.379	1.496	E+0
75	1.318	1.460	1.653	1.781	1.931	2.098	2.221	2.269	2.276	2.271	2.272	2.321	2.467	2.747	3.104	3.457	3.728	E+0
70	2.748	3.057	3.452	3.796	4.161	4.613	4.952	5.080	5.090	5.073	5.062	5.191	5.596	6.202	6.979	7.709	8.239	E+0
65	0.557	0.621	0.702	0.774	0.878	0.990	1.070	1.097	1.096	1.092	1.093	1.124	1.198	1.317	1.457	1.587	1.681	E+1
60	1.087	1.218	1.387	1.559	1.804	2.046	2.200	2.245	2.233	2.222	2.242	2.316	2.453	2.653	2.878	3.087	3.242	E+1
55	2.051	2.315	2.673	3.067	3.612	4.070	4.333	4.377	4.339	4.326	4.394	4.551	4.798	5.121	5.470	5.791	6.021	E+1
50	0.380	0.433	0.508	0.592	0.700	0.781	0.823	0.829	0.822	0.821	0.838	0.867	0.910	0.960	1.014	1.062	1.094	E+2
45	0.716	0.817	0.967	1.140	1.341	1.482	1.552	1.564	1.555	1.554	1.580	1.633	1.702	1.785	1.868	1.938	1.983	E+2
40	1.389	1.584	1.888	2.247	2.632	2.868	2.982	3.005	2.991	2.994	3.036	3.121	3.231	3.359	3.482	3.588	3.661	E+2
35	2.800	3.187	3.845	4.661	5.418	5.784	5.934	5.949	5.910	5.937	6.018	6.164	6.326	6.515	6.690	6.849	6.970	E+2
30	0.601	0.686	0.840	1.022	1.156	1.206	1.223	1.220	1.212	1.218	1.235	1.260	1.285	1.311	1.337	1.361	1.383	E+3
25	1.449	1.636	1.962	2.290	2.497	2.565	2.594	2.590	2.578	2.587	2.617	2.659	2.700	2.736	2.773	2.806	2.835	E+3
20	3.699	3.995	4.577	5.099	5.447	5.591	5.669	5.689	5.678	5.689	5.732	5.796	5.836	5.848	5.860	5.874	5.889	E+3

JULY ZONAL MEAN DENSITY (kg m⁻³)

HEIGHT (Km)	LATITUDE																EXPONENT	
	-80	-70	-60	-50	-40	-30	-20	-10	0	10	20	30	40	50	60	70		80
80	0.982	1.093	1.242	1.341	1.464	1.595	1.694	1.728	1.729	1.724	1.730	1.783	1.932	2.206	2.541	2.854	3.082	E-5
75	2.049	2.284	2.585	2.814	3.128	3.493	3.761	3.869	3.882	3.864	3.847	3.951	4.281	4.873	5.557	6.147	6.562	E-5
70	0.413	0.461	0.520	0.575	0.660	0.750	0.819	0.842	0.842	0.837	0.837	0.860	0.918	1.010	1.117	1.213	1.281	E-4
65	0.797	0.893	1.014	1.146	1.340	1.538	1.662	1.701	1.691	1.686	1.698	1.756	1.855	1.989	2.139	2.276	2.377	E-4
60	1.464	1.657	1.923	2.229	2.657	3.010	3.202	3.223	3.186	3.165	3.227	3.351	3.524	3.723	3.935	4.126	4.269	E-4
55	2.638	3.018	3.583	4.237	5.084	5.647	5.915	5.912	5.847	5.859	6.003	6.222	6.507	6.805	7.105	7.373	7.540	E-4
50	0.487	0.560	0.670	0.799	0.944	1.038	1.082	1.089	1.083	1.083	1.106	1.141	1.186	1.234	1.282	1.320	1.339	E-3
45	0.955	1.090	1.305	1.560	1.818	1.980	2.057	2.079	2.076	2.075	2.093	2.151	2.215	2.295	2.363	2.422	2.458	E-3
40	1.950	2.214	2.673	3.250	3.792	4.030	4.131	4.147	4.127	4.147	4.206	4.278	4.369	4.475	4.567	4.652	4.725	E-3
35	4.169	4.761	5.887	7.304	8.325	8.626	8.660	8.606	8.525	8.599	8.705	8.875	9.013	9.139	9.260	9.387	9.526	E-3
30	1.000	1.147	1.418	1.693	1.828	1.852	1.864	1.855	1.847	1.855	1.878	1.904	1.925	1.937	1.959	1.976	1.997	E-2
25	2.817	3.050	3.463	3.778	3.968	4.044	4.085	4.101	4.094	4.093	4.129	4.171	4.204	4.222	4.232	4.235	4.233	E-2
20	6.910	7.176	7.863	8.409	8.822	9.118	9.365	9.469	9.482	9.483	9.486	9.496	9.400	9.193	9.020	8.905	8.831	E-2

(note that 1 N m⁻² = 1 Pa = 0.01 mb = 10 dynes cm⁻²; 1000 kg m⁻³ = 1 g cm⁻³)

ORIGINAL PAGE IS
OF POOR QUALITY

TABLE 11 (continued)

HEIGHT COORDINATES

AUGUST ZONAL MEAN TEMPERATURE (K)

HEIGHT (Km)	LATITUDE																
	-80	-70	-60	-50	-40	-30	-20	-10	0	10	20	30	40	50	60	70	80
80	217.8	217.9	218.4	215.4	211.1	207.9	205.4	202.8	203.2	204.5	205.3	203.9	196.8	187.7	179.8	177.7	179.8
75	221.7	221.2	222.6	220.7	216.9	213.3	210.2	207.0	207.0	208.2	209.9	209.7	206.4	202.1	199.2	199.4	202.0
70	227.4	225.9	226.6	224.4	220.6	217.3	215.0	213.4	214.8	216.5	217.1	216.4	215.6	215.0	218.8	221.1	224.3
65	239.5	235.3	231.7	229.2	225.6	223.7	224.9	226.4	228.2	229.2	229.5	228.0	226.7	229.0	235.0	240.6	244.8
60	255.4	249.2	241.1	235.3	231.8	234.5	238.2	242.5	244.2	244.7	243.8	241.4	240.7	243.2	248.9	254.8	258.8
55	270.7	264.1	254.3	245.9	244.2	250.1	255.1	259.0	259.6	258.1	254.1	252.6	253.1	256.5	260.9	265.1	268.7
50	275.2	270.5	263.4	255.9	256.3	261.3	266.1	267.4	267.1	266.0	263.8	263.1	263.8	266.1	269.2	272.4	275.5
45	269.1	267.5	263.1	256.8	257.0	261.1	265.2	265.6	265.0	263.7	263.6	262.9	264.9	266.9	269.5	271.6	273.0
40	258.9	259.7	255.8	247.8	245.7	249.0	253.3	255.0	254.9	253.5	251.9	252.5	255.5	257.2	259.5	261.6	262.2
35	244.9	245.7	240.8	233.5	233.0	236.3	240.0	241.3	241.4	240.6	240.4	240.2	241.9	245.1	247.3	248.6	248.7
30	219.5	221.0	218.9	220.0	224.8	228.1	228.3	228.6	227.9	228.3	228.5	229.6	230.8	233.5	234.7	235.8	236.4
25	183.2	192.8	204.3	215.4	221.0	221.7	220.7	219.2	218.2	218.7	219.5	221.1	222.7	224.5	226.3	227.9	229.4
20	187.6	194.5	204.3	213.4	217.0	214.6	211.3	209.9	209.4	209.3	210.4	212.6	216.1	221.0	225.0	227.7	229.8
15	191.4	196.7	205.8	214.4	215.9	210.5	204.4	202.0	202.0	202.4	204.1	207.2	212.4	219.2	223.9	226.9	229.3
10	201.0	204.9	210.6	217.2	223.0	229.3	235.3	237.7	237.9	238.5	239.1	238.6	234.8	229.6	227.0	226.4	227.1
5	229.3	234.4	241.0	247.9	254.5	262.1	269.4	271.8	271.6	271.9	272.4	271.9	268.8	263.2	256.5	254.8	251.5
0			273.0	278.2	285.3	291.0	295.8	299.0	299.9	300.9	300.2	298.9	294.8	287.0	283.8	279.3	273.4

AUGUST ZONAL MEAN PRESSURE (N m⁻²)

HEIGHT (Km)	LATITUDE																	EXPONENT
	-80	-70	-60	-50	-40	-30	-20	-10	0	10	20	30	40	50	60	70	80	
80	0.681	0.764	0.843	0.875	0.916	0.980	1.041	1.054	1.061	1.069	1.067	1.060	1.057	1.085	1.147	1.230	1.324	E+0
75	1.456	1.634	1.797	1.881	1.995	2.158	2.316	2.373	2.389	2.396	2.379	2.371	2.418	2.556	2.770	2.989	3.183	E+0
70	3.074	3.455	3.780	3.980	4.275	4.685	5.073	5.251	5.269	5.258	5.201	5.191	5.333	5.682	6.165	6.628	6.986	E+0
65	6.631	0.716	0.786	0.833	0.905	1.000	1.085	1.123	1.121	1.113	1.100	1.102	1.137	1.205	1.290	1.369	1.427	E+1
60	1.246	1.432	1.600	1.714	1.882	2.079	2.237	2.293	2.276	2.254	2.228	2.247	2.329	2.452	2.579	2.692	2.777	E+1
55	2.359	2.756	3.153	3.448	3.812	4.155	4.407	4.465	4.421	4.383	4.363	4.429	4.587	4.801	4.984	5.141	5.250	E+1
50	4.363	5.164	6.033	6.728	7.450	7.995	8.375	8.425	8.337	8.296	8.333	8.485	8.778	9.118	9.396	9.605	9.740	E+1
45	0.810	0.965	1.142	1.295	1.431	1.518	1.573	1.579	1.564	1.560	1.573	1.603	1.656	1.709	1.752	1.784	1.798	E+2
40	1.535	1.831	2.187	2.521	2.795	2.932	3.003	3.006	2.982	2.985	3.015	3.078	3.160	3.250	3.312	3.356	3.379	E+2
35	3.000	3.567	4.313	5.087	5.656	5.881	5.946	5.931	5.878	5.901	5.982	6.102	6.226	6.367	6.454	6.512	6.551	E+2
30	0.621	0.736	0.900	1.074	1.185	1.218	1.224	1.217	1.206	1.212	1.229	1.254	1.274	1.292	1.304	1.312	1.319	E+3
25	1.446	1.683	2.020	2.341	2.535	2.582	2.599	2.589	2.573	2.585	2.615	2.657	2.691	2.712	2.724	2.734	2.740	E+3
20	3.666	4.060	4.632	5.169	5.496	5.613	5.681	5.689	5.672	5.692	5.738	5.798	5.825	5.813	5.790	5.770	5.749	E+3

AUGUST ZONAL MEAN DENSITY (kg m⁻³)

HEIGHT (Km)	LATITUDE																	EXPONENT
	-80	-70	-60	-50	-40	-30	-20	-10	0	10	20	30	40	50	60	70	80	
80	1.089	1.221	1.344	1.415	1.511	1.641	1.765	1.810	1.818	1.821	1.811	1.811	1.872	2.014	2.222	2.410	2.566	E-5
75	2.288	2.572	2.811	2.969	3.205	3.525	3.838	3.993	4.021	4.010	3.949	3.939	4.081	4.404	4.844	5.223	5.489	E-5
70	0.471	0.533	0.581	0.618	0.675	0.751	0.822	0.857	0.855	0.846	0.835	0.835	0.862	0.916	0.982	1.044	1.085	E-4
65	0.918	1.059	1.182	1.266	1.398	1.557	1.680	1.728	1.712	1.692	1.670	1.683	1.747	1.834	1.912	1.982	2.030	E-4
60	1.700	2.002	2.312	2.537	2.828	3.088	3.272	3.294	3.247	3.209	3.184	3.242	3.370	3.513	3.609	3.681	3.738	E-4
55	3.036	3.635	4.319	4.884	5.439	5.788	6.019	6.007	5.932	5.915	5.962	6.109	6.314	6.520	6.655	6.756	6.807	E-4
50	0.552	0.665	0.798	0.916	1.013	1.066	1.096	1.098	1.087	1.086	1.100	1.124	1.159	1.189	1.216	1.228	1.232	E-3
45	1.048	1.256	1.512	1.756	1.940	2.025	2.066	2.070	2.056	2.060	2.078	2.125	2.178	2.231	2.264	2.288	2.294	E-3
40	2.066	2.456	2.979	3.543	3.962	4.103	4.130	4.107	4.076	4.102	4.170	4.247	4.309	4.402	4.447	4.470	4.490	E-3
35	4.268	5.057	6.240	7.588	8.456	8.670	8.630	8.564	8.482	8.544	8.668	8.852	8.966	9.050	9.091	9.126	9.177	E-3
30	0.986	1.160	1.433	1.700	1.837	1.861	1.868	1.854	1.844	1.850	1.873	1.903	1.923	1.928	1.935	1.939	1.944	E-2
25	2.750	3.041	3.444	3.787	3.996	4.057	4.102	4.114	4.108	4.118	4.149	4.187	4.210	4.208	4.193	4.178	4.161	E-2
20	6.807	7.273	7.899	8.440	8.824	9.112	9.366	9.440	9.434	9.474	9.500	9.501	9.389	9.163	8.964	8.829	8.716	E-2

(note that 1 N m⁻² = 1 Pa = 0.01 mb = 10 dynes cm⁻²; 1000 kg m⁻³ = 1 g cm⁻³)

TABLE 11 (continued)

HEIGHT COORDINATES

SEPTEMBER ZONAL MEAN TEMPERATURE (K)

HEIGHT (Km)	LATITUDE															
	-80	-70	-60	-50	-40	-30	-20	-10	0	10	20	30	40	50	60	80
80	212.8	213.6	214.5	211.5	209.7	208.0	206.6	205.5	205.9	206.3	206.0	206.8	205.3	201.8	199.3	199.1
75	218.6	220.0	223.0	221.6	218.1	214.2	210.5	207.5	207.6	209.1	210.2	211.5	210.7	209.2	208.8	209.4
70	226.4	226.2	228.1	227.0	224.1	220.1	217.1	213.9	214.4	216.1	218.3	218.6	217.0	216.8	219.4	220.6
65	236.4	233.4	232.6	231.9	229.6	227.6	226.6	226.5	226.9	228.5	230.1	229.8	226.9	226.2	229.6	232.8
60	252.6	245.8	239.8	237.1	236.2	237.3	238.5	241.4	242.4	242.3	242.8	240.2	238.6	238.8	241.1	243.6
55	270.8	261.2	250.9	246.9	248.2	252.4	255.5	258.4	258.9	257.9	254.5	253.3	252.1	251.6	252.0	253.7
50	278.0	269.4	260.7	256.7	259.0	263.2	266.7	268.1	268.4	267.4	266.0	265.3	264.4	263.5	262.5	262.2
45	277.2	270.9	263.5	258.3	259.1	263.2	267.1	268.2	268.2	267.1	265.6	263.5	263.2	262.8	260.9	258.3
40	273.5	268.3	258.6	249.4	248.0	251.6	256.6	258.4	258.4	257.2	255.2	252.9	253.2	252.3	249.6	246.0
35	262.7	257.3	246.1	236.6	235.3	238.8	242.9	244.5	244.0	243.1	241.7	240.4	239.6	239.7	238.5	234.8
30	237.4	235.0	229.0	225.1	225.7	228.3	229.5	229.7	229.6	229.7	229.7	228.7	228.7	228.4	228.0	226.7
25	202.4	208.1	214.1	220.8	222.9	221.8	220.2	219.2	218.2	218.3	219.1	220.1	221.0	221.6	222.0	221.8
20	196.6	200.5	208.3	216.7	218.3	214.6	210.8	209.0	208.7	208.8	210.2	212.8	216.0	219.6	222.0	223.0
15	193.8	198.7	207.2	215.8	216.7	210.6	204.4	201.7	201.6	201.8	203.2	206.3	212.0	218.2	222.2	224.1
10	201.6	205.2	211.3	218.2	223.7	229.8	235.5	238.1	238.5	238.8	238.6	236.6	231.4	226.4	224.1	223.6
5	229.5	234.2	241.2	248.3	255.6	263.4	269.6	271.9	272.0	272.3	272.2	270.8	266.1	259.3	253.8	249.5
0			274.1	278.8	285.3	291.0	295.9	299.1	299.8	300.8	300.3	298.5	293.5	286.1	281.3	275.5

SEPTEMBER ZONAL MEAN PRESSURE (N m⁻²)

HEIGHT (Km)	LATITUDE																	EXPONENT
	-80	-70	-60	-50	-40	-30	-20	-10	0	10	20	30	40	50	60	70	80	
80	0.881	0.898	0.931	0.962	1.007	1.052	1.084	1.089	1.087	1.092	1.093	1.077	1.041	1.005	0.989	0.971	0.960	E+0
75	1.910	1.939	1.995	2.077	2.194	2.316	2.411	2.437	2.434	2.436	2.435	2.388	2.316	2.262	2.243	2.192	2.175	E+0
70	4.055	4.106	4.182	4.368	4.664	4.990	5.258	5.381	5.367	5.343	5.306	5.191	5.062	4.957	4.898	4.775	4.739	E+0
65	0.838	0.852	0.866	0.906	0.975	1.053	1.117	1.149	1.145	1.133	1.118	1.094	1.076	1.056	1.034	1.000	0.986	E+1
60	1.667	1.720	1.763	1.852	2.002	2.165	2.296	2.350	2.334	2.305	2.267	2.228	2.208	2.172	2.107	2.022	1.972	E+1
55	3.169	3.338	3.498	3.711	4.008	4.294	4.519	4.589	4.548	4.501	4.447	4.398	4.377	4.309	4.171	3.978	3.851	E+1
50	5.849	6.289	6.748	7.227	7.762	8.217	8.578	8.660	8.574	8.506	8.459	8.388	8.375	8.263	8.007	7.631	7.369	E+1
45	1.072	1.173	1.282	1.387	1.481	1.554	1.606	1.617	1.600	1.591	1.588	1.580	1.580	1.563	1.521	1.456	1.410	E+2
40	1.981	2.193	2.444	2.690	2.877	2.982	3.049	3.058	3.024	3.017	3.027	3.027	3.030	3.003	2.944	2.844	2.770	E+2
35	3.712	4.167	4.767	5.391	5.782	5.937	5.982	5.973	5.913	5.916	5.964	5.996	6.017	5.970	5.887	5.747	5.633	E+2
30	0.730	0.827	0.972	1.124	1.207	1.225	1.223	1.217	1.206	1.208	1.220	1.233	1.239	1.230	1.217	1.198	1.181	E+3
25	1.586	1.786	2.096	2.404	2.568	2.596	2.596	2.586	2.564	2.570	2.594	2.621	2.633	2.617	2.591	2.559	2.530	E+3
20	3.740	4.121	4.693	5.218	5.535	5.641	5.686	5.692	5.667	5.672	5.709	5.732	5.721	5.652	5.574	5.499	5.436	E+3

SEPTEMBER ZONAL MEAN DENSITY (Kg m⁻³)

HEIGHT (Km)	LATITUDE																		EXPONENT
	-80	-70	-60	-50	-40	-30	-20	-10	0	10	20	30	40	50	60	70	80		
80	1.442	1.464	1.513	1.585	1.673	1.762	1.828	1.846	1.840	1.844	1.848	1.814	1.766	1.734	1.729	1.687	1.679	E-5	
75	3.043	3.071	3.117	3.265	3.505	3.766	3.989	4.091	4.084	4.059	4.035	3.933	3.829	3.766	3.742	3.640	3.618	E-5	
70	6.239	6.324	6.387	6.702	7.250	7.895	8.438	8.761	8.723	8.614	8.467	8.272	8.127	7.967	7.777	7.542	7.453	E-5	
65	1.235	1.272	1.297	1.362	1.479	1.611	1.717	1.767	1.758	1.728	1.692	1.658	1.652	1.627	1.569	1.497	1.454	E-4	
60	2.300	2.438	2.562	2.720	2.953	3.178	3.354	3.391	3.355	3.315	3.252	3.231	3.224	3.169	3.044	2.892	2.780	E-4	
55	4.076	4.451	4.857	5.236	5.625	5.928	6.161	6.187	6.119	6.080	6.087	6.048	6.048	5.965	5.767	5.463	5.240	E-4	
50	0.733	0.813	0.902	0.981	1.044	1.088	1.121	1.126	1.113	1.108	1.108	1.101	1.103	1.092	1.063	1.014	0.981	E-3	
45	1.347	1.508	1.695	1.871	1.991	2.057	2.094	2.101	2.078	2.075	2.083	2.088	2.092	2.072	2.032	1.964	1.916	E-3	
40	2.523	2.847	3.292	3.758	4.041	4.129	4.139	4.123	4.077	4.085	4.132	4.170	4.169	4.146	4.108	4.026	3.949	E-3	
35	4.923	5.642	6.748	7.937	8.560	8.661	8.579	8.510	8.442	8.478	8.595	8.689	8.749	8.676	8.598	8.525	8.426	E-3	
30	1.071	1.226	1.479	1.739	1.863	1.869	1.856	1.846	1.829	1.833	1.851	1.877	1.887	1.876	1.859	1.841	1.824	E-2	
25	2.729	2.991	3.411	3.793	4.013	4.078	4.107	4.110	4.093	4.102	4.124	4.149	4.150	4.114	4.066	4.019	3.980	E-2	
20	6.627	7.162	7.849	8.388	8.833	9.157	9.397	9.485	9.459	9.466	9.462	9.386	9.226	8.969	8.747	8.592	8.481	E-2	

(note that 1 N m⁻² = 1 Pa = 0.01 mb = 10 dynes cm⁻²; 1000 Kg m⁻³ = 1 g cm⁻³)

ORIGINAL PAGE IS OF POOR QUALITY

TABLE II (continued)

HEIGHT COORDINATES

OCTOBER ZONAL MEAN TEMPERATURE (K)

HEIGHT (Km)	LATITUDE															
	-80	-70	-60	-50	-40	-30	-20	-10	0	10	20	30	40	50	60	80
80	200.2	201.9	203.8	202.7	204.7	205.9	206.3	208.3	211.3	211.0	208.4	208.8	210.7	213.4	215.1	220.8
75	215.6	217.3	219.1	217.5	219.5	212.7	208.9	207.2	208.4	209.6	210.6	212.5	214.3	216.8	220.6	223.6
70	228.2	228.8	229.1	227.6	224.7	221.4	217.9	212.9	211.8	212.9	216.0	218.2	219.0	221.0	225.6	228.0
65	236.5	236.4	236.6	235.9	233.9	231.7	228.8	226.0	224.7	225.3	228.1	229.7	227.7	227.4	231.8	236.1
60	251.3	248.3	245.2	243.3	242.0	241.1	240.0	241.6	241.9	241.5	241.2	239.7	239.0	238.3	240.0	244.0
55	267.2	261.7	256.5	254.7	254.6	255.1	255.4	257.5	258.6	258.1	256.3	254.4	252.4	249.7	247.8	253.3
50	279.3	273.1	267.7	264.9	266.3	267.5	268.1	268.1	268.6	268.0	266.5	266.0	263.7	259.0	256.5	255.8
45	284.0	277.1	269.8	266.2	266.1	267.5	268.3	268.5	268.8	268.1	266.4	263.9	261.3	257.1	252.5	249.2
40	283.6	274.1	261.6	255.0	254.6	255.7	258.3	260.0	260.3	259.3	256.4	252.3	249.1	245.4	239.2	232.6
35	269.0	260.0	247.5	240.0	239.2	241.7	245.0	247.1	247.2	245.9	242.9	239.3	235.8	231.8	227.0	219.2
30	242.8	238.5	232.0	226.7	225.8	228.9	231.1	230.8	231.4	231.5	230.7	228.0	225.1	222.1	218.5	215.6
25	216.6	220.2	225.8	224.6	222.9	221.5	220.3	219.6	218.9	219.2	219.9	220.2	219.5	218.2	216.4	213.7
20	209.0	212.0	216.4	218.6	218.4	213.9	210.1	208.3	208.1	208.1	209.4	211.7	214.5	217.2	218.4	217.1
15	203.1	207.6	214.0	218.5	216.8	210.2	203.9	200.5	200.1	200.4	202.1	206.3	212.0	216.9	220.0	220.6
10	203.6	209.1	214.4	220.2	224.8	230.2	235.8	238.4	238.7	238.7	237.5	233.4	227.3	223.2	221.4	220.6
5	233.1	236.9	242.9	249.8	257.4	264.4	269.4	271.9	272.1	272.4	271.8	268.2	262.0	254.8	248.4	243.3
0			276.4	280.5	286.4	292.1	296.5	299.3	300.1	300.9	300.1	297.0	291.1	283.5	277.0	268.3

OCTOBER ZONAL MEAN PRESSURE (N m⁻²)

HEIGHT (Km)	LATITUDE																EXPONENT
	-80	-70	-60	-50	-40	-30	-20	-10	0	10	20	30	40	50	60	70	
80	1.121	1.132	1.133	1.109	1.121	1.126	1.109	1.093	1.096	1.098	1.091	1.061	1.000	0.928	0.878	0.831	0.799
75	2.504	2.511	2.491	2.453	2.479	2.498	2.479	2.437	2.424	2.424	2.418	2.338	2.190	2.014	1.889	1.761	1.680
70	5.317	5.314	5.248	5.193	5.290	5.386	5.419	5.402	5.370	5.346	5.285	5.080	4.739	4.323	3.998	3.700	3.504
65	1.094	1.092	1.078	1.069	1.097	1.126	1.144	1.156	1.156	1.147	1.122	1.072	1.003	0.912	0.832	0.762	0.715
60	2.182	2.185	2.162	2.152	2.217	2.286	2.336	2.365	2.367	2.351	2.289	2.185	2.055	1.877	1.694	1.533	1.418
55	4.171	4.222	4.230	4.226	4.359	4.494	4.596	4.624	4.617	4.592	4.487	4.311	4.072	3.733	3.375	3.028	2.768
50	7.716	7.919	8.031	8.063	8.300	8.531	8.708	8.739	8.708	8.665	8.510	8.197	7.793	7.223	6.568	5.893	5.356
45	1.403	1.459	1.500	1.516	1.557	1.595	1.625	1.630	1.624	1.618	1.596	1.542	1.475	1.382	1.270	1.145	1.043
40	2.544	2.689	2.825	2.890	2.970	3.030	3.073	3.076	3.061	3.058	3.030	2.958	2.854	2.702	2.519	2.308	2.118
35	4.682	5.057	5.489	5.718	5.881	5.973	6.005	5.973	5.943	5.952	5.958	5.875	5.724	5.486	5.210	4.892	4.571
30	0.908	0.997	1.113	1.183	1.219	1.226	1.220	1.211	1.203	1.206	1.215	1.211	1.193	1.158	1.115	1.069	1.020
25	1.908	2.098	2.340	2.510	2.594	2.599	2.583	2.564	2.549	2.556	2.573	2.577	2.558	2.503	2.438	2.360	2.284
20	4.242	4.600	5.023	5.379	5.591	5.655	5.669	5.652	5.627	5.641	5.658	5.644	5.585	5.461	5.323	5.194	5.084

OCTOBER ZONAL MEAN DENSITY (Kg m⁻³)

HEIGHT (Km)	LATITUDE																EXPONENT
	-80	-70	-60	-50	-40	-30	-20	-10	0	10	20	30	40	50	60	70	
80	1.950	1.954	1.937	1.907	1.907	1.905	1.873	1.828	1.808	1.813	1.823	1.770	1.653	1.515	1.422	1.310	1.244
75	4.046	4.027	3.961	3.928	4.007	4.090	4.134	4.099	4.053	4.029	3.999	3.833	3.560	3.237	2.982	2.744	2.591
70	8.116	8.093	7.980	7.949	8.202	8.473	8.663	8.840	8.833	8.750	8.523	8.112	7.538	6.814	6.174	5.653	5.295
65	1.612	1.610	1.587	1.579	1.633	1.692	1.741	1.782	1.791	1.774	1.714	1.625	1.535	1.398	1.251	1.125	1.036
60	3.025	3.065	3.072	3.080	3.192	3.302	3.390	3.411	3.409	3.391	3.306	3.175	2.995	2.744	2.459	2.189	1.982
55	5.439	5.619	5.745	5.780	5.964	6.137	6.269	6.257	6.221	6.198	6.099	5.903	5.621	5.207	4.744	4.225	3.807
50	0.962	1.010	1.045	1.061	1.086	1.111	1.132	1.135	1.130	1.126	1.112	1.073	1.030	0.971	0.892	0.803	0.728
45	1.721	1.834	1.937	1.984	2.038	2.077	2.110	2.115	2.104	2.102	2.087	2.036	1.966	1.872	1.752	1.601	1.466
40	3.125	3.417	3.763	3.947	4.064	4.129	4.145	4.122	4.096	4.108	4.117	4.085	3.991	3.836	3.668	3.455	3.224
35	6.063	6.774	7.725	7.299	8.564	8.608	8.539	8.420	8.373	8.432	8.544	8.551	8.456	8.245	7.996	7.775	7.479
30	1.302	1.456	1.671	1.818	1.881	1.866	1.839	1.827	1.811	1.815	1.835	1.850	1.846	1.817	1.778	1.727	1.681
25	3.069	3.320	3.610	3.892	4.054	4.086	4.085	4.067	4.056	4.063	4.076	4.077	4.059	3.996	3.924	3.847	3.779
20	7.071	7.561	8.087	8.534	8.917	9.208	9.400	9.451	9.420	9.443	9.413	9.287	9.070	8.758	8.491	8.333	8.234

(note that 1 N m⁻² = 1 Pa = 0.01 mb = 10 dynes cm⁻²; 1000 Kg m⁻³ = 1 g cm⁻³)

TABLE II (continued)

HEIGHT COORDINATES

NOVEMBER ZONAL MEAN TEMPERATURE (K)

HEIGHT (Km)	LATITUDE																
	-80	-70	-60	-50	-40	-30	-20	-10	0	10	20	30	40	50	60	70	80
80	182.1	184.7	187.5	190.8	196.4	201.8	205.2	208.7	211.8	211.8	209.8	211.2	215.4	219.9	222.4	226.1	228.6
75	206.5	207.9	209.1	208.4	208.3	208.1	208.4	207.8	208.1	208.7	210.5	213.9	218.4	223.0	227.3	227.3	227.9
70	226.3	225.6	223.9	221.9	220.3	218.5	216.6	213.4	210.9	211.0	213.9	218.3	222.9	227.1	231.6	230.4	230.9
65	240.6	239.1	236.9	235.3	233.3	231.0	229.7	228.2	226.1	225.4	227.2	229.1	229.7	232.5	237.1	236.8	236.5
60	259.3	255.9	251.4	248.7	245.6	244.4	243.2	245.0	244.8	244.2	242.2	240.2	238.3	239.8	243.1	246.0	247.1
55	273.7	270.2	266.2	263.5	261.5	258.8	256.8	257.6	258.6	258.3	256.0	253.1	250.3	249.8	250.5	254.3	256.2
50	283.7	280.3	276.7	274.2	273.0	271.9	269.8	267.0	266.5	266.4	265.3	263.3	259.5	256.9	256.6	260.2	261.7
45	284.4	281.4	278.4	276.4	275.1	272.6	269.8	267.6	266.7	266.6	266.9	263.6	259.2	252.5	249.8	251.4	253.2
40	277.7	274.2	269.5	267.0	265.3	262.2	261.0	260.3	260.0	259.6	257.8	252.7	245.6	239.0	234.9	232.4	231.4
35	263.3	259.9	255.1	250.7	247.9	246.6	246.9	247.8	247.9	246.8	243.9	238.1	231.5	223.9	219.4	215.0	211.2
30	246.6	243.6	238.6	232.5	229.4	229.9	230.5	229.9	230.6	230.8	228.9	225.8	220.4	215.1	209.9	205.4	201.0
25	235.5	234.6	230.4	226.9	222.9	221.0	219.9	219.3	219.0	219.3	219.5	218.6	216.9	214.5	210.6	206.1	201.9
20	233.8	231.8	227.9	222.0	216.6	211.8	208.6	207.2	206.7	206.8	208.5	210.7	213.8	215.6	215.3	212.2	208.7
15	226.1	225.4	223.4	220.4	215.2	208.6	202.8	199.3	198.9	199.3	201.6	206.6	212.4	216.5	217.9	216.6	214.5
10	214.8	216.5	219.0	222.5	226.2	231.1	236.3	238.5	238.9	238.6	236.0	230.4	223.9	220.5	219.3	218.1	216.9
5	235.6	238.7	244.5	252.1	259.8	266.1	270.5	271.9	272.1	272.5	270.9	265.2	257.5	249.8	243.3	238.7	236.0
0		274.4	280.2	287.3	292.9	297.2	299.7	299.7	300.2	300.6	299.3	295.0	288.5	281.0	271.8	261.2	255.7

NOVEMBER ZONAL MEAN PRESSURE (N m⁻²)

HEIGHT (Km)	LATITUDE																	EXPONENT
	-80	-70	-60	-50	-40	-30	-20	-10	0	10	20	30	40	50	60	70	80	
80	1.396	1.376	1.312	1.247	1.198	1.160	1.131	1.101	1.086	1.082	1.066	1.023	0.947	0.873	0.827	0.768	0.715	E+0
75	3.303	3.221	3.043	2.874	2.731	2.617	2.532	2.449	2.400	2.388	2.356	2.240	2.044	1.855	1.738	1.605	1.486	E+0
70	7.141	6.961	6.579	6.242	5.953	5.725	5.556	5.419	5.330	5.295	5.175	4.849	4.353	3.898	3.603	3.338	3.092	E+0
65	1.466	1.432	1.361	1.299	1.245	1.204	1.175	1.155	1.147	1.141	1.105	1.025	0.912	0.808	0.737	0.685	0.635	E+1
60	2.870	2.826	2.708	2.595	2.505	2.433	2.383	2.341	2.332	2.325	2.255	2.090	1.867	1.643	1.482	1.373	1.273	E+1
55	5.394	5.348	5.182	4.999	4.856	4.739	4.656	4.553	4.526	4.521	4.416	4.128	3.707	3.263	2.928	2.687	2.480	E+1
50	9.858	9.843	9.624	9.330	9.091	8.906	8.787	8.617	8.557	8.553	8.392	7.891	7.158	6.327	5.676	5.164	4.751	E+1
45	1.782	1.792	1.762	1.716	1.676	1.647	1.635	1.612	1.603	1.603	1.574	1.490	1.366	1.223	1.101	0.996	0.911	E+2
40	3.247	3.286	3.260	3.187	3.123	3.087	3.076	3.042	3.032	3.033	2.982	2.855	2.661	2.423	2.209	1.999	1.829	E+2
35	6.066	6.185	6.207	6.118	6.024	5.987	5.970	5.901	5.881	5.895	5.840	5.676	5.401	5.034	4.654	4.272	3.942	E+2
30	1.178	1.212	1.233	1.233	1.225	1.218	1.211	1.196	1.190	1.194	1.193	1.177	1.142	1.090	1.026	0.958	0.900	E+2
25	2.394	2.473	2.545	2.583	2.596	2.583	2.570	2.541	2.526	2.533	2.537	2.522	2.482	2.405	2.305	2.197	2.102	E+3
20	4.934	5.122	5.345	5.502	5.613	5.644	5.658	5.607	5.585	5.599	5.591	5.549	5.453	5.289	5.115	4.941	4.802	E+3

NOVEMBER ZONAL MEAN DENSITY (Kg m⁻³)

HEIGHT (Km)	-80	-70	-60	-50	-40	-30	-20	LATITUDE -10				0	10	20	30	40	50	60	70	80	EXPONENT
80	2.671	2.596	2.438	2.276	2.125	2.002	1.920	1.838	1.787	1.780	1.770	1.687	1.532	1.383	1.295	1.184	1.090	E-5			
75	5.572	5.399	5.070	4.805	4.568	4.381	4.232	4.107	4.018	3.986	3.899	3.648	3.260	2.898	2.664	2.461	2.271	E-5			
70	1.099	1.075	1.024	0.980	0.941	0.913	0.894	0.885	0.880	0.874	0.843	0.774	0.680	0.598	0.542	0.505	0.468	E-4			
65	2.122	2.087	2.001	1.922	1.859	1.815	1.782	1.763	1.767	1.764	1.695	1.559	1.384	1.210	1.082	1.007	0.936	E-4			
60	3.856	3.846	3.753	3.635	3.553	3.468	3.413	3.330	3.318	3.316	3.244	3.031	2.729	2.387	2.123	1.944	1.794	E-4			
55	6.865	6.895	6.782	6.608	6.469	6.379	6.317	6.157	6.095	6.096	6.009	5.682	5.159	4.552	4.072	3.681	3.372	E-4			
50	1.210	1.223	1.212	1.185	1.160	1.141	1.135	1.124	1.119	1.118	1.102	1.044	0.961	0.858	0.771	0.691	0.632	E-3			
45	2.183	2.218	2.205	2.163	2.123	2.105	2.111	2.098	2.094	2.094	2.055	1.969	1.835	1.687	1.536	1.380	1.253	E-3			
40	4.073	4.175	4.214	4.159	4.100	4.101	4.106	4.071	4.062	4.071	4.030	3.935	3.774	3.532	3.276	2.997	2.753	E-3			
35	8.026	8.289	8.476	8.501	8.465	8.458	8.423	8.298	8.262	8.320	8.341	8.302	8.128	7.832	7.389	6.921	6.502	E-2			
30	1.665	1.733	1.800	1.847	1.861	1.845	1.830	1.811	1.798	1.803	1.815	1.816	1.806	1.766	1.704	1.625	1.559	E-2			
25	3.542	3.674	3.848	3.965	4.058	4.072	4.072	4.037	4.019	4.025	4.027	4.018	3.986	3.905	3.813	3.713	3.628	E-2			
20	7.351	7.696	8.170	8.632	9.026	9.283	9.449	9.425	9.410	9.434	9.341	9.174	8.884	8.547	8.276	8.112	8.016	E-2			

(note that 1 N m⁻² = 1 Pa = 0.01 mb = 10 dynes cm⁻²; 1000 Kg m⁻³ = 1 g cm⁻³)

ORIGINAL PAGE IS
OF POOR QUALITY

TABLE 11 (continued)

HEIGHT COORDINATES

DECEMBER ZONAL MEAN TEMPERATURE (K)

HEIGHT (Km)	LATITUDE																
	-80	-70	-60	-50	-40	-30	-20	-10	0	10	20	30	40	50	60	70	80
80	171.6	173.4	176.2	182.2	190.7	199.0	203.9	206.2	208.3	207.9	206.6	209.9	215.8	220.6	222.8	226.1	229.3
75	200.4	200.8	201.1	201.5	202.9	205.3	207.8	207.6	207.9	207.8	208.7	212.3	219.2	223.9	227.6	228.3	229.8
70	225.0	223.9	221.8	218.6	216.0	214.4	214.3	214.6	214.0	213.3	213.5	217.3	221.7	227.7	232.9	233.3	233.6
65	245.7	243.4	240.2	236.5	232.3	229.1	229.4	231.8	231.8	230.2	229.5	228.5	227.3	231.3	238.5	239.6	239.5
60	266.3	262.5	257.7	253.5	248.8	246.7	246.8	250.3	250.6	249.2	244.9	239.7	233.9	237.0	244.2	248.6	249.4
55	281.2	276.8	271.8	267.8	263.7	260.8	259.1	260.8	261.5	260.6	257.0	251.7	246.2	245.6	250.2	256.4	258.5
50	288.8	284.9	280.6	276.6	273.8	271.0	268.9	266.4	265.7	265.8	265.7	262.9	258.2	253.5	254.2	258.6	260.1
45	287.2	284.5	281.6	278.3	276.3	272.5	268.7	264.9	263.8	264.1	266.8	264.7	259.6	249.4	246.6	249.1	250.5
40	277.8	275.7	272.8	269.9	266.7	263.6	260.0	257.3	256.9	257.2	258.6	255.3	247.1	236.9	233.0	233.6	235.6
35	263.4	261.8	258.4	254.7	251.6	248.9	246.1	244.8	245.3	245.3	244.4	240.1	233.7	223.8	219.3	217.6	219.5
30	245.0	244.9	242.7	238.0	234.7	231.7	230.2	228.6	228.6	229.2	228.3	227.5	223.1	217.1	211.3	203.6	201.0
25	236.2	235.4	232.8	228.4	224.7	222.2	220.4	219.5	218.7	218.8	219.2	218.7	217.4	214.5	209.0	201.1	193.8
20	236.1	234.0	229.3	222.3	215.7	211.0	208.0	206.5	205.6	206.0	207.8	210.5	214.2	215.9	214.1	209.2	204.3
15	231.9	230.1	226.8	220.9	213.5	206.9	202.2	199.4	198.9	199.2	201.6	207.2	213.5	217.0	216.7	213.6	210.4
10	223.1	222.6	222.7	224.0	227.6	232.9	237.3	238.8	238.9	238.3	235.3	228.2	222.2	219.3	217.9	216.1	214.8
5	240.9	243.0	247.0	253.9	261.7	267.7	271.2	272.1	272.3	272.4	270.1	263.1	254.1	246.3	240.9	236.7	233.4
0			275.0	281.3	288.6	294.6	298.2	300.2	300.5	300.3	298.1	293.0	286.0	279.1	268.1	257.0	251.6

DECEMBER ZONAL MEAN PRESSURE (N m⁻²)

HEIGHT (Km)	LATITUDE																	EXPONENT
	-80	-70	-60	-50	-40	-30	-20	-10	0	10	20	30	40	50	60	70	80	
80	1.563	1.492	1.391	1.285	1.207	1.150	1.121	1.108	1.102	1.086	1.064	1.014	0.924	0.830	0.796	0.736	0.688	E+0
75	3.845	3.650	3.366	3.066	2.815	2.623	2.516	2.478	2.451	2.418	2.372	2.234	1.987	1.758	1.672	1.535	1.425	E+0
70	8.439	8.019	7.417	6.793	6.245	5.812	5.550	5.468	5.416	5.349	5.232	4.864	4.237	3.685	3.455	3.172	2.935	E+0
65	1.722	1.643	1.533	1.417	1.318	1.237	1.181	1.157	1.147	1.137	1.114	1.030	0.892	0.764	0.703	0.645	0.597	E+1
60	3.318	3.189	3.005	2.809	2.644	2.497	2.380	2.315	2.292	2.285	2.253	2.104	1.846	1.565	1.410	1.284	1.188	E+1
55	6.124	5.946	5.665	5.340	5.085	4.832	4.610	4.447	4.396	4.396	4.390	4.163	3.715	3.137	2.779	2.496	2.301	E+1
50	1.105	1.081	1.040	0.989	0.949	0.908	0.869	0.839	0.829	0.830	0.832	0.798	0.722	0.615	0.541	0.480	0.440	E+2
45	1.983	1.954	1.892	1.813	1.747	1.681	1.620	1.576	1.561	1.562	1.563	1.506	1.381	1.197	1.058	0.929	0.850	E+2
40	3.603	3.563	3.475	3.349	3.244	3.145	3.058	2.997	2.975	2.975	2.958	2.872	2.680	2.393	2.138	1.871	1.703	E+2
35	6.731	6.684	6.558	6.370	6.213	6.069	5.952	5.857	5.811	5.811	5.782	5.673	5.412	4.989	4.521	3.964	3.585	E+2
30	1.309	1.304	1.291	1.266	1.246	1.226	1.209	1.195	1.184	1.183	1.181	1.169	1.136	1.076	0.994	0.887	0.802	E+3
25	2.662	2.653	2.638	2.624	2.607	2.587	2.565	2.542	2.525	2.520	2.517	2.498	2.452	2.365	2.235	2.065	1.916	E+3
20	5.463	5.472	5.507	5.577	5.630	5.650	5.641	5.616	5.591	5.577	5.557	5.496	5.377	5.205	4.988	4.728	4.500	E+3

DECEMBER ZONAL MEAN DENSITY (Kg m⁻³)

HEIGHT (Km)	LATITUDE																	EXPONENT
	-80	-70	-60	-50	-40	-30	-20	-10	0	10	20	30	40	50	60	70	80	
80	3,174	2,998	2,750	2,457	2,204	2,014	1,915	1,872	1,843	1,819	1,794	1,684	1,491	1,311	1,245	1,134	1,045	E-5
75	6,684	6,335	5,832	5,302	4,833	4,451	4,219	4,159	4,105	4,054	3,960	3,667	3,199	2,736	2,559	2,343	2,160	E-5
70	1,307	1,248	1,165	1,082	1,007	0,944	0,902	0,888	0,881	0,873	0,854	0,780	0,666	0,564	0,517	0,474	0,438	E-4
65	2,441	2,350	2,223	2,087	1,977	1,881	1,793	1,740	1,724	1,721	1,691	1,370	1,368	1,151	1,028	0,938	0,868	E-4
60	4,340	4,232	4,062	3,859	3,702	3,527	3,360	3,222	3,185	3,194	3,205	3,037	2,750	2,301	2,011	1,799	1,659	E-4
55	7,587	7,484	7,260	6,947	6,717	6,454	6,198	5,941	5,857	5,877	5,950	5,761	5,256	4,450	3,870	3,392	3,101	E-4
50	1,333	1,322	1,292	1,246	1,207	1,167	1,126	1,097	1,087	1,088	1,091	1,058	0,975	0,845	0,741	0,646	0,589	E-3
45	2,405	2,392	2,341	2,270	2,202	2,150	2,101	2,073	2,061	2,061	2,041	1,981	1,853	1,673	1,495	1,300	1,182	E-3
40	4,518	4,502	4,438	4,323	4,237	4,156	4,097	4,058	4,034	4,029	3,985	3,920	3,778	3,519	3,196	2,791	2,519	E-3
35	8,902	8,894	8,841	8,713	8,603	8,494	8,425	8,333	8,252	8,254	8,241	8,229	8,068	7,764	7,181	6,346	5,689	E-3
30	1,861	1,854	1,852	1,853	1,850	1,843	1,830	1,821	1,805	1,799	1,802	1,790	1,773	1,727	1,639	1,518	1,390	E-2
25	3,926	3,927	3,948	4,002	4,041	4,056	4,055	4,034	4,020	4,012	4,000	3,978	3,930	3,840	3,725	3,577	3,444	E-2
20	8,061	8,144	8,367	8,739	9,092	9,325	9,448	9,474	9,470	9,433	9,316	9,098	8,744	8,398	8,116	7,874	7,673	E-2

(note that 1 N m⁻² = 1Pa = 0.01mb = 10dynes cm⁻²; 1000Kg m⁻³ = 1g cm⁻³)

2.3.1a PLANETARY WAVES

J. J. Barnett and M. Corney

Department of Atmospheric Physics, Clarendon Laboratory
Oxford OX1 3PU, Great Britain

CLIMATOLOGICAL DISTRIBUTION

Figures 1 and 2 show the mean temperature field at various pressure levels for January and July for both hemispheres. In summer (July in the Northern Hemisphere, January in the Southern Hemisphere) the fields are nearly zonally symmetric, but in winter large longitudinal variations are evident. These are mainly of low wave number, i.e., they may be represented by Fourier analysis around the globe using just a few (one or two) waves. This is the basis for representing the climatology of longitudinal variation in terms of wave components, since the fields may be defined with fewer values than by using a grid in longitude that has a sufficiently small interval to adequately represent the smooth variations.

Figures 3.1-3.24 and Table I give the amplitude and phase of temperature and geopotential height for wave numbers one and two, with $\ln(\text{pressure})$ as the vertical coordinate. The fields were calculated and plotted at pressure intervals of 0.2 in $\ln(\text{pressure})$ and at latitude intervals of 4 deg, but were interpolated to intervals of 0.5 in $\ln(\text{pressure})$ (approximately 3.5 km) and 10 deg latitude for tabulation.

These tables and figures give wave coefficients for the monthly mean temperature fields. Thus they represent the quasi-stationary planetary waves.

The convention used for phase angle is such that the reconstructed temperature is given by:

$$T(\lambda) = T_0 + T_1 \cos(\lambda - \phi_1) + T_2 \cos(2\lambda - \phi_2)$$

where T_0 is the zonal mean, T_1 and T_2 are wave number one and two amplitudes, ϕ_1 and ϕ_2 are wave number one and two phases, and λ is longitude (deg E). T_0 , T_1 , T_2 , ϕ_1 and ϕ_2 all depend on latitude and pressure and are to be found from the tables (T_0 are given in Table I in Section 2.2). Thus for wave number one the maximum occurs at longitude ϕ_1 , and the minimum at $\phi_1 + 180$ deg E. For wave number two the maxima are at $\phi_2/2$ and $\phi_2/2 + 180$ deg E, and the minima at $\phi_2/2 + 90$ and $\phi_2/2 + 270$. The same convention applies to geopotential height.

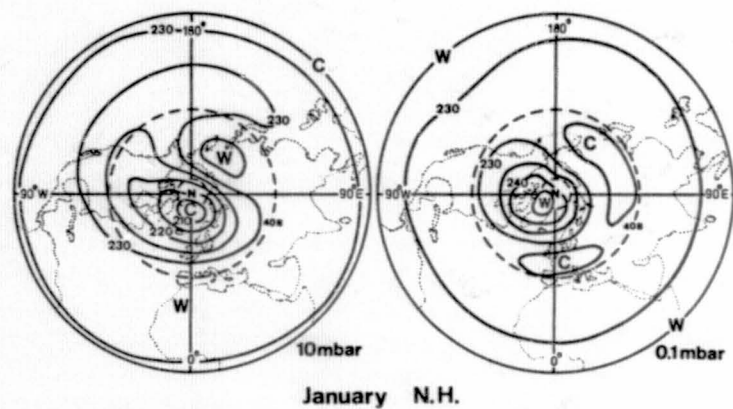
Contour levels for the amplitude figures are: temperature: 0.5, 1, 2, 4, 6, 8, 10, etc. geopotential height: 2, 4, 8, 16, 32, 64, 80, etc. Phase is contoured at 30 deg intervals; however phases are only given in the figures at places where the amplitude exceeds 0.5 K for temperature and 4 dam for geopotential height. This contour is given as a dashed line on the phase figures to mark the edge of the contoured regions. The tables contain phase values at all locations, and amplitudes are plotted over the whole domain irrespective of their size.

For a discussion of the relation between geometric and geopotential height and the extent to which they can be used interchangeably, see Section 2.2.

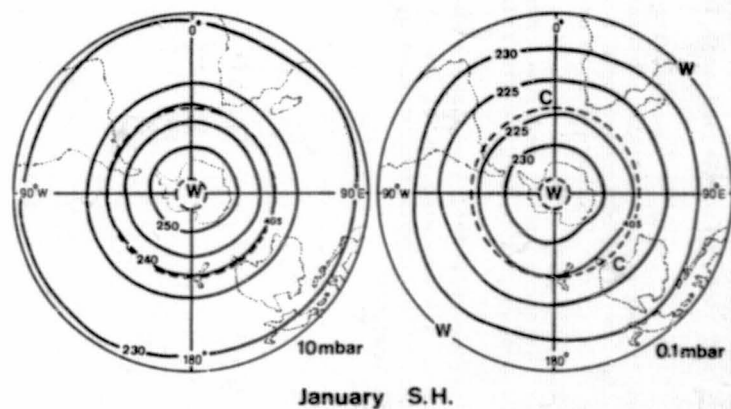
GENERAL FEATURES OF MEAN PLANETARY WAVE DATA

The following general observations can be made from the amplitude and phase sections of temperature and geopotential height (Figures 3.1-3.24):

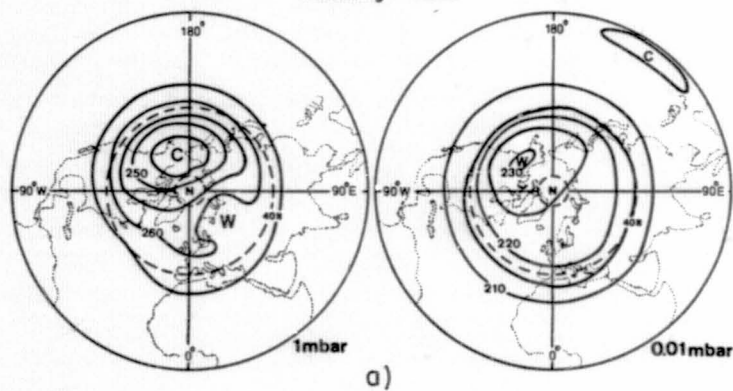
- 1) Wave amplitudes are small in the tropics throughout the year, slightly larger in the summer season at mid- and high latitudes and much larger during the winter season.
- 2) Maximum amplitudes occur at about 60-70 deg north or south during winter.
- 3) In the Northern Hemisphere wave number two amplitudes are substantially smaller than wave number one. In the Southern Hemisphere both wave number one and two amplitudes are smaller than in the Northern Hemisphere, but their amplitudes are comparable with each other.
- 4) Amplitudes are generally largest in the stratosphere and lower mesosphere and although they decay above the mid-mesosphere, they remain relatively large up to the top level.
- 5) Where the amplitude is large (midlatitude winter), the phase normally tilts westward with increasing height, and for wave number one with decreasing distance from the equator. Wave number two phase does not exhibit a clear overall latitudinal tendency.



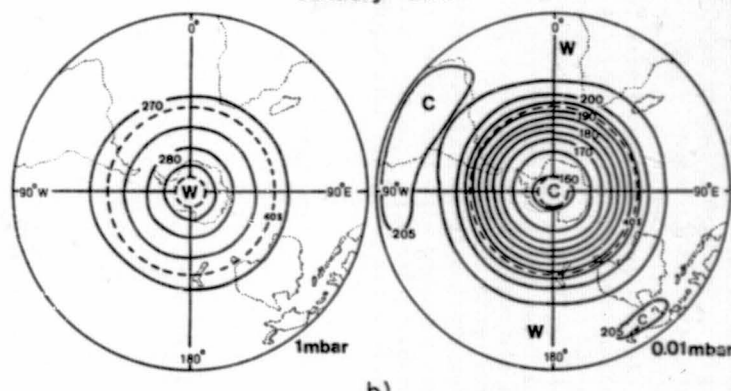
January N.H.



January S.H.



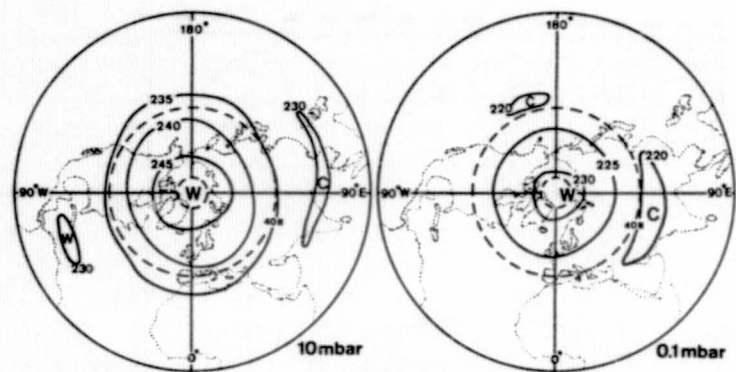
a)



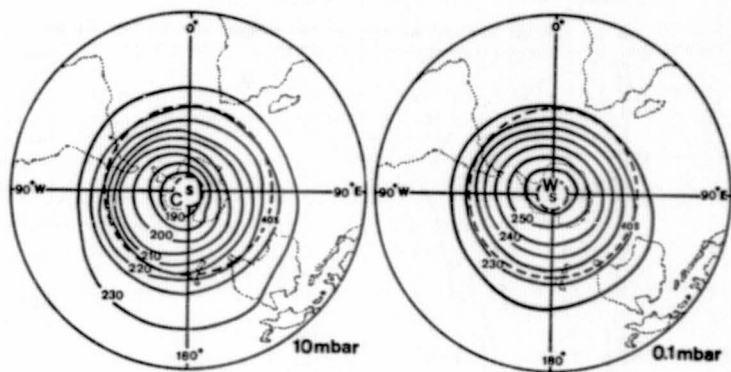
b)

Figure 1.

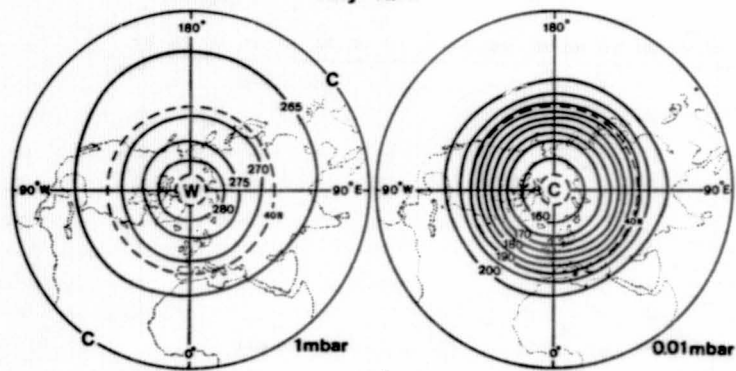
2-2



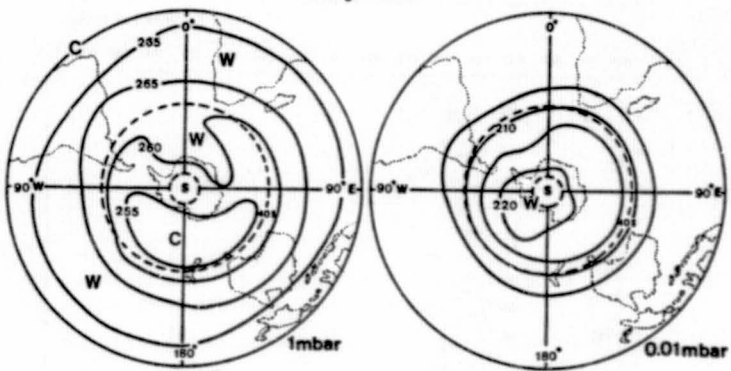
July N.H.



July S.H.



a)



b)

Figure 2.

ORIGINAL PAGE IS
OF POOR QUALITY

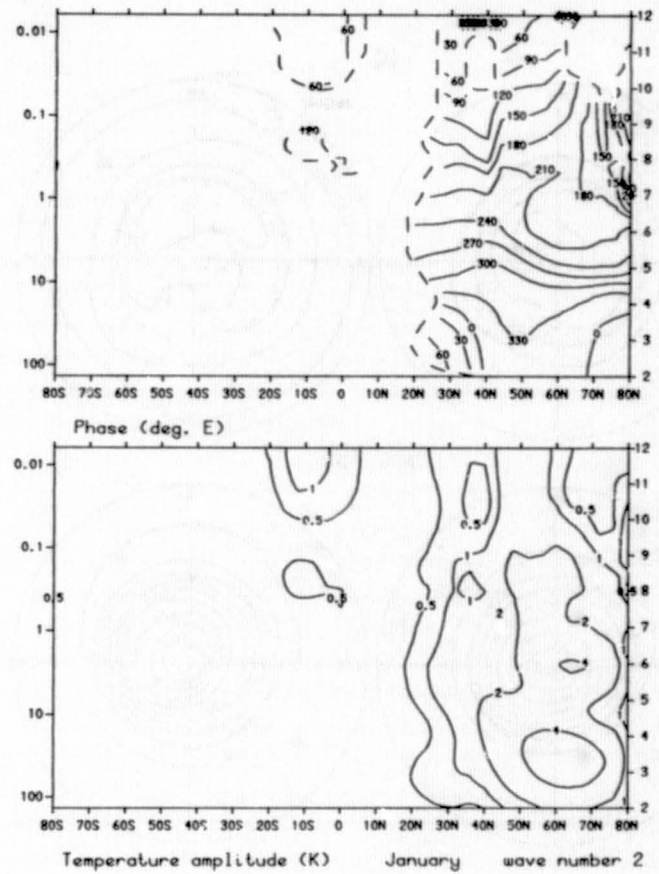
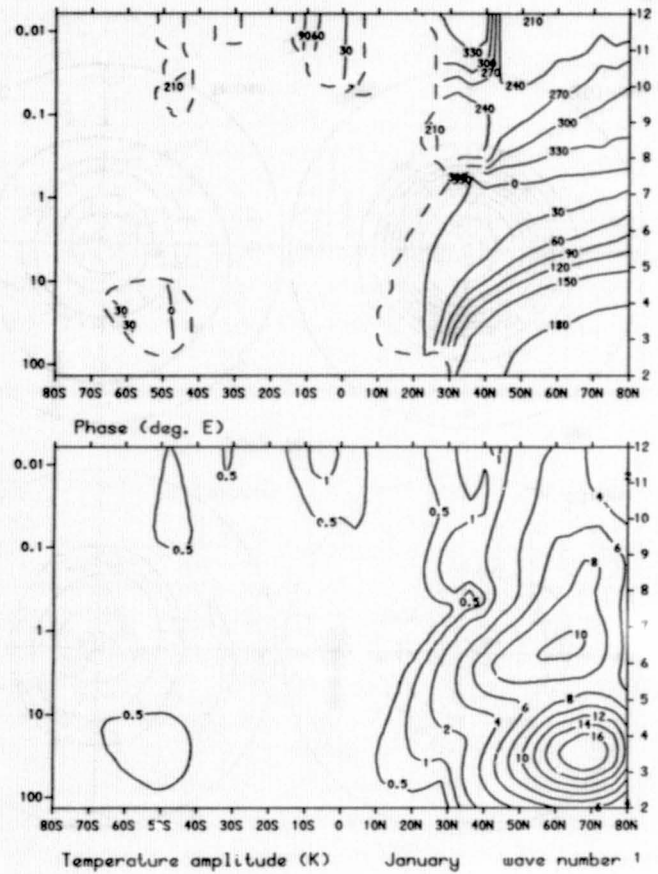


Figure 3.1

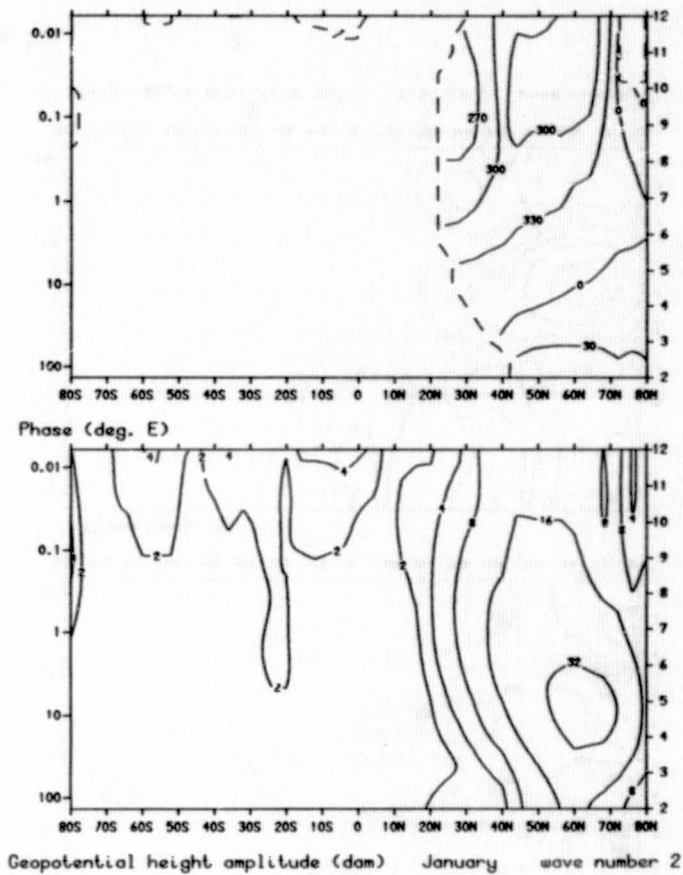
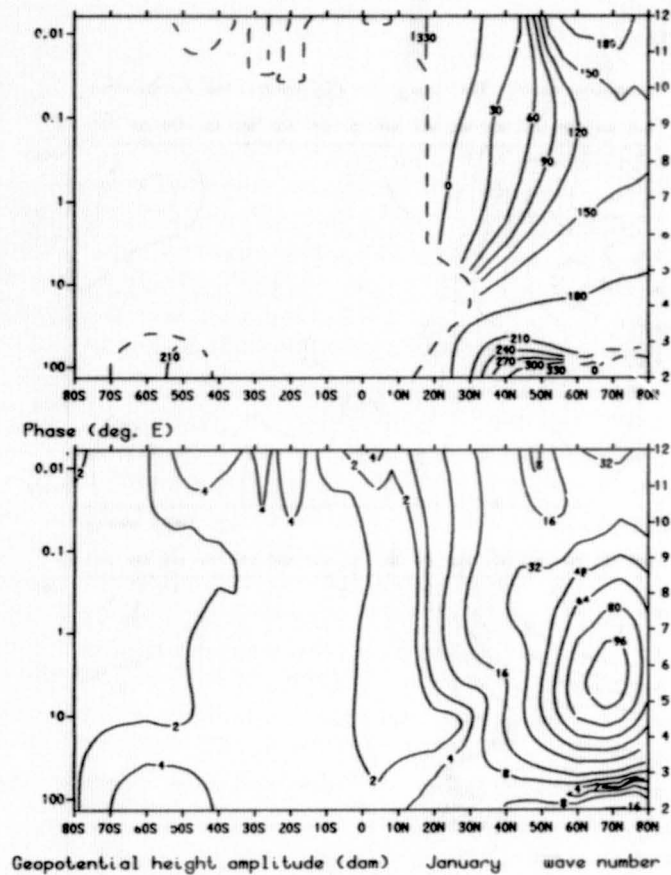


Figure 3.2

ORIGINAL PAGE IS
OF POOR QUALITY

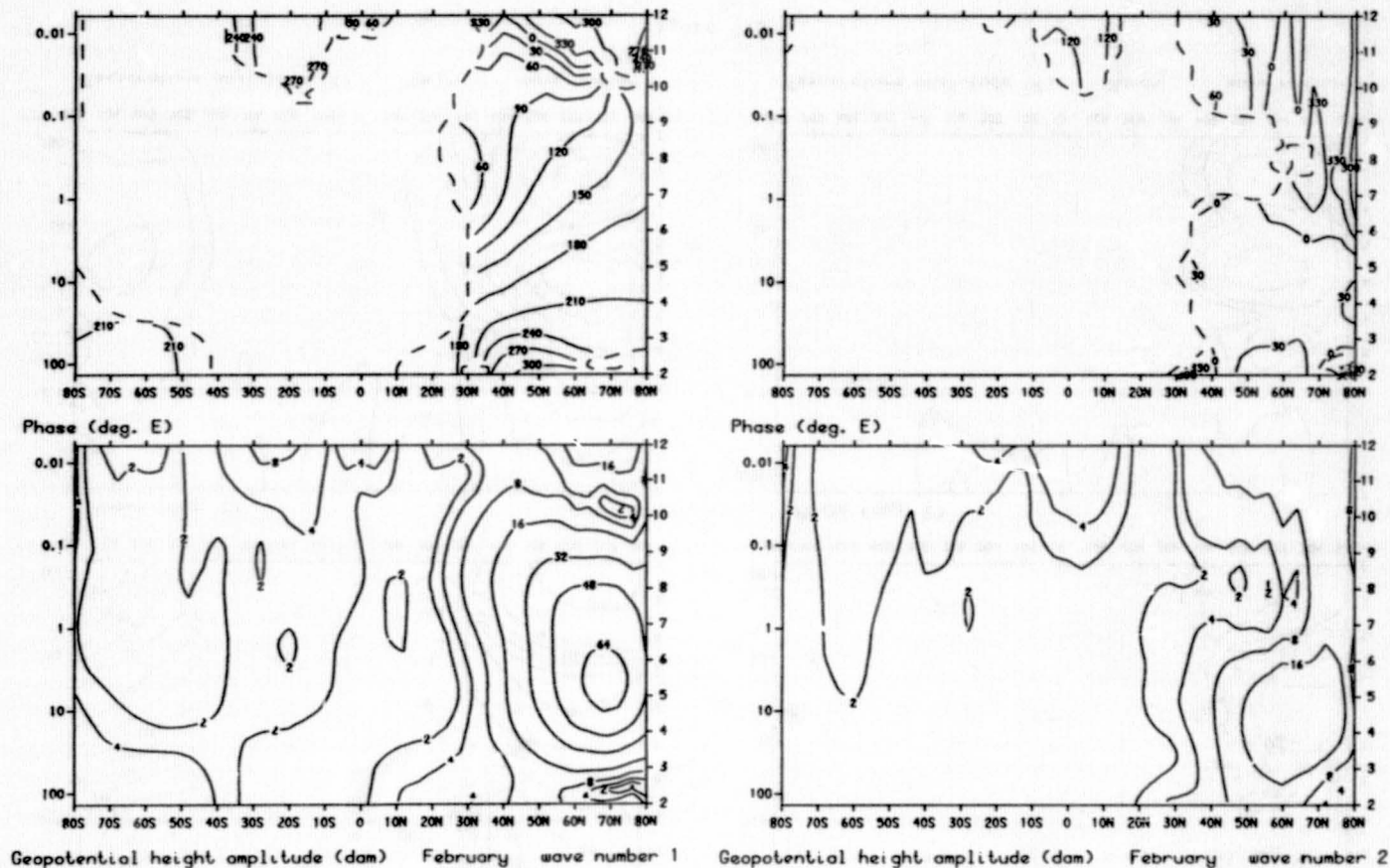


Figure 3.4

ORIGINAL PAGE IS
OF POOR QUALITY

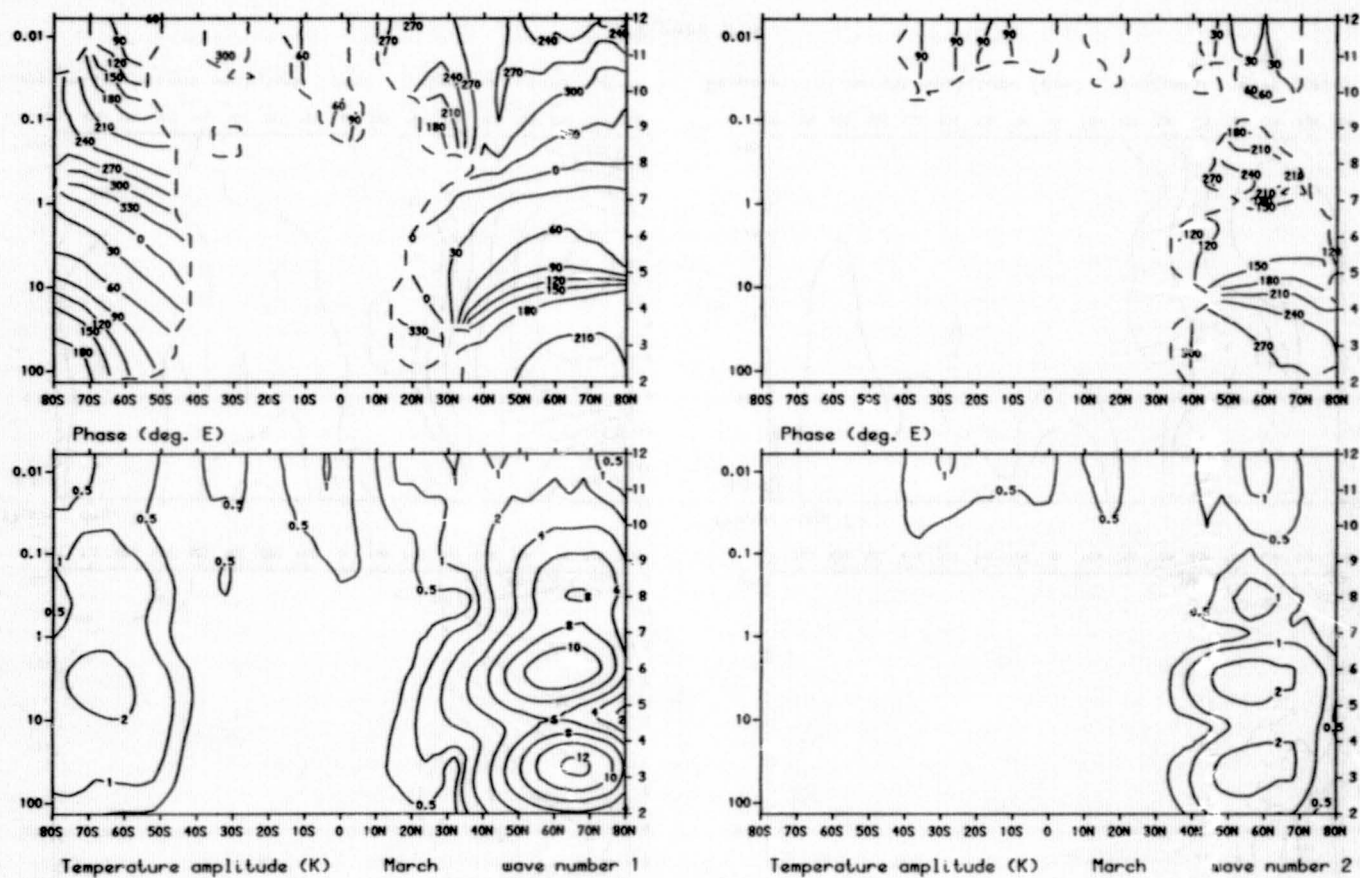


Figure 3.5

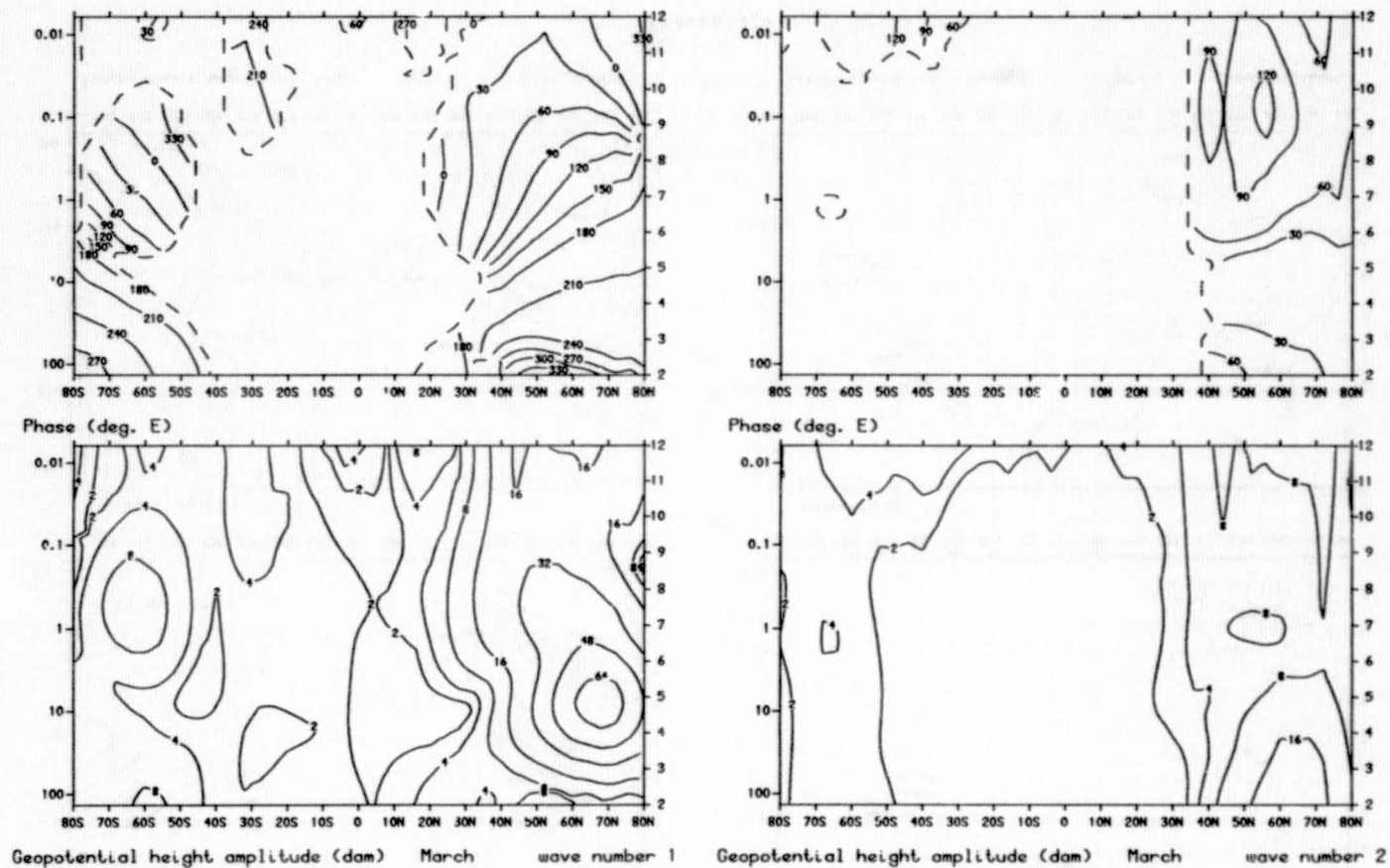
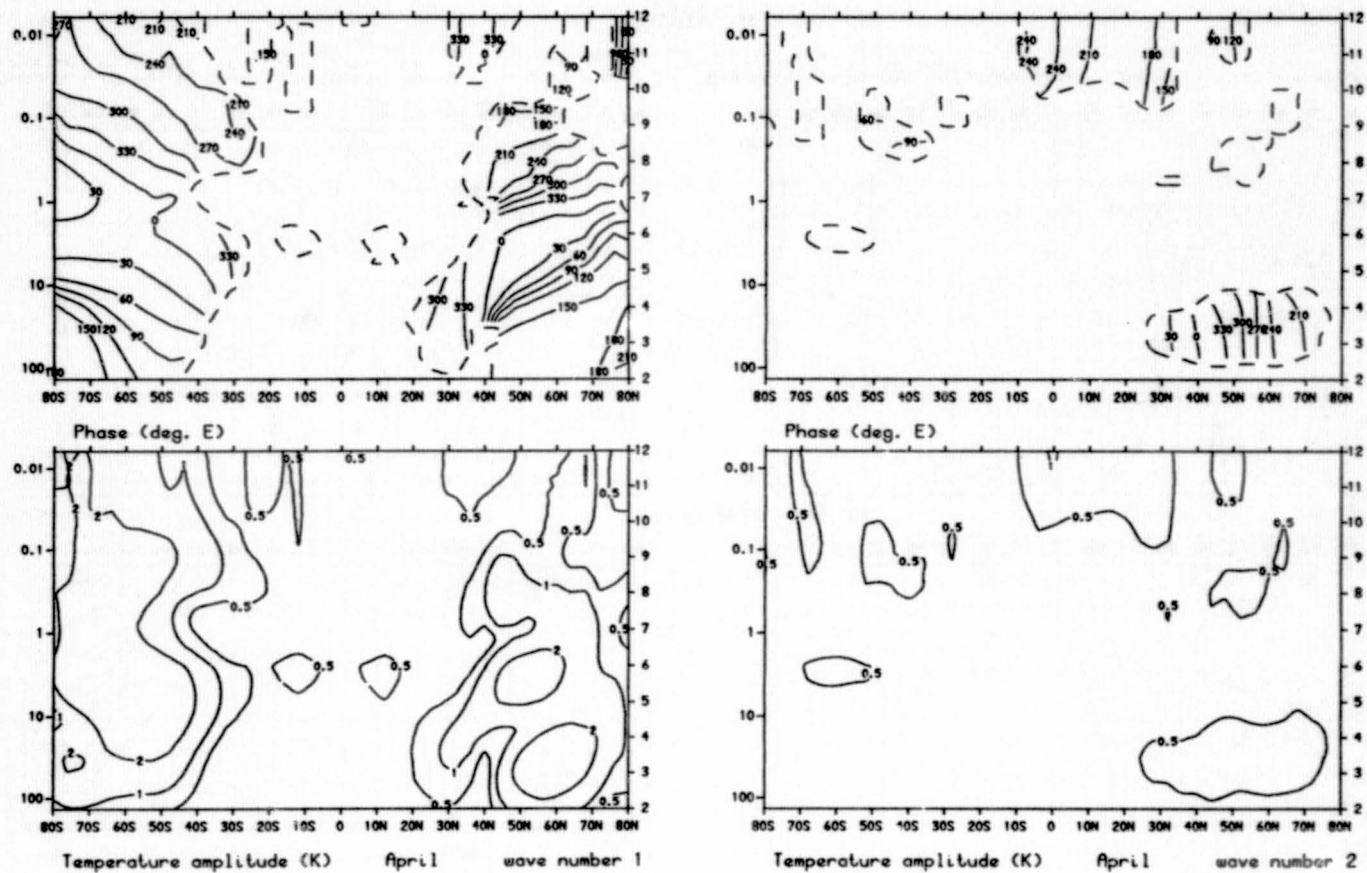


Figure 3.6

ORIGINAL PAGE IS
OF POOR QUALITY



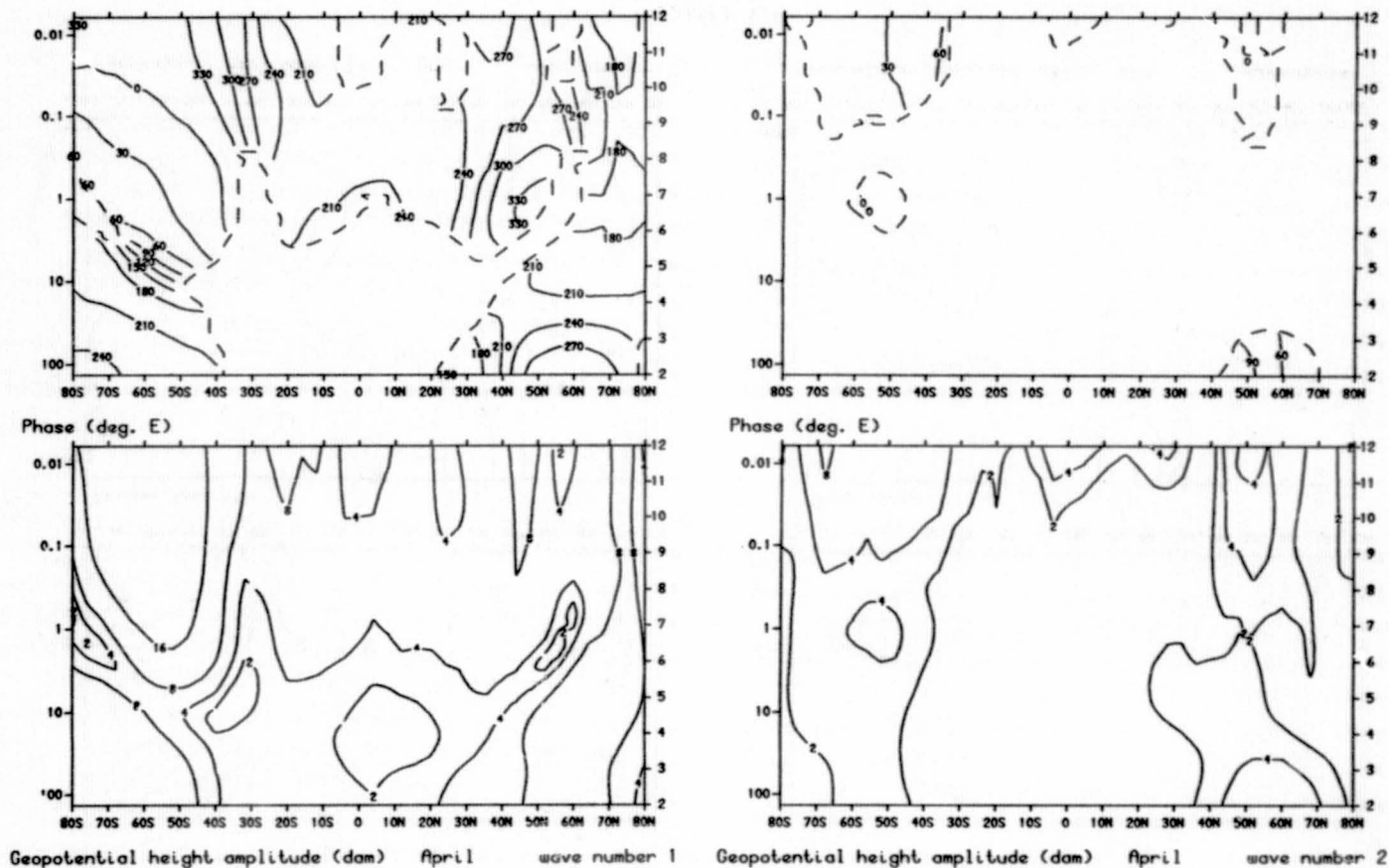


Figure 3.8

ORIGINAL PAGE IS
OF POOR QUALITY

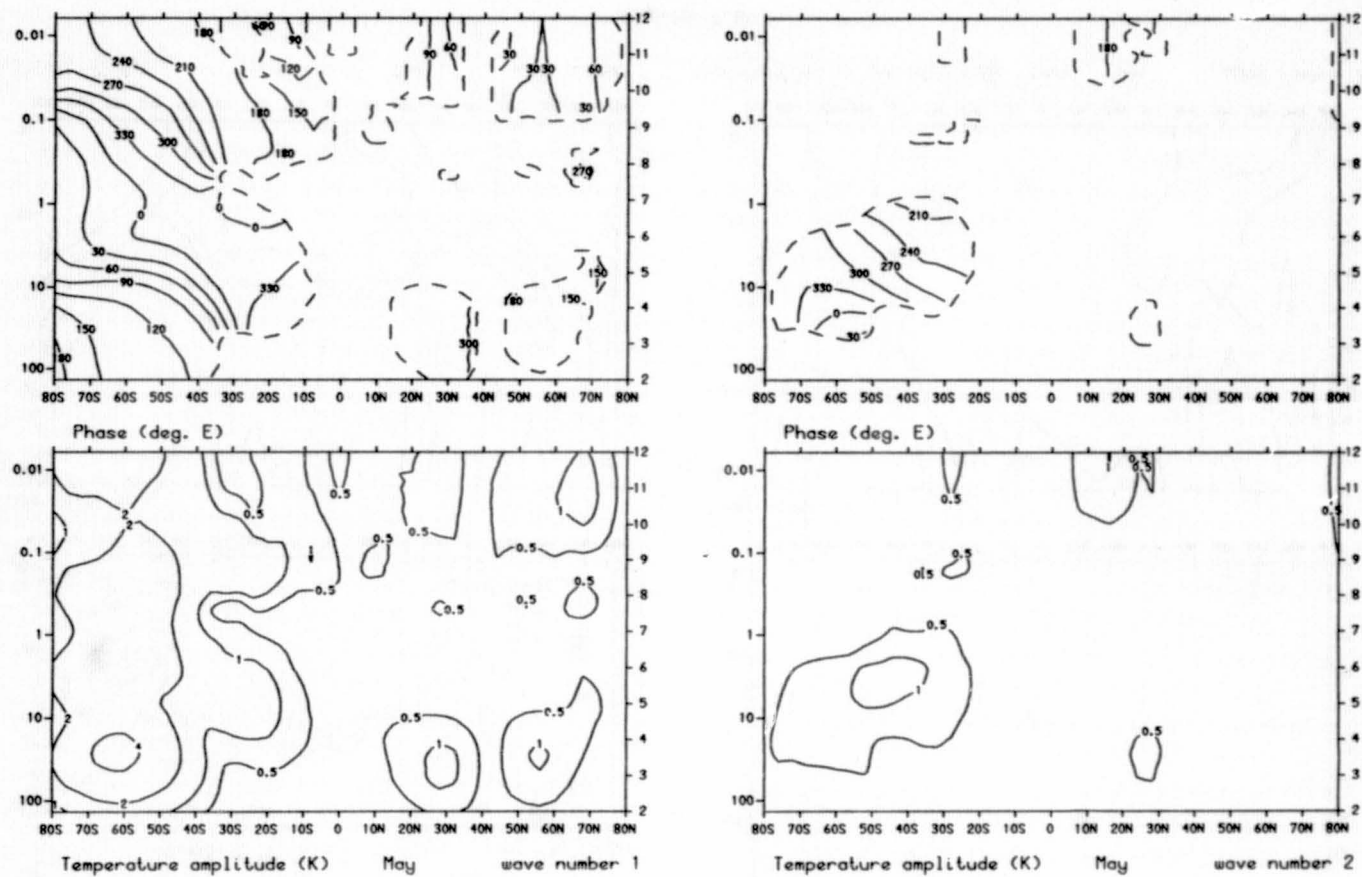
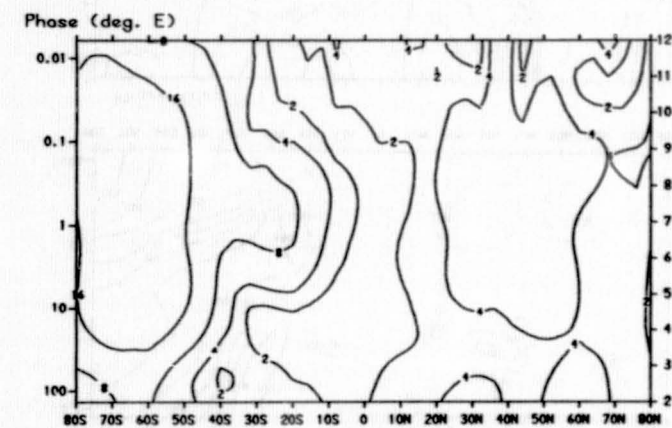
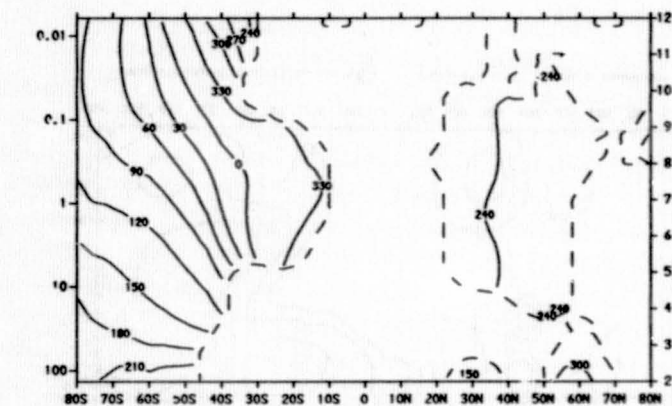
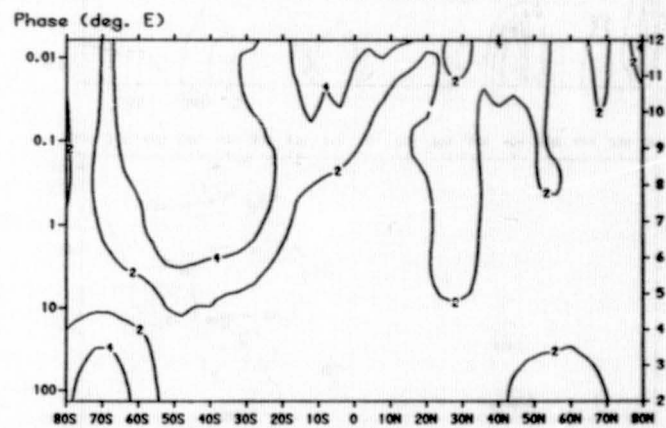
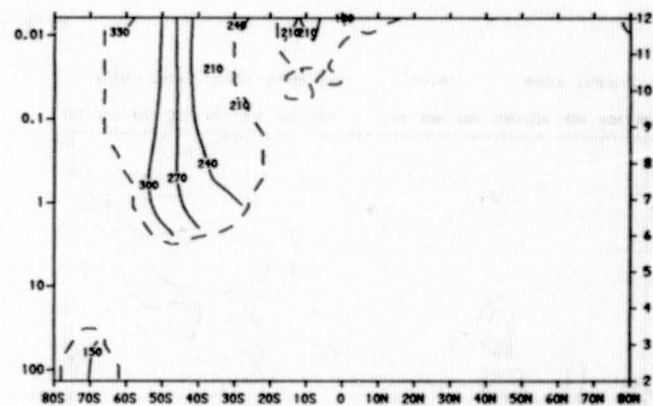


Figure 3.9



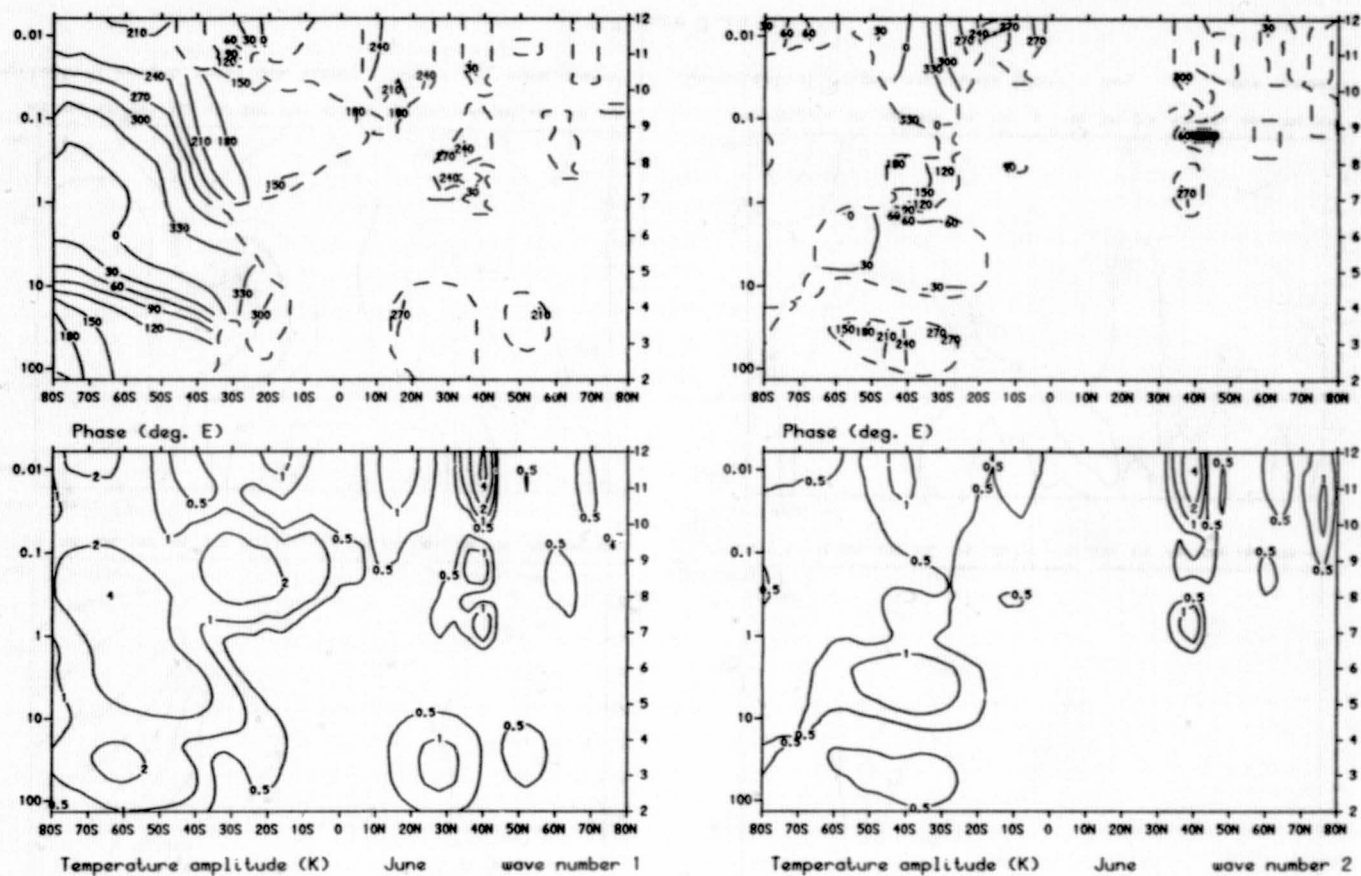
Geopotential height amplitude (dam) May wave number 1



Geopotential height amplitude (dam) May wave number 2

Figure 3.10

ORIGINAL PAGE IS
OF POOR QUALITY



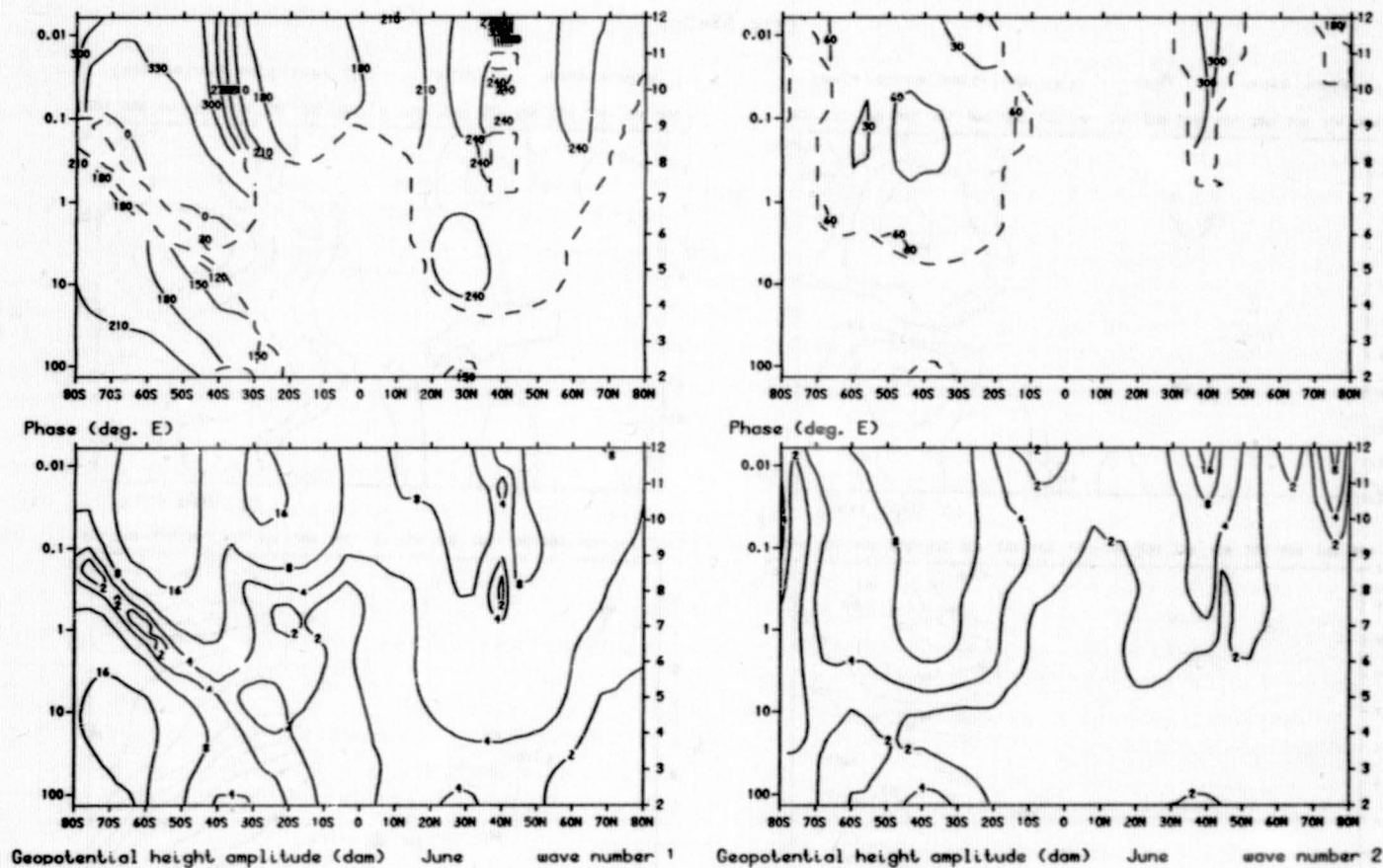
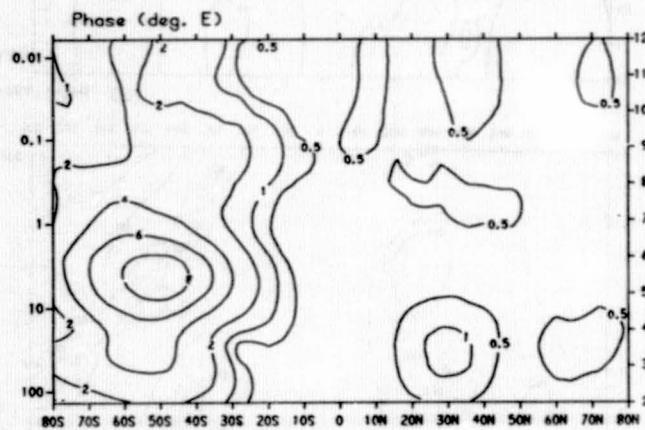
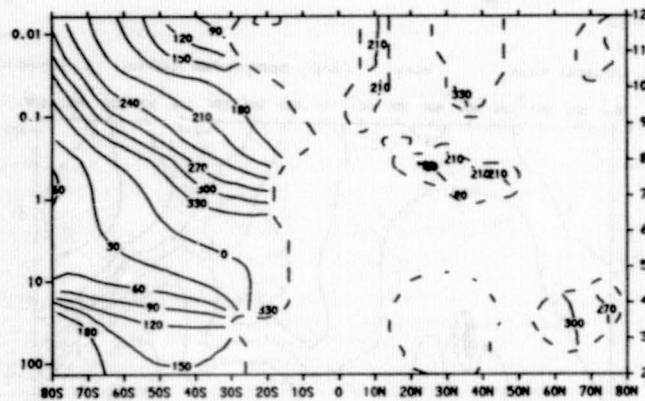
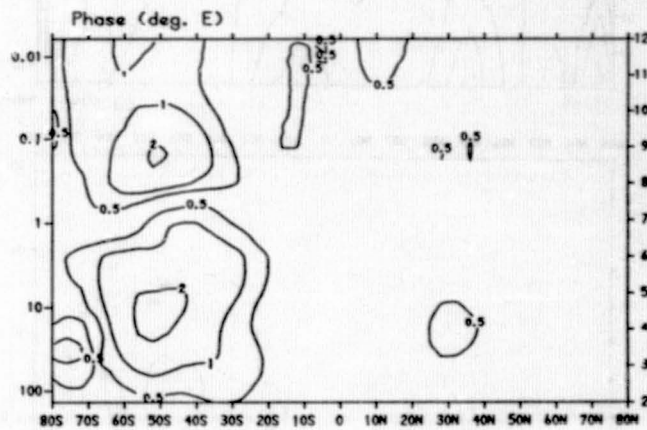
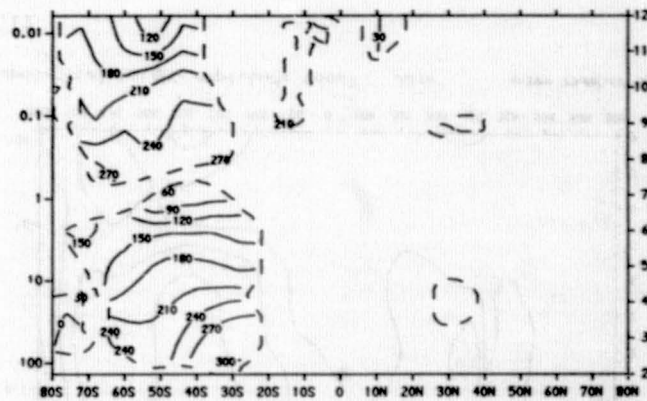


Figure 3.12



Temperature amplitude (K) July wave number 1



Temperature amplitude (K) July wave number 2

Figure 3.13

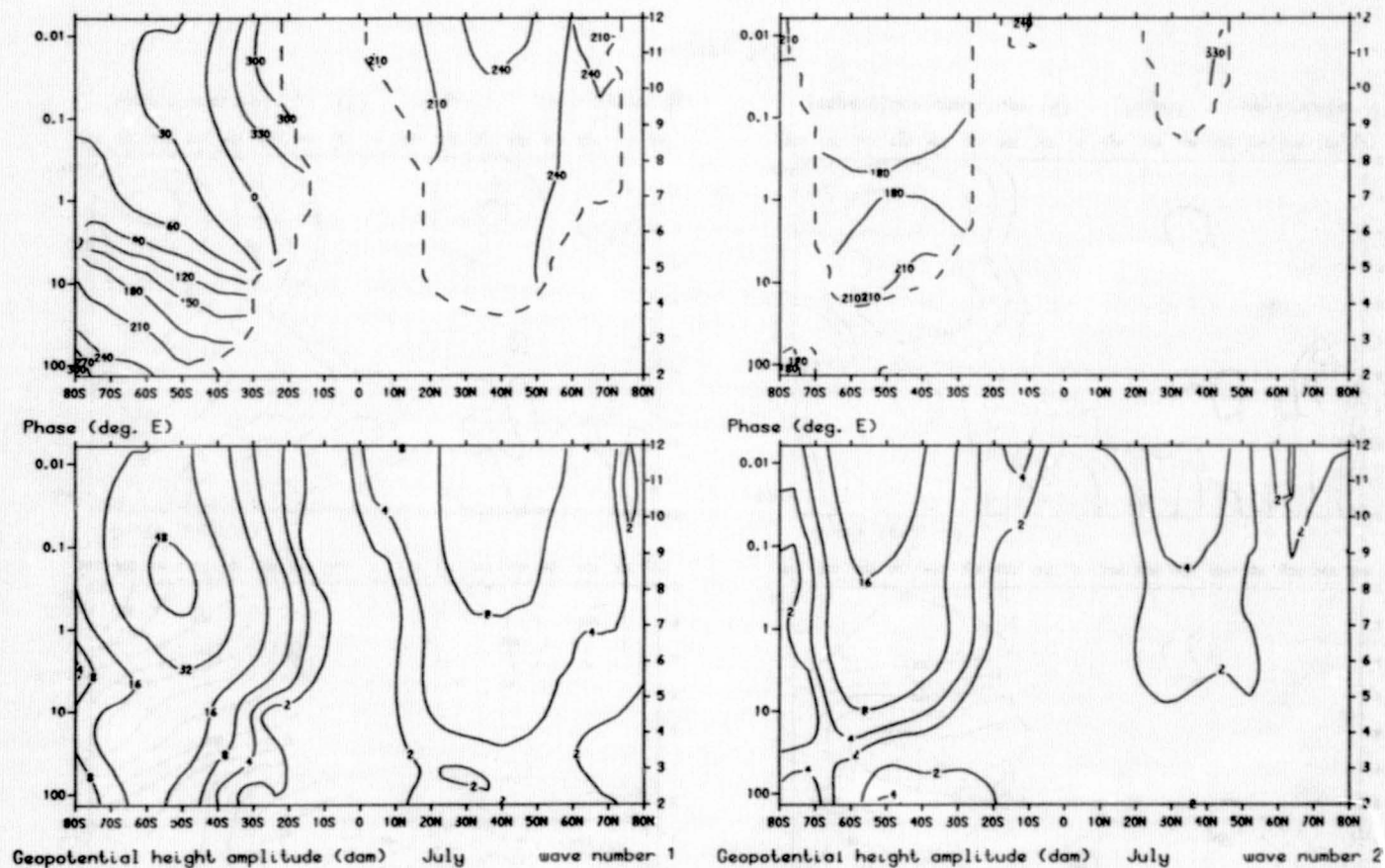
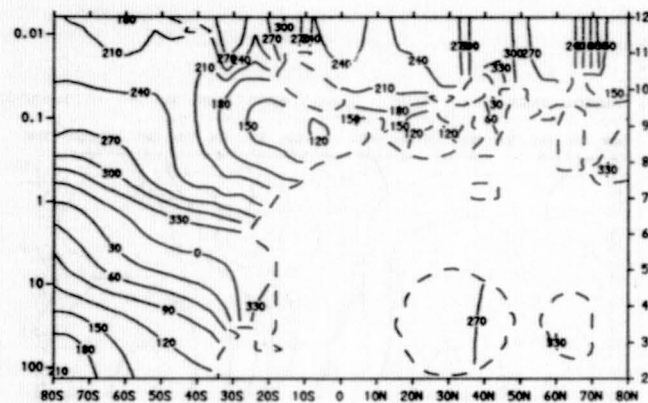


Figure 3.14

ORIGINAL PAGE IS
OF POOR QUALITY



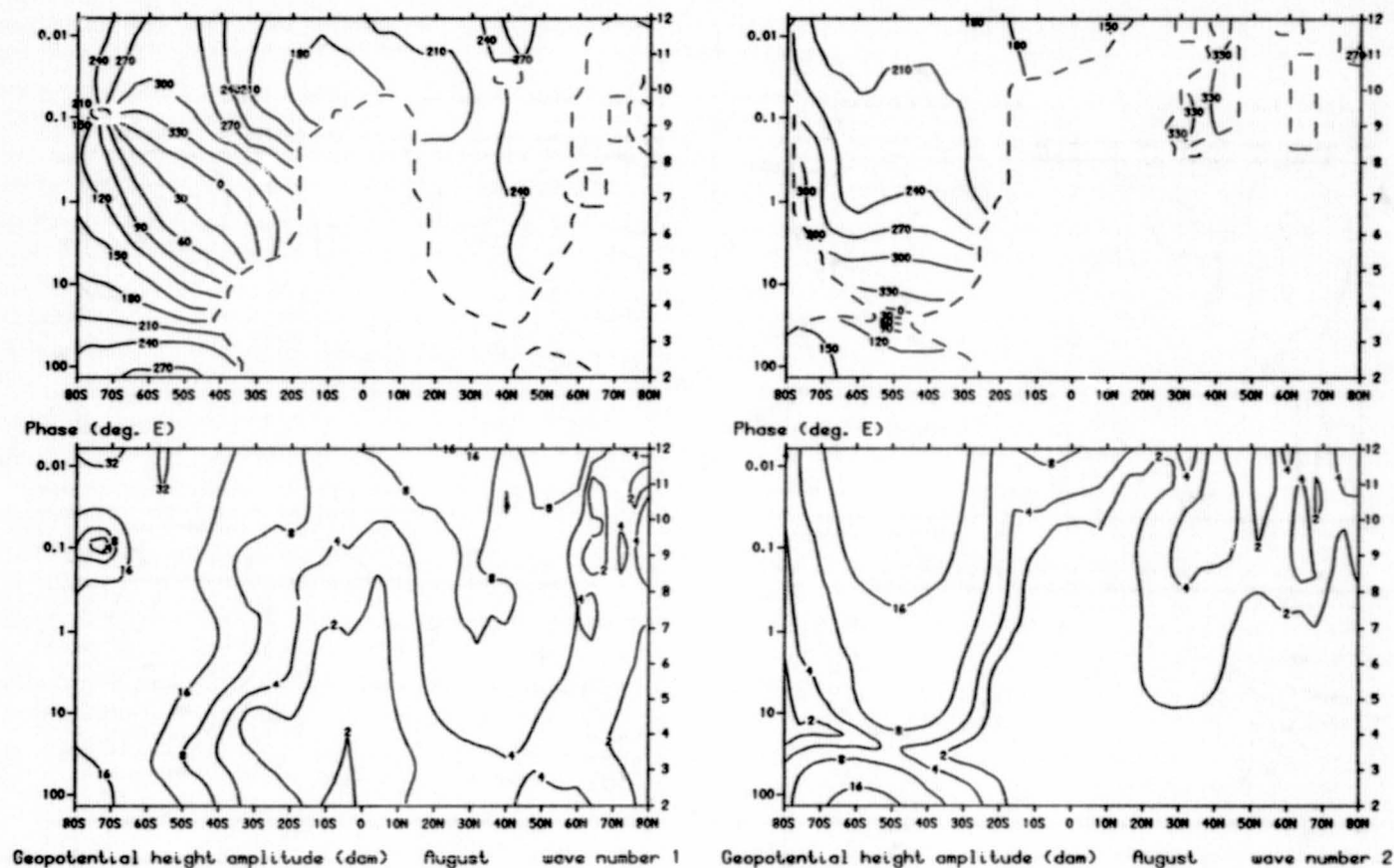


Figure 3.16

ORIGINAL PAGE IS
OF POOR QUALITY

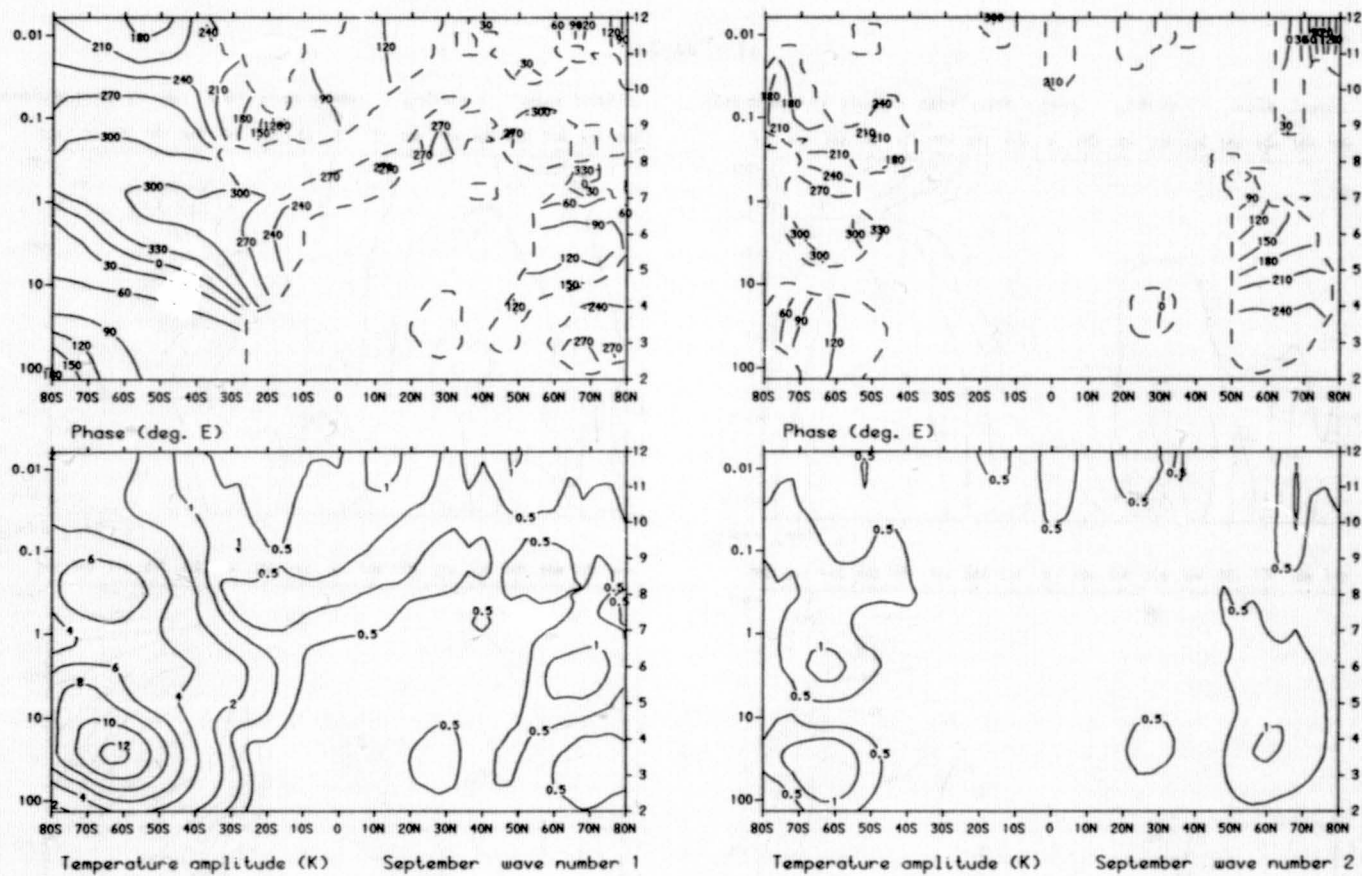
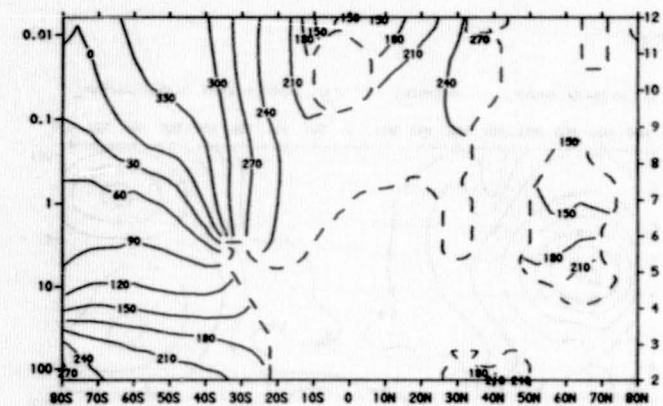
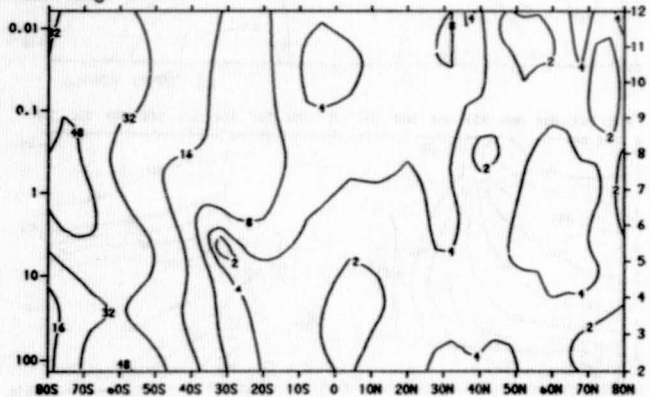


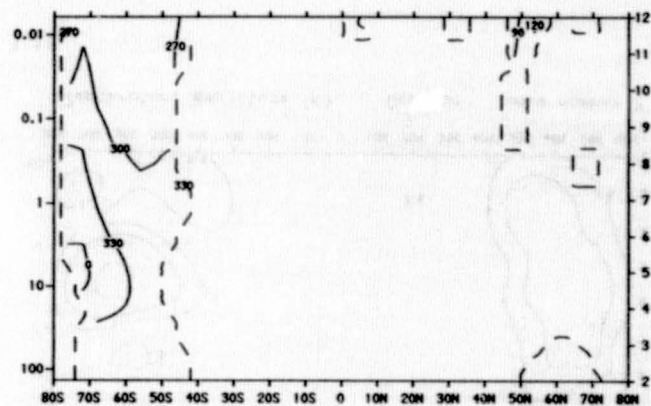
Figure 3.17



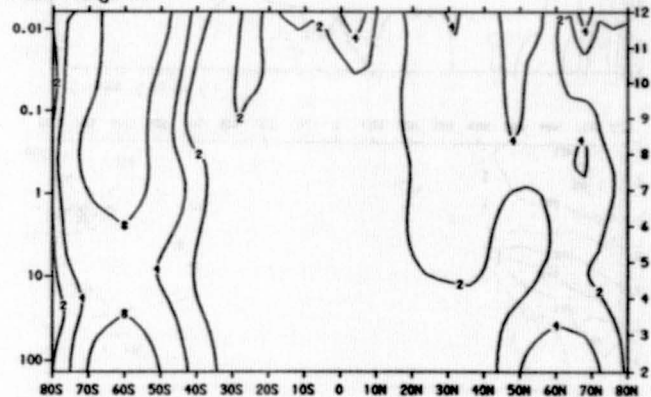
Phase (deg. E)



Geopotential height amplitude (dam) September wave number 1



Phase (deg. E)



Geopotential height amplitude (dam) September wave number 2

Figure 3.18

ORIGINAL PAGE IS
OF POOR QUALITY

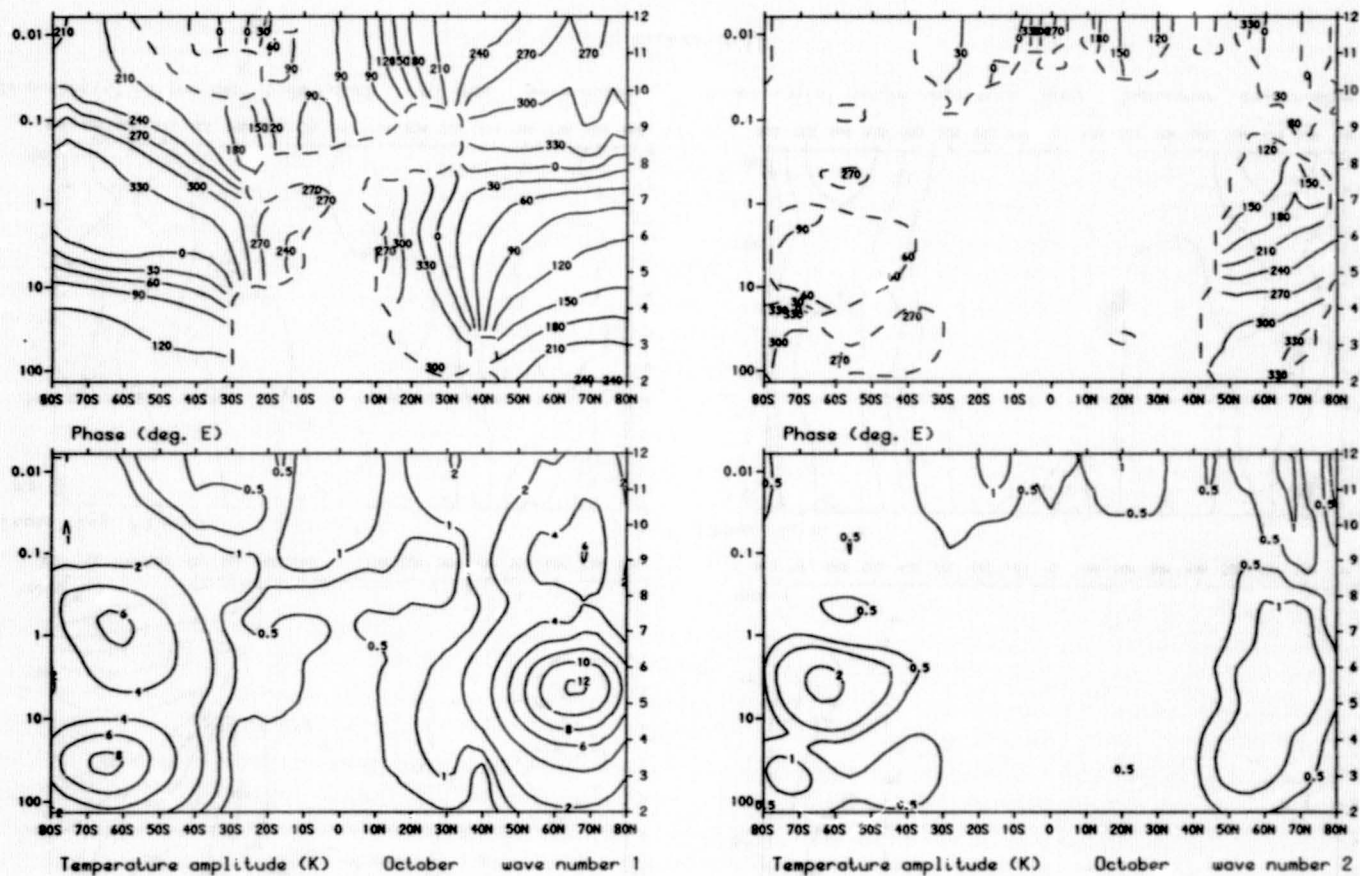


Figure 3.19

ORIGINAL PAGE IS
OF POOR QUALITY

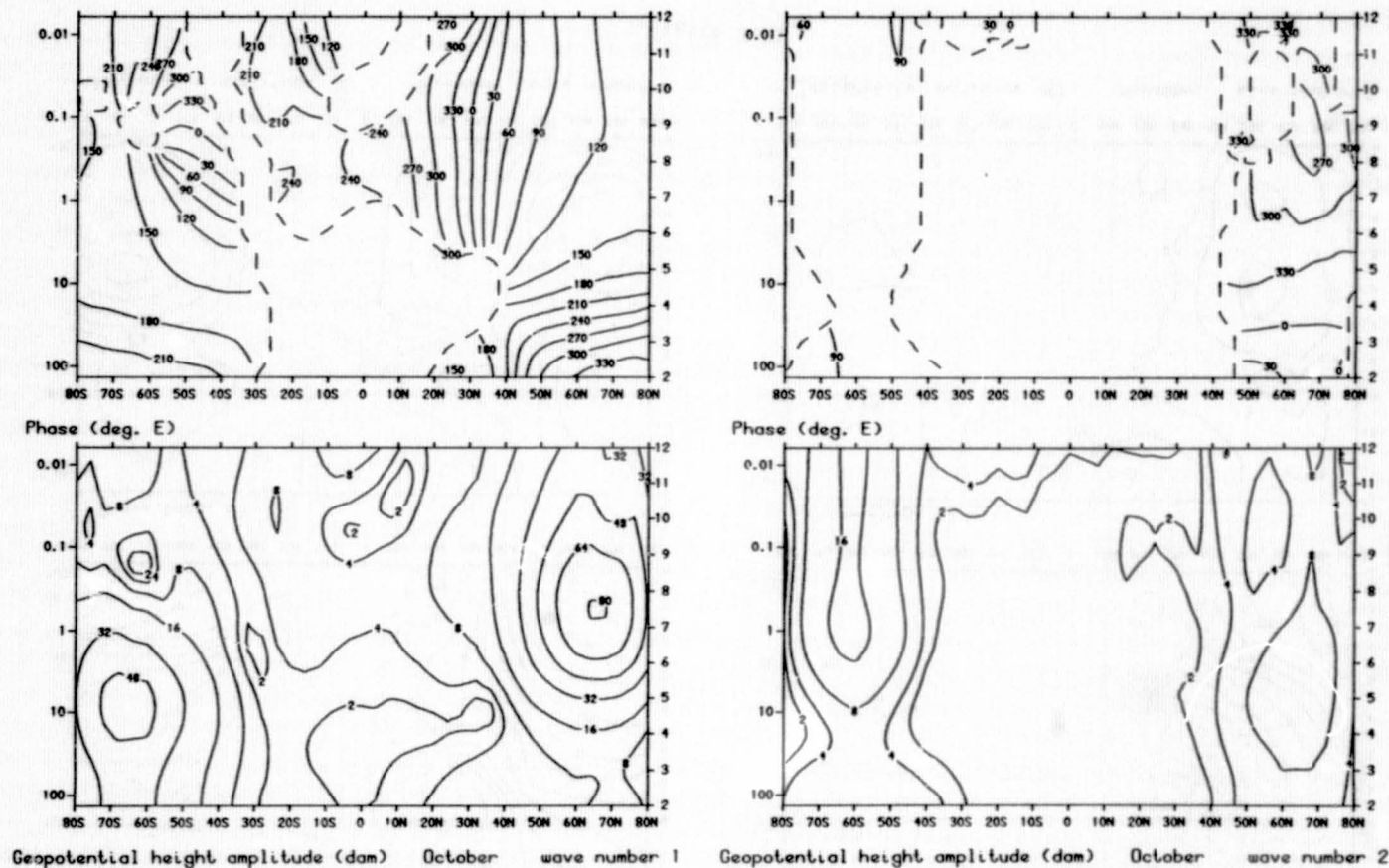


Figure 3.20

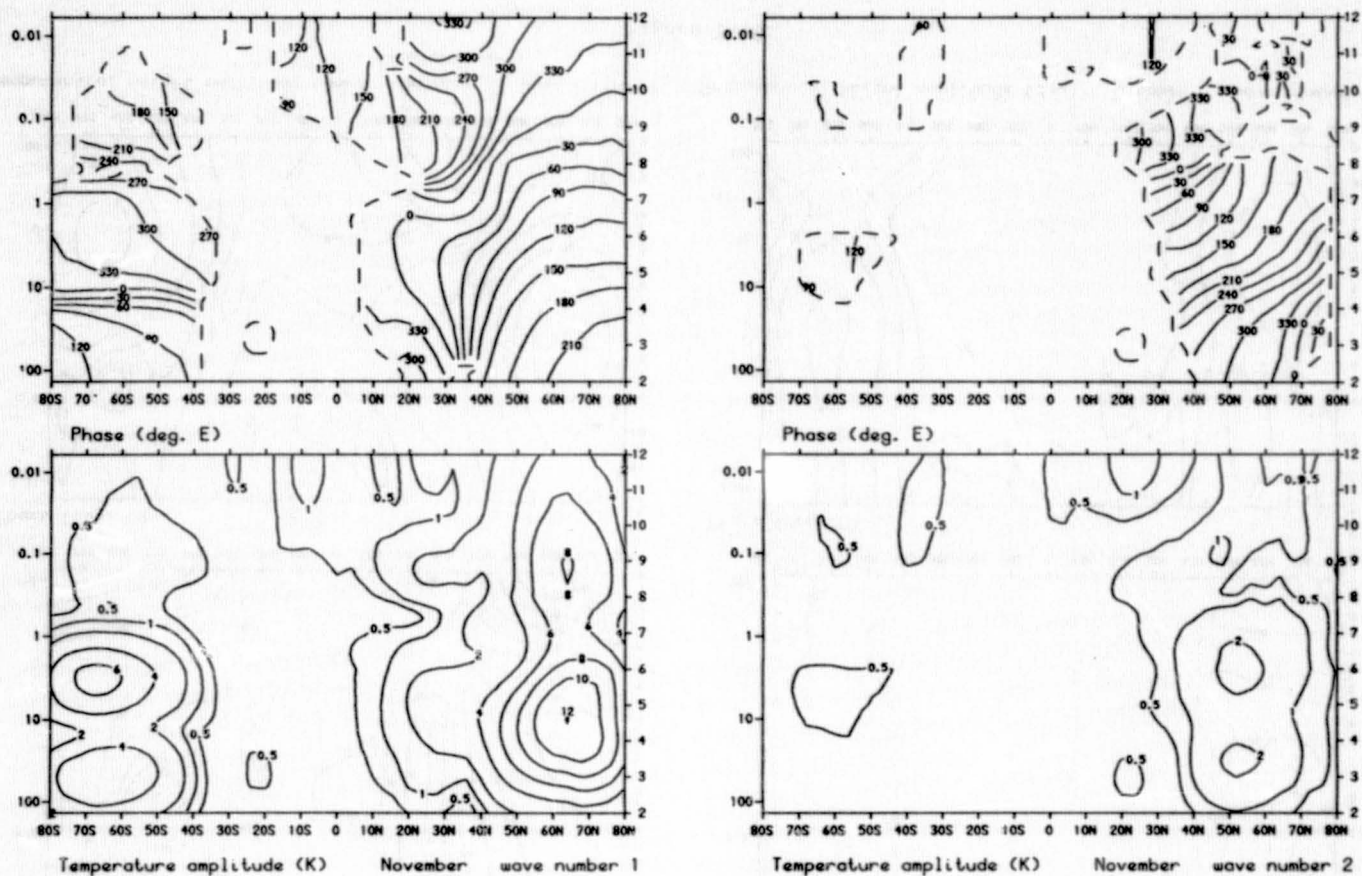


Figure 3.21

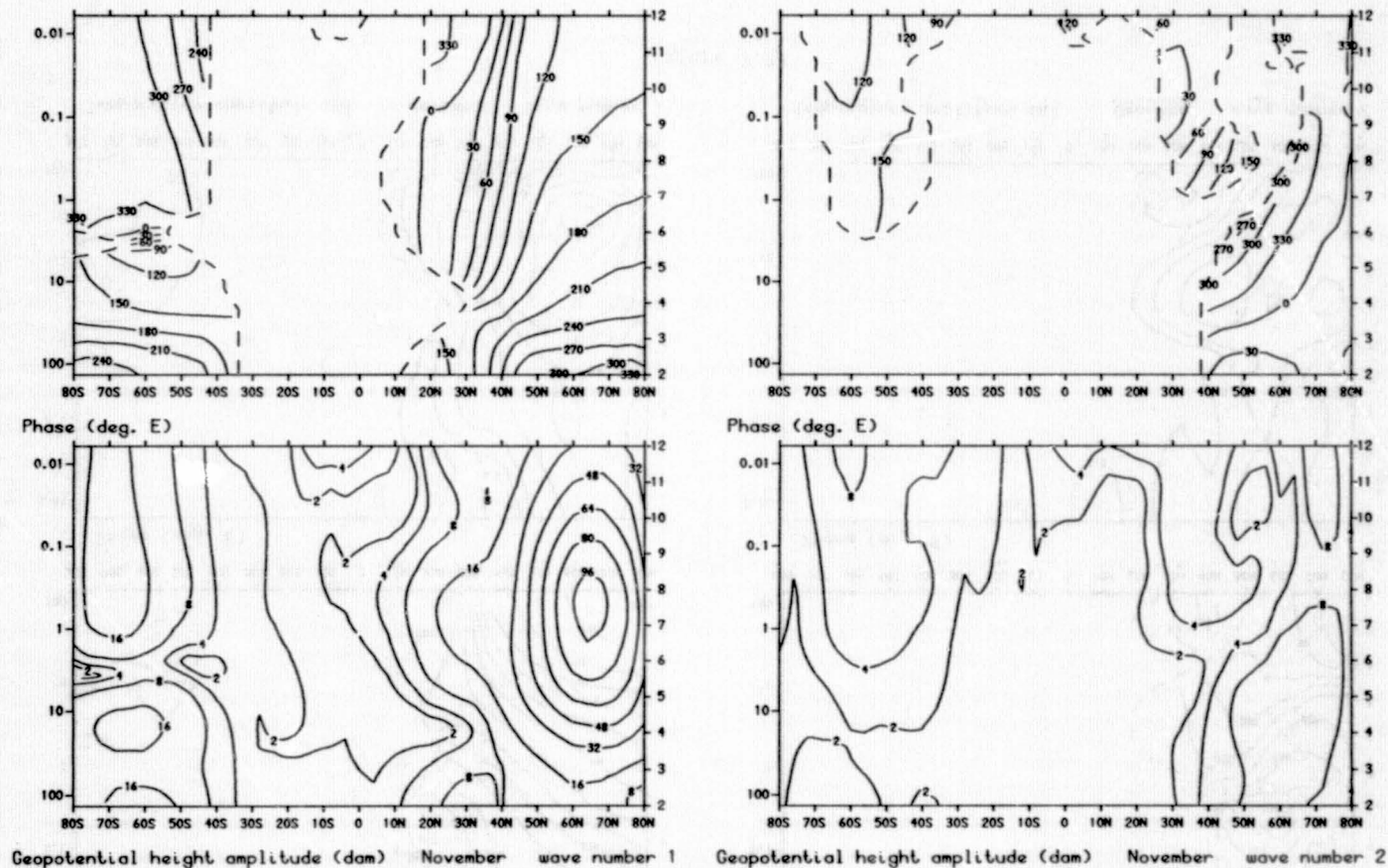


Figure 3.22

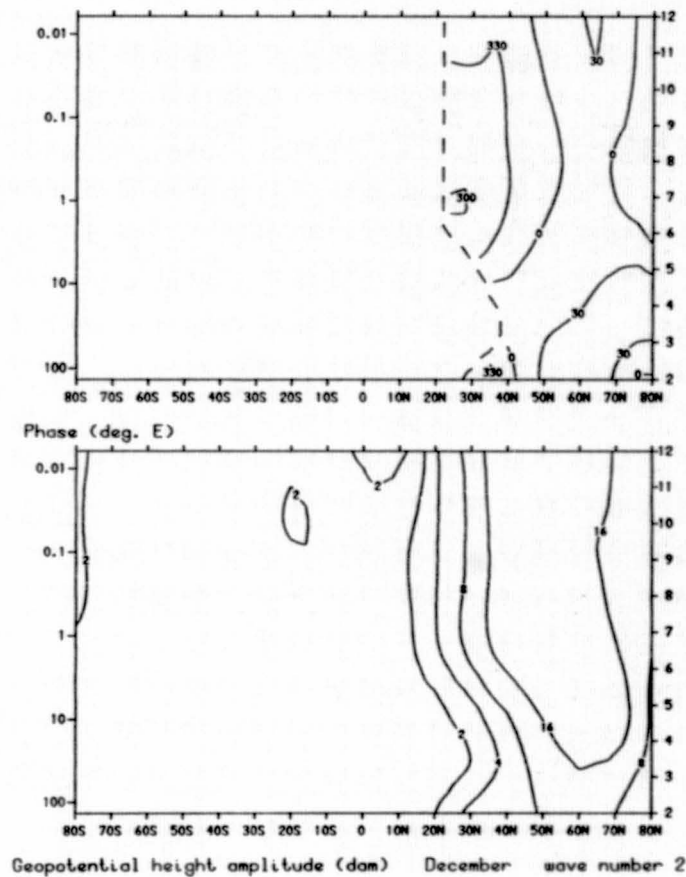
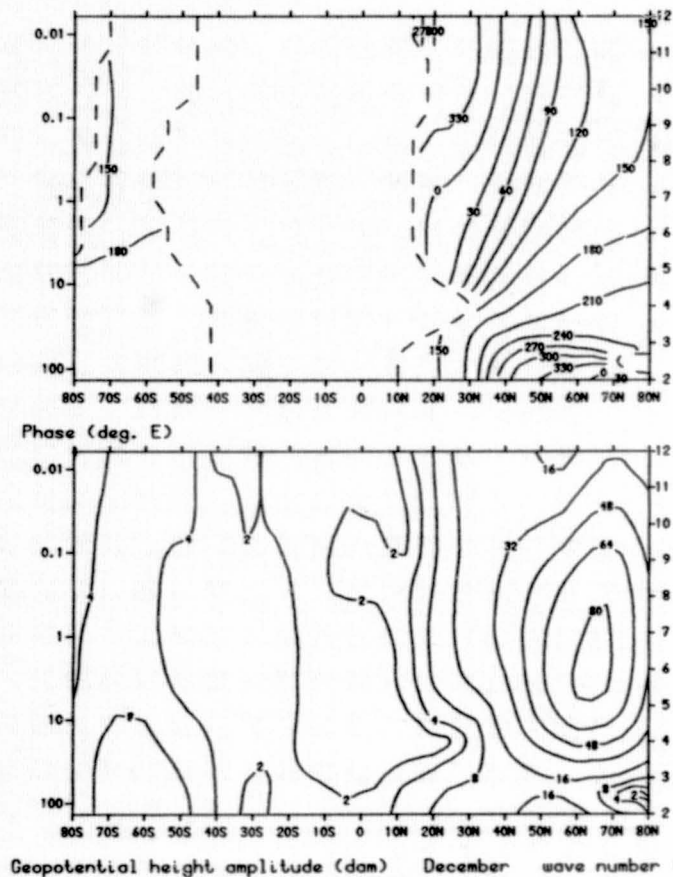


Figure 3.24

ORIGINAL PAGE IS
OF POOR QUALITY

Table 1. Amplitudes and phases of height and temperature waves 1 and 2 for 12 months.

ORIGINAL PAGE IS
OF POOR QUALITY

JANUARY		MEAN TEMPERATURE AMPLITUDE (K) AND PHASE WAVE																
SCALE	PRESSURE	-80	-70	-60	-50	-40	-30	-20	-10	0	10	20	30	40	50	60	70	80
HEIGHT	(mb)																	
12.0	0.0022	0.28 339	0.13 336	0.07 117	0.40 213	0.31 228	0.49 302	0.16 215	0.84 79	0.93 35	0.35 349	0.33 327	0.87 337	1.10 345	2.55 211	4.13 215	5.32 217	2.09 211
11.5	0.0103	0.33 338	0.14 335	0.07 132	0.47 213	0.35 221	0.46 299	0.18 207	0.79 77	0.92 35	0.37 348	0.31 325	0.82 331	1.02 336	2.84 216	4.40 223	5.49 229	2.00 228
11.0	0.0169	0.35 338	0.13 334	0.06 149	0.53 211	0.37 213	0.39 293	0.22 202	0.67 73	0.84 35	0.37 344	0.27 321	0.70 318	0.89 320	3.09 223	4.58 233	5.78 246	2.08 255
10.5	0.0279	0.34 336	0.10 335	0.08 173	0.56 211	0.40 203	0.28 281	0.24 191	0.48 82	0.68 33	0.38 340	0.20 311	0.58 290	0.86 289	3.33 231	4.83 247	4.41 264	2.64 281
10.0	0.0460	0.27 332	0.05 328	0.12 211	0.58 211	0.44 191	0.18 246	0.28 184	0.30 35	0.48 30	0.36 334	0.13 283	0.67 263	1.11 259	3.62 242	5.31 263	5.45 281	3.63 299
9.5	0.0758	0.16 318	0.04 180	0.17 224	0.54 209	0.47 178	0.23 186	0.31 178	0.28 336	0.27 30	0.33 330	0.13 231	0.97 229	1.55 243	3.89 254	5.96 280	6.67 296	4.73 312
9.0	0.1250	0.10 253	0.12 175	0.22 236	0.43 205	0.47 165	0.35 161	0.28 182	0.40 304	0.10 336	0.26 329	0.18 202	1.25 220	1.86 237	4.03 271	6.61 298	7.74 310	5.56 321
8.5	0.2061	0.20 212	0.12 179	0.23 250	0.21 189	0.35 144	0.41 147	0.18 207	0.42 286	0.16 261	0.10 356	0.18 196	1.28 217	1.74 238	4.01 292	7.01 318	8.25 324	5.70 332
8.0	0.3398	0.26 212	0.09 193	0.19 264	0.13 81	0.23 92	0.32 136	0.19 279	0.31 262	0.21 247	0.16 110	0.11 207	0.93 222	1.15 253	4.07 318	7.30 338	8.29 341	5.20 346
7.5	0.5603	0.18 232	0.05 299	0.06 315	0.25 55	0.24 43	0.12 81	0.28 310	0.14 206	0.13 261	0.23 121	0.10 243	0.40 276	1.34 340	5.13 351	8.30 0	8.59 3	4.88 11
7.0	0.9237	0.08 284	0.10 6	0.09 32	0.20 54	0.20 27	0.14 18	0.22 321	0.15 156	0.07 262	0.17 137	0.14 291	0.97 348	3.21 4	6.95 11	9.45 17	9.15 22	5.06 36
6.5	1.52	0.14 12	0.17 28	0.12 28	0.06 60	0.08 30	0.13 9	0.10 354	0.07 142	0.05 248	0.07 192	0.26 331	1.88 359	5.28 12	8.74 23	10.16 31	9.37 40	5.26 57
6.0	2.51	0.26 29	0.22 32	0.15 360	0.04 310	0.03 342	0.10 21	0.11 34	0.03 333	0.06 261	0.08 278	0.55 348	2.82 4	7.10 17	9.66 34	9.75 46	8.74 61	5.24 84
5.5	4.14	0.29 34	0.32 34	0.27 9	0.18 350	0.12 328	0.06 346	0.07 15	0.09 290	0.09 257	0.09 303	0.12 352	0.83 352	3.17 9	6.70 25	8.02 49	7.77 75	5.43 95
5.0	6.83	0.28 35	0.40 33	0.39 15	0.36 359	0.24 327	0.10 290	0.09 291	0.15 287	0.10 264	0.22 322	1.06 352	3.05 14	5.19 38	6.00 80	7.70 119	8.86 136	6.73 146
4.5	11.25	0.24 34	0.44 33	0.51 22	0.55 3	0.35 325	0.19 275	0.21 276	0.24 289	0.13 284	0.34 332	1.17 351	2.44 22	3.38 69	6.00 127	10.63 153	12.56 162	8.89 166
4.0	18.95	0.17 33	0.44 33	0.58 27	0.67 6	0.42 326	0.27 273	0.32 274	0.32 291	0.15 302	0.44 337	1.15 350	1.67 36	3.16 120	8.08 157	14.13 169	16.23 175	10.82 179
3.5	30.59	0.09 27	0.38 33	0.57 30	0.71 8	0.43 325	0.31 272	0.37 273	0.35 293	0.17 311	0.49 349	1.01 341	1.04 61	4.11 149	9.48 171	15.56 178	17.49 184	11.23 188
3.0	50.43	0.04 0	0.29 34	0.49 33	0.63 10	0.39 324	0.31 272	0.38 273	0.34 295	0.16 317	0.47 343	0.81 346	0.75 98	4.45 161	9.06 178	13.83 184	15.17 189	9.24 195
2.5	85.15	0.02 288	0.19 33	0.35 36	0.48 11	0.31 325	0.25 272	0.31 274	0.28 296	0.14 321	0.36 344	0.53 344	0.61 125	3.67 167	6.92 182	9.98 188	10.52 193	6.11 200

JANUARY		MEAN GEOPOTENTIAL HEIGHT AMPLITUDE (dam) AND PHASE WAVE 1																
SCALE	PRESSURE	-80	-70	-60	-50	-40	-30	-20	-10	0	10	20	30	40	50	60	70	80
HEIGHT	(mb)																	
12.0	0.0062	2.8 318	0.7 331	1.8 249	5.0 224	4.7 213	4.1 230	5.2 211	0.5 140	3.7 10	2.9 337	6.5 338	15.1 349	24.2 20	7.6 149	31.2 188	35.1 190	26.8 180
11.5	0.0103	2.3 314	0.5 330	1.8 252	4.4 226	4.3 212	3.9 221	4.9 211	1.1 232	2.4 358	2.4 335	6.1 339	13.9 350	23.0 22	6.9 118	26.1 181	31.0 186	24.6 175
11.0	0.0169	1.9 308	0.3 326	1.9 254	3.7 228	3.7 211	3.8 211	4.6 212	2.1 244	1.4 328	1.8 332	5.7 340	12.9 352	22.2 25	8.9 89	22.1 168	28.0 177	23.6 169
10.5	0.0279	1.5 298	0.1 310	1.9 257	2.9 233	3.2 211	3.7 204	4.3 213	2.9 245	1.3 277	1.3 327	5.3 341	12.3 353	22.0 28	12.8 75	21.0 150	27.5 165	24.4 161
10.0	0.0460	1.1 284	0.0 215	1.8 261	2.2 242	2.6 216	3.6 199	4.0 215	3.5 243	1.8 246	0.8 320	5.2 343	12.2 359	22.6 31	17.6 70	23.9 133	30.5 152	27.6 154
9.5	0.0758	0.9 271	0.0 198	1.7 266	1.5 257	2.0 224	3.3 198	3.6 219	3.7 238	2.2 231	0.3 299	5.2 345	12.9 44	24.2 23	23.1 69	30.6 123	37.5 143	33.2 149
9.0	0.1250	0.8 266	0.1 345	1.5 272	1.2 284	1.7 243	3.0 202	3.3 224	3.6 231	2.5 222	0.2 187	5.3 347	14.2 8	26.5 36	28.8 72	39.6 120	47.5 138	40.6 147
8.5	0.2061	0.6 280	0.2 353	1.2 280	1.3 305	1.8 305	2.6 263	3.0 211	3.4 228	2.4 221	0.5 171	5.5 348	15.9 29	29.0 38	34.0 77	49.4 121	59.3 141	48.9 148
8.0	0.3398	0.6 312	0.4 358	0.9 288	1.4 309	1.4 270	2.1 223	2.5 227	2.8 213	3.1 210	2.2 182	0.5 350	5.7 17.4	14.0 31.0	38.2 40	59.0 83	71.1 126	56.7 141
7.5	0.5603	0.7 339	0.5 3	0.8 290	1.5 299	2.4 267	2.6 229	2.8 220	2.9 210	2.0 208	0.5 219	5.8 351	18.0 16	31.3 42	40.5 92	67.5 133	81.7 145	63.1 152
7.0	0.9237	0.7 354	0.4 6	0.7 284	1.7 289	2.6 261	2.7 229	2.8 212	2.7 213	1.8 209	0.6 252	5.8 352	17.5 18	29.1 47	41.4 104	75.5 141	90.9 151	67.8 156
6.5	1.52	0.6 355	0.2 352	0.8 272	1.8 284	2.8 258	2.9 226	2.9 208	2.6 216	1.7 210	0.6 267	5.6 354	15.6 21	24.5 56	42.2 120	83.0 150	98.3 158	70.6 162
6.0	2.51	0.4 332	0.2 293	0.9 260	1.8 283	2.8 256	3.0 225	3.0 220	2.6 217	1.6 209	0.5 272	5.0 355	12.4 26	18.7 75	44.7 138	89.5 158	103.4 165	71.4 168
5.5	4.14	0.4 264	0.6 225	1.0 242	1.8 279	2.8 254	3.1 223	3.2 208	2.6 215	1.6 206	0.4 265	4.0 357	8.4 36	8.4 108	15.1 153	48.0 166	92.4 171	103.7 174
5.0	6.83	0.7 258	1.1 219	1.3 226	1.7 266	2.7 249	3.1 222	3.2 207	2.6 212	1.5 201	0.3 227	2.6 359	4.6 62	15.8 141	49.3 165	89.5 173	97.8 177	62.8 179
4.5	11.25	1.1 230	1.7 217	2.0 217	1.9 246	2.6 240	3.0 218	3.0 203	2.5 205	1.5 193	0.5 180	1.0 11	3.3 120	3.3 162	16.9 45.8	78.9 78.9	84.0 84.0	52.4 52.4
4.0	18.55	1.4 227	2.3 216	2.8 213	2.5 227	2.6 227	2.8 212	3.0 196	3.0 196	1.7 185	1.7 167	0.8 146	4.6 162	15.9 172	37.4 182	61.7 182	63.6 182	38.3 185
3.5	30.59	1.6 225	2.9 215	3.6 212	3.3 216	3.8 214	2.7 204	3.0 186	2.6 185	1.9 178	1.8 164	2.4 161	5.7 179	12.2 192	25.2 190	40.0 187	38.8 189	22.1 191
3.0	50.43	1.6 223	3.4 215	4.4 212	4.2 210	3.1 203	2.5 195	3.0 176	2.8 175	2.2 172	2.5 163	3.7 164	6.1 191	8.1 220	12.5 207	18.3 207	14.5 193	6.7 192
2.5	85.15	1.7 222	3.8 215	5.0 212	5.0 207	3.4 196	2.5 186	3.1 166	3.1 168	2.4 169	3.1 163	4.7 164	5.9 200	6.8 267	9.6 257	2.3 257	4.3 257	4.5 26

JANUARY	MEAN TEMPERATURE	AMPLITUDE (K)	AND PHASE	WAVE 2															
SCALE	PRESSURE	-80	-70	-60	-50	-40	-30	-20	-10	0	10	20	30	40	50	60	70	80	
HEIGHT	(mb)																		
12.0	0.0062	0.32	0.19	0.18	0.15	0.25	0.26	0.52	1.30	0.80	0.36	0.36	0.78	0.58	1.10	0.92	0.33	0.25	
		9	325	112	21	127	90	40	37	55	22	27	18	309	50	62	286	209	
11.5	0.0103	0.37	0.21	0.22	0.17	0.27	0.29	0.49	1.24	0.79	0.34	0.35	0.78	0.49	1.10	0.88	0.29	0.42	
		9	328	111	27	124	88	37	38	55	28	31	23	314	59	74	278	221	
11.0	0.0169	0.41	0.21	0.24	0.19	0.26	0.29	0.39	1.09	0.72	0.31	0.31	0.73	0.34	1.06	0.85	0.23	0.67	
		10	335	109	34	119	84	36	41	55	40	40	33	328	75	93	257	228	
10.5	0.0279	0.40	0.20	0.27	0.20	0.26	0.29	0.23	0.82	0.60	0.26	0.27	0.67	0.21	1.11	0.94	0.21	0.98	
		9	343	110	42	105	79	28	46	54	63	61	50	28	98	121	214	231	
10.0	0.0460	0.32	0.16	0.26	0.21	0.26	0.27	0.07	0.50	0.44	0.27	0.28	0.67	0.44	1.33	1.28	0.39	1.30	
		9	7	106	54	90	73	344	61	54	94	90	74	84	122	146	178	232	
9.5	0.0758	0.16	0.17	0.23	0.22	0.26	0.23	0.18	0.28	0.24	0.34	0.34	0.75	0.80	1.69	1.77	0.70	1.51	
		2	41	109	68	76	65	240	114	60	119	118	100	102	142	164	164	232	
9.0	0.1250	0.08	0.22	0.18	0.21	0.24	0.15	0.34	0.43	0.10	0.39	0.42	0.87	1.08	2.03	2.30	1.11	1.21	
		240	64	103	79	62	63	225	172	135	137	138	124	111	158	119	161	229	
8.5	0.2061	0.30	0.21	0.13	0.14	0.16	0.02	0.38	0.60	0.30	1.37	0.46	0.92	1.17	2.16	2.68	1.48	0.45	
		210	66	99	81	60	148	217	191	191	154	155	146	122	177	193	161	278	
8.0	0.3398	0.50	0.16	0.07	0.05	0.04	0.20	0.32	0.60	0.52	0.50	0.44	0.90	0.99	2.10	2.85	1.70	1.13	
		208	46	74	53	146	216	202	203	192	180	171	141	140	199	208	167	21	
7.5	0.5603	0.48	0.14	0.06	0.08	0.14	0.26	0.16	0.33	0.49	0.24	0.47	1.08	1.20	2.04	2.45	1.65	1.11	
		203	359	24	314	199	214	176	226	194	224	187	195	185	213	209	163	78	
7.0	0.9237	0.40	0.13	0.08	0.09	0.17	0.21	0.06	0.20	0.32	0.25	0.47	1.19	1.49	2.02	2.49	1.90	1.07	
		196	333	7	315	197	207	135	271	204	241	205	213	211	215	199	178	12	
6.5	1.52	0.29	0.07	0.06	0.04	0.09	0.08	0.01	0.17	0.16	0.24	0.52	1.29	1.62	2.09	3.16	2.82	0.53	
		188	327	23	336	183	180	360	289	232	239	226	232	230	211	191	192	157	
6.0	2.51	0.24	0.02	0.04	0.02	0.03	0.06	0.03	0.12	0.10	0.23	0.66	1.50	1.73	2.17	3.93	3.73	1.19	
		195	326	90	135	135	90	45	280	253	239	248	251	256	216	202	220		
5.5	4.14	0.21	0.03	0.07	0.08	0.04	0.11	0.09	0.05	0.05	1.45	1.82	1.92	3.22	3.17	1.09			
		204	225	146	159	146	99	87	273	229	239	262	270	263	249	213	215	235	
5.0	6.83	0.19	0.06	0.13	0.14	0.05	0.16	0.16	0.04	0.06	0.10	0.49	1.28	2.03	3.20	2.52	2.18	0.85	
		216	209	162	163	143	99	94	124	121	231	278	290	305	286	252	244	260	
4.5	11.25	0.16	0.09	0.18	0.19	0.07	0.21	0.25	0.13	0.14	0.05	0.27	1.00	2.17	3.10	3.11	2.09	0.76	
		231	206	171	167	148	100	96	108	107	152	310	317	320	309	299	304	309	
4.0	18.55	0.14	0.11	0.21	0.23	0.07	0.23	0.30	0.20	0.20	0.13	0.24	0.85	2.10	3.75	4.50	3.47	1.14	
		249	205	175	167	146	100	96	106	100	97	24	353	331	321	323	340	350	
3.5	30.59	0.12	0.10	0.22	0.23	0.07	0.22	0.31	0.23	0.22	0.19	0.41	0.89	1.84	3.85	5.29	4.55	1.53	
		263	207	177	168	146	100	96	104	100	90	60	25	339	327	334	353		
3.0	50.43	0.09	0.09	0.19	0.19	0.06	0.20	0.29	0.23	0.21	0.22	0.51	0.91	1.42	3.36	4.90	4.44	1.48	
		276	208	177	168	141	100	96	104	101	87	70	44	344	330	339	359	15	
2.5	83.15	0.07	0.06	0.14	0.14	0.05	0.15	0.23	0.19	0.17	0.18	0.45	0.75	0.94	2.42	3.63	3.31	1.07	
		287	209	180	170	143	100	96	103	100	88	76	55	349	333	342	2	19	

JANUARY	MEAN GEOPOTENTIAL	HEIGHT	AMPLITUDE (dam) AND PHASE										WAVE 2									
SCALE	PRESSURE	-80	-70	-60	-50	-40	-30	-20	-10	0	10	20	30	40	50	60	70	80				
HEIGHT	(mb)																					
12.0	0.0062	2.0	1.7	4.0	2.4	3.0	3.5	2.2	5.1	4.5	1.4	1.6	4.8	13.8	11.6	10.2	8.0	5.2				
		223	16	116	89	118	97	84	65	86	118	221	289	311	307	287	334	296				
11.5	0.0103	2.5	1.5	3.7	2.3	2.7	3.1	1.8	3.6	3.5	1.5	2.1	4.9	13.0	12.2	11.2	7.7	5.1				
		216	27	116	94	116	98	101	79	95	138	218	275	311	300	283	337	301				
11.0	0.0169	3.0	1.4	3.4	2.2	2.3	2.7	1.6	2.5	2.7	1.7	2.6	5.5	12.4	13.2	12.4	7.6	5.0				
		211	38	117	100	116	100	122	105	109	154	218	265	311	294	281	340	310				
10.5	0.0279	3.6	1.3	3.0	2.0	1.9	2.3	1.7	2.2	2.1	1.8	3.0	6.2	12.1	14.6	13.7	7.6	4.9				
		208	50	118	107	117	104	138	139	127	166	220	258	310	291	282	342	324				
10.0	0.0460	4.1	1.1	2.6	1.9	1.5	2.0	1.8	2.4	1.9	1.8	3.3	7.7	12.3	16.3	15.0	8.0	5.3				
		205	61	119	115	121	109	144	163	148	178	223	256	308	291	285	343	343				
9.5	0.0758	4.4	1.0	2.3	1.7	1.3	1.7	1.9	2.3	1.8	1.7	3.6	8.2	13.0	18.4	16.5	8.8	6.3				
		204	69	121	123	132	118	140	175	163	191	230	257	306	294	291	344	1				
9.0	0.1250	4.5	0.7	2.0	1.6	1.1	1.5	1.9	1.9	1.6	1.6	3.7	9.2	14.4	20.7	18.1	10.1	7.9				
		203	75	123	132	149	126	128	181	172	209	238	262	304	298	299	344	1				
8.5	0.2061	4.2	0.4	1.7	1.4	1.2	1.5	2.0	1.2	1.3	1.4	3.8	10.0	16.0	22.8	19.8	12.0	9.3				
		202	82	126	141	164	130	113	180	173	230	248	268	303	304	309	343	18				
8.0	0.3398	3.6	0.2	1.6	1.4	1.2	1.5	2.1	0.4	0.8	1.3	3.8	10.5	17.6	24.3	21.5	14.3	10.0				
		201	117	128	146	170	124	98	141	162	250	258	274	304	311	319	343	18				
7.5	0.5603	2.9	0.3	1.4	1.4	1.1	1.5	2.2	0.7	0.4	1.1	3.7	10.6	18.8	25.2	23.1	16.7	9.7				
		200	161	131	146	167	111	90	69	113	264	269	282	307	317	328	343	11				
7.0	0.9237	2.3	0.5	1.7	1.5	0.9	1.6	2.1	1.0	0.7	0.8	3.5	10.4	19.5	26.0	25.2	19.3	9.5				
		200	162	134	145	160	98	86	67	73	277	279	291	313	324	335	344	2				
6.5	1.52	1.8	0.6	1.7	1.6	0.7	1.7	2.1	1.2	0.9	0.6	3.3	9.9	19.6	27.3	26.5	22.6	9.9				
		203	159	137	145	152	91	85	74	67	300	290	301	319	330	340	347	356				
6.0	2.51	1.4	0.7	1.7	1.7	0.7	1.6	2.1	1.4	1.1	0.5	2.8	9.0	19.3	28.8	33.0	26.8	10.9				
		206	158	140	146	149	89	86	79	68	338	304	312	326	335	345	352	359				
5.5	4.14	1.1	0.7	1.7	1.6	0.6	1.5	2.0	1.5	1.2	0.6	2.3	7.9	18.0	29.6	37.3	31.1	12.1				
		209	156	140	145	150	89	86	80	68	7	322	324	333	341	350	358	5				
5.0	6.83	0.8	0.7	1.5	1.4	0.6	1.3	1.9	1.6	1.3	0.8	1.9	6.6	15.9	28.9	39.5	33.9	12.8				
		208	152	139	144	150	87	86	80	66	19	342	337	339	346	355	3	10				
4.5	11.25	0.6	0.6	1.3	1.2	0.5	1.0	1.6	1.5	1.2	0.9	1.7	5.3	13.2	26.3	38.7	33.9	12.8				
		201	143	134	139	150	84	84	77	62	20	356	347	345	352	361	7	15				
4.0	18.55	0.4	0.6	1.1	1.0	0.4	0.7	1.2	1.0	0.9	1.3	1.4	4.1	10.5	22.5	35.3	31.1	11.1				
		182	130	124	131	151	76	80	72	54	13	359	341	351	0	7	12	11				
3.5	30.59	0.4	0.5	1.0	0.7	0.5	0.5	0.7	1.0	0.9	0.9	1.1	2.9	7.5	18.3	29.9	25.8	10.8				
		156	115	109	114	154	59	70	62	59	357	341	342	357	11	16	18	20				
3.0	50.43	0.5	0.6	0.9	0.6	0.2	0.3	0.4	0.8	0.8	0.9	1.2	2.4	5.2	14.7	24.5	19.7	7.7				
		140	101	91	89	159	16	41	44	19	338	308	316	4	25	27	25	2				
2.5	83.15	0.6	0.6	0.9	0.6	0.1	0.4	0.4	0.7	0.8	1.1	1.8	2.7	3.6	12.6	20.6	14.7	6.3				
		133	92	76	65	176	331	339	20	358	323	289	290	13	40	40	34	6				

FEBRUARY MEAN TEMPERATURE AMPLITUDE (K) AND PHASE WAVE 1

SCALE HEIGHT	PRESSURE (mb)	-80	-70	-60	-50	-40	-30	-20	-10	0	10	20	30	40	50	60	70	80
12.0	0.0062	0.24 272	0.48 8	0.65 22	0.14 86	0.21 239	1.10 245	0.96 260	0.04 340	1.46 63	0.36 26	0.62 271	1.57 288	1.95 295	2.55 264	3.96 257	3.30 265	2.67 317
11.5	0.0103	0.27 270	0.54 8	0.70 22	0.13 85	0.25 241	1.10 246	0.95 260	0.03 326	1.46 63	0.38 33	0.62 271	1.60 288	2.09 292	2.76 270	4.47 266	3.68 276	3.04 320
11.0	0.0169	0.29 262	0.59 9	0.71 24	0.12 76	0.29 243	1.03 248	0.86 259	0.01 90	1.37 61	0.38 41	0.60 258	1.54 277	2.13 289	3.49 277	5.05 277	4.65 287	3.41 324
10.5	0.0279	0.28 253	0.58 10	0.66 27	0.10 63	0.35 248	0.87 251	0.70 258	0.03 138	1.23 59	0.40 50	0.56 246	1.40 266	2.11 284	4.00 286	5.82 289	5.65 298	3.81 328
10.0	0.0460	0.27 236	0.52 13	0.56 33	0.09 41	0.40 249	0.68 257	0.49 258	0.06 135	1.05 54	0.42 61	0.54 230	1.28 250	2.03 278	4.59 294	6.83 300	6.87 307	4.25 333
9.5	0.0758	0.25 205	0.41 19	0.40 44	0.08 22	0.41 252	0.45 267	0.28 258	0.06 135	0.83 47	0.44 70	0.52 211	1.16 230	1.85 272	5.09 302	7.64 310	7.96 316	4.56 337
9.0	0.1250	0.30 166	0.25 38	0.25 76	0.06 27	0.35 254	0.24 291	0.14 274	0.01 315	0.60 32	0.41 75	0.45 192	1.00 206	1.49 263	5.20 310	8.50 320	8.50 325	4.59 343
8.5	0.2061	0.40 139	0.16 103	0.22 130	0.08 110	0.17 248	0.09 349	0.17 304	0.18 319	0.43 1	0.28 65	0.29 158	0.74 169	0.86 259	4.55 322	8.32 334	8.10 339	4.07 351
8.0	0.3398	0.50 121	0.29 145	0.29 155	0.21 124	0.12 90	0.11 87	0.31 303	0.41 319	0.16 324	0.16 0	0.28 73	0.74 104	0.04 153	3.23 344	7.37 353	7.10 353	3.10 1
7.5	0.5603	0.34 125	0.35 175	0.27 163	0.34 127	0.29 84	0.13 133	0.45 289	0.37 318	0.34 300	0.34 307	0.47 19	0.98 49	1.03 37	3.00 57	6.26 18	6.37 18	2.60 38
7.0	0.9237	0.09 111	0.24 205	0.20 195	0.31 142	0.28 90	0.12 145	0.24 282	0.31 316	0.26 288	0.37 290	0.48 0	1.25 26	2.05 33	4.02 45	6.57 46	7.07 55	3.07 64
6.5	1.52	0.20 339	0.19 293	0.24 254	0.24 182	0.17 108	0.10 119	0.03 270	0.07 301	0.14 264	0.26 339	0.28 17	1.26 263	2.90 310	5.37 320	7.88 325	8.13 325	3.84 343
6.0	2.51	0.41 352	0.42 335	0.40 282	0.28 219	0.15 132	0.13 99	0.12 76	0.11 165	0.11 202	0.29 212	0.07 297	1.26 212	3.50 287	6.38 315	8.95 343	8.45 343	4.21 80
5.5	4.14	0.45 11	0.53 357	0.41 314	0.18 257	0.10 117	0.09 114	0.11 54	0.10 182	0.13 198	0.27 211	0.09 342	1.27 30	3.35 54	6.39 82	8.57 93	7.20 94	3.55 108
5.0	6.83	0.43 34	0.57 16	0.47 354	0.24 343	0.07 45	0.05 174	0.08 7	0.10 233	0.13 209	0.18 227	0.23 353	1.16 39	2.96 107	6.05 120	7.69 130	6.08 149	3.79 149
4.5	11.25	0.39 66	0.56 38	0.66 25	0.54 12	0.19 358	0.11 242	0.15 301	0.18 268	0.11 236	0.15 297	0.44 351	0.92 47	2.65 105	5.94 137	7.75 155	7.32 155	5.36 180
4.0	18.55	0.42 101	0.55 61	0.89 42	0.83 21	0.30 348	0.20 257	0.25 281	0.28 281	0.13 274	0.30 333	0.61 349	0.63 61	2.72 135	6.29 163	9.12 183	10.23 195	7.43 197
3.5	30.59	0.49 125	0.53 80	1.01 52	0.99 26	0.37 345	0.25 262	0.34 274	0.34 287	0.45 292	0.45 342	0.73 347	0.40 83	2.91 155	6.47 180	9.90 199	12.06 207	8.54 207
3.0	50.43	0.47 138	0.47 95	0.93 58	0.95 29	0.37 343	0.26 265	0.36 270	0.35 288	0.18 304	0.51 346	0.74 347	0.26 116	2.73 167	5.88 191	9.07 209	10.92 214	7.06 214
2.5	85.15	0.38 145	0.35 104	0.71 61	0.74 31	0.30 341	0.22 266	0.30 265	0.29 291	0.16 307	0.42 347	0.56 345	0.19 145	2.09 175	4.42 198	6.74 215	7.65 219	4.43 219

FEBRUARY MEAN GEOPOTENTIAL HEIGHT AMPLITUDE (dam) AND PHASE WAVE 1

SCALE HEIGHT	PRESSURE (mb)	-80	-70	-60	-50	-40	-30	-20	-10	0	10	20	30	40	50	60	70	80
12.0	0.0062	4.7 182	3.0 13	3.5 28	1.6 167	4.1 225	8.7 243	9.0 265	3.5 287	5.4 46	2.0 58	3.2 255	4.3 309	5.7 359	8.2 395	21.7 293	22.7 288	10.7 279
11.5	0.0103	4.7 178	2.2 15	2.5 31	1.6 174	3.7 224	7.1 242	7.5 266	3.5 287	4.0 40	1.6 68	2.3 250	2.3 332	5.2 307	5.7 352	16.7 304	17.8 304	7.9 260
11.0	0.0169	4.7 173	1.4 19	1.5 36	1.6 181	3.4 222	5.5 241	6.2 267	3.4 286	2.7 28	1.1 83	2.4 242	2.0 36	6.5 258	5.5 314	11.5 323	11.8 323	7.1 224
10.5	0.0279	4.7 167	0.6 32	0.5 56	1.7 186	2.9 218	4.1 238	5.1 269	3.5 287	1.8 3	0.8 110	0.6 227	0.6 65	8.9 73	8.9 84	7.4 64	4.4 6	9.8 192
10.0	0.0460	4.6 163	0.4 159	0.5 178	1.8 190	2.5 212	3.1 235	4.2 272	3.5 287	1.5 325	0.6 160	0.2 89	0.2 70	5.6 80	11.6 80	13.9 83	9.9 69	14.7 176
9.5	0.0758	4.4 159	1.0 183	1.1 202	1.9 201	2.1 224	2.4 244	3.7 274	3.6 288	1.8 297	0.9 203	0.9 50	7.3 68	14.4 83	20.1 95	18.2 98	15.6 127	20.9 170
9.0	0.1250	4.1 156	1.5 190	1.5 212	2.0 191	1.8 187	2.1 213	3.4 275	3.6 288	2.1 283	1.4 223	1.6 38	6.7 63	16.9 84	26.9 103	28.7 113	27.5 133	27.5 167
8.5	0.2061	3.6 157	1.6 198	1.6 222	2.0 193	1.6 174	2.1 208	3.2 274	3.5 287	2.2 275	1.9 230	2.0 28	2.0 57	9.5 84	18.6 110	33.2 123	39.6 139	33.9 167
8.0	0.3398	3.0 163	1.5 209	1.6 236	2.0 199	1.6 172	2.0 208	2.9 270	3.2 283	2.0 265	2.2 230	2.1 20	2.1 95	19.3 84	37.7 115	49.0 131	49.2 145	39.1 169
7.5	0.5603	2.6 172	1.2 225	1.6 251	1.9 211	1.6 184	2.3 212	2.5 266	2.7 275	2.2 251	1.6 220	2.2 14	1.6 89	8.4 85	18.7 95	39.6 98	55.4 140	42.5 172
7.0	0.9237	2.4 177	0.9 242	1.5 263	1.9 226	1.7 198	2.2 217	2.1 261	2.3 265	1.6 235	2.1 206	0.9 18	0.9 52	6.8 91	17.4 128	39.6 148	58.7 162	44.6 176
6.5	1.52	2.5 177	0.7 241	1.3 270	1.7 237	1.8 208	2.2 217	2.1 260	2.5 260	1.5 225	2.0 194	0.4 52	0.4 62	5.3 102	15.7 138	38.7 158	60.0 172	46.3 182
6.0	2.51	2.9 175	0.7 188	0.9 232	1.5 249	1.8 228	2.3 228	2.3 259	1.9 265	2.1 228	1.3 228	0.5 180	4.2 92	14.5 105	38.2 140	61.0 165	66.0 182	48.3 195
5.5	4.14	3.6 177	1.4 188	0.4 185	1.1 239	1.8 224	2.3 224	2.1 256	2.1 268	1.1 232	1.4 170	0.5 113	3.4 136	14.0 159	37.4 179	61.4 193	68.6 200	49.2 201
5.0	6.83	4.2 180	2.2 188	0.8 185	1.0 234	1.9 220	2.3 220	2.3 250	2.0 268	0.9 232	1.2 170	0.6 113	3.5 136	15.6 159	35.7 179	59.9 193	68.0 200	47.5 201
4.5	11.25	4.6 186	3.0 193	1.6 189	2.0 220	2.0 221	2.2 230	2.2 253	1.8 270	0.8 230	1.2 161	1.0 138	1.2 161	12.8 176	31.8 192	54.3 202	62.0 206	42.1 206
4.0	18.55	4.7 193	3.6 201	2.7 199	2.4 210	2.3 214	2.6 228	1.9 248	1.5 268	0.6 217	1.5 157	1.7 157	1.7 176	11.1 193	26.0 206	44.6 211	50.4 211	33.4 211
3.5	30.59	4.6 201	4.2 209	4.0 209	3.7 208	2.6 206	1.8 223	1.6 240	1.1 262	0.7 191	2.1 157	2.2 157	2.7 158	4.5 185	18.8 213	31.6 221	34.1 211	21.7 215
3.0	50.43	4.4 209	4.6 217	5.3 216	5.2 208	3.1 199	1.5 213	1.2 226	0.7 241	0.9 241	2.8 191	3.8 160	4.5 191	6.9 246	18.4 230	17.0 220	10.0 221	
2.5	85.15	4.2 217	4.9 223	6.4 220	6.4 208	3.5 194	1.3 204	0.9 197	0.5 162	1.2 161	3.5 161	4.7 161	4.3 194	6.6 271	9.8 285	8.2 257	3.5 230	1.8 242

FEBRUARY MEAN TEMPERATURE AMPLITUDE (K) AND PHASE WAVE 2

SCALE HEIGHT	PRESSURE (mb)	-80	-70	-60	-50	-40	-30	-20	-10	0	10	20	30	40	50	60	70	80
12.0	0.0062	0.37 133	0.04 188	0.28 314	0.07 297	0.38 30	0.39 59	1.04 97	0.86 79	0.51 36	0.43 114	0.54 343	0.54 293	1.03 333	0.93 354	0.53 14	0.16 79	0.23 247
11.5	0.0103	0.46 135	0.03 160	0.29 316	0.06 304	0.38 33	0.39 59	0.99 97	0.82 79	0.50 41	0.47 113	0.11 360	0.48 298	1.00 337	0.99 359	0.63 10	0.18 75	0.11 270
11.0	0.0169	0.55 139	0.05 139	0.29 316	0.06 325	0.34 34	0.36 59	0.85 98	0.72 82	0.48 50	0.51 113	0.13 18	0.35 308	0.91 346	1.01 5	0.35 2	0.24 9	0.10 39
10.5	0.0279	0.61 142	0.07 103	0.26 320	0.06 342	0.27 40	0.30 58	0.62 100	0.56 85	0.47 63	0.54 112	0.15 48	0.20 345	0.76 4	1.00 15	0.82 2	0.36 9	0.30 39
10.0	0.0460	0.65 146	0.11 87	0.21 331	0.07 16	0.18 52	0.21 62	0.35 108	0.37 95	0.48 80	0.59 110	0.22 68	0.30 60	0.70 35	0.99 26	0.91 357	0.49 2	0.50 44
9.5	0.0758	0.63 152	0.13 76	0.13 353	0.10 39	0.11 98	0.10 61	0.09 164	0.18 130	0.52 98	0.62 110	0.29 81	0.57 80	0.83 67	0.97 40	0.96 357	0.58 0	0.69 46
9.0	0.1250	0.49 165	0.14 63	0.13 45	0.13 53	0.15 152	0.01 180	0.25 180	0.22 198	0.54 113	0.63 110	0.35 95	0.81 89	1.07 87	0.93 54	0.90 358	0.59 2	0.76 46
8.5	0.2061	0.28 196	0.11 37	0.18 67	0.13 61	0.22 164	0.07 226	0.35 262	0.31 219	0.51 127	0.57 115	0.38 110	0.89 95	1.17 100	1.07 70	0.71 10	0.45 5	0.65 43
8.0	0.3398	0.31 270	0.12 340	0.21 67	0.12 70	0.21 161	0.10 227	0.28 262	0.31 224	0.38 145	0.44 124	0.39 130	0.75 105	1.03 113	0.50 101	0.41 25	0.22 41	0.36 36
7.5	0.5603	0.37 288	0.15 316	0.15 38	0.10 76	0.14 129	0.05 198	0.08 266	0.19 238	0.18 151	0.21 169	0.39 165	0.42 161	0.61 212	0.57 150	0.36 36	0.65 141	0.17 142
7.0	0.9237	0.26 281	0.12 318	0.13 4	0.09 86	0.12 85	0.03 108	0.03 90	0.11 259	0.19 249	0.19 217	0.41 203	0.69 222	0.98 226	1.41 216	1.72 186	1.58 185	0.65 221
6.5	1.52	0.13 225	0.07 0	0.12 358	0.08 55	0.11 68	0.06 75	0.03 90	0.10 277	0.18 267	0.24 243	0.46 236	0.95 243	1.12 236	2.11 206	3.56 194	3.13 208	1.46 239
6.0	2.51	0.16 176	0.11 59	0.11 45	0.06 45	0.06 51	0.07 70	0.01 90	0.08 274	0.11 275	0.26 251	0.60 261	1.06 257	0.88 241	2.58 195	5.11 198	4.73 220	2.36 248
5.5	4.14	0.11 162	0.16 64	0.16 74	0.03 111	0.03 141	0.10 96	0.07 124	0.02 120	0.02 270	0.20 253	0.50 277	0.78 267	2.46 238	4.72 191	3.42 203	4.46 229	2.48 252
5.0	6.83	0.06 108	0.22 66	0.22 87	0.09 164	0.11 185	0.16 114	0.15 122	0.13 101	0.09 96	0.09 260	0.35 303	0.34 289	1.04 166	1.54 192	3.23 211	3.15 242	2.06 255
4.5	11.25	0.11 49	0.28 65	0.29 96	0.16 173	0.21 191	0.22 126	0.23 123	0.24 104	0.21 69	0.06 5	0.27 5	0.33 44	0.58 68	1.23 215	1.44 253	1.09 292	1.59 259
4.0	18.55	0.17 31	0.30 63	0.32 99	0.22 175	0.29 192	0.28 133	0.28 120	0.32 99	0.30 94	0.21 73	0.44 49	0.78 68	0.60 64	0.79 359	2.17 346	2.73 346	0.33 43
3.5	30.59	0.21 22	0.30 62	0.32 101	0.24 175	0.32 191	0.30 137	0.29 120	0.35 97	0.34 95	0.31 75	0.62 64	1.16 68	1.50 347	3.71 367	4.62 347	1.65 4	2.69 72
3.0	50.43	0.20 18	0.25 61	0.27 103	0.22 175	0.29 190	0.28 141	0.27 118	0.33 97	0.35 95	0.35 76	0.67 72	1.17 62	1.73 348	4.03 348	4.73 4	2.03 33	1.54 73
2.5	85.15	0.15 18	0.17 59	0.19 104	0.16 174	0.23 189	0.22 142	0.21 118	0.26 96	0.25 95	0.28 77	0.55 76	0.93 79	1.46 62	3.21 348	3.50 6	1.54 35	1.54 73

FEBRUARY MEAN GEOPOTENTIAL HEIGHT AMPLITUDE (dam) AND PHASE WAVE 2

SCALE HEIGHT	PRESSURE (mb)	-80	-70	-60	-50	-40	-30	-20	-10	0	10	20	30	40	50	60	70	80
12.0	0.0062	5.2 170	2.3 55	3.4 41	2.2 74	3.0 93	3.6 84	5.3 109	4.5 117	6.1 106	6.6 117	0.8 67	1.9 19	8.7 27	11.4 21	12.9 356	13.0 339	7.4 316
11.5	0.0103	4.7 174	2.4 54	3.4 48	2.3 76	2.8 103	3.1 89	5.9 114	5.5 115	5.7 119	5.9 118	0.8 79	2.0 42	7.9 26	10.1 32	12.1 34	13.0 354	7.2 318
11.0	0.0169	4.2 180	2.4 53	3.4 55	2.4 78	2.7 113	2.6 95	5.2 122	5.2 130	5.2 121	5.2 118	0.8 91	2.8 58	8.2 45	11.1 28	12.9 353	13.0 337	7.1 318
10.5	0.0279	3.6 189	2.3 51	3.5 62	2.4 80	2.6 123	2.3 102	1.7 137	4.7 149	4.4 124	4.4 119	0.7 119	2.2 68	6.5 54	7.4 31	10.0 352	12.5 335	7.1 316
10.0	0.0460	3.0 202	2.2 49	3.6 67	2.4 82	2.5 130	2.0 109	1.2 158	4.0 168	3.6 127	3.6 121	0.5 125	2.0 74	6.0 60	6.0 34	8.1 351	12.0 334	7.1 311
9.5	0.0758	2.5 219	2.1 46	3.6 71	2.3 85	2.4 134	1.9 114	0.9 168	1.7 179	3.2 130	2.7 125	0.4 74	1.4 46	4.5 34	7.4 34	11.3 350	11.3 332	7.2 304
9.0	0.1250	2.3 238	1.9 44	3.5 73	2.2 88	2.3 135	1.8 116	0.9 156	1.5 181	2.4 134	1.9 132	0.6 224	0.5 47	3.3 55	3.2 29	6.0 348	10.5 330	7.5 296
8.5	0.2061	2.1 252	1.7 43	3.3 74	2.0 91	2.0 131	1.9 114	1.1 172	1.1 138	1.5 148	1.1 252	1.0 291	1.0 23	2.3 27	2.2 11	4.9 345	9.9 327	7.9 288
8.0	0.3398	1.7 256	1.6 46	3.0 75	1.8 93	1.8 125	1.9 110	1.4 143	0.9 143	0.6 188	1.4 269	2.2 284	2.5 340	2.1 346	4.1 346	9.6 325	8.2 325	8.2 284
7.5	0.5603	1.3 246	1.6 53	2.7 76	1.7 95	1.5 122	2.0 107	1.7 112	0.9 138	0.5 238	0.4 285	1.8 290	2.9 340	3.5 346	2.5 346	4.2 336	10.1 324	8.4 282
7.0	0.9237	1.0 227	1.6 60	2.6 80	1.6 97	1.6 124	1.9 106	1.7 112	1.1 117	0.6 119	0.4 272	1.9 302	3.0 351	4.3 351	5.5 341	11.4 341	8.3 327	8.3 785
6.5	1.52	0.8 217	1.6 64	2.6 84	1.5 99	1.3 130	1.9 107	1.6 112	1.2 114	0.8 109	0.2 333	0.8 320	2.8 328	5.2 7	6.0 35	9.1 354	13.8 338	7.9 295
6.0	2.51	0.6 224	1.5 66	2.6 87	1.4 103	1.2 135	1.8 109	1.6 113	1.3 112	1.0 105	0.4 36	1.8 343	2.9 357	6.2 18	9.5 17	15.1 3	17.6 354	6.1 315
5.5	4.14	0.5 242	1.3 67	2.4 89	1.4 104	1.2 138	1.7 111	1.6 112	1.4 111	1.1 102	0.7 52	1.8 9	3.3 21	7.0 13	13.1 16	22.2 7	22.5 7	5.6 351
5.0	6.83	0.5 255	1.1 67	2.1 90	1.3 102	1.1 135	1.5 111	1.4 111	1.2 101	1.0 98	0.9 29	1.8 34	3.7 34	7.5 15	16.0 12	28.0 12	26.8 16	7.0 20
4.5	11.25	0.7 254	0.7 68	1.7 89	1.2 94	1.0 123	1.2 108	1.1 108	0.8 115	0.8 102	0.9 58	1.6 37	3.5 22	7.1 15	17.5 15	30.7 28	28.4 22	8.5 33
4.0	18.55	0.8 245	0.3 74	1.3 86	1.2 81	0.9 102	0.9 100	0.8 101	0.6 126	0.5 106	0.7 54	1.2 44	2.8 31	6.6 18	17.3 17	29.8 18	26.6 25	8.9 37
3.5	30.59	1.1 236	0.2 227	0.8 78	1.3 66	1.0 77	0.6 75	0.4 184	0.3 177	0.1 35	0.4 19	0.4 2	2.0 6	15.9 12	25.8 22	21.0 22	7.6 26	7.6 32
3.0	50.43	1.3 228	0.6 236	0.5 57	1.4 53	1.3 58	0.5 31	0.3 6	0.6 247	0.5 262	0.3 313	0.8 275	2.2 315	5.4 4	13.9 25	20.4 23	14.0 23	5.6 13
2.5	85.15	1.6 224	0.9 237	0.3 14	1.6 45	0.8 47	0.8 3	0.5 321	0.5 260	0.7 267	1.6 279	3.5 263	5.0 292	12.1 356	15.6 32	8.1 35	4.9 15	4.9 345

MARCH		MEAN TEMPERATURE AMPLITUDE (K) AND PHASE WAVE																
SCALE	PRESSURE	-80	-70	-60	-50	-40	-30	-20	-10	0	10	20	30	40	50	60	70	80
HEIGHT	(mb)																	
12.0	0.0062	0.25 313	0.34 120	0.89 70	0.45 58	0.37 53	0.65 320	0.46 116	0.72 55	0.81 33	0.51 279	1.10 271	0.97 265	1.06 293	1.01 246	1.67 229	1.31 229	0.80 213
11.5	0.0103	0.28 296	0.37 139	0.88 76	0.53 65	0.34 310	0.63 316	0.40 117	0.72 55	0.82 36	0.47 277	1.07 269	1.01 299	1.23 255	1.33 245	1.89 255	1.49 244	0.73 220
11.0	0.0169	0.36 276	0.46 162	0.80 86	0.37 76	0.29 304	0.56 310	0.51 119	0.69 56	0.80 39	0.73 273	0.95 265	1.02 251	1.35 230	1.53 265	1.74 262	2.24 273	1.90 273
10.5	0.0279	0.50 261	0.63 182	0.70 109	0.31 98	0.19 287	0.47 298	0.16 125	0.62 56	0.76 265	0.26 258	0.76 259	1.00 289	1.49 279	2.27 281	2.70 293	3.06 307	1.30 321
10.0	0.0460	0.68 251	0.89 197	0.71 141	0.30 138	0.13 243	0.38 274	0.58 256	0.54 57	0.40 55	0.54 232	0.54 242	0.55 224	0.51 228	0.91 289	1.61 291	3.82 307	3.85 321
9.5	0.0758	0.87 246	1.16 209	0.91 172	0.43 172	0.22 194	0.37 242	0.23 285	0.41 57	0.70 64	0.16 155	0.43 212	1.05 212	1.73 289	3.57 350	5.03 310	5.20 319	3.05 335
9.0	0.1250	0.98 246	1.34 222	1.19 196	0.62 192	0.32 178	0.42 215	0.40 291	0.25 56	0.67 73	0.26 127	0.43 179	1.00 198	1.73 292	4.11 299	6.26 322	6.51 331	4.00 340
8.5	0.2061	0.92 250	1.33 259	1.34 218	0.76 209	0.37 175	0.45 196	0.41 191	0.55 41	0.53 81	0.30 118	0.40 163	0.75 187	1.59 301	4.39 314	7.22 334	7.44 356	4.65 349
8.0	0.3398	0.66 265	1.23 269	1.38 245	0.81 226	0.33 171	0.39 180	0.37 290	0.14 253	0.31 86	0.22 99	0.25 162	0.27 161	1.32 317	4.45 334	7.69 352	7.88 358	4.83 359
7.5	0.5603	0.45 334	1.32 314	1.34 285	0.73 253	0.20 180	0.24 168	0.19 273	0.25 265	0.07 321	0.14 335	0.24 276	0.36 341	1.28 344	4.43 415	7.26 415	7.32 415	4.19 428
7.0	0.9237	0.88 21	1.62 349	1.50 321	0.71 289	0.09 254	0.14 272	0.12 228	0.23 270	0.26 295	0.32 304	0.42 306	0.52 355	0.88 356	2.03 37	5.62 40	8.16 43	4.60 45
6.5	1.52	1.31 37	1.95 349	1.74 321	0.86 289	0.17 299	0.19 191	0.12 204	0.15 272	0.17 293	0.17 293	0.34 352	0.44 351	1.36 31	3.49 31	7.62 48	10.14 55	9.85 53
6.0	2.51	1.56 49	2.25 36	2.04 342	1.14 317	0.33 203	0.16 213	0.17 213	0.22 249	0.27 292	0.51 279	1.96 359	5.10 23	9.44 38	11.80 66	10.05 63	6.25 58	6.25 44
5.5	4.14	1.62 62	2.32 49	2.19 35	1.29 357	0.39 322	0.17 213	0.16 216	0.15 246	0.19 284	0.26 278	0.67 5	2.32 28	5.23 46	8.79 66	10.23 74	8.71 68	4.61 45
5.0	6.83	1.22 83	2.07 63	2.15 39	1.34 13	0.30 325	0.21 226	0.18 235	0.16 253	0.24 293	0.26 255	0.80 273	0.80 288	1.31 30	4.48 67	7.77 85	7.24 99	5.23 70
4.5	11.25	1.02 119	1.61 84	1.94 56	1.30 56	0.30 329	0.21 248	0.19 259	0.21 267	0.17 267	0.29 308	0.29 352	0.88 352	1.89 77	5.11 77	9.41 126	6.18 153	2.85 168
4.0	18.55	1.14 154	1.28 115	1.68 74	1.21 74	0.17 335	0.25 252	0.24 272	0.26 274	0.15 266	0.33 317	0.90 340	1.23 123	2.17 123	5.86 91	9.13 191	8.98 198	5.32 205
3.5	30.59	1.29 173	1.17 145	1.41 93	1.07 63	0.40 360	0.26 258	0.28 282	0.28 287	0.14 266	0.36 325	0.89 329	0.59 6	2.55 165	7.49 104	11.42 115	11.68 205	7.32 208
3.0	50.43	1.22 184	1.07 165	1.11 108	0.87 66	0.06 121	0.25 261	0.28 285	0.28 291	0.12 270	0.36 331	0.81 320	2.09 304	2.89 184	7.59 104	11.10 112	11.51 215	7.41 218
2.5	83.15	0.94 190	0.84 177	0.78 120	0.62 86	0.08 135	0.22 264	0.23 285	0.23 297	0.09 277	0.29 333	0.59 314	0.59 260	2.49 192	6.05 209	8.58 216	8.76 216	5.10 210

MARCH		MEAN GEOPOTENTIAL HEIGHT AMPLITUDE (dam) AND PHASE																WAVE 1	
SCALE	PRESSURE	-80	-70	-60	-50	-40	-30	-20	-10	0	10	20	30	40	50	60	70	80	
HEIGHT	(mb)																		
12.0	0.0062	5.3 253	0.2 284	5.4 39	2.4 338	3.6 235	5.6 232	3.5 216	2.1 72	4.4 62	3.5 259	7.4 284	5.5 347	21.1 13	16.1 25	15.2 5	18.5 345	16.4 324	
11.5	0.0103	5.0 249	0.7 302	4.4 29	2.5 323	3.5 227	5.7 223	3.7 225	1.2 88	3.4 66	2.8 254	5.8 288	5.6 2	20.9 18	17.3 29	16.9 12	19.1 351	16.6 331	
11.0	0.0169	4.7 246	1.3 315	3.8 14	2.7 310	3.5 219	5.7 214	3.9 233	0.6 150	2.4 73	2.2 248	4.5 295	6.2 16	20.8 23	18.8 34	18.6 20	19.2 358	16.5 333	
10.5	0.0279	4.1 242	1.9 329	3.8 358	3.0 304	3.4 214	5.8 207	4.0 237	1.2 205	1.5 86	1.8 243	3.5 306	7.2 24	21.0 28	20.7 40	20.0 30	18.5 350	15.1 335	
10.0	0.0460	3.3 239	2.9 344	4.5 347	3.5 303	3.3 210	5.7 200	4.1 239	1.9 218	0.8 119	1.5 241	3.0 321	8.6 29	21.5 34	23.1 48	21.5 43	17.3 22	13.0 335	
9.5	0.0758	2.2 234	4.1 357	5.6 345	3.9 307	3.1 210	5.5 196	3.9 237	2.6 223	0.8 186	1.4 247	3.1 334	10.1 30	22.3 40	26.1 57	23.4 59	16.1 45	9.3 343	
9.0	0.1250	0.9 215	5.7 9	7.1 350	4.4 316	2.7 214	5.0 192	3.6 231	3.1 225	1.4 219	1.5 257	3.6 340	11.6 29	23.3 46	29.6 66	26.5 76	16.9 75	4.3 353	
8.5	0.2061	0.8 100	7.3 19	8.6 357	4.9 327	2.3 222	4.4 190	3.4 224	3.3 226	1.9 232	1.9 267	4.2 341	12.8 28	24.3 52	33.1 75	30.8 94	20.8 104	12.8 104	
8.0	0.3398	2.0 86	8.5 29	9.9 6	5.4 338	2.0 234	3.7 191	3.2 211	3.2 225	2.2 238	2.2 271	4.7 341	13.5 26	24.9 56	36.0 85	36.1 111	27.2 126	9.6 161	
7.5	0.5603	2.6 93	8.9 40	10.4 17	5.7 349	1.9 244	3.3 193	3.0 205	2.2 222	2.3 239	2.3 269	4.8 344	13.5 26	24.9 61	37.1 94	40.7 125	33.4 143	15.1 170	
7.0	0.9237	2.7 112	8.3 54	10.1 28	5.6 360	1.7 249	3.1 195	3.0 201	2.8 216	2.1 233	2.1 262	4.5 348	12.7 29	23.8 65	35.9 105	43.5 140	38.7 159	20.1 186	
6.5	1.52	2.9 145	6.9 71	8.8 40	5.0 10	1.6 246	1.9 196	2.0 201	2.6 211	1.9 223	1.7 253	4.0 353	11.3 32	20.8 72	32.7 121	45.7 157	44.9 175	27.0 195	
6.0	2.51	3.9 176	9.5 55	7.0 55	2.5 234	1.5 196	2.0 200	2.6 207	2.5 213	1.8 203	1.4 242	3.5 354	9.0 36	16.3 86	30.4 143	50.5 175	54.1 189	35.0 203	
5.5	4.14	5.5 197	4.1 135	4.8 77	2.6 44	1.5 214	2.4 194	2.3 199	2.3 204	1.7 203	1.1 231	1.5 350	5.9 42	12.0 112	31.5 168	57.5 141	64.0 200	42.6 207	
5.0	6.83	6.8 211	4.7 177	3.5 119	1.7 91	1.8 197	2.4 192	2.1 196	2.0 200	1.6 194	0.9 212	1.4 340	2.6 58	10.6 149	34.4 188	62.5 202	69.9 207	47.1 210	
4.5	11.25	7.5 222	6.0 203	3.8 167	2.1 152	2.2 187	2.0 186	2.0 190	2.1 193	1.6 184	0.9 186	0.8 285	1.5 152	11.4 177	34.7 201	61.2 210	68.5 212	46.1 214	
4.0	18.55	7.5 234	6.8 220	5.1 198	3.3 183	2.5 182	1.9 177	1.9 181	2.0 183	1.6 175	1.2 182	1.5 185	3.4 186	11.4 196	30.5 212	52.7 217	59.6 216	41.6 214	
3.5	30.59	7.1 247	7.0 234	6.3 217	4.0 200	2.6 181	1.8 166	2.0 170	2.1 173	1.7 167	1.7 162	2.4 168	4.7 189	9.6 211	22.0 223	38.4 224	44.6 220	32.1 216	
3.0	50.43	6.6 263	6.9 248	7.3 230	5.9 211	2.6 182	1.5 155	2.2 161	2.4 164	1.9 169	2.2 158	3.6 160	5.2 187	6.7 231	12.6 244	22.6 235	27.8 227	21.1 212	
2.5	83.15	6.4 277	6.7 259	8.0 238	6.3 219	2.6 184	1.4 147	2.4 153	2.6 157	2.1 157	2.7 145	4.5 152	5.2 187	7.6 267	9.7 276	10.4 264	13.7 241	12.0 230	

MARCH	MEAN TEMPERATURE AMPLITUDE (K) AND PHASE																		WAVE 2																	
SCALE	PRESSURE	-80	-70	-60	-50	-40	-30	-20	-10	0	10	20	30	40	50	60	70	80																		
HEIGHT	(mb)																																			
12.0	0.0062	0.02 63	0.20 159	0.09 117	0.36 123	0.49 101	1.02 76	0.66 93	0.60 98	0.67 118	0.51 141	0.50 145	0.14 90	0.38 30	0.67 30	1.09 31	0.46 24	0.23 167																		
11.5	0.0103	0.05 107	0.20 161	0.11 131	0.39 123	0.51 98	0.99 76	0.63 92	0.57 96	0.65 118	0.49 139	0.52 142	0.16 102	0.41 32	0.67 35	1.13 35	0.50 26	0.26 178																		
11.0	0.0169	0.11 124	0.19 163	0.12 145	0.41 125	0.52 99	0.87 76	0.55 90	0.49 93	0.58 119	0.44 137	0.52 139	0.20 113	0.38 35	0.61 39	1.06 37	0.51 20	0.28 172																		
10.5	0.0279	0.19 134	0.16 169	0.17 165	0.41 127	0.49 98	0.68 76	0.43 87	0.38 87	0.47 118	0.36 135	0.48 135	0.24 127	0.35 42	0.48 50	0.89 44	0.48 18	0.32 159																		
10.0	0.0460	0.36 158	0.13 185	0.24 178	0.41 128	0.47 97	0.42 75	0.27 75	0.24 72	0.34 122	0.26 127	0.44 128	0.30 136	0.29 55	0.33 75	0.67 58	0.43 16	0.36 148																		
9.5	0.0758	0.36 139	0.09 224	0.28 187	0.37 130	0.44 95	0.14 68	0.12 21	0.13 32	0.18 119	0.16 106	0.39 120	0.35 142	0.21 79	0.26 129	0.41 91	0.33 19	0.41 136																		
9.0	0.1250	0.58 138	0.13 268	0.28 197	0.31 130	0.38 92	0.14 276	0.22 313	0.13 323	0.04 124	0.10 57	0.32 108	0.33 146	0.18 133	0.40 183	0.41 165	0.16 34	0.47 124																		
8.5	0.2061	0.28 135	0.19 287	0.20 214	0.19 123	0.28 86	0.32 271	0.35 297	0.20 281	0.10 309	0.14 10	0.22 89	0.21 143	0.28 176	0.65 215	0.86 206	0.14 156	0.49 112																		
8.0	0.3398	0.08 97	0.24 293	0.09 288	0.07 62	0.16 74	0.36 275	0.40 290	0.25 250	0.21 315	0.15 352	0.13 42	0.04 96	0.43 199	0.94 235	1.37 223	0.43 181	0.46 101																		
7.5	0.5603	0.12 355	0.17 318	0.23 8	0.17 10	0.07 74	0.14 285	0.26 285	0.23 307	0.21 315	0.12 327	0.14 319	0.19 244	0.44 235	0.81 256	1.00 229	0.40 165	0.30 89																		
7.0	0.9237	0.12 340	0.11 3	0.31 27	0.21 14	0.06 99	0.04 56	0.11 280	0.17 240	0.20 294	0.17 279	0.22 291	0.19 301	0.32 198	0.25 200	0.62 174	0.66 138	0.27 98																		
6.5	1.52	0.04 196	0.10 58	0.27 24	0.18 118	0.09 108	0.11 143	0.03 276	0.11 277	0.18 258	0.23 270	0.31 176	0.11 176	0.53 118	1.19 123	1.47 129	1.19 132	0.43 98																		
6.0	2.51	0.19 174	0.11 108	0.14 60	0.14 33	0.09 108	0.14 143	0.10 276	0.05 277	0.16 258	0.25 270	0.34 176	0.11 176	1.09 123	2.31 123	2.41 129	1.77 132	0.68 98																		
5.5	4.14	0.20 179	0.11 149	0.05 127	0.05 17	0.05 84	0.13 104	0.14 129	0.03 145	0.09 267	0.21 250	0.27 269	0.14 124	1.14 118	2.27 131	2.32 143	1.76 147	0.63 107																		
5.0	6.83	0.16 180	0.14 180	0.17 201	0.07 242	0.04 346	0.11 98	0.19 122	0.12 121	0.03 162	0.13 233	0.12 270	0.20 83	0.85 119	1.66 145	1.92 165	1.57 168	0.48 127																		
4.5	11.25	0.11 185	0.17 197	0.32 209	0.19 227	0.10 313	0.08 92	0.24 114	0.12 116	0.08 117	0.07 166	0.29 81	0.29 59	0.28 118	0.96 195	1.64 204	1.47 200	0.40 171																		
4.0	18.55	0.04 194	0.18 208	0.42 211	0.28 224	0.14 306	0.06 80	0.27 110	0.28 113	0.21 109	0.15 116	0.25 85	0.36 44	0.38 299	1.47 257	1.97 240	1.63 230	0.52 210																		
3.5	30.59	0.01 315	0.17 219	0.45 215	0.31 220	0.15 302	0.04 68	0.25 106	0.30 112	0.27 107	0.23 101	0.37 87	0.39 35	0.86 298	2.18 274	2.34 259	1.75 228	0.63 237																		
3.0	50.43	0.03 342	0.14 218	0.38 213	0.29 220	0.14 300	0.03 68	0.23 105	0.28 112	0.27 107	0.26 97	0.41 86	0.36 29	1.24 298	2.27 269	2.27 262	1.64 237	0.62 241																		
2.5	83.15	0.04 353	0.09 223	0.28 214	0.21 219	0.10 298	0.02 56	0.17 102	0.22 112	0.22 107	0.22 93	0.34 87	0.28 24	0.90 298	1.90 284	1.77 275	1.26 269	0.50 241																		

MARCH	MEAN GEOPOTENTIAL HEIGHT	AMPLITUDE (dam) AND PHASE																	WAVE 2
SCALE	PRESSURE	-80	-70	-60	-50	-40	-30	-20	-10	0	10	20	30	40	50	60	70	80	
HEIGHT	(mb)																		
12.0	0.0062	4.2 135	3.9 151	4.8 144	5.2 122	6.1 92	4.9 70	2.8 77	2.2 93	2.3 120	1.9 137	3.2 122	3.6 82	7.0 70	8.0 92	9.9 73	10.2 55	8.0 81	
11.5	0.0103	4.2 136	3.6 150	4.6 144	4.7 122	5.3 91	3.5 68	1.9 68	1.4 81	1.6 123	1.1 135	2.6 116	3.4 81	6.6 86	7.6 98	8.8 80	9.6 57	8.0 79	
11.0	0.0169	4.1 136	3.3 149	4.4 145	4.1 121	4.6 89	2.1 62	1.1 51	0.6 87	0.9 131	0.4 131	1.9 107	3.1 79	6.3 63	7.2 105	8.7 88	9.0 60	8.1 76	
10.5	0.0279	3.9 137	3.0 148	4.2 144	3.5 120	3.9 88	1.0 47	0.7 13	0.0 325	0.4 157	0.2 333	1.3 90	2.9 74	6.0 111	6.8 97	6.8 73	8.4 63	8.1 70	
10.0	0.0460	3.5 137	2.9 146	4.0 142	2.9 119	3.2 85	0.5 356	0.7 332	0.5 264	0.3 249	0.3 317	0.6 61	0.9 27	5.6 67	6.5 115	6.1 105	8.0 66	8.0 69	
9.5	0.0758	3.0 136	2.8 144	3.7 138	2.3 117	2.5 82	0.6 312	0.8 312	0.7 255	0.6 277	0.5 311	0.9 21	0.9 57	5.4 106	6.1 116	5.5 110	7.6 70	6.9 65	
9.0	0.1250	2.5 136	2.0 141	3.5 133	1.9 113	1.9 79	0.5 309	0.6 303	0.8 242	0.8 285	1.0 304	1.0 351	2.6 46	5.1 100	5.8 113	5.1 108	7.4 72	6.1 61	
8.5	0.2061	2.0 136	3.0 138	3.4 127	1.5 109	1.4 75	0.3 349	0.1 308	0.6 224	0.8 290	1.0 294	1.2 333	2.7 38	4.9 97	5.9 105	5.1 84	7.3 69	7.2 52	
8.0	0.3398	1.7 137	3.3 135	3.4 124	1.3 109	1.1 74	0.5 55	0.4 108	0.5 197	0.7 293	1.0 282	1.3 322	2.7 34	5.0 91	6.5 97	6.0 84	7.4 69	6.8 52	
7.5	0.5603	1.8 140	3.6 134	3.6 126	1.3 116	1.0 74	0.8 72	0.9 109	0.3 147	0.6 296	0.9 272	1.2 316	2.7 37	5.4 85	7.7 92	7.5 76	7.6 64	6.4 49	
7.0	0.9237	1.9 143	3.8 135	3.7 132	1.4 127	0.9 73	0.9 76	1.2 107	0.4 103	0.3 303	0.7 266	0.9 320	2.7 44	5.8 81	8.4 90	8.3 71	7.6 59	6.1 46	
6.5	1.52	2.0 143	3.8 138	3.8 139	1.5 138	0.8 68	0.8 75	1.3 106	0.6 93	0.1 349	0.4 262	0.7 342	2.8 47	5.7 76	7.8 85	7.9 79	7.3 49	5.8 43	
6.0	2.51	1.9 140	3.7 139	3.8 144	1.6 145	0.7 60	0.6 66	1.2 103	0.7 93	0.2 61	0.0 254	0.7 24	2.9 46	5.0 66	5.9 70	7.3 40	7.3 32	5.4 36	
5.5	4.14	1.7 134	3.6 140	3.8 145	1.7 150	0.6 54	0.5 51	1.1 98	0.7 92	0.4 71	0.3 75	1.0 49	3.0 43	4.2 47	5.0 35	8.4 16	8.5 15	5.1 26	
5.0	6.83	1.5 126	3.4 139	3.7 144	1.7 149	0.6 55	0.4 33	0.9 91	0.7 87	0.5 68	0.5 58	1.2 39	2.9 26	4.0 26	6.2 7	10.9 5	10.5 6	5.2 17	
4.5	11.25	1.4 120	3.3 136	3.5 139	1.7 143	0.6 65	0.4 13	0.6 77	0.5 72	0.4 55	0.6 61	1.2 59	2.5 41	4.7 25	7.9 35	13.3 21	12.6 6	6.1 12	
4.0	18.55	1.3 115	3.2 131	3.4 130	1.7 131	0.7 78	0.4 357	0.4 42	0.3 22	0.4 23	0.6 54	1.0 31	2.1 41	4.1 15	9.0 10	15.4 10	14.6 10	6.2 12	
3.5	30.59	1.3 114	3.1 126	3.4 119	1.8 117	0.9 88	0.3 345	0.4 342	0.5 329	0.5 342	0.5 20	0.7 16	1.6 29	4.0 29	9.9 25	17.1 20	16.3 24	7.0 20	
3.0	50.43	1.4 115	3.1 122	3.5 109	1.9 104	1.0 95	0.3 337	0.7 316	0.9 312	0.8 319	0.6 343	0.6 338	1.0 27	4.2 48	11.3 27	18.8 29	17.7 24	7.7 20	
2.5	83.15	1.4 117	3.2 119	3.6 102	2.1 95	1.2 98	0.3 332	0.9 306	1.3 306	1.1 309	0.8 318	0.9 303	0.5 28	4.9 64	13.2 54	20.3 37	18.8 30	8.4 23	

APRIL	MEAN TEMPERATURE AMPLITUDE (K) AND PHASE																			WAVE
SCALE	PRESSURE	-80	-70	-60	-50	-40	-30	-20	-10	0	10	20	30	40	50	60	70	80		
HEIGHT	(mb)																			
12.0	0.0062	2,21	1,92	1,20	0,85	0,59	0,18	0,85	0,37	0,48	0,21	0,13	0,58	0,72	0,44	0,45	0,61	0,52	0,32	
		265	248	209	208	197	136	147	154	5	22	113	350	358	321	73	82			
11.5	0.0103	2,19	1,99	1,21	0,94	0,67	0,19	0,83	0,40	0,47	0,19	0,13	0,58	0,69	0,40	0,49	0,66	0,57	0,37	
		269	254	222	220	208	158	149	153	5	25	112	331	351	319	81	85			
11.0	0.0169	2,03	1,99	1,26	1,09	0,77	0,23	0,73	0,41	0,43	0,15	0,13	0,53	0,59	0,30	0,51	0,65	0,57	0,37	
		275	262	240	236	220	186	151	151	5	27	115	336	360	312	91	90	26		
10.5	0.0279	1,77	1,99	1,45	1,35	0,95	0,32	0,58	0,42	0,37	0,08	0,11	0,45	0,38	0,15	0,55	0,59	0,53	0,23	
		285	275	262	250	232	206	155	149	9	36	111	342	359	277	106	98	20		
10.0	0.0460	1,56	2,06	1,86	1,71	1,18	0,47	0,58	0,43	0,30	0,02	0,10	0,34	0,09	0,25	0,57	0,49	0,44	0,8	
		301	290	281	265	242	219	166	146	9	117	114	354	360	198	125	111	8		
9.5	0.0758	1,44	2,23	2,36	2,07	1,39	0,62	0,23	0,40	0,24	0,08	0,07	0,23	0,27	0,54	0,57	0,33	0,40	0,8	
		324	307	296	274	250	230	208	142	8	191	111	19	186	186	150	134	342		
9.0	0.1250	1,49	2,42	2,84	2,29	1,51	0,74	0,29	0,30	0,18	0,13	0,04	0,17	0,62	0,84	0,57	0,24	0,43	0,8	
		350	324	309	284	258	239	260	136	0	214	45	58	190	192	187	203	308		
8.5	0.2061	1,69	2,58	3,06	2,21	1,36	0,77	0,43	0,11	0,18	0,15	0,10	0,13	0,88	1,12	0,76	0,46	0,52	0,8	
		15	345	323	299	269	251	243	107	328	244	348	100	196	207	233	259	285		
8.0	0.3398	1,95	2,75	3,02	1,92	0,97	0,67	0,46	0,20	0,25	0,20	0,17	0,10	0,96	1,37	1,19	0,77	0,60	0,8	
		36	8	341	323	290	269	277	345	307	280	339	169	205	227	264	283	272		
7.5	0.5605	1,85	2,51	2,39	1,40	0,45	0,36	0,36	0,27	0,28	0,21	0,13	0,26	0,85	1,26	1,33	1,02	0,43	0,8	
		48	26	360	346	316	262	256	304	275	279	299	192	202	242	290	313	290		
7.0	0.9237	1,76	2,49	2,22	1,37	0,42	0,20	0,32	0,30	0,30	0,25	0,16	0,35	0,40	0,88	1,43	1,11	0,28	0,8	
		47	34	14	1	355	322	334	261	244	242	227	191	205	293	329	341	354		
6.5	1.52	1,88	2,62	2,61	1,81	0,77	0,27	0,35	0,43	0,38	0,4	0,32	0,35	0,27	1,53	1,91	1,15	0,47	0,8	
		33	27	15	359	349	329	231	224	219	215	204	185	344	350	1	10	51		
6.0	2.51	2,23	3,62	3,51	2,75	1,45	0,57	0,49	0,56	0,44	0,36	0,42	0,25	0,92	2,49	2,36	1,14	0,70	0,8	
		19	18	12	357	343	313	242	214	211	212	204	195	353	4	17	40	80		
5.5	4.14	1,94	3,59	3,90	3,30	1,82	0,69	0,46	0,52	0,42	0,54	0,41	0,25	1,37	2,61	2,12	1,09	0,75	0,8	
		26	26	23	10	354	323	247	218	216	216	217	272	353	10	32	78	107		
5.0	6.83	1,74	2,89	3,83	3,47	1,90	0,67	0,41	0,43	0,38	0,49	0,40	0,55	1,53	2,10	1,59	1,35	0,81	0,8	
		43	39	35	22	4	528	252	225	223	225	238	303	354	21	63	116	135		
4.5	11.25	0,73	1,95	3,31	3,17	1,66	0,30	0,35	0,35	0,32	0,33	0,43	0,86	1,35	1,23	1,68	1,79	0,87	0,8	
		104	66	51	34	14	331	254	240	234	243	261	311	355	55	118	141	160		
4.0	18.55	1,29	1,68	2,67	2,62	1,25	0,26	0,27	0,29	0,26	0,25	0,49	1,06	0,91	1,33	2,56	2,10	0,90	0,8	
		156	111	69	49	28	333	255	263	249	279	279	315	358	124	148	155	181		
3.5	30.59	1,75	1,88	2,09	2,01	0,86	0,04	0,19	0,26	0,20	0,26	0,51	1,09	0,41	2,07	3,13	2,10	0,86	0,8	
		170	141	89	64	48	328	253	285	269	315	291	317	7	151	160	163	196		
3.0	50.43	1,66	1,80	1,58	1,48	0,61	0,12	0,13	0,24	0,17	0,30	0,49	0,97	0,09	2,32	2,95	1,77	0,72	0,8	
		174	156	107	80	75	158	252	302	287	334	298	318	78	159	166	169	206		
2.5	83.15	1,22	1,39	1,11	1,00	0,44	0,17	0,08	0,19	0,13	0,26	0,38	0,73	0,18	1,94	2,26	1,26	0,52	0,8	
		179	163	120	94	97	157	247	312	299	342	303	318	149	163	169	173	213		

APRIL	MEAN GEOPOTENTIAL HEIGHT AMPLITUDE (dam) AND PHASE																	WAVE 1	
SCALE HEIGHT	PRESSURE (mb)	-80	-70	-60	-50	-40	-30	-20	-10	0	10	20	30	40	50	60	70	80	
12.0	0.0062	14.2 322	24.3 338	28.5 346	25.5 332	12.8 300	7.4 255	9.6 205	7.6 191	2.6 233	4.6 220	4.2 213	5.2 283	6.2 291	8.3 275	5.4 204	7.7 166	2.5 204	
11.5	0.0103	12.6 334	24.3 345	29.4 348	24.2 335	12.9 304	7.5 255	9.0 205	7.1 193	2.9 227	4.9 219	4.2 215	5.7 275	7.9 281	5.9 272	5.9 212	7.6 173	3.5 206	
11.0	0.0169	11.5 348	24.4 352	30.3 351	24.6 338	12.9 308	7.4 258	8.5 208	6.7 197	3.3 222	5.1 218	4.3 218	5.4 286	7.5 272	4.5 269	7.5 220	4.4 180	2.6 206	
10.5	0.0279	10.8 2	24.2 359	30.5 355	24.8 342	12.8 314	7.2 260	8.2 225	6.3 201	3.7 219	5.3 218	4.3 220	5.2 296	7.8 265	7.3 268	4.8 228	7.6 187	4.9 206	
10.0	0.0460	10.3 15	25.7 36	30.5 359	24.8 342	12.6 321	6.9 264	7.9 230	5.9 206	4.0 217	5.3 218	4.3 222	5.2 249	7.8 261	7.1 269	5.2 236	7.6 193	5.6 205	
9.5	0.0758	9.5 26	22.7 13	29.5 55	24.4 354	12.2 329	6.3 268	7.6 232	5.7 211	4.3 213	5.3 218	4.3 225	5.4 244	7.8 262	7.0 273	5.4 245	7.4 198	6.2 202	
9.0	0.1250	8.3 38	21.1 21	28.0 12	25.7 12	11.8 340	5.5 274	7.3 232	5.5 216	4.5 217	5.1 219	4.4 224	5.7 242	7.6 249	7.0 282	5.3 254	7.1 198	6.5 195	
8.5	0.2061	6.5 49	18.7 29	25.8 20	22.8 9	11.5 350	4.5 281	6.9 229	5.5 219	4.6 217	4.9 218	4.5 225	5.9 243	7.5 280	6.9 294	6.6 261	6.8 197	6.6 192	
8.0	0.3398	4.2 64	15.6 37	23.0 28	21.5 16	11.1 358	3.6 288	6.5 224	5.7 219	4.7 215	4.8 216	4.6 221	5.0 244	7.5 295	6.7 300	6.3 266	6.6 189	6.8 185	
7.5	0.5603	1.9 94	12.1 42	20.1 35	19.8 21	10.7 391	2.9 290	6.0 220	5.7 216	4.7 211	4.7 213	4.7 217	4.8 247	7.6 309	6.5 326	1.5 252	7.2 179	6.7 178	
7.0	0.9237	1.9 183	8.6 47	17.2 40	18.0 23	10.2 290	2.5 290	5.6 218	4.6 212	4.5 208	4.5 210	4.5 217	4.6 252	7.0 317	6.1 339	1.7 177	8.6 174	7.8 175	
6.5	1.52	4.3 205	5.0 60	14.2 46	16.0 27	9.3 285	2.2 285	5.1 217	5.1 209	4.0 206	4.0 208	4.2 218	4.4 258	5.9 319	5.9 342	4.1 172	10.2 174	7.5 178	
6.0	2.51	7.3 205	3.1 124	10.7 59	13.2 34	7.9 274	1.8 274	4.6 215	4.4 208	3.3 205	3.3 207	3.7 220	5.8 264	7.3 314	5.2 315	1.9 180	11.7 178	7.8 183	
5.5	4.14	10.4 204	6.8 175	7.5 88	9.5 88	5.6 177	1.3 244	4.0 210	3.6 207	2.5 203	2.5 205	3.1 222	4.0 266	5.0 298	4.0 317	10.2 217	12.5 187	7.9 185	
5.0	6.83	12.7 206	11.0 190	6.6 139	5.9 73	3.1 204	1.5 204	3.5 203	3.0 203	2.1 198	1.8 199	2.5 221	3.5 262	5.3 286	3.4 295	12.5 195	12.5 192	7.6 199	
4.5	11.25	13.7 209	13.8 199	8.6 172	8.2 128	1.4 89	2.1 185	3.2 195	2.5 197	1.6 188	1.3 186	2.9 212	2.9 212	3.9 247	3.8 233	13.1 208	11.6 204	6.9 202	
4.0	18.55	13.3 215	15.0 208	11.1 193	5.9 174	2.1 162	2.6 178	3.0 180	2.2 187	1.5 174	1.5 168	1.7 193	2.7 218	5.0 216	9.6 216	12.3 210	10.2 215	5.9 219	
3.5	30.59	12.0 223	14.7 218	12.9 208	8.0 196	3.2 185	2.8 176	2.9 182	2.2 177	1.6 163	1.5 158	1.9 179	3.3 219	5.8 211	9.2 231	11.0 232	8.8 237	4.8 221	
3.0	50.43	10.5 234	14.0 229	14.0 218	9.7 209	3.9 197	2.8 176	2.8 177	2.4 180	1.8 156	1.9 156	2.4 195	4.4 174	6.1 210	9.0 252	10.7 261	8.1 251	3.7 228	
2.5	83.15	9.5 244	13.4 238	14.6 225	10.7 217	4.5 207	2.6 178	2.8 174	2.7 165	2.1 153	2.4 156	3.0 148	5.5 166	6.1 212	9.5 280	11.6 280	8.0 267	2.9 233	

WAVE PERIOD	MEAN TEMPERATURE	AMPLITUDE (K) AND PHASE										WAVE 2									
SCALE	PRESSURE	-80	-70	-60	-50	-40	-30	-20	-10	0	10	20	30	40	50	60	70	80			
HEIGHT	(mb)																				
12.0	0.0062	0.21 113	0.48 63	0.58 6	0.12 43	0.17 0	0.22 77	0.18 61	0.48 238	1.03 243	0.95 212	0.70 194	0.69 174	0.18 218	0.60 122	0.30 135	0.02 146	0.40 101			
11.5	0.0103	0.20 130	0.51 60	0.42 5	0.47 49	0.17 26	0.20 70	0.25 53	0.19 239	0.46 243	1.00 210	0.91 193	0.70 172	0.73 216	0.18 122	0.62 138	0.28 76	0.01 0.40			
11.0	0.0169	0.20 153	0.52 56	0.44 5	0.46 49	0.23 23	0.29 61	0.39 43	0.18 241	0.39 242	0.89 208	0.80 191	0.66 168	0.72 210	0.16 119	0.57 149	0.21 7	0.04 9			
10.5	0.0279	0.26 178	0.55 51	0.46 1	0.37 50	0.28 38	0.34 52	0.17 24	0.31 244	0.72 241	0.62 205	0.61 189	0.58 163	0.68 196	0.14 117	0.46 172	0.11 355	0.09 5			
10.0	0.0460	0.36 193	0.54 49	0.46 1	0.50 52	0.35 43	0.39 53	0.19 357	0.19 253	0.54 237	0.40 196	0.46 186	0.46 157	0.61 170	0.11 106	0.27 274	0.13 350	0.05 270			
9.5	0.0708	0.47 202	0.51 39	0.43 5	0.60 56	0.43 40	0.43 38	0.22 240	0.09 286	0.34 250	0.18 164	0.52 178	0.51 151	0.11 143	0.11 29	0.30 294	0.20 350	0.22 203			
9.0	0.1250	0.55 204	0.44 34	0.55 64	0.64 62	0.49 73	0.49 33	0.26 320	0.08 0	0.14 201	0.19 78	0.16 158	0.34 147	0.09 111	0.32 331	0.45 303	0.22 351	0.38 198			
8.5	0.2061	0.52 199	0.27 27	0.23 48	0.77 55	0.92 92	0.26 32	0.29 306	0.11 120	0.32 0	0.10 72	0.12 179	0.04 40	0.56 324	0.50 313	0.21 352	0.46 194				
8.0	0.3398	0.43 185	0.03 303	0.28 109	0.43 111	0.54 115	0.01 63	0.28 288	0.05 72	0.14 98	0.34 32	0.18 29	0.27 280	0.13 321	0.69 324	0.44 328	0.16 4	0.38 194			
7.5	0.5603	0.23 172	0.18 238	0.21 146	0.30 161	0.38 132	0.15 222	0.24 275	0.10 237	0.04 0	0.15 1	0.11 18	0.20 249	0.18 310	0.46 325	0.28 346	0.11 8	0.09 187			
7.0	0.9237	0.11 170	0.24 250	0.11 229	0.21 217	0.14 144	0.16 236	0.19 267	0.19 243	0.19 245	0.11 263	0.04 256	0.34 272	0.16 277	0.17 321	0.20 15	0.11 180	0.07 15			
6.5	1.52	0.11 203	0.29 286	0.35 301	0.27 295	0.36 356	0.15 283	0.13 270	0.15 254	0.19 249	0.12 236	0.27 227	0.12 251	0.23 229	0.21 193	0.11 45	0.18 24	0.02 247			
6.0	2.51	0.18 207	0.46 309	0.62 316	0.62 323	0.49 338	0.38 316	0.19 275	0.11 207	0.13 248	0.16 234	0.15 236	0.14 234	0.24 212	0.36 200	0.28 74	0.19 68	0.05 265			
5.5	4.14	0.13 189	0.40 316	0.51 322	0.49 326	0.39 332	0.16 311	0.07 257	0.05 241	0.08 238	0.13 243	0.10 276	0.12 253	0.12 225	0.20 229	0.35 111	0.14 172	0.04 244			
5.0	6.83	0.07 153	0.29 333	0.33 333	0.32 328	0.37 326	0.12 310	0.04 180	0.06 128	0.04 166	0.09 257	0.11 345	0.12 358	0.20 267	0.32 351	0.17 273	0.35 211	0.25 192	0.21 223		
4.5	11.25	0.06 75	0.12 21	0.14 10	0.31 330	0.31 320	0.05 323	0.09 133	0.14 109	0.10 110	0.04 300	0.21 15	0.31 25	0.31 329	0.31 298	0.53 252	0.44 200	0.56 200	0.27 211		
4.0	18.55	0.10 37	0.25 52	0.16 90	0.16 334	0.21 311	0.02 63	0.13 117	0.20 105	0.16 101	0.06 26	0.31 27	0.48 31	0.53 349	0.71 309	0.69 239	0.70 204	0.31 202			
3.5	30.59	0.12 21	0.29 70	0.24 112	0.06 345	0.06 299	0.13 99	0.06 112	0.16 103	0.22 96	0.20 96	0.10 35	0.35 35	0.56 356	0.67 317	0.77 244	0.80 242	0.72 207	0.32 197		
3.0	50.43	0.11 10	0.27 77	0.25 119	0.03 107	0.07 108	0.09 103	0.15 103	0.21 102	0.20 96	0.12 96	0.36 38	0.54 35	0.66 359	0.69 318	0.72 244	0.62 209	0.28 193			
2.5	85.15	0.09 7	0.20 80	0.20 122	0.05 133	0.04 247	0.08 103	0.16 105	0.16 101	0.11 94	0.11 52	0.28 41	0.43 36	0.53 31	0.51 319	0.55 245	0.45 211	0.45 190	0.20 193		

APRIL		MEAN GEOPOTENTIAL HEIGHT AMPLITUDE (dam) AND PHASE WAVE 2																	
SCALE	PRESSURE	-80	-70	-60	-50	-40	-30	-20	-10	0	10	20	30	40	50	60	70	80	
HEIGHT	(mb)																		
12.0	0.0062	4.1 174	7.6 26	7.9 9	7.1 33	5.5 49	3.6 46	2.1 334	2.5 239	5.8 232	3.8 181	3.2 162	4.1 16	0.6 29	3.5 2	2.2 2	0.8 64	1.9 205	
11.5	0.0103	4.0 177	7.0 22	7.3 9	6.8 33	5.3 51	3.3 43	2.1 327	1.9 239	4.5 229	2.5 207	2.2 175	3.0 159	0.9 22	3.7 15	2.5 355	0.8 62	2.5 201	
11.0	0.0169	3.7 180	6.4 18	6.7 10	6.5 32	5.0 53	3.0 40	2.1 320	1.2 239	3.3 225	1.2 204	1.3 161	2.0 152	1.1 24	4.0 351	2.8 351	0.6 64	1.9 199	
10.5	0.0279	3.4 181	5.8 14	6.1 10	6.1 31	4.7 55	2.5 37	2.0 313	0.7 236	2.3 218	0.2 189	0.7 119	1.3 139	1.4 24	4.4 354	3.0 350	0.7 70	3.5 198	
10.0	0.0460	3.0 180	5.2 9	5.4 12	5.9 29	4.2 56	2.0 34	1.9 306	0.3 224	1.5 207	0.5 27	0.6 57	0.4 71	1.5 22	3.5 348	3.1 351	0.7 84	3.5 197	
9.5	0.0758	2.4 175	4.6 4	4.7 13	4.8 24	3.6 36	1.4 51	1.9 299	0.2 190	1.0 191	0.8 19	1.2 35	0.9 359	1.6 18	4.7 347	3.0 357	0.8 104	3.3 196	
9.0	0.1250	1.8 164	4.0 358	4.2 13	4.1 17	3.0 54	0.8 28	1.4 292	0.3 177	0.7 176	1.0 6	1.5 26	1.4 346	1.7 14	4.5 345	2.7 345	0.9 121	2.9 196	
8.5	0.2061	1.3 141	3.6 353	3.8 12	3.6 6	2.4 46	0.3 19	0.3 283	0.4 183	0.6 178	1.5 346	1.0 21	1.7 343	1.8 21	3.8 349	2.4 21	1.2 134	2.3 195	
8.0	0.3398	1.0 107	3.4 352	3.7 7	3.6 355	2.1 28	0.1 349	0.6 274	0.5 191	0.6 196	0.7 309	1.4 17	1.8 349	1.6 12	3.0 356	2.2 37	1.4 141	1.6 195	
7.5	0.5603	1.0 80	3.4 354	3.8 2	3.8 350	2.2 10	0.2 18	0.3 263	0.5 187	0.6 209	0.7 280	1.1 16	1.7 6	1.5 20	2.3 20	2.0 90	1.5 146	1.2 196	
7.0	0.9237	1.0 66	3.6 359	4.0 2	4.3 351	2.5 3	0.4 34	0.1 127	0.4 161	0.5 206	0.6 272	1.1 17	1.8 25	1.5 30	2.0 16	1.8 59	1.6 150	1.1 198	
6.5	1.52	1.1 59	3.6 356	4.0 6	4.3 355	2.5 3	0.6 47	0.3 96	0.5 125	0.3 182	0.3 285	1.2 20	2.0 35	1.7 35	2.1 18	1.6 63	1.5 155	1.0 198	
6.0	2.51	1.3 54	3.4 31	3.6 15	4.0 15	2.1 8	0.7 86	0.4 94	0.7 110	0.3 135	0.3 321	1.4 24	2.3 38	2.1 36	2.3 18	2.3 64	1.5 158	0.9 192	
5.5	4.14	1.4 49	3.1 23	3.2 27	3.4 8	1.7 18	0.8 83	0.6 93	0.8 104	0.4 108	0.4 357	1.5 29	2.5 41	2.6 36	2.7 20	1.1 60	1.7 159	1.2 182	
5.0	6.83	1.5 44	2.9 32	3.0 38	2.9 16	1.4 36	1.0 92	0.7 89	0.8 101	0.4 96	0.4 17	1.5 34	2.6 43	2.9 39	3.0 26	1.2 54	1.4 153	0.8 167	
4.5	11.25	1.5 42	2.7 37	2.8 43	2.5 26	1.3 57	0.6 97	0.6 82	0.6 99	0.6 86	0.5 28	1.3 40	2.3 46	2.9 35	3.1 37	1.6 51	1.6 126	0.6 140	
4.0	18.59	1.4 41	3.3 35	2.6 43	2.4 32	1.4 72	1.1 99	0.5 90	0.4 94	0.2 69	0.4 32	0.9 47	1.7 52	2.7 57	3.3 53	2.4 53	1.2 79	0.6 96	
3.5	30.59	1.2 40	2.0 32	2.5 37	2.3 36	1.6 79	1.0 99	0.4 99	0.1 58	0.1 30	0.3 32	0.5 65	1.1 67	2.5 76	3.7 56	3.5 51	2.1 54	0.8 62	
3.0	50.43	1.1 48	1.7 23	2.5 28	2.3 28	1.7 82	0.9 99	0.4 99	0.3 92	0.3 298	0.2 19	0.2 157	0.6 116	2.5 100	4.2 84	4.7 84	3.0 46	1.2 46	
2.5	83.15	1.0 53	1.5 13	2.5 21	2.3 21	1.8 82	0.8 99	0.4 94	0.5 289	0.5 288	0.1 298	0.6 200	0.9 173	2.7 118	4.8 93	5.6 57	3.7 43	1.5 38	

MAY		MEAN TEMPERATURE AMPLITUDE (K) AND PHASE WAVE 1																
SCALE	PRESSURE	-80	-70	-60	-50	-40	-30	-20	-10	0	10	20	30	40	50	60	70	80
HEIGHT	(mb)																	
12.0	0.0062	2.25	2.90	2.79	2.06	1.18	0.18	0.63	0.50	0.64	0.28	0.46	0.71	0.40	0.62	0.76	0.92	0.25
		250	237	214	186	178	79	96	76	35	74	109	58	320	36	40	59	117
11.5	0.0103	2.05	2.68	2.66	1.98	1.23	0.20	0.66	0.51	0.61	0.28	0.50	0.75	0.43	0.70	0.90	1.06	0.27
		253	241	221	194	185	136	104	86	36	83	108	60	322	35	40	58	114
11.0	0.0169	1.62	2.23	2.37	1.80	1.25	0.41	0.64	0.52	0.53	0.28	0.51	0.75	0.42	0.74	0.97	1.12	0.26
		257	247	232	206	189	171	118	100	46	98	106	62	325	34	38	57	106
10.5	0.0279	1.12	1.66	2.06	1.65	1.26	0.77	0.67	0.58	0.42	0.32	0.52	0.69	0.38	0.75	0.98	1.08	0.23
		267	261	250	227	199	183	137	118	60	117	104	66	328	32	36	55	95
10.0	0.0460	0.64	1.24	1.98	1.74	1.29	1.21	0.80	0.71	0.34	0.39	0.51	0.61	0.32	0.69	0.90	0.91	0.17
		298	292	276	253	212	188	156	134	88	137	101	72	334	29	33	53	65
9.5	0.0758	0.66	1.35	2.27	2.09	1.36	1.63	1.00	0.86	0.36	0.49	0.47	0.45	0.24	0.55	0.71	0.62	0.15
		1	333	302	275	226	190	171	145	122	148	98	77	344	22	28	44	14
9.0	0.1250	1.14	1.91	2.71	2.50	1.41	1.85	1.19	0.92	0.46	0.55	0.36	0.24	0.15	0.31	0.44	0.30	0.23
		31	359	321	292	241	193	178	153	148	152	93	79	4	9	16	14	326
8.5	0.2061	1.59	2.49	3.07	2.74	1.41	1.61	1.20	0.76	0.50	0.49	0.16	0.08	0.06	0.14	0.16	0.32	0.34
		44	12	337	307	260	195	180	161	164	152	76	330	39	280	333	296	301
8.0	0.3398	1.89	2.88	3.24	2.71	1.33	0.88	0.94	0.39	0.39	0.32	0.14	0.39	0.02	0.41	0.28	0.57	0.43
		52	22	353	323	285	201	178	176	179	141	306	298	180	226	243	271	281
7.5	0.5603	1.62	2.58	3.06	2.42	1.10	0.14	0.42	0.07	0.11	0.18	0.23	0.50	0.11	0.42	0.37	0.50	0.35
		57	25	3	341	315	18	150	324	177	81	279	292	259	228	235	270	258
7.0	0.9237	1.52	2.43	3.05	2.38	1.19	0.77	0.35	0.31	0.13	0.20	0.16	0.30	0.13	0.26	0.28	0.26	0.28
		58	25	6	353	340	14	46	358	18	40	263	282	261	255	249	260	229
6.5	1.52	1.73	2.65	3.25	2.50	1.41	0.96	0.71	0.35	0.20	0.13	0.04	0.10	0.07	0.22	0.13	0.12	0.22
		54	22	3	354	345	1	8	360	13	20	187	191	250	313	301	165	207
6.0	2.51	2.13	3.02	3.39	2.59	1.67	1.14	0.97	0.36	0.16	0.07	0.06	0.22	0.07	0.21	0.18	0.37	0.22
		54	23	2	353	339	342	351	343	346	321	99	148	172	333	34	126	202
5.5	4.14	2.09	2.74	2.71	2.22	1.68	1.41	1.24	0.50	0.23	0.19	0.11	0.10	0.06	0.07	0.18	0.51	0.19
		62	40	25	14	350	341	343	329	317	298	307	173	180	262	98	135	197
5.0	6.85	1.72	2.38	2.46	2.00	1.44	1.45	1.32	0.59	0.31	0.30	0.32	0.23	0.09	0.28	0.37	0.59	0.16
		79	70	68	52	8	341	336	322	302	295	292	280	249	186	139	141	187
4.5	11.25	1.42	2.66	3.32	2.39	1.20	1.23	1.22	0.61	0.35	0.39	0.55	0.59	0.20	0.58	0.66	0.58	0.13
		114	108	105	88	38	345	329	314	292	296	287	291	279	178	154	146	171
4.0	18.55	1.76	3.49	4.22	2.90	1.21	0.88	0.96	0.55	0.36	0.43	0.72	0.91	0.32	0.80	0.88	0.50	0.11
		153	133	127	107	72	352	320	307	284	298	284	293	286	176	161	151	142
3.5	30.59	2.06	3.76	4.45	2.98	1.31	0.54	0.68	0.45	0.32	0.40	0.79	1.08	0.39	0.87	0.95	0.37	0.11
		173	144	130	117	93	6	306	299	277	300	282	294	290	175	165	156	126
3.0	50.43	1.78	3.14	3.71	2.60	1.25	0.31	0.46	0.35	0.27	0.35	0.77	1.09	0.39	0.78	0.84	0.23	0.10
		183	151	134	123	105	33	288	290	272	303	280	294	293	174	168	162	114
2.5	85.15	1.24	2.14	2.58	1.89	0.99	0.20	0.29	0.22	0.19	0.26	0.60	0.89	0.32	0.58	0.61	0.12	0.08
		188	155	137	126	112	68	266	282	267	304	280	294	293	174	170	170	105

MAY		MEAN GEOPOTENTIAL HEIGHT AMPLITUDE (dam) AND PHASE WAVE 1																
SCALE	PRESSURE	-80	-70	-60	-50	-40	-30	-20	-10	0	10	20	30	40	50	60	70	80
HEIGHT	(mb)																	
12.0	0.0062	11.4 109	11.6 72	7.8 25	7.9 330	6.2 280	3.4 237	1.5 136	3.3 116	2.7 128	3.7 151	2.4 161	1.1 324	5.3 268	2.4 278	3.3 9	4.0 54	2.7 255
11.5	0.0103	14.0 101	15.6 69	11.7 29	10.4 341	6.7 295	3.6 240	0.9 175	2.7 125	2.6 141	3.6 158	2.1 177	1.6 281	5.0 262	3.0 261	2.4 353	2.5 51	3.0 260
11.0	0.0169	16.5 97	19.2 68	15.3 33	12.7 348	7.5 308	3.6 246	1.0 234	2.1 136	2.6 153	3.4 164	2.0 198	2.5 265	4.7 256	3.8 249	1.7 318	0.9 41	3.3 263
10.5	0.0279	18.4 95	22.1 68	18.2 38	14.5 356	8.4 319	3.3 260	1.6 270	1.4 151	2.4 165	3.2 170	2.1 218	3.5 259	4.5 249	4.7 241	2.0 274	0.8 255	3.6 265
10.0	0.0460	19.7 95	23.9 70	20.3 43	15.7 4	9.3 330	3.2 285	2.3 292	0.7 186	2.2 177	2.8 234	2.6 257	4.5 242	4.5 236	5.7 232	3.0 251	2.2 241	3.9 265
9.5	0.0758	20.1 97	24.8 74	21.7 51	16.3 13	10.2 340	4.0 316	3.3 311	0.8 283	1.7 191	2.3 186	3.1 244	5.2 256	4.6 237	6.5 232	3.9 240	3.3 237	4.1 263
9.0	0.1250	19.9 101	24.7 79	22.5 60	16.7 25	11.0 350	5.9 337	4.6 325	2.0 311	1.2 212	1.8 201	3.7 249	5.8 257	4.7 234	7.0 229	4.7 234	3.9 234	4.0 259
8.5	0.2061	19.1 106	24.0 87	23.0 71	16.8 38	11.5 1	8.1 348	6.1 334	3.2 321	1.1 263	1.4 225	4.0 250	5.9 256	4.8 233	7.1 227	4.9 230	4.0 228	3.8 254
8.0	0.3398	17.9 113	22.9 96	23.1 82	16.8 52	11.7 10	9.8 354	7.6 340	4.0 327	1.4 295	1.4 251	4.1 249	5.7 254	4.8 233	6.8 226	4.8 228	3.6 220	3.4 248
7.5	0.5603	16.7 121	22.0 106	23.1 93	16.6 65	11.3 19	10.3 355	8.6 341	4.1 328	1.6 303	1.6 259	3.9 247	5.2 249	4.8 233	6.1 226	4.3 227	3.2 209	2.9 244
7.0	0.9237	15.7 128	21.8 116	23.4 104	16.2 77	10.3 26	9.6 353	8.8 339	3.9 327	1.5 298	1.9 256	3.6 245	4.7 244	4.6 232	5.7 225	3.8 225	2.9 226	2.4 244
6.5	1.52	15.2 137	22.2 125	24.6 115	16.1 89	9.0 34	8.4 351	8.2 335	3.5 322	1.5 287	2.0 251	3.5 245	4.5 243	4.5 231	5.5 223	3.6 223	2.7 197	2.1 249
6.0	2.51	15.1 147	23.5 135	26.9 125	16.9 102	7.8 47	6.9 351	7.1 331	3.1 317	1.5 277	2.1 247	3.5 246	4.5 246	4.4 231	5.6 219	3.7 221	2.6 204	1.9 255
5.5	4.14	15.4 159	24.9 145	28.9 133	111.5 113	17.8 65	7.0 354	5.0 332	2.5 327	1.3 313	2.0 267	3.5 245	4.5 245	4.3 249	5.6 232	3.9 218	2.5 222	1.8 219
5.0	6.85	15.7 169	25.2 153	29.0 140	17.7 123	6.4 85	3.0 4	3.7 320	1.7 307	1.0 252	1.8 234	3.3 241	4.4 249	4.2 233	5.4 218	4.0 227	2.5 237	1.7 272
4.5	11.25	15.2 177	23.8 160	26.6 147	15.9 131	5.8 101	1.4 35	1.9 308	0.9 297	0.7 221	1.6 217	2.9 232	3.9 244	4.1 231	4.9 223	3.9 238	2.7 256	1.7 279
4.0	18.55	13.7 184	20.5 168	22.0 154	12.8 141	4.8 116	1.2 110	1.6 239	0.2 212	0.8 178	1.6 196	2.5 214	3.5 229	3.9 226	4.3 233	3.9 250	3.0 255	1.8 284
3.5	30.59	11.1 188	16.0 178	16.6 165	9.2 154	3.4 133	1.8 141	1.8 164	0.8 138	1.1 153	1.9 177	2.3 187	3.0 203	3.7 219	3.8 249	4.1 274	3.4 281	1.9 286
3.0	50.43	8.3 192	11.8 190	11.9 181	6.3 166	2.1 163	1.2 24	1.6 143	1.3 128	1.4 140	2.2 165	2.7 162	3.4 175	3.5 210	3.6 268	4.7 290	3.6 287	2.1 287
2.5	83.15	6.1 195	9.0 205	9.3 201	4.9 209	1.7 213	2.4 162	2.4 152	1.7 132	1.7 134	2.6 159	3.5 146	4.4 158	4.5 201	3.8 283	5.3 299	3.7 299	2.2 287

MAY		MEAN TEMPERATURE AMPLITUDE (K) AND PHASE																	WAVE 2	
SCALE	PRESSURE	-80	-70	-60	-50	-40	-30	-20	-10	0	10	20	30	40	50	60	70	80		
HEIGHT	(mb)																			
12.0	0.0062	0.21 357	0.15 46	0.47 62	0.08 67	0.21 352	0.54 305	0.42 305	0.42 281	0.16 222	0.74 171	0.77 200	0.28 194	0.59 6	0.19 28	0.17 211	0.28 114	0.81 238		
11.5	0.0103	0.21 1	0.13 49	0.42 54	0.07 59	0.18 337	0.49 307	0.38 307	0.41 278	0.20 218	0.73 171	0.76 200	0.29 195	0.42 2	0.21 35	0.23 215	0.31 117	0.92 240		
11.0	0.0169	0.19 12	0.08 60	0.35 39	0.06 27	0.09 347	0.39 314	0.28 311	0.37 270	0.23 214	0.66 170	0.68 199	0.29 354	0.41 44	0.22 215	0.28 120	0.32 245	0.95 295		
10.5	0.0279	0.17 27	0.04 104	0.30 13	0.08 358	0.05 90	0.25 336	0.14 327	0.31 256	0.29 205	0.56 167	0.57 197	0.28 204	0.41 344	0.21 60	0.33 216	0.30 127	0.89 253		
10.0	0.0460	0.15 48	0.06 180	0.35 342	0.12 346	0.18 128	0.20 32	0.07 74	0.27 232	0.38 198	0.43 161	0.40 194	0.25 210	0.39 329	0.23 77	0.37 216	0.23 140	0.75 268		
9.5	0.0758	0.14 67	0.11 199	0.41 322	0.16 346	0.32 134	0.33 76	0.24 112	0.31 203	0.45 196	0.28 149	0.21 181	0.20 311	0.37 311	0.24 311	0.38 220	0.18 167	0.59 293		
9.0	0.1250	0.13 94	0.14 209	0.47 312	0.19 348	0.14 134	0.48 92	0.36 124	0.39 186	0.47 193	0.15 116	0.10 119	0.12 223	0.34 291	0.21 104	0.22 229	0.17 203	0.49 352		
8.5	0.2061	0.12 137	0.13 221	0.45 312	0.21 350	0.38 130	0.48 103	0.39 139	0.43 179	0.39 192	0.14 61	0.18 71	0.22 49	0.25 266	0.11 95	0.18 247	0.17 229	0.45 11		
8.0	0.3398	0.17 187	0.08 245	0.34 323	0.19 357	0.27 121	0.35 121	0.35 167	0.40 178	0.24 189	0.14 34	0.23 70	0.18 53	0.14 214	0.11 342	0.13 333	0.14 243	0.48 53		
7.5	0.5603	0.19 215	0.05 311	0.12 350	0.09 173	0.26 170	0.36 202	0.30 182	0.24 192	0.06 215	0.06 38	0.14 92	0.21 55	0.13 146	0.21 333	0.24 15	0.03 290	0.42 83		
7.0	0.9237	0.19 231	0.11 331	0.07 297	0.33 211	0.51 202	0.53 203	0.31 218	0.16 225	0.05 259	0.04 167	0.07 146	0.13 45	0.12 110	0.15 345	0.22 34	0.05 37	0.30 96		
6.5	1.52	0.15 240	0.27 319	0.34 283	0.65 241	0.85 217	0.66 210	0.32 215	0.14 234	0.09 225	0.10 200	0.06 198	0.06 242	0.06 48	0.06 45	0.10 78	0.01 105	0.11 105		
6.0	2.51	0.11 243	0.55 315	0.79 293	1.11 262	1.17 230	0.80 219	0.39 212	0.17 216	0.15 212	0.13 216	0.04 236	0.10 210	0.10 345	0.05 107	0.13 156	0.12 236	0.12 222		
5.5	4.14	0.14 266	0.72 319	0.94 302	1.19 276	1.09 244	0.77 231	0.41 219	0.16 203	0.14 188	0.12 225	0.08 343	0.18 357	0.14 333	0.02 246	0.12 187	0.19 224	0.18 214		
5.0	6.83	0.20 288	0.83 323	0.95 314	1.05 291	0.90 259	0.71 245	0.38 225	0.15 188	0.14 163	0.10 242	0.20 0	0.20 11	0.18 326	0.13 283	0.25 225	0.24 216	0.23 209		
4.5	11.25	0.30 300	0.82 328	0.83 332	0.75 312	0.66 281	0.61 260	0.32 232	0.13 166	0.14 136	0.07 279	0.32 9	0.42 19	0.20 323	0.27 290	0.24 254	0.27 211	0.22 203		
4.0	18.55	0.39 308	0.73 332	0.69 353	0.54 346	0.50 312	0.51 276	0.24 240	0.10 141	0.16 117	0.08 328	0.42 12	0.49 24	0.20 319	0.27 293	0.27 272	0.27 208	0.22 201		
3.5	30.59	0.40 311	0.54 337	0.58 357	0.49 21	0.44 341	0.42 290	0.17 254	0.10 117	0.16 103	0.10 354	0.45 15	0.50 27	0.18 316	0.42 282	0.31 282	0.24 203	0.19 197		
3.0	50.43	0.31 315	0.34 342	0.46 340	0.47 43	0.40 1	0.33 302	0.11 270	0.10 99	0.15 94	0.12 5	0.44 16	0.47 29	0.14 318	0.38 297	0.27 287	0.18 199	0.13 193		
2.5	83.15	0.20 317	0.19 348	0.32 349	0.37 54	0.31 14	0.22 312	0.07 295	0.08 88	0.12 80	0.11 18	0.34 31	0.36 313	0.10 298	0.28 291	0.21 195	0.19 195	0.08 191		

MAY	MEAN GEOPOTENTIAL HEIGHT AMPLITUDE (dam) AND PHASE WAVE 2																	
SCALE	PRESSURE	-80	-70	-60	-50	-40	-30	-20	-10	0	10	20	30	40	50	60	70	80
HEIGHT	(mb)																	
12.0	0.0062	1.2 190	2.1 313	7.3 333	6.2 300	5.0 232	4.1 240	3.4 210	4.8 214	4.3 183	4.7 161	2.6 172	1.2 56	4.1 343	3.3 38	1.5 223	2.6 150	4.9 258
11.5	0.0103	1.5 187	2.1 307	7.3 328	6.3 300	5.1 229	3.8 230	3.5 208	4.6 208	4.1 184	3.6 156	1.7 154	1.5 46	3.6 340	3.0 39	1.2 225	2.3 156	2.6 266
11.0	0.0169	1.8 167	2.2 304	7.2 324	6.3 299	5.2 227	3.8 220	3.7 193	4.4 201	3.8 185	2.6 153	1.2 116	1.9 40	3.0 336	2.7 39	0.8 231	1.9 165	2.6 277
10.5	0.0279	2.0 189	2.2 302	7.0 320	6.3 298	5.3 227	3.9 213	3.9 189	4.2 195	3.5 185	1.8 145	1.4 76	2.3 36	2.4 332	2.3 37	0.4 249	1.6 175	1.5 302
10.0	0.0460	2.2 191	2.3 303	6.7 318	6.2 297	5.3 228	4.1 211	4.0 189	3.9 190	3.1 186	1.1 132	1.9 57	2.7 35	1.8 331	2.1 32	0.3 350	1.3 187	1.0 355
9.5	0.0758	2.4 195	2.3 306	6.2 317	6.1 295	5.4 232	4.5 213	4.0 192	3.6 187	2.6 177	1.1 113	2.2 48	3.0 35	1.3 336	1.9 24	0.8 23	1.1 196	1.2 44
9.0	0.1250	2.5 199	2.4 311	5.5 317	5.9 293	5.5 238	4.9 219	3.9 198	3.1 186	2.1 187	0.4 96	2.3 44	3.2 35	0.9 355	1.9 14	1.3 31	0.9 199	1.5 75
8.5	0.2061	2.5 203	2.4 315	4.8 318	5.8 291	5.6 244	5.3 225	3.7 207	2.5 187	1.6 186	0.2 103	2.1 40	3.3 35	0.9 22	1.9 6	1.6 36	0.6 192	1.6 99
8.0	0.3398	2.3 206	2.4 319	4.2 318	5.6 288	5.9 248	5.6 231	3.4 214	1.9 190	1.3 182	0.2 156	1.9 35	3.2 35	1.1 32	1.8 27	1.7 48	0.5 160	1.4 152
7.5	0.5603	2.1 207	2.3 321	4.0 317	5.6 288	6.0 251	5.5 236	3.0 218	1.4 192	1.1 175	0.3 179	1.7 29	2.9 33	1.3 27	1.6 10	1.5 48	1.0 160	1.2 150
7.0	0.9237	1.8 204	2.2 320	3.9 316	5.6 291	5.7 256	5.0 241	2.6 220	1.2 189	1.1 168	0.3 182	1.7 24	2.7 31	1.3 19	1.4 16	1.2 95	0.5 162	1.0 177
6.5	1.52	1.6 199	1.9 320	3.6 318	5.3 297	5.1 264	4.3 247	2.1 220	1.0 181	1.0 161	0.2 175	1.8 22	2.6 31	1.3 14	1.2 17	1.0 96	0.6 167	1.0 193
6.0	2.51	1.4 194	1.4 321	3.0 326	4.5 308	4.1 277	3.5 257	1.6 223	0.9 170	0.9 151	0.2 128	1.8 23	2.5 33	1.2 15	1.2 14	0.9 50	0.5 159	1.0 196
5.5	4.14	1.4 188	0.4 330	1.9 344	3.4 327	3.0 298	2.5 270	1.0 226	0.7 157	0.8 139	0.2 73	1.8 25	2.4 37	1.0 21	1.2 13	0.4 43	0.5 134	0.5 190
5.0	6.83	1.4 178	0.7 135	1.2 30	2.4 355	2.3 327	1.7 290	0.5 232	0.5 141	0.7 127	0.4 64	1.6 29	2.1 41	0.9 33	1.7 17	1.2 40	0.6 102	0.7 177
4.5	11.25	1.6 166	1.9 142	1.4 91	2.0 27	1.9 356	1.1 321	0.1 20	0.4 124	0.6 118	0.5 67	1.3 35	1.6 49	0.8 51	1.3 31	1.4 44	0.8 76	0.8 136
4.0	18.55	2.0 156	3.1 147	2.0 122	1.7 54	1.7 22	0.9 8	0.5 51	0.3 105	0.4 110	0.6 51	0.8 65	1.1 70	0.9 51	1.4 50	1.7 51	1.1 61	0.3 66
3.5	30.59	2.5 150	4.0 147	2.6 140	1.4 78	1.4 45	1.1 46	0.8 57	0.1 81	0.2 108	0.6 103	0.5 106	1.0 85	1.8 67	2.0 60	1.4 52	0.6 43	0.6 58
3.0	50.43	3.1 147	4.6 149	3.0 153	1.0 107	1.2 70	1.4 68	0.9 62	0.1 357	0.1 30	0.6 105	0.8 157	1.2 157	2.2 94	2.3 79	1.7 68	0.7 47	0.8 35
2.5	83.15	3.4 146	5.0 150	3.3 162	0.9 145	1.0 97	1.6 80	1.1 67	0.7 278	0.1 234	0.6 120	1.3 173	1.4 179	1.3 99	2.6 86	2.6 73	1.9 44	0.9 31

JUNE	MEAN TEMPERATURE	AMPLITUDE (K)	AND PHASE	WAVE 1															
SCALE	PRESSURE	-80	-70	-60	-50	-40	-30	-20	-10	0	10	20	30	40	50	60	70	80	
HEIGHT	(mb)																		
12.0	0.0062	1.16 213	2.33 217	1.82 208	0.72 205	0.47 46	0.95 37	1.18 345	0.68 338	0.17 277	0.96 246	1.15 229	0.17 107	4.20 43	0.41 73	0.35 75	0.43 258	0.21 211	
11.5	0.0103	1.02 223	2.10 224	1.76 215	0.78 213	0.30 62	0.75 51	0.97 345	0.54 337	0.16 257	0.87 243	1.13 228	0.15 102	4.70 43	0.45 72	0.36 72	0.49 256	0.25 213	
11.0	0.0169	0.85 243	1.71 236	1.59 226	0.83 223	0.21 141	0.59 88	0.57 349	0.26 331	0.16 227	0.83 240	1.03 227	0.11 87	3.77 43	0.45 71	0.28 63	0.53 253	0.28 218	
10.5	0.0279	0.85 275	1.35 261	1.45 245	0.90 235	0.58 185	0.86 139	0.10 108	0.17 181	0.25 195	0.74 234	0.85 226	0.07 37	2.17 41	0.39 68	0.18 24	0.51 250	0.27 227	
10.0	0.0460	1.05 305	1.37 299	1.44 270	1.01 250	1.08 196	1.55 160	0.84 155	0.69 167	0.39 177	0.64 223	0.63 223	0.13 337	0.71 31	0.28 63	0.25 320	0.42 241	0.24 235	
9.5	0.0758	1.38 323	1.87 327	1.72 297	1.16 269	1.52 202	2.34 168	1.70 158	1.24 164	0.53 172	0.55 206	0.37 217	0.24 311	0.36 239	0.10 44	0.48 294	0.31 227	0.17 248	
9.0	0.1250	1.70 336	2.55 344	2.25 319	1.43 290	1.80 208	2.94 173	2.38 159	1.67 163	0.64 171	0.50 183	0.18 196	0.37 295	1.33 230	0.10 259	0.69 205	0.23 203	0.11 236	
8.5	0.2061	1.85 348	3.15 355	2.98 336	1.88 310	1.88 218	2.97 177	2.56 159	1.72 161	0.57 173	0.48 163	0.13 178	0.49 276	1.19 230	0.29 236	0.74 279	0.20 202	0.13 162	
8.0	0.3398	1.85 3	3.52 5	3.73 348	2.48 326	1.28 240	2.32 182	2.10 159	1.34 158	0.35 185	0.42 149	0.19 201	0.60 258	0.15 332	0.41 220	0.62 273	0.22 231	0.34 148	
7.5	0.5603	1.40 16	2.92 11	3.48 357	2.39 332	1.10 258	1.31 191	1.08 155	0.57 143	0.03 225	0.30 124	0.58 206	1.40 235	0.38 39	0.30 208	0.23 251	0.28 251	0.38 152	
7.0	0.9237	1.06 26	2.29 15	3.09 297	2.33 269	1.11 202	0.55 168	0.39 136	0.20 83	0.15 16	0.18 98	0.29 196	0.46 209	1.47 239	0.27 44	0.18 208	0.28 209	0.26 171	
6.5	1.52	0.89 28	1.91 15	2.87 338	2.54 308	1.45 277	0.36 96	0.23 58	0.12 54	0.12 99	0.13 166	0.21 175	0.35 235	0.43 235	0.15 200	0.15 200	0.22 200	0.19 233	
6.0	2.51	0.91 24	1.82 14	2.97 356	3.11 341	2.14 325	0.66 309	0.14 98	0.11 170	0.11 146	0.14 144	0.18 137	0.29 152	0.29 190	0.14 260	0.10 204	0.25 107	0.30 230	
5.5	4.14	0.82 44	1.64 29	2.81 3	3.24 350	2.59 341	1.12 331	0.23 342	0.14 202	0.12 199	0.13 223	0.10 223	0.15 189	0.24 204	0.21 238	0.15 215	0.27 198	0.35 258	
5.0	6.83	0.66 68	1.35 53	2.14 20	2.65 352	2.43 337	1.33 319	0.48 266	0.24 232	0.18 236	0.21 266	0.32 266	0.31 266	0.28 266	0.33 221	0.23 221	0.28 221	0.34 215	
4.5	11.25	0.51 117	1.24 97	1.51 63	1.66 30	1.69 50	1.18 340	0.67 306	0.32 275	0.24 247	0.28 250	0.59 272	0.67 280	0.36 238	0.48 209	0.32 227	0.28 232	0.30 248	
4.0	18.55	0.82 173	1.62 136	1.90 111	1.33 82	0.96 41	0.82 342	0.75 295	0.36 281	0.27 255	0.33 260	0.80 274	0.98 283	0.44 250	0.59 202	0.39 228	0.28 252	0.22 236	
3.5	30.59	1.11 192	1.88 155	2.40 129	1.63 116	0.85 99	0.41 342	0.73 286	0.33 283	0.26 262	0.32 266	0.88 274	1.12 284	0.46 257	0.61 199	0.30 230	0.27 267	0.14 213	
3.0	50.43	0.95 202	1.59 164	2.20 158	1.70 130	1.05 128	0.67 340	0.29 279	0.22 285	0.29 267	0.85 271	1.11 274	0.43 284	0.54 263	0.35 195	0.23 231	0.25 280	0.19 180	
2.5	85.15	0.62 207	1.06 169	1.60 142	1.37 137	0.97 159	0.10 169	0.49 272	0.20 288	0.17 273	0.22 274	0.70 274	0.92 284	0.35 266	0.41 194	0.26 230	0.17 250	0.07 155	

JUNE	MEAN GEOPOTENTIAL	HEIGHT	AMPLITUDE (dam)	AND PHASE	WAVE 1														
SCALE	PRESSURE	-80	-70	-60	-50	-40	-30	-20	-10	0	10	20	30	40	50	60	70	80	
HEIGHT	(mb)																		
12.0	0.0062	10.9 279	13.7 310	21.4 314	21.2 315	9.1 263	16.3 172	12.7 164	9.9 170	6.2 189	9.9 210	12.9 225	9.1 245	14.3 35	5.8 214	6.6 259	8.1 235	5.2 218	
11.5	0.0103	10.3 287	14.0 323	22.2 320	21.5 318	9.6 262	17.1 176	14.3 164	10.8 169	6.4 185	8.9 206	11.2 225	9.3 245	7.9 218	6.3 258	7.2 235	7.5 233	4.8 218	
11.0	0.0169	9.6 294	14.5 334	22.7 327	21.8 321	9.9 262	17.5 164	15.5 168	11.4 168	6.6 182	7.9 200	9.7 224	9.5 246	6.3 243	6.9 221	7.6 258	6.8 231	4.4 219	
10.5	0.0279	8.6 298	14.6 343	22.9 332	21.8 325	9.9 265	17.0 181	15.8 168	11.4 168	6.4 180	7.0 224	8.3 246	9.6 254	5.7 223	7.4 255	7.9 227	6.1 228	4.0 218	
10.0	0.0460	7.3 300	13.8 350	22.5 337	21.7 328	9.6 272	15.6 184	15.2 165	10.8 168	6.0 180	6.2 190	7.2 224	9.6 245	5.6 241	7.9 224	5.4 255	3.7 226	3.7 217	
9.5	0.0758	5.6 295	12.0 356	21.1 342	21.1 332	9.2 283	12.9 189	13.4 166	9.4 168	5.2 181	5.9 186	6.5 224	9.6 244	5.1 239	8.1 225	7.6 252	4.9 225	3.4 215	
9.0	0.1250	4.0 276	9.0 187	18.8 347	20.1 336	9.1 299	10.4 196	7.3 168	7.3 170	4.1 184	4.7 184	6.1 225	9.3 242	4.1 241	6.2 224	6.9 247	4.5 226	3.2 213	
8.5	0.2061	3.8 237	5.0 14	15.2 351	18.2 341	9.2 315	6.8 213	4.8 173	2.9 174	4.0 191	5.9 186	8.9 227	8.9 239	7.3 251	7.9 224	6.0 242	4.2 228	3.1 214	
8.0	0.3398	5.6 212	1.2 91	10.4 355	15.3 345	9.5 328	3.0 299	3.5 186	2.6 187	2.1 202	3.5 191	5.8 228	8.2 236	1.3 263	7.4 224	5.2 235	3.9 229	3.0 219	
7.5	0.5603	7.8 206	4.7 174	5.1 358	11.9 350	9.3 339	3.4 308	1.8 223	1.7 209	1.8 198	3.2 230	5.4 235	7.3 239	2.3 224	6.8 224	4.7 231	3.6 227	2.8 230	
7.0	0.9237	9.6 205	8.4 186	0.4 180	8.7 185	8.8 9	4.0 339	1.8 334	1.7 263	1.9 231	3.2 208	5.0 235	6.6 235	4.5 240	6.3 228	4.4 236	3.2 233	2.7 244	
6.5	1.52	11.0 205	11.4 186	4.0 185	5.5 189	7.8 9	4.0 339	2.1 334	2.0 263	2.2 231	3.3 208	4.8 235	6.2 240	5.9 228	6.1 226	4.2 233	2.8 235	2.5 244	
6.0	2.51	12.3 205	14.1 187	8.3 181	2.8 55	6.1 15	3.4 341	2.4 264	2.0 233	2.2 211	3.3 211	4.8 238	6.1 244	6.0 228	5.9 225	4.0 234	2.6 226	2.1 242	
5.5	4.14	13.6 206	16.5 189	12.5 180	4.6 130	4.1 48	2.2 351	2.5 260	1.9 235	2.1 213	3.2 213	4.8 240	6.1 247	5.7 230	5.6 224	3.9 235	2.2 231	1.7 238	
5.0	6.83	14.5 208	18.4 193	16.0 183	8.3 152	4.1 103	0.7 40	2.3 249	1.7 231	1.9 212	2.9 212	4.5 239	5.8 248	5.3 231	5.2 224	3.5 237	1.9 237	1.2 231	
4.5	11.25	14.9 211	19.4 197	18.3 187	10.8 163	5.6 134	1.6 137	2.1 137	1.4 227	1.6 219	2.6 207	4.0 234	5.2 244	4.9 241	4.7 225	3.2 238	1.5 241	0.8 218	
4.0	18.55	14.5 214	19.1 203	18.7 194	11.6 173	6.7 149	3.1 149	2.0 198	1.2 198	1.4 195	2.4 200	3.2 222	4.3 234	4.3 229	3.9 229	2.7 240	1.1 241	0.5 198	
3.5	30.59	13.3 217	17.7 210	18.0 204	11.1 183	6.5 159	3.9 152	2.4 170	1.2 172	1.3 180	2.2 189	2.6 201	3.5 214	3.7 225	3.2 237	2.1 243	0.7 230	0.3 173	
3.0	50.43	11.8 219	16.2 218	17.1 215	10.0 195	5.6 159	4.3 152	2.9 151	1.5 157	1.3 165	2.1 177	2.6 188	3.3 186	3.2 218	2.6 249	1.6 247	0.5 247	0.2 144	
2.5	85.15	10.7 221	15.1 223	16.6 224	9.1 208	4.4 180	4.2 152	3.5 140	1.7 148	1.4 155	2.2 168	3.0 150	3.8 163	2.8 210	2.3 264	1.1 254	0.6 254	0.1 99	

ORIGINAL PAGE IS OF POOR QUALITY

125

JUNE		MEAN TEMPERATURE AMPLITUDE (K) AND PHASE										WAVE 2									
SCALE	PRESSURE	-80	-70	-60	-50	-40	-30	-20	-10	0	10	20	30	40	50	60	70	80			
HEIGHT	(mb)																				
12.0	0.0062	0.81	0.66	0.57	0.52	1.04	0.82	0.55	0.70	0.42	0.24	0.46	0.30	3.53	0.33	0.58	0.41	0.30			
		28	61	41	33	1	290	233	278	245	91	101	333	278	251	28	141	189			
11.5	0.0103	0.71	0.58	0.51	0.61	1.07	0.84	0.54	0.71	0.39	0.23	0.43	0.30	3.99	0.37	0.60	0.47	0.36			
		30	62	43	32	359	295	237	279	245	81	98	333	278	251	30	141	188			
11.0	0.0169	0.54	0.44	0.41	0.57	1.05	0.83	0.51	0.65	0.30	0.22	0.36	0.26	3.26	0.37	0.54	0.48	0.37			
		35	69	45	30	356	301	243	281	244	70	92	332	278	254	34	142	189			
10.5	0.0279	0.32	0.27	0.28	0.49	0.99	0.79	0.45	0.54	0.14	0.23	0.24	0.19	2.04	0.34	0.37	0.43	0.35			
		51	85	55	28	352	312	257	285	250	52	75	328	280	259	45	145	190			
10.0	0.0460	0.17	0.17	0.15	0.40	0.88	0.75	0.40	0.39	0.04	0.26	0.17	0.12	0.94	0.27	0.16	0.32	0.27			
		111	139	79	25	345	326	273	292	34	30	25	310	284	270	104	150	193			
9.5	0.0758	0.29	0.24	0.11	0.28	0.69	0.70	0.35	0.21	0.23	0.31	0.25	0.08	0.58	0.20	0.37	0.14	0.13			
		170	187	129	21	337	343	296	313	62	17	336	264	350	292	175	163	189			
9.0	0.1250	0.48	0.31	0.10	0.15	0.39	0.60	0.31	0.16	0.37	0.33	0.35	0.11	0.53	0.17	0.64	0.07	0.07			
		188	207	156	23	318	4	327	37	66	10	317	238	89	330	188	286	56			
8.5	0.2061	0.58	0.27	0.04	0.05	0.22	0.45	0.28	0.34	0.37	0.25	0.33	0.15	0.41	0.18	0.67	0.19	0.24			
		203	220	157	90	213	42	14	82	75	13	300	257	93	352	189	318	44			
8.0	0.3398	0.59	0.16	0.10	0.19	0.78	0.53	0.35	0.52	0.25	0.10	0.23	0.24	0.51	0.17	0.44	0.20	0.36			
		216	254	6	161	171	102	63	98	104	51	270	283	274	353	185	328	52			
7.5	0.5603	0.41	0.17	0.30	0.14	0.90	0.57	0.32	0.44	0.20	0.16	0.18	0.28	1.46	0.12	0.05	0.08	0.30			
		240	345	360	148	158	136	105	114	173	152	202	297	274	316	77	349	61			
7.0	0.9237	0.25	0.27	0.44	0.20	0.69	0.49	0.28	0.29	0.23	0.21	0.16	0.22	1.42	0.15	0.24	0.02	0.16			
		256	5	360	44	127	128	122	132	193	162	176	302	274	292	12	90	72			
6.5	1.52	0.13	0.29	0.58	0.68	0.88	0.59	0.25	0.13	0.12	0.12	0.03	0.15	0.58	0.16	0.18	0.03	0.03			
		225	11	2	26	66	69	83	138	185	167	162	308	277	297	352	232	112			
6.0	2.51	0.23	0.33	0.75	1.26	1.66	1.24	0.56	0.14	0.06	0.05	0.14	0.19	0.16	0.17	0.11	0.08	0.08			
		173	13	8	26	43	44	44	46	51	45	356	331	317	317	315	253	203			
5.5	4.14	0.24	0.38	0.71	1.20	1.68	1.34	0.67	0.19	0.10	0.09	0.25	0.27	0.25	0.22	0.12	0.10				
		168	20	16	30	43	43	44	47	55	33	359	340	327	331	312	238	203			
5.0	6.83	0.14	0.42	0.56	0.84	1.29	1.13	0.64	0.22	0.14	0.14	0.35	0.36	0.34	0.29	0.12	0.16	0.13			
		159	27	33	38	41	39	40	46	56	27	360	346	350	342	318	229	203			
4.5	11.25	0.13	0.48	0.41	0.35	0.63	0.68	0.48	0.22	0.17	0.17	0.43	0.43	0.42	0.35	0.11	0.19	0.14			
		5	33	69	68	33	26	30	42	57	26	1	349	333	350	322	233	200			
4.0	18.55	0.43	0.48	0.46	0.33	0.19	0.36	0.30	0.19	0.17	0.19	0.46	0.46	0.46	0.38	0.10	0.19	0.15			
		352	38	113	161	306	336	4	38	59	23	1	350	334	356	323	221	200			
3.5	30.59	0.58	0.39	0.53	0.55	0.52	0.49	0.23	0.14	0.17	0.18	0.44	0.44	0.43	0.35	0.08	0.17	0.13			
		348	42	135	185	250	281	316	35	60	23	360	352	335	0	350	219	202			
3.0	50.43	0.50	0.25	0.47	0.60	0.68	0.63	0.28	0.09	0.14	0.16	0.39	0.38	0.37	0.30	0.06	0.14	0.11			
		347	45	145	192	243	265	285	29	60	24	360	352	336	3	329	216	202			
2.5	83.15	0.34	0.14	0.34	0.48	0.62	0.58	0.27	0.05	0.10	0.12	0.29	0.29	0.27	0.21	0.04	0.09	0.07			
		346	49	150	195	241	259	270	18	63	22	360	352	336	5	337	215	200			

JUNE		MEAN GEOPOTENTIAL HEIGHT AMPLITUDE (dm) AND PHASE										WAVE 2									
SCALE	PRESSURE	-80	-70	-60	-50	-40	-30	-20	-10	0	10	20	30	40	50	60	70	80			
HEIGHT	(mb)																				
12.0	0.0062	2.3	5.3	8.2	11.0	13.9	10.8	5.6	1.8	1.7	3.5	3.2	4.7	25.1	3.8	2.1	2.5	2.2			
		176	46	37	45	33	18	14	354	86	52	17	327	283	314	73	152	153			
11.5	0.0103	3.3	4.4	7.4	10.1	12.6	10.8	4.3	1.9	2.1	3.2	3.2	4.3	17.6	3.6	1.6	1.9	1.9			
		187	67	37	47	37	25	21	26	82	49	6	327	284	322	95	156	144			
11.0	0.0169	4.2	3.6	6.7	9.3	11.4	10.8	4.9	2.4	2.5	2.9	3.2	3.9	12.1	3.4	1.5	1.2	1.5			
		192	68	36	48	42	31	27	50	81	45	355	326	287	330	126	165	130			
10.5	0.0279	4.7	3.1	6.3	8.5	10.5	10.8	5.4	3.0	2.8	2.6	3.3	3.6	8.4	3.3	1.6	0.6	1.3			
		196	67	35	50	48	38	32	64	81	44	348	326	291	339	151	187	110			
10.0	0.0460	4.9	2.9	6.0	8.0	9.8	10.6	5.8	3.5	2.9	2.2	3.2	3.3	6.2	3.2	1.6	0.4	1.3			
		199	63	33	52	54	44	36	71	83	44	343	326	295	347	164	250	90			
9.5	0.0758	4.7	3.0	5.9	7.5	9.6	10.3	6.1	3.8	2.8	1.8	2.9	3.2	5.5	3.1	1.3	0.5	1.4			
		202	58	32	53	61	49	41	76	87	49	342	327	295	353	165	286	79			
9.0	0.1250	4.2	3.3	6.0	7.3	9.6	9.8	6.1	3.8	2.5	1.5	2.5	3.2	5.9	2.9	0.6	0.6	1.4			
		204	53	30	55	66	54	46	79	93	59	345	330	293	356	145	296	76			
8.5	0.2061	3.4	3.7	6.1	7.1	9.8	9.2	5.9	3.5	2.1	1.3	2.1	3.2	6.6	2.7	0.7	0.4	1.2			
		206	51	30	55	67	56	49	80	100	74	353	333	290	357	49	289	82			
8.0	0.3398	2.6	4.0	6.0	7.1	10.1	8.6	5.5	2.9	1.7	1.1	1.9	3.1	6.6	2.4	1.5	0.2	0.9			
		205	51	30	54	64	55	50	78	104	85	5	338	290	358	27	233	98			
7.5	0.5603	1.9	4.0	5.8	7.2	10.4	8.3	5.1	2.3	1.4	1.0	2.1	2.8	5.2	2.2	1.7	0.3	0.6			
		197	53	31	52	57	50	47	70	99	80	10	343	295	359	22	194	129			
7.0	0.9237	1.7	3.9	5.3	7.1	10.5	8.3	5.0	2.0	1.3	1.0	2.4	2.5	3.2	2.1	1.5	0.4	0.6			
		184	57	34	51	50	45	42	57	85	64	10	349	309	4	22	193	162			
6.5	1.52	1.6	3.6	4.7	6.5	9.8	7.9	4.8	1.9	1.3	1.1	2.5	2.4	2.2	2.1	1.2	0.3	0.6			
		175	62	39	43	46	41	38	49	73	51	9	354	332	10	27	193	175			
6.0	2.51	1.4	3.3	4.0	5.3	8.0	6.6	4.3	1.9	1.3	1.1	2.4	2.2	1.9	2.0	1.1	0.3	0.5			
		173	68	47	60	45	39	36	46	69	47	9	357	342	16	35	181	173			
5.5	4.14	1.0	3.0	3.1	3.9	5.5	4.7	3.4	1.6	1.1	1.0	2.1	1.9	1.6	1.1	0.3	0.4				

JULY	MEAN TEMPERATURE AMPLITUDE (K) AND PHASE WAVE																	
SCALE	PRESSURE	-80	-70	-60	-50	-40	-30	-20	-10	0	10	20	30	40	50	60	70	80
HEIGHT	(mb)																	
12.0	0.0062	1.04 261	1.68 210	2.16 173	1.98 125	1.43 90	0.78 65	0.55 347	0.28 341	0.37 153	0.54 203	0.34 306	0.67 354	0.64 336	0.24 263	0.22 141	0.49 137	0.13 225
11.5	0.0103	0.96 274	1.61 218	2.18 181	1.89 136	1.30 105	0.69 94	0.41 349	0.22 341	0.35 142	0.57 204	0.34 301	0.69 352	0.68 336	0.25 264	0.25 146	0.57 136	0.14 226
11.0	0.0169	0.87 296	1.45 229	2.11 192	1.75 155	1.20 131	0.67 118	0.15 356	0.13 305	0.31 158	0.59 207	0.33 297	0.65 347	0.69 335	0.26 268	0.23 157	0.60 133	0.13 228
10.5	0.0279	0.93 325	1.28 248	2.03 207	1.80 182	1.42 167	0.97 154	0.24 158	0.02 229	0.29 183	0.57 211	0.29 290	0.56 340	0.67 336	0.25 273	0.22 180	0.56 128	0.11 236
10.0	0.0460	1.18 349	1.21 273	1.99 226	2.16 207	2.07 191	1.55 174	0.73 164	0.20 173	0.36 212	0.55 214	0.25 275	0.45 323	0.59 333	0.22 279	0.24 215	0.46 120	0.07 278
9.5	0.0758	1.51 6	1.28 303	1.92 248	2.57 226	2.84 206	2.18 185	1.22 167	0.39 168	0.46 226	0.53 215	0.22 244	0.57 295	0.48 328	0.20 282	0.34 241	0.28 103	0.08 342
9.0	0.1250	1.80 20	1.52 332	1.85 279	2.70 244	3.29 217	2.51 195	1.53 171	0.54 166	0.50 230	0.47 210	0.26 205	0.37 257	0.33 310	0.17 270	0.43 255	0.12 50	0.13 4
8.5	0.2061	1.96 35	1.96 360	2.16 320	2.44 273	3.12 235	2.55 208	1.47 180	0.56 165	0.38 220	0.38 192	0.46 177	0.29 224	0.29 259	0.24 243	0.45 264	0.16 312	0.12 5
8.0	0.3398	1.99 52	2.59 21	3.22 351	2.63 317	2.52 261	2.09 231	1.05 199	0.43 159	0.25 168	0.37 160	0.53 254	0.55 200	0.47 225	0.21 226	0.33 270	0.31 268	0.06 329
7.5	0.5603	1.84 66	3.07 30	4.11 6	3.35 338	2.53 291	1.81 261	0.75 238	0.17 144	0.32 104	0.32 127	0.51 156	0.55 185	0.60 210	0.51 217	0.11 234	0.35 243	0.09 214
7.0	0.9237	1.95 65	3.77 33	5.07 13	4.46 351	3.11 322	1.71 298	0.60 281	0.09 92	0.32 83	0.25 105	0.40 148	0.47 171	0.53 200	0.49 210	0.18 171	0.30 222	0.09 212
6.5	1.52	2.43 54	4.73 34	6.28 67	6.08 358	4.47 341	2.23 331	0.63 330	0.16 15	0.19 52	0.13 74	0.25 131	0.34 159	0.38 183	0.36 205	0.27 178	0.23 205	0.08 266
6.0	2.51	3.17 45	5.79 36	7.68 20	8.24 5	6.52 353	3.39 347	1.07 351	0.23 356	0.12 0	0.07 25	0.14 111	0.23 158	0.25 168	0.27 204	0.26 191	0.22 202	0.20 297
5.5	4.14	3.04 47	5.89 43	8.10 28	9.11 9	7.33 16	3.99 357	1.42 356	0.32 349	0.13 342	0.08 332	0.05 236	0.20 202	0.23 195	0.27 221	0.21 225	0.26 227	0.31 289
5.0	6.83	2.51 52	5.33 31	7.49 39	8.48 29	6.66 16	3.75 4	1.47 356	0.37 344	0.15 323	0.13 302	0.29 262	0.43 240	0.33 230	0.30 240	0.27 272	0.36 251	0.40 280
4.5	11.25	1.52 70	4.06 68	6.01 58	6.59 59	4.79 34	2.64 13	1.21 351	0.38 336	0.18 312	0.19 290	0.56 261	0.76 249	0.53 247	0.44 257	0.50 298	0.46 266	0.47 271
4.0	18.55	1.13 158	2.84 109	4.90 91	5.02 81	3.19 68	1.35 32	0.80 339	0.35 328	0.20 307	0.23 285	0.76 259	1.02 252	0.71 253	0.38 268	0.61 208	0.60 275	0.47 263
3.5	30.59	2.46 198	3.09 162	4.61 126	4.52 113	2.84 109	0.67 95	0.48 311	0.30 318	0.19 303	0.24 282	0.83 258	1.11 252	0.78 256	0.37 275	0.67 313	0.63 281	0.43 255
3.0	50.43	2.34 205	3.10 185	4.13 148	4.20 134	2.96 148	1.00 266	0.39 309	0.24 303	0.17 281	0.22 258	0.80 253	1.08 257	0.75 280	0.32 316	0.61 285	0.55 285	0.35 250
2.5	83.15	1.53 207	2.23 193	3.05 159	3.32 147	2.55 146	1.09 161	0.37 239	0.16 299	0.13 301	0.17 279	0.65 257	0.88 253	0.59 283	0.24 318	0.45 318	0.40 287	0.24 244

JULY	MEAN GEOPOTENTIAL HEIGHT	AMPLITUDE (dam)	AND PHASE	WAVE 1														
SCALE	PRESSURE	-80	-70	-60	-50	-40	-30	-20	-10	0	10	20	30	40	50	60	70	80
HEIGHT	(mb)																	
12.0	0.0062	22.6 37	26.4 39	31.3 32	34.5 31	21.1 0	7.8 316	3.3 269	0.3 172	3.6 197	7.7 203	7.2 222	8.8 244	9.7 257	10.2 238	6.9 241	4.8 200	3.5 268
11.5	0.0103	23.6 40	28.8 39	33.9 29	35.1 27	21.5 355	8.4 309	3.2 256	0.6 166	3.2 202	6.9 203	7.1 218	9.2 238	9.6 252	9.8 234	6.9 249	4.5 205	3.4 270
11.0	0.0169	24.2 43	31.0 39	36.8 27	36.4 23	22.4 351	9.2 306	3.3 249	0.9 164	2.9 208	6.0 203	7.1 214	9.6 233	9.5 246	9.5 236	6.9 246	4.3 220	3.2 273
10.5	0.0279	24.3 46	32.9 40	39.8 27	38.5 22	24.2 350	10.4 308	3.3 250	1.0 162	2.4 212	5.2 202	7.0 210	9.9 228	9.6 240	9.2 235	6.9 249	4.4 231	3.1 275
10.0	0.0460	23.7 49	34.3 42	42.7 27	41.4 20	26.6 351	11.8 313	3.4 262	0.8 159	1.9 214	4.4 200	6.9 227	10.2 224	9.7 234	9.7 234	6.7 251	4.7 240	3.0 276
9.5	0.0758	22.5 53	35.1 45	45.2 29	44.7 22	29.8 354	13.9 321	3.8 284	0.4 149	1.2 210	3.6 197	6.7 205	10.1 221	9.9 230	9.7 232	6.3 253	5.0 245	2.9 275
9.0	0.1250	20.7 58	35.0 48	46.9 32	48.0 24	33.5 359	16.4 331	5.0 306	0.3 14	0.5 189	2.9 192	6.4 204	9.8 218	9.8 226	9.3 231	5.7 253	3.3 246	2.9 272
8.5	0.2061	18.4 62	33.8 52	47.1 35	50.3 28	37.0 4	19.1 340	6.7 320	1.1 353	0.4 93	2.3 190	6.0 205	9.3 217	9.7 224	8.3 230	5.1 252	3.3 245	2.9 268
8.0	0.3398	15.7 65	31.4 55	45.2 39	50.7 32	39.2 9	21.1 348	8.1 330	1.8 349	0.6 48	1.8 193	5.4 209	8.6 218	9.2 223	7.8 230	4.5 250	2.9 242	2.6 266
7.5	0.5603	12.9 66	27.9 60	41.2 44	48.8 36	39.5 15	21.8 355	8.7 338	2.2 347	0.7 15	1.5 208	4.9 216	7.8 220	8.4 224	7.2 231	4.2 249	2.4 241	2.8 266
7.0	0.9237	10.2 66	23.6 65	35.8 50	45.4 42	38.1 20	21.4 1	8.5 344	2.3 344	0.8 224	1.6 223	4.7 224	7.3 224	7.6 226	6.5 233	4.1 252	2.4 242	2.8 269
6.5	1.52	7.0 69	18.6 75	29.4 59	40.5 49	34.6 27	19.5 7	7.9 348	2.2 341	0.9 314	1.7 230	4.6 229	7.0 228	7.1 229	5.9 235	4.1 256	2.4 245	2.7 270
6.0	2.51	3.5 93	13.6 96	22.6 76	34.3 62	28.9 37	16.0 13	6.7 348	1.9 338	0.8 301	1.9 231	4.7 232	6.9 232	6.8 232	5.5 232	4.0 262	3.6 248	2.5 269
5.5	4.14	3.4 176	11.5 135	18.1 107	28.2 83	21.7 53	11.0 63	4.9 346	1.6 334	0.7 291	1.9 228	4.7 233	6.8 234	6.6 234	5.2 240	3.8 266	3.3 251	2.2 265
5.0	6.83	6.7 205	14.0 172	18.7 144	24.8 111	15.9 80	6.1 85	2.8 338	1.1 328	0.6 277	1.9 224	4.9 232	6.3 234	6.2 236	4.8 240	3.5 267	2.9 263	1.7 259
4.5	11.25	9.4 215	17.9 192	24.0 170	23.9 137	13.2 112	5.6 95	1.0 306	0.5 315	0.4 253	1.9 217	4.9 227	5.5 232	5.6 233	4.3 239	2.6 264	2.3 251	1.1 249
4.0	18.55	10.0 223	20.0 206	24.3 188	23.0 157	11.9 138	4.0 140	1.0 210	0.2 229	0.4 213	1.8 207	3.2 218	4.3 227	4.7 232	3.8 236	2.5 252	1.5 241	0.5 222
3.5	30.59	8.1 234	18.7 217	23.9 205	20.4 173	9.6 157	4.1 157	1.6 180	0.5 161	0.5 180	1.7 196	2.5 200	2.9 213	3.7 226	3.4 231	2.2 230	1.0 206	0.4 124
3.0	50.43	5.3 256	15.6 229	22.3 220	16.9 190	6.6 178	3.2 167	1.9 163	0.9 149	0.7 185	1.7 171	2.1 202	2.8 214	3.1 224	2.3 235	1.2 206	0.9 158	0.9 93
2.5	83.15	4.1 288	12.9 240	20.7 234	13.9 207	4.2 214	1.7 178	1.9 146	1.1 143	0.9 155	1.8 176	2.3 143	2.0 139	2.2 196	2.9 217	2.6 190	1.7 139	1.3 85

JULY	MEAN TEMPERATURE AMPLITUDE (K) AND PHASE										WAVE 2									
SCALE	PRESSURE	-80	-70	-60	-50	-40	-30	-20	-10	0	10	20	30	40	50	60	70	80		
HEIGHT	(mb)																			
12.0	0.0062	0.19 225	0.62 171	1.20 133	0.91 107	0.59 143	0.17 158	0.26 295	0.48 251	0.13 238	0.69 35	0.48 38	0.27 34	0.18 273	0.13 242	0.22 219	0.19 182	0.33 110		
11.5	0.0103	0.25 231	0.68 177	1.14 140	0.78 121	0.57 155	0.17 170	0.26 285	0.51 249	0.14 226	0.65 34	0.46 34	0.27 27	0.20 276	0.14 253	0.25 216	0.22 182	0.37 107		
11.0	0.0169	0.35 237	0.72 182	1.00 151	0.64 150	0.54 175	0.17 188	0.26 274	0.51 247	0.14 214	0.55 32	0.39 29	0.27 12	0.22 283	0.15 266	0.28 215	0.24 181	0.41 103		
10.5	0.0279	0.42 242	0.76 189	0.85 171	0.76 192	0.60 204	0.19 213	0.27 256	0.51 244	0.16 196	0.40 30	0.28 14	0.28 352	0.24 292	0.18 286	0.31 216	0.23 181	0.38 99		
10.0	0.0460	0.51 247	0.80 197	0.84 199	1.18 218	0.81 227	0.26 235	0.31 239	0.49 240	0.19 183	0.19 18	0.20 340	0.31 329	0.26 300	0.23 305	0.32 214	0.21 180	0.30 90		
9.5	0.0758	0.56 250	0.80 206	1.00 222	1.67 230	1.11 242	0.37 251	0.37 224	0.46 238	0.23 171	0.06 265	0.22 289	0.39 311	0.32 309	0.30 318	0.17 213	0.19 179	0.60 60		
9.0	0.1250	0.52 252	0.73 217	1.22 236	2.00 236	1.31 251	0.49 260	0.39 216	0.40 238	0.23 170	0.23 221	0.28 260	0.44 297	0.33 316	0.34 327	0.22 210	0.12 187	0.17 3		
8.5	0.2061	0.37 257	0.62 238	1.35 245	1.96 241	1.27 258	0.57 266	0.32 215	0.27 245	0.16 173	0.31 207	0.26 239	0.42 281	0.42 316	0.31 334	0.12 207	0.11 205	0.21 333		
8.0	0.3398	0.14 270	0.55 271	1.33 251	1.51 247	0.91 269	0.55 273	0.17 225	0.13 275	0.05 217	0.27 187	0.20 198	0.35 258	0.23 310	0.20 340	0.02 154	0.15 218	0.19 317		
7.5	0.5603	0.02 63	0.44 291	0.73 262	0.23 299	0.40 28	0.21 347	0.11 27	0.08 358	0.05 302	0.17 139	0.17 143	0.23 225	0.15 285	0.08 303	0.03 39	0.14 212	0.07 287		
7.0	0.9237	0.11 146	0.19 278	0.10 270	0.72 62	0.75 75	0.43 81	0.21 62	0.05 58	0.02 0	0.16 104	0.14 124	0.14 212	0.13 279	0.09 284	0.01 90	0.13 203	0.04 207		
6.5	1.52	0.25 180	0.32 164	0.52 121	0.94 94	1.18 108	0.80 117	0.30 111	0.08 153	0.06 132	0.10 110	0.02 117	0.08 279	0.15 298	0.11 288	0.03 189	0.08 189	0.07 184		
6.0	2.51	0.40 187	0.77 153	1.26 139	1.31 144	1.63 147	1.25 142	0.49 139	0.13 175	0.09 139	0.06 149	0.07 326	0.21 323	0.24 324	0.14 331	0.05 331	0.07 191	0.09 189		
5.5	4.14	0.30 177	0.75 145	1.52 149	1.66 168	1.81 169	1.30 159	0.49 156	0.12 175	0.07 117	0.04 192	0.16 329	0.33 329	0.33 336	0.31 12	0.18 158	0.05 189	0.08 152		
5.0	6.83	0.14 150	0.63 133	1.66 160	2.06 184	1.88 187	1.17 178	0.41 176	0.10 174	0.06 72	0.04 270	0.26 332	0.44 333	0.39 345	0.39 35	0.28 130	0.08 188	0.04 166		
4.5	11.25	0.21 33	0.40 107	1.67 173	2.27 195	1.73 205	0.92 205	0.30 209	0.06 170	0.09 43	0.07 302	0.35 335	0.54 335	0.46 349	0.37 47	0.12 110	0.07 182	0.03 243		
4.0	18.55	0.63 14	0.37 35	1.58 191	2.15 204	1.48 225	0.30 242	0.30 255	0.03 141	0.12 31	0.10 317	0.40 337	0.57 336	0.48 353	0.44 53	0.14 102	0.05 169	0.07 278		
3.5	30.59	1.03 11	0.64 358	1.29 210	1.76 213	1.22 245	0.87 272	0.38 284	0.02 50	0.12 27	0.11 328	0.39 338	0.54 336	0.45 356	0.43 57	0.15 96	0.03 135	0.10 291		
3.0	50.43	0.75 6	0.66 347	0.89 229	1.25 221	0.98 264	0.91 289	0.43 298	0.03 27	0.12 24	0.11 333	0.35 340	0.47 337	0.38 357	0.36 59	0.14 94	0.02 104	0.10 294		
2.5	83.15	0.42 3	0.45 343	0.54 244	0.76 228	0.70 277	0.75 298	0.37 305	0.04 23	0.09 22	0.09 338	0.27 341	0.35 336	0.28 358	0.26 62	0.10 90	0.02 76	0.08 292		

JULY	MEAN GEOPOTENTIAL HEIGHT AMPLITUDE (dam) AND PHASE WAVE 2																		
SCALE	PRESSURE	-80	-70	-60	-50	-40	-30	-20	-10	0	10	20	30	40	50	60	70	80	
HEIGHT	(mb)																		
12.0	0.0062	5.0	11.7	25.1	24.1	16.7	7.6	3.0	4.4	0.3	2.0	3.2	6.3	5.7	2.9	3.0	3.1	2.2	
		226	191	189	199	201	191	209	247	202	42	348	321	318	351	190	183	82	
11.5	0.0103	4.7	10.8	22.1	24.0	16.2	7.4	3.0	3.7	0.2	1.1	2.8	6.2	5.5	3.0	2.7	2.8	1.7	
		226	192	193	202	203	192	201	246	196	49	338	317	320	354	186	184	75	
11.0	0.0169	4.3	9.8	21.1	25.7	15.6	7.2	2.9	2.9	0.2	0.3	2.5	6.0	5.3	3.0	2.4	2.5	1.2	
		226	193	196	204	205	192	194	245	186	102	326	314	322	358	181	184	62	
10.5	0.0279	3.7	8.7	20.0	22.9	14.8	6.9	2.8	2.2	0.1	0.7	2.3	5.7	5.0	3.0	2.0	2.1	0.9	
		224	194	198	206	206	192	186	245	150	185	315	311	324	3	174	184	36	
10.0	0.0460	3.1	7.6	18.8	21.5	13.8	6.6	2.7	1.5	0.1	1.1	2.0	5.4	4.7	2.9	1.7	1.8	0.8	
		219	194	199	206	205	191	178	247	75	193	308	309	326	8	164	185	1	
9.5	0.0758	2.5	6.4	17.5	19.5	12.6	6.4	2.4	0.8	0.3	1.2	1.8	4.9	4.3	2.7	1.4	1.5	0.8	
		210	193	198	204	202	187	169	254	52	192	307	307	329	15	150	186	334	
9.0	0.1250	1.9	5.3	16.2	17.3	11.4	6.2	2.1	0.2	0.5	1.1	1.5	4.3	3.8	2.4	1.3	1.3	0.7	
		194	190	195	199	195	182	157	302	46	184	315	308	331	24	134	187	316	
8.5	0.2061	1.7	4.6	14.9	15.1	10.6	6.1	1.9	0.4	0.7	0.7	1.4	3.7	3.4	2.2	1.2	1.1	0.5	
		174	182	190	192	186	175	143	31	46	169	331	311	333	34	123	185	299	
8.0	0.3398	1.7	4.4	13.9	13.7	10.3	6.2	1.8	0.7	0.9	0.4	1.5	3.2	3.0	2.0	1.2	1.0	0.2	
		161	172	183	183	178	167	131	48	48	136	343	318	335	43	118	180	264	
7.5	0.5603	1.8	4.7	13.6	13.4	10.6	6.5	1.8	0.7	0.9	0.2	1.7	3.2	2.8	2.0	1.2	0.8	0.2	
		159	163	177	179	175	164	131	58	51	92	344	325	338	49	120	172	212	
7.0	0.9237	1.7	5.0	13.6	13.7	11.1	6.7	1.8	0.6	0.8	0.1	1.9	3.3	2.7	2.0	1.2	0.7	0.1	
		160	159	175	180	180	166	138	63	51	0	340	329	342	51	121	162	187	
6.5	1.52	1.5	4.8	13.4	14.0	11.1	6.3	1.6	0.6	0.7	0.2	2.0	3.3	2.6	2.1	1.2	0.6	0.0	
		159	158	176	185	188	174	148	57	45	311	338	332	345	54	121	153	177	
6.0	2.51	1.0	4.0	12.5	13.5	10.3	5.4	1.1	0.7	0.8	0.3	2.0	3.1	2.4	2.2	1.2	0.5	0.1	
		147	158	180	191	197	184	158	44	36	309	338	333	349	58	118	146	345	
5.5	4.14	0.7	2.9	10.9	11.8	8.4	3.9	0.4	0.8	0.8	0.4	1.8	2.7	2.0	2.1	1.1	0.4	0.2	
		121	161	186	197	206	200	175	34	28	314	339	334	353	64	115	135	334	
5.0	6.83	0.5	2.0	9.0	9.3	6.2	2.6	0.3	0.9	0.8	0.4	1.5	2.1	1.5	1.8	1.1	0.3	0.3	
		94	172	194	202	220	222	326	28	21	321	341	334	357	70	113	119	335	
4.5	11.25	0.4	1.6	6.9	6.2	3.9	1.5	0.7	1.0	0.7	0.3	1.1	1.4	0.9	1.4	0.9	0.3	0.3	
		101	192	203	209	236	253	356	24	16	327	344	335	3	79	112	101	340	
4.0	18.55	0.7	1.9	4.8	3.0	2.0	0.8	1.0	1.1	0.7	0.2	0.5	0.6	0.3	1.0	0.7	0.3	0.3	
		163	205	214	220	261	305	16	22	10	337	353	334	36	96	114	85	353	
3.5	30.59	1.9	2.6	2.8	0.6	0.9	0.9	1.2	1.1	0.6	0.1	0.2	0.2	0.5	0.6	0.5	0.3	0.3	
		182	201	224	291	338	30	39	20	4	12	90	161	155	137	120	74	18	
3.0	50.43	3.3	3.5	1.2	2.1	1.8	1.9	1.5	1.0	0.5	0.1	0.6	1.0	1.1	0.8	0.3	0.3	0.3	
		185	193	232	21	43	76	61	20	356	130	145	157	166	185	136	68	47	
2.5	83.15	4.1	4.2	0.2	3.5	2.7	3.0	1.9	1.0	0.4	0.3	1.1	1.6	1.6	1.1	0.2	0.2	0.4	
		185	188	210	30	62	91	77	20	346	144	152	157	170	205	166	65	66	

AUGUST	MEAN TEMPERATURE AMPLITUDE (K) AND PHASE WAVE																	
SCALE	PRESSURE	-80	-70	-60	-50	-40	-30	-20	-10	0	10	20	30	40	50	60	70	80
HEIGHT	(mb)																	
12.0	0.0062	2.43 214	3.63 203	2.29 178	0.55 192	0.38 263	1.20 292	1.08 274	0.78 257	1.29 252	1.54 237	2.11 245	1.95 260	0.97 302	0.81 284	1.60 266	0.52 171	2.33 171
11.5	0.0103	2.80 221	4.00 210	2.54 191	0.85 211	0.50 242	1.05 286	0.94 267	0.70 254	1.21 250	1.50 235	2.01 244	1.86 259	0.89 306	0.85 284	1.70 267	0.57 171	2.47 171
11.0	0.0169	3.19 228	4.34 219	2.88 207	1.28 224	0.69 224	0.77 269	0.77 250	0.54 246	1.03 245	1.35 231	1.75 240	1.63 256	0.70 313	0.80 285	1.64 267	0.59 171	2.37 171
10.5	0.0279	3.66 235	4.78 250	3.47 224	1.91 232	1.05 213	0.80 221	0.54 205	0.35 221	0.76 235	1.11 224	1.32 234	1.22 251	0.47 339	0.70 287	1.45 268	0.55 169	1.92 169
10.0	0.0460	4.14 243	5.34 242	4.35 238	2.74 258	1.55 208	1.01 177	0.86 160	0.32 164	0.51 207	0.84 209	0.84 217	0.75 236	0.44 36	0.54 290	1.08 272	0.43 169	1.15 158
9.5	0.0758	4.41 251	5.85 253	5.36 249	3.72 241	2.20 206	1.71 164	1.42 146	0.56 133	0.48 161	0.63 185	0.55 170	0.40 188	0.73 66	0.35 300	0.58 281	0.24 166	0.34 84
9.0	0.1250	4.27 261	6.07 265	5.19 258	4.70 243	2.94 208	2.32 164	1.89 143	0.80 126	0.64 132	0.52 154	0.66 126	0.52 130	0.95 75	0.19 316	0.18 348	0.31 151	1.09 10
8.5	0.2061	3.59 279	5.75 280	6.46 267	5.38 245	3.60 213	2.58 172	1.99 149	0.86 132	0.67 128	0.40 132	0.66 115	0.60 114	0.84 75	0.11 327	0.36 37	0.19 344	1.61 358
8.0	0.3398	2.96 312	5.06 300	6.00 279	5.41 248	3.92 220	2.47 188	1.74 165	0.73 150	0.47 140	0.14 117	0.35 127	0.32 114	0.38 43	0.38 272	0.35 69	0.31 345	1.46 349
7.5	0.5603	2.79 355	4.06 331	4.54 299	4.02 258	3.20 232	1.99 215	1.20 196	0.47 185	0.18 193	0.12 300	0.24 220	0.17 238	0.44 288	0.26 254	0.02 63	0.27 340	0.62 330
7.0	0.9237	2.89 24	4.01 5	4.16 334	2.92 294	2.16 261	1.50 246	0.82 226	0.33 221	0.15 259	0.15 291	0.29 232	0.29 241	0.53 267	0.31 239	0.17 234	0.12 353	0.27 273
6.5	1.52	2.64 48	4.49 27	5.28 360	3.82 336	2.03 313	1.04 288	0.38 253	0.14 249	0.06 305	0.02 234	0.17 190	0.23 199	0.31 234	0.29 230	0.17 219	0.02 212	0.14 278
6.0	2.51	2.38 73	4.88 41	6.49 12	5.21 352	3.73 345	2.71 338	1.12 346	0.25 348	0.06 329	0.04 56	0.08 155	0.16 152	0.25 180	0.32 218	0.13 241	0.06 231	0.27 315
5.5	4.14	2.96 69	5.02 55	6.59 25	5.42 7	3.12 359	1.49 351	0.48 344	0.13 315	0.04 278	0.09 195	0.19 211	0.31 214	0.23 247	0.32 254	0.13 272	0.07 258	0.31 317
5.0	6.83	2.69 104	4.83 71	6.05 43	4.93 26	3.01 14	1.58 358	0.66 338	0.20 309	0.10 259	0.13 228	0.33 241	0.51 237	0.39 264	0.33 274	0.25 310	0.19 299	0.29 322
4.5	11.25	2.90 122	4.66 96	5.49 73	4.31 56	2.53 36	1.35 5	0.75 328	0.24 305	0.15 258	0.18 250	0.52 252	0.76 248	0.61 272	0.36 295	0.44 322	0.37 310	0.24 332
4.0	18.55	3.95 143	5.31 127	6.03 106	4.38 88	2.15 64	0.94 13	0.74 318	0.25 302	0.17 260	0.22 262	0.68 237	0.95 253	0.77 274	0.41 311	0.60 327	0.54 313	0.16 353
3.5	30.59	4.21 166	6.34 153	6.75 129	4.73 110	2.08 90	0.57 29	0.69 309	0.24 299	0.17 260	0.23 270	0.72 259	1.01 256	0.83 276	0.43 321	0.67 329	0.61 315	0.12 28
3.0	50.43	2.42 191	5.11 170	6.13 143	4.49 122	1.97 108	0.30 60	0.59 300	0.21 298	0.14 262	0.22 275	0.68 261	0.95 258	0.75 276	0.38 326	0.61 330	0.57 317	0.10 61
2.5	83.15	1.17 206	3.07 181	4.33 151	3.44 130	1.58 118	0.21 103	0.41 293	0.15 295	0.11 265	0.17 278	0.54 259	0.75 261	0.59 276	0.29 330	0.46 331	0.43 318	0.09 74

AUGUST	MEAN GEOPOTENTIAL HEIGHT AMPLITUDE (dam) AND PHASE WAVE 1																		
SCALE	PRESSURE	-80	-70	-60	-50	-40	-30	-20	-10	0	10	20	30	40	50	60	70	80	
HEIGHT	(mb)																		
12.0	0.0062	33.3 225	35.3 240	30.1 273	28.9 277	18.1 244	12.3 220	11.1 195	6.6 192	8.2 209	11.7 215	15.7 221	16.7 233	6.2 277	11.5 265	13.6 268	3.9 217	5.5 179	
11.5	0.0103	29.5 226	30.7 245	30.2 279	28.6 279	17.4 244	11.8 212	10.8 187	6.2 182	6.9 200	9.6 211	13.0 216	14.3 228	5.1 270	10.4 263	11.1 269	3.4 227	1.9 181	
11.0	0.0169	25.1 226	25.7 252	29.8 287	27.9 282	16.6 244	11.3 206	10.5 181	5.9 174	5.8 189	7.7 205	10.6 209	12.1 222	4.2 260	9.3 260	8.7 269	3.0 240	1.7 340	
10.5	0.0279	20.1 225	20.0 261	28.5 296	26.6 286	15.5 246	10.7 203	10.0 177	5.6 168	5.1 178	6.1 198	8.7 202	10.4 216	3.9 249	8.3 257	6.4 270	2.8 256	4.9 346	
10.0	0.0460	14.6 219	13.7 274	26.6 307	24.6 292	14.0 251	9.6 204	9.1 177	5.2 166	4.5 170	4.7 192	7.3 196	9.2 211	4.2 242	7.5 253	4.5 270	2.9 271	7.1 345	
9.5	0.0758	9.5 202	7.3 304	24.2 322	22.0 302	12.2 260	8.1 212	7.6 183	4.6 169	3.8 167	3.7 191	6.4 210	8.4 214	5.0 241	7.0 250	3.3 268	3.0 280	8.0 343	
9.0	0.1250	7.7 160	6.4 23	22.5 342	19.6 318	10.4 276	6.5 232	5.9 198	3.9 179	3.2 173	2.9 196	5.9 203	8.1 214	6.2 243	6.8 247	2.9 263	3.1 283	7.4 338	
8.5	0.2061	11.1 130	12.5 64	22.8 125	18.9 28	9.5 340	5.9 304	4.7 265	3.3 227	2.6 195	2.6 186	5.8 208	8.2 212	7.6 220	6.8 245	3.2 258	3.1 281	5.6 329	
8.0	0.3398	15.6 125	18.9 81	25.1 28	20.9 2	10.8 335	6.8 298	4.6 261	2.8 216	2.3 202	2.6 218	6.0 220	8.4 225	8.5 240	6.7 245	3.7 254	2.9 274	3.6 314	
7.5	0.5603	19.2 131	27.3 94	27.5 43	24.2 18	13.5 357	7.9 322	4.8 286	2.4 231	2.1 209	2.6 217	5.8 222	8.4 226	8.4 243	6.4 243	4.0 256	2.8 266	2.4 297	
7.0	0.9237	21.6 141	25.5 106	28.0 56	26.0 28	15.5 340	8.4 304	4.7 240	1.9 207	1.9 212	2.5 221	5.4 225	8.0 240	7.8 243	6.0 245	3.8 256	2.7 260	1.9 292	
6.5	1.52	22.9 150	26.1 120	26.1 70	24.7 38	15.4 20	8.1 352	4.4 314	1.6 241	1.8 203	2.5 210	5.1 221	7.7 225	7.2 238	5.6 244	3.6 258	2.7 258	1.7 295	
6.0	2.51	23.2 159	26.4 135	25.6 89	21.4 52	13.4 31	7.1 359	4.1 316	1.5 239	2.0 203	2.5 211	4.9 224	7.4 227	6.9 239	5.2 245	3.5 261	2.6 260	1.4 294	
5.5	4.14	22.7 168	27.0 151	22.2 113	17.8 73	10.4 46	5.2 4	3.7 312	1.5 233	1.8 203	2.4 213	4.7 226	7.1 228	6.6 239	4.7 245	3.3 254	2.6 261	1.0 285	
5.0	6.83	21.8 178	27.7 166	22.4 137	15.1 98	7.5 69	3.0 11	3.0 304	1.4 224	1.7 201	2.2 213	4.4 225	6.5 228	6.2 238	4.3 243	3.1 245	2.4 259	0.7 254	
4.5	11.25	20.4 188	26.6 180	22.4 158	12.9 124	5.4 50	0.9 34	2.1 291	1.4 211	1.7 196	2.0 210	3.8 221	5.6 226	5.6 234	3.9 239	2.8 258	2.1 251	0.6 230	
4.0	18.55	18.2 200	25.9 195	20.9 179	10.5 152	4.2 138	1.0 163	1.3 264	1.5 197	1.7 189	1.8 203	3.1 212	4.5 219	4.5 227	4.9 237	3.7 234	1.7 233	0.8 209	
3.5	30.59	14.7 216	21.8 213	18.1 206	8.1 182	3.8 183	1.9 182	1.0 213	1.6 184	1.6 173	1.9 195	3.4 204	4.2 212	3.7 240	3.0 216	2.0 207	2.0 205	1.1 205	
3.0	50.43	11.3 233	17.8 255	17.3 237	9.2 228	4.5 225	2.5 191	1.4 171	1.8 174	1.7 174	2.2 182	2.8 170	3.8 188	3.7 199	3.9 211	3.5 219	2.4 187	1.1 208	
2.5	83.15	9.4 242	15.4 257	19.1 261	12.6 263	6.0 240	2.6 198	1.9 159	1.9 167	1.7 167	2.7 173	2.4 184	3.8 194	3.7 205	4.1 213	4.0 209	2.2 192	1.2 176	1.2 212

AUGUST		MEAN GEOPOTENTIAL HEIGHT AMPLITUDE (dam) AND PHASE																WAVE 2	
SCALE HEIGHT	PRESSURE (mb)	-80	-70	-60	-50	-40	-30	-20	-10	0	10	20	30	40	50	60	70	80	
12.0	0.0062	3.8 253	15.1 199	22.4 192	28.5 198	26.8 196	18.1 180	7.7 188	9.0 152	8.6 161	5.9 148	3.5 93	4.6 66	5.2 349	2.3 189	5.4 256	2.2 286	7.1 286	
11.5	0.0103	4.1 251	14.3 203	22.4 197	28.7 202	27.2 202	17.3 186	7.1 194	7.5 154	6.7 164	4.7 152	2.4 79	3.2 45	5.4 340	2.2 188	4.2 251	2.1 276	5.1 276	
11.0	0.0169	4.2 250	13.3 209	22.3 201	28.8 207	27.4 207	16.5 191	6.6 195	6.0 157	5.5 168	3.5 156	1.6 49	2.7 11	5.6 333	2.2 315	3.1 260	2.0 251	2.0 251	
10.5	0.0279	4.2 250	12.2 216	22.1 205	28.5 211	27.1 212	15.9 197	6.2 199	4.6 161	3.5 172	2.6 159	1.6 11	3.2 343	5.7 327	2.3 351	2.4 242	1.9 267	3.5 235	
10.0	0.0460	4.0 251	10.9 224	21.5 209	27.6 214	26.0 216	15.2 202	6.0 202	3.4 162	3.2 176	1.8 170	2.0 351	3.0 350	5.6 329	2.4 342	2.4 276	1.9 277	3.4 204	
9.5	0.0758	3.7 255	9.7 235	20.5 213	26.3 217	24.1 220	14.5 207	5.9 205	2.5 169	1.3 172	1.2 151	2.3 343	4.3 326	5.2 324	2.5 358	2.9 299	2.0 281	3.5 187	
9.0	0.1250	3.4 260	8.6 247	18.9 216	23.7 220	23.4 224	13.7 210	5.8 206	1.8 170	1.8 141	1.0 128	2.4 346	4.4 327	4.5 327	2.5 335	3.1 313	2.2 303	2.2 262	
8.5	0.2061	3.1 266	7.6 258	16.8 219	20.7 223	18.4 228	12.7 211	5.7 203	1.3 162	0.9 109	1.1 359	2.3 352	4.1 333	3.7 335	2.3 336	3.0 332	2.4 314	2.4 241	
8.0	0.3398	2.9 271	6.7 266	14.3 220	17.7 226	16.1 231	11.7 212	5.3 193	1.2 146	1.2 96	1.0 101	2.1 358	3.0 340	3.9 347	2.1 340	2.6 327	2.3 321	1.1 111	
7.5	0.5603	2.7 273	5.9 267	12.1 223	15.6 231	15.1 236	10.8 213	4.8 191	1.2 131	1.2 96	1.0 101	2.1 0	3.7 349	2.8 356	1.8 344	2.1 329	1.8 326	1.1 108	
7.0	0.9237	2.6 275	5.4 267	10.4 229	14.5 241	15.1 244	9.9 220	4.0 188	1.2 120	1.0 95	0.7 104	2.1 358	3.6 347	2.7 341	1.7 348	1.4 328	1.1 333	0.8 115	
6.5	1.52	2.3 282	5.0 272	9.2 243	14.2 256	15.0 256	8.8 233	1.9 192	1.0 107	0.8 89	0.4 104	2.5 356	3.5 348	2.6 354	1.6 354	1.5 325	1.1 340	0.8 130	
6.0	2.51	1.9 295	4.7 287	8.5 266	14.4 276	14.7 273	7.6 253	0.9 210	0.7 87	0.3 76	0.2 88	2.0 356	3.0 350	1.0 350	2.4 10	1.4 325	1.1 340	0.8 130	
5.5	4.14	1.4 316	4.3 308	8.3 291	14.7 295	14.0 291	6.7 278	0.8 262	0.9 66	0.7 64	0.2 61	2.0 356	2.9 352	2.0 352	1.2 16	1.2 8	1.0 329	0.8 358	
5.0	6.83	1.0 378	3.7 329	7.9 311	14.0 311	12.6 306	5.9 300	1.0 328	1.0 55	0.7 56	0.2 40	2.0 356	2.9 353	2.0 353	1.2 24	1.2 19	1.0 339	0.9 345	
4.5	11.25	0.7 42	2.5 358	6.0 330	11.1 326	9.8 319	4.7 319	1.2 359	1.0 51	0.6 50	0.2 25	1.3 356	1.6 354	1.4 33	1.0 33	0.9 356	0.9 361	0.6 40	
4.0	18.55	1.2 112	1.8 86	2.8 19	6.6 350	6.1 357	3.0 341	1.0 29	1.0 51	0.5 45	0.1 8	0.7 355	0.8 353	0.9 46	0.9 48	0.9 21	0.8 29	0.3 45	
3.5	30.59	2.8 148	5.4 138	5.6 113	6.2 65	2.6 28	1.5 39	1.0 73	0.9 95	0.4 94	0.1 324	0.2 346	0.1 276	0.5 77	0.9 63	1.0 45	0.7 37	0.3 31	
3.0	50.43	4.6 161	9.9 151	11.5 131	8.9 113	4.3 89	4.3 107	1.6 111	0.7 112	0.2 62	0.1 30	0.4 263	0.4 184	0.7 184	0.4 149	0.9 73	1.3 58	0.7 45	
2.5	83.15	5.5 166	12.8 156	16.7 137	13.8 126	7.6 126	7.6 126	2.2 129	0.6 72	0.1 14	0.2 242	0.8 181	1.3 182	0.7 181	0.9 80	1.5 65	0.6 50	0.1 14	

SEPTEMBER MEAN TEMPERATURE AMPLITUDE (K) AND PHASE WAVE 1

SCALE HEIGHT	PRESSURE (mb)	-80	-70	-60	-50	-40	-30	-20	-10	0	10	20	30	40	50	60	70	80
12.0	0.0062	1.94 210	2.72 197	2.27 180	1.29 172	0.53 223	0.34 249	0.34 322	0.41 95	0.44 121	1.08 115	0.89 133	0.39 126	0.53 29	1.02 45	0.91 59	0.57 126	0.78 74
11.5	0.0103	2.26 221	2.79 206	2.25 189	1.27 185	0.65 224	0.41 234	0.27 322	0.47 92	0.51 116	1.08 115	0.85 134	0.33 133	0.46 25	0.97 12	0.88 51	0.57 129	0.82 75
11.0	0.0169	2.66 233	2.79 221	2.08 206	1.22 202	0.77 228	0.51 219	0.14 326	0.54 326	0.57 89	1.02 109	0.74 112	0.25 136	0.34 155	0.84 12	0.75 38	0.51 51	0.79 133
10.5	0.0279	3.23 246	2.94 241	2.08 235	1.31 231	0.92 232	0.66 206	0.04 120	0.64 120	0.66 86	0.90 104	0.56 108	0.21 140	0.22 204	0.62 329	0.56 29	0.40 39	0.68 139
10.0	0.0460	3.95 258	3.53 263	2.64 263	1.78 259	1.08 259	0.85 197	0.25 135	0.73 135	0.76 83	0.74 98	0.33 104	0.37 155	0.32 244	0.40 277	0.37 1	0.25 3	0.53 159
9.5	0.0758	4.73 269	4.63 281	3.86 285	2.62 276	1.23 249	0.96 192	0.45 136	0.81 81	0.81 94	0.52 96	0.18 218	0.58 258	0.55 259	0.39 309	0.45 310	0.17 225	0.34 89
9.0	0.1250	5.34 279	5.97 294	5.39 294	3.62 288	1.41 265	0.91 191	0.55 134	0.77 79	0.70 90	0.21 81	0.35 267	0.73 265	0.66 257	0.58 281	0.69 288	0.32 278	0.10 61
8.5	0.2061	5.51 291	7.10 303	6.77 302	4.51 297	1.68 286	0.54 197	0.47 129	0.52 76	0.35 86	0.22 245	0.52 278	0.69 271	0.55 268	0.67 276	0.79 281	0.51 299	0.28 324
8.0	0.3398	5.21 306	7.56 312	7.50 309	5.00 305	2.10 306	0.25 311	0.20 101	0.20 39	0.23 275	0.63 271	0.56 277	0.45 323	0.34 323	0.54 282	0.64 284	0.63 315	0.60 322
7.5	0.5603	3.93 317	6.35 308	6.41 302	4.29 301	2.11 304	0.62 312	0.17 291	0.41 257	0.62 264	0.70 262	0.36 263	0.09 301	0.51 18	0.32 339	0.34 344	0.58 357	0.58 340
7.0	0.9237	2.96 348	4.81 317	5.53 301	4.08 297	2.40 300	0.51 293	0.59 267	0.60 247	0.52 295	0.21 249	0.10 223	0.51 93	0.37 23	0.55 51	0.49 1	0.68 48	0.47 18
6.5	1.52	3.60 26	4.50 347	5.30 309	4.53 298	3.08 281	1.86 251	0.89 251	0.54 232	0.36 235	0.31 224	0.18 177	0.10 135	0.27 4	0.31 36	0.85 79	1.03 82	0.57 64
6.0	2.51	5.55 40	6.40 13	5.86 328	5.22 308	3.93 301	2.62 279	1.28 245	0.51 215	0.27 202	0.26 202	0.17 192	0.10 313	0.19 59	0.22 100	1.13 101	1.31 101	0.73 80
5.5	4.14	6.73 49	8.01 32	6.04 360	4.65 336	3.66 320	2.52 290	1.29 251	0.46 218	0.24 217	0.24 209	0.11 188	0.15 247	0.17 301	0.25 101	1.13 101	1.17 112	0.50 81
5.0	6.83	7.27 57	9.18 47	7.21 32	4.91 16	3.20 349	2.02 303	1.13 257	0.39 226	0.23 232	0.21 222	0.16 252	0.29 273	0.13 299	0.38 118	0.93 122	0.80 127	0.17 87
4.5	11.25	7.34 67	10.02 62	9.36 56	6.61 48	3.28 27	1.29 329	0.85 266	0.31 242	0.23 292	0.18 246	0.30 272	0.47 284	0.05 319	0.49 123	0.59 141	0.41 172	0.19 250
4.0	18.35	7.28 81	10.75 76	11.57 72	8.31 65	3.88 54	0.98 21	0.52 281	0.25 265	0.23 268	0.18 275	0.43 278	0.61 289	0.06 59	0.55 122	0.37 191	0.55 258	0.48 254
3.5	30.59	7.04 107	10.36 94	12.19 82	8.87 74	4.28 69	0.28 59	0.23 316	0.23 289	0.18 279	0.23 293	0.18 280	0.55 291	0.11 75	0.52 121	0.45 241	0.80 259	0.64 255
3.0	50.43	4.79 143	8.27 111	10.43 89	7.95 80	4.03 78	1.47 75	0.25 7	0.23 306	0.21 287	0.19 287	0.49 304	0.61 282	0.14 294	0.43 78	0.52 131	0.84 260	0.62 256
2.5	83.15	2.66 169	4.92 124	7.27 94	5.91 84	3.13 83	1.28 82	0.24 31	0.18 316	0.16 290	0.15 309	0.39 281	0.47 294	0.12 76	0.31 117	0.46 269	0.68 273	0.47 256

SEPTEMBER MEAN GEOPOTENTIAL HEIGHT AMPLITUDE (dam) AND PHASE WAVE 1

SCALE HEIGHT	PRESSURE (mb)	-80	-70	-60	-50	-40	-30	-20	-10	0	10	20	30	40	50	60	70	80
12.0	0.0062	26.0 353	35.5 346	33.0 321	27.5 315	21.3 303	15.5 257	9.6 232	4.7 151	4.0 150	6.2 156	6.6 195	7.9 235	4.2 278	2.1 17	3.3 90	4.9 139	5.5 52
11.5	0.0103	28.3 358	38.9 350	35.6 325	28.9 317	21.1 305	15.0 257	9.6 229	4.4 158	4.1 157	5.1 168	6.1 205	8.0 239	4.0 275	1.0 130	2.3 108	4.1 141	4.5 46
11.0	0.0169	30.8 3	41.9 353	37.6 329	30.0 320	21.0 300	14.5 259	9.6 227	4.1 168	3.5 168	4.4 184	5.8 216	8.1 262	4.7 265	1.3 137	1.9 139	3.3 143	3.5 37
10.5	0.0279	33.3 9	44.3 358	38.7 333	30.4 323	20.8 311	13.9 261	9.7 227	4.1 180	3.2 185	4.3 203	5.7 226	8.0 244	4.7 258	2.1 143	2.1 166	2.7 145	2.8 21
10.0	0.0460	35.9 16	45.7 3	38.6 358	30.0 327	20.5 315	13.4 263	9.7 228	4.3 193	3.3 204	4.6 218	5.7 232	7.6 245	4.5 259	2.7 152	2.7 175	2.2 144	2.5 3
9.5	0.0758	38.8 25	46.1 11	36.7 344	28.5 333	20.0 320	13.0 271	9.7 231	4.8 206	5.1 220	5.5 227	6.9 235	9.8 244	3.8 254	2.8 172	3.0 199	2.0 139	2.5 349
9.0	0.1250	42.1 34	45.8 20	33.3 354	25.8 341	19.2 325	12.8 277	9.8 235	5.6 216	4.7 230	5.5 231	6.0 234	9.4 241	2.5 253	2.7 161	3.7 132	2.2 341	2.6 341
8.5	0.2061	45.3 44	45.4 33	29.2 9	22.3 352	17.8 330	10.0 282	6.3 240	5.3 222	5.5 234	4.7 231	5.1 229	9.4 235	2.1 249	2.5 187	4.5 149	2.8 127	2.4 341
8.0	0.3398	48.1 53	45.1 46	26.2 30	18.7 336	15.6 284	12.6 242	10.3 224	6.7 224	5.4 233	5.1 226	4.2 220	4.4 226	1.6 237	2.7 167	5.2 140	3.6 127	1.8 348
7.5	0.5603	50.0 61	48.2 58	27.2 52	17.1 30	13.1 343	12.1 282	10.3 242	6.5 222	4.9 218	4.4 212	5.8 224	7.2 223	2.0 160	3.1 138	5.8 138	4.4 152	1.0 4
7.0	0.9237	50.4 66	51.3 74	31.3 77	18.2 65	10.8 15	10.9 278	9.9 215	5.9 215	4.1 209	3.7 208	3.5 224	4.3 217	2.8 164	3.6 143	6.1 143	4.7 142	0.3 27
6.5	1.52	48.1 70	52.3 87	36.1 77	21.4 76	9.2 15	8.7 239	6.9 215	5.1 215	3.5 204	3.2 209	3.2 226	4.3 226	3.3 214	4.0 169	5.9 153	4.6 157	0.5 235
6.0	2.51	42.9 76	50.4 82	40.6 87	26.0 79	9.5 77	5.5 278	7.4 237	4.4 213	3.1 215	2.8 202	3.0 213	4.2 228	3.5 210	4.2 173	5.4 167	4.1 179	1.4 248
5.5	4.14	35.4 83	45.8 94	43.3 98	29.9 91	11.5 103	1.8 135	5.5 263	3.7 233	2.7 213	2.5 202	2.9 215	4.1 228	3.5 205	4.2 177	4.8 184	4.0 205	2.3 253
5.0	6.83	27.0 94	39.7 109	43.0 111	31.3 103	13.5 97	2.1 142	3.9 223	3.0 211	2.3 215	2.1 200	2.7 215	3.8 225	3.6 202	4.1 183	4.5 203	2.2 226	2.8 255
4.5	11.25	18.8 112	33.4 128	39.5 127	29.2 118	14.0 115	4.5 137	2.9 205	2.6 207	1.9 211	1.9 195	2.5 209	3.5 218	3.6 200	3.8 192	4.3 217	2.2 237	2.8 255
4.0	18.35	12.4 144	28.5 155	35.1 149	25.8 140	13.5 137	5.8 146	2.7 185	2.3 200	1.8 188	1.8 187	2.4 197	3.3 205	3.6 200	3.6 203	3.6 203	2.4 241	2.3 256
3.5	30.59	9.9 199	27.1 188	34.0 179	24.5 169	13.2 163	2.9 160	2.3 175	2.3 191	1.8 194	1.9 180	2.4 180	3.4 189	3.7 201	3.6 216	3.6 226	2.7 237	1.5 256
3.0	50.43	11.6 246	29.8 217	38.8 204	27.9 196	14.5 188	6.7 173	3.2 183	2.4 183	1.8 173	2.0 173	2.6 173	3.7 203	3.8 203	3.7 219	2.8 219	1.7 218	0.5 258
2.5	83.15	12.7 270	32.8 233	45.4 220	33.3 212	16.8 205	7.3 194	3.6 176	2.6 178	1.9 177	2.2 168	3.0 153	4.2 165	4.0 206	3.9 239	2.3 207	1.3 177	0.3 71

SEPTEMBER MEAN TEMPERATURE AMPLITUDE (K) AND PHASE WAVE 2

SCALE HEIGHT	PRESSURE (mb)	-80	-70	-60	-50	-40	-30	-20	-10	0	10	20	30	40	50	60	70	80
12.0	0.0062	0.32 145	0.20 174	0.17 303	0.44 301	0.24 275	0.20 240	0.52 318	0.36 270	0.84 167	0.27 149	0.76 108	0.50 100	0.21 175	0.14 39	0.26 358	0.68 36	0.75 74
11.5	0.0103	0.37 152	0.28 173	0.14 290	0.47 296	0.28 268	0.20 240	0.47 320	0.36 266	0.80 190	0.27 152	0.71 107	0.50 101	0.21 172	0.13 41	0.28 360	0.73 34	0.77 73
11.0	0.0169	0.43 158	0.38 172	0.11 260	0.46 288	0.30 261	0.18 239	0.34 322	0.34 256	0.73 194	0.24 158	0.59 107	0.47 104	0.19 159	0.11 45	0.31 2	0.75 32	0.72 71
10.5	0.0279	0.49 165	0.49 172	0.12 204	0.45 276	0.36 252	0.15 239	0.17 333	0.32 244	0.62 203	0.21 168	0.41 103	0.39 107	0.18 145	0.09 56	0.34 4	0.73 28	0.58 70
10.0	0.0460	0.55 171	0.60 171	0.23 178	0.45 259	0.41 242	0.09 234	0.09 90	0.34 228	0.54 215	0.18 187	0.31 90	0.17 112	0.05 123	0.35 96	0.68 8	0.40 22	0.63
9.5	0.0758	0.57 172	0.68 173	0.35 175	0.48 238	0.45 228	0.03 197	0.27 124	0.35 214	0.46 234	0.17 210	0.10 342	0.23 122	0.18 103	0.07 130	0.36 15	0.60 17	0.21 43
9.0	0.1250	0.51 170	0.69 180	0.48 184	0.56 219	0.50 210	0.06 95	0.37 131	0.35 202	0.40 248	0.17 231	0.26 307	0.15 140	0.20 87	0.16 132	0.35 29	0.49 16	0.16 330
8.5	0.2061	0.54 159	0.58 197	0.59 199	0.64 204	0.56 188	0.12 90	0.28 145	0.28 198	0.27 256	0.18 243	0.31 304	0.11 146	0.16 79	0.28 119	0.32 54	0.50 13	0.27 298
8.0	0.3398	0.15 106	0.50 233	0.72 220	0.68 193	0.64 166	0.15 90	0.14 231	0.15 199	0.11 225	0.16 244	0.20 307	0.10 118	0.08 76	0.45 110	0.33 88	0.07 37	0.35 290
7.5	0.5603	0.15 135	0.68 272	0.70 243	0.30 191	0.43 125	0.18 66	0.31 275	0.05 235	0.15 148	0.09 218	0.03 117	0.11 98	0.03 53	0.51 93	0.42 102	0.23 156	0.22 278
7.0	0.9237	0.31 299	0.82 288	0.77 271	0.16 311	0.35 72	0.19 90	0.27 274	0.04 240	0.17 144	0.07 180	0.14 120	0.10 87	0.05 53	0.51 86	0.50 115	0.41 147	0.14 234
6.5	1.52	0.35 282	0.84 295	0.95 290	0.46 325	0.37 26	0.16 48	0.09 232	0.06 187	0.10 159	0.07 169	0.09 126	0.06 49	0.11 52	0.49 93	0.62 129	0.53 153	0.18 191
6.0	2.51	0.29 272	0.81 299	1.16 293	0.60 316	0.32 356	0.11 66	0.13 148	0.08 152	0.04 153	0.03 171	0.05 338	0.14 352	0.17 45	0.56 109	0.80 141	0.64 162	0.23 185
5.5	4.14	0.17 296	0.59 314	0.91 295	0.44 306	0.19 325	0.08 128	0.14 124	0.07 117	0.05 84	0.01 101	0.16 349	0.26 353	0.19 39	0.49 129	0.83 166	0.71 186	0.26 192
5.0	6.83	0.16 349	0.40 351	0.43 292	0.20 283	0.15 266	0.13 164	0.16 104	0.10 81	0.09 58	0.04 36	0.28 352	0.39 356	0.21 31	0.42 160	0.88 193	0.80 208	0.28 199
4.5	11.25	0.28 21	0.49 51	0.27 130	0.20 162	0.21 221	0.15 172	0.18 83	0.13 64	0.13 48	0.08 26	0.39 353	0.50 357	0.22 25	0.43 203	0.97 218	0.83 226	0.26 205
4.0	18.55	0.49 32	0.90 79	1.01 122	0.50 140	0.24 199	0.15 176	0.18 71	0.15 55	0.15 42	0.11 22	0.45 354	0.56 359	0.22 22	0.55 231	1.06 237	0.85 240	0.23 209
3.5	30.59	0.67 37	1.28 92	1.54 121	0.68 133	0.25 186	0.12 178	0.17 57	0.15 48	0.16 40	0.12 19	0.47 347	0.54 15	0.20 15	0.63 245	1.03 250	0.77 250	0.19 213
3.0	50.43	0.44 28	1.18 101	1.60 129	0.69 175	0.22 176	0.08 48	0.15 44	0.14 36	0.14 36	0.12 35	0.42 17	0.47 355	0.16 18	0.59 253	0.88 259	0.61 258	0.14 216
2.5	83.15	0.24 24	0.74 104	1.23 121	0.55 129	0.16 166	0.05 171	0.11 41	0.10 42	0.10 35	0.09 19	0.32 355	0.35 3	0.11 18	0.46 258	0.63 265	0.42 264	0.09 220

SEPTEMBER MEAN GEOPOTENTIAL HEIGHT AMPLITUDE (dam) AND PHASE WAVE 2

SCALE HEIGHT	PRESSURE (mb)	-80	-70	-60	-50	-40	-30	-20	-10	0	10	20	30	40	50	60	70	80
12.0	0.0062	2.4 181	5.6 286	11.2 287	9.7 279	3.1 255	0.9 82	1.3 30	2.2 239	4.1 197	1.9 182	3.1 49	4.2 56	3.0 55	4.7 96	2.1 83	3.4 33	2.6 65
11.5	0.0103	2.0 189	5.7 289	10.9 287	9.0 278	2.7 253	1.2 76	1.2 63	1.7 231	3.2 201	1.5 29	2.7 48	3.7 50	3.2 48	4.6 95	2.1 95	2.4 32	1.5 59
11.0	0.0169	1.6 201	6.0 293	10.8 287	8.4 277	2.3 251	1.4 73	1.5 87	1.3 219	2.3 205	1.2 200	2.7 8	3.3 38	3.3 46	4.5 100	2.1 107	3.3 31	0.5 31
10.5	0.0279	1.1 222	6.3 298	10.7 288	7.7 276	1.8 250	1.7 71	1.7 98	0.9 203	1.6 212	2.8 212	3.2 354	3.2 27	4.1 41	4.4 101	2.3 101	3.3 36	0.6 283
10.0	0.0460	0.9 263	6.8 304	10.7 289	7.1 277	1.2 251	1.8 69	1.7 101	0.6 176	0.8 220	3.0 224	3.0 345	3.1 18	3.4 37	4.3 102	2.5 129	3.6 202	1.3 264
9.5	0.0758	1.3 304	7.5 309	10.9 291	6.5 280	0.6 266	1.9 68	1.5 99	0.4 120	0.3 227	0.6 234	3.0 343	3.0 31	3.2 33	4.2 101	2.8 138	1.7 201	1.7 257
9.0	0.1250	1.9 322	8.2 314	11.1 294	6.0 286	0.5 339	1.9 67	1.1 87	0.7 68	0.2 54	0.3 245	2.7 345	3.3 7	3.2 28	4.1 100	3.1 147	2.5 199	1.8 251
8.5	0.2061	2.5 328	8.8 319	11.3 298	5.9 294	1.2 294	1.8 3	0.9 61	1.0 48	0.6 58	0.1 270	2.4 352	3.5 5	3.1 24	3.8 98	3.3 155	3.1 198	1.7 241
8.0	0.3398	2.8 327	9.0 324	11.4 303	6.1 303	2.1 303	1.6 0	1.3 63	0.9 46	0.2 41	0.2 59	2.2 56	3.6 2	3.0 3	3.3 21	3.3 163	3.4 198	1.4 227
7.5	0.5603	2.8 325	8.7 329	11.1 308	6.4 309	2.7 352	1.4 60	1.2 56	1.5 40	1.1 53	0.4 55	2.1 2	3.6 2	2.9 20	2.6 97	3.1 185	3.3 208	1.3 201
7.0	0.9237	2.4 327	8.1 335	10.4 312	6.4 311	2.9 342	1.1 61	1.6 66	1.5 41	1.1 45	0.4 47	2.2 359	3.6 358	2.9 20	1.9 97	2.9 185	3.1 208	1.1 201
6.5	1.52	2.0 335	7.2 341	9.4 316	5.9 310	2.8 332	0.8 64	1.8 69	1.8 41	1.2 39	0.5 38	2.3 355	3.6 357	2.8 19	1.2 102	2.6 201	2.8 220	0.9 199
6.0	2.51	1.8 349	6.4 349	8.0 320	5.1 308	2.4 324	0.6 68	1.9 65	1.6 38	1.3 35	0.6 32	2.3 354	3.5 356	2.6 16	3.0 105	2.4 224	2.5 237	0.6 205
5.5	4.14	1.7 359	9.7 356	6.6 326	4.4 307	2.0 321	0.5 63	1.8 59	1.6 34	1.3 33	0.6 30	2.1 355	3.2 357	2.4 13	3.4 312	2.3 254	2.2 260	0.3 225
5.0	6.83	1.6 4	5.1 360	5.9 351	3.9 308	1.8 324	0.6 47	1.7 53	1.2 30	0.6 29	1.8 29	2.7 355	2.7 357	2.1 11	3.1 319	2.3 286	2.0 289	0.2 326
4.5	11.25	1.3 2	4.6 357	5.7 333	3.9 311	1.8 331	0.7 33	1.5 47	1.5 26	1.1 24	0.5 29	1.3 357	2.0 357	1.8 8	1.5 334	2.4 319	2.0 324	0.5 4
4.0	18.55	0.8 345	4.4 345	6.6 329	4.4 312	2.0 339	0.9 24	1.3 42	1.3 21	0.9 18	0.3 31	0.7 360	1.3 357	1.5 4	1.9 353	2.8 350	2.3 356	0.9 14
3.5	30.59	0.7 274	5.0 313	8.3 318	5.3 313	2.4 344	1.0 19	1.1 37	1.1 16	0.7 9	0.2 44	0.1 80	0.5 351	1.2 360	2.4 12	3.6 15	3.0 18	1.2 18
3.0	50.43	1.4 242	6.3 313	10.5 318	6.3 313	2.7 346	1.2 16	0.8 32	0.9 27	0.6 357	0.1 158	0.7 168	0.3 195	1.0 355	3.0 357	4.5 30	3.6 31	1.4 21
2.5	83.15	1.8 232	7.6 307	12.5 315	7.2 312	3.0 347	1.3 15	0.7 29	0.6 2	0.5 342	0.2 179	1.2 171	0.9 187	0.8 349	3.6 36	5.2 40	4.2 39	1.6 23

OCTOBER MEAN TEMPERATURE AMPLITUDE (K) AND PHASE WAVE 1

SCALE HEIGHT	PRESSURE (mb)	-80	-70	-60	-50	-40	-30	-20	-10	0	10	20	30	40	50	60	70	80
12.0	0.0062	0.97 196	1.19 212	0.84 204	0.19 213	0.87 205	0.74 139	0.58 351	1.38 97	1.69 88	1.12 107	1.14 196	1.94 219	1.73 228	1.48 239	1.83 259	2.49 253	1.62 273
11.5	0.0103	1.09 204	1.36 213	1.06 205	0.19 139	0.77 351	0.65 45	0.56 96	1.45 88	1.70 105	1.14 183	1.10 218	1.91 235	1.73 251	1.64 268	2.14 261	2.96 261	1.78 276
11.0	0.0169	1.10 214	1.48 214	1.29 206	0.42 181	0.50 2	0.44 352	0.54 59	1.47 99	1.62 89	1.11 102	1.00 178	1.72 218	1.64 242	1.88 265	2.51 278	3.52 270	1.89 280
10.5	0.0279	1.24 228	1.51 218	1.49 209	0.80 197	0.08 352	0.12 358	0.53 80	1.47 93	1.49 90	1.06 97	0.81 169	1.38 218	1.52 256	2.25 280	3.02 288	4.23 278	2.00 284
10.0	0.0460	1.31 247	1.39 228	1.61 215	1.26 205	0.46 191	0.30 170	0.64 103	1.47 91	1.34 92	0.99 91	0.62 153	0.96 218	1.48 275	2.78 302	3.63 307	5.04 293	2.09 300
9.5	0.0758	1.43 272	1.24 255	1.60 235	1.67 218	1.03 196	0.76 174	0.76 119	1.41 89	1.16 94	0.88 81	0.46 122	0.45 219	1.56 294	3.30 302	4.20 307	5.69 293	2.11 300
9.0	0.1250	1.72 301	1.65 301	1.75 269	1.94 236	1.94 205	1.47 177	0.82 130	1.22 87	0.89 96	0.67 70	0.41 80	0.04 324	1.64 311	3.54 312	4.48 317	5.81 303	2.01 315
8.5	0.2061	2.31 326	3.10 327	2.91 306	2.26 268	1.67 124	1.30 183	0.67 136	0.77 85	0.52 99	0.34 49	0.34 34	0.34 13	1.51 327	3.18 325	4.18 331	5.05 318	1.89 343
8.0	0.3398	3.05 345	4.97 358	4.93 325	3.20 301	1.80 254	1.15 194	0.30 147	0.15 72	0.08 113	0.23 304	0.42 359	0.46 311	1.51 351	2.43 352	3.55 355	3.97 351	2.18 20
7.5	0.5603	3.11 347	5.57 331	6.02 321	4.29 293	2.16 236	0.72 267	0.26 269	0.47 283	0.29 280	0.52 311	0.60 349	0.36 311	1.16 349	2.56 32	3.54 54	4.26 42	2.76 51
7.0	0.9237	2.78 349	5.35 338	6.24 335	4.85 332	2.62 318	0.80 289	0.49 274	0.66 264	0.41 281	0.56 277	0.65 307	0.70 357	1.61 42	3.57 58	4.83 69	5.78 79	3.35 78
6.5	1.52	2.31 354	4.71 340	5.91 337	4.80 339	2.86 334	1.03 311	0.56 262	0.57 253	0.35 270	0.47 275	0.64 315	0.98 12	2.24 50	4.89 72	7.24 90	7.83 97	4.41 107
6.0	2.51	1.95 9	4.06 346	5.49 341	4.34 345	2.93 345	1.11 322	0.59 255	0.50 236	0.31 248	0.45 264	0.74 318	1.29 17	2.87 57	6.35 84	10.20 103	10.55 112	6.19 118
5.5	4.14	1.90 41	3.20 358	4.40 2	3.86 2	2.63 0	1.05 333	0.59 259	0.49 233	0.36 242	0.47 261	0.82 314	1.37 14	3.12 65	7.11 95	11.34 113	11.75 123	7.06 128
5.0	6.83	2.25 76	2.81 35	3.33 38	3.18 35	2.22 24	0.86 346	0.57 261	0.46 234	0.37 244	0.46 265	0.90 310	1.36 5	2.94 70	6.94 105	10.81 122	10.97 134	6.64 139
4.5	11.25	3.07 103	4.18 98	4.88 88	3.59 77	2.05 59	0.59 8	0.40 263	0.36 241	0.43 251	0.93 278	1.29 308	2.34 352	5.79 117	8.76 135	8.71 147	5.29 152	
4.0	18.55	4.16 121	6.35 118	6.56 111	4.65 102	2.25 89	0.41 51	0.40 263	0.52 253	0.32 261	0.40 297	0.89 306	1.21 337	1.50 77	4.31 134	6.56 155	6.53 167	4.01 169
3.5	30.59	4.91 133	7.80 128	7.92 121	5.20 124	2.43 107	0.44 94	0.30 263	0.25 271	0.27 274	0.39 315	0.79 304	1.12 323	7.71 81	3.07 156	4.54 180	4.85 190	2.90 189
3.0	50.43	4.34 142	7.27 134	7.26 121	4.81 128	2.28 117	0.50 115	0.21 262	0.22 288	0.23 298	0.37 303	0.66 312	0.99 312	0.13 56	2.25 91	3.45 181	3.62 206	2.05 213
2.5	83.15	2.89 147	5.21 137	5.52 130	3.66 124	1.78 123	0.45 124	0.12 261	0.16 301	0.17 297	0.29 336	0.46 302	0.74 305	0.16 247	1.62 200	2.57 224	2.60 229	1.40 226

OCTOBER MEAN GEOPOTENTIAL HEIGHT AMPLITUDE (den) AND PHASE WAVE 1

SCALE HEIGHT	PRESSURE (mb)	-80	-70	-60	-50	-40	-30	-20	-10	0	10	20	30	40	50	60	70	80
12.0	0.0062	11.1 199	14.9 212	11.6 207	3.8 279	4.0 312	4.9 171	4.2 113	10.4 101	10.2 110	4.0 257	5.3 289	7.3 307	11.8 301	26.1 81	39.7 110	31.2 145	25.5 135
11.5	0.0103	9.5 199	13.0 212	10.4 230	4.0 279	5.3 296	5.7 210	4.7 179	8.5 105	7.7 113	2.4 275	5.1 312	5.1 312	14.2 34	28.3 79	42.3 109	32.9 139	27.5 131
11.0	0.0169	7.9 197	10.9 212	8.8 235	4.2 284	5.3 279	6.3 206	5.4 186	10.4 124	11.1 111	0.8 134	5.4 292	7.5 333	16.5 37	30.9 108	45.5 133	35.9 128	29.7 128
10.5	0.0279	6.3 191	8.7 211	7.1 243	4.3 296	5.7 271	6.7 204	5.7 193	4.8 136	3.3 126	1.0 254	6.1 303	8.7 346	17.5 41	33.8 81	49.5 107	40.5 128	32.3 126
10.0	0.0460	5.2 176	6.6 208	5.3 256	4.7 315	5.0 276	6.6 204	5.9 201	3.6 161	2.5 166	6.9 266	9.9 308	9.9 354	20.1 45	37.1 83	54.4 108	46.7 124	35.2 125
9.5	0.0758	5.3 154	5.1 197	3.5 276	5.6 337	5.1 297	6.0 208	6.0 211	3.5 196	2.5 216	3.9 266	7.7 309	10.7 358	21.3 50	40.9 87	59.9 109	54.4 122	38.2 124
9.0	0.1250	7.0 140	5.2 176	1.8 313	7.0 358	3.8 326	4.8 218	6.0 222	4.5 220	3.8 236	5.0 307	8.2 359	10.9 399	22.1 56	44.8 91	65.9 111	62.8 121	41.2 124
8.5	0.2061	9.9 144	8.2 158	1.7 127	8.2 143	5.1 266	5.6 239	6.1 235	5.6 244	4.7 259	5.7 301	8.4 359	10.6 399	22.5 62	48.3 95	71.3 114	70.8 122	43.8 125
8.0	0.3398	13.7 149	14.0 158	6.9 139	9.2 174	6.5 34	2.7 293	6.2 240	6.2 233	5.1 242	5.8 256	8.2 299	10.1 359	22.5 71	50.5 103	75.3 121	76.5 129	45.4 133
7.5	0.5603	18.0 149	21.8 158	14.7 139	10.7 174	7.3 34	2.3 293	6.0 240	6.0 233	4.8 242	5.3 256	7.5 299	9.3 359	21.7 71	50.4 103	76.4 121	78.3 129	45.6 133
7.0	0.9237	22.2 153	29.9 158	23.6 144	14.7 101	8.0 60	1.5 313	5.5 237	5.3 227	4.2 237	4.5 252	6.6 298	8.4 359	20.2 74	48.1 107	74.4 125	76.0 134	44.2 138
6.5	1.52	25.7 155	37.2 158	32.4 147	19.2 118	9.1 86	0.3 14	4.9 232	4.6 221	3.7 231	3.9 247	5.7 295	7.2 358	17.7 78	43.6 113	68.2 130	69.5 139	40.5 144
6.0	2.51	28.6 158	43.7 158	40.6 150	24.6 129	11.1 108	1.4 127	4.1 227	3.9 217	3.2 226	3.3 243	4.8 291	5.6 353	14.4 84	37.1 120	58.0 137	59.0 147	34.3 151
5.5	4.14	30.5 162	48.7 160	47.5 153	29.4 133	13.3 124	3.0 138	3.4 220	3.2 213	2.7 223	2.6 238	3.8 284	3.9 342	10.4 94	29.0 130	44.6 147	45.2 157	26.0 151
5.0	6.83	31.3 163	51.5 164	51.8 145	32.3 145	15.1 136	4.3 145	2.8 209	2.5 207	2.2 218	2.0 230	2.7 271	2.5 319	6.7 111	20.6 144	31.4 161	31.6 172	17.6 176
4.5	11.25	30.5 174	51.1 169	52.0 162	32.4 154	15.6 147	5.3 151	2.4 194	2.0 198	1.8 209	1.6 214	1.9 245	1.5 263	4.4 144	13.8 166	20.9 183	20.9 203	11.1 200
4.0	18.55	28.4 183	47.7 177	48.6 164	30.2 164	15.0 159	5.7 156	2.3 178	1.7 185	1.5 192	1.5 192	1.7 201	2.2 208	4.3 192	9.6 217	14.3 213	13.9 223	7.4 237
3.5	30.59	29.2 196	42.3 189	43.0 182	26.7 177	13.6 162	5.6 162	2.3 171	1.7 179	1.4 176	1.9 176	2.3 183	3.4 183	4.9 201	7.5 230	10.6 245	9.9 258	6.4 278
3.0	50.43	22.3 211	37.5 203	36.2 196	23.8 192	12.1 185	5.3 168	2.4 156	1.8 161	1.6 166	2.3 166	3.2 156	4.7 169	5.2 207	6.7 261	7.8 278	8.4 296	6.8 310
2.5	83.15	20.8 224	35.1 217	35.8 211	22.5 207	11.2 199	4.9 175	2.5 151	2.0 155	1.8 159	2.8 165	3.9 150	5.7 160	5.1 206	6.3 285	7.5 309	8.4 327	7.3 330

OCTOBER		MEAN TEMPERATURE AMPLITUDE (K) AND PHASE WAVE 2																	
SCALE	PRESSURE	-80	-70	-60	-50	-40	-30	-20	-10	0	10	20	30	40	50	60	70	80	
HEIGHT	(mb)																		
12.0	0.0062	0.63 45	0.27 269	0.06 72	0.03 149	0.30 69	0.91 51	1.02 8	0.87 4	0.73 275	0.50 209	1.03 146	0.71 123	0.24 312	0.50 298	0.75 0	0.54 3	1.43 141	
11.5	0.0103	0.69 46	0.29 272	0.10 102	0.07 153	0.31 66	0.92 49	0.99 9	0.82 3	0.72 274	0.49 206	0.98 147	0.58 123	0.23 314	0.47 301	0.77 3	0.63 4	1.39 139	
11.0	0.0169	0.68 46	0.28 278	0.16 120	0.10 160	0.27 62	0.85 45	0.87 11	0.69 0	0.63 274	0.44 201	0.84 147	0.63 121	0.21 317	0.43 310	0.75 5	0.71 4	1.25 137	
10.5	0.0279	0.59 47	0.25 289	0.27 130	0.15 161	0.21 57	0.73 37	0.70 13	0.51 355	0.37 272	0.51 192	0.37 150	0.61 118	0.50 327	0.17 327	0.34 9	0.70 5	1.03 133	
10.0	0.0460	0.46 48	0.22 304	0.38 135	0.21 165	0.12 42	0.57 25	0.48 20	0.31 338	0.36 270	0.30 176	0.33 160	0.33 110	0.14 343	0.14 357	0.31 19	0.61 8	0.83 126	
9.5	0.0758	0.29 42	0.20 321	0.44 142	0.27 172	0.04 333	0.45 6	0.25 35	0.18 291	0.20 266	0.24 151	0.10 233	0.14 86	0.12 7	0.33 31	0.30 36	0.60 12	0.55 111	
9.0	0.1250	0.14 12	0.19 328	0.38 157	0.31 187	0.12 296	0.32 347	0.12 90	0.21 244	0.03 198	0.21 124	0.27 304	0.10 331	0.12 31	0.39 54	0.44 73	0.60 24	0.37 85	
8.5	0.2061	0.17 302	0.16 304	0.25 208	0.37 211	0.19 227	0.16 343	0.09 131	0.16 239	0.14 92	0.15 98	0.35 316	0.24 297	0.12 15	0.37 73	0.62 113	0.33 77	0.27 48	
8.0	0.3398	0.26 288	0.20 257	0.47 271	0.45 238	0.24 208	0.15 90	0.02 63	0.10 332	0.22 82	0.05 34	0.23 326	0.32 276	0.14 352	0.30 100	0.93 133	0.68 147	0.24 2	
7.5	0.5603	0.22 275	0.28 213	0.59 280	0.43 254	0.19 186	0.30 103	0.16 339	0.22 357	0.08 62	0.11 293	0.04 90	0.22 258	0.13 351	0.33 115	1.14 140	1.16 164	1.0 273	
7.0	0.9237	0.09 186	0.40 130	0.15 344	0.09 301	0.14 115	0.30 96	0.19 328	0.18 341	0.07 278	0.15 276	0.14 155	0.16 235	0.05 0	0.46 129	1.19 150	1.32 177	0.30 222	
6.5	1.52	0.31 127	1.04 97	0.94 83	0.59 71	0.36 74	0.21 62	0.12 302	0.13 285	0.17 268	0.13 263	0.16 197	0.13 227	0.08 155	0.63 144	1.18 167	1.33 195	0.47 222	
6.0	2.51	0.46 114	1.74 87	1.95 86	1.29 77	0.64 71	0.20 71	0.09 270	0.12 272	0.15 270	0.13 259	0.19 234	0.17 234	0.20 174	0.79 166	1.23 191	1.48 217	0.55 236	
5.5	4.14	0.41 108	1.78 82	2.13 83	1.38 76	0.56 62	0.10 76	0.07 225	0.05 302	0.09 277	0.09 265	0.12 261	0.12 245	0.20 193	0.77 191	1.26 215	1.52 233	0.60 255	
5.0	6.83	0.25 95	1.51 76	1.92 81	1.17 74	0.33 41	0.06 235	0.09 174	0.05 49	0.02 333	0.03 315	0.12 336	0.05 331	0.18 225	0.75 228	1.29 242	1.34 250	0.54 268	
4.5	11.25	0.16 356	0.95 62	1.35 78	0.68 72	0.25 315	0.24 248	0.13 148	0.13 67	0.08 58	0.08 47	0.27 12	0.19 79	0.21 266	0.92 265	1.38 269	1.07 271	0.40 281	
4.0	18.55	0.50 317	0.50 3	0.58 67	0.08 47	0.54 276	0.40 249	0.16 133	0.18 76	0.13 67	0.17 55	0.41 22	0.34 37	0.28 291	1.17 286	1.48 289	0.90 298	0.25 299	
3.5	30.59	0.86 311	0.88 305	0.23 312	0.40 259	0.67 267	0.47 249	0.18 125	0.19 78	0.16 72	0.21 60	0.49 27	0.42 40	0.32 305	1.27 298	1.43 302	0.79 321	0.13 331	
3.0	50.43	0.92 309	1.15 290	0.59 278	0.62 257	0.78 263	0.46 250	0.17 118	0.19 81	0.17 73	0.22 60	0.50 30	0.44 42	0.30 311	1.16 304	1.19 312	0.65 339	0.09 18	
2.5	83.15	0.65 308	0.97 284	0.62 272	0.59 256	0.64 260	0.37 251	0.13 115	0.15 82	0.13 74	0.18 62	0.40 31	0.34 43	0.24 316	0.88 309	0.86 318	0.49 350	0.08 45	

OCTOBER		MEAN GEOPOTENTIAL HEIGHT AMPLITUDE (dam) AND PHASE WAVE 2																	
SCALE	PRESSURE	-80	-70	-60	-50	-40	-30	-20	-10	0	10	20	30	40	50	60	70	80	
HEIGHT	(mb)																		
12.0	0.0062	5.6	11.2	18.0	9.6	4.0	6.5	5.6	4.9	2.2	2.3	2.6	2.0	4.5	6.1	6.1	8.5	3.7	
		50	77	82	90	69	44	16	350	280	197	142	92	330	325	338	316	134	
11.5	0.0103	4.6	11.6	17.9	9.6	3.5	5.1	4.2	3.7	1.5	1.6	1.1	1.2	4.2	5.5	5.1	8.0	1.7	
		51	77	82	90	70	42	19	345	279	192	138	66	332	328	333	312	127	
11.0	0.0169	3.6	12.0	17.7	9.6	3.1	3.8	2.8	2.7	0.8	0.9	0.3	1.1	3.9	4.9	4.2	7.4	0.5	
		52	78	81	89	71	40	24	338	278	184	2	17	333	331	325	306	6	
10.5	0.0279	2.7	12.3	17.5	9.5	2.7	2.7	1.7	1.9	0.3	0.4	1.3	1.5	3.6	4.3	3.5	6.9	2.0	
		54	79	81	88	72	40	32	329	279	163	336	344	334	332	314	298	325	
10.0	0.0460	1.9	12.6	17.2	9.4	2.5	1.7	0.9	1.3	0.1	0.2	2.0	1.9	3.4	3.9	3.1	6.6	3.3	
		57	80	79	87	74	45	48	320	340	48	335	350	334	331	298	288	319	
9.5	0.0758	1.4	12.8	16.9	9.4	2.4	1.1	0.5	1.0	0.2	0.5	2.3	2.2	3.2	3.6	3.2	6.5	4.2	
		61	81	78	85	76	63	72	319	26	5	337	324	332	326	284	277	314	
9.0	0.1250	1.1	12.9	16.7	9.4	2.5	1.0	0.2	0.9	0.3	0.8	2.1	2.2	3.1	3.5	3.6	6.8	4.8	
		68	82	76	82	77	93	91	333	359	347	342	321	330	318	275	269	310	
8.5	0.2061	1.1	13.1	16.8	9.7	2.8	1.2	0.1	1.0	0.5	0.9	1.7	1.9	3.0	3.7	4.3	7.2	5.0	
		77	83	74	79	75	109	64	350	332	333	350	322	328	309	276	265	305	
8.0	0.3398	1.4	13.3	17.3	10.2	3.0	1.2	0.1	1.0	0.7	1.0	1.4	1.6	2.9	4.0	5.3	7.7	4.9	
		85	83	74	78	72	114	21	359	316	326	360	331	325	305	281	268	301	
7.5	0.5603	1.8	13.6	18.1	10.8	3.2	0.9	0.1	0.7	0.7	0.9	1.3	1.5	2.7	4.5	6.7	8.3	4.8	
		88	82	75	77	67	120	106	0	307	326	2	345	323	303	289	277	300	
7.0	0.9237	2.0	13.6	18.5	11.2	3.2	0.5	0.3	0.4	0.6	0.8	1.4	1.5	2.6	5.0	8.1	9.0	4.7	
		87	81	76	77	63	139	144	6	309	337	358	355	322	303	296	288	303	
6.5	1.52	1.8	12.7	17.9	10.8	2.9	0.4	0.5	0.3	0.4	0.7	1.6	1.6	2.6	5.8	9.5	9.6	4.7	
		80	79	76	78	61	188	141	34	330	352	358	1	322	305	303	299	310	
6.0	2.51	1.4	10.7	15.8	9.5	2.2	0.5	0.7	0.5	0.3	0.7	1.8	1.8	2.8	6.7	10.6	9.9	4.6	
		65	77	75	78	57	218	135	55	8	7	3	6	323	309	311	311	319	
5.5	4.14	1.1	8.1	12.8	7.5	1.3	0.7	0.7	0.5	0.4	0.8	1.9	1.9	3.0	7.5	11.3	10.0	4.4	
		39	74	73	78	51	228	127	64	31	18	9	11	327	316	320	324	330	
5.0	6.83	1.0	5.7	9.8	5.6	0.7	0.8	0.7	0.5	0.4	0.8	1.8	2.0	3.2	7.9	11.5	10.0	4.2	
		11	71	70	79	48	230	119	69	38	24	13	14	331	323	329	336	341	
4.5	11.25	0.8	3.9	7.5	4.2	0.5	0.6	0.6	0.4	0.3	0.7	1.6	1.8	3.1	7.7	11.0	9.7	4.0	
		1	72	67	81	76	224	109	72	33	23	15	14	336	332	339	346	350	
4.0	18.55	0.5	3.1	6.1	3.7	1.0	0.2	0.4	0.2	0.2	0.6	1.1	1.4	3.0	6.9	10.1	9.1	3.8	
		28	80	65	83	94	167	93	72	2	2	14	14	8	342	342	349	354	
3.5	30.59	1.0	3.6	5.7	3.5	2.0	0.7	0.2	0.1	0.3	0.4	0.4	1.0	2.7	5.9	9.0	8.3	3.6	
		104	94	66	83	92	90	56	264	305	348	358	352	348	355	360	0	359	
3.0	50.43	2.3	5.0	6.2	4.7	3.1	1.3	0.3	0.4	0.5	0.5	0.4	0.8	2.3	5.1	8.0	7.4	3.4	
		119	100	70	82	89	80	356	260	280	307	241	312	356	12	11	4	359	
2.5	83.15	3.5	6.6	7.1	5.6	4.1	1.9	0.4	0.6	0.7	0.6	1.0	0.9	2.0	4.7	7.2	6.6	3.3	
		122	102	73	81	87	77	330	261	272	282	222	275	3	29	21	7	358	

NOVEMBER MEAN TEMPERATURE AMPLITUDE (K) AND PHASE		WAVE 1																
SCALE	PRESSURE	-80	-70	-60	-50	-40	-30	-20	-10	0	10	20	30	40	50	60	70	80
HEIGHT	(mb)																	
12.0	0.0062	0.36 132	0.01 90	0.31 135	0.16 135	0.22 135	0.52 313	0.18 174	1.14 121	0.70 130	0.41 158	0.97 314	1.21 332	1.53 314	3.26 294	4.82 305	4.05 316	1.73 318
11.5	0.0103	0.41 135	0.07 170	0.41 140	0.23 142	0.20 12	0.51 314	0.19 161	1.14 120	0.73 150	0.48 137	0.88 304	1.11 324	1.64 307	3.56 299	5.32 312	4.50 324	1.95 327
11.0	0.0169	0.42 144	0.18 175	0.55 172	0.34 148	0.17 40	0.45 315	0.17 140	1.07 118	0.75 130	0.56 157	0.74 285	0.96 307	1.72 297	3.79 304	5.80 320	4.97 333	2.21 337
10.5	0.0279	0.43 157	0.32 162	0.69 175	0.48 152	0.21 94	0.34 319	0.19 110	0.94 115	0.73 129	0.67 157	0.72 249	0.92 274	1.88 285	4.00 312	6.36 331	5.57 344	2.58 348
10.0	0.0460	0.41 174	0.52 165	0.85 177	0.64 157	0.38 117	0.17 334	0.27 86	0.77 110	0.72 129	0.80 157	1.02 216	1.24 243	2.11 276	4.22 321	7.03 342	6.34 354	3.07 357
9.5	0.0758	0.42 197	0.68 189	0.97 182	0.77 162	0.57 128	0.09 54	0.35 68	0.57 99	0.70 129	0.92 157	1.52 201	1.76 227	2.30 271	4.36 333	7.58 354	7.08 4	3.65 7
9.0	0.1250	0.45 220	0.76 196	0.97 189	0.82 172	0.66 129	0.21 102	0.39 55	0.35 76	0.63 129	0.95 159	1.90 193	2.17 221	2.24 274	4.38 350	7.81 38	7.56 16	4.21 17
8.5	0.2061	0.46 241	0.67 213	0.81 205	0.72 190	0.55 111	0.28 111	0.36 32	0.22 21	0.45 127	0.79 163	1.82 189	2.09 221	1.84 293	4.33 13	7.62 26	7.50 32	4.58 29
8.0	0.3398	0.47 268	0.57 256	0.63 245	0.60 230	0.20 101	0.21 114	0.32 351	0.31 328	0.19 126	0.43 175	1.21 187	1.46 230	1.77 336	4.55 40	7.53 54	7.19 54	4.66 43
7.5	0.5603	0.49 267	0.68 277	0.68 277	0.64 258	0.10 336	0.09 336	0.39 324	0.34 316	0.16 346	0.19 307	0.25 244	1.14 284	2.34 351	3.93 44	6.62 77	6.06 82	3.68 67
7.0	0.9257	1.18 311	2.04 308	1.98 303	1.36 286	0.43 288	0.02 63	0.33 329	0.29 344	0.36 338	0.53 346	0.76 327	1.36 346	2.34 327	3.32 1	6.20 68	6.14 90	3.52 106
6.5	1.52	2.56 324	4.21 315	3.95 307	2.54 294	0.86 279	0.03 218	0.25 2	0.29 355	0.43 353	0.67 347	1.24 2	1.57 358	2.05 18	3.23 82	6.59 110	7.24 118	4.44 147
6.0	2.51	3.89 330	6.26 318	5.83 310	3.73 297	1.30 281	0.10 225	0.22 50	0.32 360	0.40 357	0.68 349	1.65 13	2.06 24	2.28 46	4.14 58	8.08 98	9.17 101	5.90 125
5.5	4.14	3.94 335	6.23 324	5.78 317	3.70 306	1.38 290	0.17 248	0.10 39	0.29 350	0.39 348	0.75 347	1.99 13	2.71 35	3.21 71	5.82 118	9.90 138	10.31 140	6.36 141
5.0	6.83	3.14 342	4.89 334	4.51 330	2.88 321	1.17 302	0.25 257	0.06 231	0.28 331	0.39 334	0.79 344	2.08 9	3.03 37	3.92 85	7.25 134	11.20 153	10.80 153	6.37 161
4.5	11.25	1.66 2	2.73 5	2.73 8	1.91 4	0.76 330	0.25 262	0.31 236	0.39 305	0.78 317	1.91 339	2.87 0	4.05 34	7.85 96	11.50 147	10.96 178	6.44 184	
4.0	18.55	1.21 88	2.67 77	3.44 68	2.54 61	0.67 33	0.32 265	0.43 239	0.37 287	0.39 300	0.71 333	1.60 27	2.39 106	3.68 159	7.64 181	10.90 196	10.99 196	6.73 204
3.5	30.59	2.63 123	4.71 106	5.19 92	3.69 83	1.01 266	0.29 243	0.53 275	0.39 286	0.38 326	0.61 326	1.32 116	1.79 116	2.92 168	6.66 193	9.45 208	9.94 217	6.24
3.0	50.43	3.32 131	5.60 115	5.68 101	4.03 91	1.19 79	0.25 264	0.55 244	0.40 269	0.37 276	0.50 320	1.15 307	1.29 357	2.05 127	5.14 176	7.05 202	7.78 218	4.97
2.5	85.15	2.84 135	4.73 119	4.66 106	3.30 95	1.04 84	0.18 269	0.45 247	0.32 264	0.28 271	0.33 313	0.87 292	0.84 340	1.27 138	3.45 183	4.62 209	5.27 224	3.42

NOVEMBER MEAN GEOPOTENTIAL HEIGHT AMPLITUDE (dam) AND PHASE		WAVE 1																
SCALE	PRESSURE	-80	-70	-60	-50	-40	-30	-20	-10	0	10	20	30	40	50	60	70	80
HEIGHT	(mb)																	
12.0	0.0062	9.5 306	18.1 308	12.2 295	6.8 258	2.1 193	1.3 229	1.5 89	5.8 104	4.8 118	2.4 145	7.3 317	12.1 341	11.2 23	18.6 110	32.6 126	36.5 134	21.1 143
11.5	0.0103	10.1 307	18.2 308	12.5 297	6.9 260	2.4 192	1.4 197	1.5 79	4.2 97	3.6 114	1.8 141	6.0 318	10.4 343	10.7 35	23.5 111	40.0 127	42.5 135	23.8 143
11.0	0.0169	10.7 307	18.3 309	12.9 300	7.1 263	2.6 193	1.9 177	1.4 69	2.7 85	2.3 106	1.1 129	4.9 323	9.1 347	11.1 48	28.8 113	48.1 128	49.2 137	26.8 144
10.5	0.0279	11.3 309	18.5 309	13.5 303	7.3 267	2.8 197	2.3 168	1.3 60	1.7 57	1.3 86	0.5 75	4.4 334	8.4 355	12.5 58	34.4 115	56.6 131	56.5 140	30.1 146
10.0	0.0460	11.8 310	18.9 311	14.2 307	7.7 273	2.8 206	2.7 165	1.1 50	1.4 26	0.9 26	1.1 4	4.9 348	8.8 348	14.8 66	40.1 119	65.6 135	64.2 144	33.9 149
9.5	0.0758	12.1 313	19.4 313	15.1 311	8.2 280	2.8 221	2.8 165	0.7 34	1.8 337	1.4 344	2.3 350	6.4 359	10.3 14	17.8 122	45.7 139	74.8 148	72.5 158	38.1 153
9.0	0.1250	12.3 316	20.0 316	15.9 315	8.7 287	3.0 239	2.8 170	0.3 341	2.1 320	2.2 332	3.7 345	8.9 4	12.9 20	20.9 74	50.8 127	83.6 144	80.8 153	42.7 158
8.5	0.2061	12.3 319	20.4 318	16.6 319	9.1 294	3.4 253	2.6 177	0.5 258	2.2 311	2.7 328	5.0 344	11.6 5	16.0 24	23.6 77	54.7 132	90.7 150	88.2 159	47.5 164
8.0	0.3398	12.0 322	20.4 321	16.8 322	9.1 299	3.8 260	2.5 184	0.8 226	1.9 304	2.9 328	5.9 345	13.9 6	18.5 27	25.1 82	56.9 138	94.9 156	93.5 165	52.0 169
7.5	0.5603	11.7 325	20.0 323	16.5 325	8.7 304	3.9 259	2.5 189	1.1 200	1.5 298	2.7 329	6.1 346	14.8 346	19.7 31	25.7 89	57.3 145	95.6 162	95.0 170	54.8 175
7.0	0.9257	10.8 327	18.4 325	15.0 328	7.5 309	3.7 256	2.5 191	1.5 182	1.1 289	2.3 328	5.5 348	14.4 8	19.6 36	26.0 96	57.0 150	93.8 168	93.3 176	55.4 180
6.5	1.52	8.1 330	13.9 329	11.0 337	4.8 320	2.8 248	2.5 191	1.9 178	0.9 267	1.8 322	4.7 348	13.0 9	18.3 41	26.1 103	56.0 155	90.1 173	89.3 181	53.8 186
6.0	2.51	3.4 334	6.6 343	5.9 15	2.0 30	1.7 219	1.4 240	2.2 181	2.0 140	1.3 308	3.7 348	10.9 10	16.1 46	25.3 110	53.9 146	84.9 179	83.8 188	51.0 194
5.5	4.14	2.5 152	4.0 103	7.6 92	5.8 102	2.1 156	2.3 186	2.4 184	1.3 222	0.9 282	2.6 348	8.2 9	12.8 50	22.9 117	49.5 166	76.8 186	76.6 197	47.2 203
5.0	6.83	7.7 156	11.5 134	13.8 117	10.4 115	3.7 136	2.2 179	2.4 185	1.5 208	0.8 242	1.5 350	5.2 7	8.7 56	19.1 127	42.7 174	66.0 195	67.2 207	42.3 213
4.5	11.25	11.2 160	16.4 144	17.6 129	13.0 125	5.1 136	2.1 168	2.3 180	1.7 204	0.4 19	2.3 144	4.8 74	14.8 141	33.9 185	53.1 206	95.6 217	95.6 223	35.8 223
4.0	18.55	12.2 166	17.5 154	18.1 142	13.3 138	5.8 142	2.2 156	2.1 169	1.9 179	1.3 178	0.9 138	0.8 116	3.3 127	11.1 161	25.0 199	40.0 218	42.4 228	27.8 233
3.5	30.59	10.7 178	15.3 171	15.7 163	11.9 158	5.9 154	2.4 146	2.0 148	2.0 164	1.6 161	1.8 144	2.7 146	5.0 163	8.7 185	17.5 219	28.1 234	29.2 241	19.3 244
3.0	50.43	8.6 202	13.2 201	14.3 193	11.4 187	5.8 170	2.6 139	2.2 127	2.3 150	2.0 148	2.6 144	5.1 142	7.1 170	13.2 210	19.8 248	18.7 255	12.0 260	7.3 259
2.5	85.15	8.1 234	14.5 233	16.3 221	13.0 211	5.9 186	2.8 134	2.6 113	2.3 139	3.2 140	5.2 142	8.7 137	7.7 170	12.3 228	15.7 276	12.3 279	7.3 287	7.3

NOVEMBER MEAN TEMPERATURE AMPLITUDE (K) AND PHASE WAVE 2

SCALE HEIGHT	PRESSURE (mb)	-80	-70	-60	-50	-40	-30	-20	-10	0	10	20	30	40	50	60	70	80
12.0	0.0062	0.08 187	0.30 61	0.18 74	0.01 0	0.41 54	0.49 39	0.12 194	0.17 82	0.60 115	0.77 102	1.27 92	1.02 116	0.52 97	0.64 42	0.37 3	0.47 67	0.29 8
11.5	0.0103	0.10 183	0.36 62	0.4 71	0.04 28	0.47 52	0.51 40	0.10 183	0.17 78	0.61 114	0.74 101	1.22 93	0.94 116	0.44 91	0.64 29	0.45 3	0.49 57	0.25 354
11.0	0.0169	0.09 180	0.39 67	0.30 75	0.08 43	0.55 49	0.50 43	0.06 162	0.14 71	0.58 114	0.65 102	1.05 92	0.75 113	0.32 70	0.65 11	0.52 0	0.51 45	0.19 325
10.5	0.0279	0.08 176	0.41 70	0.39 73	0.15 45	0.61 45	0.47 47	0.08 98	0.10 63	0.54 113	0.50 102	0.77 92	0.47 106	0.28 19	0.73 349	0.58 360	0.54 29	0.21 281
10.0	0.0460	0.05 169	0.39 75	0.45 75	0.24 48	0.57 42	0.41 53	0.15 74	0.07 36	0.48 114	0.32 104	0.41 90	0.15 55	0.48 339	0.89 332	0.60 359	0.58 16	0.32 256
9.5	0.0758	0.04 144	0.33 82	0.54 74	0.31 52	0.68 58	0.32 36	0.21 63	0.05 65	0.40 118	0.13 114	0.01 333	0.41 327	0.76 329	0.99 323	0.51 359	0.95 5	0.44 243
9.0	0.1250	0.03 162	0.24 95	0.52 78	0.33 58	0.56 56	0.22 78	0.22 63	0.07 274	0.29 131	0.10 240	0.39 274	0.79 318	0.95 327	0.89 322	0.28 19	0.40 353	0.52 238
8.5	0.2061	0.06 209	0.13 122	0.41 87	0.26 73	0.26 58	0.13 116	0.14 72	0.12 217	0.21 173	0.23 249	0.62 272	0.96 319	0.93 334	0.45 338	0.28 116	0.11 301	0.50 234
8.0	0.3398	0.13 225	0.09 202	0.24 118	0.19 121	0.17 201	0.12 178	0.08 173	0.22 192	0.30 217	0.28 240	0.60 273	0.87 326	0.71 355	0.50 85	0.78 140	0.44 189	0.35 226
7.5	0.5603	0.17 224	0.12 236	0.19 163	0.21 152	0.37 196	0.09 191	0.16 207	0.19 180	0.30 237	0.14 236	0.26 315	0.70 315	0.90 11	1.37 50	1.29 101	0.93 145	0.19 182
7.0	0.9237	0.21 219	0.09 190	0.18 161	0.27 147	0.33 175	0.06 151	0.14 216	0.10 183	0.22 254	0.03 252	0.22 21	0.74 46	1.25 76	1.67 112	1.62 154	1.17 188	0.14 201
6.5	1.52	0.19 201	0.24 124	0.28 116	0.35 130	0.29 130	0.11 106	0.04 225	0.03 287	0.10 279	0.02 315	0.16 57	0.67 69	1.41 93	2.06 127	1.84 167	1.20 203	0.20 257
6.0	2.51	0.19 174	0.10 113	0.56 105	0.51 105	0.39 127	0.13 113	0.03 342	0.04 353	0.06 329	0.04 270	0.14 159	0.53 102	1.46 159	2.21 146	1.97 182	1.20 224	0.44 286
5.5	4.14	0.17 175	0.54 107	0.60 103	0.52 132	0.34 126	0.11 133	0.03 121	0.04 94	0.04 30	0.04 169	0.26 156	0.53 135	2.05 156	2.01 199	1.80 241	1.06 305	0.42 162
5.0	6.83	0.11 175	0.52 97	0.61 103	0.49 137	0.26 152	0.12 178	0.11 131	0.12 108	0.08 76	0.09 119	0.29 159	0.59 146	1.14 162	1.73 193	1.52 288	0.85 270	0.34 330
4.5	11.25	0.04 187	0.45 82	0.56 103	0.39 140	0.25 200	0.18 203	0.20 131	0.15 109	0.17 82	0.28 96	0.49 116	1.03 147	1.60 196	1.50 234	0.80 267	0.25 310	0.25 9
4.0	18.55	0.05 323	0.38 61	0.47 105	0.26 140	0.34 234	0.24 216	0.27 129	0.26 107	0.20 84	0.25 83	0.37 77	1.06 332	1.06 228	1.88 267	1.96 296	0.96 340	0.27 54
3.5	30.59	0.12 326	0.32 36	0.35 106	0.12 135	0.42 249	0.27 221	0.30 129	0.27 105	0.30 82	0.22 76	0.30 57	0.50 86	1.22 251	2.08 284	1.95 310	1.02 355	0.31 79
3.0	50.43	0.14 326	0.27 13	0.22 108	0.03 101	0.42 296	0.27 224	0.31 128	0.26 103	0.21 82	0.32 71	0.58 48	1.03 45	2.82 265	2.94 319	1.70 319	0.88 4	0.28 92
2.5	83.15	0.12 332	0.21 1	0.12 111	0.03 350	0.34 261	0.21 225	0.24 129	0.16 102	0.26 79	0.50 67	0.52 43	0.78 32	1.44 273	1.22 300	0.62 324	0.21 9	0.21 98

NOVEMBER MEAN GEOPOTENTIAL HEIGHT AMPLITUDE (dam) AND PHASE WAVE 2

SCALE HEIGHT	PRESSURE (mb)	-80	-70	-60	-50	-40	-30	-20	-10	0	10	20	30	40	50	60	70	80
12.0	0.0062	3.6 208	5.6 106	8.9 108	5.9 130	4.7 97	3.7 86	2.6 126	2.2 121	4.7 120	4.2 103	5.3 85	6.3 53	6.2 45	3.7 18	5.6 334	10.1 350	5.0 327
11.5	0.0103	3.5 209	5.3 110	8.6 109	5.9 131	4.3 103	3.2 96	2.5 123	2.0 126	4.0 101	3.1 123	5.5 80	5.7 54	5.8 39	2.8 51	5.1 330	9.9 346	4.6 325
11.0	0.0169	3.3 210	4.9 114	8.3 110	5.9 131	3.9 111	2.8 108	2.5 121	1.9 131	3.3 127	2.0 105	6.8 57	5.5 35	5.4 35	1.9 9	4.5 326	9.6 342	4.3 323
10.5	0.0279	3.2 211	4.5 120	7.9 112	5.9 133	3.6 123	2.6 122	2.4 131	1.8 136	2.6 131	1.2 107	0.8 30	5.5 18	5.0 34	0.9 39	3.9 319	9.2 359	4.1 324
10.0	0.0460	3.2 212	4.1 126	7.4 116	5.9 136	3.6 138	2.5 136	2.3 140	1.8 137	2.1 142	0.6 112	0.9 326	5.4 49	4.6 38	0.7 108	3.3 309	8.6 335	3.9 329
9.5	0.0758	3.1 213	3.8 131	6.9 120	5.9 140	3.8 153	2.4 149	2.1 129	1.9 142	1.6 142	0.3 117	1.1 313	5.1 49	4.3 34	2.0 134	2.8 297	7.9 351	3.9 337
9.0	0.1250	3.1 214	3.5 136	6.4 125	5.8 145	4.3 164	2.4 158	2.0 138	1.9 141	1.2 144	0.2 103	0.9 325	4.7 24	4.3 66	3.4 137	2.6 285	7.3 349	4.0 348
8.5	0.2061	3.1 215	3.3 139	5.9 129	5.8 149	4.7 170	2.3 164	1.9 146	1.9 137	0.9 137	0.5 85	0.7 23	4.3 84	4.7 84	4.4 139	2.8 281	6.9 328	4.4 357
8.0	0.3398	2.9 215	3.2 138	5.5 132	5.6 152	4.8 171	2.1 165	1.9 148	1.8 130	0.7 110	0.8 76	1.3 62	4.3 59	5.1 97	4.6 144	3.5 288	7.1 330	4.8 3
7.5	0.5603	2.7 214	3.2 135	5.2 131	5.3 152	4.4 169	2.0 163	1.7 143	1.7 122	0.9 86	1.1 72	1.6 75	4.0 74	4.8 109	3.7 160	4.9 298	8.0 334	5.1 6
7.0	0.9237	2.4 213	3.2 133	5.0 129	5.0 152	3.9 166	1.9 162	1.7 136	1.6 115	1.2 80	1.2 70	1.8 85	3.4 98	3.9 126	3.0 200	6.8 308	9.4 359	5.3 6
6.5	1.52	2.1 213	3.0 132	4.7 129	4.6 154	3.5 168	1.8 165	1.7 132	1.6 113	1.3 81	1.3 71	1.6 95	2.5 98	2.7 154	3.8 317	9.0 344	10.8 344	5.5 8
6.0	2.51	1.9 216	2.5 135	4.1 132	4.0 158	3.2 174	1.7 170	1.7 132	1.6 114	1.4 84	1.3 72	1.5 93	1.7 105	2.2 203	5.8 278	11.4 325	12.0 351	5.5 13
5.5	4.14	1.7 222	1.8 146	3.4 139	3.4 164	2.9 183	1.6 175	1.7 132	1.6 115	1.4 87	1.3 71	1.4 81	1.9 94	2.7 251	7.9 298	13.5 334	12.9 357	5.4 19
5.0	6.83	1.6 228	1.3 169	2.7 150	2.8 171	2.6 190	1.5 177	1.6 132	1.5 113	1.3 88	1.3 68	1.4 65	0.7 36	3.6 280	9.6 312	14.9 342	13.3 342	5.2 24
4.5	11.25	1.5 231	1.4 199	2.2 166	2.2 180	2.3 192	1.3 174	1.3 133	1.3 116	1.1 89	1.1 62	1.1 48	1.3 360	4.1 301	10.2 325	15.1 350	13.0 350	4.0 27
4.0	18.55	1.5 231	1.8 214	2.0 186	1.9 189	1.9 186	1.1 164	1.0 133	1.0 119	0.8 89	0.9 53	1.1 29	4.8 348	4.4 321	9.8 339	14.4 358	12.1 358	4.5 27
3.5	30.59	1.5 226	2.3 217	2.0 204	1.7 196	1.7 170	0.9 144	0.6 136	0.5 128	0.5 90	0.5 33	0.5 353	4.0 335	4.4 353	8.8 342	12.9 356	10.8 358	4.2 15
3.0	50.43	1.5 218	2.7 215	2.1 215	1.7 199	1.7 149	1.7 118	0.9 158	0.2 162	0.3 97	0.3 335	0.7 284	0.7 330	4.5 350	8.1 326	11.5 319	9.4 317	4.0 18
2.5	83.15	1.6 212	3.0 212	2.1 222	1.7 200	2.0 153	1.0 100	0.3 293	0.3 233	0.1 251	0.6 286	1.3 253	1.9 218	4.8 18	8.0 34	10.5 29	8.3 18	3.9 12

DECEMBER MEAN TEMPERATURE AMPLITUDE (K) AND PHASE WAVE 1

SCALE HEIGHT	PRESSURE (mb)	-80	-70	-60	-50	-40	-30	-20	-10	0	10	20	30	40	50	60	70	80
12.0	0.0062	0.20 180	0.21 273	0.31 184	0.14 168	0.43 339	0.03 0	0.22 342	0.23 170	0.52 154	0.39 229	0.28 302	0.84 349	0.07 74	2.52 248	4.88 264	4.39 281	2.31 301
11.5	0.0103	0.22 175	0.23 274	0.34 184	0.18 164	0.44 343	0.05 346	0.25 359	0.25 169	0.52 153	0.40 222	0.28 358	0.75 276	0.18 295	2.95 270	5.24 286	4.63 290	2.40 307
11.0	0.0169	0.23 170	0.25 279	0.36 183	0.20 161	0.42 349	0.08 338	0.26 337	0.26 166	0.47 152	0.37 210	0.30 268	0.65 313	0.57 274	3.38 263	5.47 278	4.73 292	2.42 315
10.5	0.0279	0.21 159	0.20 283	0.30 179	0.24 158	0.36 2	0.11 335	0.28 332	0.26 162	0.37 152	0.35 194	0.37 243	0.74 275	1.12 274	3.95 272	5.67 289	4.78 302	2.46 326
10.0	0.0460	0.18 139	0.14 299	0.19 171	0.27 150	0.31 25	0.17 333	0.30 327	0.25 158	0.24 152	0.37 175	0.53 227	1.17 290	1.83 275	4.58 281	5.89 300	4.83 313	2.54 338
9.5	0.0758	0.14 100	0.09 348	0.08 137	0.28 149	0.30 60	0.20 358	0.31 329	0.19 149	0.08 137	0.41 160	0.74 220	1.79 241	2.64 278	5.19 291	6.08 314	4.81 327	2.67 352
9.0	0.1250	0.16 55	0.12 31	0.08 60	0.28 147	0.37 90	0.20 350	0.30 332	0.07 118	0.10 343	0.40 154	0.93 218	2.33 241	3.40 283	5.54 303	6.11 331	4.72 347	2.77 8
8.5	0.2061	0.16 18	0.12 33	0.11 45	0.25 147	0.40 111	0.17 22	0.23 346	0.19 354	0.30 340	0.28 162	1.02 221	2.54 249	3.85 291	5.49 319	6.05 354	4.80 13	2.78 27
8.0	0.3398	0.20 336	0.11 3	0.05 53	0.16 146	0.35 130	0.21 69	0.16 22	0.48 344	0.47 339	0.16 230	0.95 231	2.41 265	3.80 302	5.25 342	6.28 320	5.45 41	2.79 49
7.5	0.5603	0.22 312	0.21 320	0.21 270	0.03 129	0.15 156	0.22 91	0.16 73	0.53 342	0.38 335	0.30 283	0.89 245	2.55 284	4.19 314	5.92 357	6.89 300	5.94 313	2.77 358
7.0	0.9237	0.18 351	0.23 4	0.11 45	0.07 30	0.02 243	0.18 93	0.18 90	0.35 344	0.21 331	0.28 296	0.64 304	2.36 335	4.39 355	6.89 15	8.05 44	6.73 63	3.21 84
6.5	1.52	0.36 46	0.49 54	0.39 58	0.15 54	0.07 21	0.12 77	0.16 97	0.09 10	0.04 315	0.11 313	0.36 305	2.22 330	5.25 0	8.55 35	10.00 57	8.28 74	4.33 98
6.0	2.51	0.65 61	0.86 70	0.68 65	0.29 66	0.15 62	0.14 69	0.16 97	0.11 109	0.05 191	0.02 90	0.51 2	2.88 395	6.77 20	10.47 50	12.09 71	10.34 88	5.77 110
5.5	4.14	0.73 64	0.98 69	0.79 61	0.40 52	0.17 60	0.12 81	0.10 102	0.04 115	0.07 283	0.15 340	1.03 9	3.24 15	7.14 40	10.69 73	11.91 52	10.57 108	6.09 128
5.0	6.83	0.69 64	0.92 66	0.81 66	0.53 53	0.17 39	0.08 122	0.02 207	0.08 285	0.17 303	0.37 333	1.46 5	3.67 26	6.88 100	10.39 122	11.39 155	10.36 149	6.13
4.5	11.25	0.53 62	0.70 56	0.75 39	0.65 28	0.15 31	0.10 191	0.15 259	0.22 288	0.30 306	0.62 330	1.76 357	3.52 32	6.12 84	10.36 130	12.10 155	10.95 166	6.35 176
4.0	18.55	0.32 58	0.45 34	0.66 21	0.73 19	0.13 4	0.20 27	0.28 262	0.35 288	0.40 307	0.82 328	1.88 347	2.91 36	5.58 112	11.14 156	14.05 180	12.26 192	6.71 200
3.5	30.59	0.11 41	0.33 350	0.59 2	0.72 13	0.13 338	0.25 223	0.35 262	0.42 289	0.44 307	0.91 326	1.80 338	2.04 38	5.28 138	11.45 174	14.92 195	12.46 208	6.52 220
3.0	50.43	0.07 267	0.35 315	0.49 315	0.62 346	0.13 8	0.29 318	0.38 227	0.43 289	0.43 306	0.89 326	1.61 329	1.15 39	4.80 156	10.25 186	12.95 209	10.74 220	5.49 234
2.5	85.15	0.11 267	0.32 300	0.37 334	0.45 4	0.11 311	0.25 229	0.32 262	0.37 290	0.33 306	0.68 325	1.17 323	0.47 323	3.69 167	7.59 194	9.36 212	7.63 227	3.81 243

DECEMBER MEAN GEOPOTENTIAL HEIGHT AMPLITUDE (dm) AND PHASE WAVE 1

SCALE HEIGHT	PRESSURE (mb)	-80	-70	-60	-50	-40	-30	-20	-10	0	10	20	30	40	50	60	70	80
12.0	0.0062	4.1 137	4.1 162	7.1 169	5.6 167	1.4 115	1.5 147	0.7 324	0.8 219	0.7 234	2.5 236	8.2 300	23.5 325	30.3 5	13.2 53	16.3 133	29.8 148	24.9 154
11.5	0.0103	3.8 133	4.3 158	6.7 168	5.3 167	1.9 129	1.5 148	0.4 310	0.6 247	0.8 284	2.0 239	7.8 301	22.4 324	30.2 6	17.0 57	22.1 121	34.8 140	27.9 150
11.0	0.0169	3.6 130	4.4 154	6.2 166	5.0 168	2.5 138	1.6 149	0.2 244	1.3 281	1.5 308	7.4 307	21.4 323	30.3 27	21.4 7	19.4 62	40.4 113	31.3 135	24.9 148
10.5	0.0279	3.3 127	4.6 151	6.7 165	4.7 167	2.9 145	1.8 150	0.4 179	0.9 304	1.8 318	1.2 265	7.1 305	20.6 325	30.3 9	26.3 67	37.4 111	47.5 133	34.8 147
10.0	0.0460	3.1 124	4.8 149	6.4 164	4.4 169	3.3 151	2.0 165	0.8 314	1.2 321	2.2 310	1.2 291	6.9 310	20.1 328	30.6 13	31.8 73	45.9 111	54.5 132	38.4 148
9.5	0.0758	2.8 125	5.0 149	6.2 164	4.0 171	3.4 157	2.2 151	1.3 159	1.5 319	2.5 322	1.6 308	7.0 317	20.0 334	31.1 39	38.0 72	54.3 114	61.5 133	42.1 149
9.0	0.1250	2.7 128	5.1 150	6.5 165	3.3 174	3.6 165	2.5 152	1.7 157	2.7 319	2.2 321	7.3 316	20.4 327	32.0 343	39.0 27	44.5 85	62.3 118	67.9 135	45.5 152
8.5	0.2061	2.7 133	5.2 152	6.2 167	3.3 177	3.2 175	2.7 155	2.1 157	1.7 315	2.5 319	7.8 320	21.2 337	32.5 353	33.3 36	50.4 91	68.8 123	72.9 139	48.4 155
8.0	0.3398	2.9 136	5.3 153	6.3 168	3.0 180	2.9 184	2.8 160	2.4 160	1.3 304	2.1 313	2.9 323	8.5 346	22.0 2	34.8 45	54.9 98	73.3 129	75.9 144	50.5 159
7.5	0.5603	3.2 136	5.5 153	6.3 168	2.9 181	2.6 189	2.8 166	2.4 165	0.8 270	1.6 304	2.7 329	9.0 355	22.1 12	36.0 54	58.1 106	76.0 136	77.4 150	51.5 164
7.0	0.9237	3.5 137	5.8 153	6.3 168	2.9 182	2.5 190	2.7 172	2.4 170	0.9 225	1.2 292	2.4 336	9.3 21	21.7 64	36.6 21	60.4 115	78.2 144	78.4 157	51.6 169
6.5	1.52	3.6 142	6.0 157	6.5 172	3.0 184	2.6 190	2.7 177	2.4 176	1.1 212	1.0 284	2.1 340	9.2 20	20.5 29	35.5 6	61.3 125	79.9 154	78.8 165	50.6 175
6.0	2.51	3.6 154	6.2 166	6.8 179	3.2 189	2.7 191	2.8 180	2.3 182	1.2 253	1.0 285	2.1 341	8.8 37	18.3 7	32.7 138	61.2 175	81.5 165	78.5 175	48.6 183
5.5	4.14	3.8 169	6.5 178	6.3 188	3.6 195	2.9 195	2.8 184	2.3 187	1.2 220	0.9 287	2.0 340	7.6 7	14.8 45	28.6 107	59.4 153	81.4 177	76.4 186	45.4 193
5.0	6.83	4.2 183	7.1 189	7.2 195	4.2 200	3.1 198	2.8 187	2.3 189	1.2 220	0.8 285	1.6 342	5.8 7	10.3 57	24.6 127	55.3 178	77.7 189	71.5 197	41.0 203
4.5	11.25	4.7 193	7.9 196	8.2 199	5.0 202	3.3 200	2.7 188	2.2 186	1.1 210	0.5 268	0.9 350	3.4 12	6.1 80	20.7 149	47.6 182	68.0 200	61.7 207	34.6 213
4.0	18.55	5.2 198	8.6 199	9.2 201	6.0 202	3.5 200	2.5 187	2.2 178	1.0 188	0.4 188	0.4 188	1.3 57	4.4 131	16.8 172	36.7 197	52.9 211	47.5 217	26.3 221
3.5	30.59	5.4 200	9.1 199	10.1 200	7.1 201	3.6 201	2.2 198	2.2 182	1.4 165	0.9 164	1.6 149	2.7 135	5.9 135	12.8 169	24.0 199	34.1 218	30.4 225	16.8 227
3.0	50.43	5.5 200	9.5 197	10.8 198	8.1 200	3.8 198	1.9 173	2.3 152	1.8 148	1.5 141	2.9 140	5.1 141	7.6 234	10.0 259	14.9 254	17.4 241	14.1 241	7.9 227
2.5	85.15	5.5 198	9.6 194	11.3 196	8.8 199	3.8 194	1.7 162	2.5 140	2.3 138	2.1 142	4.0 145	7.2 187	8.6 270	10.0 270	15.8 309	12.9 317	4.4 313	1.9 179

DECEMBER MEAN TEMPERATURE AMPLITUDE (K) AND PHASE WAVE 2

SCALE HEIGHT	PRESSURE (mb)	-80	-70	-60	-50	-40	-30	-20	-10	0	10	20	30	40	50	60	70	80
12.0	0.0062	0.30 104	0.02 0	0.06 342	0.16 309	0.15 318	0.20 306	0.35 292	0.41 292	0.41 105	0.75 115	0.21 59	0.86 53	0.69 13	1.11 44	1.33 53	0.06 38	0.46 179
11.5	0.0103	0.36 101	0.03 338	0.09 341	0.18 315	0.16 321	0.19 304	0.31 290	0.41 294	0.41 101	0.74 116	0.20 57	0.88 52	0.66 13	1.12 48	1.35 56	0.14 34	0.41 172
11.0	0.0169	0.41 100	0.06 345	0.12 346	0.18 321	0.15 323	0.17 298	0.21 289	0.36 298	0.36 96	0.65 118	0.65 61	0.83 52	0.58 12	1.07 55	1.26 59	0.26 34	0.34 163
10.5	0.0279	0.42 95	0.08 341	0.16 348	0.20 333	0.13 326	0.14 286	0.08 300	0.29 305	0.29 82	0.51 121	0.14 62	0.74 51	0.44 10	0.97 65	1.09 77	0.41 77	0.24 138
10.0	0.0460	0.39 89	0.11 339	0.22 352	0.19 350	0.11 333	0.11 259	0.10 101	0.21 319	0.23 61	0.34 128	0.09 58	0.52 50	0.26 9	0.89 81	0.88 81	0.53 80	0.24 95
9.5	0.0758	0.31 86	0.14 333	0.26 358	0.21 350	0.08 313	0.08 217	0.27 106	0.13 351	0.21 53	0.18 190	0.05 68	0.49 51	0.08 53	0.86 103	0.72 107	0.62 85	0.33 64
9.0	0.1250	0.16 84	0.15 330	0.26 7	0.22 32	0.07 56	0.11 177	0.37 109	0.12 40	0.19 12	0.11 212	0.04 76	0.40 57	0.19 122	0.94 127	0.72 142	0.60 90	0.49 47
8.5	0.2061	0.10 169	0.12 322	0.24 16	0.22 50	0.13 90	0.12 146	0.31 110	0.10 86	0.13 16	0.13 258	0.09 56	0.40 69	0.43 119	1.01 148	0.90 171	0.45 100	0.63 40
8.0	0.3398	0.27 202	0.07 298	0.19 39	0.19 70	0.18 99	0.12 107	0.11 124	0.11 149	0.07 124	0.09 270	0.19 54	0.49 82	0.65 111	1.03 169	1.09 192	0.23 128	0.71 34
7.5	0.5603	0.37 199	0.03 261	0.12 65	0.12 83	0.10 105	0.14 80	0.12 274	0.16 213	0.02 166	0.21 324	0.26 35	0.85 62	0.07 135	0.85 228	1.08 213	0.43 197	0.43 43
7.0	0.9237	0.35 198	0.02 198	0.07 82	0.04 83	0.06 108	0.07 73	0.18 276	0.16 249	0.14 192	0.03 333	0.16 259	0.42 299	0.90 272	1.20 272	1.15 225	0.92 318	0.12 318
6.5	1.52	0.26 201	0.02 113	0.04 82	0.01 117	0.00 143	0.02 124	0.09 263	0.14 275	0.10 256	0.13 260	0.37 279	1.16 289	2.02 307	1.58 299	1.18 242	1.57 242	0.72 273
6.0	2.51	0.21 208	0.05 114	0.07 117	0.05 148	0.03 270	0.03 198	0.03 298	0.10 293	0.13 266	0.22 272	0.65 272	1.80 179	3.04 319	1.94 332	1.05 293	2.19 271	1.45 287
5.5	4.14	0.18 213	0.08 128	0.11 131	0.07 164	0.06 260	0.04 208	0.06 151	0.03 308	0.07 309	0.17 272	0.62 272	2.96 179	2.06 319	0.98 332	2.10 293	1.57 271	1.57 287
5.0	6.83	0.15 222	0.10 137	0.15 143	0.09 171	0.09 257	0.05 204	0.11 257	0.06 104	0.04 45	0.08 295	0.47 275	1.31 292	2.43 325	2.07 342	1.20 332	1.63 294	1.34 294
4.5	11.25	0.09 238	0.11 141	0.18 147	0.10 180	0.13 257	0.06 203	0.17 129	0.16 106	0.12 83	0.08 279	0.22 295	0.66 303	1.57 332	1.92 356	1.68 341	1.29 313	0.77 313
4.0	18.55	0.06 270	0.11 144	0.20 150	0.11 183	0.14 258	0.06 198	0.21 125	0.23 106	0.19 90	0.19 54	0.19 32	0.26 35	0.67 355	1.67 357	2.14 8	1.70 25	0.45 33
3.5	30.59	0.03 315	0.10 148	0.19 151	0.10 185	0.15 258	0.06 191	0.21 123	0.26 107	0.23 94	0.26 61	0.26 59	0.40 88	0.72 88	1.30 2	2.25 13	2.10 43	0.87 78
3.0	50.43	0.05 349	0.08 148	0.16 153	0.08 188	0.13 261	0.06 185	0.21 119	0.26 108	0.23 97	0.29 63	0.53 65	0.99 90	0.75 122	0.88 5	1.90 16	2.00 52	1.05 89
2.5	83.15	0.04 360	0.05 155	0.11 156	0.05 192	0.10 261	0.04 183	0.16 120	0.21 107	0.19 98	0.24 65	0.47 67	0.88 92	0.74 131	0.52 6	1.33 18	1.50 57	0.86 93

DECEMBER MEAN GEOPOTENTIAL HEIGHT AMPLITUDE (dam) AND PHASE WAVE 2

SCALE HEIGHT	PRESSURE (mb)	-80	-70	-60	-50	-40	-30	-20	-10	0	10	20	30	40	50	60	70	80
12.0	0.0062	3.7 149	0.4 230	0.9 33	0.7 12	0.4 320	0.6 211	1.2 127	1.4 311	2.4 76	2.8 109	3.6 333	10.9 347	23.6 337	24.3 11	23.1 29	15.3 15	8.8 360
11.5	0.0103	3.4 155	0.4 227	0.8 39	0.6 32	0.1 321	0.7 187	1.6 122	0.8 324	2.0 69	1.7 105	3.6 328	10.4 341	22.8 341	23.0 8	21.3 26	15.2 15	9.5 360
11.0	0.0169	3.1 163	0.4 220	0.7 49	0.6 57	0.1 143	0.9 170	2.0 120	0.4 120	1.6 62	0.7 89	3.6 323	10.0 334	22.1 335	21.9 5	19.7 23	15.0 14	10.0 359
10.5	0.0279	2.9 174	0.5 210	0.6 66	0.7 82	0.3 143	1.0 160	2.2 119	0.5 119	1.4 55	0.4 359	3.6 319	9.9 327	21.5 333	21.0 20	18.4 20	14.8 13	10.4 358
10.0	0.0460	2.9 186	0.6 199	0.6 91	0.8 103	0.5 145	1.1 151	2.2 122	0.7 96	1.1 51	0.9 326	3.6 317	9.8 322	21.0 333	20.6 359	17.6 16	14.5 10	10.5 357
9.5	0.0758	3.0 196	0.7 188	0.7 119	0.9 121	0.6 149	1.1 145	2.0 122	0.9 109	0.9 53	1.3 323	3.7 315	9.8 317	20.9 332	20.7 355	17.3 13	14.3 6	10.5 354
9.0	0.1250	3.1 202	0.9 180	1.0 139	1.0 139	0.7 156	1.0 139	1.5 126	0.9 120	0.6 64	1.5 327	3.7 314	9.9 313	20.9 332	21.4 352	17.7 10	14.2 3	10.2 351
8.5	0.2061	3.1 205	1.1 174	1.3 153	1.1 156	0.7 168	0.9 135	1.0 135	0.8 129	0.5 79	1.5 334	3.7 313	10.1 310	21.3 331	22.6 350	18.7 8	14.2 360	9.7 348
8.0	0.3398	2.8 206	1.2 169	1.5 163	1.2 171	0.6 188	0.7 136	0.7 144	0.7 132	0.5 82	1.4 340	3.8 310	10.5 307	22.0 330	24.1 349	20.2 7	14.4 358	9.1 343
7.5	0.5603	2.4 207	1.2 166	1.6 170	1.2 181	0.7 209	0.6 147	0.8 139	0.6 121	0.5 63	1.4 342	3.8 305	10.9 305	22.4 329	25.2 351	21.7 8	14.8 358	8.6 338
7.0	0.9237	1.8 210	1.2 165	1.6 175	1.2 186	0.7 221	0.6 160	1.0 128	0.7 106	0.7 48	1.4 343	3.7 302	10.7 304	22.0 330	25.4 354	23.1 11	15.6 360	8.4 336
6.5	1.52	1.4 213	1.2 165	1.6 177	1.2 187	0.7 224	0.6 166	1.0 122	0.9 101	0.9 49	1.4 348	3.4 303	9.6 306	20.1 333	24.6 358	24.3 13	16.7 5	8.2 340
6.0	2.51	1.1 216	1.1 167	1.6 179	1.2 188	0.7 223	0.6 166	1.0 119	0.9 102	1.0 56	1.4 359	2.8 310	7.5 311	16.7 338	23.0 352	25.2 17	18.0 13	7.6 350
5.5	4.14	0.8 218	1.1 178	1.5 183	1.1 191	0.7 219	0.5 162	1.1 117	1.2 103	1.1 62	1.4 326	2.1 321	5.2 345	12.7 345	20.6 358	25.5 8	19.3 20	7.0 22
5.0	6.83	0.5 219	1.0 175	1.4 189	1.0 193	0.6 213	0.4 156	1.0 114	1.2 104	1.1 65	1.4 348	1.7 341	3.4 341	9.1 355	18.1 352	24.9 12	20.0 23	6.9 25
4.5	11.25	0.4 214	0.9 181	1.2 197	0.9 196	0.5 201	0.4 147	0.8 110	0.9 104	1.0 65	1.4 348	1.6 340	2.6 340	6.7 340	15.5 340	23.3 17	19.6 26	6.9 38
4.0	18.55	0.3 201	0.8 188	1.1 209	0.7 199	0.4 177	0.3 135	0.6 101	0.7 102	0.7 58	1.2 360	1.4 354	2.3 354	5.3 354	13.2 354	20.8 22	17.8 29	6.5 44
3.5	30.59	0.3 186	0.6 197	0.9 223	0.6 203	0.4 148	0.3 120	0.3 77	0.3 98	0.5 36	1.0 354	1.1 354	2.0 354	4.7 354	11.2 354	17.7 354	14.8 354	5.7 40
3.0	50.43	0.3 179	0.6 207	0.9 239	0.5 207	0.4 128	0.3 103	0.2 4	0.1 339	0.4 347	0.8 338	1.1 319	2.4 323	4.9 323	9.6 323	14.8 323	12.0 323	4.7 28
2.5	83.15	0.4 178	0.5 216	0.9 251	0.4 211	0.7 211	0.3 88	0.4 329	0.4 296	0.6 313	0.9 290	1.5 305	3.5 305	5.6 353	8.8 353	12.6 353	9.5 40	4.3 11

D7

N86-12821

2.3.1b PLANETARY WAVES

K. Labitzke

Meteorological Institute, Free University Berlin
Federal Republic of Germany

J. J. Barnett

Department of Atmospheric Physics, Clarendon Laboratory
Oxford, Great Britain

INTERANNUAL VARIABILITY

The zonal wave fields given in Section 2.3.1a show the climatology of the quasi-stationary planetary waves. The middle atmosphere exhibits variation on a time scale of a few days, and such short-term variations are missing from these means. Short-term variations include travelling waves which are found at all seasons (although those occurring in summer have very small amplitudes), e.g., see MADDEN (1978) or RODGERS and PRATA (1981). However, stratospheric warmings which are connected with a very strong intensification of the planetary waves one or two, have the largest effect. They affect the stratosphere and mesosphere over periods varying between a few days and several months. They are described in reviews by QUIROZ et al. (1975), SCHOEBERL (1978), LABITZKE (1981) and MCINTYRE (1982).

Figure 1 shows the magnitude of temperature changes which can occur. In this case at some level (e.g. 50 km) changes exceed 70 K over 15 days from 28 December to 18 January. The sudden warming is such a large phenomenon that it strongly affects individual monthly means, giving larger planetary wave amplitudes than for months without large warmings. However, sudden warmings are part of the climatology, and their mean effect needs to be included (it would be difficult to do otherwise), but an average over a small number of years for a given month can possibly be inadequate to obtain a reliable mean. Consequently, the means given here must be treated with caution.

During the summer season, planetary wave amplitudes are small (a few K) so the year-to-year variability will cause little absolute error in the amplitude. Year-to-year variability of the monthly mean is illustrated by Figures 2 - 7, which are derived from Nimbus 6 PMR retrieved temperature fields. Figures 2 - 4 are temperature analyses on constant pressure surfaces for 1 and 0.01 mb for December and January for the three Northern Hemisphere winters measured by the PMR. Figures 5 - 7 are the corresponding wave number one amplitude and phase components.

Fortunately, three very different types of stratospheric warmings took place (cf. Section 2.3.7, Figure 7), which are also reflected in the very different maps of the 0.01-mb temperatures. The first winter, 1975/76 (Figure 2) belongs in the group with several "minor" warmings, no breakdown of the stratospheric polar vortex, and a late reversal into summer. The maps of the stratosphere show a typical wave one situation, particularly well developed in January. This wave is obvious also in the upper mesosphere with the typical westward slope with height, as discussed in Section 2.3.1a. Overall, the amplitude of wave one is, however, not very large (Figure 5) and the pattern of the temperature still rather regular. It is of interest to note that a correlation exists between the polar minima at the 1-mb level and the polar maxima at the 0.01-mb level. This confirms earlier studies based on rocketsonde data (LABITZKE, 1972).

The second winter, 1976/77 (Figure 3) belongs to the group of "major" warmings which commonly terminate with the "breakdown" of the stratospheric

polar vortex and a "late winter cooling period". This time the warming developed already in December 1976 and this is reflected in the mean map of the 0.01-mb temperatures for December. A large wave one had developed and this wave is very pronounced also at the 0.01-mb level, i.e., in the upper mesosphere where the pattern is now very asymmetric compared with December 1975 (Figure 2).

January 1977 (Figure 3) is a period of "late winter cooling". The polar vortex was broken down at that time, the planetary waves were weak in the troposphere and stratosphere, no wave energy was therefore transported upwards and the radiational cooling resulted in a very cold polar stratosphere. At the same time we observe a very warm polar mesosphere with a rather symmetric temperature pattern, undisturbed by planetary waves.

The third winter, 1977/78 (Figure 4), belongs again in the group with "minor" warmings without a "breakdown", but the minor warming is very intense in January 1978. Accordingly, we find a rather undisturbed, regular December and a highly disturbed January, both in the stratosphere and in the upper mesosphere.

Thus the amplitude structure of the three winters is seen to be very different (Figures 5 - 7), and there is as much difference among the different sections for January and for December as between January and December. It is interesting that the phase fields are quite similar; if they were not, the three-year mean amplitude would be much reduced. Hence reference to Figures 3.1 and 3.12 in Section 2.3.1a shows that the three-year mean amplitude approximately equals the arithmetic mean of the amplitudes for the three years.

As pointed out before, "minor" warmings take place during the southern winters but they are not so intense as to be reflected in a monthly mean at upper mesospheric levels.

REFERENCES

- Labitzke, K. (1972), The interaction between stratosphere and mesosphere in winter, J. Atmos. Sci., **29**, 1395-1399.
- Labitzke, K. (1981), Stratospheric-mesospheric midwinter disturbances: A summary of observed characteristics, J. Geophys. Res., **86**, 9665-9678.
- Madden, R. A. (1979), Observation of large-scale traveling Rossby waves, Rev. Geophys. Space Phys., **17**, 1935-1949.
- McIntyre, M. E. (1982), How well do we understand the dynamics of stratospheric warmings? J. Meteorol. Soc. Japan, **60**, 37-65.
- Quiroz, R. S., A. J. Miller, and R. M. Nagatani (1975), A comparison of observed and simulated properties of sudden stratospheric warmings, J. Atmos. Sci., **32**, 1723-1736.
- Rodgers, C. D., and A. J. Prata (1981), Evidence for a traveling two-day wave in the middle atmosphere, J. Geophys. Res., **86**, 9661-9664.

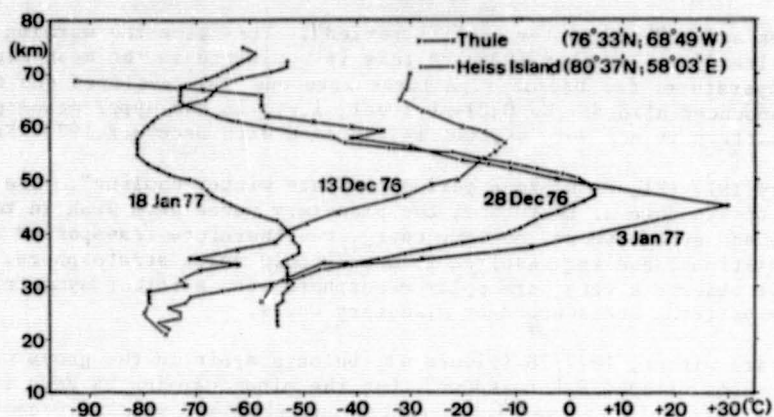


Figure 1. Rocketsonde measurements during the winter 1976/77.

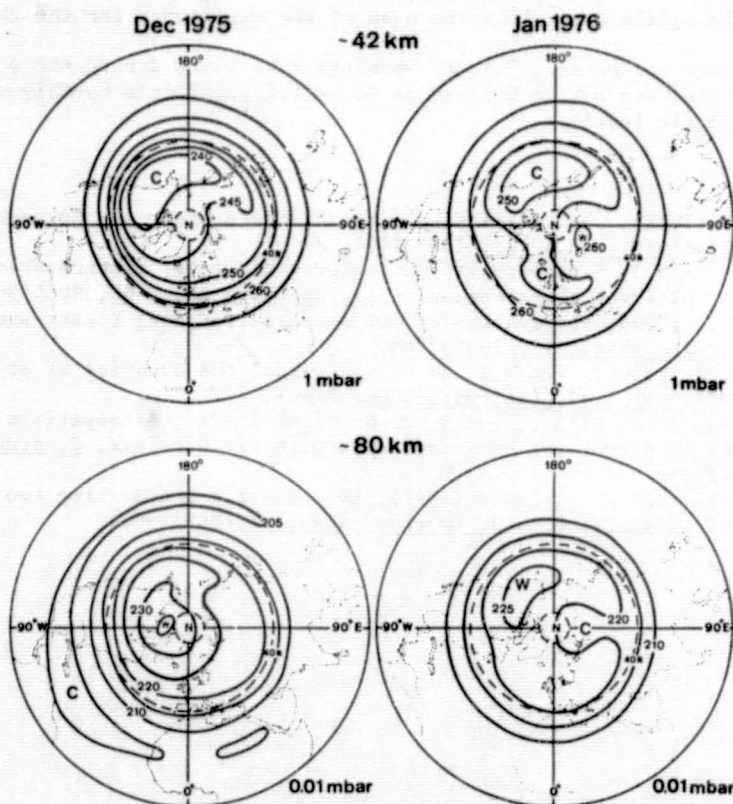


Figure 2. Monthly mean 1- and 0.01-mb temperature maps for December 1975 and January 1976.

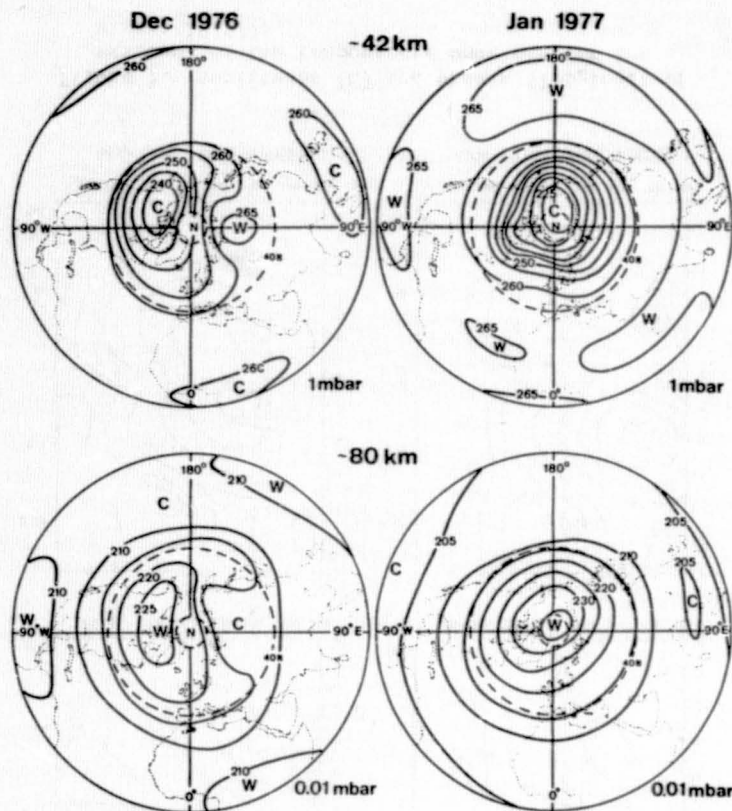


Figure 3. As Figure 2, but for the winter 1976/77.

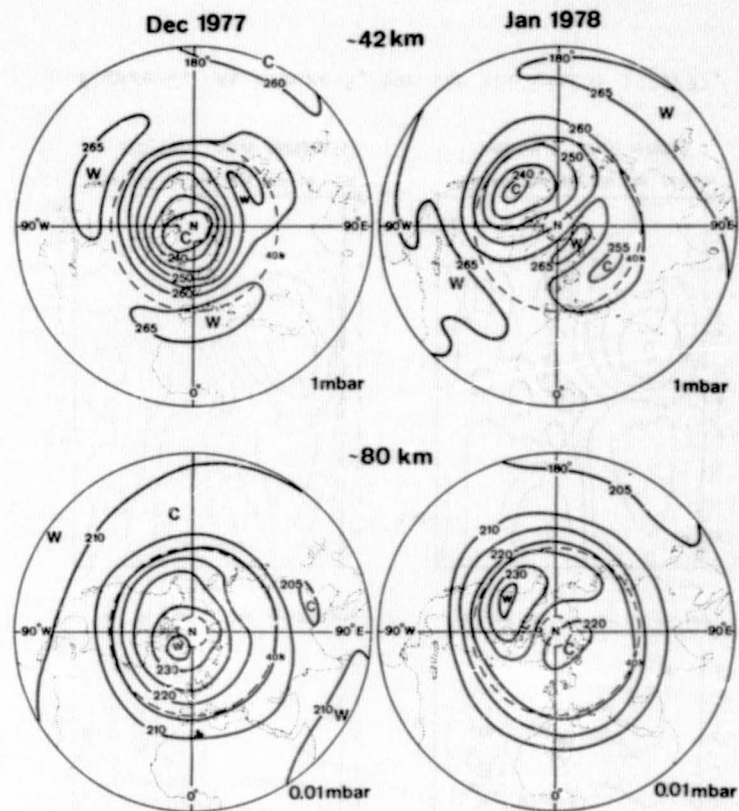


Figure 4. As Figure 2, but for the winter 1977/78.

ORIGINAL PAGE IS
OF POOR QUALITY

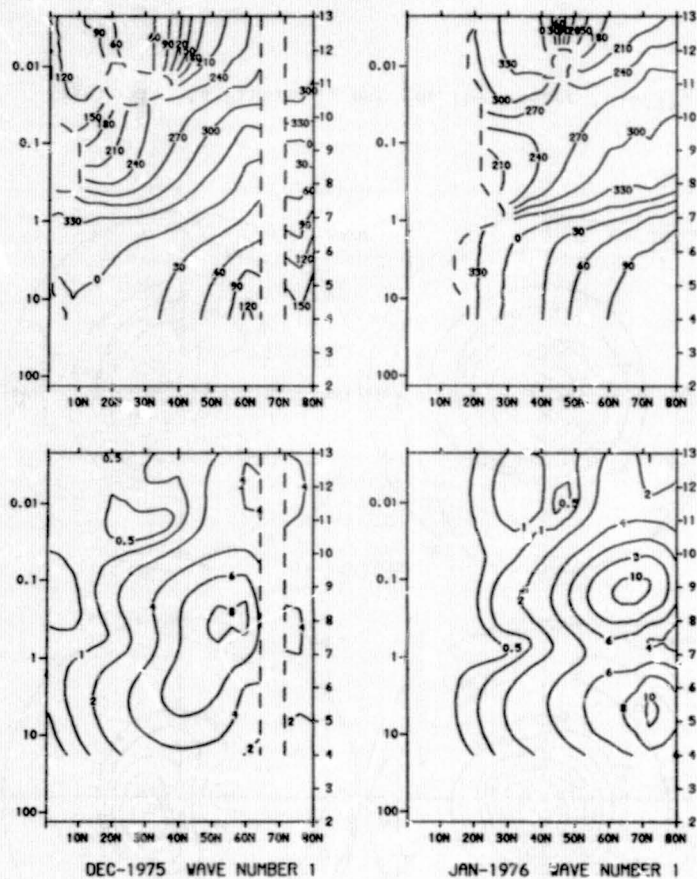


Figure 5. Amplitudes (K) and phases (longitude of maximum) of the temperature wave one for the winter 1975/76.

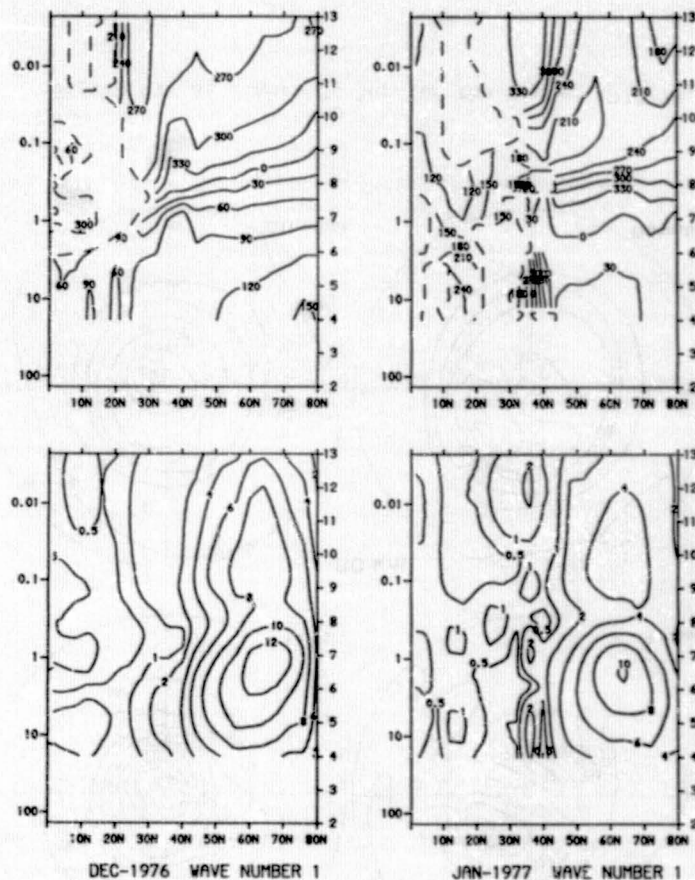


Figure 6. As Figure 5, but for the winter 1976/77.

ORIGINAL PAGE IS
OF POOR QUALITY

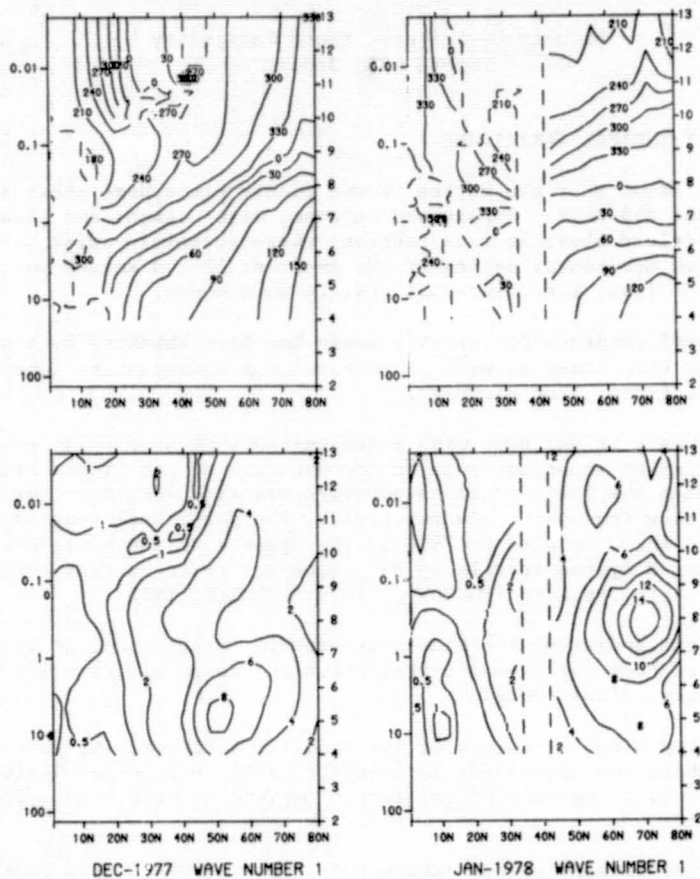


Figure 7. As Figure 5, but for the winter 1977/78.

D8

N86-12822

2.3.2a GRAVITY WAVES

I. Hirota

Faculty of Science, Kyoto University
Kyoto 606, Japan

SEASONAL AND LATITUDINAL VARIATIONS

It is well known that the motion in the middle atmosphere shows a broad spectrum in space and time. Superposed on zonal mean motions and planetary-scale waves described above in this section, there certainly exist wind fluctuations with horizontal scales of the order of 10-100 km and periods of the order of hours or less, i.e., internal gravity wave modes.

Observational evidence for gravity waves has been obtained by a wide variety of radar techniques as well as rocket-borne measurements (see the review of FRITTS et al. (1984), for example).

In recent years it has been widely recognized that vertically propagating gravity waves play an important role in the dynamics of the middle atmosphere in partly determining the large-scale temperature and wind structure through their energy and momentum transport. In particular, the meridional temperature distribution and the mean wind profile in the upper mesosphere are considered to be largely affected by the turbulence diffusion and friction that gravity waves induce through their breaking (HOUGHTON, 1978; LINDZEN, 1981).

For an understanding of the middle atmosphere circulation, it is therefore very important to know the global distribution and temporal variation of gravity waves in a climatological sense.

In this subsection the result of the statistics for gravity wave activity in the stratosphere and mesosphere is presented as a function of latitude and month, with the aid of meteorological rocket network observations. For detail see HIROTA (1984).

High altitude meteorological data supplied by the World Data Center A are used in these statistics for the 4-year period from 1977 to 1980. Thirteen stations covering a wide range of latitudes are selected for which a large number of rocket data are available. The average number of observation days at each station is about 360 for the four years.

Rocket observations of zonal wind component U , meridional wind component V and temperature T are used at an interval of 1 km. The height range is between 20 and 65 km in most cases.

First, in order to remove the contribution of large-scale components such as the mean field, planetary waves and tides, a high-pass filter is applied to the daily data with respect to height. By this filtering, the fluctuations with characteristic vertical scales less than about 10 km are separated.

Figure 1 shows an example of the wind and temperature fluctuations at Thule (77°N). In the filtered data, wave-like disturbances with a vertical scale close to or less than 10 km are seen. They are considered to be due to internal gravity waves.

Then, as a measure of the gravity wave intensity, an estimate is made of the root-mean-square (rms) of the second-order derivatives with respect to height for each component (U, V, T) and for each observation day.

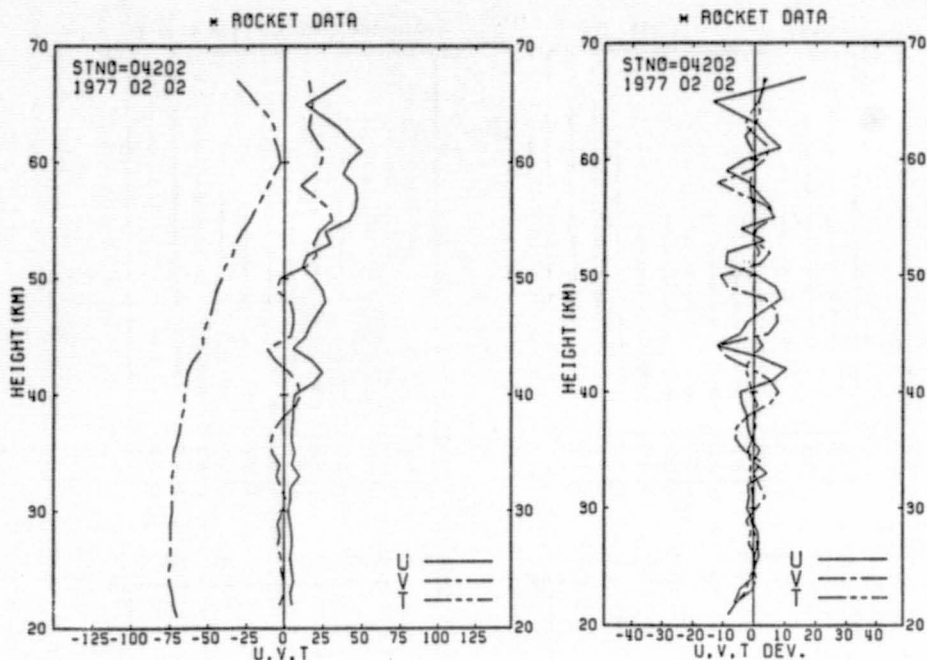


Figure 1. An example of the vertical distribution of wind and temperature at Thule (77°N) for February 2, 1977. (left) raw data, (right) filtered data. Units are m/s for wind and K for temperature.

It is found that the daily values of the intensity of zonal and meridional wind components are considerably variable and random with each other, but the rms values of the two components are almost equal in magnitude in a statistical sense. This is an indication of the isotropy of gravity waves in their orientation. Hence, in the following statistics, the two components are averaged to give a measure of the intensity of wind fluctuations.

The gravity wave intensity thus defined is again averaged for each month (of the four years) to obtain climatological mean values at each station, together with the estimate of the standard deviation around the monthly mean.

Figure 2 shows the seasonal variation of the gravity wave intensity, i.e., rms amplitudes of wind and temperature, for four typical stations. The standard deviation around the monthly mean is denoted by vertical bars.

In high latitudes (Thule, 77°N and Primrose Lake, 55°N), it can be seen that both the wind and temperature rms value show a notable annual cycle with the maximum in winter. Roughly speaking, the maximum value in winter is twice as large as the minimum in summer for wind, while the annual variation in percent for temperature seems to be larger than that for wind.

On the other hand, in lower latitudes (White Sands, 32°N and Ascension Island, 8°S), such a notable annual variation cannot be seen. Results of harmonic analysis indicate that the semiannual component is rather larger than the annual component, especially in the temperature variation. The maximum value of the semiannual cycle appears near the equinox. This fact is probably

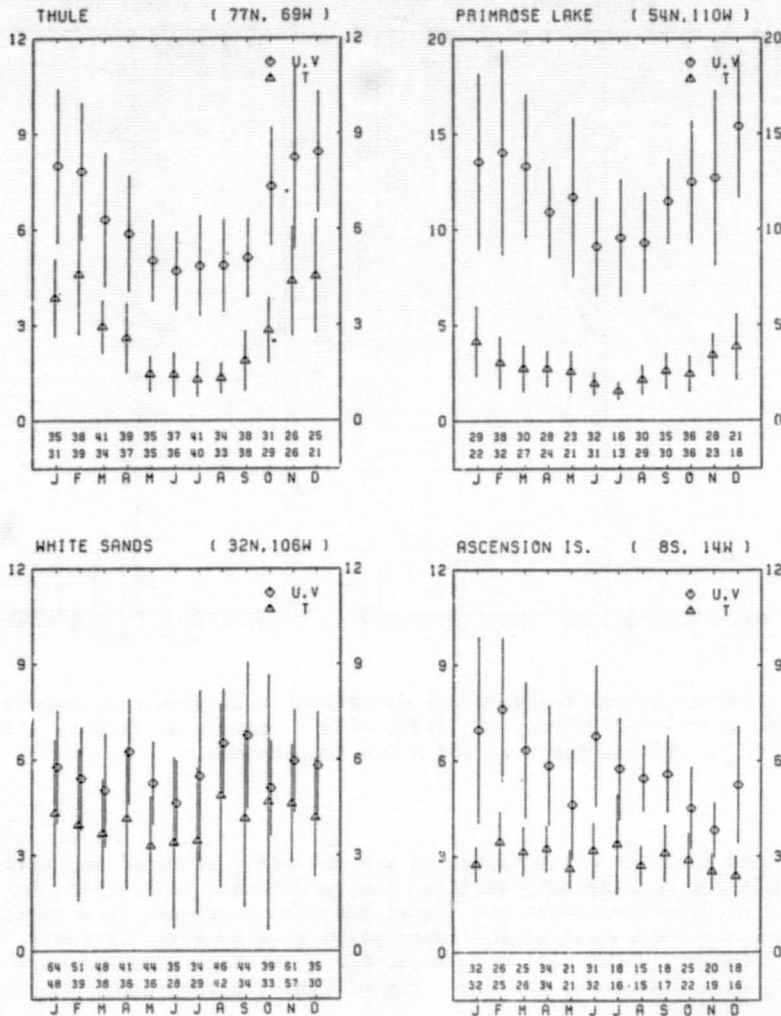


Figure 2. Seasonal variation of rms values of gravity wave intensity at four stations. Vertical bars denote the standard deviation. Units are $\text{m sec}^{-1} \text{ km}^{-2}$ for wind and K km^{-2} for temperature. Figures above the abscissa are total number of rocket observations used in these statistics for wind (above) and temperature (below).

related to the seasonal variation of the mean zonal wind in the middle atmosphere presented in a previous subsection.

The seasonal and latitudinal dependency of the gravity wave intensity is summarized in Figure 3. The values at two stations adjacent in latitude are not always close to each other, so that in this figure the latitudinal variation is smoothed to some extent. Moreover, there are no data in a latitude zone between 38°N and 54°N . Nevertheless, the contrast in the seasonal change is clearly seen between high and low latitudes.

Another interesting aspect of gravity wave activity is transiency. In the middle atmosphere, gravity waves are likely to be as variable as their generation

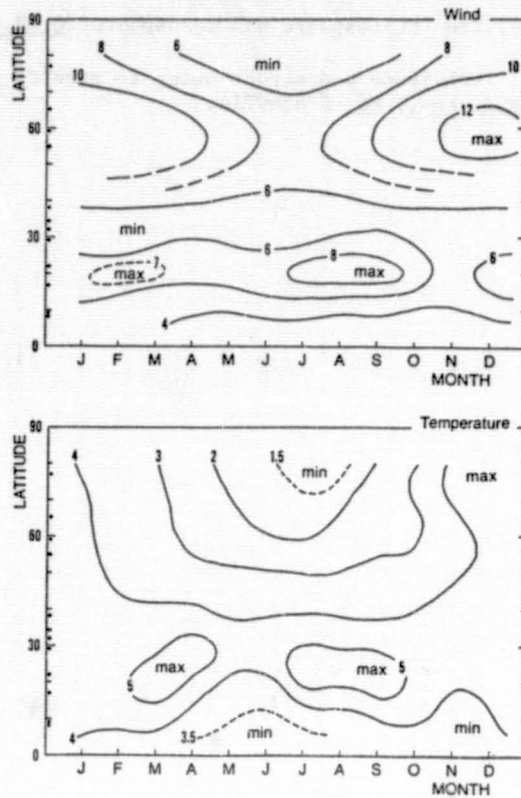


Figure 3. Latitude-time section of rms values for wind (above) and temperature (below) in the same units as those of Figure 2. Circles on the ordinate denote the rocket stations.

processes in the lower atmosphere which have a wide range of time scales from hours to days.

Such transient variability can indeed be observed in Figure 2. With regard to the wind fluctuation, the standard deviation is about one third as large as the monthly mean value throughout a year. Since the launch frequency for the present rocket network is approximately once per four days on the average, the typical time scale of the gravity wave transiency cannot be inferred.

In conclusion, the climatology of gravity waves in the middle atmosphere as shown in Figures 2 and 3 should be regarded as an ensemble mean of time-dependent, stochastic processes, in contrast to the quasi-steady state of large-scale motions such as mean zonal wind and planetary waves.

REFERENCES

- Fritts, D. C. et al. (1984), Research status and recommendations from the Alaska Workshop on Gravity Waves and Turbulence in the Middle Atmosphere, Bull. Am. Meteorol. Soc., **65**, 149-159.
- Hirota, I. (1984), Climatology of gravity waves in the middle atmosphere, J. Atmos. Terr. Phys., **46**, 767-773.

- Houghton, J. T. (1978), The stratosphere and mesosphere, Q. J. Roy. Meteorol. Soc., 104, 1-29.
- Lindzen, R. S. (1981), Turbulence and stress owing to gravity wave and tidal breakdown, J. Geophys. Res., 86, 9707-9714.

2.3.2b GRAVITY WAVES

T. E. VanZandt

Aeronomy Laboratory
National Oceanic and Atmospheric Administration
Boulder, Colorado 80303

SPECTRAL DESCRIPTION OF MESOSCALE FLUCTUATIONS

Atmospheric parameters fluctuate on all scales. In the mesoscale these fluctuations are occasionally sinusoidal so that they can be interpreted as gravity waves. Usually, however, the fluctuations are noise-like, so that their cause is not immediately evident. VANZANDT (1982) and others have suggested that they are due to a random field of gravity waves. GAGE (1979) suggested that they are the result of two-dimensional turbulence. See LILLY (1983) for a review of the situation.

For the purposes of this section, the term mesoscale is defined as including motions with vertical scales ranging from roughly 5 km down to less than 40 m, horizontal scales from a few hundred kilometers down to about a kilometer, and time scales from roughly a day down to the buoyancy (Brunt-Vaisala) frequency of 5 - 10 minutes.

Results of mesoscale observations in the 20 to 120 km altitude range that are suitable for incorporation into a model atmosphere are very limited. In the stratosphere and lower mesosphere observations are sparse and very little data has been summarized into appropriate form. There is much more data in the upper mesosphere and lower thermosphere, but again very little of it has been summarized.

A convenient and commonly used statistical description of these fluctuations is in terms of power spectra. This description is made simpler and more useful because it turns out that both the shape and amplitude of the spectra appear to be remarkably insensitive to variations of related geophysical variables, such as background wind, atmospheric stability, altitude, latitude, underlying topography, etc.

Spectral amplitudes will be denoted by F . The dependent variables to be considered are the horizontal and vertical velocity, u and w , and the independent variables are the horizontal wave number k , the vertical wave number m , and the frequency ω . In the graphs the independent variable is $\log k$, $\log m$, or $\log \omega$, as is usual. The amplitude of the spectra is plotted as $\log(kF(k))$, $\log(mF(m))$ or $\log F(\omega)$.

$$mF_u(m)$$

The available mesoscale spectra of horizontal wind u versus vertical wave number m in the 20 to 120 km altitude range are shown in Figure 1, together with a spectrum from the lower atmosphere for comparison. Further information about these spectra is given in Table 1. In spite of the large range of altitudes and latitudes, the spectra from the lower atmosphere (NASA, 1971 and DEWAN, 1984) are remarkably similar in both shape and amplitude. The mean slopes of -2.38 for the NASA spectrum and -2.7 for the Dewan spectra are supported by the mean slope of -2.75 found by ROSENBERG et al. (1974).

The mesospheric spectrum (VINCENT, 66-96 km) is too short to establish a shape. Its amplitude is about an order of magnitude larger than the NASA

spectrum in the same wave number range.

The NASA and Dewan spectra suggest that the mesoscale spectra in the lower atmosphere are insensitive to meteorological conditions. Meteorological data of the Dewan spectra were not given, but presumably the conditions for the five spectra were diverse. The NASA spectra were taken throughout the year under a wide variety of weather conditions at Cape Kennedy, yet the standard deviation of the 1200 independent spectra about the mean spectrum is only about a factor of two. Moreover, ENDLICH et al. (1969) show mean spectra (from the same data set as the NASA spectrum) on three days with peak winds of 18, 41, and 62 m/s, that is, with energy densities per unit mass in synoptic scales ranging over about a factor of 10. Yet the spectral shapes for scales smaller than 5 km were essentially identical and the spectral densities ranged over a factor of only 2 - 3, with the 18 m/s day always the smallest but with the 41 m/s day the largest in the 1 to 5 km range.

HIROTA (1983) also studied the climatology of mesoscale fluctuations between 20 and 65 km using vertical profiles of horizontal wind data from the Meteorological Rocket Network. In order to characterize the amplitude of the fluctuations, he used the rms value of the second derivative of the wind versus altitude, which emphasizes the smaller scale fluctuations. The range of amplitudes of this quantity was found to be about a factor of three, from a minimum at low latitudes to a maximum at about 60 deg latitude in winter. This result is not inconsistent with the weak dependence of the amplitude of spectra found in the present study.

$$\frac{kF_u(k)}{u}$$

Because of obvious experimental difficulties, no spectra of $F(k)$ are available in the altitude range from 20 to 120 km. There are many studies of $F(k)$ at lower altitudes, however, which, because of the apparent insensitivity of the spectra to altitude, should be relevant to the 20 to 120 km range. The definitive study of NASTROM and GAGE (1985) used very extensive, homogeneous, aircraft data between 9 and 14 km. A straight line approximation to the sum of their zonal and meridional spectra, that is, to the spectrum of the vector wind, is shown in Figure 1 as "NG, 9-14 km". Further information is given in Table 1. They found that the mean zonal and meridional spectra were the same, that the amplitude of the mean spectra depended only weakly on atmospheric stability (the stratospheric amplitude was 1.2 to 1.5 times larger than the tropospheric amplitude) and season (with summer being smallest), and that there was an apparent latitude variation of a factor of 2 to 4 between the 15°S to 15°N zone and the 45°N to 60°N zone. The standard deviation of 2718 independent spectra was about a factor of 2.5.

It may be noted that the same spectral energy density is found in the $kF(k)$ and $mF(m)$ spectra but at values of k from 10 to 100 times smaller than the corresponding values of m (that is, at horizontal scales from 100 to 10 times larger than the vertical scales). This is a result of the horizontal elongation of the mesoscale motions relative to the vertical because of the suppression of vertical motions by buoyancy forces. Such stratification is also evident in the stratosphere and lower mesosphere in horizontally separated simultaneous wind profiles (LESTER and TOLEFSON, 1964; MAHONEY and BOER, 1968; MARSHALL, 1969) and sequential profiles (WEINSTEIN et al., 1966; ENDLICH et al., 1969; JOHNSON and VAUGHAN, 1978).

$$\frac{F_u(\omega)}{u}$$

Table 1 Information on the Spectra

Fig.	Spectrum	Designation	Reference	Altitude (km)		Latitude	Method	Comments
				Range	Mean			
1.	$mF_u(m)$	NASA	NASA	4-16	10	28.5°N	Jimsphere balloon	scalar wind
		Dewan	A	29-42	36	38°N	smoke trail	scalar wind
			B	22-34	28	38°N		
			C	18-28	26	33°N		
			D	20-31	28	33°N		
			E	16-32	27	59°N		
		Vincent	(1984)	66-96	81	35°S	radar	vector wind
1.	$kF_u(k)$	NG	Nastrom & Gage (1984)	9-14	11.5	50°N ⁽¹⁾	aircraft	vector wind
2.	$F_u(\omega)$	BC	Balsley & Carter (1983)	7.0-9.2	8.1	65°N	radar	zonal wind
		Vincent	(1984)	85-87	86	65°N	radar	zonal wind
				82.75-87.25	85	$\left\{ \begin{matrix} 35^\circ S \\ 19^\circ S \end{matrix} \right\}$	radar	av. zonal + merid.
3.	$F_w(\omega)$	Ecklund et al.	(1983)	3.9-6.1 10.6-12.9	5.0 11.8	43.5°N	radar	
		Röttger	(1981)	21.75-23.25	22.5	52°N	radar	} plotted on a relative scale
	$\omega F_w(\omega)$	Tolstoy & Montes	(1971)	---	130	41°N	radio	
				---	175			
				---	240			

(1) Mean latitude. The range was 22°N to 61°N.

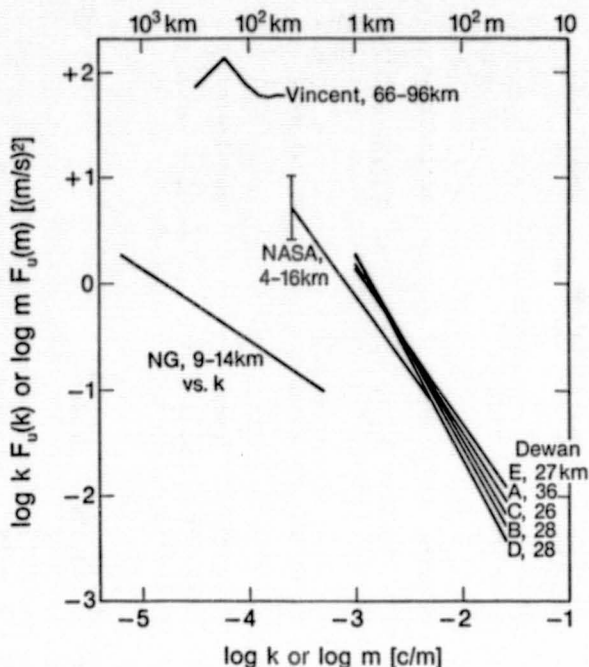


Figure 1. Spectra of $\log k F_u(k)$ or $\log m F_u(m)$ versus $\log k$ or $\log m$, where u is the horizontal wind and k and m are the horizontal and vertical wave numbers, respectively. For further information see Table 1.

The available mesoscale spectra of horizontal wind u versus frequency in the 20 to 120 km altitude range are shown in Figure 2, together with a typical tropospheric spectrum. Further information on these spectra are given in Table 1. Again, in spite of the wide range of latitudes and season, the spectra from Townsville, Adelaide and Poker Flat are essentially identical in both shape and amplitude. Vincent finds that all of the published mesospheric spectra have powers between -1.5 and -2. Tropospheric spectra also have slopes in the same range, as is shown in Figure 2. Indeed, LARSEN et al. (1982) find an average slope of $1.60 \pm .27$ over the frequency range from 4.2×10^{-6} (c/s) (66 2/3 hr) to 1.25×10^{-4} (c/s) (2 2/9 hr).

$$F_w(\omega)$$

Spectra of vertical wind w versus frequency ω present a problem different from the other spectra considered. When the wind is small, the $F_w(\omega)$ spectra have similar shapes throughout the atmosphere from near the ground up to at least 250 km. When the wind is strong, however, the shape changes and becomes much more variable and the amplitude increases. The reasons for these changes are not fully understood, but they may be due to the vertical component of lee waves and to tilted isentropic surfaces that project properly horizontal motions onto the vertical. In Figure 3 are shown the available $F_w(\omega)$ spectra under light wind conditions. Geophysical parameters for these spectra are given in Table 1. Note that some of the spectra are plotted on relative scales and that the TOLSTOY and MONTES (1971) spectra are multiplied by ω .

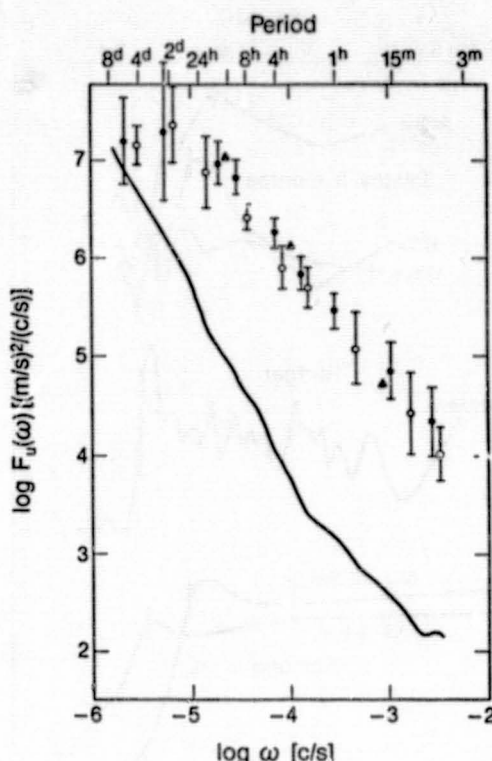


Figure 2. Spectra of $\log F_u(\omega)$ versus $\log \omega$, where u is the horizontal velocity and ω is the frequency. The curve is from 8.1 km; the points, from about 85 km. The triangles are from 65°N (BALSLEY and CARTER, 1982); the filled circles, from 35°S (VINCENT, 1984); and the open circles from 10°S (VINCENT, 1984). For further information see Table 1.

The similarity of shape is apparent. In every case the peak in the spectrum is near the local buoyancy frequency. It has been shown that the very similar peaks observed in oceanic vertical current spectra are due to the behavior of gravity waves near their turning point (DESAUBIES, 1975). There can be little doubt that the atmospheric peak has the same explanation. Therefore the high frequency part, at least, of the $F_w(\omega)$ spectra under light wind conditions must be due to gravity waves.

VARIATION OF SPECTRAL AMPLITUDE WITH ALTITUDE

Since the spectra shown in Figures 1-3 tend to have constant shapes in the mesoscale range, the variation of spectral amplitude with altitude can be simply characterized by the ratio of amplitudes at a typical wave number or frequency. The results are shown in Figure 4, where the logarithm of the ratio of amplitudes is plotted versus the logarithm of the ratio of atmospheric densities from the USSA 1976 model atmosphere. The corresponding nearly linear altitude scale is indicated on the right-hand ordinate. For the m spectra the amplitudes are referred to the NASA spectrum, which is taken to be at 10 km. For the ω spectra the amplitudes are referred to the BALSLEY and CARTER (1982) 8.1 km spectrum. This ratio is plotted as though the 8.1 km spectrum were actually at

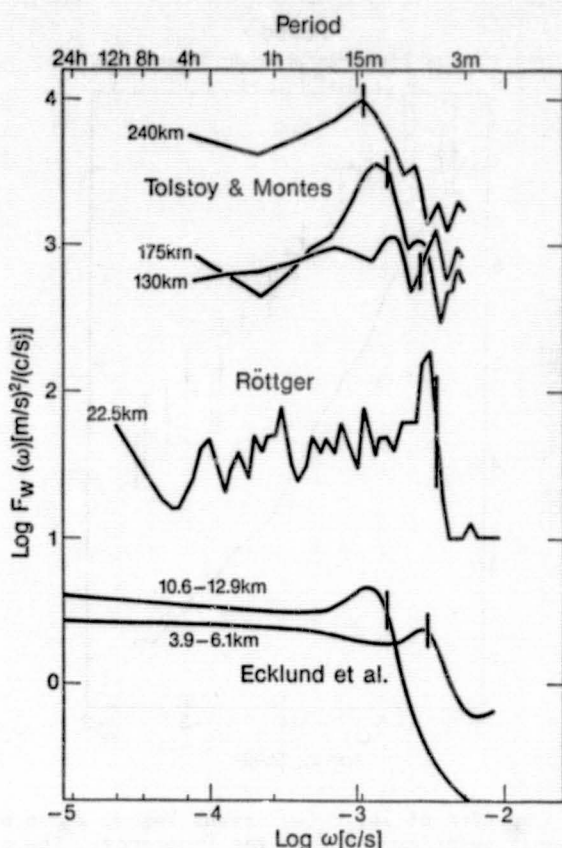


Figure 3. Spectra of $\log F_w(\omega)$ versus $\log \omega$, where w is the vertical velocity and ω is the frequency. Note that the Röttger and the Tolstoy and Montes curves are plotted on a relative scale and that the Tolstoy and Montes curves are multiplied by ω . For further information see Table 1.

10 km, which makes a negligible error. The bars through the points extend a factor of two on either side, in order to indicate in a very rough way the uncertainty of the points. The m points also extend over a considerable vertical distance, but this does not affect the conclusions.

The m ratios show very little variation with altitude. Indeed, a constant amplitude would not be inconsistent with the m ratios when all of the uncertainties are taken into account. The ω ratio indicates a larger variation with altitude, approximately as $(\rho(z))^{-0.4}$. The solid line with unit slope $((\rho(z))^{-1})$ to 60 km and the constant line above 60 km indicate the standard scenario for the growth of gravity waves in the atmosphere (FRITTS et al., 1984), corresponding to constant energy density per unit volume up to, say, 60 km and saturation with constant energy density per unit mass above. It is clear that the spectral data are inconsistent with this picture. If the observed fluctuations are indeed entirely due to gravity waves then the data indicate that there is considerable loss of wave energy at all heights above 10 km.

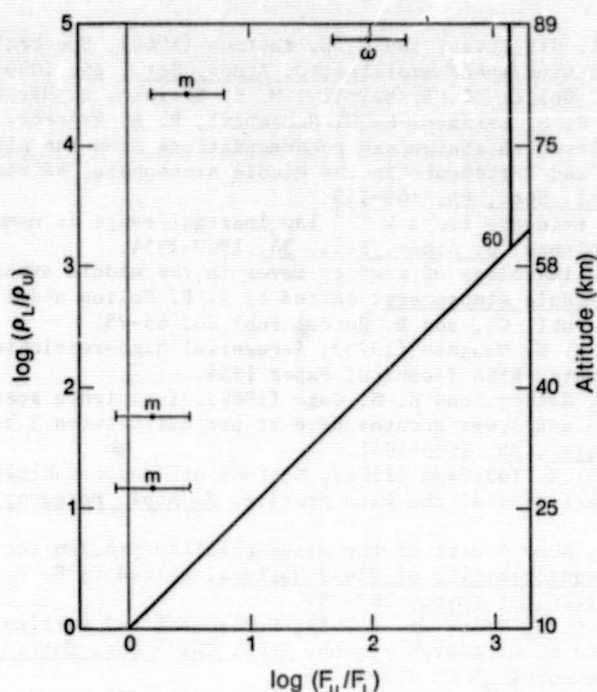


Figure 4. The ratio of spectral amplitudes in the mesoscale as a function of altitude. A 45° line corresponds to constant energy per unit volume, J/m^3 ; a constant line corresponds to constant energy per unit mass, $J/kg = (m/s)^2$, implying saturation of spectral amplitudes.

CONCLUSION

Study of mesoscale fluctuations in the atmosphere is currently a very active field. Thus, the picture described here will be significantly augmented and perhaps changed in the next few years. In the meantime, if a spectrum is needed in a region where it has not been observed, the best alternative would be to use the observed spectral shape scaled with altitude according to Figure 4.

REFERENCES

- Balsley, B. B., and D. A. Carter (1982), The spectrum of atmospheric velocity fluctuations at 8 km and 86 km, *Geophys. Res. Lett.*, **9**, 465-468.
- Desaubies, Y. J. F. (1975), A linear theory of internal wave spectra and coherences near the Vaisala frequency, *J. Geophys. Res.*, **80**, 895-899.
- Dewan, E. M., N. Grossbard, A. F. Quesada, and R. E. Good (1984), Spectral analysis of 10 m resolution scalar velocity profiles in the stratosphere, *Geophys. Res. Lett.*, **11**, 80-83.
- Dewan, E. M., N. Grossbard, A. F. Quesada, and R. E. Good (1984), Errata to "Spectral analysis of 10 m resolution scalar velocity profiles in the stratosphere", submitted to *Geophys. Res. Lett.*
- Ecklund, W. L., B. B. Balsley, M. Crochet, D. A. Carter, A. C. Riddle, and R. Garelo (1983), Vertical wind speed power spectra from the troposphere and stratosphere obtained under light wind conditions, *Handbook for MAP, VOL. 9*, 269.

- Endlich, R. M., R. C. Singleton, and J. W. Kaufman (1969), Spectral analysis of detailed vertical wind speed profiles, J. Atmos. Sci., **26**, 1030-1041.
- Fritts, D. C., M. A. Geller, B. B. Balsley, M. L. Chainin, I. Hirota, J. R. Holton, S. Kato, R. S. Lindzen, M. R. Schoeberl, R. A. Vincent, and R. F. Woodman (1984), Research status and recommendations from the Alaska Workshop on Gravity Waves and Turbulence in the Middle Atmosphere, Fairbanks, Alaska, Bull. Am. Meteorol. Soc., **65**, 149-159.
- Gage, K. S. (1979), Evidence for a $k^{-5/3}$ law inertial range in mesoscale two-dimensional turbulence, J. Atmos. Sci., **36**, 1950-1954.
- Hirota, I. (1984), Climatology of gravity waves in the middle atmosphere, in Dynamics of the Middle Atmosphere, edited by J. R. Holton and T. Matsuno. Terra Scientific Publ. Co. and D. Reidel Publ. Co. 65-75.
- Johnson, D. L., and W. W. Vaughan (1978), Sequential high-resolution wind profile measurements, NASA Technical Paper 1354.
- Larsen, M. F., M. C. Kelley, and K. S. Gage (1982), Turbulence spectra in the upper troposphere and lower stratosphere at periods between 2 hours and 40 days, J. Atmos. Sci., **39**, 1035-1041.
- Lester, H. C., and H. B. Tolefson (1964), A study of launch-vehicle responses to detailed characteristics of the wind profile, J. Appl. Meteorol., **3**, 491-498.
- Lilly, D. K. (1984), Some facets of the predictability problem for atmospheric mesoscales, in Predictability of Fluid Motions, edited by G. Holloway and B. J. West, Am. Inst. of Phys., 287-294.
- Mahoney, J. R., and G. J. Boer, Jr. (1968), Horizontal and vertical scales of winds in the 30 to 60 kilometer region, Proc. Third Nat. Conf. on Aerospace Meteorol., Am. Meteorol. Soc, 457-464.
- Marshall, J. C. (1981), Behavior of smoke trails, 30 to 70 km, J. Appl. Meteorol., **4**, 641-648.
- NASA (1971), Terrestrial Environment (Climatic) Criteria Guidelines for use in Aerospace Vehicle Development, 1971, 1973, and 1982 revisions. NASA TM X-64589 (1971), Daniels, G. E.; NASA TM X-64757 (1973), Daniels, G. E.; NASA TM 83473 (1982), Turner, R. E., and C. K. Hill.
- Nastrom, G. D., and K. S. Gage (1985), A climatology of atmospheric wavenumber spectra of wind and temperature observed by commercial aircraft, J. Atmos. Sci., **42**, 950-960.
- Rosenberg, N. W., R. E. Good, W. K. Vickery, and E. M. Dewan (1974), Experimental investigation of small scale transport mechanisms in the stratosphere, AIAA J., **12**, 1094-1099.
- Rottger, J. (1981), Wind variability in the stratosphere deduced from spaced antenna VHF radar measurements, Preprint Vol. 20th Conf. on Radar Meteorology, Nov. 30-Dec 3, Boston, MA, Am. Meteorol. Soc., 22-29.
- Tolstoy, I. and H. Montes (1971), Phase height fluctuations in the ionosphere between 130 and 250 km, J. Atmos. Terr. Phys., **33**, 775-781.
- VanZandt, T. E. (1982), A universal spectrum of buoyancy waves in the atmosphere, Geophys. Res. Lett., **9**, 575-578.
- Vincent, R. A., Gravity-wave motions in the mesosphere, submitted to J. Atmos. Terr. Phys.
- Weinstein, A. I., E. R. Reiter, and J. R. Scoggins (1966), Mesoscale structure of 11-20 km winds, J. Appl. Meteorol., **5**, 49-57.

2.3.3 ATMOSPHERIC TIDES BELOW 80 KM

Jeffrey M. Forbes

N86-12824

Department of Electrical, Computer, and System Engineering
Boston University
Boston, MA 02215

Gerald V. Groves

Department of Physics and Astronomy
University College London, Gower Street
London WC1E 6BT, Great Britain

ABSTRACT

Measurements of diurnal and semidiurnal tidal oscillations between about 25 and 80 km are reviewed. At latitudes greater than about 30 deg, S-N wind components are consistently in quadrature with and similar to the W-E components. The tidal structures are interpreted as a superposition of quasi-steady higher-order modes excited in the troposphere by sources of limited extent ($\sim 10^3$ km). At latitudes less than about 30 deg, steady or quasi-steady diurnal and semidiurnal components are not necessarily the dominant components of daily variation. At high latitudes diurnal phases generally show little change with height in comparison with observations at lower latitudes in accord with the latitudinal properties of positive and negative diurnal modes.

DATA SOURCES

Above 80 km the main body of tidal data comes from meteor partial reflection drift, MST, and incoherent scatter radar measurements. Most of the mesosphere, however, is inaccessible to these techniques, at least for the purposes of extracting tidal information (data series covering a significant fraction ($\geq 70\%$) of the day). Below 35 km ST radars are beginning to provide tidal information, but here the tidal amplitudes are relatively small and are sought after more for theoretical than practical reasons. In the intervening altitude region the primary source of tidal data is from a number of rocket launch series which have been performed between 1965 and 1974 (see Table 1). Of particular interest are 70 rockets equipped with standard Datasonde instrumentation which were launched on 19-20 March 1974 at eight Western Hemisphere sites by the NASA Wallops Flight Center in cooperation with other agencies, to study atmospheric tides and their latitudinal variations (SCHMIDLIN et al., 1957). All of these data are analyzed by GROVES (1980), and a representative sampling plus the major conclusions to emerge from that study are presented here.

SUMMARY OF TIDAL CHARACTERISTICS

Middle Latitudes

The diurnal wind oscillations derived for 23-25 October 1968 and 13-15 December 1967 at Cape Kennedy are shown in Figure 1 in comparison with theoretical phase profiles for the migrating Hough modes (1,1,1) to (1,1,5); observed phases are seen to correspond most nearly with modes of higher order than the leading (1,1,1) mode. Amplitudes lie in the range 5 - 15 m/s between 25 and 60 km. The slope of the phases with respect to height points to a tropospheric source for the oscillation. A notable property of the Cape Kennedy results of 23-25 October 1968 is that the profiles of S-N and W-E

Table 1. Diurnal launch series 1965-74.

Site	Latitude	Longitude W	Date	Number of successful launchings
Thule	76° 33' N	68° 49'	24-26 Oct 1968	14
Fort Churchill	58° 44'	93° 49'	6-8 Sept. 1966	10
			8-9 Sept. 1966	10
			4-5 Jan. 1968	12
			23-25 Oct. 1968	18
			19-20 Mar. 1974	8
Wallops Island	37° 50'	75° 29'	19-20 Mar. 1974	13
Arenosillo	37° 06'	06° 44'	24-28 Feb. 1970	27
White Sands	32° 23'	106° 29'	30 June-2 July 1965	17
			9-11 Oct. 1965	16
Cape Kennedy	28° 27'	80° 32'	13-15 Dec. 1967	25
			23-25 Oct. 1968	17
Antigua	17° 09'	61° 47'	19-20 Mar. 1974	8
Fort Shrmann	09° 20'	79° 59'	19-20 Mar. 1974	8
Kourou	05° 08'	52° 37'	19-22 Sept. 1971	13
			19-20 Mar. 1974	10
Natal	05° 55' S	35° 10'	1966-68	24
			19-20 Mar. 1974	8
Ascension Island	07° 59'	14° 25'	11-12 Apr. 1966	13
			12-13 Apr. 1966	13
			24-26 Oct. 1968	14
			19-20 Mar. 1974	8
Mar Chiquita	37° 45'	57° 25'	19-20 Mar. 1974	7

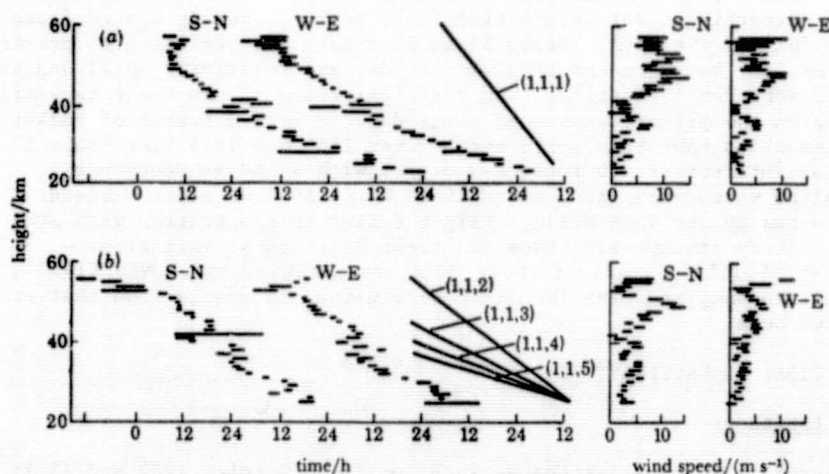


Figure 1. Diurnal wind components at Cape Kennedy. The straight lines indicate the approximate theoretical slopes of the phase profiles of the first five positive migrating modes. (a) 23-25 October 1968, 17 launchings in 48 hours. (b) 13-15 December 1967, 25 launchings in 48 hours (GROVES, 1980).

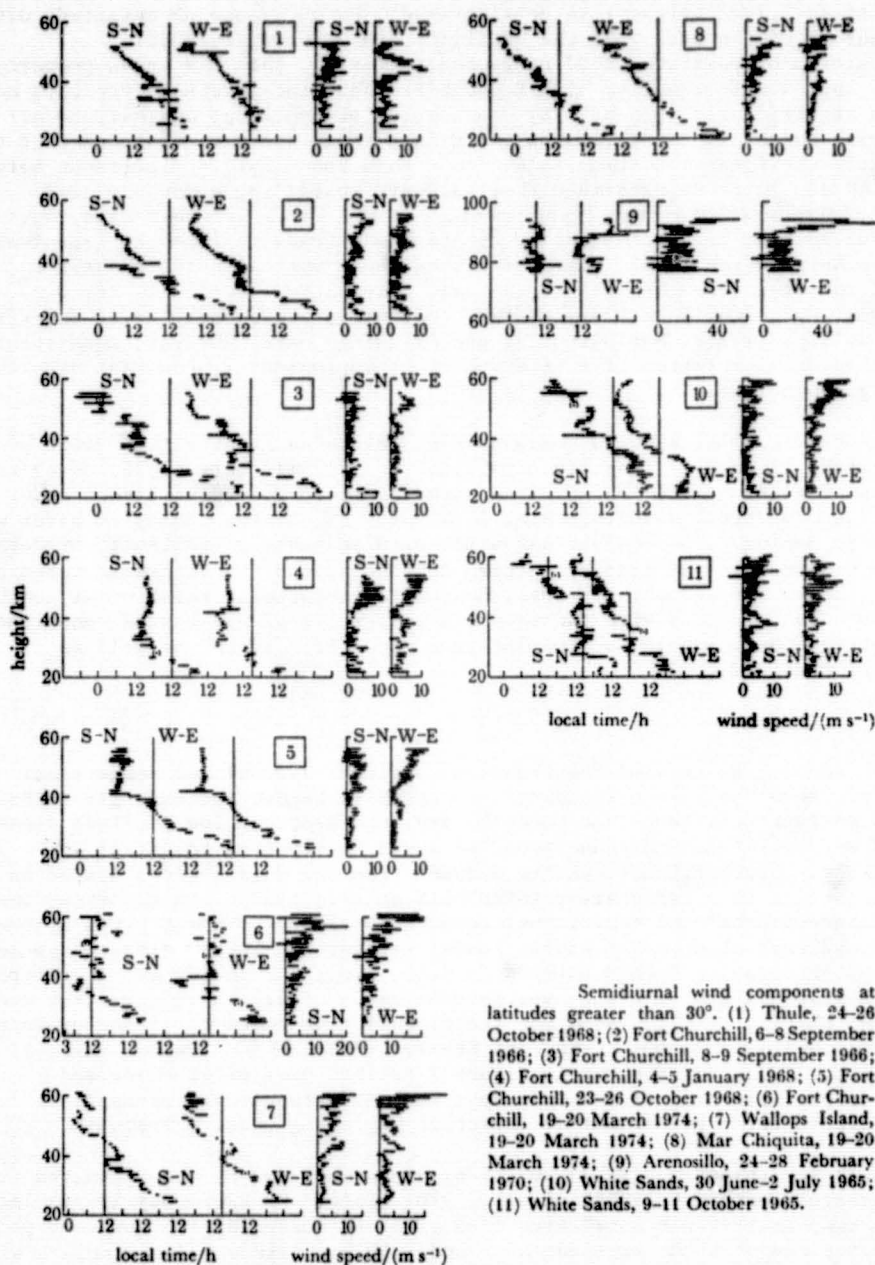
amplitudes show no significant differences and that W-E phases at all heights are later than S-N phases by close to 6 h. In other words, the diurnal wind vector at any given height rotates clockwise with no change of magnitude within the accuracy of the data. If the oscillation may be regarded as a superposition of positive ($n > 0$) Hough modes ($1, s, n$), then the above property implies approximate equality of W-E and S-N Hough wind functions for each mode that is significantly present. By examination of numerical evaluations of Hough wind functions for various s and n (not shown here) it is found that this apparently stringent condition holds (to within about 20%) at latitudes between 20 and 40 deg latitude, provided that eastward travelling modes are small compared with westward travelling modes. For the 13-15 December data, however, a clockwise rotating wind vector of constant magnitude is found at less than half the heights analysed. This was traced to an unsteadiness in the W-E diurnal component from one day to the next, the cause of which is unknown. Additional data from launchings at the other midlatitude stations of the White Sands, Wallops Island, Mar Chiquita, and Arensillo, are, however, consistent with the diurnal rotation of a wind vector of approximately constant magnitude at any given height.

The measured semidiurnal wind components at latitudes greater than about 30 deg latitude (Figure 2) indicate amplitudes of 3-12 m/s between 25 and 60 km, and phase variations with height indicative of the presence of higher order modes (i.e., vertical wavelengths of 15 km or less, corresponding to modes with n as large as 10). The semidiurnal winds also indicate a similarity between S-N and W-E profiles at middle and high latitudes, and the clockwise rotation of the wind vector at northern latitudes and anticlockwise rotation at southern latitudes are in accord with the expected properties of Hough wind functions. The above properties hold for nonmigrating modes ($2, s, n$) $s \neq 2$ as well as migrating modes ($2, 2, n$).

Low Latitudes

S-N and W-E Hough wind functions for positive diurnal and semidiurnal modes (not shown here) are found by inspection to become increasingly different in form at latitudes less than about 15 deg, and hence at low latitude sites S-N and W-E amplitude and phase profiles would be expected to differ appreciably. Observational results deduced from the data sources listed in Table 1 confirm this expectation (SCHMIDLIN et al., 1957). In addition, the low-latitude diurnal and semidiurnal components are not characterized by the quasi-steadiness observed at midlatitudes; rather, day-to-day differences occur which appear to arise from a nontidal source, i.e., one that does not correlate with the hour angle of the sun over several days. This confirms earlier conclusions (BEYERS, et al., 1966) for the diurnal tide based on a smaller data set. Diurnal wind components at Fort Sherman (9°N, 80°W), Kourou (5°N, 52°W), and Natal (6°S, 35°W) as shown in Figure 3 exhibit dissimilar phase and amplitude profiles even on the same day; such differences are perhaps explicable in terms of asymmetric and/or nonmigrating tidal components.

Lower stratospheric (12-35 km) tidal winds measured by the Jicamarca (12°S) radar are reported by FUKAO et al., (1978, 1981). On 23-24 May 1974 a large diurnal component in the zonal wind (1-5 m/s) was observed with downward phase progression and vertical wavelength of order 10 km. These values compare with theoretical estimates (LINDZEN, 1967) for the migrating diurnal tides of order .2 - .5 m/s and vertical wavelength near 28 km. The observations are interpreted as being connected with topographically induced nonmigrating diurnal tides similarly revealed in radiosonde data (WALLACE and TADD, 1974). The 23-24 May 1974 data show a predominance of the semidiurnal oscillation below the tropopause. By way of contrast, Jicamarca horizontal wind data for 3 - 4 October and 6 - 8 December 1977 exhibit characteristics strikingly similar to those expected of the migrating diurnal tide (LINDZEN, 1967). The observed



Semidiurnal wind components at latitudes greater than 30° . (1) Thule, 24-26 October 1968; (2) Fort Churchill, 6-8 September 1966; (3) Fort Churchill, 8-9 September 1966; (4) Fort Churchill, 4-5 January 1968; (5) Fort Churchill, 23-26 October 1968; (6) Fort Churchill, 19-20 March 1974; (7) Wallops Island, 19-20 March 1974; (8) Mar Chiquita, 19-20 March 1974; (9) Arenosillo, 24-28 February 1970; (10) White Sands, 30 June-2 July 1965; (11) White Sands, 9-11 October 1965.

Figure 2. Semidiurnal wind components derived from rocket launchings at latitudes greater than 30° (CROVES, 1980).

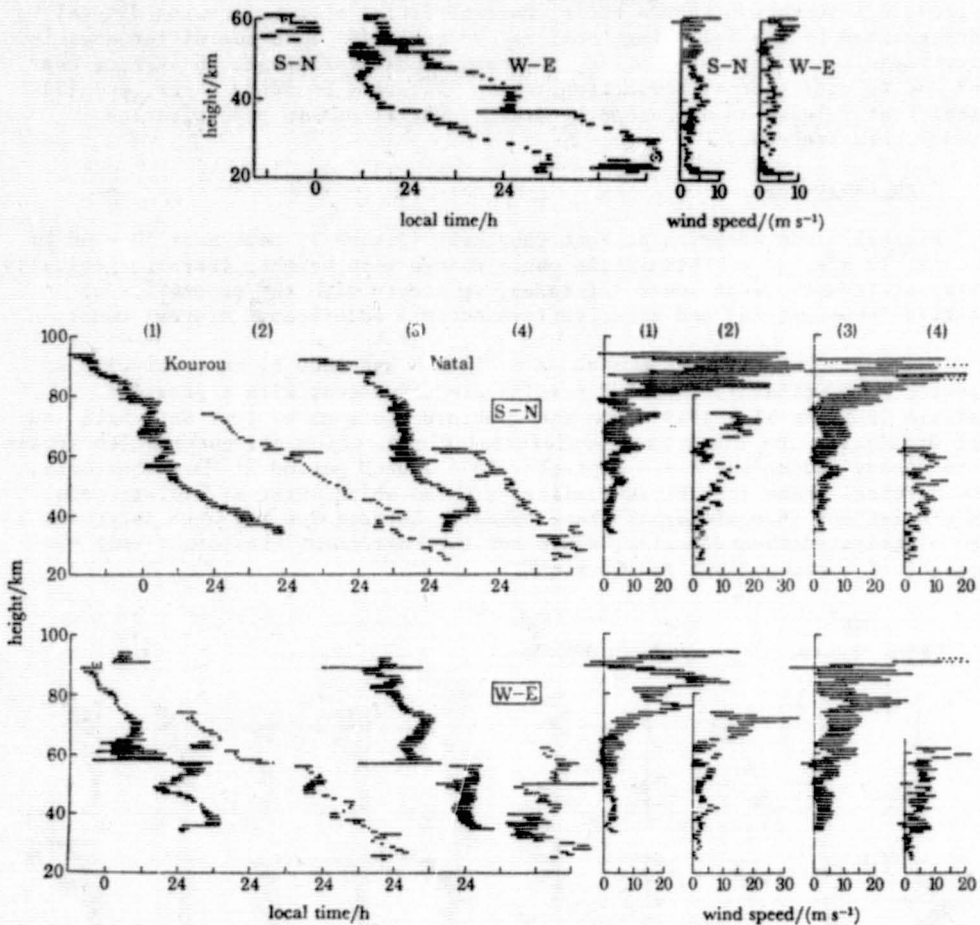


Figure 3. Diurnal wind components at (top) Fort Sherman, 19-27 March 1974, and at (middle and bottom) Kourou and Natal: (1) Kourou, 19-22 September 1971; (2) Kourou, 19-20 March 1974; (3) Natal, 1966-1968; Natal, 19-20 March 1974 (GROVES, 1980).

semidiurnal amplitudes ($.5 - 1.0$ m/s) are several times larger than estimated theoretically by LINDZEN and HONG (1974), and do not exhibit the characteristic mode near 30 km. The observed tendency of the semidiurnal phase to remain approximately constant with height over this altitude regime is consistent with behavior expected theoretically for the semidiurnal migrating tide.

KATO et al. (1982) investigated the generation and propagation characteristics of diurnal nonmigrating tides due to geographically localized sources of excitation. Their simulations reveal short vertical wavelength (~ 10 km) oscillations similar to the observations or stratospheric tides observed at Jicamarca and cited above. The perturbations are almost stationary and tend to increase in horizontal scale with altitude. The result of KATO et al. (1982) are semiquantitative in that the heat sources are poorly known, and somewhat arbitrary distributions have been adopted for the simulations. However, they

do provide information on the basic characteristics of nonmigrating diurnal tides excited by the following localized sources: (1) land-sea differences in water vapor insolation absorption, (2) topographic variations in surface heat flux due to eddy thermal conduction in the planetary boundary layer, and (3) latent heat release as suggested by diurnal variations in precipitation thunderstorm frequency.

High Latitudes

Diurnal winds observed at Fort Churchill (Figure 4) peak near 50 - 60 km at about 10 m/s and exhibit little phase change with height, characteristically different from those at lower latitudes, in accord with the properties of positive (propagating) and negative (evanescent) sequence of diurnal modes.

The S-N and W-E phases are close to 1200 h and 1800 h, respectively, as expected theoretically. The S-N results are consistent with a previous analysis (REED et al., 1969) from the combined stations of Fort Churchill and Fort Greely. On the other hand semidiurnal winds, which are observed to remain quite steady during the 6 - 9 September 1966 launch period at Fort Churchill, show vertical phase structures similar to those which exist at midlatitudes. This consistency in semidiurnal phase behavior between low and high latitudes is also anticipated theoretically, since for the semidiurnal component only one sequence of (propagating) modes exists.

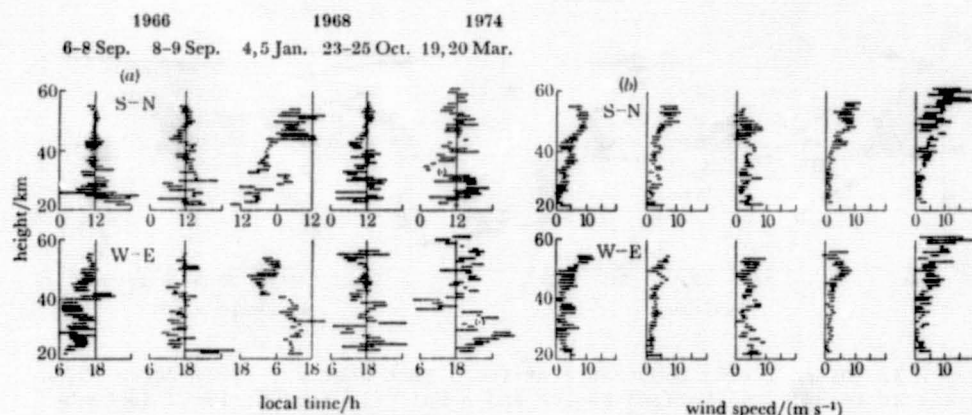


Figure 4. Diurnal wind components derived from rocket launchings at Fort Churchill (a) phases, (b) amplitudes (GROVES, 1980).

CONCLUSIONS

Atmospheric tides in the stratosphere and lower mesosphere are characterized by smaller amplitudes (5-15 m/s) shorter vertical scales (10 - 20 km), greater unsteadiness, and greater spatial variability than exhibited in the upper mesosphere and above. These properties reflect the influences of variable tropospheric excitations which occur over more local ($\sim 10^3$ km) than global scales. The associated short vertical scale oscillations are significantly damped by turbulent dissipation before they reach the mesopause region (ca. 85 km).

ACKNOWLEDGEMENTS

J. M. Forbes received support for this work under Grant ATM-8113078 from the National Science Foundation. G. V. Groves gratefully acknowledges the

award of a National Research Council Research Associateship at the Atmospheric Sciences Division, Air Force Geophysics Laboratory, Hanscom AFB, MA.

REFERENCES

- Beyers, N. J., B. T. Miers, and R. J. Reed (1966), Diurnal tidal motions near stratopause during 84 hours at White Sands Missile Range, J. Atmos. Terr. Phys., **23**, 325.
- Fukao, S., K. Aoki, K. Wakasugi, T. Tsuda, S. Kato, and D. A. Fleisch (1981), Some further results on the lower stratospheric winds and waves over Jicamarca, J. Atmos. Terr. Phys., **43**, 649.
- Fukao, S., S. Kato, S. Yokoi, R. M. Harper, R. F. Woodman, and W. E. Gordon (1978), One full-day radar measurement of lower stratospheric winds over Jicamarca, J. Atmos. Terr. Phys., **50**, 1331.
- Groves, G. V. (1980), Seasonal and diurnal variations of middle atmosphere winds, Phil. Trans. R. Soc. Lond., **A296**, 19.
- Kato, S., T. Tsuda, and F. Watanabe (1982), Thermal excitation of nonmigrating tides, J. Atmos. Terr. Phys., **44**, 131.
- Lindzen, R. S. (1967), Thermally driven diurnal tide in the atmosphere, Q. J. Roy. Meteorol. Soc., **93**, 18.
- Lindzen, R. S., and S. S. Hong (1974), Effects of mean winds and horizontal temperature gradients on solar and lunar semidiurnal tides in the atmosphere, J. Atmos. Sci., **31**, 1421.
- Reed, R. J., M. J. Oard, and M. Sieminski (1969), A comparison of observed and theoretical diurnal tidal motions between 30 and 60 kilometers, Mon. Weather Rev., **97**, 456.
- Schmidlin, F. J., Y. Yamasaki, A. Motta, and S. Brynzstein, NASA Rep. SP-3095, Washington, D. C.
- Wallace, J. M., and R. F. Tadd (1974), Some further results concerning the vertical structure of atmospheric tidal motions within the lowest 30 km, Mon. Weather Rev., **102**, 795.

2.3.4 COMPARISON OF TIME-PERIODIC VARIATIONS IN TEMPERATURE AND WIND FROM
METEOROLOGICAL ROCKETS AND SATELLITES

A. D. Belmont

Control Data Corporation, P. O. Box 1249,
Minneapolis, MN. 55440 USA

(shortened for this publication by K. Labitzke, Editor)

ABSTRACT

Although the Meteorological Rocket Network operated by or in cooperation with the United States has decreased from fourteen to nine stations in the past five years, there have been many observations accumulated in the ten years since CIRA 1972 was prepared with data up to 1969. The mean, annual and semi-annual variations of temperature and wind are presented and special attention is directed to the polar semiannual wave. The results are compared with the Oxford SCR-PMR five-year data set, the CDC-SCR seven-year data, and CIRA 1972 with respect to both temperature and zonal winds, as far as presently available. The agreement among the data sets is very good.

INTRODUCTION

The purpose of this paper is to review the available variability statistics for temperature and wind in the region from 20 to 70 km to help in the selection of the best information available for a revised CIRA. There are many different data sources but they will be limited here to those with at least five years of record. They will be intercompared with respect to their means, and periodic time variations. The satellite data were not operational, real-time data, but were processed years after the observations were made, taking account of all corrections that became known in the interim. These three sets are:

Variables	Source	Abbr.	Instrument & Period of Record
T, H, W	Oxford	OXF	2 years of SCR (1973-1974) plus 3 years PMR (1975-1977)
T	CDC	SCR	7 years of SCR (April 1970- April 1977)
T, W	WDC-A	MRN	Meteorological rockets (MRN) (1960-1982)

(T = temperature, H = geopotential altitude, W = wind)

These data sets have only recently been compiled and an evaluation of their differences has begun. The preliminary results will be reviewed here.

CIRA 1972 contained no satellite data for the range 25 to 60 km. Tables and graphs were based entirely on meteorological rocket data. In revising CIRA it was agreed that both satellite and rocket data would be examined and compared before deciding which data or combination of data would suit the purpose most reliably at this time.

Each instrument has its advantages and disadvantages. Satellite data, taken by a single instrument during the life of a given satellite, are consis-

tent with each other and observations are on a global scale. Satellite radiometers, however, generally need to be recalibrated during their lifetimes because of degradation problems. Downward sensing radiometers have relatively coarse vertical resolution of 10-20 km. Scanning radiometers provide excellent horizontal coverage but the SCR and PMR instruments, for which data sets are now available, provided orbital plane data only, consisting of 13 and a fraction orbits a day separated by about 26° of longitude. The orbits shift continually from day to day returning to the same observation orbits at approximately two-week intervals. Data for fixed grids can be obtained by interpolation between orbits on a daily basis. It is not possible to obtain tidal variations from a single orbiting satellite.

For climatological purposes, variations are primarily required as a function of altitude, latitude, and time, although longitudinal variations may also be important. Meteorological satellite temperature observations have only been available since about 1970. The reduction of the radiance data to provide temperatures is generally done by one or two methods. The first is the inversion of the radiative transfer equation which requires estimates of the instrument's weighting function for each frequency observed, and a good first guess of the temperature profile in advance. It should be stressed that the inversion technique does not provide a unique solution, and that the first guess strongly influences the final result. First guesses are commonly based on climatology derived from meteorological rocket and radiosonde data. The second technique is a statistical approach which simply regresses observed radiances in several channels against coincidental rocket observations as close as possible in space and time to the radiance observations. These statistics generally produce reasonable results at those locations where there are adequate rocket observations. As will be seen below, this is not always possible. The method, however, is simple and straightforward and involves few assumptions, but depends largely on adequate samples to provide reliable regression coefficients.

Meteorological rocket data provide direct measurements of temperature and wind as a function of altitude at a given place. Vertical resolution is 1 to 2 km. The main limitation is paucity of rocket stations. Unfortunately for scientific users, rocket observation locations have been grouped mainly in the latitude belt from 30° to 40°N . North American rocket observations began about 1960, and the network gradually increased to its maximum density about 1975, and thereafter declined rapidly over North America losing five stations from 1979-82. At present, there are no operational stations in North America north of 55° and only two remain in the Southern Hemisphere, at 8°S and 68°S , although there are Russian rocket-launching ships which are gradually accumulating observations grouped by latitude and month (KOSHELKOV, 1984; cf. Section 2.1.3). The available rocket data used in this report is given in Table 1. It will be noticed that most of the Northern Hemisphere stations used here are in North America. Three Russian stations, at 80°N , 48°N , and 68°S , use the M-100 instrument which appears not to be compatible above 50 km with the sensors used in the North American rockets. Continuing efforts at intercalibration have been made, but necessary corrections to be applied to the past M-100 observations are apparently not available. The correction history changes in time, and it is difficult to learn whether data provided by the World Data Center-A have been corrected and if so, by how much, and whether this correction varied in time. A variety of sensors has also been used in American rockets. A rocket's errors and intercalibration can be found in KOSHELKOV (1984) and SCHMIDLIN (1980).

So long as one depends upon satellite data for future requirements, there will be a need for direct rocket measurements at a wide range of latitudes and throughout the year with which to verify and calibrate satellite data.

Table 1. Rocketsonde stations used.

	Latitude	Longitude	N	Period of Record
Heiss Island	80°37'N	58°03'E	601	1957-75*
Thule	76°33'N	68°49'W	1199	1965-80
Poker Flat	65°07'N	147°29'W	838	1972-79
Fort Greely	64°00'N	145°44'W	1222	1960-72
Fort Churchill	58°44'N	93°49'W	2005	1960-79
Primerose Lake	54°45'N	110°03'W	1238	1964-82
Shemya	52°43'N	174°06'E	532	1975-82
Volgograd	48°41'N	44°21'E	423	1965-75*
Ryori	39°02'N	141°50'E	175	1970-72, 79-82
Wallops Island	37°50'N	75°29'W	2890	1960-82
Pt. Mugu	34°07'N	119°07'W	3432	1960-82
White Sands	32°23'N	106°29'W	4698	1959-82
Cape Kennedy	28°27'N	80°32'W	3792	1960-82
Barking Sands	22°02'N	159°47'W	2580	1960-82
Grand Turk Island	21°26'N	71°09'W	223	1963-66
Antigua	17°09'N	61°47'W	1319	1963-82
Fort Sherman	09°20'N	79°59'W	1554	1966-79
Kwajalein	08°44'N	167°44'E	1668	1963-82
Katal	05°55'S	35°10'W	78	1969-76
Ascension Island	07°59'S	14°25'W	2316	1962-82
Woomera	30°56'S	136°31'E	96	1962-72
Mar Chiquita	37°45'S	57°25'W	58	1969-76
Molodezhnaya	67°40'S	45°51'E	253	1969-75*

* Later data exist but unavailable from WDC-A

DATA

OXF

The Oxford satellite temperatures and derived heights and winds were assembled from two years (1973-74) of radiances from the Selective Chopper Radiometer plus three years (1975-77) from the Pressure Modulated Radiometer. A discussion of the data is given in Section 2.1.1. It should be noted, however, that the PMR instrument retrieves temperatures up to near 85 km, and thus provides information beyond the reach of standard meteorological rockets. This means that only radiative equation inversions can be used to obtain temperature with PMR.

SCR

The SCR temperature data from CDC for the seven years (1970-77) were obtained from radiances calibrated by Oxford, or by CDC with Oxford calibration factors, and the use of a multiple nonlinear regression against rocket data. The regressions were done by winter and summer seasons with April 1 and October 1 being the dividing dates. To account for possible drifts in the radiances, the regressions were recomputed every six months. The errors of regression were generally 2 to 4 C as estimated from five different, random, independent sets of rocket data, each set consisting of 15% of the total data available. As there are so few reliable rocket data in the Southern Hemisphere, the regressions for the Northern Hemisphere were applied to the Southern Hemisphere

radiances six months later. This means that for any Northern Hemisphere winter which experienced large sudden warmings, the regression coefficients may be slightly different from true Southern Hemisphere winter coefficients where warmings are not as frequent or as intense. To extend the cross section downward from 30 to 20 km, north of 20°N, NMC radiosonde data were added to the altitude-latitude sections for the same dates.

MRN

Only meteorological network data as available from World Data Center-A were used here. Unfortunately, despite very long delays in processing rocket data at WDC-A, there is no real quality control of the observations. It is assumed that each individual station, or its processing center, carefully does this. Meteorological rocket data received by teletype for operational use frequently contain serious errors and are not recommended for any scientific purpose when there is time to obtain more reliable data. Russian rocket data taken since 1975 are not available from WDC-A, so it is doubly unfortunate that many North American stations at high latitudes have been closed since 1977. This also prevents the future use of rocket data to retrieve satellite temperatures at high latitudes.

With respect to possible solar cycle influences above 50 km, the dates of the establishment and the reduction of the rocket network were not helpful. The major solar maximum of 1959, and the recent one of 1980, both occurred at a time when there were few rocket stations, especially at high latitudes where any solar effect is likely to be strongest.

Only stations with the most observations were used at a given latitude where there were several to choose from (e.g., Thumba was not used). Stations with less than 150 observations were generally not used unless there was no other station near that latitude; also if the distribution of observations was not spread over the year, the station was not used (Can). It is highly recommended that meteorological rocket network stations be distributed more evenly with respect to latitude, including the Southern Hemisphere.

The influence of standing planetary waves introduces much irregularity when stations from all longitudes are combined onto a single cross section. Elimination of five Pacific region stations (Poker Flat/Ft. Greely, Shemya, Ryori, Barking Sands, Kwajalein), despite the many observations at the latter two stations, would have produced smoother analyses. The five stations were analysed separately from the continental stations and the altitude-latitude patterns were very similar although absolute values differed, due to planetary wave influence, as shown in Section 2.3.1.

A further caveat in the interpretation of all rocket and satellite data is that so far no tidal corrections have been applied although the regions to which the data apply are known to have large tides. It is possible that in the near future tidal estimates, as discussed in Section 2.3.3., can be applied to both past and future observations.

ANALYTICAL METHOD

A multiple regression is used to determine the amplitudes and phases of periodic features in the bi-weekly averages of daily data. Sine and cosine function pairs are used to represent the annual, semiannual, and terannual oscillations; a mean and trend are also determined during the regression. The QBO is represented by two empirically determined time series of amplitudes derived from tropical data. The method by which these series are generated requires further elaboration.

The QBO is observed to have a continuously variable period and amplitude. For these reasons, the QBO signal in the tropical lower stratosphere was used to define a reference signal with variable period and amplitude from cycle to cycle. This signal was then used in the regression. A second time series of equal variance which was orthogonal to and 90° out-of-phase with the original QBO signal was created using a Hilbert transform. This transformed signal was also used in the regression. The original QBO reference signal was obtained from the zonal winds at 30 km altitude from Fort Sherman (9.33°N), Kwajalein (8.73°N), and Ascension (7.98°S). Thirty-day means were obtained from each station, and the mean, trend, annual, semiannual, and terannual signal were removed using the regression technique. The residual means were then averaged over the three stations to provide a continuous QBO record from late 1962 through 1982. The exact values of the series at bi-weekly intervals are obtained through three-point Lagrangian interpolation.

The errors in fitting periodic functions to the data were used to evaluate the reliability of the data in the contouring of amplitudes and phases. Diagrams of the annual, semiannual, terannual and QBO were made using only those amplitudes (and corresponding phases) that were equal to or larger than the associated standard deviation. Also, at least 45 bi-weekly periods of data were required. The means for all stations were adjusted to a common reference data (1972) to avoid the effect of long period trends. In Figures 1-10, tick marks along the upper edge indicate rocket launch sites.

COMPARISON OF VARIATIONS

Figures 1-10 present the amplitudes of the means, annual and semiannual waves. The values in Figures 1-6 are for SCR and MRN temperature, and those in Figures 7-10 are for MRN wind. The values of OXF are discussed in more detail in Section 2.3.5.

All these data sets are preliminary and may be revised before use in a new CIRA. Periodic variations of the wind are presently available only from MRN. Note that these cross sections are machine contoured and lack smoothness, especially at highest altitudes due to the inhomogeneity of the data. The general patterns of maxima are not affected, however, and the amplitude and phase values discussed below were taken from tabulations rather than the plots, whenever possible.

Sample values at three latitudes are summarized in Table 2. The agreement is far better than expected considering the different sensors, data sources, methods of reduction of the raw data, interpolations to latitude-altitude grids for automated contouring, graphical smoothing techniques, and problems of different longitudes of the stations, periods of record, sample size and uneven distribution of data in space and time.

For the annual variation in temperature (Figures 3 and 4, also Figure 1 in Section 2.3.5.), the most noticeable difference is in the altitudes of the maximum amplitude shown by SCR and OXF. SCR shows a maximum near 3 mb (40 km) at 80°S , while the OXF maximum lies near 11 mb (29 km). OXF is in fair agreement with MRN, where their data overlap. Phase dates are at the solstices. The corresponding annual amplitude of the wind (Figure 8) shows large midlatitude maxima centered near 60 km, in general agreement with Figure 38 in CIRA 1972.

The semiannual wave in temperature (Figures 5, 6, Table 2; cf. 2.3.5, Figure 1) is of interest because it is as strong or stronger at both polar regions than at the equator. Although the polar waves have generally not been recognized, they are shown by VAN LOON et al. (1972) and BELMONT et al. (1975), and are strongly confirmed by all three present data sources. The phase of the

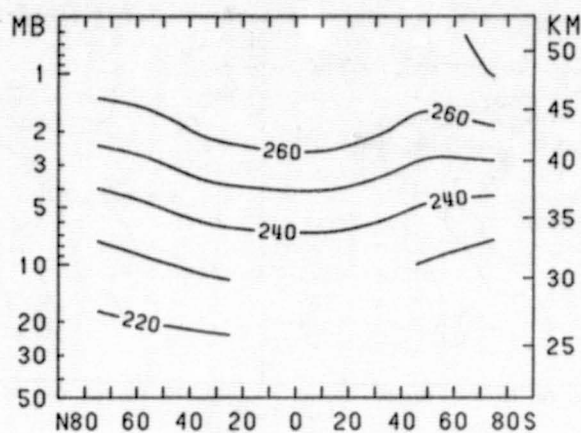


Figure 1. Mean temperature, K, 1970-1977, from SCR.

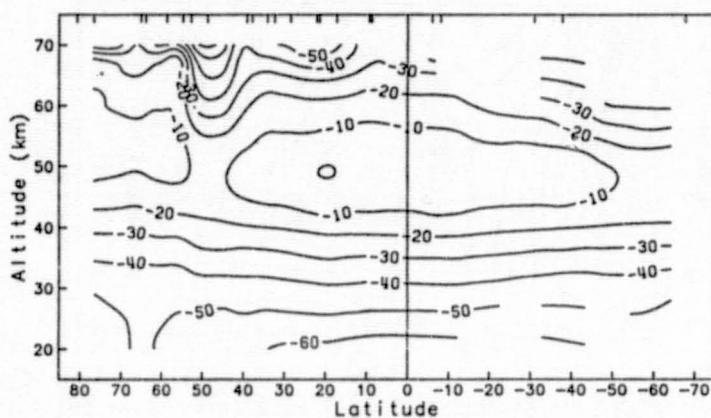


Figure 2. Mean temperature, C, 1960-1982, from MRN.

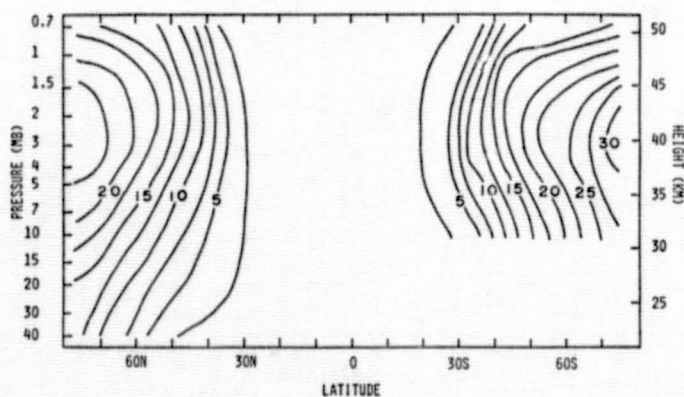


Figure 3. Amplitude of the annual wave in temperature, K, from SCR, 1970-1977.

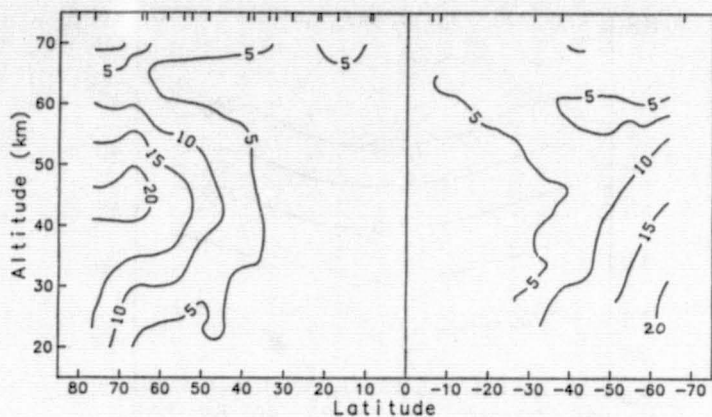


Figure 4. Amplitude of the annual wave in temperature, K, from MRN, 1960-1982.

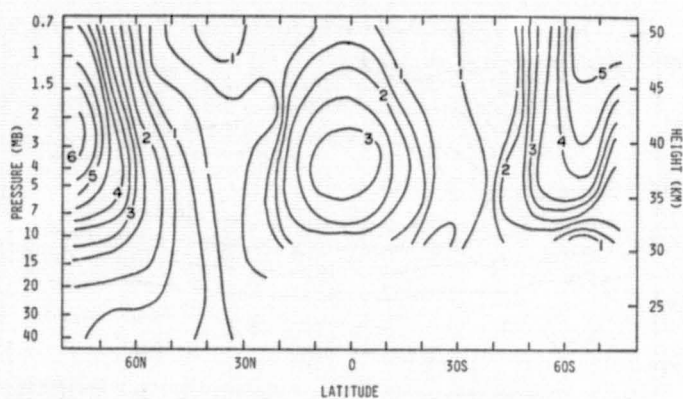


Figure 5. Amplitude of the semiannual wave in temperature, K from SCR, 1970-1977.

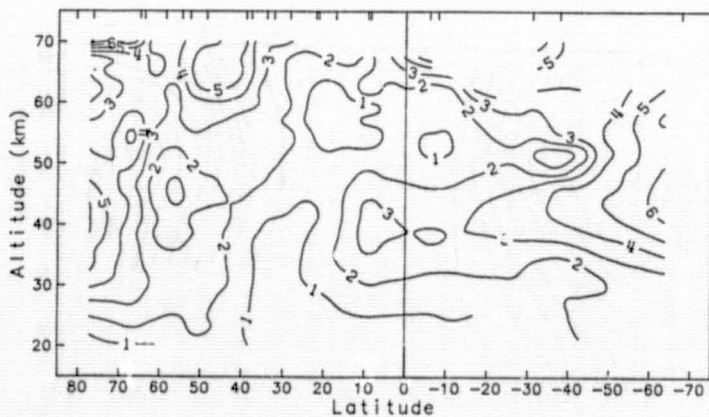


Figure 6. Amplitude of the semiannual wave in temperature, K from MRN, 1960-1982.

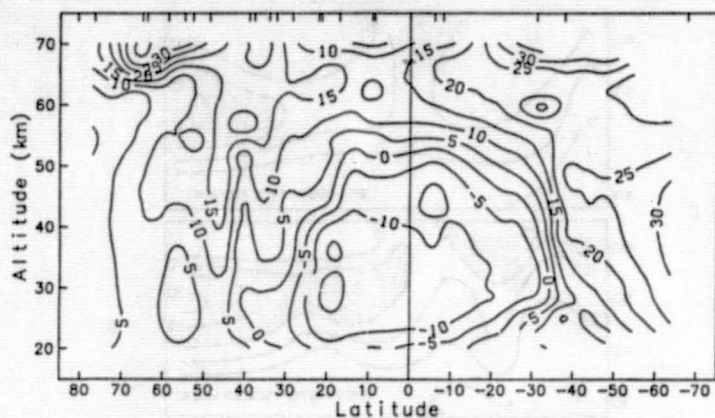


Figure 7. Amplitude of the mean zonal wind, m/s, from MRN, 1960-1982.

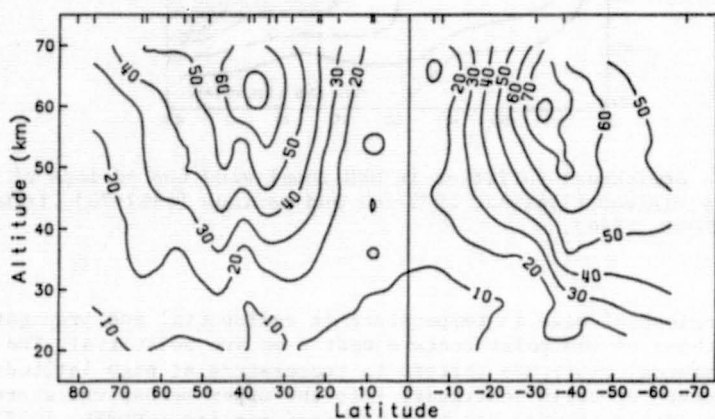


Figure 8. Amplitude of the annual wave in zonal wind, m/s, from MRN, 1960-1982.

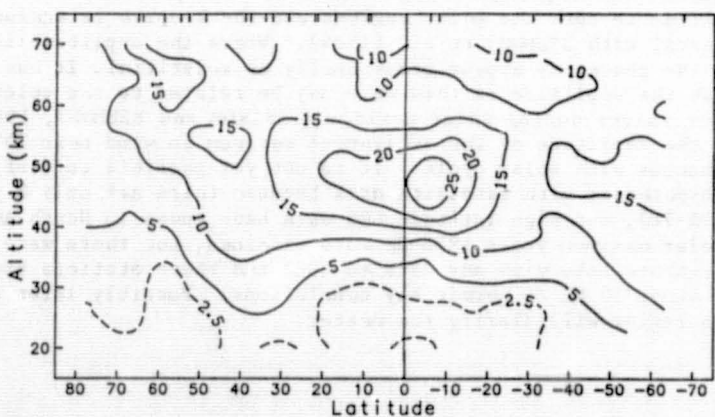


Figure 9. Amplitude of the semiannual wave in zonal wind, m/s, from MRN, 1960-1982.

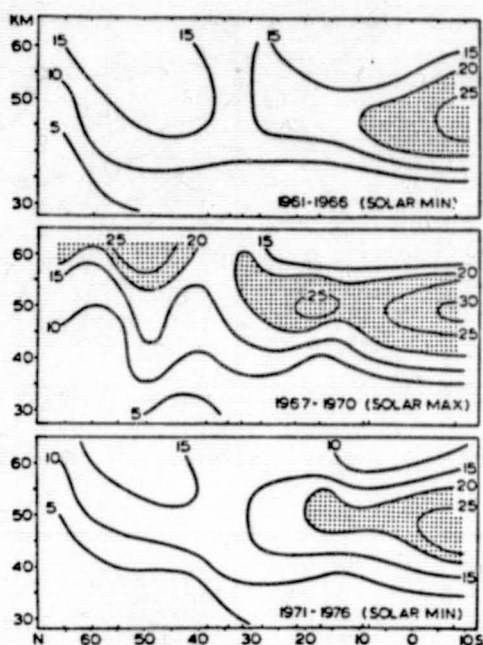


Figure 10. Semiannual variation in MRN zonal wind for periods of solar activity minimum (1961-66, 1971-76) and maximum (1967-70), from NASTROM and BELMONT, 1980).

equatorial semiannual wave in temperature is equinoctial and propagates downward, while those of the polar centers near 3 mb are solstitial. The OXF data show the semiannual amplitude pattern in temperature at high latitudes as a vertical sequence of cells continuing into the upper mesosphere where the semiannual variation in wind has been reported earlier (GROVES, 1972).

The MRN semiannual wave in the wind (Figure 9) shows the well-known tropical maximum near 50 km, south of the equator, with bands of maxima extending poleward (BELMONT et al., 1974). The semiannual wind phase at these centers of maximum amplitude in both the polar regions and the tropics is equinoctial and agrees in general with BELMONT et al. (1974). Where the amplitude is weak, below 35 km, the phase may appear occasionally as solstitial. It has been suggested that the amplitude of this wave may be related to the solar cycle, showing higher values during solar maximum (NASTROM and BELMONT, 1980). Figure 10 shows how the amplitude of the semiannual maximum in wind near 50°N apparently changes with solar cycle. It is not yet possible to confirm this solar cycle hypothesis with satellite data because there are only 8 years of SCR data (1970-78), and high latitude MRN data have ended in North America. The recent solar maximum years 1978-82 were examined, but there were only Shemya and Primrose Lake with any data to 1982 and these stations had too few observations above 50 km to permit any conclusions. Possibly later satellite data for this region will clarify the matter.

Table 2. Comparison of OXF, SCR, MRN, CIRA 1972.

	Temperature (K)				Wind (m/s)		
	OXF	SCR	MRN	CIRA	OXF	MRN	CIRA
	<u>Annual (1 MB)</u>						
80°N	263	264	263	(264)	70°N	18	5 (1)
0	268	270	271	(269)	10°N	-	-5 (-13)
80°S	270	271	263	-	70°S	30	30 -
	<u>Annual (10 MB)</u>						
80°N	224	227	224	(223)	70°N	10	5 (17)
0	233	234	232	(231)	10°N	-	-10 (-21)
80°S	222	226	226	-	70°S	35	30 -
	<u>July Mean (1 MB)</u>						
80°N	284	285	-	283			
0	263	268	-	269			
80°S	254	259	-	-			
	<u>December Mean (1 MB)</u>						
80°N	247	250	-	257			
0	265	269	-	271			
80°S	288	291	-	-			

	OXF	SCR	MRN
	<u>Maximum Annual Temperature Amplitude K (at any altitude)</u>		
80°N	42 (.006 mb)	-	-
80°N	26 (2.5 mb)	24 (3 mb)	28 (44 km) (1.3 mb)
0	3 (0.1 mb)	1 (1 mb)	4 (42 km) (2.5 mb)
80°S	41 (.006 mb)	-	-
80°S	-	31 (3 mb)	-
80°S	35 (11 mb)	-	24 (26 km) (25 mb)
	<u>Maximum Semi-Annual Amplitude K (at any altitude)</u>		
80°N	11 (4 mb)	6 (3 mb)	6 (40 km) (3 mb)
0	4 (1.5 mb)	3 (3 mb)	3 (40 km) (3 mb)
80°S	6 (0.3 mb)	-	-
80°S	4 (1.5 mb)	6 (1 mb)	7 (46 km) (1.5 mb)

Notes to Table 2

1. Values are taken from tables, if available, interpolating when necessary. Figures are used if tables not available.
2. Values in parentheses were estimated from mean of January and July values read from tables.
3. No SCR data available below 10 mb south of 15°S.

SUMMARY OF RESULTS

The three sets of data agree remarkably well. This may be due in part to ultimate reliance upon a climatology based on meteorological rocket profiles which still serves as the only large body of independent data for the middle atmosphere.

Semiannual variations in wind and temperature at high altitudes of both hemispheres are confirmed, but the cause of the semiannual oscillation at high latitudes is still unknown.

Possible solar modulation of the semiannual wave during the 1979-81 maximum could not be detected at high latitudes due to reduction in the MRN rocket network.

Meaningful comparisons of data require data for the same years and place, not just for equal periods of records.

Resultant, observed temperatures or winds are made up of many periodic and quasi periodic components, possibly including solar effects, that modeling must take into account.

RECOMMENDATIONS

Best present estimates of middle atmosphere climate are from satellite global data. A data set consisting of PMR and SAMS to 85 km for 8 years, plus 5 years of SCR, plus continued SSU and similar instruments which sense to 50 km, is now within reach. Resumption of the PMR type measurements is highly recommended.

MRN data must be separated by region. Longitudinal variations due to planetary waves may be large. Thus the sparse MRN data are best used for vertical resolution at a given place, and not for representative global coverage.

Added MRN stations are needed for satellite temperature retrievals, calibration and verification, especially at high latitudes.

MRN data need to be carefully quality controlled. Tidal corrections are needed to adjust single observations per day into more representative values.

ACKNOWLEDGEMENT

Thanks are extended to D. E. Venne and J. Roe for computation and figure preparation.

REFERENCES

- Belmont, A. D., D. G. Dartt, and G. D. Nastrom (1974), Periodic variations in stratospheric zonal wind from 20 to 65 km, at 80°N to 70°S, Q. J. Roy. Meteorol. Soc., **100**, 203-211.
- CIRA (1972), The Committee for the COSPAR International Reference Atmosphere (CIRA) of COSPAR Working Group 4, CIRA 1972, Akademie-Verlag Berlin.
- Groves, G. V. (1972), Annual and semiannual zonal wind components and corresponding temperature and density variations, 60-130 km, Planet. Space Sci., **20**, 2099-2112.
- Koshelkov, Yu. P. (1984), Reference Middle Atmospheres for the Southern Hemisphere, COSPAR, 25.
- Nastrom, G. D., and A. D. Belmont (1975), Periodic variations in stratospheric-mesospheric temperature from 20-65 km at 80°N to 30°S, J. Atmos. Sci., **32**, 1715-1722.
- Nastrom, G. D., and A. D. Belmont (1980), Apparent solar cycle influence on long-period oscillations in stratospheric zonal wind speed, Geophys. Res. Lett., **7**, 457-460.
- Schmidlin, F. J., J. R. Duke, A. I. Ivanovsky, and Y. M. Chewrnyshenko (1980), Results of the August 1977 Soviet and American Meteorological Rocketsonde Intercomparison, held at Wallops Island, Virginia; NASA Ref. Publ., **1053**, NASA, Washington, D. C.
- van Loon, H., K. Labitzke, and R. L. Jenne (1972), Half-yearly wave in the stratosphere, J. Geophys. Res., **77**, 3846-3855.

2.3.5 ANNUAL AND SEMIANNUAL CYCLES BASED ON THE MIDDLE ATMOSPHERE REFERENCE MODEL IN SECTION 2.2

J. J. Barnett and M. Corney

Department of Atmospheric Physics, Clarendon Laboratory
Oxford OX1 3PU, Great Britain

K. Labitzke

Meteorological Institute, Free University Berlin
Berlin, Federal Republic of Germany

The SCR/PMR monthly temperature mean values have been Fourier analysed at each latitude and pressure level to obtain the annual mean and the amplitude and phase of the annual and semiannual cycles (Figure 1 and Table I). The phase is the month of the maximum, such that 1 = January 1, 1.5 = January 16, 2 = February 1, etc. There are some very marked hemispheric differences, notably:

(a) At 80°N there is a maximum amplitude of the annual cycle of 26 K at 2.5 mb, the corresponding maximum at 80°S is much stronger (35 K) and at a lower altitude (11 mb).

(b) The semiannual amplitudes show the well-known maximum over the tropics in the upper stratosphere, but also maxima at high latitudes. There the maximum in the Southern Hemisphere, which is at 65°S, is weaker than that in the Northern Hemisphere; (cf. also Section 2.3.4).

(c) The annual mean shows a minimum at 50°S, 1 mb, and a corresponding weaker minimum at 60°N. This has already been noted in Section 2.1.1 (Figure 4), and is a general feature of the Southern Hemisphere winter, occurring to a smaller extent in the Northern Hemisphere, and clearly strong enough to affect the annual mean.

In general, the hemispheres are remarkably similar and six months out of phase above about 0.3 mb (56 km). It can be seen from Section 2.2 (Figures 1.1 to 1.12) that the two hemispheres are significantly different especially in winter after allowing for a six-month shift. However, changes from summer to winter are so large by comparison that the annual cycles appear to be very similar.

Because of the existence in winter of large longitudinal temperature variations which are repeatedly in the same phase for several months (cf. Section 2.3.1), a given longitude might be consistently warm at some levels and cold at others, leading to annual and semiannual cycles which differ markedly from those of the zonal mean. This is shown for the annual wave by means of horizontal maps of the 30-mb level (Figure 2). Over the Northern Hemisphere large changes in phase occur within the Aleutian anticyclone. Here, the amplitude of the annual wave is small because it is warm in winter as well as in summer.

Over the Southern Hemisphere large phase changes occur over the southern part of South America. Here the maximum of the annual wave is reached late because the "Final Warmings" always start over the Australian section of Antarctica and the transition into summer finishes last over South America.

The variations around the globe of annual and semiannual cycles should be largest at 60 - 70°S or N where planetary wave amplitudes are largest (cf. Section 2.3.1), and Figure 3 shows the temperature amplitudes and phase (time of maxima) for 64°N as a function of longitude and pressure. Phase variations

28881-08M

are relatively minor (except where the amplitudes are very small). However there are large amplitude variations, e.g. from 16 to 26 K at 3 mb for the annual cycle, 5 to 8.3 K at 5 mb for the semiannual cycle.

REFERENCE

Labitzke, K. (1977), Comparison of the stratospheric temperature distribution over Northern and Southern Hemispheres, *Space Res.*, XVII, 159-165.

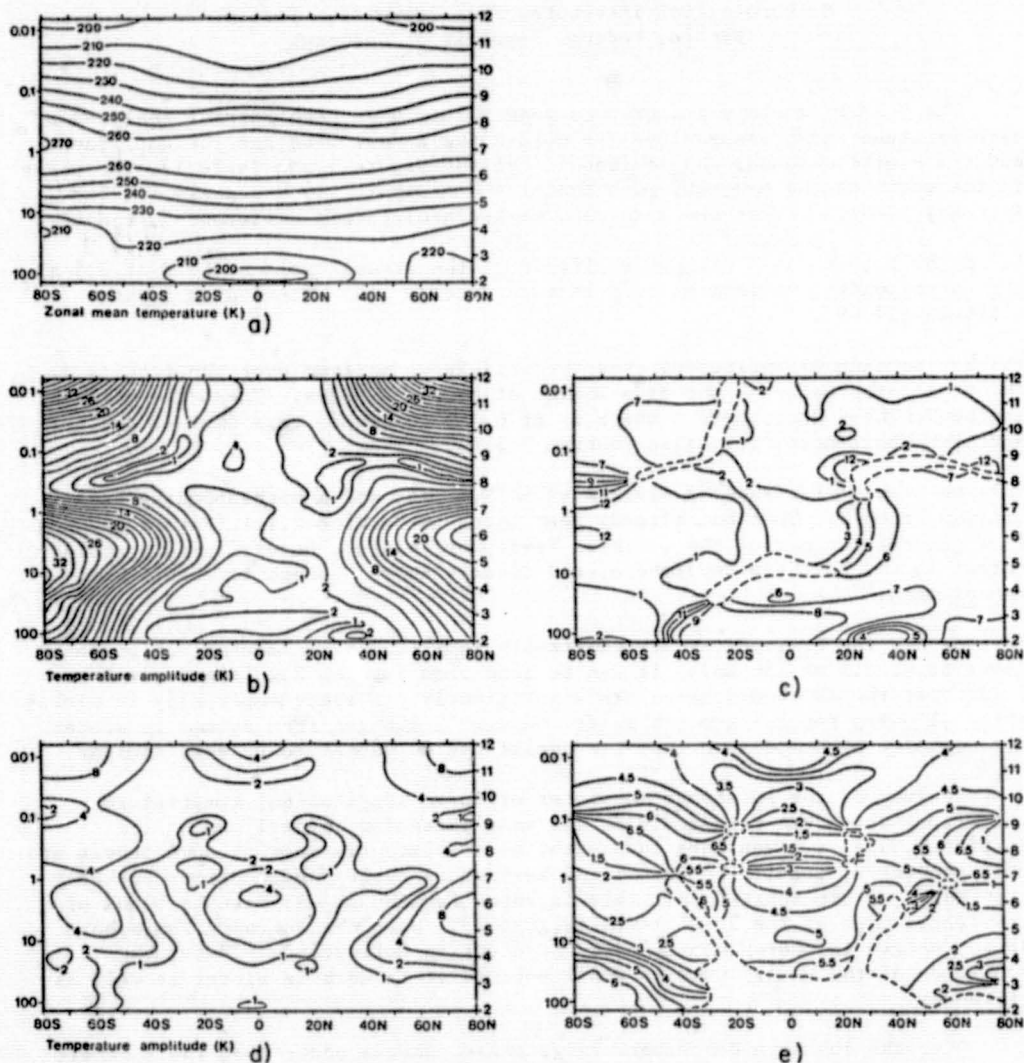


Figure 1. Components of the annual variation of temperature (K) derived from the SCR/PMR combined means. a) annual mean; b) amplitude of annual cycle; c) phase of annual cycle; d) amplitude of semiannual cycle; e) phase of semiannual cycle; phase is given as the month of maximum temperature, e.g., 12 means December 1.

Table 1.

ANNUAL MEAN TEMPERATURE (K)

SCALE HEIGHT	PRESSURE (mb)	-60	-70	-60	-50	-40	-30	-20	-10	0	10	20	30	40	50	60	70	80
12.0	0.0062	195.6	195.3	195.1	197.2	200.0	202.0	203.6	205.7	207.7	206.7	205.1	203.4	200.4	197.7	195.5	195.2	195.1
11.5	0.0103	201.5	201.4	201.7	203.0	204.3	204.9	205.0	206.1	207.6	207.1	206.4	206.3	204.5	203.1	201.6	201.0	200.9
11.0	0.0169	208.3	208.4	209.3	209.4	209.1	207.9	206.6	206.3	206.9	207.3	208.1	209.2	209.1	208.9	208.6	207.5	207.2
10.5	0.0279	216.2	216.2	217.1	216.0	213.9	211.4	209.2	207.7	207.4	208.6	210.6	212.5	213.5	214.8	215.7	214.9	214.8
10.0	0.0460	225.5	224.8	224.8	222.2	218.7	215.7	213.2	211.2	210.6	212.0	214.3	216.4	217.8	220.1	222.5	222.8	223.4
9.5	0.0758	235.4	235.7	232.1	228.6	224.8	222.3	220.3	218.7	218.3	219.3	221.2	222.7	223.5	225.7	229.2	230.9	232.7
9.0	0.1250	246.0	242.9	239.7	235.5	231.8	230.5	230.0	229.5	229.6	229.9	230.4	230.4	230.2	232.2	236.1	239.6	242.3
8.5	0.2061	256.5	252.6	247.6	243.1	239.5	239.3	240.2	241.8	242.4	241.9	240.5	238.9	236.1	240.1	243.9	246.5	251.9
8.0	0.3398	265.5	261.5	255.6	251.3	248.6	249.0	250.6	253.4	254.6	253.2	250.4	246.5	247.7	249.3	252.2	256.6	259.9
7.5	0.5603	269.9	267.0	262.5	259.2	258.5	259.5	260.9	263.0	264.0	263.8	260.4	259.1	258.3	258.6	260.1	262.6	264.4
7.0	0.9237	269.8	268.1	265.3	263.5	264.8	266.5	267.7	268.0	268.0	267.8	267.4	266.4	265.4	263.8	263.1	263.5	263.6
6.5	1.52	265.3	264.3	262.4	261.4	263.6	265.6	267.2	266.8	266.7	266.6	267.0	265.9	264.8	262.0	260.0	258.6	257.7
6.0	2.51	258.2	257.3	255.0	253.7	255.7	258.2	260.3	260.8	261.0	260.6	260.1	258.7	257.3	254.5	252.3	250.2	248.9
5.5	4.14	246.8	246.5	244.4	243.3	245.3	248.0	250.6	251.8	252.4	251.6	250.4	248.7	247.0	244.5	242.7	240.9	239.4
5.0	6.83	233.5	234.4	233.8	233.4	235.6	238.3	240.5	241.6	242.0	241.4	240.4	238.6	237.0	234.8	233.6	232.0	230.4
4.5	11.25	218.9	222.0	224.2	225.8	227.9	230.2	231.0	231.0	230.7	230.9	230.9	230.5	228.5	227.1	226.0	224.7	223.1
4.0	18.55	209.3	213.9	218.9	222.2	223.9	224.7	224.3	223.7	223.3	223.4	223.6	223.9	222.9	222.1	221.0	219.7	218.4
3.5	30.59	211.4	214.3	218.1	220.6	221.0	219.6	218.4	217.3	216.7	216.7	217.6	218.3	219.0	219.6	219.7	219.0	218.3
3.0	50.43	212.1	214.5	217.0	218.2	216.7	213.6	211.0	209.5	208.6	209.1	210.6	212.8	215.9	218.9	220.4	220.3	219.5
2.5	83.15	212.5	214.7	217.0	217.5	214.3	208.1	202.3	199.4	198.7	199.3	202.1	207.0	213.5	218.4	220.8	221.0	220.4
2.0	137.09	213.2	215.0	217.0	217.6	214.8	209.3	204.2	201.5	201.2	201.7	204.0	208.6	214.0	218.5	220.7	221.3	221.2

ANNUAL TEMPERATURE CYCLE

AMPLITUDE (K) AND PHASE (MONTH OF MAXIMUM)

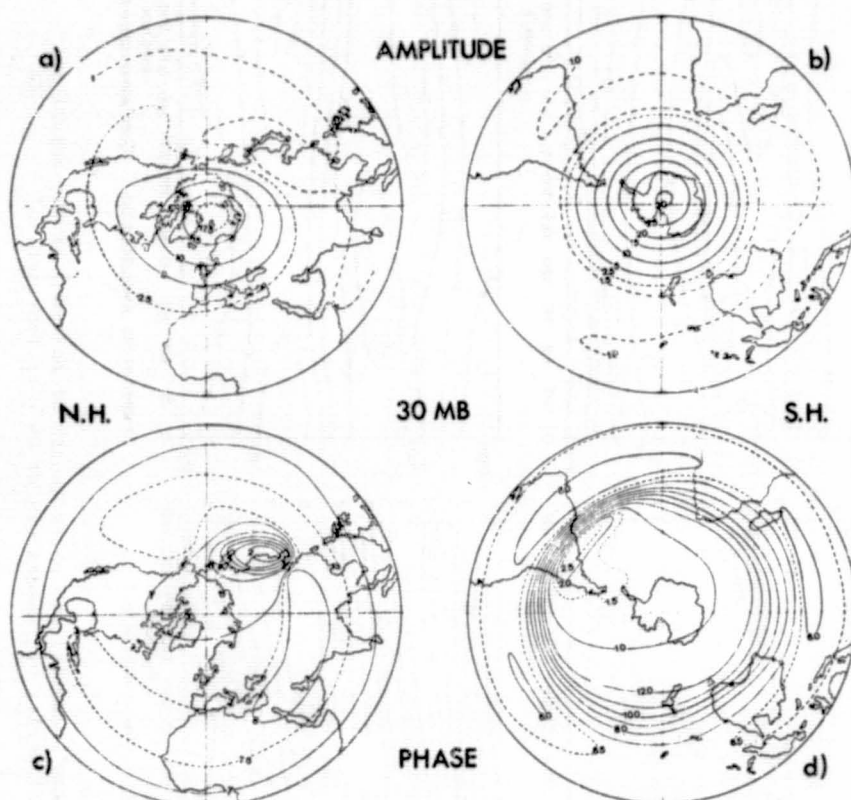
SCALE HEIGHT	PRESSURE (mb)	-60	-70	-60	-50	-40	-30	-20	-10	0	10	20	30	40	50	60	70	80
12.0	0.0062	41.35	37.39	32.30	24.41	13.95	4.45	0.94	1.99	2.10	2.37	2.81	7.57	17.41	27.66	35.42	39.51	41.99
		6.68	6.72	6.81	6.74	6.64	6.56	2.17	2.34	1.30	12.31	12.74	12.83	12.73	12.83	12.91	12.85	12.81
11.5	0.0103	35.72	32.27	28.19	21.22	11.69	3.35	0.82	1.74	2.27	2.97	2.98	6.58	15.01	24.06	30.82	33.99	35.99
		6.71	6.78	6.93	6.85	6.76	6.71	12.96	1.92	1.25	12.73	1.13	12.96	12.83	12.94	1.03	12.92	12.85
11.0	0.0169	28.80	26.12	23.52	17.51	9.72	2.72	0.96	1.84	2.44	2.60	2.93	5.80	12.50	19.46	25.17	27.04	28.44
		6.77	6.84	7.00	7.02	6.99	7.01	12.64	1.53	1.24	12.95	1.32	1.16	1.11	1.13	1.00	12.92	
10.5	0.0279	22.33	20.16	18.63	14.02	7.93	2.29	1.49	2.48	2.64	2.27	2.45	5.02	9.75	14.65	18.77	19.91	21.09
		6.84	6.90	7.05	7.20	7.27	7.55	12.66	1.36	1.21	12.98	1.55	1.46	1.23	1.30	1.22	1.08	12.97
10.0	0.0460	16.92	15.18	14.18	10.96	6.25	1.77	2.29	3.39	2.88	1.78	1.92	4.06	6.87	9.97	12.53	13.37	14.53
		6.89	6.91	7.01	7.27	7.50	8.05	12.59	1.18	1.21	1.13	2.13	1.74	1.47	1.44	1.24	1.10	12.97
9.5	0.0758	13.41	11.72	10.66	8.06	4.67	1.10	2.35	3.91	3.17	1.76	1.63	2.99	4.31	5.56	6.97	8.20	9.83
		6.85	6.81	6.86	7.34	7.65	7.27	1.00	1.10	1.23	1.37	1.88	1.56	1.74	1.72	1.12	12.88	12.69
9.0	0.1250	11.35	9.52	7.37	4.73	2.07	0.97	2.75	4.07	3.36	1.91	1.40	1.56	1.30	1.58	2.28	4.77	7.14
		6.83	6.73	6.71	7.33	7.89	4.23	1.95	1.22	1.27	1.28	12.48	12.77	2.81	2.96	12.71	12.32	12.22
8.5	0.2061	8.55	6.65	3.80	1.03	1.45	2.04	3.61	3.98	3.30	1.93	1.30	0.45	2.23	2.70	1.64	1.21	3.19
		7.51	7.22	6.73	6.35	1.54	2.13	2.23	1.50	1.41	1.11	11.09	9.01	6.96	6.87	7.52	11.73	12.24
8.0	0.3398	6.55	4.28	1.43	2.88	3.86	2.63	2.43	2.83	2.93	2.48	1.41	0.69	3.36	4.98	4.92	3.43	2.75
		9.26	9.09	10.80	1.01	1.30	1.38	2.15	1.80	1.65	1.36	12.60	6.51	6.82	6.79	6.72	6.40	6.17
7.5	0.5603	9.50	6.86	6.29	6.95	5.62	2.92	0.98	1.58	2.16	2.28	1.90	0.95	3.72	6.83	8.24	8.70	9.99
		11.42	11.57	12.25	12.85	1.01	12.98	1.21	2.38	2.15	1.82	2.09	5.12	6.25	6.53	6.59	6.65	6.69
7.0	0.9237	19.27	15.67	13.63	12.35	8.37	4.61	1.98	1.32	1.85	2.06	2.02	1.85	4.82	10.08	13.52	16.02	18.61
		12.02	12.10	12.36	12.77	12.95	12.83	12.51	2.20	2.51	2.52	3.19	5.08	6.05	6.47	6.55	6.66	6.72
6.5	1.52	27.06	23.30	20.55	17.78	12.16	6.51	2.58	1.38	1.85	2.38	2.38	3.08	7.13	13.74	18.42	21.50	23.94
		12.04	12.08	12.32	12.67	12.86	12.73	12.81	1.87	2.52	2.62	2.90	4.78	5.99	6.39	6.53	6.61	6.65
6.0	2.51	31.66	28.08	24.54	21.54	15.84	8.95	3.28	1.70	1.96	2.64	2.98	3.59	9.08	15.57	20.00	23.59	25.63
		11.96	11.97	12.24	12.66	12.88	12.90	12.97	1.74	2.32	2.40	2.64	4.81	6.06	6.41	6.51	6.53	6.53
5.5	4.14	33.19	29.93	26.21	22.63	16.06	8.84	3.44	1.33	1.41	2.11	2.38	3.75	8.82	14.95	18.81	22.35	24.38
		12.38	12.33	12.49	12.78	13.00	1.05	12.99	1.80	3.24	3.02	4.15	5.72	6.34	6.65	6.67	6.55	6.46
5.0	6.83	33.59	30.22	25.93	20.75	13.35	7.15	2.75	0.51	0.54	1.09	1.49	3.55	7.35	12.72	16.38	19.86	22.26
		12.58	12.33	12.49	12.78	13.00	1.05	12.99	1.80	3.24	3.02	4.15	5.72	6.34	6.65	6.67	6.55	6.46
4.5	11.25	34.90	30.06	23.75	16.10	8.75	3.40	0.86	0.92	0.79	0.39	1.39	2.76	5.66	9.52	13.17	17.40	21.02
		12.82	12.72	12.75	12.94	1.15	1.18	1.18	6.17	6.95	7.85	6.07	6.15	6.78	6.94	6.79	6.64	6.56
4.0	18.55	32.69	25.90	19.88	11.28	4.74	1.14	0.70	1.15	1.12	1.03	1.69	2.53	4.26	6.74	10.51	15.00	19.37
		1.13	1.04	12.97	12.93	12.97	1.20	6.30	6.50	6.27	6.57	6.66	6.72	7.00	7.00	6.84	6.71	6.64
3.5	30.59	27.66	22.34	15.32	7.62	2.37	0.29	1.00	1.01	1.07	1.21	1.58	1.96	2.59	4.37	7.75	12.20	16.47
		1.28	1.25	1.18	12.94	12.57	10.90	6.97	6.53	6.24	6.96	7.15	7.46	7.74	7.07	6.90	6.79	6.75
3.0	50.43	25.73	20.37	13.82	5.70	1.38	1.75	1.91	2.26	2.47	2.39	2.19	2.00	1.74	3.04	5.94	9.93	13.52
		1.53	1.53	1.45	1.14	10.83	8.67	8.37	8.33	8.35	8.19	8.05	7.77	7.28	6.86	6.97	6.93	6.96
2.5	83.15	23.16	19.14	12.12	3.86	2.27	2.95	2.26	2.27	2.56	2.29	1.45	0.79	1.32	1.85	4.67	8.33	11.92
		1.78	1.80	1.73	1.20	9.05	8.44	8.43	8.42	8.40	8.21	7.70	4.81	3.93	6.33	7.08	7.13	7.19

ORIGINAL PAGE IS
OF POOR QUALITY

Table 1 continued.

SEMI-ANNUAL TEMPERATURE CYCLE			AMPLITUDE (K) AND PHASE (MONTH OF MAXIMUM)																	
SCALE	PRESSURE		-80	-70	-60	-50	-40	-30	-20	-10	0	10	20	30	40	50	60	70	80	
HEIGHT	(mb)																			
12.0	0.0062	11.94	11.42	9.57	6.59	4.24	2.50	2.50	4.31	5.90	4.18	2.87	2.18	3.36	4.87	7.17	9.23	9.63		
		4.29	4.21	4.10	4.00	3.97	4.04	4.55	4.73	4.74	4.67	4.45	4.03	3.75	3.81	3.97	4.13	4.20		
11.5	0.0103	11.43	10.97	9.28	6.04	3.98	2.42	1.58	3.06	4.31	2.94	2.01	2.44	3.40	4.64	7.30	9.24	9.49		
		4.31	4.26	4.20	4.12	3.96	3.70	3.96	4.75	4.90	4.67	3.94	3.63	3.71	3.92	4.06	4.17	4.22		
11.0	0.0169	9.32	9.16	8.18	5.22	3.41	2.73	1.70	1.68	1.90	1.68	2.04	2.88	3.26	4.46	6.72	8.05	7.99		
		4.35	4.36	4.39	4.25	3.97	3.56	3.34	4.20	4.57	4.07	3.41	3.48	3.67	4.01	4.24	4.26	4.25		
10.5	0.0279	6.64	6.75	6.31	3.94	2.82	2.82	2.38	2.16	2.12	2.31	2.67	3.19	3.03	3.87	5.52	6.30	6.02		
		4.48	4.58	4.67	4.54	4.19	3.70	3.33	3.24	3.12	3.17	3.36	3.56	3.80	4.17	4.44	4.41	4.35		
10.0	0.0460	3.97	4.43	4.47	3.02	2.60	2.85	3.20	3.01	3.67	3.19	3.37	3.31	2.98	3.06	3.96	4.40	4.01		
		4.72	4.98	5.14	5.18	4.67	4.03	3.50	2.94	2.72	2.90	3.47	3.79	4.10	4.45	4.68	4.64	4.51		
9.5	0.0745	0.85	2.83	4.15	3.44	2.76	2.87	2.51	2.77	3.88	2.90	2.67	3.15	2.81	2.66	2.82	2.21	1.58		
		5.70	5.85	5.87	5.83	5.24	4.49	3.58	2.69	2.38	2.65	3.53	4.11	4.45	4.78	5.16	5.07	4.57		
9.0	0.1250	3.44	4.12	5.16	4.58	3.28	2.52	0.53	2.24	3.63	2.39	0.74	2.33	2.80	2.89	2.65	1.70	1.93		
		1.51	6.82	6.41	6.18	5.69	5.04	3.49	1.99	1.82	2.00	3.23	4.43	4.77	5.14	5.74	6.49	1.58		
8.5	0.2061	5.58	5.86	5.96	5.25	3.30	2.04	1.38	3.10	3.51	3.17	1.31	0.84	2.41	3.14	2.85	3.28	3.78		
		1.60	1.13	6.77	6.43	6.09	5.95	1.07	1.35	1.43	1.39	1.32	5.25	5.02	5.45	6.15	6.89	1.38		
8.0	0.3398	5.45	6.19	6.39	4.79	2.97	1.86	1.63	2.60	2.74	2.59	1.44	0.76	2.47	3.15	3.17	3.94	3.97		
		1.70	1.31	1.05	6.63	6.19	6.32	1.10	1.46	1.56	1.55	1.36	5.73	5.17	5.58	6.35	6.83	1.17		
7.5	0.5603	3.62	4.53	4.92	2.93	1.70	1.06	0.47	1.42	1.79	1.60	0.38	1.13	2.43	2.53	2.49	3.50	3.81		
		1.90	1.53	1.34	6.92	5.92	5.74	1.04	2.42	2.57	2.58	2.45	4.89	5.02	5.44	6.12	6.43	6.57		
7.0	0.9237	2.97	3.66	3.67	1.74	0.64	1.13	0.67	1.95	3.03	2.27	1.03	1.49	1.80	1.48	0.99	2.91	4.53		
		2.34	2.03	1.95	1.96	5.44	5.19	4.41	3.60	3.62	3.60	4.01	4.80	4.80	4.75	5.71	6.54	6.67		
6.5	1.52	3.54	4.58	4.63	2.30	0.51	1.04	1.35	3.38	4.35	3.53	1.58	1.12	0.99	0.93	1.37	4.77	7.37		
		2.44	2.22	2.22	2.44	6.30	5.51	4.36	3.99	3.93	4.00	4.24	5.15	5.22	4.08	1.44	1.18	1.13		
6.0	2.51	3.32	4.97	5.62	3.11	0.49	1.01	1.91	3.57	4.05	3.66	2.02	0.99	0.29	0.82	5.91	7.82	10.59		
		2.67	2.30	2.25	2.47	2.36	5.84	4.64	4.27	4.19	4.30	4.64	5.54	4.37	2.53	1.59	1.42	1.36		
5.5	4.14	2.71	4.51	5.55	3.77	1.23	0.44	1.78	3.18	3.18	3.25	1.97	0.83	0.31	1.93	5.13	8.84	11.16		
		2.89	2.48	2.43	2.60	2.73	5.45	4.78	4.64	4.68	4.69	4.86	5.33	2.55	2.06	1.73	1.62	1.59		
5.0	6.83	2.05	3.45	4.67	3.80	1.66	0.26	1.29	2.65	2.97	2.74	1.50	0.47	1.03	3.03	5.58	8.17	9.63		
		3.52	2.85	2.67	2.65	2.46	3.15	4.75	4.92	5.07	4.98	4.93	5.27	1.63	1.90	1.84	1.85	1.86		
4.5	11.25	2.55	2.35	2.80	3.07	2.27	0.80	1.09	1.61	2.30	1.59	1.29	0.31	1.95	3.72	5.10	6.00	6.54		
		4.48	3.69	2.99	2.60	2.31	2.38	4.61	4.92	4.97	5.02	4.88	6.93	1.65	1.78	1.91	2.14	2.29		
4.0	18.55	2.18	1.87	1.80	1.50	1.62	0.78	0.61	1.04	1.36	0.98	0.98	0.51	1.64	2.58	2.96	3.33	3.80		
		5.21	4.86	4.22	3.09	2.50	2.48	4.71	4.85	4.85	5.23	5.34	6.98	1.69	1.87	2.11	2.57	2.77		
3.5	30.59	2.41	2.61	2.08	0.92	0.70	0.28	0.26	0.60	0.76	0.86	1.02	0.52	0.96	1.57	1.25	1.38	1.83		
		5.79	5.72	5.12	4.34	3.15	3.07	5.37	5.27	5.22	5.82	5.81	6.37	1.66	2.00	2.45	3.25	3.69		
3.0	50.43	3.43	3.20	1.81	0.69	0.80	0.51	0.14	0.10	0.34	0.26	0.26	0.05	0.52	0.93	0.83	0.68	0.25		
		6.07	6.12	5.96	4.66	3.72	3.46	2.43	6.01	4.79	5.34	5.34	3.90	2.00	2.05	2.11	2.00	1.39		
2.5	83.15	3.57	3.20	2.05	0.84	0.59	0.47	0.11	0.61	0.67	0.55	0.22	0.21	0.05	0.60	0.44	0.22	0.64		
		6.27	6.23	6.14	5.38	4.54	4.50	2.86	2.26	2.44	2.46	2.59	4.73	1.56	2.00	2.06	1.16	6.10		

ORIGINAL PAGE IS
OF POOR QUALITY



AMPLITUDE AND PHASE OF THE ANNUAL TEMPERATURE WAVE

Figure 2. a) and b): amplitude (K); c) and d): phases (month of maximum) of the annual temperature wave at the 30-mb level (LABITZKE, 1977).

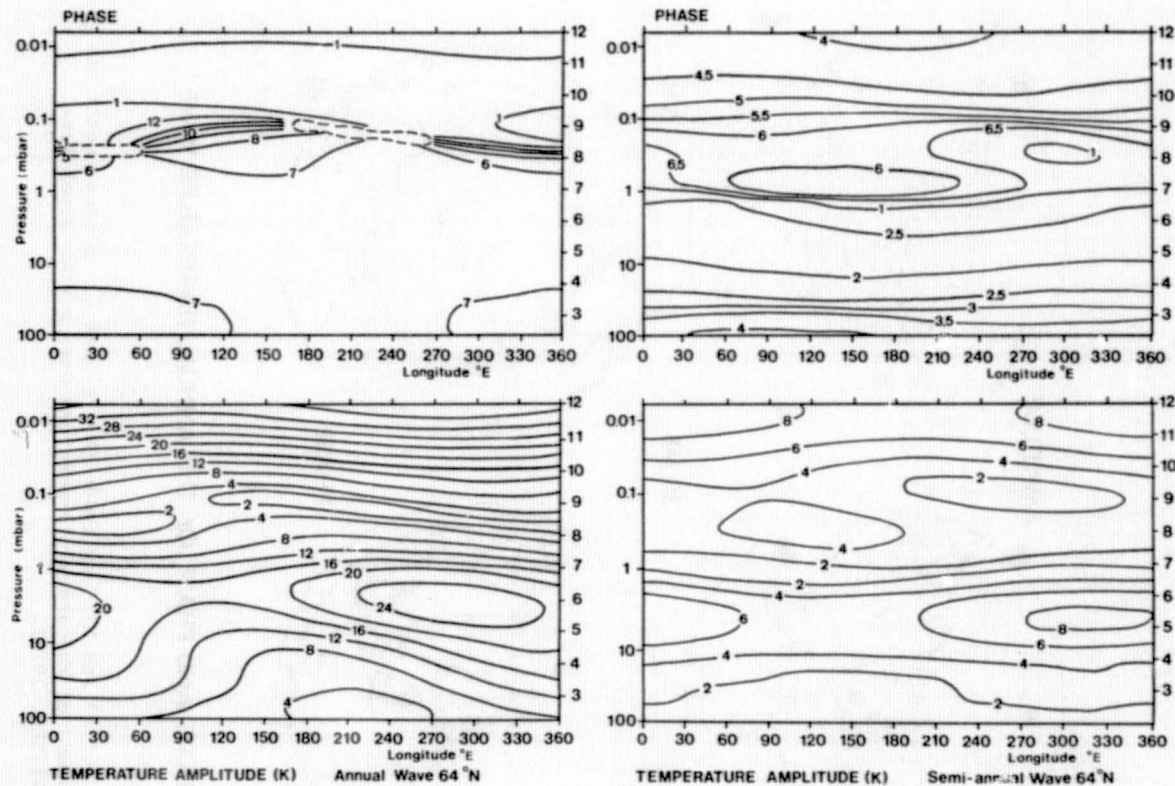


Figure 3. Amplitude (K) and phase (month of maximum) of the annual and semiannual cycles of temperature at 64°N as functions of longitude and pressure.

ORIGINAL PAGE IS
OF POOR QUALITY

2.3.6 ON THE QUASI-BIENNIAL OSCILLATION, QBO

K. Labitzke

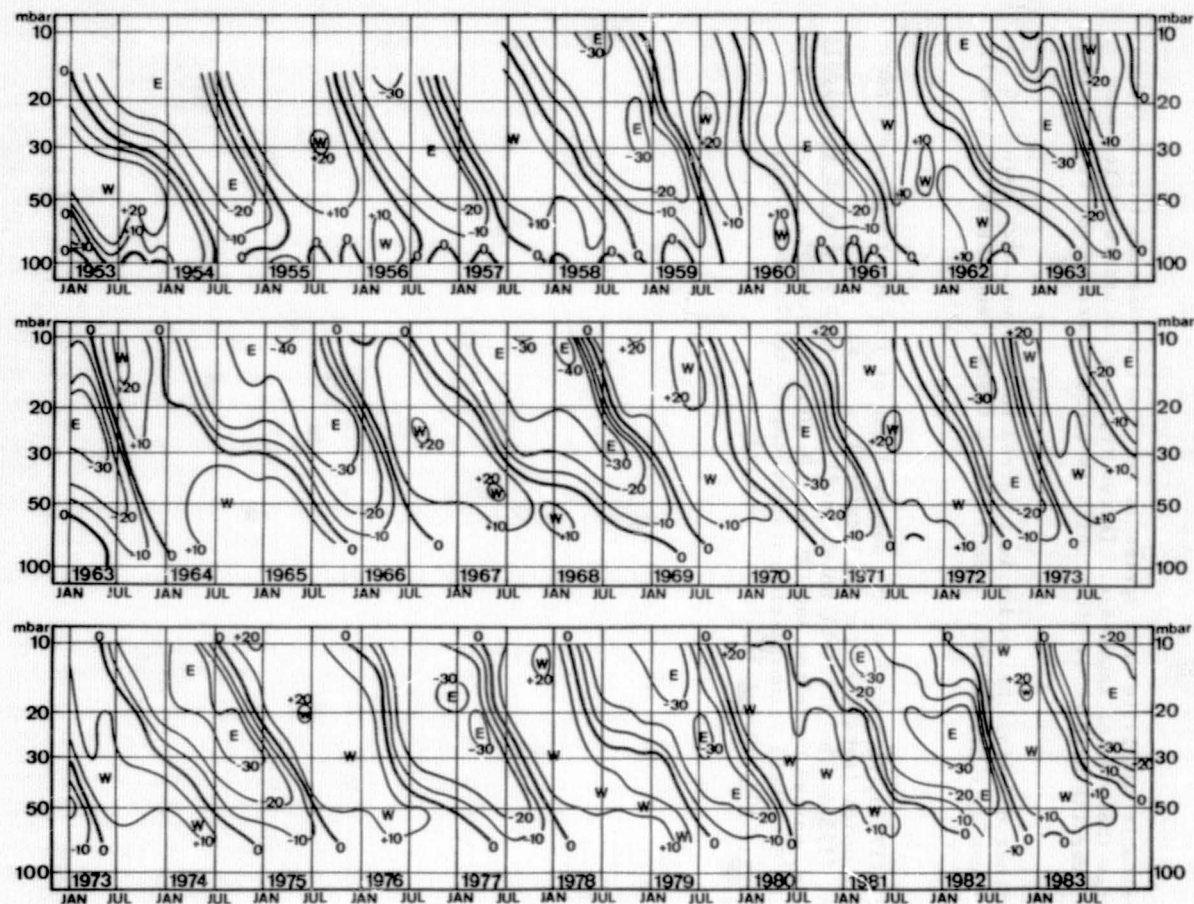
Meteorological Institute, Free University Berlin
Berlin, Federal Republic of Germany

The available satellite data series is too short to discuss this cycle and to enlarge the present knowledge. Therefore, only an update of the mean zonal winds over the tropics is given which is based on radiosonde data (Figure 1).

For further details, the reader is referred to reviews which have been published recently, e.g., NAUJOKAT (1985), PLUMB (1984), and TRENBERTH (1980).

REFERENCES

- Naujokat, B. (1985), An update of the observed QBO of the stratospheric winds over the tropics (submitted for publication).
Plumb, R. A. (1984), The quasi-biennial oscillation, in Dynamics of the Middle Atmosphere, edited by Holton and Matsuno, D. Reidel, 217-251.
Trenberth, K. E. (1980), Atmospheric quasi-biennial oscillations, Mon. Weather Rev., 108, 1370-1377.



TIME-HEIGHT CROSS SECTION OF MONTHLY MEAN ZONAL WINDS [ms^{-1}] AT EQUATORIAL STATIONS (UNTIL 1963
 FIGURE WAS TAKEN FROM REED, 1965) [JAN 53-AUG 67: CANTON ISLAND, $3^{\circ}\text{S}/172^{\circ}\text{W}$; SEP 67-DEC 75: GAN/MALEDIVE
 ISLANDS, $1^{\circ}\text{S}/73^{\circ}\text{E}$; JAN 76-DEC 83: SINGAPORE, $1^{\circ}\text{N}/104^{\circ}\text{E}$]

Figure 1.

ORIGINAL PAGE IS
 OF POOR QUALITY

2.3.7 ON THE INTERANNUAL VARIABILITY AND ON TRENDS OF THE TEMPERATURE IN THE MIDDLE ATMOSPHERE

K. Labitzke and B. Naujokat

N86-12827

Meteorological Institute, Free University Berlin
Berlin, Federal Republic of Germany

The new Reference Atmosphere presented here is based on global satellite data and forms a very useful basis for climatological studies. When using such climatologies it is important to be aware of the well-known interannual variability which in the middle atmosphere is particularly large during the northern winters and southern springs.

(a) VARIABILITY OF THE LOWER STRATOSPHERE

For a discussion of the interannual variability of the lower stratosphere a long-term series of temperature data is available for the Northern Hemisphere. This series is based on daily maps derived largely from radiosonde data (Free University Berlin). For the Southern Hemisphere only data of single radiosonde stations are available.

Variability of the Polar Regions: For a comparison of the two polar regions, the monthly mean temperature data for 90°N and 90°S are shown in Figure 1 (update of Figure 1 of NAUJOKAT, 1981) and 2 (Figure 1b, LABITZKE and NAUJOKAT, 1983) in the form of frequency distributions. The time-scale is shifted by six months so that both polar regions can be compared easily. The monthly mean values for the North Pole are based on daily 30-mbar charts derived from radiosonde data, while for the South Pole a radiosonde station is available directly.

The main features to be noted and which have been pointed out previously (e.g., BARNETT, 1974; LABITZKE, 1974; KNITTEL, 1976) are:

- (1) In the lower stratosphere the interannual variability during the northern midwinters (Figure 1) is much larger than during the southern midwinters (Figure 2), due to the major midwinter warmings which take place only during the northern winters; the largest interannual variations over Antarctica are observed during late spring, i.e., October and November when very intense "Final Warmings" bring about the transition into summer.
- (2) The variability in the middle stratosphere is very small in summer when the planetary waves of the troposphere cannot propagate upwards into the stratosphere due to the prevailing easterly winds. This is true for both polar regions.

Variability over Middle and Low Latitudes: The frequency distributions of 30-mbar temperatures for middle northern latitudes (not shown), reveal less disturbed winters and very regular summers.

Although a similar long-term series of temperatures is not available for the Southern Hemisphere, data of single radiosonde stations and satellite data indicate a similar behaviour.

At 30°N (Figure 3) the variability is small throughout the year (note the changed interval in the frequency distribution), although still smallest in summer.

This is no longer valid for 10°N (Figure 4) where the variability is enlarged by the quasi-biennial oscillation (QBO).

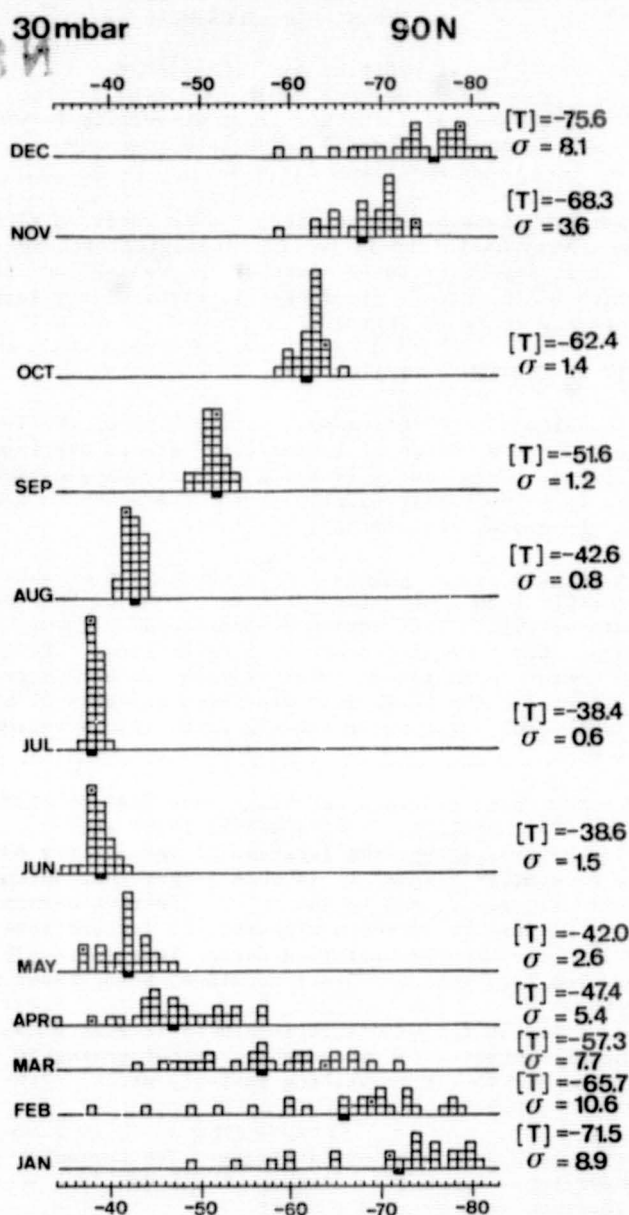
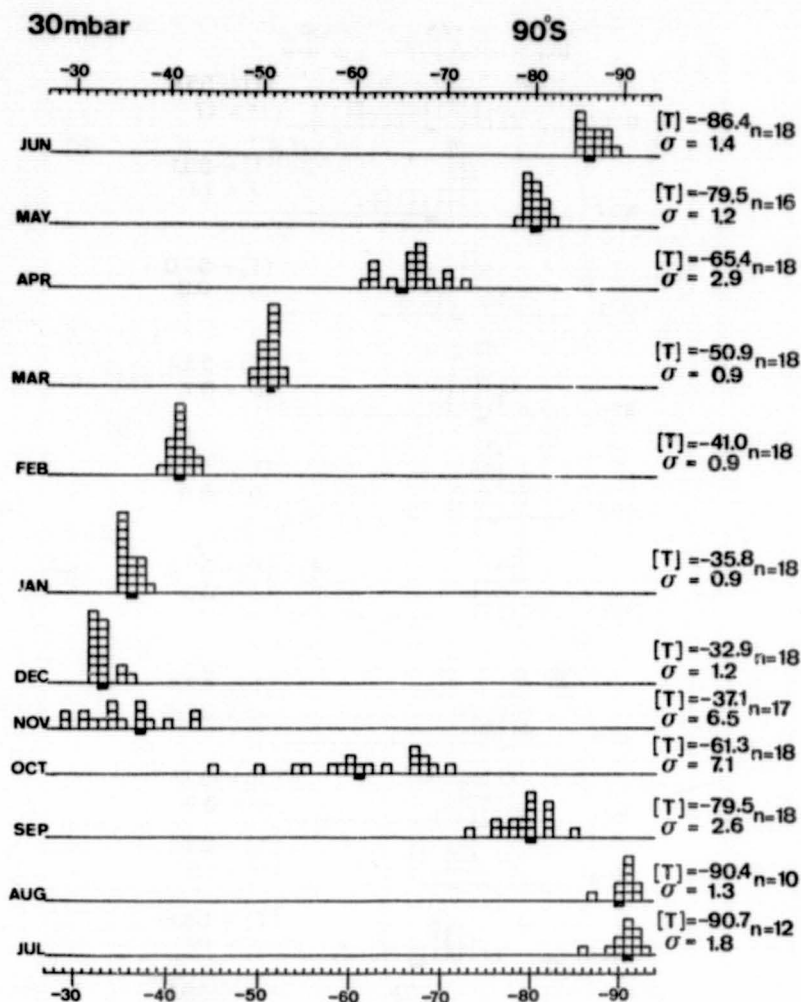


Figure 1. Frequency distribution of the monthly mean 30-mb temperatures ($^{\circ}\text{C}$) over the North Pole, for the period July 1955 through December 1982. Interval is 1 K. The long-term average $[T]$ is given at the righthand side of the picture, together with the standard deviation σ , and $[T]$ is also marked as a black box in the frequency distribution. The data of 1982 are marked and are not included in the long-term average $[T]$. (Update of Figure 1, NAUJOKAT, 1981).



AMUNDSON-SCOTT, TEMPERATURE, 30mbar, 1961-1978

Figure 2. Frequency distribution of the monthly mean 30-mb temperatures (°C) over the South Pole, for the period 1961-1978. (Based on radiosonde data, not all months are complete, because of the very low temperatures in winter). Otherwise same notation as in Figure 1 (Figure 1b LABITZKE and NAUJOKAT, 1983).

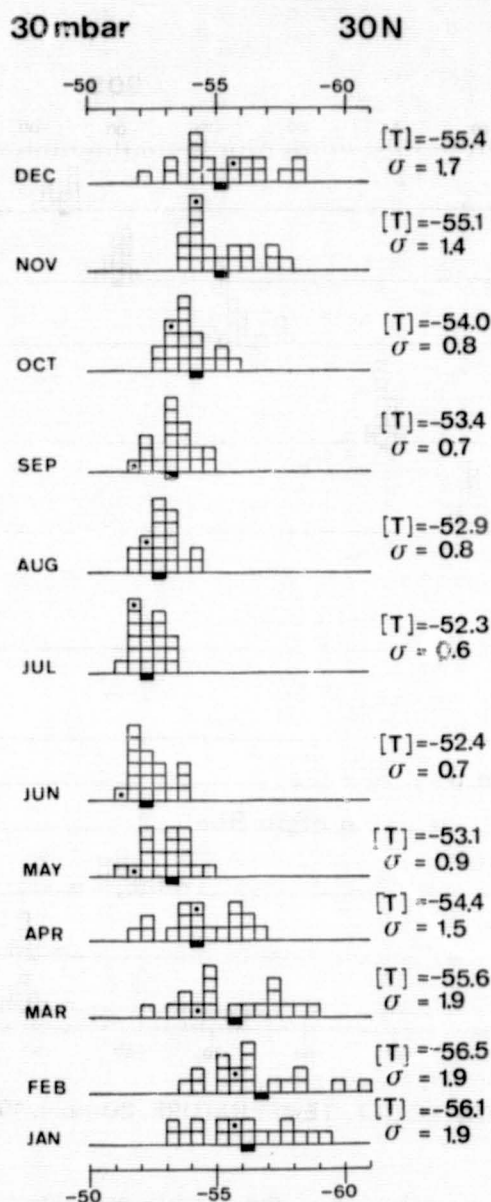


Figure 3. Frequency distribution of the monthly mean 30-mb temperatures ($^{\circ}\text{C}$), averaged along 30°N , for the period July 1964 through December 1982, with an interval of $1/2$ K. Otherwise same notation as in Figure 1. (Figure 1c LABITZKE and NAUJOKAT, 1983).

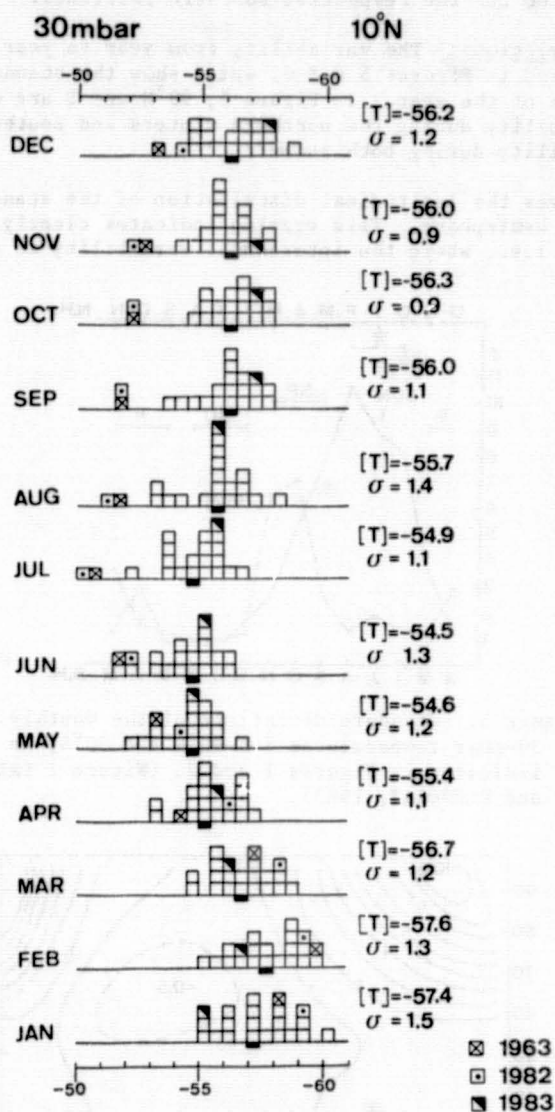


Figure 4. As Figure 3, but for 10°N, and for the period January 1963 through December 1982; the long-term average [T] is based on January 1964 through December 1981. The values for 1963 are marked ☒, for 1982 □, for 1983 ■. (Update of Figure 1d, LABITZKE and NAUJOKAT, 1983).

At 10°N large positive deviations from the long-term mean are noticeable from July through December in 1963 and 1982. This will be discussed below in part (c). The frequency distributions at 30° and 10°N can be taken as being representative also for the respective southern latitudes.

Standard Deviations: The variability from year to year as discussed above is summarized in Figures 5 and 6, which show the standard deviations during the course of the year. In Figure 5, 90°N and S are compared, with the very large variability during the northern winters and southern springs, and the small variability during both summers.

Figure 6 gives the latitudinal distribution of the standard deviations for the Northern Hemisphere. This drawing indicates clearly where one should look for trends, i.e., where the interannual variability is smallest: at $60^{\circ} - 70^{\circ}\text{N}$, in summer.

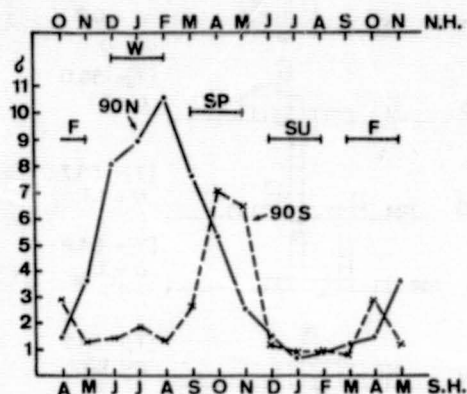


Figure 5. Standard deviations of the monthly mean 30-mbar temperatures for 90°N and 90°S , as indicated in Figures 1 and 2. (Figure 2 LABITZKE and NAUJOKAT, 1983).

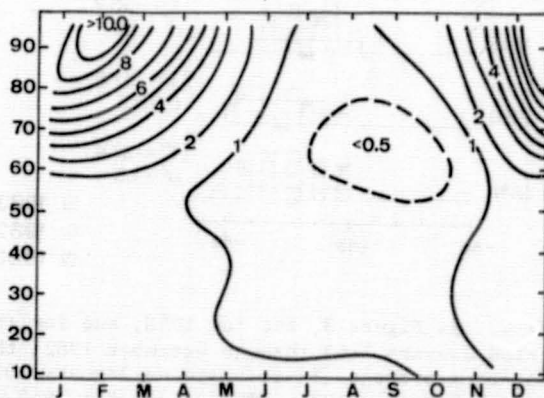


Figure 6. Latitudinal distribution of the standard deviations (K) of the monthly mean 30-mbar temperatures throughout the year. (90°N ; July 1955-December 1981, $n = 26$ or 27 years; $80^{\circ}-10^{\circ}\text{N}$: July 1964-December 1981; $n = 17$ or 18 years.) (Figure 3, LABITZKE and NAUJOKAT, 1983).

(b) VARIABILITY OF THE UPPER STRATOSPHERE

The discussion of the interannual variability of the upper stratosphere will concentrate on satellite data which are available for this region since the winter of 1970/71.

Variability of the Polar Regions: The same features as discussed for the lower stratosphere can be found in the upper stratosphere, namely highly disturbed northern winters. This is shown with daily zonal means of radiances at 80°N from different upper stratospheric channels of the SCR (Selective Chopper Radiometer) and PMR (Pressure Modulated Radiometer) (Nimbus 4,5,6) (Figure 7). They are compared with the 10- and 30-mbar temperatures over the North Pole (LABITZKE, 1983). The data set used for the preparation of the new Reference Atmosphere (cf. Sections 2.1.1 and 2.2) includes most of these winters.

This survey over eight northern winters illustrates distinctly their high variability of the stratospheric winters with the different timing and intensity of the stratospheric warmings. The "major warmings(*)" are connected with a breakdown of the stratospheric polar vortex, followed by a "late winter cooling", thus influencing the whole winter season.

In contrast, the southern winters show very little variation from year to year over the polar region. The temperature minimum is reached in early winter and therefore in the upper stratosphere the transition into summer starts much earlier over the Antarctic than over the Arctic. This is shown in Figure 8 where the march of radiances at 80°N and 80°S is compared (LABITZKE, 1977).

These differences are most obvious in spring. Therefore the 1-mbar temperature charts of March/N.H. and September/S.H. are compared in Figure 9 (Data: New Reference Atmosphere).

(c) Temperature Trends

Much attention has been directed recently towards the detectability of changes in temperature because theoretical calculations suggest that changing concentrations of a number of anthropogenically influenced tract gases may presently be altering the global temperature structure, mostly warming the troposphere and cooling the stratosphere (greenhouse effect). A variety of natural processes and phenomena are also known to affect the middle atmosphere, e.g., variation in the solar ultraviolet flux over the 11-year sunspot cycle, or the increase of the stratospheric aerosol load due to volcanic eruptions.

Lower Stratosphere: For the investigation of long-term temperature changes in the lower stratosphere a series of temperature data for the Northern Hemisphere is available from the Stratospheric Research Group, Free University Berlin. This data set which starts in July 1964 for most pressure levels consists of daily hemispheric analyses of temperatures (and geopotential heights), based largely on radiosonde observations. The daily hemispheric analyses have been analyzed by hand and have been digitized into a latitude-longitude grid. Monthly mean statistics have been derived afterwards.

Figure 10 shows filtered zonal mean 30-mb temperatures (°C). A 39-point filter has removed the annual and the quasi-biennial cycles. Looking at these curves, several features can be noticed:

Large variations with a time scale of several years still exist.

The causes of these variations are not clear.

At higher latitudes the variations appear to be connected with the appearance of intense midwinter warmings or undisturbed cold winters.

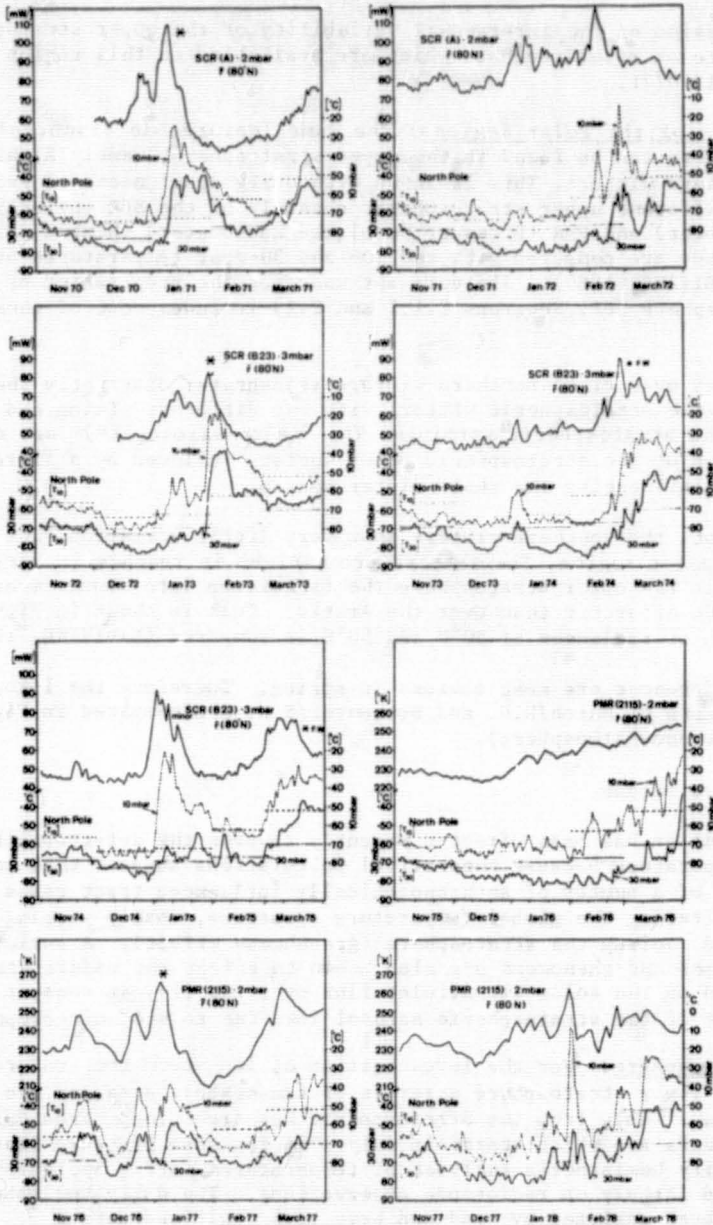
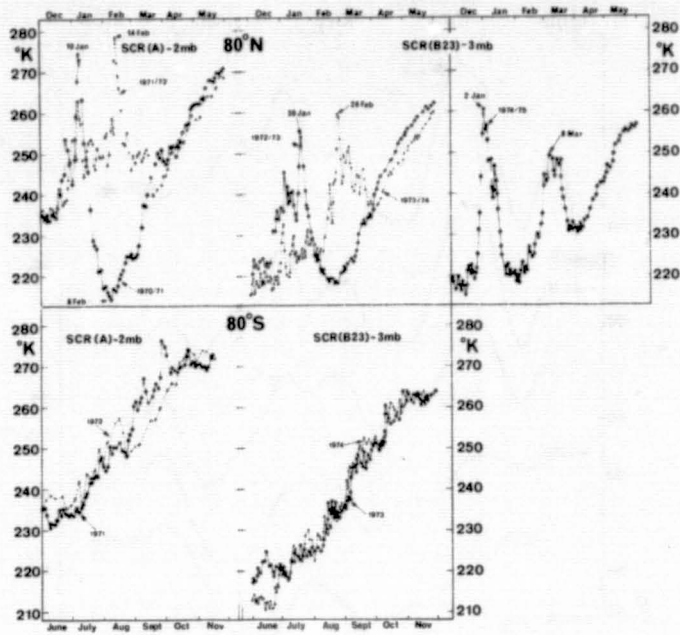


Figure 7. Course of radiances or temperatures over the polar region: zonal mean radiances at 80°N in $[\text{mW(m}^2\text{sr(cm}^2\text{))}^{-1}]$ or (K), i.e., equivalent blackbody temperature, from different experiments representing the upper stratosphere as indicated. Temperatures ($^{\circ}\text{C}$) of the 10- and 30-mbar level over the North Pole. (Radiance data: Oxford University, UK; temperature data: Free University Berlin.) (LABITZKE, 1983).



Daily zonal means at 80 deg. latitude of radiances of upper stratospheric channels of the SCR, flown on Nimbus 4 and 5.
(The radiances are converted into equiv. black body temperatures (°K)).

Figure 8. Daily zonal means at 80° latitude of radiances of upper stratospheric channels of the SCR flown on Nimbus 4 and 5. The radiances are converted into equivalent blackbody temperatures (from LABITZKE, 1977).

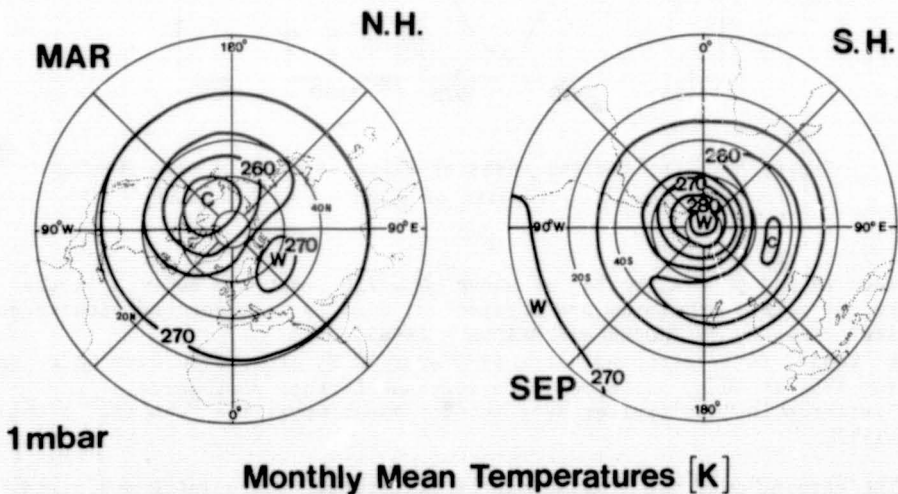


Figure 9. Monthly mean 1-mbar temperatures from March/N.H. and September/S.H. (Data are from the new Reference Atmosphere).

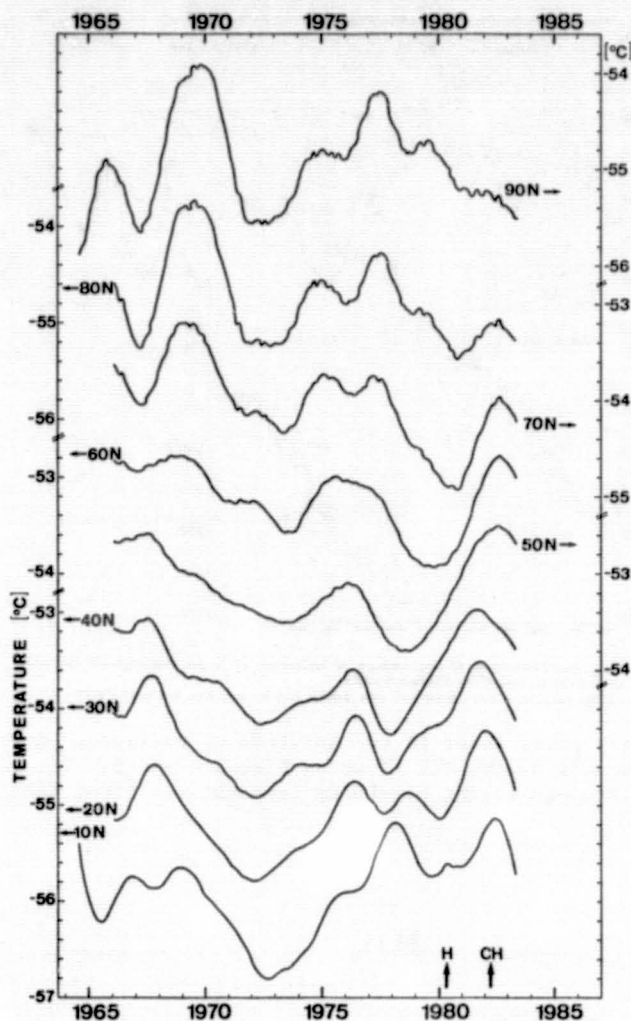


Figure 10. Latitudinal means of filtered monthly mean 30-mbar temperatures ($^{\circ}\text{C}$). (Update of Figure 4 of NAUJOKAT, 1981).

Between 70°N and 40°N a "trend" of about $-0.6^{\circ}/10$ years can be seen in the data, if maxima or minima are considered; this is in agreement with recent calculations by De RUDDER and BRASSEUR (1985).

This "trend" is interrupted after 1979 over 40°N , after 1980 over 50°N , and after 1981 at 60°N , but appears to continue further northwards.

The interruption was earlier over low latitudes where the "cooling" stopped in 1972.

The warming over the tropics can be attributed to the increased aerosol load after volcanic eruptions. This was demonstrated for the summer and fall of 1963 and 1982, when the stratosphere warmed markedly over the tropics after the eruptions of Agung and El Chichón (Figures 4 and 11) (LABITZKE et al., 1983; LABITZKE and NAUJOKAT, 1983).

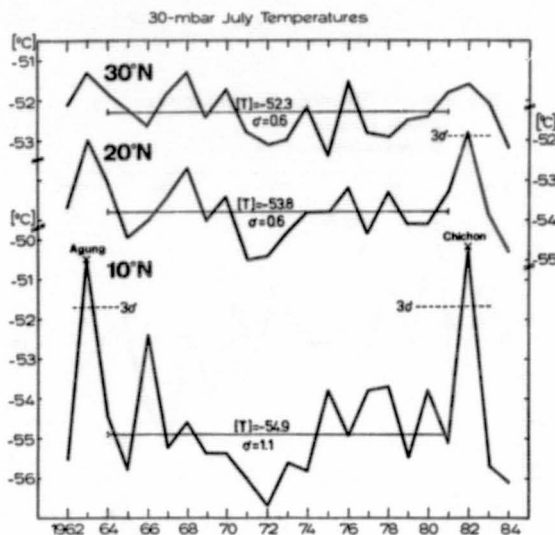


Figure 11. Zonal mean 30-mbar temperatures ($^{\circ}\text{C}$) during July at 10, 20, and 30°N , for the period 1962 through 1984. The 18-year average $[T]$ is for the period 1964-1981. (Update of Figure 8 from LABITZKE and NAUJOKAT, 1983).

The filtered 30-mb temperatures (Figure 10) show that the effect of the warming is noticeable as far as 60°N . Probably the region between 40 and 60°N was also strongly affected by the increased aerosol from the eruption of Mt. St. Helens in May 1980.

Looking at the annual averages of the single years directly (Figure 12) the strong cooling over the tropics and subtropics is especially worth noting. The temperatures are as cold or even colder than during the years 1971 and 1972.

The departures of the annual mean temperatures, averaged over two years, are summarized in a time-latitude section (Figure 13). The warming episode due to the increased volcanic aerosol appears to be finished and the cooling has resumed over almost all latitudes.

An even clearer picture emerges, if only July, i.e., a relatively quiet summer month, is considered (Figure 14). The data series for July starts in 1962, cf. Figure 11, and the time-latitude section shows clearly the warming after Agung (March 1963) and after El Chichon (March 1982). If an overall cooling of approximately $0.6^{\circ}/10$ years is accepted, it is not surprising that negative deviations are observed earlier after El Chichon than after Agung, if the deviations are made from the same long-term average.

Upper Stratosphere: Attempts have been made to detect a temperature trend in the upper stratosphere using US rocketsonde data (eg., QUIROZ, 1979; ANGELL and KORSHOVER, 1983; JOHNSON and GELMAN, 1984). Unfortunately, a noticeable temperature decrease coincides with a change in the principal observing system from the Arcasonde system to the Datasonde system, and therefore a clear answer cannot be given at this point.

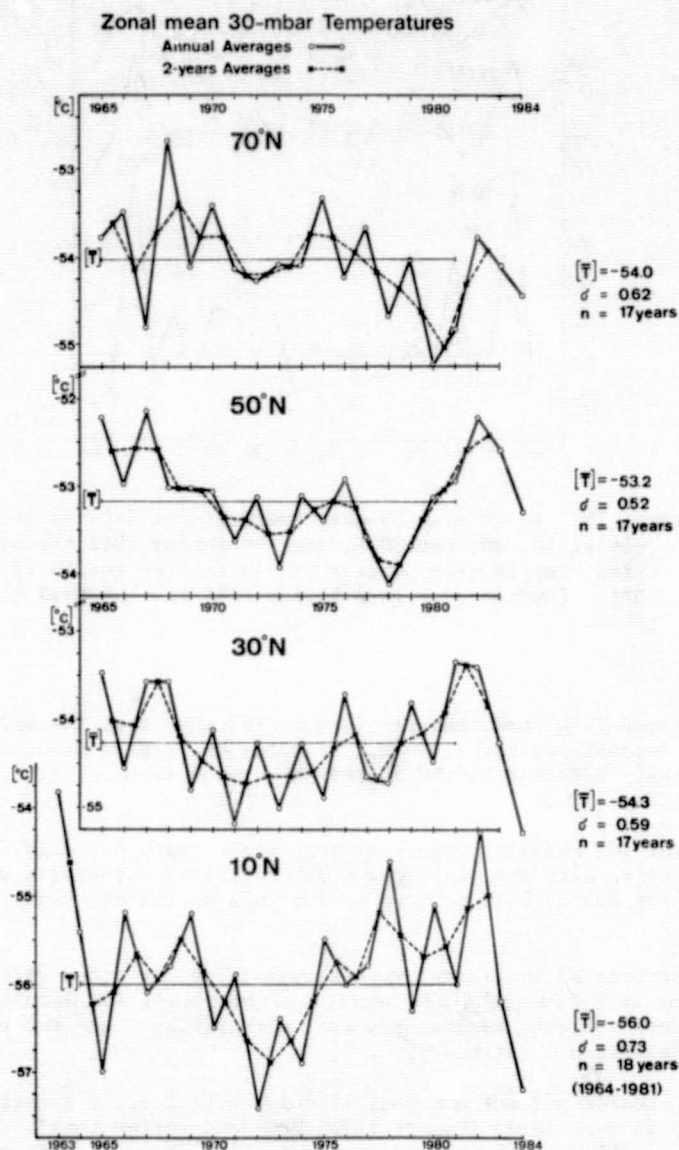


Figure 12. Annual and biennial averages of the 30-mbar temperatures (°C) at 70, 50, 30 and 10°N for the period 1965 through 1984, except for 10°N which starts in 1963. (Update of Figure 4b of LABITZKE and NAUJOKAT, 1983).

Departures ($\frac{1}{10}$ K) of the 30-mbar Temperatures, averaged over 2 years, from the 17-year mean 1965-1981

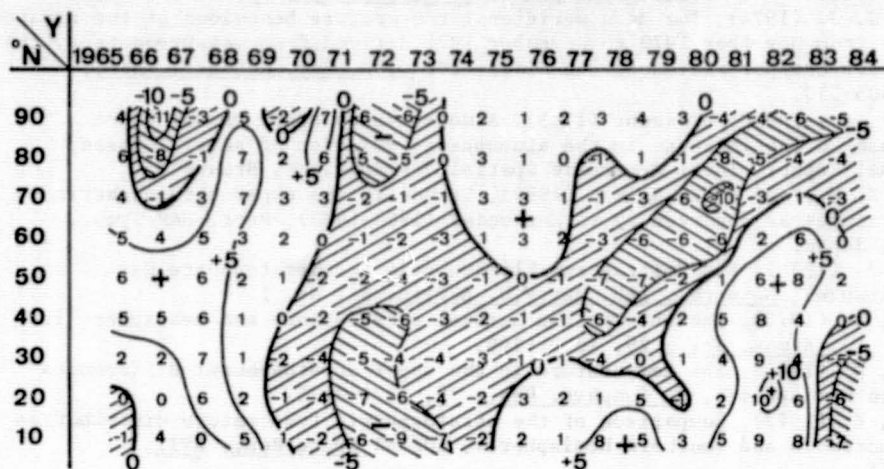


Figure 13. Time-latitude distribution of the deviations ($\frac{1}{10}$ K) of the annual averages, smoothed over two years, from the 17-year mean 1965-1981. (Update of Figure 5, LABITZKE and NAUJOKAT, 1983).

Departures ($\frac{1}{10}$ K) of the 30-mbar July Temperatures, averaged over 2-years, from the 18-year mean 1964-1981

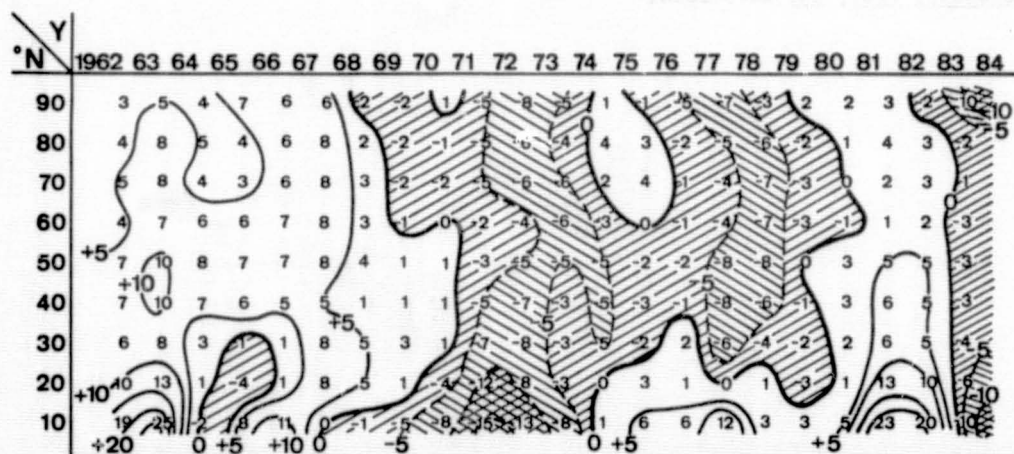


Figure 14. Time-latitude distribution of the deviations ($\frac{1}{10}$ K) of the July averages, smoothed over two years, from the 18-year mean 1964-1981. (Update of Figure 6, LABITZKE and NAUJOKAT, 1983).

REFERENCES

- Angell, J. K., and J. Korshover (1978), Recent rocketsonde-derived temperature variations in the Western Hemisphere, J. Atmos. Sci., **35**, 1758-1764.
- Barnett, J. J. (1974), The mean meridional temperature behaviour of the stratosphere from November 1970 to November 1971 derived from measurements by the selective chopper radiometer on Nimbus IV, Q. J. Roy. Meteorol. Soc., **100**, 505-530.
- De Rudder, A., and G. Brasseur (1985), A model calculation of the ozone response to the increase in the atmospheric emission of several gases, Internal Report, Inst. Aeronomie Spatiale de Belgique, Brussels.
- Johnson, K. W., and M. E. Gelman (1984), Trends in the upper stratospheric temperatures as observed by rocketsondes (1965-1983), Proc. MAP Symp., Kyoto, Japan.
- Knittel, J. (1976), Ein Beitrag zur Klimatologie der Stratosphäre der Sudhalbkugel, Meteorol. Abh. der F.U. Berlin, **A2**, Nr. 1.
- Labitzke, K. (1972), The interaction between stratosphere and mesosphere in winter, J. Atmos. Sci., **29**, 1359-1399.
- Labitzke, K. (1974), The temperature in the upper stratosphere: Differences between hemispheres, J. Geophys. Res., **79**, 2171-2175.
- Labitzke, K. (1977), Comparison of the stratospheric temperature distribution over northern and southern hemispheres, COSPAR Space Res., **XVII**, 159-165.
- Labitzke, K. (1983), A survey over the PMP-1 winters 1978/79-1981/82 in comparison with earlier winters, Adv. Space Res., **2**, 149-157.
- Labitzke, K., B. Naujokat, and M. P. McCormick (1983), Temperature effects on the stratosphere of the April 4, 1982 eruption of El Chichon, Mexico, Geophys. Res. Lett., **10**, 24-26.
- Labitzke, K., and B. Naujokat (1983), On the variability and on trends of the temperature in the middle stratosphere, Contributions to Atmos. Phys., **56**, 495-507.
- Naujokat, B. (1981), Long-term variations in the stratosphere of the northern hemisphere during the last two sunspot cycles, J. Geophys. Res., **86**, 9811-9816.
- Quiroz, R. S. (1979), Stratospheric temperatures during solar cycle 20, J. Geophys. Res., **84**, 2415-2420.

2.4 A PROPOSED INTERNATIONAL TROPICAL REFERENCE ATMOSPHERE UP TO 80 KM

M. R. Ananthasayanam and R. Narasimha

Department of Aerospace Engineering
Indian Institute of Science
Bangalore 560 012, India

N86-12828

1. INTRODUCTION

With the large number of balloonsonde and meteorological rocket network (MRN) stations over the globe and satellite soundings, it is presently possible to characterise the atmosphere typical of a season, a month or even a day. However, a standard atmosphere representative of the mean annual conditions is still essential for many aerospace and remote sensing applications. An International Standard Atmosphere (ISA: see US STANDARD ATMOSPHERE, 1962; ICAO, 1964) specified up to 32 km, and its proposed extension to higher altitudes such as US STANDARD ATMOSPHERE (1976), have been formulated for meeting these needs. These have been generally inspired by conditions in the temperate region around mid-northern latitudes. However, conditions over the tropics can be substantially different from those specified in the International Standards; over the past several years the authors have sought to answer the question "Is it possible to define a standard atmosphere which is close to the mean conditions over tropical India and elsewhere?". During summer, tropical conditions prevail up to about 35 N and during winter the change from extratropical to tropical conditions occurs somewhere between 27°N and 35°N and probably around 30°N (KRISHNA RAO, 1952). Thus with the available data, a suitable Indian Standard Tropical Atmosphere (ISTA) up to 80 km and about 30°N in latitude was specified by ANANTHASAYANAM and NARASIMHA (1979, 1980, 1983, 1984a).

The following facts suggest that, with minor modification, it should be possible to provide an International Tropical Reference Atmosphere (ITRA) suitable for the whole of the tropical regions in both the Northern and Southern Hemispheres. Firstly, a study of the balloonsonde results up to 20 km for stations at other longitudinal locations in North America (see Table 1) show that conditions are not very different from those prevailing over India. Further, even at altitudes up to 80 km, COLE and KANTOR (1978) show that longitudinal variations during summer are small at all latitudes and at all altitudes above 20 km; during winter longitudinal variations become important only in arctic and subarctic latitudes.

We have considered the data at the available longitudinal stations in the tropics in formulating the present proposal. Many reference atmospheres have been formulated for the tropics: e.g., PISHAROTY (1959), ARB (1966), USSA (1966), CIRA (1972), COLE and KANTOR (1978), SASI and SEN GUPTA (1979), COLE et al. (1979), and KOSHELOV (1980); none of these cover the latitude and altitude range of the present proposal.

Finally, it is well known (COLE and KANTOR, 1978) that latitudinal variations are weaker in the tropics than in the temperate regions; hence it should be possible to formulate a meaningful global standard for the tropics. The subsequent section discusses the nature, accuracy and consistency of the data available for the present study.

2. DATA BASE FOR PRESENT WORK

2.1 Temperature data: The present standard is developed in three parts,

Table 1. Station temperature data for the proposed ITRA.

ALT IN KM ----->			STATION	1.5	3.1	5.8	9.7	12.4	14.2	16.6	20.7
STATION	LAT	LONG	PERIOD & DATA								
TRIVANDRUM	9 N	77 E	50-71 B 300	291	283	268	242	221	208	198	211
NAGPUR	21 N	79 E	50-71 B 300	294	283	267	242	222	210	199	210
NEW DELHI	29 N	77 E	50-71 B 297	292	281	264	240	223	214	204	214
SRINAGAR	34 N	75 E	50-71 B 286		278	260	236	222	217	211	
TRIVANDRUM	9 N	77 E	73-78 B 299	290	282	267	242	220	205	194	210
NAGPUR	21 N	79 E	73-78 B 300	294	283	267	243	222	209	197	209
NEW DELHI	29 N	77 E	73-78 B 298	291	280	264	239	221	211	200	211
KWAJALEIN	9 N	168 W	69-76 B 304	293	285	269	243	221	207	195	208
BROWNSVILLE	26 N	97 W	71-80 B 293	289	281	264	237	217	207	200	211
AP.CHICOLA	30 N	85 W	71-80 B 290	286	278	263	236	217	209	204	212
ALT IN KM ----->			25	30	35	40	45	50	55	60	65
ASCENSION	8 S	14 W	69-76 T 221	232	243	258	269	270	264	254	238
THUMBA (a)	9 N	168 E	70-76 T 221	232	244	258	264	262	248	218	209
KWAJALEIN	9 N	77 E	69-76 T 220	230	240	255	266	270	261	246	230
FT.SHERMAN	9 N	80 W	69-76 T 222	231	243	257	268	271	267	259	
ANTIGUA	17 N	62 W	69-76 T 222	232	242	256	267	269	264	253	236
BARK.SANDS	22 N	160 W	69-76 T 221	231	241	254	266	268	263	254	234
CP.KENNEDY	28 N	80 W	69-76 : 222	231	242	255	267	268	263	255	239
WHT. SANDS	32 N	106 W	69-76 T 221	229	240	254	266	268	262	254	246
ALT IN KM ----->			40	45	50	55	60	65	70	75	80
ASCENSION(b)	8 S	14 W	60-71 G(251	(261	(263	(257	(242	(222	(202	(191	(188
and NATAL			-259)-271)	-271)	-263)	-252)	-234)	-220)	-211)	-206)	
THUMBA (c)	9 N	77 E	71-77 T 259	267	269	256	242	227	213	205	193
KWAJALEIN	9 N	168 W	56-78 * 255	266	270	261	246	230	213	200	196
WOOMERA (d)	31 S	137 E	57-63 S 254	267	267	259	249	232	218	204	191
WOOMERA (e)	31 S	137 E	57-63 G(239	(258	(235	(205	(185				
			-263)	-281)	-255)	-235)	-208)				

+ B = Balloon, G = Grenade, P = Pitot, S = Sphere, T = Thermistor,
 * = T & S (a) Without adjustment of FINGER et al. (1975); (b) Mean
 +/- standard deviation; (c) With adjustment of FINGER et al. (1975);
 (d) Approximate values from Figure 3 of PEARSON (1974); (e) Approximate range from Figure 3 of GROVES (1966).

namely, (i) in the troposphere and lower stratosphere, using balloonsonde data, (ii) in the upper stratosphere, utilising rocketsonde data, and (iii) in the mesosphere, considering grenade and falling sphere data.

Table 1 also shows the details of the station, type of instrumentation used, duration of available data and reference from which the data have been obtained.

2.2 Remarks on the quality and consistency of data. Table 1 shows the pre- and post-1970 IMD data when it switched from chronometric and fan type recorders to the audio-modulated type in the radiosonde. The effect of this, as noticed by ANANTHASAYANAM and NARASIMHA (1979) and by Van de Boogard (1977), is that during July over Nagpur, e.g., the later temperature values are lower by about 5 C at the 100 mb level. However, considering the variation of temperature over the range of stations in the Indian subcontinent and during a year, such discrepancies lower the grand mean among stations only by about 2 - 3 C, and thus would not strongly alter the present proposal. Table 1 further shows data of some typical stations in India and in the American region; these are broadly consistent and confirm that a proposal (up to 20 km) valid for the whole tropical region over the world should be feasible.

For the 20 to 50 km range, commencing from the late sixties when several MRN stations were set up, extensive (generally once-weekly) rocketsonde data are available, as mentioned earlier. The wire type thermistor probe used on the Russian M-100 rocketsonde and the bead type thermistor probe on American

rocketsondes are fairly consistent up to 50 km. However, these probes have shown differences of as much as 15°C around 70 km during the many intercomparison experiments carried out at Wallops Island and reported by FINGER et al. (1975), IVANOVSKY et al. (1979) and SCHMIDLIN et al. (1980). It is possible that these differences are due to the free molecular conditions prevailing at altitudes beyond about 50 km, but no universally accepted resolution of these differences is yet available. Thus, rocketsonde data available at many stations over the globe have been used only in the range from about 20 to 50 km.

For the higher altitude range of 50 to 80 km we have used mainly the falling sphere and grenade data, which are consistent among themselves and possess an accuracy of about $2 - 3^{\circ}\text{C}$ (CIRA, 1972). SMITH et al. report pitot tube data as well, but these lead to temperatures which are about 5°C higher on an average from the grenade data; as the reason for this is not clear, we have not considered the pitot data. Data in this altitude range are not as extensive as one would wish, but are perhaps barely adequate to propose a reasonable standard for describing the mean conditions.

Beyond an altitude of 80 km molecular dissociation commences, and above 100 km molecular diffusion predominates, and so air can no longer be treated as a perfect gas. It is then necessary to specify at each level the (varying) concentration of different species constituting air. Hence an altitude of 80 km is a natural limit to the present kind of standard.

3. PROPOSED INTERNATIONAL TROPICAL REFERENCE ATMOSPHERE (ITRA) UP TO 80 KM

The philosophy adopted by the authors in proposing the reference has been that it should: (a) be reasonably close to mean conditions, (b) be within the range of variation inherent in the atmosphere over space and time and the uncertainty in the data be as simple as possible, and (c) adopt, where no physical principles are violated, as many of the parameters in the ISA as possible.

3.1 Temperature distribution with altitude. Table 1 and Figure 1 show, respectively, the station mean data, and the grand mean among themselves, for the temperature between sea level and about 90 km. In the mesospheric region the grand mean is weighted towards low latitude stations. But Wallops Island data in USSA (1976) indicated that the latitudinal variations (at least between 50 and 70 km) is weak. Usually straight lines best fitting the data are used to describe the temperature distribution with altitude. This is because closed form integration of the governing equation to obtain other atmospheric properties is then possible.

As the data indicate, the proposed standard has a sea level temperature of 27°C , and a lapse rate of $6^{\circ}\text{C}/\text{km}$ up to 6 km. Beyond this altitude the lapse rate is $6.5^{\circ}\text{C}/\text{km}$ (as in ISA) up to 16 km, the tropopause height. This tropopause height, and the corresponding temperature of -74°C seems quite appropriate as noticed by us, and is also consistent with the various monthly reference atmospheres at the equator, 15°N and 30°N proposed by COLE and KANTOR (1978). Further, in the stratosphere, a single lapse rate of $-2.3^{\circ}\text{C}/\text{km}$ all the way up to a stratopause height of 46 km, with a temperature of -5°C , fits the data very well. Though this temperature is somewhat higher than indicated by the Thumba value (IMD, 1976), we consider it appropriate because of the fact that the stratopause temperature decreased with increasing latitudes (COLE and KANTOR, 1978). The available data in the mesosphere indicate that it would be worthwhile to extend the constant temperature stratopause up to 52 km. It should be noted that in the mesosphere inversions occur during some months and there are well-known double mesopauses with different temperature values as

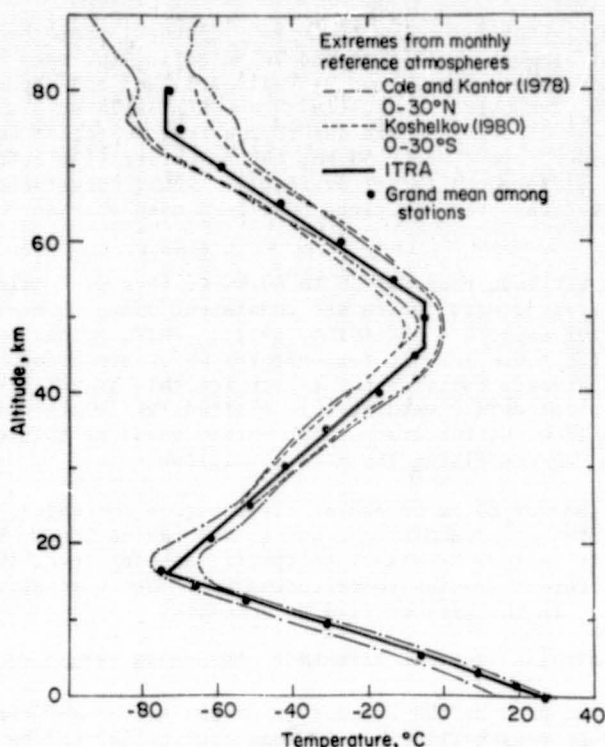


Figure 1. Comparison of ITRA with station data and monthly reference atmospheres.

well (WDC, 1969:76). But considering the totality of the data, and the average value that can be assigned at different levels over many stations, it is seen that once again a constant lapse rate of $3^{\circ}\text{C}/\text{km}$ from 52 km to 75 km, leading to a temperature of -74°C (as at tropopause) by the beginning of the mesopause, is justified. The constant temperature mesopause extends up to 80 km, which is the limit of the present proposal.

The present tropical reference is within the range of the extremes based on the temperature values in the monthly reference atmospheres for the tropical regions proposed for the Northern and Southern Hemispheres by COLE and KANTOR (1978) and by KOSHELKOV (1980), respectively; these are also shown in Figure 1.

3.2 Mean sea level pressure. Seasonal pressure variations like those of the temperature increase with latitude, the mean pressure being lower during summer and higher during winter. Consideration of the mean annual station level pressures at Indian stations, extrapolated to sea level conditions, gives a value of about 1010 mb based on hourly data (ANANTHASAYANAM and NARASIMHA, 1984b). In ISTA, we had used a lower value of 1005 mb, consistent with the somewhat higher sea level temperature value of 30°C to provide a slight bias towards the hot day that was considered desirable for aeronautical work. The more appropriate sea level temperature of 27°C now proposed, goes with the higher value of 1010 mb for sea level pressure. COLE and KANTOR (1978), using mostly data from western longitudes, also obtain a mean pressure close to this value. Only towards 30°N and beyond does the mean pressure increase

appreciably. A further study of the Southern and Northern Hemisphere data for the years 1951 to 1960 from the WORLD WEATHER RECORDS (1967) for nearly 200 tropical stations shows that the above annual value is justified. It may be noted that the yearly variation of pressure at a given station is of the order of a few mb. Different countries adopt slightly different methods for reducing the station level pressure to sea level conditions (WMO, 1968). But these are even smaller than 1 mb and thus do not affect our proposal.

3.3 Acceleration due to gravity (g). For this we suggest a value corresponding to the Tropic of Cancer, which from Lambert's formula given in LIST (1968) gives 9.78852 m/s (to five decimal places).

4. ATMOSPHERIC TABLES

Table A below specifies the temperature distribution for the present International Tropical Reference Atmosphere, as also the other constants adopted for generating the atmospheric table.

Table A. Defining parameters and constants for the proposed ITRA

Altitude (km)	0	6	16	46	52	75	80
Temp (°C)	27(-6.0)	-9(-6.5)	-74(2.3)	-5(0.0)	-5(3.0)	-74(0.0)	-74

The bracketed quantities denote lapse rate in °C/km. Sea level pressure = 1010 mb; Acceleration due to gravity = 9.78852 ms^{-2} . The molecular weight and the ratio of the specific heats of air, the gas constant and the other constants for the transport properties are assumed to be the same as in US STANDARD ATMOSPHERE (1976).

Tables 2 and 3 give the atmospheric properties useful in meteorological and aerospace applications. More detailed atmospheric tables and the computer code used are available on request from the authors.

ACKNOWLEDGEMENT

The authors thank the Aeronautics Research and Development Board (ARDB) for having supported this study through a grant for the project "SITA".

ORIGINAL PAGE IS
OF POOR QUALITY

Table 2. Atmospheric properties of ITRA (SI units).

PRESSURE	GEOPT	NUMBER	MEAN	MEAN	MEAN	DYNAMIC	KINMATIC	THERMAL	
	ALT	DENSITY	PARTICLE	COLLSN	FREE	VISCY	VISCY	CONDVTY	
(mb)	(m)	(m ⁻³)	(m/s)	(s ⁻¹)	(m)	kg/(m.s)	(m ² /s)	W/(m.K)	
1,010	3	00	2,437 25	4,684 2	6,757 9	6,932-8	1,847-5	1,575-5	2,626-2
8,500	2	1500	2,114 25	4,614 2	5,774 9	7,990-8	1,804-5	1,774-5	2,556-2
7,000	2	3130	1,802 25	4,535 2	4,837 9	9,377-8	1,757-5	2,027-5	2,479-2
5,000	2	5820	1,365 25	4,403 2	3,559 9	1,237-7	1,677-5	2,553-5	2,350-2
3,000	2	9610	9,028 24	4,195 2	2,241 9	1,871-7	1,551-5	3,571-5	2,151-2
2,000	2	12360	6,502 24	4,036 2	1,553 9	2,598-7	1,455-5	4,653-5	2,002-2
1,500	2	14190	5,151 24	3,926 2	1,197 9	3,280-7	1,390-5	5,609-5	1,902-2
1,000	2	16610	3,611 24	3,829 2	8,185 8	4,678-7	1,332-5	7,666-5	1,814-2
5,000	1	20790	1,723 24	3,919 2	3,998 8	9,804-7	1,386-5	1,672-4	1,896-2
3,000	1	23990	9,989 23	3,988 2	2,358 8	1,691-6	1,426-5	2,969-4	1,958-2
2,000	1	26610	6,480 23	4,042 2	1,550 8	2,607-6	1,459-5	4,682-4	2,008-2
1,000	1	31260	3,092 23	4,138 2	7,573 7	5,464-6	1,517-5	1,020-3	2,098-2
5,000	0	36140	1,475 23	4,236 2	3,699 7	1,145-5	1,576-5	2,221-3	2,190-2
2,000	0	42940	5,548 22	4,369 2	1,435 7	3,045-5	1,656-5	6,206-3	2,317-2
1,000	0	48350	2,701 22	4,427 2	7,078 6	6,255-5	1,691-5	1,302-2	2,374-2
5,000-1	53780	1,378 22	4,383 2	3,575 6	1,226-4	1,664-5	2,511-2	2,331-2	
2,000-1	60570	5,975 21	4,210 2	1,489 6	2,827-4	1,560-5	5,428-2	2,165-2	
1,000-1	65350	3,175 21	4,083 2	7,675 5	5,320-4	1,484-5	9,715-2	2,046-2	
5,000-2	69850	1,688 21	3,961 2	3,956 5	1,001-3	1,410-5	1,737-1	1,933-2	
2,000-2	75390	7,274 20	3,815 2	1,643 5	2,323-3	1,324-5	3,784-1	1,802-2	
1,000-2	79440	3,637 20	3,815 2	8,214 4	4,645-3	1,324-5	7,567-1	1,802-2	

ORIGINAL PAGE IS OF POOR QUALITY

Table 3. Atmospheric properties of ITRA (largely SI units).

GEOPT ALT (m)	PRES ALT (m)	TEMP DEGREE (K)	PRESSURE (mb)	PRESSURE RATIO	DENSITY (kg/m ³)	DENSITY RATIO	SONIC VELOCITY (m/s)	UNIT REY NUMBER (s/m ²)
-2000	-1890	312.15	1.262 3	1.250 0	1.408 0	1.202 0	354.18	7.402 0
00	30	300.15	1.010 3	1.000 0	1.172 0	1.000 0	347.31	6.348 0
2000	1940	288.15	8.010 2	7.930-1	9.684-1	8.261-1	340.29	5.412 0
4000	3840	276.15	6.290 2	6.227-1	7.934-1	6.769-1	333.13	4.584 0
6000	5740	264.15	4.886 2	4.838-1	6.444-1	5.497-1	325.81	3.856 0
8000	7640	251.15	3.750 2	3.712-1	5.201-1	4.437-1	317.70	3.240 0
10000	9540	238.15	2.837 2	2.809-1	4.150-1	3.540-1	309.36	2.700 0
12000	11430	225.15	2.113 2	2.093-1	3.270-1	2.790-1	300.80	2.228 0
14000	13410	212.15	1.547 2	1.532-1	2.540-1	2.167-1	291.99	1.819 0
16000	15520	199.15	1.110 2	1.099-1	1.942-1	1.657-1	282.90	1.467 0
18000	17660	203.75	7.914 1	7.836-2	1.353-1	1.154-1	286.15	1.002 0
20000	19760	208.35	5.684 1	5.628-2	9.503-2	8.107-2	289.36	6.908-1
22000	21820	212.95	4.112 1	4.071-2	6.726-2	5.738-2	292.54	4.800-1
24000	23860	217.55	2.995 1	2.965-2	4.796-2	4.091-2	295.68	3.362-1
26000	25870	222.15	2.196 1	2.175-2	3.444-2	2.938-2	298.79	2.373-1
28000	27860	226.75	1.621 1	1.605-2	2.490-2	2.124-2	301.87	1.686-1
30000	29820	231.35	1.203 1	1.192-2	1.812-2	1.546-2	304.92	1.207-1
32000	31770	235.95	8.988 0	8.899-3	1.327-2	1.132-2	307.93	8.697-2
34000	33700	240.55	6.750 0	6.683-3	9.776-3	8.339-3	310.92	6.307-2
36000	35640	245.15	5.097 0	5.047-3	7.244-3	6.179-3	313.88	4.602-2
38000	37590	249.75	3.869 0	3.831-3	5.397-3	4.604-3	316.81	3.378-2
40000	39550	254.35	2.952 0	2.923-3	4.043-3	3.449-3	319.71	2.494-2
42000	41510	258.95	2.263 0	2.241-3	3.045-3	2.597-3	322.59	1.851-2
44000	43480	263.55	1.743 0	1.726-3	2.304-3	1.966-3	325.44	1.381-2
46000	45460	268.15	1.349 0	1.335-3	1.752-3	1.495-3	328.27	1.036-2
48000	47470	268.15	1.046 0	1.035-3	1.359-3	1.159-3	328.27	8.034-3
50000	49480	268.15	8.110-1	8.030-4	1.054-3	8.988-4	328.27	6.230-3
52000	51490	268.15	6.289-1	6.226-4	8.170-4	6.969-4	328.27	4.831-3
54000	53500	262.15	4.862-1	4.814-4	6.462-4	5.512-4	324.58	3.870-3
56000	55510	256.15	3.737-1	3.700-4	5.083-4	4.336-4	320.84	3.117-3
58000	57520	250.15	2.855-1	2.826-4	3.975-4	3.391-4	317.06	2.485-3
60000	59540	244.15	2.166-1	2.145-4	3.091-4	2.637-4	313.24	1.970-3
62000	61560	238.15	1.633-1	1.616-4	2.388-4	2.037-4	309.36	1.553-3
64000	63580	232.15	1.222-1	1.209-4	1.833-4	1.564-4	305.44	1.218-3
66000	65610	226.15	9.071-2	8.981-5	1.397-4	1.192-4	301.47	9.484-4
68000	67640	220.15	6.682-2	6.616-5	1.057-4	9.020-5	297.44	7.339-4
70000	69670	214.15	4.881-2	4.832-5	7.940-5	6.773-5	293.36	5.640-4
72000	71710	208.15	3.533-2	3.499-5	5.914-5	5.045-5	289.22	4.302-4
74000	73760	202.15	2.534-2	2.509-5	4.367-5	3.725-5	285.02	3.257-4
76000	75830	199.15	1.802-2	1.784-5	3.151-5	2.688-5	282.90	2.381-4
78000	77870	199.15	1.279-2	1.266-5	2.238-5	1.909-5	282.90	1.690-4
80000	79850	199.15	9.082-3	8.992-6	1.589-5	1.355-5	282.90	1.200-4

REFERENCES

- Air Registration Board, BCAR (1966).
- Ananthasayanam, M. R., and R. Narasimha (1979), Rep. 79 FM 5, Dept. of Aeronautical Engineering, Indian Inst. of Science, Bangalore.
- Ananthasayanam, M. R., and R. Narasimha (1980), Space Res., XX, 25.
- Ananthasayanam, M. R., and R. Narasimha (1983), Adv. Space Res., 3, (1), 17.
- Ananthasayanam, M. R., and R. Narasimha (1984a), Rep. 84 FM 1, Dept. of Aerospace Engineering, Indian Inst. of Science, Bangalore.
- Ananthasayanam, M. R., and R. Narasimha (1984b), ARDB Rep. (to be published).
- COSPAR International Reference Atmosphere (1972), Academie Verlag, Berlin
- Cole, A. E., and A. J. Kantor (1978), Air Force Reference Atmosphere, AFGL-TR-78-0051.
- Cole, A. E., A. J. Kantor, and C. R. Philbrick (1979), Kwajalein Reference Atmospheres, AFGL-TR-79-0241.
- Faire, A. C., and K. S. W. Champion (1965, 1966, 1967, 1968, 1969), Space Res., V, 1039; VI, 1048; VII, 1046; VIII, 845; IX, 343.
- Finger, F. G., et al. (1975), J. Atmos. Sci., 32, 1705.
- Groves, G. V. (1966), Space Res., VII, 1111.
- Manual of the ICAO Standard Atmosphere (1964), Doc. 7488/2, Second Edition.
- IMD (1972), Normals of Climat. Temp. based on Morning and Afternoon/Evening Radiosonde Data for the Period 1951-1970.
- IMD (1976), Climatology of the Stratosphere in the Equatorial Region over India, Meteorol. Monograph. Climatology No. 9.
- Ivanovsky, A. I., et al. (1979), Space Res., XIX, 127.
- Koshelkov, Yu. P. (1980), Space Res., XX, 41.
- Krishna Rao, P. R. (1952), Indian J. Meteorol. Geophys., 3, 173.
- List, R. J. (1968), Smithsonian Meteorological Tables, Sixth Edition.
- National Climatic Data Center (1973-1978), Monthly Climatic Data for the World.
- Pearson, P. H. O. (1974), Space Res., XIV, 67.
- Pisharoty, P. R. (1959), Indian J. Meteorol. Geophys., 19, 243.
- Sasi, M. N., and K. Sen Gupta (1979), VSSC TR 46-157-79, Trivandrum, India.
- Schmidlin, F. J., et al. (1980), NASA RP-1053.
- Smith, W., et al. (1964, 1966, 1967, 1968, 1969, 1970, 1971, 1972), NASA TR R-211, 245, 263, 288, 316, 340, 360, 391.
- US Standard Atmosphere (1962).
- US Standard Atmosphere Supplements (1966).
- US Standard Atmosphere (1976)
- Van de Boogard, H. (1977)0, NCAR/TN-118+STR, Boulder, CO.
- World Data Center A (1969-1976), High altitude meteorological data reports.
- World Meteorological Organization (1968), Tech. Note 91.
- World Weather Records (1967), US Dept. of Commerce.

2.5 INTERIM REFERENCE OZONE MODELS FOR THE MIDDLE ATMOSPHERE

G. M. Keating

NASA Langley Research Center
Hampton, VA 23665

N86-12829

D. F. Young

Systems and Applied Sciences Corporation
Hampton, VA 23666

1. INTRODUCTION

Over the last 50 years, a number of measurements of ozone in the middle atmosphere have been obtained from the ground, and from balloons, rockets and satellites. Numerous models have been developed to summarize various portions of these measurements since detailed knowledge of the global distribution of ozone is important for studies of atmospheric circulation, dynamic processes, and the radiation balance and the photochemistry of the atmosphere. From the ground-based ozone network the latitudinal-seasonal variations of total column ozone were summarized by DUTSCH (1974) and the longitudinal variations were included in a series of monthly atlases for the period 1957 to 1967 by LONDON et al. (1976). Measurements of vertical structure obtained from balloonsondes and rocket data at midlatitudes in the Northern Hemisphere were summarized in a 45 deg annual model generated by A. Krueger and R. Minzner contained in the United States Standard Atmosphere Supplements, 1976 (KRUEGER and MINZNER, 1976). BOJKOV (1969) generated models of ozone vertical structure related to total column ozone amount based on Dobson data and early Umkehr measurements. Models relating the vertical structure of ozone to total ozone based on approximately 7000 balloonsondes and a number of rocketsondes were generated (HILSEN RATH et al., 1977) as a "first guess" for the Nimbus 4 Backscattered Ultraviolet (BUV) ozone experiment retrievals of total ozone and vertical structure and for the Nimbus 7 SBUV/TOMS total ozone retrievals. Similar models based on essentially the same data base were generated (MATEER et al., 1980) as a "first guess" for inversion of "short" Umkehr observations to determine vertical structure of ozone from the ground. The 22 vertical profiles of MATEER et al. were given as a function of latitude (low, mid and high) and total column ozone, but not season. Inconsistencies between rocket and balloon data were handled differently by MATEER et al. (1980) than by HILSEN RATH et al. (1977). BHARTIA et al. (1984c) have developed similar models using both ozonesonde and satellite data. KLENK et al. (1983) developed a model of ozone vertical structure based on Nimbus 4 BUV data at pressures less than 15.6 mb and on balloon data at lower altitudes. This model was used as a "first guess" for vertical structure retrievals from the Nimbus 7 Solar Backscattered Ultraviolet (SBUV) ozone experiment. The model consisted of a simple parametric representation of the annual and latitudinal variations of ozone as a function of pressure and assumed symmetry between the Northern and Southern Hemispheres. Also included in this model is the ozone covariance matrix which describes the variance of ozone in individual atmospheric layers and the covariances between adjacent layers. An ozone covariance matrix is also included in the models of MATEER et al. (1980). DUTSCH (1978) compiled data on the vertical ozone distribution using chemical-type balloon soundings and early BUV results. A tabulation of monthly Nimbus 7 SBUV ozone profiles for the period November 1978 through October 1979 is provided by McPETERS et al. (1984) in 10 deg latitude increments from 0.17 mb to the surface. Results are given in terms of column density and its standard deviation, volume mixing ratio and number density. HEATH et al. (1982) have generated a set of atlases of total ozone for the period April 1970 - December 1976 based on Nimbus 4 BUV data. TOLSON (1981) has generated a ninth-order, ninth-degree spherical

harmonic model to represent the monthly mean total columnar ozone field over the 7-year period of the Nimbus 4 BUV data set. Annual and semiannual components are determined for both latitudinal and longitudinal variations, and the biennial and longer term variations are determined as a function of latitude. HASEBE (1983) has modeled the latitudinal and longitudinal variations in the total columnar ozone field over the 7-year period of the Nimbus 4 BUV data set using filtering techniques. Global mean total columnar ozone and its annual, semiannual, quasi-biennial and longer term components have been determined through spherical harmonic analysis (KEATING et al., 1981; TOLSON, 1981).

Data on total ozone and its vertical structure have been obtained from a number of satellite experiments. Shown in Table 1 (KRUEGER et al., 1980) is a tabulation of satellite ozone experiments through 1978. Included are solar and stellar occultation, solar backscatter ultraviolet, and infrared types. Since then, other satellites have been launched with ozone measurement capability including Applications Explorer 2 (McCORMICK et al., 1984), Dynamics Explorer 1 (KEATING et al., 1983b), Solar Mesosphere Explorer (BARTH et al., 1983), EXOS-C (MAKINO et al., 1984, and the NOAA series of satellites (PLANET et al., 1984).

With the wealth of recent satellite data allowing high precision determination of ozone variations with pressure, latitude and time, it was decided to generate models of ozone vertical structure based not just on one satellite experiment, but on multiple data sets from satellites. This is the first time such models have been generated. The very good absolute accuracy of the individual data sets allowed the data to be directly combined to generate these models. The data used for generation of these models are from some of the most recent satellite measurements over the period 1978-1982. A discussion is provided of validation and error analyses of these data sets. Also, inconsistencies in data sets are indicated which in some cases may be associated with inaccuracies in assumed ozone cross sections. The models cover the pressure range from 20 to 0.003 mb (25 to 90 km). The models for pressures less than 0.4 mb are only provisional since there was limited longitudinal coverage at these levels. The models start near 25 km in accord with previous CIRA models. The standard deviation and interannual variations relative to zonal means are also provided.

In addition to the models of monthly latitudinal variations in vertical structure based on satellite measurements, monthly models of total column ozone and its characteristic variability as a function of latitude based on 4 years of Nimbus 7 measurements, models of the relation between vertical structure and total column ozone (MATEER et al., 1980), and a midlatitude annual mean model (KRUEGER and MINZNER, 1976) are incorporated in this set of ozone reference atmospheres. Other variations of ozone in addition to the monthly latitudinal variations such as the quasi-biennial oscillation are also briefly discussed.

Future refinements which are planned for the final CIRA models are also enumerated. Among these are the inclusion of improved ozone determinations from Nimbus 7 SBUV and TOMS data based on recent determinations of ozone cross sections (KLENK et al., 1984), the incorporation of the results of intercomparison studies presently being performed on recent satellite data sets (FLEIG et al., 1984b), and the inclusion of additional data which should become available. However, considering the present fine agreement among satellite data sets (generally within 10% of the interim reference models below 0.4 mb) it is expected that the present tables will be useful for many applications.

2. SATELLITE DATA FOR REFERENCE MODELS

The reference models provided here of monthly latitudinal variations of vertical structure are based on ozone data from five satellite experiments (see

Table 1. Satellite experiments to measure ozone (KRUEGER et al., 1980).

Type	Satellite	Wavelengths nm	Latitude Coverage	Comments	References
Occulta- tion					
Solar	Echo 1	590,529.5	17 N	Dec.1960	VENKATESWARAN et al. (1961)
	USAF 1962	260	33 S-13 S	July 1962	RAWCLIFFE et al. (1963)
	Ariel 2	200-400	50 S-50 N	Apr.,May, Aug. 1964	MILLER & STEWART (1965)
Stellar	AE-5	255.5	5 N	Dec. 1976	GUENTHER et al. (1977)
	OA0-2	250	16 S-43 N	Jan. 1970 Aug. 1971	HAYS and ROBLE (1973)
	OA0-3	258-343	12 S-3 N	July 1975	RIEGLER et al. (1976)
Back- scatter uv					
Profile	USAF 1965	284	60 S-60 N	Feb.-Mar 1965	RAWCLIFFE & ELLIOTT (1966)
	USSR	225-307	60 S-60 N	Apr. 1965	IOZENAS et al. (1969)
		250-330	60 S-60 N	June 1966	IOZENAS et al. (1969)
	1966-111B	175-310	80 S-80 N	1966	ELLIOTT et al. (1967)
	OGO-4	110-340	80 S-80 N	Sept.1967- Jan.1969	ANDERSON et al. (1969)
	Nimbus 4 b.u.v.	255.5-305.8	80 S-80 N	Apr. 1970- July 1977	HEATH et al. (1973)
	AE-5 b.u.v.	255.5-305.8	20 S-20 N	Nov. 1975- Apr.1977	FREDERICK et al. (1977a)
	Nimbus 7 s.b.u.v.	255.5-305.8	80 S-80 N	Nov. 1978	HEATH et al. (1975)
	Total Nimbus 4 b.u.v.	312.5-339.8	80 S-80 N	Apr. 1970- July 1977	MATEER et al. (1971)
	AE-5 b.u.v.	312.5-339.8	20 S-20 N	Nov. 1974- Apr. 1976	
	Nimbus 7 t.o.m.s.	312.5-339.8	global	Nov. 1976	HEATH et al. (1975)
Infrared Emission Profile					
	Nimbus 6 l.r.i.r.	9.6	65 S-90 N	June 1975- Jan. 1976	GILLE et al. (1980)
	Nimbus 7 l.i.m.s.	9.6	65 S-90 N	Oct. 1978- May 1979	NIMBUS PROJECT (1978)
Total	Nimbus 3 i.r.i.s.	9-10 spec- tral scan	80 S-80 N		HANEL et al. (1970)
	Nimbus 4 i.r.i.s.	9-10 spec- tral scan	80 S-80 N	Apr. 1970- Jan. 1971	PRABHAKARA et al. (1976)
	Block 5 m.f.r. (4 flights)		global	Mar. 1977	LOVILL et al. (1978)
	Tiros N h.i.r.s.	9.71	global	Nov. 1978	

Table 2): Nimbus 7 Solar Backscatter Ultraviolet (SBUV), Nimbus 7 Limb Infrared Monitor of the Stratosphere (LIMS), Applications Explorer Mission-2 Stratospheric Aerosol and Gas Experiment (SAGE), Solar Mesosphere Explorer UV Spectrometer (SME-UVS), and Solar Mesosphere Explorer 1.27 μ Airglow (SME-IR). Other ozone data sets are included to define the nature of systematic variations other than the latitudinal-seasonal variation.

The nadir-viewing SBUV experiment determines the vertical structure of ozone from absorption of solar ultraviolet backscattered radiation between 250 and 340 nm. The resolution of the ozone measurements is about 8 km in the vertical. For these studies the first four years of SBUV data were employed (November 1978 - September 1982) using daily zonal averages every 10 deg in latitude over the illuminated portion of the earth from 20 mb to 0.4 mb. This data set includes the refinements given in the third and fourth year addendum to the SBUV User's Guide (SYSTEMS and APPLIED SCIENCES CORP., 1984) and refinements at high latitudes between 7 and 15 mb to remove an artifact in these data (P. K. Bhartia, private communication, 1984). Data contaminated by volcanic emissions after October 1980 (including El Chichon) have been removed (SYSTEMS and APPLIED SCIENCES CORP., 1984).

Validation studies have been performed on the SBUV data employing balloon, rocket and ground-based Umkehr measurements (BHARTIA et al., 1984b). The precision of the SBUV measurements is found to be better than 8% for pressures between 1 and 64 mb. Constant biases of generally less than 10% between the SBUV results and the balloon and Umkehr results may be largely due to errors in ozone absorption cross sections. It is planned to employ improved ozone absorption cross sections agreed upon recently by the International Ozone Commission of IANAP for these experiments in the near future (KLENK et al., 1984; BASS and PAUR, 1984; PAUR and BASS, 1984).

The LIMS instrument, a six-channel cryogenically cooled radiometer measured O_3 and temperature in the stratosphere and mesosphere and H_2O , HNO_3 , and NO_2 distributions in the stratosphere from 84°N to 64°S latitude from October 25, 1978 to May 28, 1979 (RUSSELL, 1984; GILLE and RUSSELL, 1984). The LIMS ozone channel measures emission near 9.6 μ m with a field of view which at the limb is about 1.8 km in the vertical and 18 km in the horizontal (perpendicular to the line of sight).

Table 2. Satellite data used for interim reference ozone models.

Instrument	Incorporated Pressure Range	Incorporated Time Interval
NIMBUS 7 LIMS	0.4 - 20 mb	11/78 - 5/79
NIMBUS 7 SBUV	0.4 - 20 mb	11/78 - 9/82
AE -2 SAGE	4 - 20 mb	2/79 - 12/79
SME UVS	0.07 - 0.5 mb	1/82 - 12/83
SME IR	0.003 - 0.5 mb	1/82 - 12/83
NIMBUS 7 TOMS	TOTAL	11/78 - 9/82

Monthly zonal means of Kalman-filtered LIMS ozone values are incorporated in the model for the period November 1978 through May 1979 from 60°S to 80°N and from 20 mb to 0.4 mb. Validation studies have been performed using balloon and rocket underflights, Umkehr soundings, and Dobson measurements (REMSBERG et al., 1984). Comparison with the correlative measurements shows mean differences of less than 10% at midlatitudes for balloon-borne sensors and less than 16% up to 0.3 mb for rocket data. The comparison with balloon measurements near 20 mb indicates LIMS data may be high by about 8% at low latitudes. At greater pressures there is evidence of a significant bias relative to balloon data in this region.

The SAGE instrument is a four-channel sun photometer which measured solar intensity at sunrise and sunset to derive ozone, aerosol, and NO₂ concentrations. Absorption of 0.6 μ m solar radiation by ozone allowed determination of the vertical structure of ozone to be obtained up to 30 times per day from February 1979 until September 1981. After data processing, the vertical resolution of the data is 1 km up to approximately 40 km altitude and 5 km above 40 km. The horizontal resolution is 200 to 300 km in the viewing direction and 200 km perpendicular to the field of view (CUNNOLD et al., 1984). Monthly latitudinal coverage depends on the time of year and solar geometry, but can extend from 78°S to 78°N. However, on any particular day, the vertical structure is obtained at a discrete latitude for sunrises or sunsets. Comparisons were made between balloon measurements and SAGE profiles from 18 to 28 km, and average differences were found to be less than 10% (REITER and McCORMICK, 1982; McCORMICK et al., 1984). Comparisons with rocketsondes up to 60 km yielded average differences of less than 14% (McCORMICK et al., 1984). Monthly zonal means from 4 to 20 mb over the period February 1979 through December 1979 were recently refined (October 1984) and are incorporated in the model. At these altitudes significant diurnal variations are not expected. An initial comparison between SAGE and SEUV in March-April 1979 indicated agreement to generally better than 15% between 5 and 30 mb (CUNNOLD et al., 1984). A comparative study has been performed between the three data sets SEUV, SAGE and LIMS for March 1979 (FLEIG et al., 1984a). The LIMS/SEUV comparisons are shown to be very good in the upper stratosphere, while the SEUV/SAGE comparisons are shown to be very good in the lower stratosphere. A more detailed comparison study is in progress (FLEIG et al., 1984b).

Mesospheric ozone densities have recently been made available from two limb-scanning experiments aboard the Solar Mesosphere Explorer (SME) spacecraft (which was launched October 6, 1981). The first of these, the SME-UVS, is a two-channel Ebert-Fastie spectrometer. The instrument measures the Rayleigh scattering of solar photons at the earth's limb at wavelengths of 265 nm and 296.4 nm from which the ozone profile is determined between 1.0mb and 0.07 mb (RUSCH et al., 1983). The field of view of the instrument is 3.5 km in the vertical by 35 km in the horizontal at the limb. Generally zonal means are not obtained. The primary orbits were over the longitude range from 40°W to 100°W, and the local solar time of measurement at the equator is 3 PM. An error analysis indicates total errors should range from 6% at 48 km to 15% at 68 km (1.0 to 0.1 mb) (RUSCH et al., 1983, 1984). The data chosen for the model is over the range 0.5 mb at 0.07 mb over the period January 1982 through December 1983.

The second SME experiment, SME-IR, is a near-infrared experiment that measures 1.27 μ m airglow from which ozone densities from 50 to 90 km are deduced. The dayglow is principally associated with photodissociation of ozone (THOMAS et al., 1983a). Results from this experiment agree well with the SME-UVS experiment and with KRUEGER and MINZNER (1976). THOMAS et al. (1984a) describe the error analysis of this experiment in some detail. Random errors are estimated to be less than 10% from 50 to 82 km, and increase to 20% at 90 km. Systematic errors are estimated to be 15% but could be as high as 50%. The

data used for the model are monthly means over the range 0.5 mb to 0.003 mb and over the period January 1982 through December 1983. The local solar time of the measurements is again about 3 PM. Latitudinal coverage is consistent with the illuminated earth, and longitudinal coverage is principally from 40 W to 100°W. Reviews including other measurements of mesospheric ozone are found in: VALLANCE JONES (1973), THOMAS (1980), NOXON (1982), VAUGHN (1984), and ALLEN et al. (1984). Ozone measurements made in the Aladdin program (WEEKS et al., 1978) by several techniques on June 29-30, 1974 are in agreement with this model below 70 km. Above 75 km Aladdin ozone is a factor of 2-3 lower than SME-IR. It is very possible that this is a real ozone variation (R. Thomas, personal communication, 1984).

Other satellite instruments which have obtained measurements of the vertical structure of ozone include the Nimbus 4 BUV experiment (HEATH et al., 1973) and the Nimbus 6 Limb Radiance Inversion Radiometer (LRIR) (GILLE et al., 1980). Since the Nimbus 4 BUV experiment had problems with a serious drift in bias, the Nimbus 7 SBUV data were considered to be a better choice for the model. The Nimbus 7 LIMS is generally considered an improvement over the Nimbus 6 LRIR experiment and was therefore chosen for the model.

The models of total column ozone given here are based on 4 years of Nimbus 7 TOMS measurements. The TOMS instrument is used to determine total column ozone by measuring backscattered solar ultraviolet radiation attenuated by ozone employing a simple monochromator whose instantaneous field of view scans through the subsatellite point and perpendicular to the orbital plane. Backscattered and direct solar radiation are sampled at six wavelengths from 312.5 nm to 380 nm. The resolution of ozone measurements is about 50 km in the horizontal. For these studies the first 4 years of TOMS data were employed (November 1978 - September 1982) using daily zonal averages every 5 deg in latitude over the illuminated portion of the earth. Comparisons of TOMS data with ground-based Dobson and M-83 data have shown a retrieved precision of better than 2% and biases of 6% where the TOMS measurements have lower values than the Dobson measurements (BHARTIA et al., 1984a). There are indications that the absorption coefficients assumed in the TOMS experiments are somewhat in error and may be updated in the near future (KLENK et al., 1984). Global measurements of total ozone from backscattered ultraviolet measurements have also been obtained from the Nimbus 4 Backscattered Ultraviolet (BUV) and the Nimbus 7 SBUV experiments. The TOMS experiment, however, obtains more measurements per day than the other two and does not appear to have the serious drift problems which occurred on the Nimbus 4 BUV experiment. Infrared experiments which measure total column ozone from absorption of 9.6 μ m radiation have included the Nimbus 4 Infrared Interferometer Spectrometer (IRIS), the DMSP Multifilter Radiometers (MFR), and the ongoing Tiros Operation Vertical Sounders (TOVS). A study of the relative biases between a limited amount of the TOMS, MFR, TOVS and SBUV results has been performed recently (LOVILL and ELLIS, 1983) showing excellent global average agreement between the TOMS and MFR (3%) but not as good agreement between SBUV and MFR (5) or between TOVS and MFR (7%), where in each case MFR gave a lower value for total ozone. Significant latitudinal biases have been noted in the IRIS data (PRABHAKARA et al., 1976; PRIOR and OZA, 1978).

3. MODELS OF TOTAL COLUMN OZONE

The monthly latitudinal models of total column ozone are based on the archived first 4 years of data from the Nimbus 7 TOMS experiment. The total column ozone values tabulated here are 6.4% higher than the TOMS data to be in accord with Dobson measurements (BHARTIA et al., 1984a). Shown in Figure 1 is total column ozone in Dobson units (the Dobson unit is defined as 10^{-5} meters of ozone at 0°C and at standard sea level pressure) as a function of latitude and month. Note the high values in mid and high latitudes in spring in the

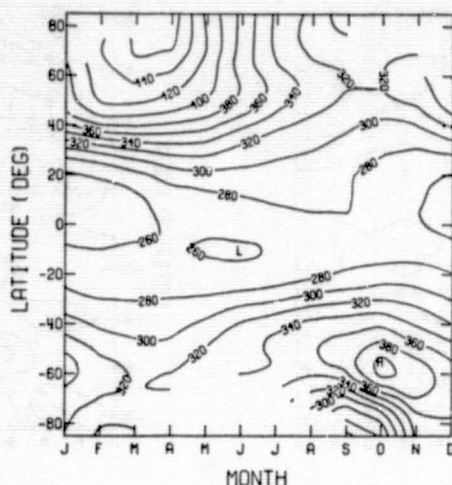


Figure 1. Zonal mean of total column ozone (Dobson units) as a function of latitude and month.

Northern Hemisphere and at midlatitudes in local spring in the Southern Hemisphere. Shown in Figure 2 is the standard deviation in percent of individual ozone measurements relative to the zonal mean obtained each month for a 1-year period (November 1978 - October 1979). A comparison of monthly ozone values from year to year over the 4-year period (November 1978 - September 1982) gives an approximate idea of patterns of interannual variability in total ozone. Shown in Figure 3 is the interannual variability expressed as standard deviation (in percent) relative to 4-year means as a function of latitude and month. The variations are generally less than 4% (except near October, 80°S) and are strongly related to quasi-biennial variation discussed briefly in the section "Other Ozone Variations."

Shown in Table 3 is a tabulation of the latitudinal variation of total column ozone in Dobson units for each month based on the dayside observations of ozone over the 4-year period. The blanks indicate no measurements were available.

4. MODELS OF VERTICAL STRUCTURE OF OZONE

As described in the section "Satellite Data for Reference Models," the vertical structure models of monthly latitudinal variations are based on the SBUV, LIMS, SAGE, SME-UVS and SME-IR data tabulated in Table 2. The 4-year mean of the SBUV data was given a weight of 2 due to the combination of extensive spatial and temporal coverage, while the other shorter data sets were each given a weight of 1.

Although there is interannual variability, comparison of the SBUV data over the 4-year period of measurements shows a remarkable similarity of structure from year to year. For example, shown in Figure 4 is the vertical structure at 0°, 20°N, 40°N and 60°N for November of 1978, 1979, 1980 and 1981. Note how the 0° and 20°N profiles come together near 4 mb. The 60°N profile changes in each case from the lowest profile at 4 mb to the highest at 1.5 mb.

Shown in Figure 5 is the interannual variability of zonal mean ozone expressed as standard deviation (in percent) relative to the mean of 4 years of

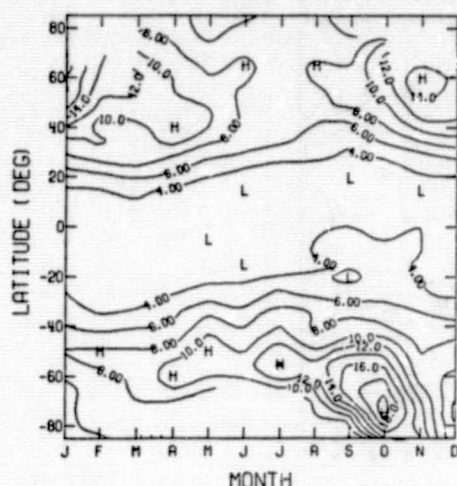


Figure 2. Standard deviation (percent) from zonal mean of total column ozone for period January 1979 through December 1979 (Nimbus 7 TOMS data).

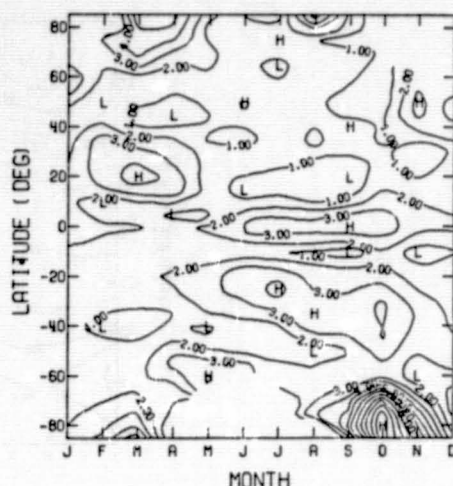


Figure 3. Interannual variability of total column ozone expressed as yearly standard deviation (percent) from 4-year zonal means (Nimbus 7 TOMS data).

Table 3. Zonal mean total column ozone (Dobson units).

LAT	JAN	FEB	MAR	APR	MAY	MONTH		AUG	SEP	OCT	NOV	DEC
85.			471	471	415	375	336	314	286			
80.			474	469	418	374	335	311	293			
75.		437	464	466	419	373	335	311	304	302		
70.		440	463	459	419	372	337	316	310	312	316	
65.	399	436	455	447	413	370	341	323	315	318	335	
60.	395	432	445	435	409	375	349	329	320	320	335	361
55.	393	429	437	425	405	378	353	333	320	320	330	356
50.	390	422	424	413	398	375	349	329	316	314	325	352
45.	379	405	405	398	385	363	338	321	309	305	314	340
40.	357	377	360	376	366	344	324	312	302	293	299	323
35.	325	344	350	351	345	326	312	306	297	285	286	302
30.	294	306	319	327	327	314	305	300	292	282	278	283
25.	271	281	293	307	310	304	298	294	286	277	272	269
20.	257	263	274	289	294	293	291	288	282	272	266	259
15.	250	253	262	277	282	284	286	286	282	270	263	254
10.	248	248	256	269	274	278	282	284	282	269	262	253
5.	249	250	257	264	266	271	276	280	280	266	260	253
0.	253	252	257	261	262	265	270	275	278	265	262	255
-5.	257	256	259	260	260	261	264	270	275	267	266	260
-10.	262	260	262	261	259	258	261	267	272	272	272	267
-15.	268	264	264	262	261	260	263	269	275	279	280	274
-20.	273	267	266	265	266	266	270	276	284	290	289	281
-25.	280	273	271	273	274	276	281	290	298	303	300	289
-30.	289	280	279	281	283	291	298	309	316	320	313	300
-35.	298	288	286	286	294	306	317	330	332	336	326	310
-40.	308	297	292	291	305	322	333	346	351	357	338	321
-45.	322	305	299	299	315	329	343	356	363	374	353	335
-50.	337	316	307	308	321	331	344	358	370	391	369	350
-55.	347	325	314	316	324	331	341	354	371	406	384	362
-60.	347	328	318	320	326	340	347	361	356	405	393	368
-65.	340	327	319	322	324		343	328	326	377	391	369
-70.	333	319	315	315				309	294	336	379	368
-75.	327	308	307	305				297	270	299	360	361
-80.	322	302	302						255	276	348	359
-85.	319	297	297						232	261	344	356

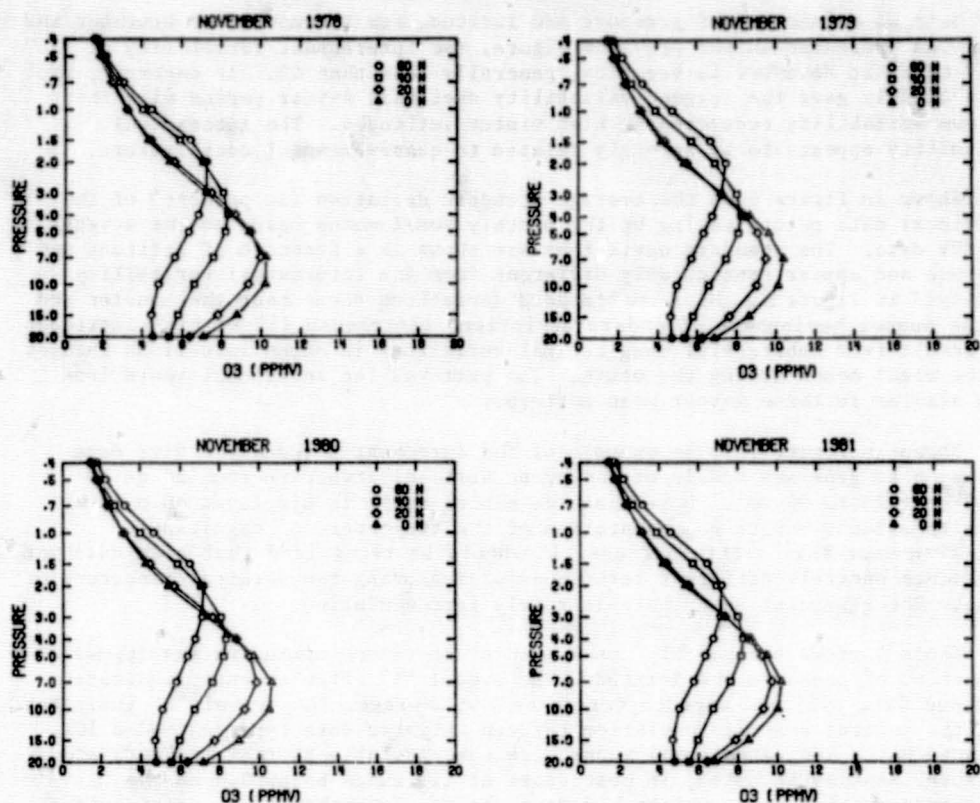


Figure 4. Similarity of ozone vertical structure in November from year to year (Nimbus 7 SBUV data).

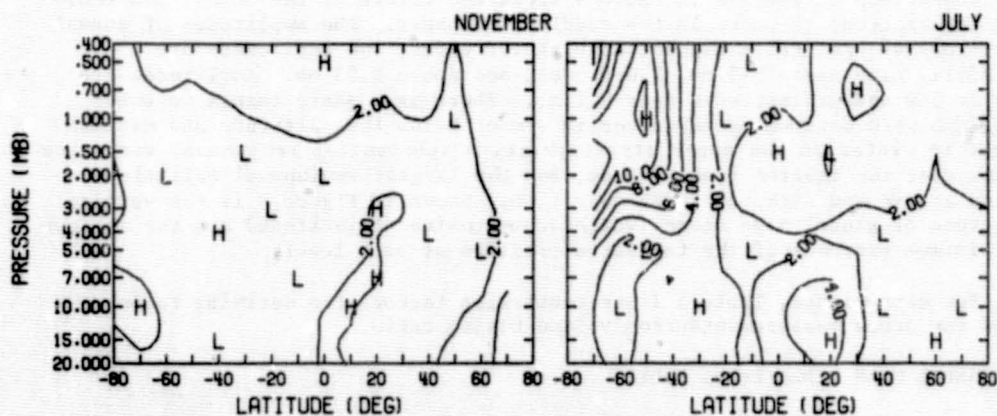


Figure 5. Interannual variability of ozone vertical structure expressed as yearly standard deviation (percent) from 4-year zonal means for the months of November and July (Nimbus 7 SBUV data).

SBUV data as a function of pressure and latitude for the months of November and July. As indicated in the previous figure, the interannual variability of zonal means in November is very low, generally less than 4%. In contrast, the month of July gave the largest variability over this 4-year period with the maximum variability occurring at high winter latitudes. The interannual variability appears to be strongly related to quasi-biennial oscillations.

Shown in Figure 6 is the average standard deviation (in percent) of the individual data points making up the monthly zonal means based on the 4 years of SBUV data. The standard deviations are shown as a function of latitude and pressure and appear considerably different from the interannual variability displayed in Figure 5. Minimum standard deviations occur near the equator and in the summer hemisphere. Standard deviations can exceed 15% at high latitudes and result from substantial longitudinal variations in ozone as well as changes in the zonal means during the month. The patterns for individual years look very similar to these 4-year mean patterns.

Shown in Figure 7 is an example of the agreement between the five data sets used to generate models of the ozone vertical structure from 20 mb to 0.003 mb (≈ 25 to 90 km). Note that the mixing ratio is displayed on a log scale to allow accurate representation of the two orders of magnitude variation over this altitude range. It should be recognized that each data set represents entirely different techniques of measuring the vertical structure of ozone. The agreement shown here is fairly representative.

Table 4 gives the monthly zonal mean ozone volume mixing ratios (ppmv) as a function of pressure and latitude. The symbol "A" after an entry indicates only one data type was used to determine the average. The symbol "B" indicates that the percent standard deviation between weighted data types exceeded 10%. A dashed entry indicates zonal means were not available at that latitude and pressure. As may be noted, in most cases at altitudes below 0.4 mb the standard deviation among weighted data types was less than 10%. Considering the difference in techniques, this is noteworthy. Owing to the lack of longitudinal coverage above 0.4 mb and the somewhat larger differences between data types, the model above 0.4 mb should be considered only provisional. Shown in Figure 8 are the ozone distributions for the equinox and solstice months.

Comparison of entries in Table 4 shows the nature of the annual and semi-annual variations of ozone in the middle atmosphere. The amplitudes of annual variations are generally highest at high latitudes, and amplitudes are especially high near 15-5 mb, 2.0-0.5 mb, and above 0.03 mb. Amplitudes are high at low and midlatitudes near 0.1 mb. There is a sharp change in phase near 4 mb with maximum ozone values in summer below this altitude and maximum values in winter in the upper stratosphere. A substantial semiannual variation occurs near the equator from 15-3 mb, but the largest semiannual variation occurs at mid and high latitudes near 1 mb. Shown in Figure 9 is the vertical structure of global mean ozone (weighted by cosine of latitude) and the maximum and minimum extremes of the tabulated profiles at each level.

For convenience, Table 5 lists conversion factors for deriving common units for ozone measurements from volume mixing ratio.

5. ANNUAL MEAN MIDLATITUDE MODEL

The KRUEGER and MINZNER (1976) annual mean ozone reference model of 45°N based on balloon and rocket data is incorporated in this set of reference models. This model has proven to be very useful and was included in the U. S. Standard Atmosphere, 1976. Data from rocket soundings in the latitude range of $45^{\circ}\text{N} \pm 15^{\circ}\text{N}$, results of balloon soundings at latitudes from 41°N to 47°N , and

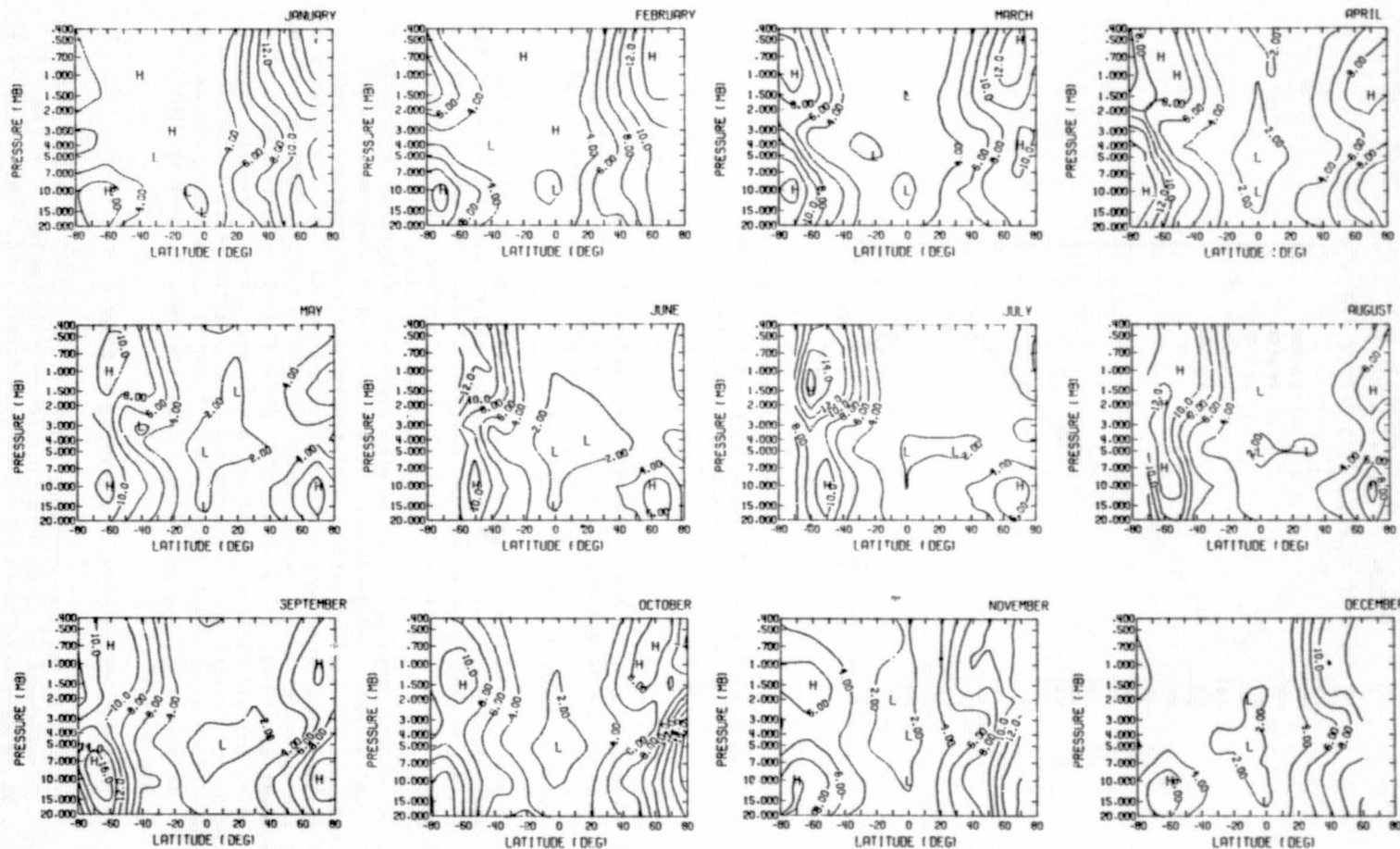


Figure 6. Average monthly standard deviation (percent) from zonal mean ozone (Nimbus 7 SBV data).

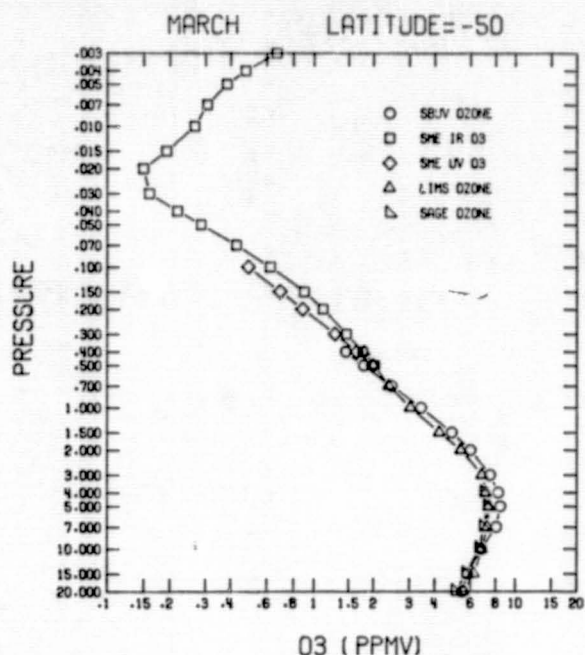


Figure 7. Comparison of measurements from five satellite experiments of zonal mean ozone volume mixing ratios for March, 50°S.

latitude gradients from Nimbus 4 BUV observations have been combined to give this estimate of the annual mean ozone concentration and its variability at heights up to 74 km for an effective latitude of 45°N. The tabulation of this model is found in KRUEGER and MINZNER (1976).

Shown in Figure 10a is a comparison of the vertical structure of the annual mean volume mixing ratio given by Krueger and Minzner with that of the annual mean determined by averaging the monthly values at 40 and 50°N based on satellite data given in Table 4. As may be detected, there is excellent agreement between the balloon and rocket measurement model and the satellite measurement model. This agreement is even more noteworthy considering the lack of longitudinal coverage in the balloon and rocket measurement model. Shown in Figure 10b are the percent differences of the Krueger and Minzner model from the annual mean model based on Table 4 values. Below altitudes of 0.2 mb, the agreement at all levels is within 10%. Below altitudes of 2.0 mb, the agreement at all levels is within 5%. Above 0.2 mb, differences as large as 45% occur, but all differences at all levels are within the error bars indicated by the Krueger and Minzner model. It is interesting to note that both models give maximum mixing ratios near 5 mb. Minimum mixing ratios occur near 0.04 mb for the Krueger and Minzner model and near 0.03 mb for the satellite data model.

6. MODELS OF TOTAL OZONE-VERTICAL STRUCTURE RELATION

As mentioned in the introduction, MATEER et al. (1980) developed models of the vertical structure of ozone as a function of total column ozone and latitude. The models were based on balloon and rocket data. These models of

ORIGINAL PAGE IS
OF POOR QUALITY

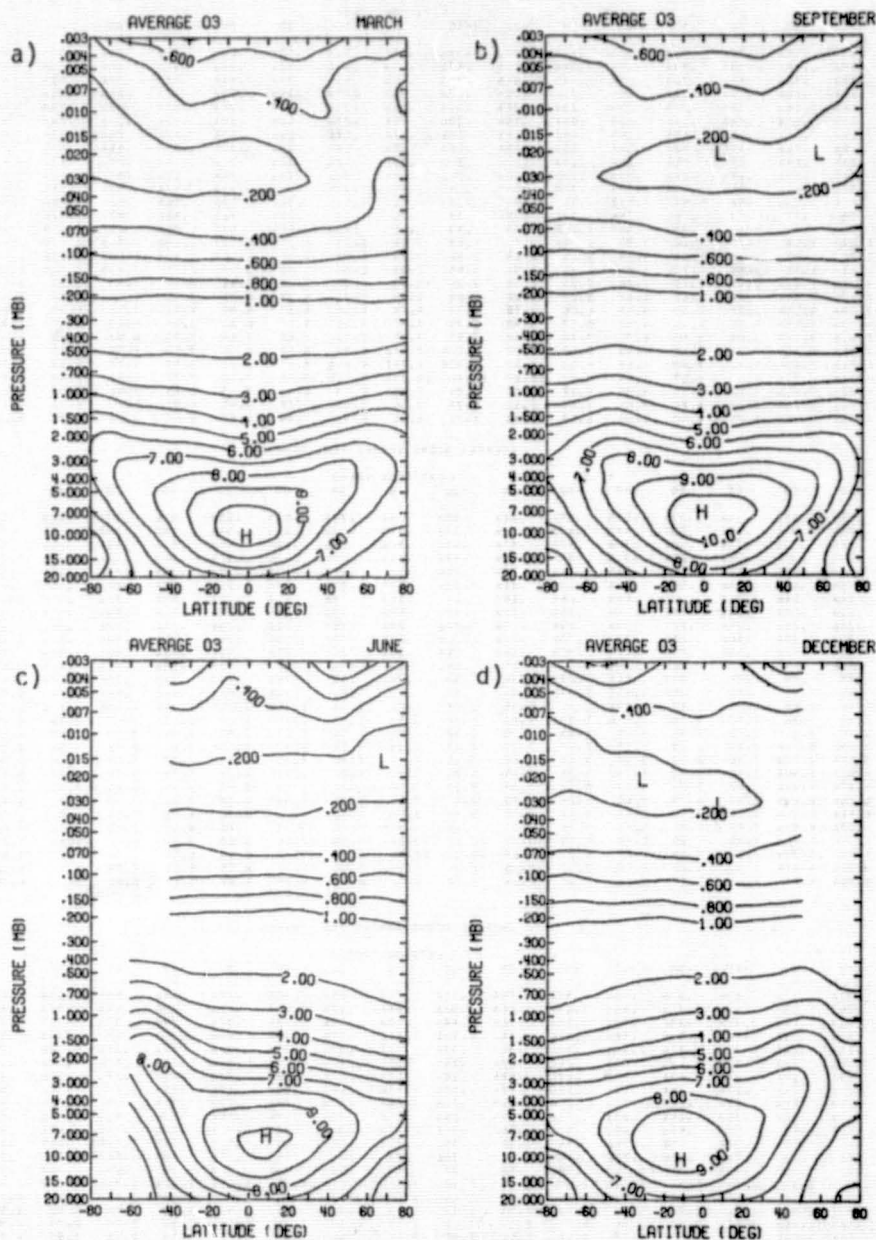


Figure 8. Monthly zonal mean ozone volume mixing ratios (ppmv) as function of latitude (deg) and pressure (mb) for (a) March, (b) September, (c) June, and (d) December.

Table 4. Zonal mean ozone volume mixing ratios (ppmv).

AVERAGE OZONE (PPMV) FOR JANUARY																	
P(MB)	LATITUDE (DEG)																
	-80	-70	-60	-50	-40	-30	-20	-10	0	10	20	30	40	50	60	70	80
.003	.59A	.72A	.60A	.71A	.73A	.64A	.58A	.54A	.54A	.52A	.52A	.66A	.81A	.84A	1.08A	--	--
.004	.39A	.48A	.38A	.43A	.50A	.54A	.50A	.47A	.46A	.43A	.42A	.50A	.62A	.68A	.85A	--	--
.005	.28A	.34A	.44A	.51A	.50A	.47A	.45A	.45A	.44A	.41A	.37A	.41A	.46A	.50A	.63A	--	--
.007	.18A	.21A	.28A	.34A	.36A	.36A	.36A	.40A	.40A	.39A	.34A	.32A	.32A	.29A	.31A	--	--
.010	.14A	.16A	.19A	.22A	.23A	.25A	.29A	.31A	.33A	.33A	.33A	.30A	.25A	.20A	.13A	--	--
.015	.13A	.15A	.16A	.16A	.16A	.16A	.18A	.20A	.21A	.23A	.26A	.28A	.27A	.24A	.24A	--	--
.020	.15A	.16A	.16A	.15A	.14A	.13A	.14A	.16A	.17A	.18A	.20A	.25A	.27A	.29A	.33A	--	--
.030	.19A	.20A	.19A	.18A	.16A	.15A	.15A	.16A	.17A	.17A	.18A	.20A	.25A	.33A	.43A	--	--
.040	.23A	.24A	.23A	.21A	.20A	.19A	.19A	.19A	.20A	.20A	.21A	.22A	.25A	.35A	.49A	--	--
.050	.28A	.29A	.28A	.26A	.25A	.24A	.23A	.24A	.24A	.24A	.24A	.24A	.26A	.32A	.44A	--	--
.070	.37A	.39A	.39A	.36A	.37A	.35A	.33A	.34A	.34A	.33A	.37A	.43A	.47A	.43A	.64A	--	--
.100	.58A	.63A	.58	.54	.52A	.53	.53	.53	.51	.51	.51	.53A	.56A	.58A	.76A	--	--
.150	.73	.77	.77	.76	.78A	.79A	.77	.73	.71	.71	.73A	.76A	.80A	.83A	.92A	--	--
.200	.86	.90	.93	.95	.98A	1.01A	.98	.93	.90	.90A	.92A	.97A	1.02A	1.05A	1.11A	--	--
.300	1.09	1.13	1.20	1.26	1.33	1.38A	1.35	1.28	1.24	1.25	1.29A	1.37A	1.45A	1.55A	1.63A	--	--
.400	1.21	1.27	1.36	1.50	1.59	1.65	1.63	1.56	1.54	1.56	1.59	1.66A	1.79A	1.90A	1.99A	1.77	1.58A
.500	1.41	1.48	1.60	1.73	1.84	1.91	1.91	1.85	1.83	1.85	1.88	1.97	2.15	2.33A	2.48	2.08	1.79A
.700	1.72A	1.82A	1.97	2.12	2.26	2.36	2.38	2.34	2.33	2.34	2.36	2.51	2.77	2.87	2.80	2.67	2.22A
1.000	2.22A	2.34A	2.50	2.68	2.87	3.02	3.08	3.09	3.09	3.11	3.17	3.42	3.81	3.92	3.74	3.52A	2.89A
1.500	3.09A	3.19A	3.37	3.59	3.84	4.06	4.20	4.27	4.29	4.34	4.50	4.90	5.32	5.36	4.97	4.65A	3.75A
2.000	4.13A	4.19A	4.36	4.61	4.90	5.17	5.40	5.53	5.57	5.61	5.77	6.11	6.34	6.23	5.69	5.30A	4.34A
3.000	5.96A	5.98A	6.09	6.43	6.79	7.15	7.52	7.77	7.77	7.71	7.95	7.98	7.93	6.92	6.25	5.83	5.06A
4.000	6.75A	6.86A	7.01	7.50	7.96	8.40	8.82	9.13A	9.48A	9.62	9.85	8.50	6.98	6.28	5.92	5.25A	4.25A
5.000	6.72A	7.00A	7.42	8.09	8.68	9.18	9.62	9.95A	9.78A	9.48A	8.91	8.21	7.57	6.90	6.19	5.86	5.10A
7.000	6.29A	6.77A	7.44	8.27	8.99	9.62	10.09	10.46	10.25A	9.40A	8.95	7.98	7.23	6.51	5.90	5.73	5.27A
10.000	4.82A	5.41A	6.52	7.50	8.35	9.11	9.57	9.99	9.95	9.47	8.44	7.40	6.66	5.94	5.39	5.28	4.74A
15.000	3.96A	4.44A	5.59	6.50	7.24	7.80	8.11	8.37	8.36	7.93	7.17	6.51	6.07	5.47	4.91	4.75	4.45A
20.000	4.05A	4.42A	5.25	5.90	6.30	6.52	6.63	6.71	6.61	6.34	5.99	5.77	5.64	5.23	4.75	4.61	4.14A
AVERAGE OZONE (PPMV) FOR FEBRUARY																	
P(MB)	LATITUDE (DEG)																
	-80	-70	-60	-50	-40	-30	-20	-10	0	10	20	30	40	50	60	70	80
.003	.42A	.56A	.64A	.65A	.61A	.59A	.62A	.69A	.74A	.72A	.69A	.68A	.69A	.73A	.82A	.98A	--
.004	.28A	.39A	.48A	.50A	.47A	.47A	.52A	.55A	.57A	.57A	.56A	.54A	.53A	.56A	.62A	.72A	--
.005	.21A	.29A	.37A	.40A	.39A	.42A	.47A	.48A	.50A	.50A	.48A	.45A	.43A	.43A	.46A	.50A	--
.007	.14A	.19A	.26A	.29A	.31A	.37A	.42A	.43A	.44A	.45A	.42A	.37A	.32A	.30A	.27A	.22A	--
.010	.14A	.14A	.16A	.19A	.23A	.25A	.34A	.35A	.35A	.35A	.37A	.39A	.35A	.30A	.25A	.19A	.12A
.015	.14A	.14A	.14A	.14A	.14A	.14A	.21A	.22A	.23A	.25A	.28A	.31A	.32A	.32A	.26A	.24A	--
.020	.16A	.16A	.15A	.14A	.14A	.14A	.16A	.17A	.18A	.19A	.21A	.25A	.29A	.31A	.33A	.33A	--
.030	.21A	.20A	.19A	.18A	.16A	.16A	.16A	.16A	.17A	.17A	.18A	.19A	.24A	.29A	.37A	.43A	--
.040	.26A	.25A	.24A	.22A	.20A	.20A	.20A	.20A	.20A	.21A	.21A	.23A	.25A	.29A	.38A	.45A	--
.050	.31A	.30A	.30A	.28A	.26A	.25A	.24A	.24A	.24A	.25A	.26A	.29A	.31A	.34A	.42A	.48A	--
.070	.41A	.42A	.41A	.38A	.36A	.36A	.36A	.36A	.36A	.37A	.37A	.41A	.45A	.45A	.51A	.55A	--
.100	.61A	.60	.58	.56A	.54A	.53	.54	.52	.52	.52	.52A	.55A	.55A	.55A	.61A	.61A	--
.150	.77	.78	.78	.80A	.81A	.80A	.78	.76	.74	.73	.74A	.78A	.78A	.77A	.80A	.80A	--
.200	.90	.92	.95	.98A	1.03A	1.03A	.99	.94	.92	.92	.94A	.94A	.93A	.96A	.98A	1.03A	--
.300	1.16	1.19	1.25	1.32	1.39A	1.41	1.35	1.28	1.26	1.28	1.33A	1.33A	1.36A	1.42A	1.47A	1.57A	--
.400	1.34	1.36	1.47	1.56A	1.64A	1.67	1.62	1.56	1.55	1.57	1.59	1.62	1.67	1.77	1.88	2.02	1.93A
.500	1.59	1.61	1.72	1.81	1.91	1.95	1.90	1.82	1.81	1.84	1.87	1.93	2.02	2.10	2.32	2.48A	2.16A
.700	2.08A	2.08A	2.14	2.25	2.38	2.44	2.37	2.27	2.25	2.26	2.33	2.45	2.65	2.92	3.04	3.02	2.60A
1.000	2.85A	2.78A	2.80	2.92	3.07	3.15	3.09	2.95	2.91	2.90	3.03	3.33	3.70	4.08	4.16	3.98	3.27A
1.500	4.02A	3.90A	3.86	3.98	4.14	4.26	4.21	4.04	3.96	4.07	4.31	4.73	5.14	5.70	5.97	5.17	4.11A
2.000	4.97A	4.93A	4.92	5.05	5.23	5.38	5.39	5.25	5.18	5.27	5.49	5.95	6.54	6.86	6.33	5.82	4.72A
3.000	6.16A	6.00A	6.02	6.15	6.35	6.50	6.43	6.29	6.25	6.42	6.76	7.40	7.80	7.98	6.83	6.33	5.69A
4.000	6.81A	6.67A	6.72	6.84	7.04	7.21	7.15	6.98	6.90	7.06	7.66	8.60	8.06	7.28	6.82	6.43	6.00A
5.000	6.09A	6.08A	6.13	6.24	6.43	6.58	6.53	6.36	6.28	6.45	7.06	8.05	7.21	6.70	6.42	6.04A	5.34A
7.000	5.39A	5.42A	5.37	5.49	5.68	5.83	5.76	5.59	5.50	5.67	6.28	7.16	6.46	6.01	5.64	5.32	6.11A
10.000	4.03A	5.00A	6.27	7.16	8.02	9.01	9.62	10.27	10.64	10.28	9.69	8.65	7.59	6.91	6.44	6.32	6.17A
15.000	3.53A	4.27A	5.40	6.17	6.95	7.75	8.16	8.54	8.59	8.16	7.57	6.78	6.15	5.69	5.32	5.77A	5.10A
20.000	3.78A	4.42A	5.14	5.57	6.08	6.49	6.84	6.78	6.72	6.43	6.17	5.88	5.69	5.55	5.24	5.10	5.10A
AVERAGE OZONE (PPMV) FOR MARCH																	
P(MB)	LATITUDE (DEG)																
	-80	-70	-60	-50	-40	-30	-20	-10	0	10	20	30	40	50	60	70	80
.003	.33A	.54A	.65A	.67A	.74A	.82A	.78A	.72A	.71A	.75A	.80A	.79A	.69A	.58A	.55A	.60A	.55A
.004	.26A	.35A	.42A	.47A	.58A	.65A	.61A	.56A	.54A	.57A	.62A	.61A	.52A	.43A	.41A	.42A	.35A
.005	.21A	.28A	.32A	.38A	.40A	.55A	.52A	.49A	.47A	.49A	.53A	.52A	.44A	.37A	.33A	.32A	.24A
.007	.10A	.21A	.24A	.31A	.40A	.45A	.44A	.42A	.41A	.42A	.44A	.44A	.39A	.34A	.29A	.24A	.17A
.010	.12A	.18A	.21A	.27A	.34A	.38A	.36A	.33A	.32A	.33A	.37A	.41A	.41A	.37A	.32A	.25A	.19A
.015	.12A	.14A	.16A	.19A	.23A	.24A	.23A	.21A	.20A	.22A	.25A	.32A	.38A	.39A	.37A	.33A	.26A
.020	.15A	.14A	.14A	.15A	.17A	.17A	.18A	.18A	.18A	.18A	.19A	.22A	.29A	.31A	.37A	.37A	.29A
.030	.21A	.19A	.17A	.16A	.15A	.16A	.18A	.17A	.17A	.18A	.18A	.19A	.22A	.29A	.37A	.37A	.29A
.040	.26A	.25A	.23A	.22A	.21A	.20A	.21A	.21A	.20A	.20A	.22A	.23A	.24A	.28A	.36A	.40A	.48A
.050	.31A	.30A	.30A	.29A	.27A	.25A	.25A	.25A	.24A	.25A	.27A	.29A	.29A	.32A	.39A	.47A	.50A
.070	.42A	.44	.43A	.43A	.40A	.37A	.36A	.34A	.33A	.34A	.38A	.41A	.42A	.44A	.47A	.45A	.54A
.100	.60	.57	.57A	.56A	.54A	.54	.54	.55	.53A	.52	.52	.52A	.54A	.57A	.58A	.60A	.61
.150	.80	.78	.78A	.78A	.78A	.78A	.78A	.78A	.77	.76	.74A	.74A	.76A	.76A	.75A	.76A	.77A
.200	.97	.96	.98A	1.00A	1.00A	.98A	.98	.97	.97	.96	.95A	.98A	.98A	.98A	.98A	.98A	.98A
.300	1.30	1.33	1.34	1.37	1.39A	1.37	1.34	1.32	1.34	1.33	1.30	1.29A	1.31A	1.30A	1.27A	1.30A	1.36A
.400	1.63	1.60	1.60	1.63A	1.65A	1.64	1.61	1.61	1.62	1.62	1.62	1.62	1.61A	1.61	1.65		

Table 4 continued.

AVERAGE OZONE (PPMV) FOR APRIL																
P(HB)	LATITUDE (DEG)															
	-80	-70	-60	-50	-40	-30	-20	-10	0	10	20	30	40	50	60	80
.003	---	---	.71A	.83A	.93A	.92A	.83A	.80A	.81A	.85A	.90A	1.05A	.88A	.61A	.52A	.50A
.004	---	---	.47A	.58A	.68A	.70A	.61A	.56A	.57A	.62A	.77A	.67A	.74A	.51A	.43A	.45A
.005	---	---	.35A	.44A	.55A	.57A	.51A	.47A	.46A	.51A	.64A	.74A	.65A	.47A	.39A	.39A
.007	---	---	.27A	.33A	.42A	.44A	.42A	.40A	.41A	.42A	.50A	.59A	.56A	.45A	.39A	.32A
.010	---	---	.28A	.31A	.34A	.34A	.33A	.35A	.35A	.35A	.39A	.47A	.51A	.40A	.33A	.28A
.015	---	---	.30A	.27A	.24A	.21A	.20A	.21A	.22A	.22A	.24A	.32A	.40A	.34A	.28A	.24A
.020	---	---	.29A	.22A	.18A	.16A	.15A	.16A	.17A	.17A	.18A	.21A	.30A	.34A	.35A	.32A
.030	---	---	.25A	.19A	.16A	.17A	.17A	.17A	.18A	.18A	.18A	.20A	.22A	.24A	.26A	.24A
.040	---	---	.27A	.22A	.21A	.22A	.22A	.21A	.21A	.22A	.23A	.24A	.25A	.26A	.27A	.31A
.050	---	---	.31A	.29A	.29A	.28A	.27A	.26A	.26A	.27A	.28A	.29A	.30A	.31A	.33A	.35A
.070	---	---	.47A	.43	.43A	.41A	.40A	.39A	.37A	.36A	.37A	.39A	.40A	.42A	.43A	.45A
.100	---	---	.58A	.58	.58A	.57	.57	.58A	.57	.54	.54	.54	.53B	.53B	.54B	.57A
.150	---	---	.73A	.62B	.63B	.61B	.61	.61	.62	.79	.70	.70B	.77B	.76B	.75B	.75B
.200	---	---	.93A	1.05	1.05B	1.02B	1.02	1.03	1.03	1.00	.99	.99B	.96B	.94B	.92B	.90B
.300	---	---	1.39A	1.51	1.50	1.43	1.40	1.40	1.39	1.37	1.36	1.35	1.32B	1.29B	1.25B	1.21B
.400	1.99A	1.90	1.84	1.79	1.71	1.66	1.65	1.67	1.67	1.60	1.60	1.64	1.59B	1.53B	1.51B	1.54
.500	2.53A	2.40	2.27	2.17	2.04	1.96	1.93	1.93	1.93	1.93	1.93	1.92	1.86	1.80	1.80	1.84
.700	3.55A	3.46A	3.06B	2.84	2.63	2.47	2.39	2.38	2.38	2.38	2.42	2.44	2.36	2.28	2.31	2.40
1.000	4.84A	4.87A	4.37B	4.02	3.64	3.33	3.13	3.04	3.02	3.04	3.12	3.19	3.12	3.06	3.14	3.30
1.500	6.14A	6.52A	6.14B	5.75	5.21	4.70	4.28	4.05	4.00	4.06	4.21	4.37	4.37	4.37	4.55	4.74
2.000	6.38A	7.03A	7.03	6.43	5.82	5.30	4.83	4.30	4.02	4.12	4.33	4.54	4.61	4.66	4.84	4.86
3.000	5.86A	6.70A	7.35	7.72	7.77	7.67	7.35	6.95	6.65	7.01	7.26	7.47	7.61	7.65	7.61	7.30
4.000	5.45A	6.22A	7.07	7.57	8.01	8.39	8.50	8.20	8.01	8.22	8.39	8.37	8.44	8.40	8.18	7.59
5.000	5.06A	5.72A	6.70	7.48	8.16	8.84	9.25	9.05	8.84	9.05	9.16	9.00	8.97	8.80	8.27	7.50
7.000	4.48A	5.02A	6.03	6.93	7.79	8.82	9.66	10.01	10.01	9.97	9.71	9.25	8.84	8.41	7.88	7.07
10.000	3.54A	4.06A	5.17	6.12	7.04	8.30	9.46	10.37	10.67	10.34	9.70	8.95	8.12	7.44	6.82	6.08
15.000	3.37A	3.80A	4.78	5.50	6.19	7.18	8.05	8.77	9.01	8.77	8.20	7.67	6.91	6.31	5.72	5.10B
20.000	3.66A	4.35A	4.75	5.17	5.36	6.17	6.83	7.02	7.15	7.08	6.84	6.53	6.08	5.70	5.30	4.80B

AVERAGE OZONE (PPMV) FOR MAY																
P(HB)	LATITUDE (DEG)															
	-80	-70	-60	-50	-40	-30	-20	-10	0	10	20	30	40	50	60	80
.003	---	---	---	1.00A	1.02A	.92A	.78A	.68A	.67A	.67A	.76A	.87A	.88A	.79A	.68A	.58A
.004	---	---	---	.69A	.75A	.68A	.56A	.51A	.50A	.51A	.61A	.72A	.75A	.68A	.57A	.48A
.005	---	---	---	.51A	.57A	.54A	.47A	.46A	.45A	.46A	.56A	.66A	.69A	.59A	.50A	.42A
.007	---	---	---	.34A	.39A	.40A	.42A	.45A	.45A	.44A	.47A	.51A	.52A	.47A	.41A	.34A
.010	---	---	---	.27A	.30A	.32A	.37A	.40A	.41A	.38A	.38A	.38A	.38A	.36A	.32A	.27A
.015	---	---	---	.23A	.22A	.22A	.24A	.26A	.25A	.24A	.24A	.24A	.24A	.24A	.23A	.21A
.020	---	---	---	.20A	.18A	.17A	.17A	.17A	.18A	.17A	.18A	.19A	.19A	.20A	.19A	.18A
.030	---	---	---	.19A	.18A	.17A	.17A	.17A	.18A	.17A	.18A	.19A	.19A	.20A	.21A	.21A
.040	---	---	---	.23A	.23A	.23A	.22A	.22A	.22A	.23A	.23A	.24A	.24A	.25A	.25A	.26A
.050	---	---	---	.29A	.30A	.29A	.28A	.28A	.27A	.28A	.28A	.28A	.29A	.29A	.30A	.31A
.070	---	---	---	.43	.43A	.43A	.41A	.40A	.39A	.39A	.40A	.39A	.40A	.40A	.41A	.42A
.100	---	---	---	.60	.59	.59	.60	.59	.57	.57	.57	.57	.57	.57	.58	.58
.150	---	---	---	.86B	.85B	.84B	.84	.82	.85	.83	.83	.81B	.79B	.79	.78	.77
.200	---	---	---	1.13B	1.08B	1.04B	1.06	1.06	1.03	1.03	1.04	1.01B	.99B	.97B	.95	.92
.300	---	---	---	1.66	1.52	1.43	1.43	1.42	1.40	1.40	1.40	1.37	1.33	1.28	1.23	1.18
.400	2.13A	2.01	2.02	1.84	1.70	1.68	1.70	1.70	1.69	1.68	1.68B	1.61B	1.55B	1.48B	1.40	1.35
.500	2.70A	2.53B	2.50	2.23	2.02	1.96	1.97	1.97	1.96	1.95	1.93	1.87	1.79	1.71	1.64	1.58
.700	3.79A	3.62B	3.45B	2.97	2.60	2.47	2.44	2.44	2.43	2.44	2.41	2.33	2.23	2.13	2.09	2.00
1.000	5.26A	5.13B	5.05B	4.26	3.60	3.25	3.13	3.11	3.11	3.12	3.09	2.99	2.86	2.75	2.67	2.61
1.500	6.85A	6.80B	6.95B	6.12	5.14	4.45	4.21	4.21	4.21	4.19	4.17	4.05	3.91	3.80	3.72	3.61
2.000	7.20A	7.26B	7.74B	7.26	6.39	5.62	5.30	5.22	5.23	5.30	5.31	5.20	5.05	4.99	4.82	4.94
3.000	6.60A	6.80	7.81	8.10	7.93	7.42	7.10	7.04	7.11	7.25	7.27	7.19	7.07	6.95	6.54	6.52
4.000	6.05A	6.24	7.25	7.90	8.24	8.18	7.99	7.93	8.30	8.45	8.40	8.29	7.93	7.53	7.19	6.90
5.000	5.37A	5.79	6.95	7.81	8.51	8.81	8.74	8.70	9.10	9.22	9.08	8.90	8.53	7.96	7.30	6.76
7.000	4.99A	5.20	6.31	7.30	8.34	9.17	9.54	9.59	9.66	9.76	9.41	9.00	8.49	7.82	7.04	6.24
10.000	4.22A	4.62	5.68	6.63	7.80	9.03	9.92	10.21	9.97	9.77	9.25	8.57	7.77	6.93	6.03	5.17
15.000	3.95A	4.38	5.28	5.98	6.85	7.99	8.48	8.79	8.86	8.43	7.86	7.17	6.61	5.91	5.02	4.10
20.000	4.11A	4.37	5.02	5.51	6.00	6.51	6.86	7.08	7.28	7.04	6.73	6.31	5.90	5.39	4.75	4.16

AVERAGE OZONE (PPMV) FOR JUNE																	
P(HB)	LATITUDE (DEG)																
	-80	-70	-60	-50	-40	-30	-20	-10	0	10	20	30	40	50	60	80	
.003	---	---	---	---	.82A	.79A	.65A	.48A	.49A	.56A	.64A	.77A	.92A	.98A	.89A	.73A	.59A
.004	---	---	---	---	.64A	.62A	.49A	.39A	.42A	.47A	.53A	.64A	.77A	.79A	.65A	.51A	.38A
.005	---	---	---	---	.51A	.50A	.42A	.36A	.40A	.43A	.46A	.55A	.65A	.63A	.49A	.38A	.33A
.007	---	---	---	---	.36A	.38A	.36A	.36A	.38A	.39A	.38A	.42A	.46A	.42A	.30A	.24A	.17A
.010	---	---	---	---	.27A	.31A	.31A	.30A	.30A	.29A	.27A	.28A	.29A	.25A	.20A	.18A	.17A
.015	---	---	---	---	.20A	.22A	.21A	.19A	.18A	.18A	.18A	.18A	.18A	.18A	.17A	.17A	.16A
.020	---	---	---	---	.17A	.17A	.16A	.15A	.15A	.15A	.15A	.15A	.16A	.16A	.16A	.16A	.17A
.030	---	---	---	---	.17A	.18A	.17A	.17A	.17A	.18A	.17A	.17A	.17A	.19A	.20A	.20A	.20A
.040	---	---	---	---	.23A	.24A	.23A	.22A	.22A	.22A	.21A	.22A	.24A	.24A	.24A	.24A	.25A
.050	---	---	---	---	.31A	.32A	.30A	.27A	.27A	.27A	.26A	.28A	.28A	.28A	.29A	.29A	.29A
.070	---	---	---	---	.45A	.46A	.43A	.40A	.38A	.38A	.39A	.40A	.40A	.39A	.40A	.40A	.40A
.100	---	---	---	---	.57B	.59B	.59	.59	.60	.61	.61	.59	.57	.58	.62B	.60B	.60B
.150	---	---	---	---	.82B	.84B	.86B	.86	.86	.88	.89	.87	.83	.82	.83	.82	.79
.200	---	---	---	---	1.05B	1.05B	1.07B	1.08	1.08	1.09	1.11	1.09	1.04	1.01	.99	.99	.99
.300	---	---	---	---	1.51	1.44	1.45	1.47	1.48	1.48	1.44	1.39	1.33	1.27	1.21	1.16	1.16
.400	---	---	---	---	1.82A	1.82A	1.68	1.67	1.70	1.70	1.69	1.68	1.57	1.50	1.41	1.33	1.27
.500	---	---	---	---	2.54A	2.50A	2.26	2.02	1.98	2.01	1.99	1.97	1.93	1.84	1.75	1.64	1.46
.700	---	---	---	---	3.68A	3.68A	3.09A	2.64A	2.52A	2.49A	2.47A	2.40A	2.28A	2.14A	1.99A	1.85A	1.74A
1.000	---	---	---	---	5.31A	5.46A	4.55A	3.72A	3.40A	3.28A	3.25A	3.23A	3.22A	3.11A	2.94A	2.78A	2.74A
1.500	---	---	---	---	7.15A	7.67A	6.61A	5.32A	4.70A	4.38A	4.37A	4.36A	4.38A	4.16A	3.96A	3.72A	3.43A
2.000	---	---	---	---	7.51A	8.37A	7.76A	6.53A	5.85A	5.57A	5.49A	5.47A	5.49A	5.32A	5.09A	4.83A	4.51A
3.000	---	---	---	---	6.72A	7.86A	6.42A	7.97A	7.57A	7.42A	7.40A	7.43A	7.50A	7.33A	7.13A	6.87A	6.50A
4.000	---	---	---	---	6.05A	7.19A	7.49	8.17	8.56A	8.62A	8.66A	8.74A	8.81A	8.62A	8.39A	7.68	7.19B
5.000	---	---	---	---	5.96A	6.63A	7.82	8.37	9.00A	9.31A	9.43A	9.59A	9.56A	9.33A	9.01A	8.29	7.66
7.000	---	---	---	---	5.00A	5.40A	7.26	8.20	9.31A	9.68A	10.12A	10.23A	10.10A	9.71A	9.61A	8.36	7.64
10.000	---	---	---	---	4.47A	5.23A	8.77	9.76	10.77A	10.77A	10.77A	10.77A	10.77A	10.77A	10.77A	10.77A	10.77A
15.000	---	---	---	---	4.88A	5.93	8.61	7.46A	8.21A	8.67A	8.69A	8.28A	7.71A	7.00A	6.44	5.09	4.68A
20.000	---	---	---	---	4.09A	4.73A	5.48	5.78	6.20A	6.58A	7.07A	7.12A	6.85A	6.50A	6.15A	5.76	5.21

Table 4 continued.

AVERAGE OZONE (PPMV) FOR JULY																		
P(NB)	-80	-70	-60	-50	-40	-30	-20	-10	LATITUDE (DEG)		10	20	30	40	50	60	70	80
									0	0								
.003	---	---	---	.57A	.05A	.05A	.57A	.50A	.48A	.51A	.63A	.70A	.73A	.87A	.96A	.80A	.59A	.49A
.004	---	---	---	.42A	.53A	.52A	.45A	.40A	.40A	.45A	.51A	.55A	.59A	.69A	.71A	.55A	.42A	.40A
.005	---	---	---	.37A	.42A	.431	.39A	.37A	.38A	.42A	.45A	.46A	.50A	.56A	.53A	.40A	.30A	.25A
.007	---	---	---	.22A	.30A	.33A	.34A	.34A	.35A	.36A	.36A	.34A	.37A	.35A	.31A	.23A	.21A	.18A
.010	---	---	---	.19A	.24A	.28A	.29A	.27A	.26A	.26A	.25A	.24A	.24A	.23A	.19A	.17A	.15A	.14A
.015	---	---	---	.20A	.20A	.20A	.19A	.17A	.16A	.16A	.16A	.15A	.15A	.15A	.15A	.15A	.15A	.14A
.020	---	---	---	.20A	.17A	.15A	.15A	.15A	.14A	.14A	.14A	.14A	.14A	.14A	.14A	.14A	.14A	.14A
.030	---	---	---	.21A	.17A	.17A	.17A	.17A	.17A	.17A	.16A	.16A	.16A	.16A	.16A	.16A	.16A	.16A
.040	---	---	---	.24A	.23A	.22A	.22A	.21A	.21A	.21A	.20A	.20A	.20A	.20A	.20A	.20A	.20A	.20A
.050	---	---	---	.28A	.31A	.30A	.28A	.25A	.25A	.26A	.25A	.25A	.25A	.27A	.29A	.29A	.26A	.24A
.070	---	---	---	.39	.47A	.40A	.41A	.38A	.38A	.37A	.36A	.37A	.40A	.40A	.40A	.39A	.35A	.34A
.100	---	---	---	.58	.60B	.62B	.60	.58	.58	.60B	.61B	.61	.59	.60	.62B	.63B	.59A	.58A
.150	---	---	---	.87B	.88B	.88B	.87B	.86	.83	.85	.89	.90	.87	.84	.84	.82B	.79B	.78B
.200	---	---	---	1.15	1.09B	1.09B	1.08B	1.06	1.05	1.07	1.12	1.13	1.09	1.04	1.00	.98	.94	.94
.300	---	---	---	1.58	1.53	1.51	1.47	1.45	1.44	1.45	1.50	1.51	1.45	1.36	1.29A	1.22	1.18	1.18
.400	---	1.62A	1.69A	1.95B	1.81	1.73B	1.69	1.68	1.68	1.68	1.69	1.69	1.62	1.52	1.42	1.33	1.25B	1.25B
.500	---	1.76A	2.11A	2.41B	2.22	2.08	2.01	2.00	1.99	1.98	1.99	1.99	1.90	1.78	1.65	1.54	1.44B	1.44B
.700	---	2.62A	2.97A	3.15A	2.96A	2.67A	2.54A	2.49A	2.48A	2.48A	2.51A	2.50A	2.38A	2.19A	2.01A	1.84A	1.70A	1.70A
1.000	---	3.51A	4.25A	4.07A	4.29A	3.74A	3.44A	3.10A	3.25A	3.25A	3.29A	3.25A	3.08A	2.93A	2.57A	2.36A	2.18A	2.18A
1.500	---	4.93A	6.04A	5.76A	6.20A	5.12A	4.51A	4.54A	4.54A	4.42A	4.45A	4.37A	4.14A	3.82A	3.49A	3.22A	3.10A	3.10A
2.000	---	5.98A	7.7A	7.72A	7.35A	6.31A	5.99A	5.71A	5.73A	5.53A	5.45A	5.45A	5.14A	4.72A	4.28A	4.02A	3.82A	3.82A
3.000	---	5.41A	6.74A	7.06A	6.20A	7.35A	7.76A	7.60A	7.53A	7.56A	7.70A	7.50A	7.22A	6.88A	6.45A	6.03A	5.76A	5.76A
4.000	---	5.65A	6.30A	7.45A	7.70	8.54A	8.71A	8.88A	8.82A	8.96A	8.96A	8.74A	8.43A	8.06A	7.52A	6.91A	6.71A	6.71A
5.000	---	5.37A	5.81A	6.74A	7.76	8.68A	9.13A	9.43A	9.63A	9.72A	9.65A	9.40A	9.03A	8.59A	7.95A	7.07A	6.74A	6.74A
7.000	---	5.08A	5.21A	6.17A	7.25	8.42A	9.28A	9.94A	10.24A	10.36A	10.12A	9.75A	9.18A	8.64A	7.88A	6.88A	6.25A	6.25A
10.000	---	4.53A	4.58A	5.42A	6.59	7.63A	8.71A	9.60A	10.06A	10.17A	9.70A	9.05A	8.26A	7.54A	6.56A	5.54A	4.83A	4.83A
15.000	---	3.58A	4.06A	4.55A	5.85	6.57A	7.38A	8.15A	8.73A	8.91A	8.12A	7.76A	7.06A	6.40A	5.55A	4.55A	3.98A	3.98A
20.000	---	3.70A	3.95A	4.06A	5.41	5.70A	6.15A	6.64A	7.13A	7.25A	6.91A	6.57A	6.23A	5.89A	5.30A	4.51A	3.95A	3.95A

AVERAGE OZONE (PPMV) FOR AUGUST																		
P(NB)	-80	-70	-60	-50	-40	-30	-20	-10	LATITUDE (DEG)		10	20	30	40	50	60	70	80
									0	10								
.003	---	---	.56A	.67A	.69A	.67A	.63A	.62A	.61A	.62A	.66A	.70A	.69A	.67A	.69A	.62A	.45A	.42A
.004	---	---	.43A	.51A	.55A	.53A	.48A	.45A	.45A	.48A	.52A	.56A	.54A	.52A	.54A	.45A	.32A	.32A
.005	---	---	.34A	.41A	.44A	.44A	.42A	.42A	.42A	.43A	.47A	.47A	.44A	.42A	.41A	.35A	.25A	.25A
.007	---	---	.27A	.30A	.33A	.35A	.36A	.37A	.37A	.37A	.39A	.36A	.32A	.30A	.28A	.23A	.19A	.19A
.010	---	---	.25A	.26A	.28A	.30A	.32A	.31A	.29A	.29A	.29A	.27A	.23A	.20A	.18A	.16A	.15A	.15A
.015	---	---	.25A	.23A	.23A	.23A	.22A	.19A	.18A	.18A	.18A	.17A	.15A	.14A	.14A	.14A	.14A	.14A
.020	---	---	.24A	.20A	.19A	.18A	.17A	.15A	.14A	.15A	.15A	.15A	.14A	.14A	.14A	.14A	.14A	.14A
.030	---	---	.23A	.19A	.17A	.17A	.18A	.17A	.16A	.17A	.18A	.17A	.15A	.14A	.14A	.14A	.14A	.14A
.040	---	---	.27A	.24A	.24A	.24A	.23A	.21A	.20A	.21A	.20A	.20A	.18A	.17A	.17A	.17A	.17A	.17A
.050	---	---	.33A	.30A	.32A	.31A	.28A	.26A	.25A	.26A	.26A	.25A	.26A	.25A	.26A	.25A	.25A	.25A
.070	---	---	.41B	.41B	.48A	.46A	.41A	.38A	.37A	.37A	.36A	.36A	.36A	.36A	.36A	.36A	.36A	.36A
.100	---	---	.56	.58B	.60B	.60B	.58	.56	.56	.57	.57	.56	.56	.57	.58A	.59	.58B	.58B
.150	---	---	.76	.83B	.87B	.88B	.85B	.82	.81	.82	.82	.83	.84B	.82	.80	.78	.76	.76
.200	---	---	.98	1.06B	1.10B	1.11B	1.08B	1.04B	1.03	1.03	1.04	1.06	1.06B	1.03B	.98	.94	.91	.91
.300	---	---	1.39	1.51	1.58B	1.54B	1.48B	1.44	1.41	1.39	1.42	1.45	1.45	1.38	1.29	1.22	1.17	1.17
.400	---	1.59A	1.69	1.78	1.81B	1.78B	1.68B	1.66	1.64	1.63	1.65	1.64	1.58	1.48	1.38	1.28	1.22	1.22
.500	---	1.93A	2.06	2.18	2.20	2.10	2.00	1.97	1.95	1.94	1.97	2.01	1.95	1.83	1.71	1.63	1.56	1.56
.700	---	2.57A	2.67A	2.86A	2.87A	2.66A	2.50A	2.44A	2.43A	2.44A	2.49A	2.53A	2.46A	2.28A	2.13A	2.04A	1.95A	1.95A
1.000	---	3.52A	3.77A	4.13A	4.09A	3.70A	3.40A	3.25A	3.20A	3.22A	3.31A	3.38A	3.28A	3.05A	2.89A	2.75A	2.64A	2.64A
1.500	---	4.80A	5.35A	5.95A	5.84A	5.24A	4.75A	4.47A	4.38A	4.41A	4.54A	4.62A	4.49A	4.23A	4.02A	3.84A	3.69A	3.69A
2.000	---	5.47A	6.29A	7.10A	7.04A	6.47A	5.97A	5.68A	5.57A	5.60A	5.76A	5.80A	5.63A	5.34A	5.11A	4.83A	4.68A	4.68A
3.000	---	5.02A	6.49A	6.02A	6.25A	6.08A	7.06A	7.75A	7.67A	7.69A	7.83A	7.86A	7.69A	7.17A	6.64A	6.04A	5.44A	5.44A
4.000	---	5.72A	6.76A	6.07A	6.61A	6.05A	6.86A	7.62A	8.20A	8.20A	8.20A	8.20A	8.20A	7.76A	7.28A	6.68A	6.08A	6.08A
5.000	---	5.45A	6.39A	7.02A	8.54A	8.98A	9.47A	9.64	9.65	9.74	9.64	9.23	8.81	8.30	7.56B	6.94A	6.04A	6.04A
7.000	---	5.15A	5.81A	7.13A	8.02A	8.76A	9.64A	10.12	10.22	10.31	10.03	9.46	8.86	8.18	7.31B	6.57A	5.72A	5.72A
10.000	---	4.57A	5.02A	6.19A	7.07A	7.93A	9.01A	10.02	10.22	10.31	9.83	9.04	8.22	7.30	6.29	5.18A	4.22A	4.22A
15.000	---	3.88A	4.28A	5.26A	6.06A	6.72A	7.57A	8.22	8.34	8.65	8.20	7.59	6.97	6.20	5.32	4.41A	3.68A	3.68A
20.000	---	3.69A	4.08A	4.88A	5.44A	5.75A	6.23A	6.60	6.94	7.05	6.77	6.44	6.13	5.66	5.02	4.51A	3.91A	3.91A

AVERAGE OZONE (PPMV) FOR SEPTEMBER																		
P(NB)	LATITUDE (DEG)																	
	-80	-70	-60	-50	-40	-30	-20	-10	0	10	20	30	40	50	60	70	80	
.003	.52A	.60A	.60A	.63A	.71A	.78A	.78A	.80A	.80A	.77A	.77A	.78A	.69A	.61A	.60A	.56A	.46A	.46A
.004	.41A	.44A	.46A	.46A	.45A	.45A	.45A	.45A	.45A	.45A	.45A	.45A	.45A	.45A	.45A	.45A	.45A	.45A
.005	.35A	.33A	.36A	.39A	.46A	.53A	.53A	.51A	.49A	.50A	.52A	.54A	.54A	.54A	.54A	.54A	.54A	.54A
.007	.29A	.28A	.31A	.34A	.40A	.43A	.44A	.42A	.39A	.39A	.41A	.43A	.39A	.29A	.24A	.22A	.19A	.19A
.010	.28A	.31A	.33A	.35A	.37A	.37A	.35A	.32A	.30A	.29A	.32A	.32A	.33A	.31A	.25A	.21A	.19A	.17A
.015	.30A	.33A	.31A	.31A	.29A	.26A	.22A	.21A	.20A	.20A	.21A	.23A	.22A	.19A	.17A	.17A	.17A	.17A
.020	.30A	.31A	.26A	.24A	.22A	.19A	.17A	.17A	.17A	.16A	.17A	.17A	.17A	.16A	.15A	.16A	.16A	.16A
.025	.29A	.28A	.22A	.19A	.16A	.17A	.17A	.17A	.17A	.17A	.17A	.17A	.17A	.16A	.16A	.17A	.18A	.22A
.030	.31A	.31A	.25A	.24A	.24A	.24A	.24A	.24A	.24A	.24A	.24A	.24A	.24A	.20A	.21A	.22A	.23A	.26A
.035	.35A	.35A	.32A	.31A	.30A	.29A	.27A	.25A	.25A	.25A	.25A	.25A	.25A	.25A	.25A	.25A	.25A	.25A
.070	.43A	.46A	.46A	.46A	.45A	.45A	.43A	.39A	.35A	.35A	.36A	.36A	.36A	.35A	.40A	.40A	.40A	.41A
.100	.59B	.60	.60B	.60B	.59B	.58B	.54	.54	.55	.55	.53	.52	.52B	.52B	.53B	.53	.53	.53
.150	.62B	.61	.62B	.64B	.64B	.62B	.60B	.70	.77	.77	.75	.74B	.75B	.75B	.75B	.73B	.71B	.71
.200	.61B	.61B	.61B	.60B	.60B	.60B	.60B	.60B	.60B	.60B	.60B	.60B	.60B	.60B	.60B	.60B	.60B	.60B
.300	.31B	.31	.31B	.31B	.31B	.31B	.31B	.31B	.31B	.31B	.31B	.31B	.31B	.31B	.31B	.31B	.31B	.31B
.400	.15B	.15B	.15B	.15B	.15B	.15B	.15B	.15B	.15B	.15B	.15B	.15B	.15B	.15B	.15B	.15B	.15B	.15B
.500	.18B	.18B	.18B	.18B	.18B	.18B	.18B	.18B	.18B	.18B	.18B	.18B	.18B	.18B	.18B	.18B	.18B	.18B
.700	.24A	.24A	.24A	.24A	.24A	.24A	.24A	.24A	.24A	.24A	.24A	.24A	.24A	.24A	.24A	.24A	.24A	.24A
1.000	.34A	.34A	.34A	.34A	.34A	.34A	.34A	.34A	.34A	.34A	.34A	.34A	.34A	.34A	.34A	.34A	.34A	.34A
1.500	.42A	.42A	.42A	.42A	.42A	.42A	.42A	.42A	.42A	.42A	.42A	.42A	.42A	.42A	.42A	.42A	.42A	.42A
2.000	.540A	.540A	.540A	.540A	.540A	.540A	.540A	.540A	.540A	.540A	.540A	.540A	.540A	.540A	.540A	.540A	.540A	.540A
3.000	.602A	.602A	.602A	.602A	.602A	.602A	.602A	.602A	.602A	.602A	.602A	.602A	.602A	.602A	.602A	.602A	.602A	.602A
4.000	.601A	.601A	.601A	.601A	.601A	.601A	.601A	.601A	.601A	.601A	.601A	.601A	.601A	.601A	.601A	.601A	.601A	.601A
5.000	.576A	.576A	.576A	.576A	.576A	.576A	.576A	.576A	.576A	.576A	.576A	.576A	.576A	.576A	.576A	.576A	.576A	.576A
6.000	.542A	.542A	.542A	.542A	.542A	.542A	.542A	.542A	.542A	.542A	.542A	.542A	.542A	.542A	.542A	.542A	.542A	.542A
10.000	.37A	.37A	.37A	.37A	.37A	.37A	.37A	.37A	.37A	.37A	.37A	.37A	.37A	.37A	.37A	.37A	.37A	.37A
15.000	.365A	.365A	.365A	.365A	.365A	.365A	.365A	.365A	.365A	.365A	.365A	.365A	.365A	.365A	.365A	.365A	.365A	.365A
20.000	.339A	.339A	.339A	.339A	.339A	.339A	.339A	.339A	.339A	.339A	.339A	.339A	.339A	.339A	.339A	.339A	.339A	.339A

Table 4 continued.

AVERAGE OZONE (PPMV) FOR OCTOBER																		
P(MB)	LATITUDE (DEG)																	
	-80	-70	-60	-50	-40	-30	-20	-10	0	10	20	30	40	50	60	70	80	
.003	.50A	.57A	.55A	.62A	.64A	.47A	.90A	.79A	.81A	.81A	.79A	.80A	.87A	.77A	.69A	.65A	.49A	
.004	.46A	.48A	.47A	.52A	.70A	.80A	.73A	.62A	.63A	.64A	.62A	.67A	.67A	.57A	.49A	.43A	.30A	
.005	.49A	.43A	.44A	.48A	.62A	.68A	.62A	.54A	.53A	.54A	.52A	.55A	.55A	.45A	.38A	.31A	.19A	
.007	.32A	.40A	.43A	.46A	.52A	.53A	.48A	.43A	.43A	.42A	.41A	.42A	.40A	.34A	.27A	.22A	.10A	
.010	.29A	.39A	.44A	.44A	.43A	.39A	.35A	.34A	.35A	.33A	.31A	.31A	.31A	.28A	.24A	.22A	.14A	
.015	.26A	.31A	.33A	.33A	.30A	.26A	.24A	.25A	.26A	.24A	.23A	.22A	.22A	.23A	.26A	.26A	.24A	
.020	.24A	.24A	.24A	.24A	.22A	.20A	.20A	.21A	.21A	.20A	.19A	.18A	.19A	.20A	.26A	.29A	.29A	
.030	.25A	.22A	.21A	.21A	.19A	.19A	.20A	.19A	.18A	.18A	.18A	.18A	.17A	.19A	.24A	.31A	.33A	
.040	.30A	.27A	.26A	.25A	.24A	.23A	.23A	.23A	.22A	.22A	.22A	.22A	.22A	.22A	.26A	.32A	.35A	
.050	.36A	.34A	.32A	.31A	.29A	.29A	.29A	.28A	.27A	.27A	.27A	.27A	.27A	.27A	.31A	.34A	.36A	
.070	.46A	.46A	.45A	.43A	.42A	.41A	.41A	.40A	.39A	.38A	.38A	.39A	.39A	.40A	.41A	.40A	.42A	
.100	.59	.58	.56B	.54B	.53B	.53B	.53B	.53B	.52B	.53	.53	.51B	.49B	.48A	.52B	.52	.53A	
.150	.78	.76	.76B	.76B	.75B	.76B	.76B	.74B	.72B	.73B	.72B	.71B	.70B	.71B	.70B	.68B	.68	
.200	.95	.92	.93B	.95B	.95B	.96B	.97B	.95B	.93B	.93B	.93B	.93B	.94B	.94B	.91B	.87B	.89	
.300	1.25	1.24	1.24	1.31B	1.33B	1.35B	1.36B	1.35B	1.33	1.32	1.33	1.36	1.36	1.38	1.37	1.34	1.41	
.400	1.47	1.47	1.52	1.57	1.58	1.58	1.60	1.61	1.62	1.60	1.59	1.60B	1.63B	1.68	1.74	1.77	1.87	
.500	1.75	1.76	1.84	1.89	1.90	1.90	1.92	1.93	1.93	1.92	1.92	1.93B	1.98B	2.06	2.19	2.25	2.40B	
.700	2.23A	2.24A	2.37A	2.44A	2.40A	2.35A	2.36A	2.38A	2.40A	2.41A	2.40A	2.39A	2.51A	2.59A	2.93A	2.97A	3.05A	
1.000	3.01A	3.04A	3.26A	3.37A	3.30A	3.18A	3.12A	3.10A	3.10A	3.14A	3.20A	3.30A	4.00A	4.24A	4.22A	4.18A		
1.500	4.19A	4.27A	4.62A	4.81A	4.72A	4.49A	4.32A	4.21A	4.24A	4.24A	4.24A	4.24A	5.23A	5.57A	6.04A	5.86A	5.50A	
2.000	5.18A	5.34A	5.79A	6.08A	6.07A	5.81A	5.56A	5.38A	5.29A	5.37A	5.61A	5.95A	6.46A	6.91A	7.04A	6.66A	5.91A	
3.000	6.44A	6.83A	7.45A	7.92A	8.13A	8.01A	7.75A	7.50A	7.34A	7.38A	7.85A	7.85A	7.96A	7.89A	7.58A	6.86A	5.75A	
4.000	6.85A	7.46A	8.20A	8.78A	9.11A	9.21A	9.14A	8.96A	8.78A	8.79A	8.64	8.59	8.20	7.70	7.50A	6.65A	5.51A	
5.000	6.75A	7.52A	8.35A	8.95A	9.34A	9.74A	9.98A	9.91A	9.77A	9.70A	9.48	9.23	8.49	7.70	7.16A	6.24A	5.20A	
7.000	8.44A	7.34A	8.18A	8.65A	9.48A	9.77A	10.48A	10.69A	10.65A	10.59A	10.06	9.37	8.16	7.17	6.47A	5.37A	4.67A	
10.000	9.31A	8.16	7.95B	7.95B	8.62A	8.66A	9.30A	10.42A	10.29	10.35	9.39	8.29	7.05	5.88	5.38A	4.50A	3.71A	
15.000	9.41A	4.84A	5.73A	6.20A	6.51A	7.34A	8.27A	8.78A	8.53	8.55	8.13	7.30	6.29	5.56	4.87A	4.14A	3.54A	
20.000	3.78A	4.43A	5.25A	5.58A	5.71A	6.15A	6.67A	7.00A	6.83	6.83	6.56	6.12	5.61	5.26	4.76A	4.35A	3.88A	

AVERAGE OZONE (PPMV) FOR NOVEMBER																		
P(MB)	LATITUDE (DEG)																	
	-80	-70	-60	-50	-40	-30	-20	-10	0	10	20	30	40	50	60	70	80	
.003	.51A	.62A	.71A	.77A	.81A	.82A	.78A	.76A	.62A	.62A	.79A	.84A	.94A	.90A	.67A	---	---	
.004	.43A	.50A	.59A	.64A	.68A	.68A	.65A	.62A	.62A	.67A	.64A	.65A	.72A	.69A	.43A	---	---	
.005	.33A	.42A	.50A	.55A	.58A	.58A	.55A	.53A	.57A	.58A	.54A	.53A	.57A	.51A	.30A	---	---	
.007	.25A	.31A	.37A	.42A	.45A	.45A	.43A	.42A	.43A	.40A	.37A	.36A	.37A	.32A	.26A	---	---	
.010	.18A	.23A	.27A	.31A	.33A	.33A	.33A	.33A	.33A	.30A	.27A	.26A	.27A	.26A	.22A	---	---	
.015	.16A	.17A	.20A	.22A	.23A	.23A	.24A	.25A	.26A	.27A	.26A	.25A	.24A	.25A	.27A	---	---	
.020	.17A	.17A	.18A	.19A	.19A	.19A	.20A	.20A	.21A	.21A	.21A	.21A	.21A	.21A	.21A	---	---	
.030	.22A	.21A	.21A	.21A	.20A	.19A	.19A	.19A	.19A	.19A	.19A	.19A	.20A	.25A	.33A	---	---	
.040	.27A	.26A	.26A	.26A	.25A	.24A	.23A	.23A	.22A	.22A	.23A	.24A	.24A	.28A	.34A	---	---	
.050	.33A	.32A	.31A	.31A	.30A	.29A	.29A	.29A	.27A	.27A	.28A	.29A	.30A	.33A	.38A	---	---	
.070	.44A	.43A	.43A	.43A	.42A	.42A	.41A	.40A	.39A	.39A	.40A	.41A	.41A	.41A	.40A	---	---	
.100	.58	.56	.55B	.53B	.51B	.52B	.53B	.54	.54	.54B	.52B	.50B	.49B	.48B	.51B	---	---	
.150	.76	.76	.76B	.75B	.73B	.74B	.75B	.74B	.75B	.73B	.72B	.71B	.71B	.71B	.73B	---	---	
.200	.91	.92	.93B	.92B	.92B	.94B	.95B	.95B	.95B	.94B	.95B	.95B	.95B	.95B	.96B	---	---	
.300	1.18	1.20	1.23B	1.26B	1.28B	1.31B	1.33B	1.35	1.34B	1.34B	1.36	1.41	1.42	1.43B	1.47	---	---	
.400	1.34	1.38	1.45	1.51	1.55	1.59	1.63	1.65	1.66	1.66	1.65	1.68B	1.72B	1.79	1.85	1.78	1.96A	
.500	1.58	1.62	1.70	1.77	1.82	1.87	1.91	1.95	1.96	1.95	1.94	1.99B	2.09	2.24B	2.36B	2.19	1.84A	
.700	1.93A	1.97A	2.08	2.15	2.21	2.28	2.33	2.39	2.42	2.41	2.36	2.43	2.67	2.94	3.07	3.02B	2.42A	
1.000	2.55A	2.59A	2.70	2.79	2.85	2.92	3.00	3.08	3.12	3.12	3.12	3.32	3.80	4.29	4.41	4.22B	3.24A	
1.500	3.57A	3.60A	3.72	3.82	3.89	3.97	4.06	4.12	4.16	4.19	4.30	4.73	5.55	6.16	6.10B	5.69B	4.14A	
2.000	4.66A	4.69A	4.82	4.96	5.04	5.11	5.20	5.23	5.23	5.27	5.44	5.96	6.74	7.14	6.83B	6.29B	4.55A	
3.000	6.44A	6.50A	6.62	6.92	7.08	7.17	7.23	7.16	7.05	7.06	7.25	7.60	7.78	7.37	6.89	6.28B	4.79A	
4.000	7.19A	7.38A	7.44B	7.61B	8.21B	8.39	8.50	8.39B	8.16B	8.06	8.26	8.04	7.92	7.35	6.51	5.91B	4.40A	
5.000	7.18A	7.54A	7.75	8.35	8.61	8.91	9.14	9.35B	9.23B	8.93B	8.78	8.69	8.41	7.83	7.03	6.14	5.55B	4.24A
7.000	8.96A	7.47A	7.66	8.31	8.88	9.48	9.48B	9.99B	9.68B	9.44	9.13	8.42	7.28	6.40	5.56	5.02B	3.87A	
10.000	9.73A	6.31A	6.78	7.39	8.02	8.88	9.65	9.47	9.85	9.60	9.02	8.02	6.49	5.68	4.90	4.37	3.42A	
15.000	4.57A	5.07A	5.78	6.25	6.76	7.54	8.24	8.63	8.62	8.15	7.64	6.87	5.81	5.23	4.58	4.10	3.19A	
20.000	4.39A	4.79A	5.34	5.62	5.90	6.36	6.76	7.00	6.96	6.60	6.31	5.88	5.34	5.02	4.52	4.15B	3.01A	

AVERAGE OZONE (PPMV) FOR DECEMBER																		
P (MB)	LATITUDE (DEG)																	
	-80	-70	-60	-50	-40	-30	-20	-10	0	10	20	30	40	50	60	70	80	
.003	.57A	.71A	.81A	.83A	.78A	.67A	.59A	.58A	.54A	.51A	.61A	.78A	.91A	.91A	--	--	--	
.004	.40A	.49A	.59A	.65A	.63A	.55A	.50A	.50A	.47A	.45A	.49A	.60A	.71A	.70A	--	--	--	
.005	.30A	.37A	.45A	.53A	.53A	.48A	.45A	.46A	.45A	.42A	.46A	.56A	.56A	.54A	--	--	--	
.007	.20A	.24A	.29A	.37A	.38A	.30A	.30A	.30A	.40A	.41A	.39A	.37A	.30A	.38A	.35A	--	--	
.010	.16A	.18A	.20A	.24A	.26A	.26A	.29A	.32A	.33A	.33A	.33A	.33A	.31A	.29A	.25A	--	--	
.015	.15A	.17A	.18A	.18A	.18A	.18A	.20A	.22A	.23A	.23A	.26A	.27A	.26A	.26A	--	--	--	
.020	.17A	.18A	.18A	.17A	.16A	.16A	.17A	.18A	.18A	.18A	.18A	.20A	.23A	.25A	.29A	--	--	
.030	.21A	.22A	.21A	.20A	.19A	.17A	.17A	.18A	.18A	.18A	.18A	.20A	.24A	.33A	--	--	--	
.040	.26A	.26A	.25A	.25A	.24A	.22A	.21A	.22A	.22A	.21A	.22A	.22A	.28A	.36A	--	--	--	
.050	.31A	.31A	.30A	.30A	.29A	.27A	.26A	.27A	.26A	.26A	.26A	.31A	.35A	.40A	--	--	--	
.070	.41A	.42A	.42A	.41A	.41A	.40A	.38A	.37A	.37A	.37A	.41A	.46A	.50A	.47B	--	--	--	
.100	.58B	.62	.58	.55B	.54B	.55B	.57	.56	.55	.54	.53B	.53B	.55B	.57B	--	--	--	
.130	.78	.80	.80	.78B	.76B	.68B	.61	.76	.75	.75B	.76B	.77B	.75B	.82B	--	--	--	
.200	.92	.94	.94	.92B	.90B	.80B	.68	.96B	.95B	.97B	.97B	.97B	.97B	.97B	--	--	--	
.300	1.16	1.20	1.25	1.25	1.25	1.32B	1.30B	1.37	1.37	1.33	1.43B	1.43B	1.43B	1.43B	--	--	--	
.400	1.27	1.32	1.40	1.40	1.57	1.63	1.66	1.66	1.65	1.65	1.65B	1.68B	1.74B	1.64B	1.64	1.49A	1.46A	
.500	1.46	1.53	1.62	1.74	1.82	1.90	1.95	1.96	1.97	1.96	1.96	1.99B	2.10B	2.29B	2.02	1.71A	1.66A	
.700	1.71A	1.81A	1.94	2.08	2.19	2.28	2.36	2.43	2.48	2.45	2.40	2.43	2.63	2.79	2.79	2.21A	2.15A	
1.000	2.19A	2.29A	2.46	2.61	2.76	2.91	3.04	3.15	3.22	3.20	3.19	3.34	3.76	4.08	3.94	3.00A	2.93A	
1.500	3.03A	3.13A	3.32	3.51	3.71	3.93	4.13	4.28	4.36	4.37	4.46	4.80	5.49B	5.99B	5.47B	4.14A	4.03A	
2.000	4.10A	4.17A	4.32	4.54	4.76	5.02	5.27	5.44	5.49	5.62	6.02	6.66	8.68B	8.72B	8.48	6.76A	6.71A	
3.000	6.11A	6.12A	6.25	6.47	6.77	7.04	7.33	7.45	7.39	7.35	7.38	7.54	7.63	7.27	6.48	5.26A	5.01A	
4.000	7.00A	7.06A	7.09	7.42	7.80	8.17	8.50	8.55	8.34	8.15	7.97	7.85	7.57	7.06	6.23	5.28A	5.07A	
5.000	7.05A	7.23A	7.30	8.04	8.52	8.94	9.29	9.31	8.99	8.70	8.39	8.08	7.51	6.76	5.94	5.19A	4.98A	
6.000	7.76A	7.16A	7.34	8.16	8.74	9.37	9.61	9.68	9.49B	9.10B	8.52B	7.92	7.05	6.18	5.46	4.81A	4.62A	
10.000	9.39A	8.58A	8.65	9.35	9.71	10.66	10.89	10.64	10.12	9.23	7.43	6.86	5.35	4.91	4.37A	4.27A	4.25A	
15.000	4.35A	4.75A	5.68	6.46	7.10	7.79	8.63	8.19	7.05	6.10	4.19	3.14	2.35	2.08	1.84	1.68A	1.67A	
20.000	4.31A	4.91A	5.26	5.75	6.12	6.45	6.83	6.69	6.35	6.11	5.93	5.71	5.50	5.27	4.55B	1.68A	1.77A	

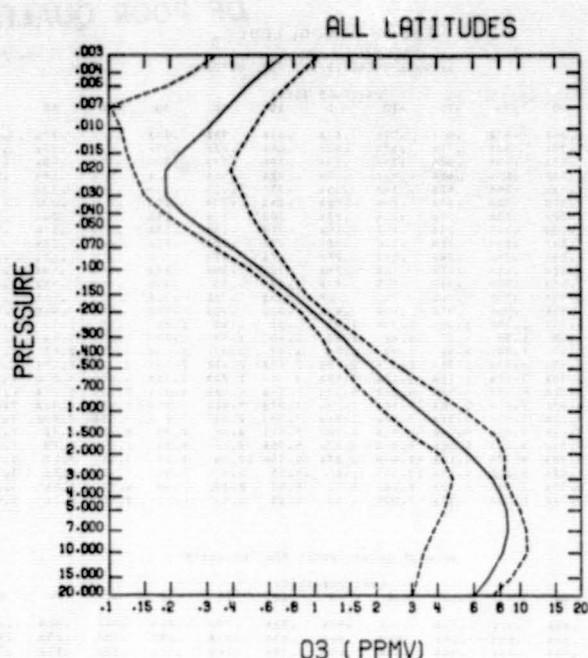


Figure 9. Global mean vertical structure of ozone volume mixing ratio (ppmv) (weighted by cosine of latitude) and the maxima and minima of Table 4 monthly latitudinal profiles.

Table 5. Ozone unit conversion table.

To convert from volume mixing ratio (ppmv) to units below, multiply by:

Mass mixing ratio (ppmm)	1.657
Mass density (kg-m^{-3})	$1.657 \times 10^{-6} \cdot \rho_t$
Number density (m^{-3})	$2.079 \times 10^{19} \cdot \rho_t$
Partial pressure (nanobars)	P_t

where P_t is the total atmospheric pressure in mb (1 mb = 100 pascals) and ρ_t is the total atmospheric density in kg-m^{-3} at a given altitude.

Total column burden (Ω) in atm-cm (1 = 1000 Dobson units) above a given pressure (P_o) can be calculated by integrating partial pressure $P(\text{O}_3)$ with respect to $\ln(P_t)$:

$$\Omega = 7.896 \times 10^{-4} \cdot \int_{P_o}^P P(\text{O}_3) d\ln(P_t).$$

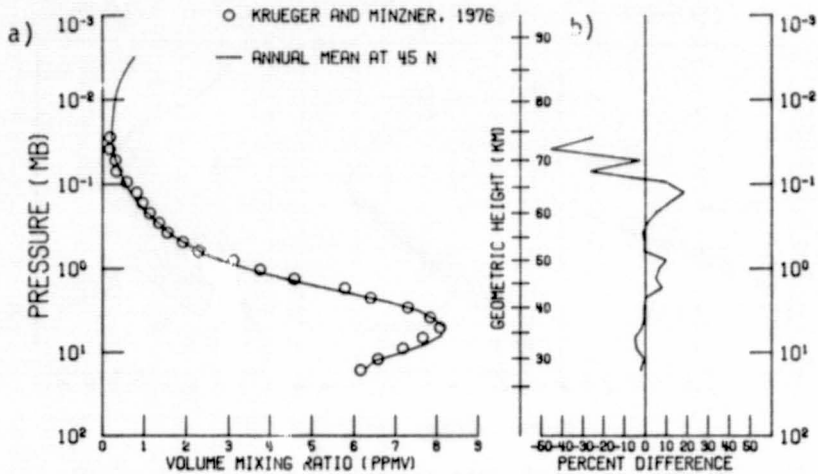


Figure 10. Comparison of annual mean ozone volume mixing ratio (ppmv) at 45°N based on the satellite data model of Table 4 and based on the balloon and rocket data model of KRUEGER and MINZNER (1976). On the left (a) is shown the vertical structure in the two models and on the right (b) the percent difference from the satellite data model of the Krueger and Minzner model.

the relation of total ozone to vertical structure are incorporated here. Shown in Figure 11a are low-latitude ($\sim 25^\circ$) profiles for ozone mixing ratios for total column ozone of 200, 230, 250 and 300 Dobson units (left to right). Shown in Figure 11b are similar midlatitude (~ 25 to 58°) profiles for total column ozone in increments of 50 Dobson units from 200 to 550 Dobson units (left to right). Finally, shown in Figure 11c are similar high-latitude (~ 58 to 80°) profiles for total column ozone in increments of 50 Dobson units from 200 to 65 Dobson units (left to right). Note that the mixing ratio variability extends to lower pressures (higher altitudes) at the higher latitudes. It should be assumed here that these profiles represent annual means since annual variability is not included. Tabulations of the models are found in MATEER et al. (1980).

7. OTHER SYSTEMATIC VARIATIONS

A number of systematic variations of ozone in addition to latitudinal seasonal variations have been analyzed. For brevity only a few references are included here. Empirical analyses have been performed on the quasi-biennial oscillation (ANGELL and KORSHOVER, 1978), solar cycle variations (KEATING, 1981), solar rotation variations (GILLE et al., 1984), diurnal variations (LEAN, 1982; REMSBERG et al., 1984), longitudinal variations (LONDON et al., 1976; WILCOX et al., 1977; HEATH et al., 1982), possible variations with volcanic eruptions (ANGELL and KORSHOVER, 1978), possible response to nuclear explosions (JOHNSON et al., 1973), long-term trends (LONDON and KELLEY, 1974; ANGELL and KORSHOVER, 1983; REINSEL et al., 1984), 4-year oscillations (HASEBE, 1983), response to stratospheric temperature (BARNETT et al., 1975; KEATING et al., 1983a; PITTS, 1981; MILLER et al., 1984), response to sudden winter warmings (GHAZI, 1974), and response to solar proton events (HEATH et al., 1977; THOMAS et al., 1983b).

The quasi-biennial variation in ozone is thought to be related to the

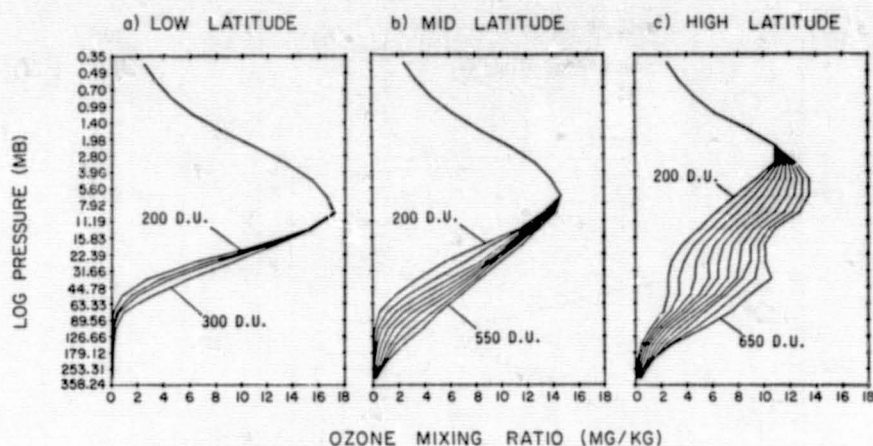


Figure 11. Variation of ozone mass mixing ratio with total ozone (from MATEER et al., 1980). (a) low-latitude ozone profiles for total ozone of 200, 230, 250 and 300 Dobson units (b) mid-latitude ozone profiles for total ozone of 200, 250, ... 550 Dobson units (c) high-latitude ozone profiles for total ozone of 200, 2500, ..., 650 Dobson units.

quasi-biennial variation in equatorial zonal winds (OLTMANS and LONDON, 1982). Shown in Figure 12 (TOLSON, 1981) is the biennial component of the zonal mean total ozone variation based on 7 years of Nimbus 4 BUUV data. The contour interval is 2 Dobson units with the solid lines positive and the shaded area with dashed lines negative. Referring back to Figure 3, it may be seen that the low and midlatitude regions of large interannual variations correspond to regions of large quasi-biennial variation. However, since the variation is only quasi-biennial, the phase indicated in Figure 12 will change with time. There is also evidence that the period of the quasi-biennial variation may vary somewhat with latitude (HILSENATH and SCHLESINGER, 1981) and that the latitude of maximum quasi-biennial variation may vary somewhat with time (HASEBE, 1983).

Evidence has accumulated that variations in ozone with a period of the order of 11 years occur at various locations. On the other hand, there has been a lack of consensus as to whether these variations are related to the 11-year solar activity cycle. The early and more recent studies which have been performed, including theoretical model results based on recent estimates of solar variations and satellite measurements of global mean ozone variations, are reviewed by KEATING (1981). It appears that there is a 2 to 3% variation in global ozone from solar maximum to minimum in accord with the photochemical effects of 11-year variations of the order of 15 to 20% from 180 to 208 nm (KEATING et al., 1981). However, studies over longer time periods of the exact variations of solar ultraviolet radiation and of ozone are needed to confirm this result. Refinement of this result is crucial for separating long-term trends of anthropogenic effects from natural variations in ozone (BLOOMFIELD et al., 1983). Latest studies on long-term variations in ozone vertical structure measured by the Nimbus 4 BUUV are consistent with the scenario of 15 to 20% solar UV variability below 210 nm (CHANDRA, 1984). In addition to a global mean increase in ozone with increasing solar activity, recent empirical and theoretical studies by SOLOMAN and GARCIA (1984) indicate that there may be a decrease in ozone at high latitudes in the upper stratosphere due to a solar cycle variation of NO transported downwards from the thermosphere which catalytically destroys ozone.

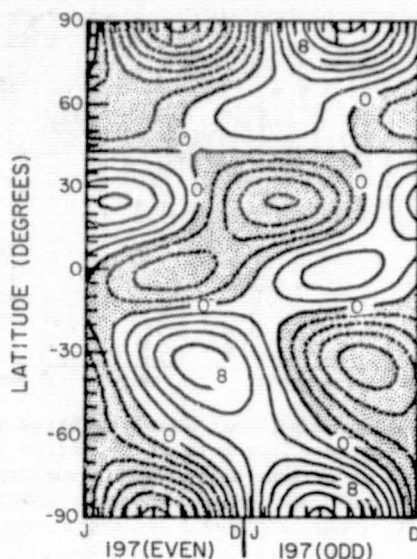


Figure 12. Biennial component of zonal mean ozone variation based on 7 years of Nimbus 4 BUV measurements. Contour interval is 2 Dobson units; solid lines are positive and the shaded area with dashed lines negative (TOLSON, 1981).

Evidence has accumulated of $\sim 3\%$ variations of solar UV between 180 and 208 nm with the 27-day solar rotation based on recent solar measurements from the Nimbus 7 and Solar Mesosphere Explorer satellites. Studies are indicating a detectable ozone response in the upper stratosphere of approximately 1% to these short-term variations (GILLE et al., 1984; HOOD, 1984).

Long-term variations in total ozone have been measured using ground-based observations from the global network. Shown in Figure 13 are estimates of percent variation in global mean ozone values based on those measurements as determined by ANGELL and KORSHOVER (1983). As may be seen, a substantial rise in total ozone occurred in the 1960s and maximum values appear to occur near the times of maxima in the 11-year solar cycle. So far there has not been a detectable decrease in total ozone associated with anthropogenic effects.

Diurnal variations of ozone are observed in the mesosphere where ozone concentrations are higher at night (LEAN, 1982; REMSBERG et al., 1984). There are also indications that the ozone mixing ratio may be higher on the dayside in the upper stratosphere.

Due to the temperature dependence of rate constants in the middle atmosphere temperature decreases result in increases of upper atmospheric ozone in regions approaching photochemical equilibrium. The latitudinal-seasonal and altitudinal relation between these two parameters has been studied in some detail using the Nimbus 4 BUV ozone measurements and Selective Chopper Radiometer (SCR) temperature measurements, and also temperature and ozone measurements from Nimbus 7 (KEATING et al., 1983a). The sensitivity of ozone to temperature variations reaches a maximum value near the stratopause of about 2% increase in ozone per $^{\circ}\text{K}$ decrease in temperature. In addition to the stratospheric ozone response, the mesospheric ozone is found to be strongly affected by temperature variations (EARTH et al., 1983).

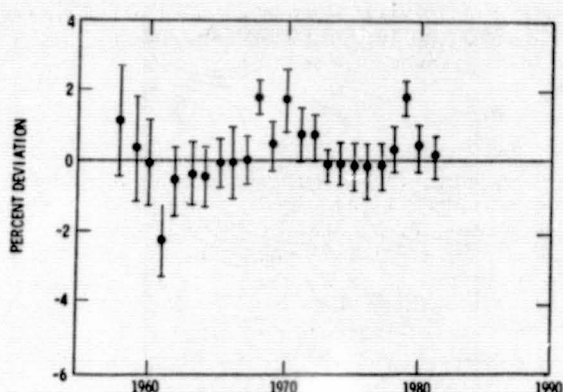


Figure 13. Variation of global yearly average total column ozone expressed as percent deviation from the mean based on ground-based Dobson spectrophotometers as well as M-83 ozonometers (ANGELL and KORSHOVER, 1983).

8. FUTURE MODEL REFINEMENTS

Currently a significant effort is under way among the investigators of contemporary satellite ozone experiments to identify and interpret relative biases among experiments (FLEIG et al., 1984b). This effort may lead to refinements in the model ozone distributions. There is evidence from studies at the National Bureau of Standards and other institutions that some of the ozone cross sections presently used for ozone determination may be in error (KLENK et al., 1984; BASS and PAUR, 1984; PAUR and BASS, 1984). This could change ozone values obtained from the SBUV experiment at some latitudes by 10% (BHARTIA et al., 1984b; KLENK et al., 1984). It is expected that more data will become available from the SME-UVS, SME-IR, SBUV, TOMS and SAGE experiments which can be incorporated later to refine the models. In addition, consideration is being given to incorporating balloon data as another data set to be included in the model, especially if the reference model is to be extended to lower altitudes.

Considering the present, very good agreement among data sets and the evidence of small interannual variability, it is expected that in many respects, refined models will not differ appreciably from those shown here.

9. CONCLUSIONS

A set of models has been generated based on six satellite experiments of the monthly latitudinal variations in total column ozone and the vertical structure of ozone from 20 mb to 0.003 mb. Generally, interannual variability in monthly zonal means is only a few percent. Comparisons of measurements using various techniques to measure global ozone reveal very good agreement between the techniques. Agreement between individual satellite experiments and the reference model of monthly zonal means is generally within 10% below altitudes of 0.4 mb. This has allowed the first global model of ozone measurements to be constructed from multiple sets of satellite measurements.

The ozone measurements based on the satellite data are in excellent agreement with the KRUEGER and MINZNER (1976) midlatitude mean annual model based on rocket and balloon data. Also, models are provided of the relation between total ozone and vertical structure (MATFER et al., 1980).

Refinements to these models will be made as more data becomes available and as algorithm improvements are incorporated considering, for example, recent reevaluations of ozone absorption cross sections.

ACKNOWLEDGEMENTS

The authors wish to acknowledge the valuable contributions of the "Ad Hoc Group on Ozone Reference Models for CIRA" in reviewing the manuscript. The Group includes C. A. Barth, P. K. Bhartia, D. F. Heath, K. Labitzke, C. A. Mateer, M. P. McCormick, A. J. Miller, and J. M. Russell III. Others offering valuable comments included J. S. Chang, R. J. Thomas, M. Allen, D. W. Rusch, and W. P. Chu. The authors also wish to thank J. Y. Nicholson III, M. C. Pitts, and B. T. Marshall of Systems and Applied Sciences Corporation for their assistance in organizing and compiling the vast amount of ozone data.

REFERENCES

- Allen, M., J. I. Lunine, and Y. L. Yung (1984), J. Geophys. Res., **89**, 4841-4872.
- Anderson, G. P., C. A. Barth, F. Cayla, and J. London (1969), Ann. Geophys., **25**, 239-243.
- Angell, J. K., and J. Korshover (1978), Mon. Weather Rev., **106**, 725-737.
- Angell, J. K., and J. Korshover (1983), J. Clim. Appl. Meteorol., **22**, 1611-1627.
- Barrett, J. J., J. T. Houghton, and J. A. Pyle (1975), Q. J. Roy. Meteorol. Soc., **101**, 245-257.
- Barth, C. A., D. W. Rusch, R. J. Thomas, G. H. Mount, G. J. Rottman, G. E. Thomas, R. W. Sanders and G. M. Lawrence, Geophys. Res. Lett., **10**, 237-240.
- Bass, A. M., and R. J. Paur (1984), Paper 7.2, Proc. Quadrennial Ozone Symposium, Halkidiki, Greece.
- Bhartia, P. K., A. J. Fleig, K. F. Klenk, C. K. Wong, and D. Gordon (1984a), J. Geophys. Res., **89**, 5239-5247.
- Bhartia, P. K., K. F. Klenk, A. J. Fleig, C. G. Wellemeyer, and D. Gordon (1984b), J. Geophys. Res., **89**, 5227-5238.
- Bhartia, P. K., B. Monosmith, D. Lee, and A. J. Fleig (1984c), paper 4.6, Proc. Quadrennial Ozone Symposium, Halkidiki, Greece.
- Bloomfield, P., G. Oehlert, M. L. Thompson, and S. Zeger (1983), J. Geophys. Res., **88**, 8512-8522.
- Bojkov, R. D. (1969), J. Appl. Meteorol., **8**, 284-292.
- Chandra, S. (1984), J. Geophys. Res., **89**, 1373-1379.
- Cunnold, D. M., M. C. Pitts, and C. R. Trepte (1984), J. Geophys. Res., **89**, 5429-5261.
- Dutsch, H. U. (1974), Can. J. Chem., **52**, 1491-1504.
- Dutsch, H. U. (1978), Pure Appl. Geophys., **116**, 511-529.
- Elliot, D. D., M. A. Clark, and R. D. Hudson (1967), Aerospace Tech. Rep. TR-0158 (3260-10).
- Fleig, A. J., P. K. Bhartia, C. K. Wong, and K. F. Klenk (1984a), Proc. 5th Conf. on Atmospheric Radiation (AMS), Oct. 31-Nov. 4, 1983, Baltimore, MD.
- Fleig, A. J., J. C. Gille, M. P. McCormick, D. W. Rusch, and J. M. Russell III (1984b), Paper 4.9, Proc. Quadrennial Ozone Symp., Halkidiki, Greece.
- Frederick, J. E., P. B. Hays, B. W. Guenther, and D. F. Heath (1977), J. Atmos. Sci., **34**, 1987-1994.
- Ghazi, A. (1974), J. Atmos. Sci., **31**, 2197-2206.
- Gille, J. C., and J. M. Russell III (1984), J. Geophys. Res., **89**, 5125-5140.
- Gille, J. C., P. L. Bailey, and J. M. Russell III (1980), Phil. Trans. R. Lond., **A296**, 205-218.

- Gille, J. C., C. M. Smythe, and D. F. Heath (1984), Science, **225**, 15-317.
- Guenther, B., R. Dasgupta, and D. F. Heath (1977), Geophys. Res. Lett., **4**, 434-437.
- Hanel, R. A., B. Schlachman, F. D. Clark, C. H. Prokesh, J. B. Taylor, W. M. Wilson, and L. Chaney (1970), Appl. Opt., **9**, 1767-1774.
- Hasebe, F. (1983), J. Geophys. Res., **88**, 6819-6834.
- Hays, P. B., and R. G. Roble (1973), Planet. Space Sci., **21**, 273-279.
- Heath, D. F., C. L. Mateer, and A. J. Krueger (1973), Pure Appl. Geophys., **106-108**, 1238-1253.
- Heath, D. F., A. J. Krueger, H. A. Roeder, and B. D. Henderson (1975), Opt. Eng., **14**, 323-331.
- Heath, D. F., A. J. Krueger, and P. J. Crutzen (1977), Science, **197**, 886.
- Heath, D. F., A. J. Fleig, A. J. Miller, T. G. Rogers, R. M. Nagatani, H. D. Bowman, V. G. Kaveeshwar, K. F. Klenk, P. K. Bhartia, K. D. Lee (1982), NASA Reference Publication 1098, A2-A163.
- Hilsenrath, E., and B. M. Schlesinger (1981), J. Geophys. Res., **86**, 12,087-12,096.
- Hilsenrath, E., P. J. Dunn, and C. L. Mateer (1977), in Collection of Extended Summaries of Contributions Presented at the Joint Assembly CMUA Sessions IAGA/IAMAP, Seattle Washington, August 1977, National Center for Atmospheric Research, Boulder, CO. 41-1-41-6.
- Hood, L. L. (1984), J. Geophys. Res., **89**, 9557-9568.
- Iozenas, V. A., V. A. Krasnopol'ski, A. P. Kuznetsov, and A. I. Lebedinsky (1969), Atmos. Oceanic Phys., **5**, 149-159.
- Johnson, M. S., G. Whitten, and J. Birks (1973), J. Geophys. Res., **78**, 6107.
- Keating, G. M. (1981), Solar Phys., **74**, 321-347.
- Keating, G. M., L. R. Lake, J. Y. Nicholson III, and M. Natarajan (1981), J. Geophys. Res., **86**, 9873-9880.
- Keating, G. M., J. J. Barnett, W. J. Borucki, J. J. Pyle, M. C. Pitts, J. Y. Nicholson III, and D. F. Young (1983a), Presented at IUGG General Assembly, Hamburg, West Germany.
- Keating, G. M., L. Frank, J. Craven, M. Shapiro, D. Young, and P. Bhartia (1983b), Adv. Space Res., **2**, 183-188.
- Klenk, K. F., P. K. Bhartia, E. Hilsenrath, and A. J. Fleig (1983), J. Clim. Appl. Meteorol., **22**, 2012-2022.
- Klenk, K. F., B. Monosmith, and P. K. Bhartia (1984), Paper 7.6, Proc. Quadrennial Ozone Symp., Halkidiki, Greece.
- Krueger, A. J., and R. A. Minzner (1976), J. Geophys. Res., **81**, 4477-4481.
- Krueger, A. J., B. Guenther, A. J. Fleig, D. F. Heath, E. Hilsenrath, R. McPeters, and C. Prabhakara (1980), Phil. Trans. R. Soc. Lond., **A296**, 191-204.
- Lean, J. L. (1982), J. Geophys. Res., **87**, 4973-4980.
- London, J., and J. Kelley (1974), Science, **184**, 987.
- London, J., R. D. Bojkov, S. Oltmans, and J. I. Kelley (1976), Atlas of the Global Distribution of Total Ozone, July 1957-June 1967, NCAR TN/113 +STR, Boulder, CO.
- Lovill, J. E., and J. S. Ellis (1983), Geophys. Res. Lett., **10**, 447-450.
- Lovill, J. E., T. J. Sullivan, R. L. Weichel, J. S. Ellis, J. G. Huebel, J. A. Korver, P. P. Werdhaas, and F. A. Phelps (1978), UCRL-52473, Lawrence Livermore Laboratory.
- Makino, T., H. Yamamoto, and H. Sekiguchi (1984), Paper 5.34, Proc. Quadrennial Ozone Symp., Halkidiki, Greece.
- Mateer, C. L., D. F. Heath, and A. J. Krueger (1971), J. Atmos. Sci., **28**, 1307-1311.
- Mateer, C. L., J. J. DeLuisi, and C. C. Porco (1980), NOAA TM ERL ARL-86.
- McCormick, M. P., T. J. Swisler, E. Hilsenrath, A. J. Krueger, and M. T. Osborn (1984), J. Geophys. Res., **89**, 5315-5320.

- McPeters, R. D., D. F. Heath, and P. K. Bhartia (1984), J. Geophys. Res., **89**, 5199-5214.
- Miller, A. J., R. M. Nagatani, and J. E. Frederick (1984), Paper 4.28 Proc. Quadrennial Ozone Symp., Halkidiki, Greece.
- Miller, D. E., and K. W. Stewart (1965), Proc. R. Soc. Lond., **A288**, 540-544.
- Nimbus Project (1978), The Nimbus 7 User's Guide, Goddard Space Flight Center, Greenbelt, MD.
- Noxon, J. F. (1982), Planet. Space Sci., **30**, 545-557.
- Oltmans, S. J., and J. London (1983), J. Geophys. Res., **87**, 8981-8989.
- Paur, R. J., and A. M. Bass (1984), Paper 7.3, Proc. Quadrennial Ozone Symp., Halkidiki, Greece.
- Pitts, M. C. (1981), Masters Thesis, Georgia Institute of Technology, Atlanta, GA.
- Planet, W. G., J. H. Lieneseh, and M. I. Hill (1984), Paper 4.2, Proc. Quad. Ozone Symp., Halkidiki, Greece.
- Prabhakara, C., E. B. Rodgers, B. J. Conrath, R. A. Hansel, and V. G. Kunde (1976), J. Geophys. Res., **81**, 6391-6399.
- Prior, E. J., and B. J. Oza (1978), Geophys. Res. Lett., **5**, 547-550.
- Rawcliffe, R. D., and D. D. Elliott (1966), J. Geophys. Res., **71**, 5077-5089.
- Rawcliffe, R. D., G. E. Meloy, R. M. Freidman, and E. H. Rogers (1963), J. Geophys. Res., **68**, 6425-6429.
- Reinsel, G. C., G. C. Tiao, J. J. DeLuisi, C. L. Mateer, A. J. Miller, and J. E. Frederick (1984), J. Geophys. Res., **89**, 4833-4840.
- Reiter, R., and M. P. McCormick (1982), Nature, **300**, 337-339.
- Remsberg, E. E., J. M. Russell III, J. C. Gille, L. L. Gordley, P. L. Bailey, W. G. Planet, and J. E. Harries (1984), J. Geophys. Res., **89**, 5161-5178.
- Riegler, G. R., J. F. Drake, S. C. Liu, and R. J. Cicerone (1976), J. Geophys. Res., **81**, 4997-5001.
- Rusch, D. W., G. H. Mount, C. A. Barth, G. J. Rottman, R. J. Thomas, G. E. Thomas, R. W. Sanders, G. M. Lawrence, and R. S. Eckman (1983), Geophys. Res. Lett., **10**, 241-244.
- Rusch, D. W., G. H. Mount, C. A. Barth, R. J. Thomas, and M. P. Callan (1984), accepted for Geophys. Res. Lett.
- Russell, J. M. III (1984), Invited paper at 25th Plenary Meeting of COSPAR and Associated Activities, Graz, Austria.
- Solomon, S., and R. R. Garcia (1984), Planet. Space Sci., **32**, 399-409.
- Systems and Applied Sciences Corp. (1984), NASA CR Contract No. NAS5-28060.
- Thomas, L. (1980), Phil. Trans. R. Soc. Lond., **A296**, 243-260.
- Thomas, R. J., C. A. Barth, G. J. Rottman, D. W. Rusch, G. H. Mount, G. M. Lawrence, R. W. Sanders, G. E. Thomas, and L. E. Clemens (1983a), Geophys. Res. Lett., **10**, 245-248.
- Thomas, R. J., C. A. Barth, G. J. Rottman, D. W. Rusch, G. H. Mount, G. M. Lawrence, R. W. Sanders, G. E. Thomas, and L. E. Clemens (1983b), Geophys. Res. Lett., **10**, 253-256.
- Thomas, R. J., C. A. Barth, D. W. Rusch, and B. W. Sanders (1984a), J. Geophys. Res., **89**, 9569-9580.
- Thomas, R. J., C. A. Barth, and S. Solomon (1984b), Geophys. Res. Lett., **11**, 673-11,676.
- Tolson, R. H. (1981), J. Geophys. Res., **86**, 7313-7330.
- Vaughn, G. (1984), Q. J. Roy. Meteorol. Soc., **110**, 239-260.
- Vallance Jones, A. (1973), Space Sci. Rev., **15**, 355.
- Venkateswaran, S. V., J. G. Moore, and A. J. Krueger (1961), J. Geophys. Res., **66**, 1751-1771.
- Weeks, L. H., R. E. Good, J. S. Randhawa, and H. Trinks (1978), J. Geophys. Res., **83**, 978-982.
- Wilcox, R. W., G. D. Nastrom, and A. D. Belmont (1977), J. Appl. Meteorol., **16**, 290-298.

3.1.1 TEMPERATURE STRUCTURE OF THE 80 km TO 120 km REGION

Jeffrey M. Forbes

Department of Electrical, Computer, and Systems Engineering
Boston University
Boston, MA 02215

INTRODUCTION

Temperatures, densities, and pressures in the COSPAR International Reference Atmosphere (CIRA) 1972 between 80 and 120 km are given as monthly averages at 5 km height increments every 10 deg in latitude for the Northern Hemisphere. However, data are extremely sparse in this region, and as Groves (see CIRA 1972) points out, CIRA 1972 suffers from the same limitations as CIRA 1965 above 60 km:

- (i) Data from all longitudes are combined without consideration of longitudinal effects. Most data are from North American sites, and so any longitudinal bias would be towards the Western Hemisphere,
- (ii) Insufficient Southern Hemisphere data were available for developing a separate mode. Therefore, Southern Hemisphere data were combined with Northern Hemisphere data with a six-month change of date.
- (iii) Due to insufficient data, no account was taken of local time in development of the models. Consequently the temperature and density fields may be diurnally biased as well.

Development of the temperature, density, and pressure specifications between 80 and 120 km for the new CIRA will involve building upon the existing CIRA 1972 model data base. Since the greatest abundance of experimental data is in the form of temperatures, and since temperature is one of the meteorological fields (besides winds) for which we have a firmer theoretical and intuitive base for understanding its behavior and structure, the temperature field will be the basis for development of the model. Following the procedure followed in CIRA 1972, given a specification of the pressure field at some lower boundary, the density and pressure fields at higher altitudes will be derived from the barometric and ideal gas laws. Available falling-sphere rocket measurements will be used to provide consistency checks on these densities and to possibly introduce adjustments in the final temperature model as appropriate. Also involved in the final stages of model development will be "matching" to temperature specifications below 80 km and above 120 km. All of these requirements will result in some iterations and adjustments in the final stages of model development, and it is anticipated that these issues will be quantitatively resolved at the IAGA/IAMAP Meeting in Prague, Czechoslovakia, in August 1985.

Without firm definition of the matching constraints at the 80 km and 120 km altitude levels, all that can be accomplished at the present time concerning the intervening altitude regime is to provide an assessment of deficiencies in CIRA 1972 given the more extensive data base now available, and to outline the scope of the new CIRA model specification between 80 and 120 km. Specifically, we will address the following questions: (i) Are there clear-cut misrepresentations in CIRA 1972 which can be rectified by the data now available? (ii) Are there sufficient data and evidence to warrant inclusion of a longitude dependence in the model? (iii) An asymmetry about the equator in the model?

SOURCES OF DATA

The following is a preliminary, and as yet incomplete, description of data which will form the basis for the 80-120 km specification of temperature,

density and pressure in the new CIRA:

- (i) The CIRA (1972) temperature model between 80 and 120 km was based heavily on data from the NASA Meteorological Sounding Rocket Program (MSRP) collected prior to 1967. The primary techniques were pitot tube and grenade measurements. The MSRP was phased out in 1973. Between 1967 and 1973 32 pitot tube and 135 rocket grenade experiments were conducted which generally yielded temperature data above 80 km. The soundings were made at Wallops Island (38°N, 75°W), Ft. Churchill (59°N, 94°W) Pt. Barrow (71°N, 157°W), Natal (6°S, 35°W), Arecibo (18°N, 67°W), Arenosillo (37°N), Eglin (30°N, 87°W), and Kourou (5°N, 53°W) (SMITH et al., 1967, 1969, 1970, 1971).
- (ii) GAIGEROV et al. (1984) present extensive analyses of temperatures from Soviet rocket measurements (mostly grenade method) north and south of the equator in the Eastern Hemisphere. Most of the Southern Hemisphere data were collected after 1970, and hence were not included in the 1972 CIRA. Gaigerov et al. also discuss the results of several intercomparisons with other independent measurements of temperature, and report that adjustments have been made for any biases which might have existed in their raw data. Monthly average data between 80 and 90-100 km are available from Heiss Island (81°N, 58°E), Volgograd (48°N, 44°E), Molodezhnaya (68°S, 45°E), and from research vessel soundings in the Pacific near 0°, 20°S, 40°S, and 50°S. These data now enable us to examine possible longitudinal and latitudinal asymmetries in the thermal structure of the mesopause region.
- (iii) Five years (1970-1975) of temperature profiles from incoherent scatter measurements in the E region (100-130 km) over Arecibo, Puerto Rico (18°N, 67°W) and Millstone Hill, Massachusetts (42°N, 71°W) are available for analysis. These data have been analyzed in parts, mostly with regard to the semidiurnal oscillation by SALAH (1974), SALAH et al. (1975), SALAH and WAND (1974), and WAND (1976, 1983). This investigator has pooled all the available data, separated mean and semidiurnal tidal components, and constructed monthly averages. A total of over 1,500 profiles (each) are available from Arecibo and Millstone Hill. These data are considered extremely important in terms of "matching" the rocket-based temperature structure of the 80-100 km region with the satellite-based density and temperature fields above 150 km.

The data described above are utilized in the preliminary analysis presented here. Some additional supplementary data between 90 and 110 km are Esrange, Sweden (68°N, 21°E) during the November/December 1980 Energy Budget Campaign (PHILBRICK et al., 1983) and between 100 and 130 km taken at St. Santin (45°N, 2°E) and at Chatanika (65°N, 147°W) may also be included at a later time, as well as several other scattered measurements taken since 1970. There also exist temperature inferences from optical emissions (5577 Å oxygen airglow and OH(8-3) band rotational temperatures in the vicinity of 85-95 km), but these are single height (slab) determinations and are generally only available at latitudes or longitudes where the rocket data are plentiful. A fairly complete list of stations from which rocket and radar data will originate for the new CIRA is included in Table I.

ANALYSIS OF THE DATA

The 80 - 100 km Region. The main focus of the current analysis is to ascertain (1) whether evidence exists for longitudinal and latitudinal asymmetries in the temperature structure of the 80 to 100 km region, and whether sufficient data are available to delineate these dependences in a reference atmosphere; and (2) whether specific deficiencies in the CIRA (1972) representation of temperature are suggested by the updated data base.

Table 1. Locations of rocket* measurements and incoherent scatter radar** measurements which will form the basis data for the new CIRA between 80 km and 120 km.

<u>Western Hemisphere</u>		<u>Eastern Hemisphere</u>	
Thule	(76°N, 69°W)	Heiss Island	(81°N, 58°E)
Pt. Barrow	(71°N, 157°W)	+Esrange	(68°N, 21°E)
+**Chatanika	(65°N, 147°W)	Volgograd	(48°N, 44°E)
Ft. Churchill	(59°N, 94°W)	**St. Santin	(45°N, 2°E)
**Millstone Hill	(42°N, 71°W)	Sardinia	(40°N, 10°E)
Wallops Island	(38°N, 75°W)	Guam	(13°N, 145°E)
White Sands	(32°N, 106°W)	Kwajalein	(9°N, 168°E)
Eglin	(30°N, 87°W)	Thumba	(8°N, 77°E)
Cape Kennedy	(28°N, 80°W)	Res. Vessels	(0°)
Barking Sands	(22°N, 159°W)	Res. Vessels	(20°)
**Arecibo	(18°N, 67°W)	Carnarvon	(25°S, 114°E)
Antigua	(17°N, 62°W)	Woomera	(31°S, 136°E)
Ft. Sherman	(9°N, 80°W)	Res. Vessels	(50°S)
Kourou	(5°N, 53°W)	Kerguelen I.	(49°S,)
Natal	(6°S, 35°W)	Res. Vessels	(50°S).
Ascension I.	(8°S, 14°W)	Molodezhnaya	(68°S, 45°E)

* With some exceptions, data are generally available between 80 - 100 km.

** Data generally available between 100 - 130 km.

+ Not included in current preliminary analysis.

In Figure 1 variations in monthly temperatures at 85 km for individual stations are compared. The comparison between Pt. Barrow (71°N, 157°W) and Heiss Island (81°N, 58°E) suggests 5-10 K higher temperatures at Heiss Island in the summer and 5-10 deg cooler temperatures between January and March. Although these two stations are separated by 10 deg in latitude, the discrepancy is opposite to what one might expect from the positive (negative) pole-to-equator temperature gradient assumed to exist in Northern Hemisphere summer (winter) months. An examination of vertical structures at the two stations indicates that the summer mesopause minimum is near 90 km at Heiss Island as opposed to 85 km at Pt. Barrow, and this in itself is an important contribution to their differences in monthly behavior at 85 km.

Although the Volgograd (48°N, 44°E) data during summer exhibit 10-15 K higher temperatures than Ft. Churchill (59°N, 94°W), their 11 deg separation in latitude is sufficient to account for more than half of this difference assuming a realistic latitude gradient in temperature (see following figures). Figure 1 also suggests a much larger temperature gradient in the Eastern than Western Hemisphere, but it must be remembered that Ft. Churchill and Pt. Barrow are only separated by 12 deg latitude, whereas the separation between Heiss Island and Volgograd is 33 deg in latitude. Obviously, to make any convincing statements about latitude structure we should examine all possible data at a given height. This will be done below.

Before leaving Figure 1, note that Southern Hemisphere data at 40°S and 50°S agree quite well with the Northern Hemisphere data at similar latitudes. Further, the monthly variation of temperature predicted by the CIRA 1972 is in excellent agreement with the measurements at Pt. Barrow, Ft. Churchill, and

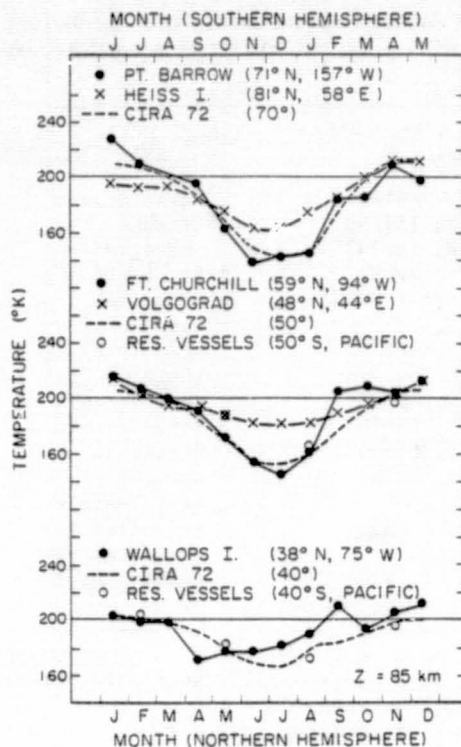


Figure 1. Temperature vs month at 85 km for various stations which allow examination of possible longitudinal or hemispheric asymmetries within specific latitude belts. CIRA 1972 values are shown for comparison.

Wallops Island. This is not surprising as considerable data from these stations prior to 1967 were used in the construction of CIRA 1972.

In Figures 2 and 3 the latitude structures of temperature during summer (mostly July) and winter (mostly January), respectively, are depicted at 80, 90, and 100 km. An obvious feature of these plots is that the Eastern/Western/Northern/Southern Hemisphere data collectively delineate fairly well-defined patterns. Further, while the CIRA 1972 curves are surprisingly successful in approximating these data in some regions, the potential for significant improvement is suggested. In particular, 100 km appears to be nearly isothermal at 200 K in January and at 190 K in summer, at least within the scatter of the data. Also, the latitude structure of temperature at 80 km and 90 km poleward of 40 deg latitude can be better modelled, and this feature is important for understanding the dynamics of the zonal mean circulation of the mesopause region.

The 100 - 130 km Region. Figure 4 depicts a selection of temperature measurements between 200 and 130 km at various latitudes during July and January. Comparisons are made with the MSIS-83 model (HEDIN et al., 1983), as this is a likely candidate for the new CIRA above 100 km or so. CIRA temperature profiles would not have compared so well with the data in Figure 4, the temperatures being some 20-60 K cooler than MSIS-83 in the 120-130 km region. The data shown in Figure 4 during January are extremely consistent

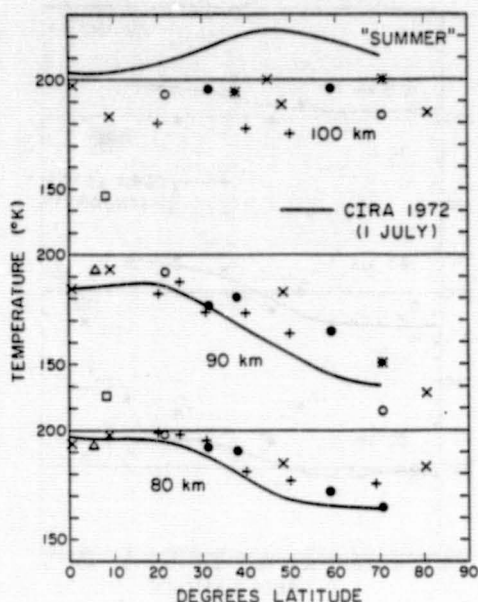


Figure 2. Temperature vs latitude for measurements representative of July north of the equator in the Western (●) and Eastern (x) Hemispheres, and January south of the equator in the Eastern Hemisphere (+). Where data under these exact conditions were not available in the Western Hemisphere, data points from 8°S August (□), 6°S August (Δ), August (*), and June (o) were inserted to allow a more complete delineation of the latitude structure. CIRA 1972 values are shown for comparison.

with each other and with the MSIS-83 model, and do not exhibit any significant latitude structure. During July, however, there appears to exist a significant positive equator-to-pole temperature gradient. At 115 km the temperature varies from about 168 K at Kwajalein (9°N) to 320 K at Arecibo (18°N) to 370 K at Wallops Island (38°N) and Millstone Hill (42°N). A small temperature difference (20 K) of this sense between 18°N and 42°N is specified in the MSIS-83 model.

CONCLUSIONS AND RECOMMENDATIONS FOR THE NEW CIRA

Between 80 and 120 km the CIRA 1972 model is based heavily on NASA Meteorological Sounding Rocket Program (MSRP) data collected prior to 1967. The data are biased towards North America, are seasonally and diurnally biased, and contain significant gaps in latitude. The MSRP was phased out in 1973. Since about 1970 an abundance of E-region (100-130 km) temperature data from the incoherent scatter facilities at Arecibo, Millstone Hill, and St. Santin have also become available. The present study examines the temperature structure of the 80-120 km region given considerable additional MSRP rocket data, thus providing better seasonal, latitudinal, and longitudinal coverage in the 80-100 km region, and a combination of incoherent scatter and rocket data in the 100-120 km region which allows a much improved delineation of lower thermosphere temperature structure. Although some individual station comparisons indicate measurable asymmetries in longitude and latitude, data are still insufficient to separate these effects; that is, to provide a reliable

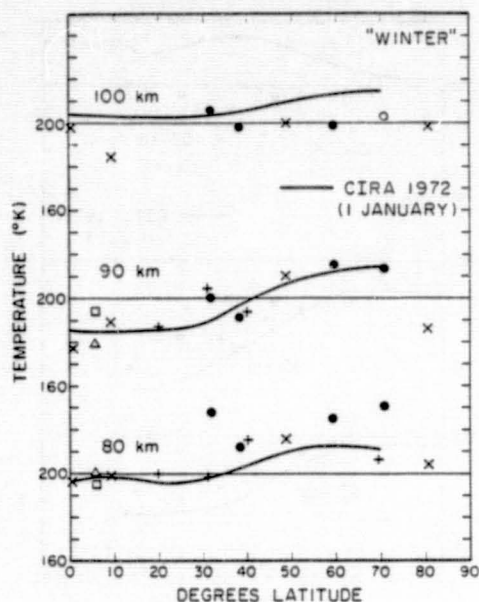


Figure 3. Temperature vs latitude for measurements representative of January north of the equator in the Western (●) and Eastern (x) Hemispheres. Where data under these exact conditions were not available in the Western Hemisphere, data points from 6°S February (□), 6°S December (Δ), and February (o) were inserted to allow a more complete delineation of the latitude structure. CIRA 1972 values are shown for comparison.

description of latitude structure as a function of longitude, or of longitude structure at any given latitude. However, by consideration of data below 70-80 km as well, GAIGEROV et al. (1984) were able to construct height-latitude temperature contours up to 100 km which are characteristic of the Asian/Pacific and American longitude sections. The Eastern Hemisphere data also extend into the Southern Hemisphere.

Specific recommendations of the new CIRA to emerge from this study are as follows:

- (i) Tabulations between 80 and 100 km should represent zonally averaged values. These can be viewed with much greater confidence than those in CIRA 1972.
- (ii) The temperature, density, and pressure specifications between 80 and 120 km should provide a smooth transition with the zonally averaged SCR/PMR data (as given in Section 2.2) below and MSIS-83 (tentative) above. In so doing, some seasonal asymmetry about the equator may be introduced via the satisfaction of matching conditions. It is anticipated that these matters will be extensively discussed and settled at the IAGA/IAMAP meeting in Prague, Czechoslovakia, in August 1985.
- (iii) To provide some measure of possible longitudinal and latitudinal asymmetries, the height-latitude contours of temperature for January, July, April and October from GAIGEROV et al. (1984) should be included in the new CIRA.

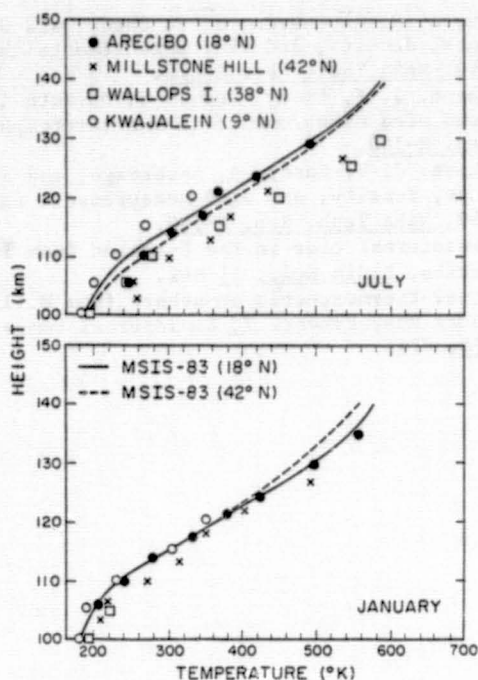


Figure 4. Vertical structures of temperature from 100 km to 130 km at various latitudes. MSIS-83 values are shown for comparison.

ACKNOWLEDGEMENTS

This work was supported under Contract F19628-82-K-0031 from the Air Force Geophysics Laboratory.

REFERENCES

- Gaigerov, S. S., E. M. Zhmulin, E. D. Zhorova, M. Ya. Kalikhman, V. G. Kidiyarova, V. V. Sadohikov, D. A. Tarasenko, and V. V. Fedorov (1984), Thermal regime in the upper atmosphere, presented at the XXV COSPAR meeting, Graz, Austria.
- Hedin, A. (1983), A revised thermospheric model based on mass spectrometer and incoherent scatter data, MSIS-83, *J. Geophys. Res.*, **88**, 10170.
- Philbrick, C. R., K. V. Grossmann, R. Hennig, G. Lange, D. Krankowsky, D. Offermann, F. J. Schmidlin, and U. von Zahn (1983), Vertical density and temperature structure over Northern Europe, *Adv. Space Res.*, **2**, 121.
- Salah, J. E. (1974), Daily oscillations of the midlatitude thermosphere studied by incoherent scatter at Millstone Hill, *J. Atmos. Terr. Phys.*, **35**, 1891.
- Salah, J. E., and R. H. Wand (1974), Tides in the temperature of the lower thermosphere at mid-latitudes, *J. Geophys. Res.*, **79**, 4295.
- Salah, J. E., R. H. Wand, and J. V. Evans (1975), Tidal effects in the E-region from incoherent scatter radar observations, *Radio Sci.*, **10**, 347.
- Smith, W. S., J. S. Theon, P. C. Swartz, L. B. Katchen, and J. J. Horvath (1968), Temperature, pressure, density and wind measurements in the stratosphere and mesosphere, 1966, *NASA Tech. Re. R-288*.

- Smith, W. S., J. S. Theon, P. C. Swartz, J. F. Casey, and J. J. Horvath (1969), Temperature, pressure, density, and wind measurements in the stratosphere and mesosphere, 1967, NASA Tech. Rep. R-316.
- Smith, W. S., J. S. Theon, J. F. Casey, and J. J. Horvath (1970), Temperature, pressure, density and wind measurements in the stratosphere and mesosphere, 1968, NASA Tech. Rep. R-340.
- Smith, W. S., J. S. Theon, J. F. Casey, A. Azcarraga, and J. J. Horvath (1971), Temperature, pressure, density, and wind measurements in the stratosphere and mesosphere, 1969, NASA Tech. Rep. R-360.
- Wand, R. H. (1976), Semidiurnal tide in the E-region from incoherent scatter measurements at Arecibo, Radio Sci., 11 641.
- Wand, R. H. (1983), Lower thermospheric structure from Millstone Hill incoherent scatter radar measurements 2, Semidiurnal temperature component, J. Geophys. Res., 88, 7211.

3.1.2 MEAN WINDS OF THE UPPER MIDDLE ATMOSPHERE (60-110 km): A GLOBAL DISTRIBUTION FROM RADAR SYSTEMS (M.F., METEOR, VHF)

A. H. Manson and C. E. Meek¹; M. Massebeuf and J. L. Fellous²;
W. G. Elford, R. A. Vincent³ and R. L. Craig⁴; R. G. Roper⁵;
S. Avery and B. B. Balsley⁵; G. J. Fraser⁶ and M. J. Smith⁶;
R. R. Clark⁷; S. Kato and T. Tsuda⁸; A. Ebel⁹

¹I.S.A.S., University of Saskatchewan, Canada; ²CNRS/CRPE and CNES, France
³University of Adelaide, Australia; ⁴Georgia Institute of Technology,
Atlanta, GA; ⁵CIRES and NOAA, Boulder, CO; ⁶University of Canterbury,
New Zealand; ⁷University of New Hampshire, Durham, NH;
⁸Kyoto University, Japan; ⁹University of Cologne, FRG

ABSTRACT

During the last decade a large number of radars (~ 12) have been developed, which have produced substantial quantities of tidally corrected mean winds data in the upper middle atmosphere. The distribution of the radars is not global, but many areas are well covered: the Americas with Poker Flat (65°N), Saskatoon (52°N), Durham (43°N), Atlanta (34°N), Puerto Rico (18°N); Europe and Kiruna (68°N), Garchy (47°N) and Monpazier (44°N); and Oceania with Christchurch (44°S), Adelaide (35°S), Townsville (20°S), and Kyoto (35°N).

Zonal and meridional wind height-time cross sections from 60-80 km (MF/meteor radar) to ~ 110 km have been prepared for the last 5-6 years. They are compared with cross sections from CIRA 1972 for zonal winds, and GROVES (1969) for meridional winds.

It is shown that while CIRA 1972 is still a useful model for many purposes, significant differences exist between it and the new radar data. The latter demonstrate important seasonal, latitudinal, longitudinal and hemispheric variations. The new meridional cross sections are of great value. The common features with GROVES (1969) are the equatorward cells in summer near 85 km; however, their strength (~ 10 m/s) and size are less. Systematic and somewhat different variations emerge at higher ($\geq 52^\circ$ N) and lower (35-44°) latitudes.

INTRODUCTION

Since the development of the last CIRA in 1972, the number of radars providing winds in the upper middle atmosphere has increased significantly. Depending on the technique, these systems fill the data gap between 60 km (the meteorological rocket network and other small rocket systems have provided winds to that height) and ~ 110 km (larger rockets, and incoherent-scatter radars provide some winds above this height). The radars include medium frequency (MF) radars or partial reflection systems giving data from 60/70-100/110 km (and MST radars operating as meteor radars). Until now MST (VHF) radars have not given winds for a sufficient number of hours per day, or heights to provide cross sections of the type shown here: however, a new extended data set from Poker Flat is discussed later. We show here data from 12 locations, which represent a good Northern Hemispheric (NH) North American chain (18-65°N, 90°W), an Oceanian chain (44°S-35°N, 140°E) which is mainly in the Southern Hemisphere (SH), and some Western Europe Data (44-68°N, $\sim 0^\circ$ E). (Of these, data are still being obtained at 7 locations, and also from two Antarctic stations not included here.) The methods of data analyses are discussed in detail elsewhere (MANSON et al., 1981a; MASSEBEUF et al., 1979; VINCENT and STUBBS, 1979; SALBY and ROPER, 1980; SMITH, 1981; CARTER and BALSLEY, 1982; CLARK, 1983; ASO and VINCENT, 1982). Generally, however, tidal

oscillations have been removed from days or groups of days, and the remaining mean winds and longer period oscillations plotted as height-time contours. Time resolution varies from 10-15 days to seasonal, and will be evident from each figure.

An attempt has been made to form composite cross sections from the years 1978-1982 so that only the major temporal features remain. Detailed study of groups of years from Adelaide (ELFORD, 1976), France (MASSEBEUF et al., 1979; MANSON et al., 1983), Saskatoon (MEEK and MANSON, 1984, 1985) suggest that, at least at middle latitudes, the main features of the circulation are repeated each year with relatively small interannual variability. Here we focus on those major features and compare these with zonal winds from CIRA 1972, and meridional winds from Groves' data compilation (GROVES, 1969). Tabulations of monthly mean values for most stations appear in the Appendix. A more detailed presentation of these data, including individual years, will be made elsewhere (MANSON et al., 1985). The sign convention is as follows: for the zonal winds, positive winds are from the west (west or westerly winds) and negative winds are east or easterly winds. For the meridional winds, positive winds are from the south (south or southerly winds), and negative winds are north or northerly winds. It is also convenient to describe these latter as poleward or equatorward winds. The figures are rather consistent, but any differences are mentioned in the captions.

ZONAL WINDS

Generally, for latitudes as low as ~ 35 deg, there are westerly/easterly flows during winter-/summer-centred months below 95/85 km, and the reverse above (Figures 1-6, 8-12) as shown in CIRA 1972 (Figures 7, 13). High latitude data, such as Kiruna and Poker Flat (Figures 1,2), which were not available for CIRA 1972, can be seen to be reasonable extrapolations of midlatitude data (e.g., Saskatoon 52°N , Figure 3). The data from Poker Flat are derived from meteor echoes. A recent analysis of the winds from meteor and turbulence echoes (BALSLEY and RIDDLE, 1984) for 1980/1 show excellent agreement; suggesting that MST radars can provide monthly mean winds, depending on their power, location and the season. For lower latitudes (≤ 35 deg) the behaviour may be similar, but in general is more complex. At midlatitudes (~ 45 deg) the reversals in the mesopause region are less clear in winter months, and are at a greater altitude (e.g., Figures 3, 4, 5, 6). There is also more systematic mesospheric variability during the ~ 7 winter-like months; this is most evident in the high resolution (7-/10-d means) large altitude-range data from Christchurch and Saskatoon (Figures 6, 3). The causes of this are planetary waves, stratospheric warmings, and annual and semiannual oscillations (MANSON et al., 1981b). This is a major difference from CIRA 1972, which due to lack of data in the lower mesosphere and averaging over years, has produced an unrealistically smooth winter vortex with a maximum in December/January. Indeed at latitudes near 50 deg, the CIRA winds for February and March are quite atypical (cf. Figure 3). The differences between winter and summer circulations, especially the variability, heights of reversal and strength of lower thermospheric circulations have important implications for theories and models which now depend upon gravity wave momentum deposition to close the westerly and easterly flows (LINDZEN, 1981; HOLTON, 1982). It is likely that the characteristics of the gravity wave fluxes, e.g., sources and group velocities, and perhaps planetary waves, also have strong seasonal variations which are reflected in these contours. Winds from most of the midlatitude stations (Figures 3, 5, 6; Saskatoon, Monpazier, Garchy, Christchurch) also illustrate the regularity of the equinoctial transitions and their rapidity. This is especially evident in the Saskatoon winds, where the composite of 4 years of continuous data differs little from individual years. Because of this, September is more winter-like and May more summer-like (Northern Hemisphere), than CIRA 1972 indicates.

**ZONAL WIND
KIRUNA (SWEDEN, 68° N)
1974 - 1975**

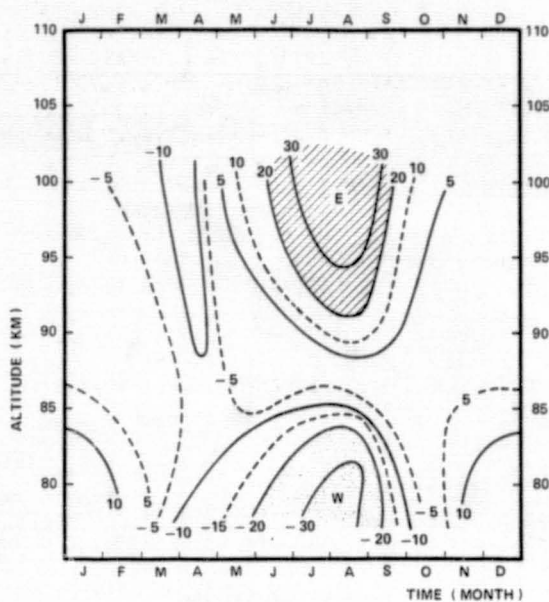


Figure 1. Kuruna, 68°N, 20°E (MASSEBEUF and FELLOUS). The positive westerly flow is marked E for eastward; and negative easterly is W for westward.

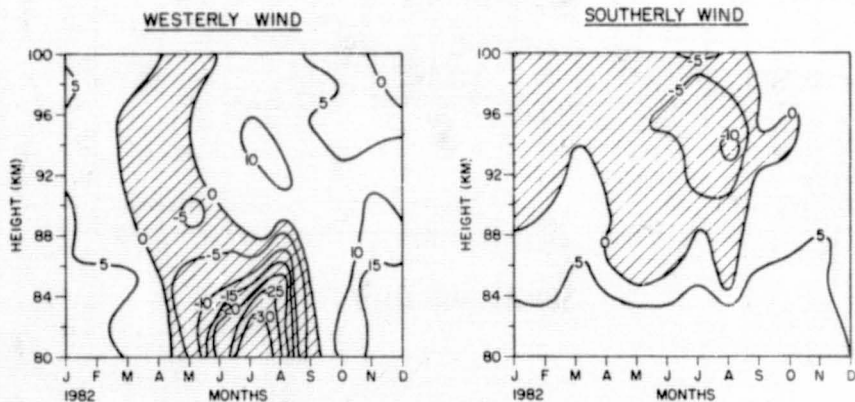


Figure 2. Poker Flat, 65°N, 147°W.

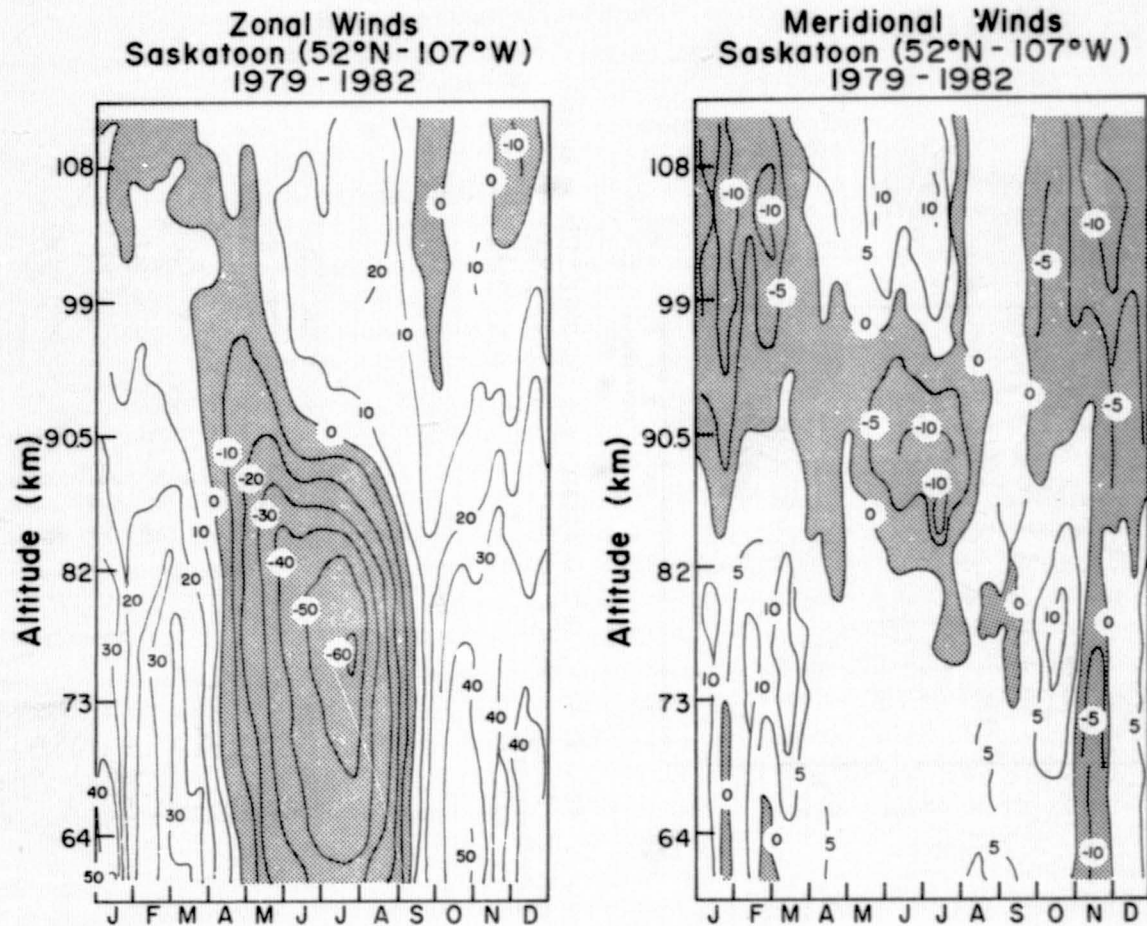


Figure 3. Saskatoon, 52°N, 107°W: 10 d means used; s.d. typically 6 ms^{-1} for EW, 4 ms^{-1} for NS at 90 km. Data above 100 km refer to a $\sim 5 \text{ km}$ layer, due to group retardation.

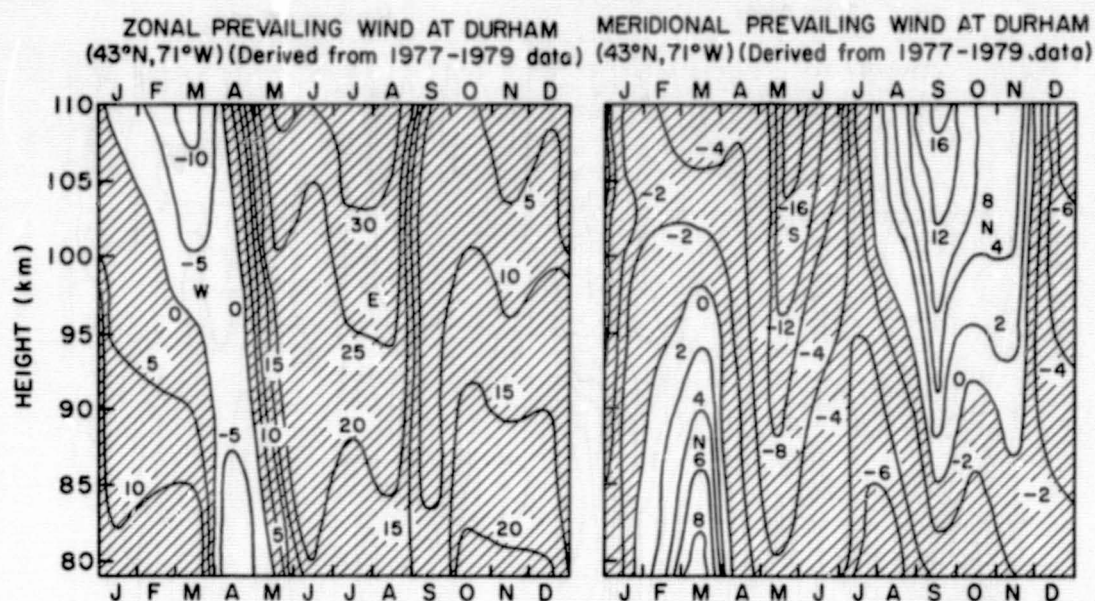


Figure 4. Durham, 43°N, 71°W: the positive easterly (E, eastward) flow is cross-hatched only in this case. Positive southerly flow is marked N for northward.

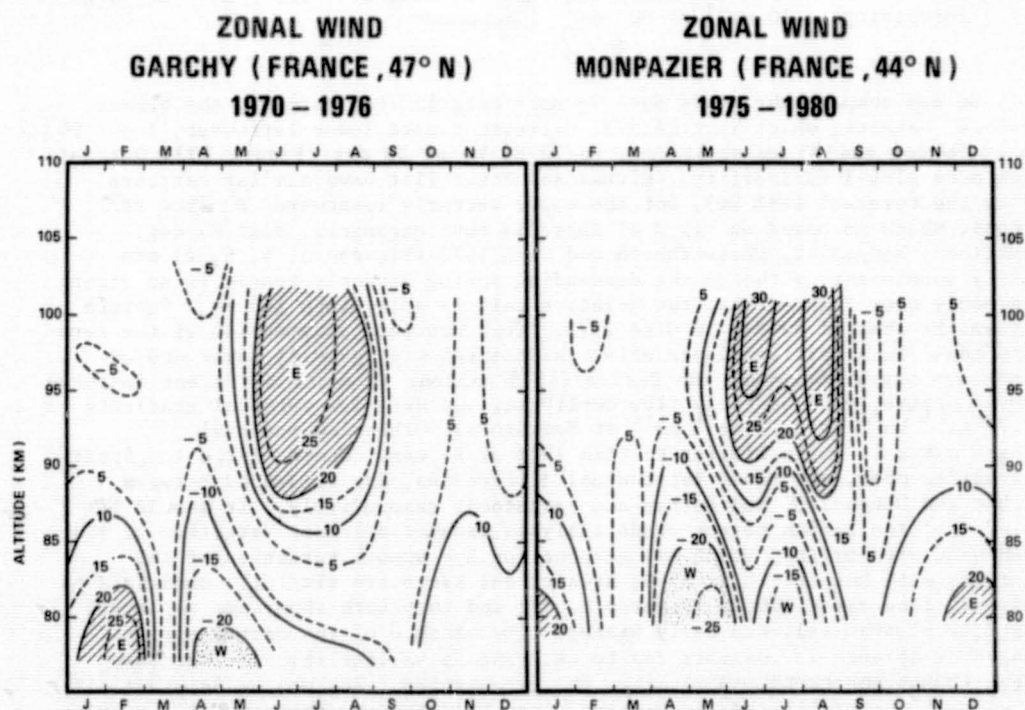


Figure 5. Monpazier, 44°N, 1°E; Garchy, 47°N, 3°E, 1970-76 (MASSEBEUF et al., 1979): westerly flow is marked E for eastward, easterly is W for westward.

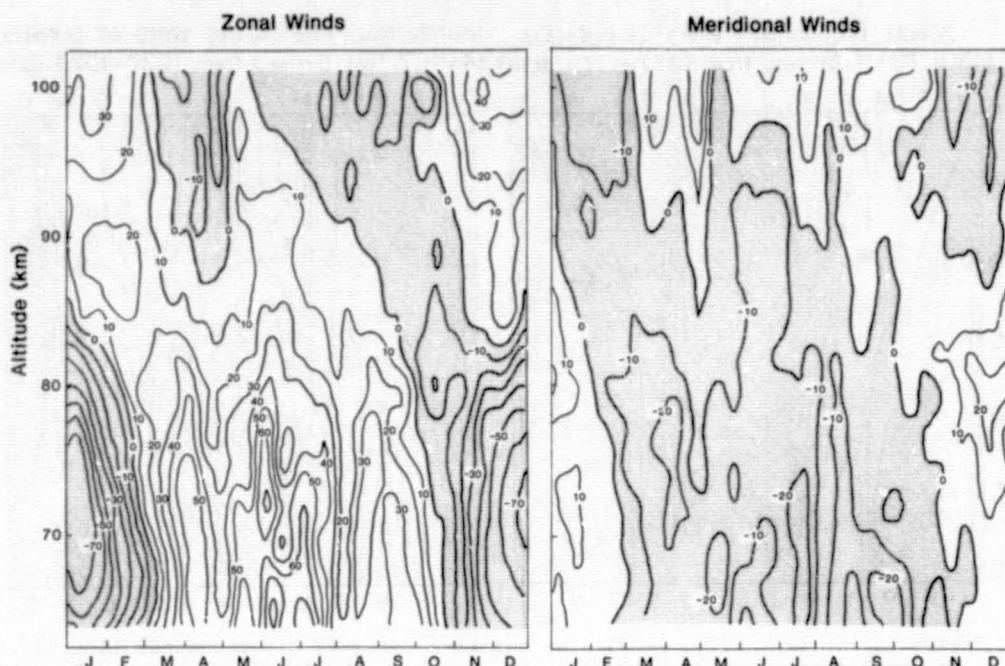
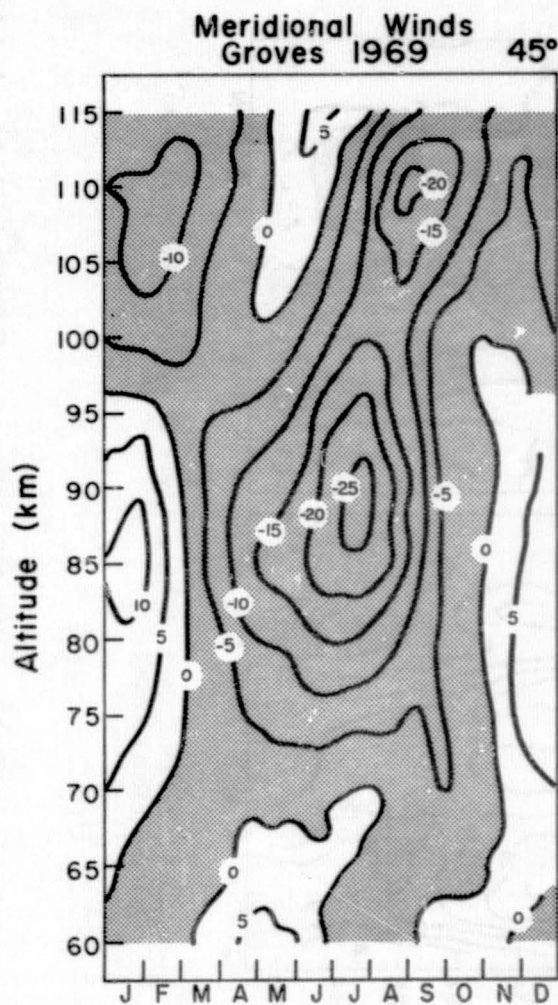
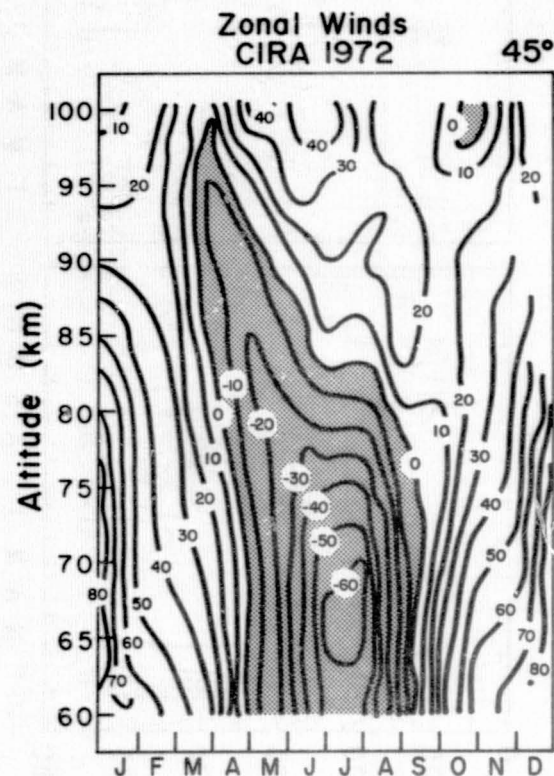


Figure 6. Christchurch, 44°S, 173°E: 7 d means used. Positive meridional flow is northward, and hence equatorward. The s.d. are 7 ms^{-1} at 90 km, increasing to 10 ms^{-1} at 80 km.

We now compare the winds data in more detail. For example, the summer reversal heights, which in CIRA 1972 decrease toward lower latitudes, from 90 km at 50 deg and 80 km at 35 deg, to 70–80 km at 20 deg (Figure 13). Our data show more global variability. Kiruna and Poker Flat have similar contours below the reversal ($\sim 88 \text{ km}$), but the upper westerly (eastward, E) flow at Kiruna, which is based on 15 d of data, is much stronger. Near 45 deg, Saskatoon, Monpazier, Christchurch and CIRA 1972 (Figures 3, 5, 6, 7) are fairly consistent, although the descending spring easterly tongue is so strong and early over France, that the negative cell is split into two -- a feature not unlike that at 20 deg in CIRA 1972. This downward progression of the zero line could be a critical layer effect associated with gravity waves and/or planetary waves. However, the Durham (43°) contour is quite different in these summer months, with westerly flow 80–110 km, and very low vertical gradients ($0.75 \text{ ms}^{-1} \text{ km}^{-1}$ vs $3.75 \text{ ms}^{-1} \text{ km}^{-1}$ at Saskatoon). This low reversal height makes it quite similar to CIRA 1972 at 35 deg. Hence, large longitudinal differences, and rapid latitudinal differences, are evidenced between Durham and Monpazier, and Durham and Saskatoon, respectively. It should be noted that the Durham meteor winds analysis assumes a linear variation of the mean wind with height, which may account for the smooth variation of the contours with height. Near 35°N, Atlanta and Kyoto are similarly dominated by westerly flow above 80 km (Figures 8, 9); and they both show some negative easterly flow in fall and early winter. The absence of the narrow spring tongue at Atlanta is possibly due to interannual variability. It has been noted (DOLAS and ROPER, 1981), that the circulation there may be tropical (Figure 13) or midlatitude in pattern: actually to form the composite contour of Figure 8, a year which was somewhat more representative of a midlatitude circulation was eliminated. At Kyoto, there is easterly flow in February --



ORIGINAL PAGE IS
OF POOR QUALITY

Figure 7. Model winds from CIRA 1972 (zonal) and GROVES (1969) (meridional): 45 deg.

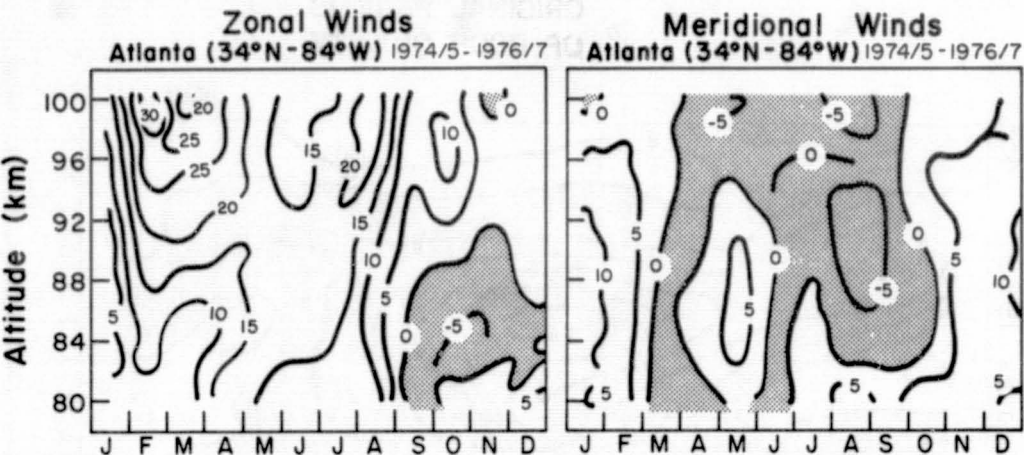


Figure 8. Atlanta, 34°N, 84°W; s.d. are 12 ms^{-1} for the zonal, 8 ms^{-1} for meridional winds.

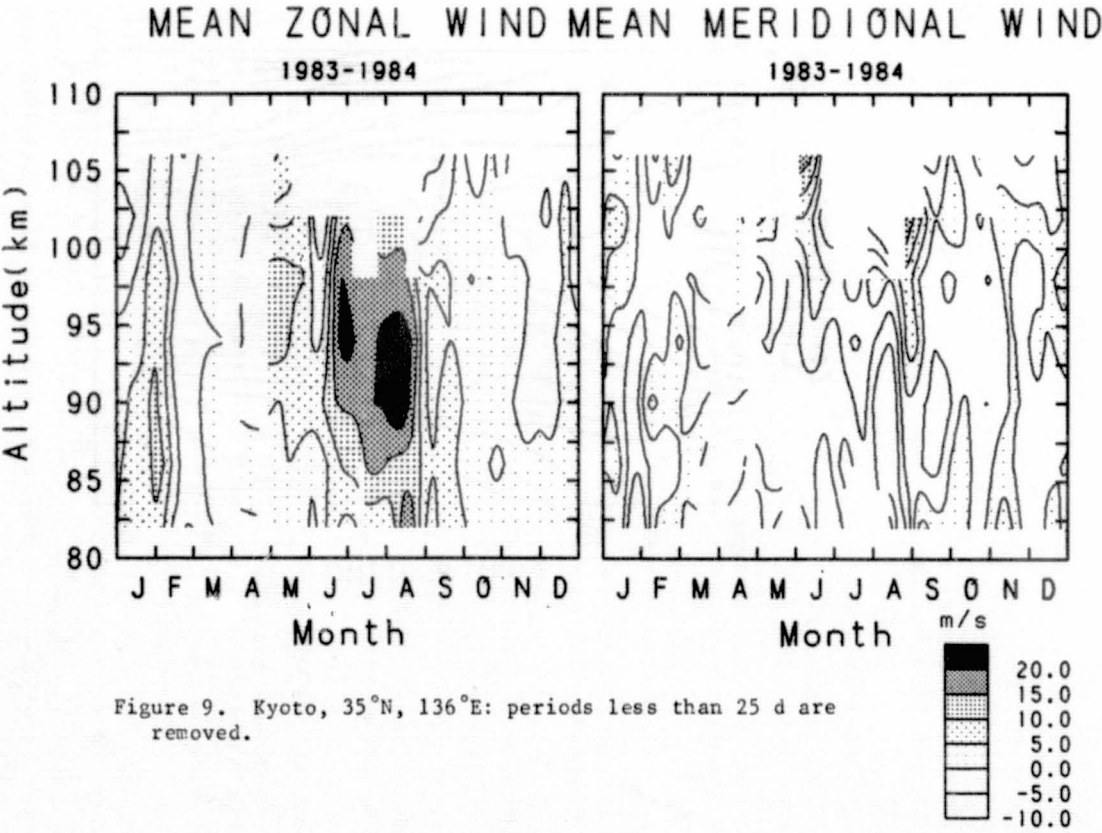
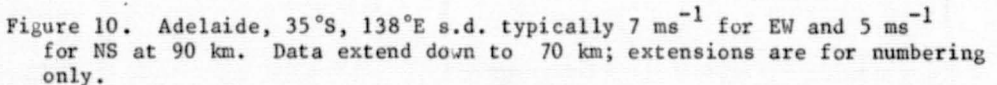


Figure 9. Kyoto, 35°N, 136°E: periods less than 25 d are removed.

The comparison between CIRA 1972 and the radar winds is well illustrated in height-latitude cross sections; and we show here December (an early solstice



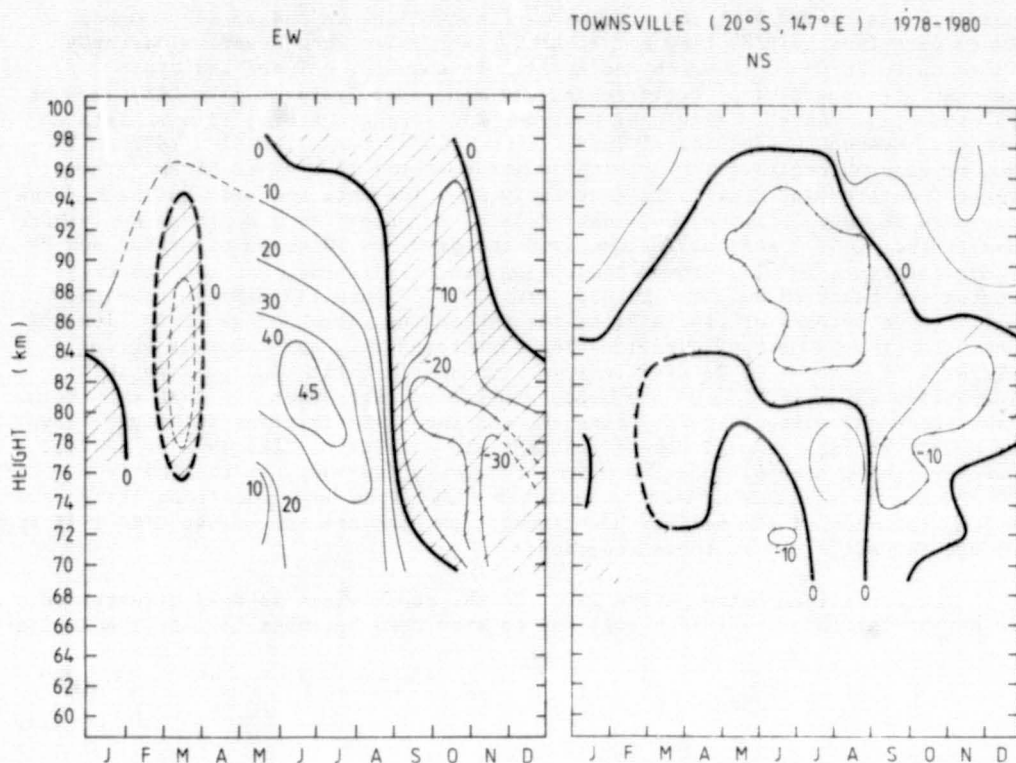


Figure 11. Townsville; 20°S, 147°E (ELFORD, VINCENT, CRAIG).

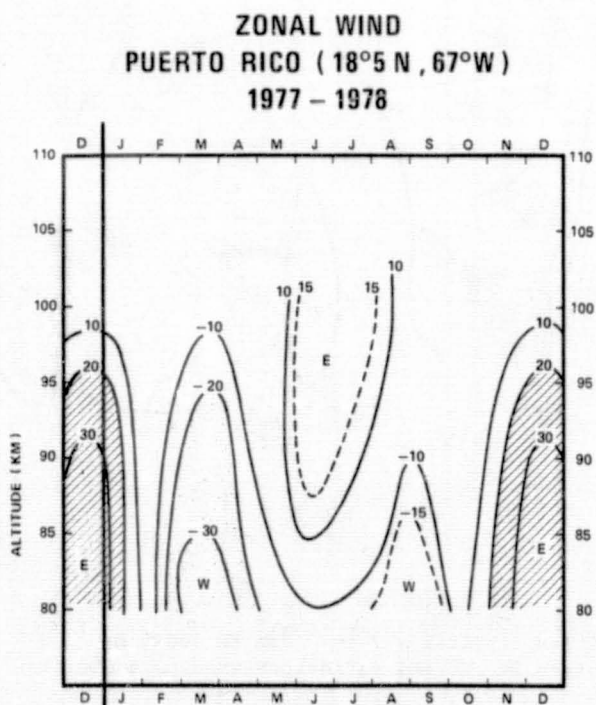


Figure 12. Puerto Rico, 18°N, 67°W (MASSEBEUF, FELLOUS): positive westerly flow is marked E for eastward.

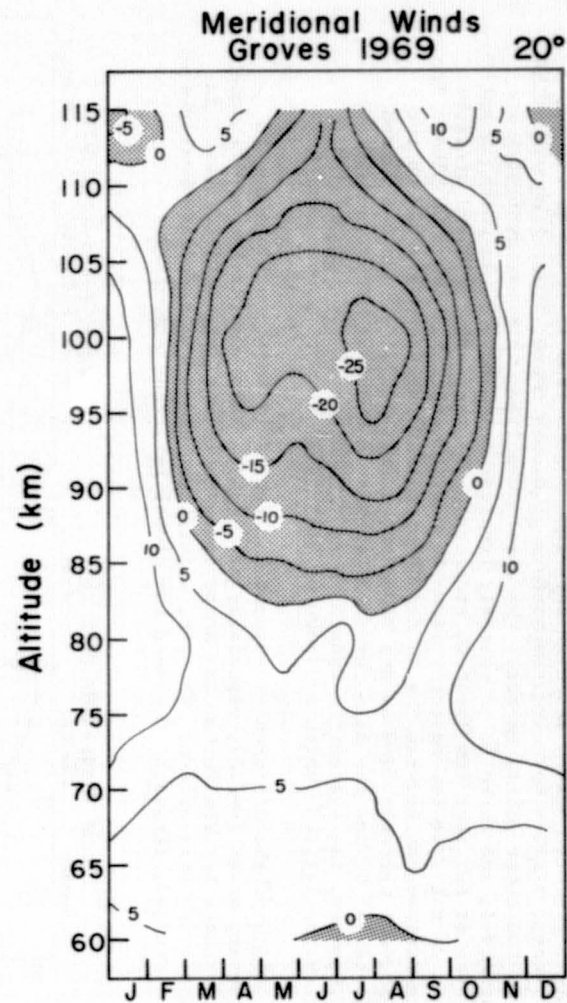
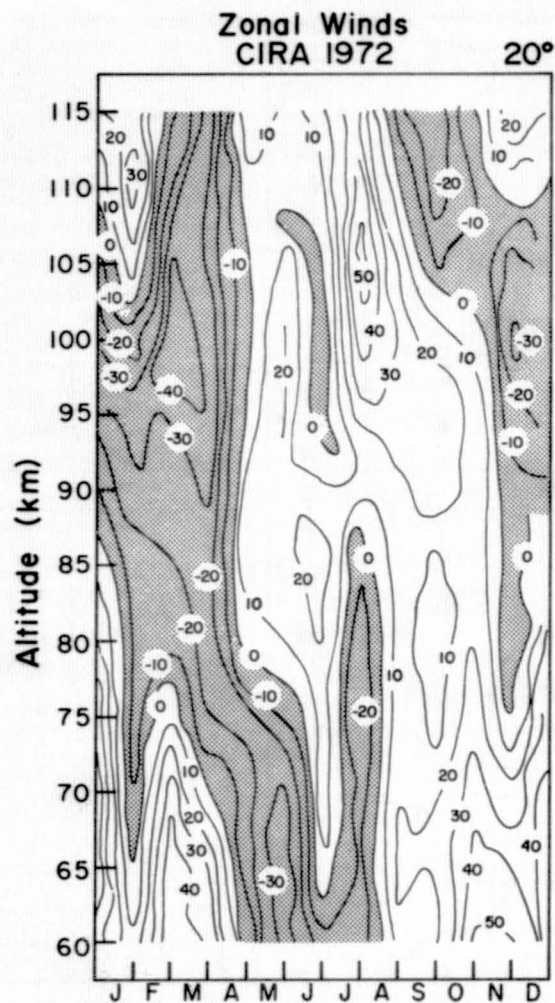


Figure 13. CIRA 1972, Groves, 1969: 20 deg.

ORIGINAL PAGE IS
OF POOR QUALITY

month, clear of NH stratospheric warmings) and July for $\sim 90^\circ\text{W}$ in the NH, and $\sim 140^\circ\text{E}$ in the SH. From CIRA, July (June 15-July 15) and January (December 15-January 15) are shown (Figures 14, 15). The time rates of change are small in midseason, so that conclusions drawn here are usually typical of the entire solstitial seasons. Only the zero contours and maxima of cells are shown for CIRA 1972. The lack of hemispheric symmetry is immediately obvious: the winters are most alike, and even then the NH zero line is 10-15 km higher, reflecting smaller poleward temperature gradients there. Comparing with CIRA 1972, two other points emerge: the upper zero lines were not available for that model; and there is an easterly tropical cell above 87 km which is not evident at our four low latitude stations. For the summers, these stations again do not have the easterly flow above 87 km, which is shown in CIRA. The main differences between the SH and NH at these longitudes are due to the consistent westerly flow at and above 80 km revealed at Durham (43°N) and Atlanta (35°N) and the high reversal heights in Oceania. Thus in both hemispheres, the systematic reduction in the height of the zero line with decreasing latitude which is shown by CIRA 1972, is not in evidence.

Some of the differences evident in Figures 14 and 15 will be due to planetary waves ($n=1,2$), especially in the NH. These could also explain the differences between Durham and Monpazier. Satellite data will be useful in quantifying this effect. However, significant differences between hemispheres have emerged, stressing the need for global reference atmospheres.

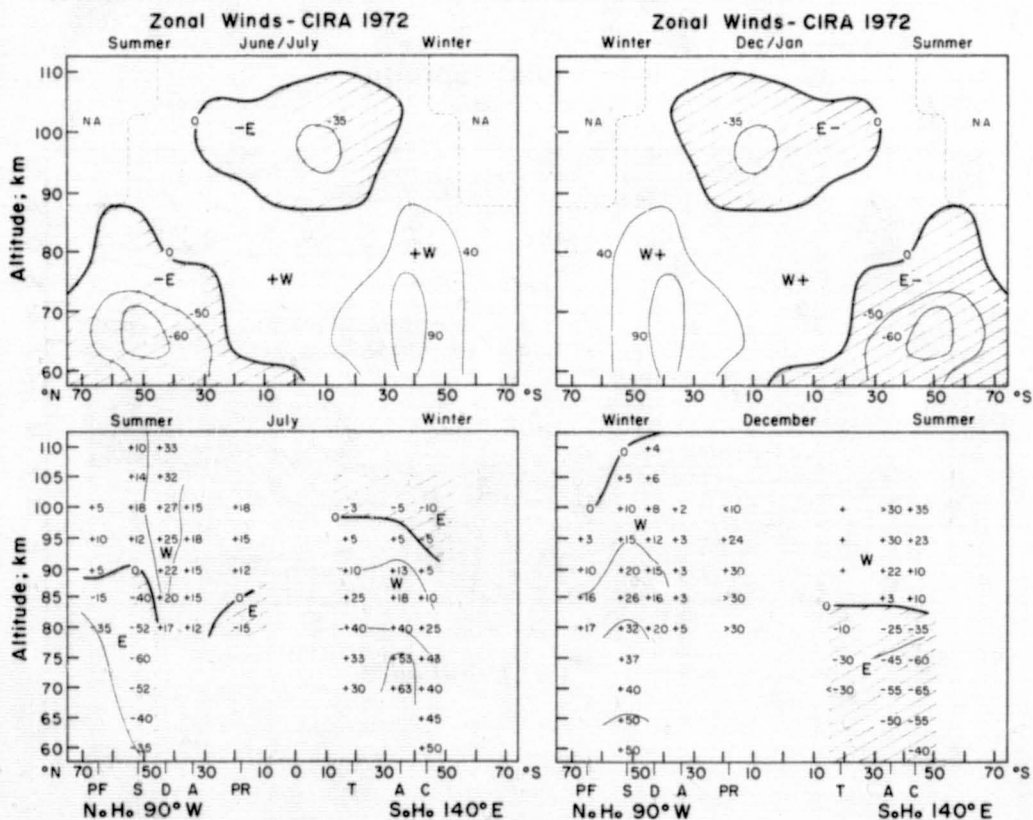


Figure 14. Zonal winds, July.

Figure 15. Zonal winds, December/January.

MERIDIONAL WINDS

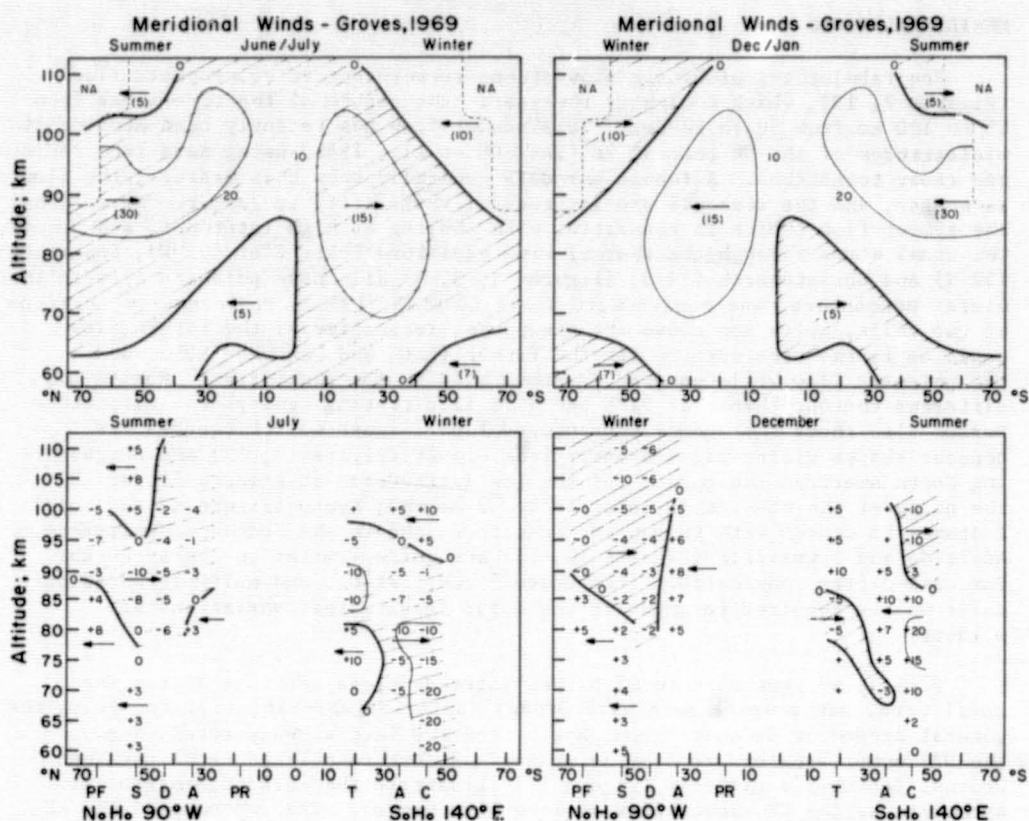
The tabulations of Groves show strong summer-centred equatorward flow (Figures 7, 13), which dominates the year: the centre of the core moves from 85 to 100 km from 50 to 20 deg. This summer flow has recently been studied at midlatitudes of the NH near 90 km (NASTROM et al., 1982) using data from radio and radar techniques. Although our data generally show this feature, the flow is weaker, and the seasonal and latitudinal variability is larger. As well as the summer flow (which is consistent with cooling at high latitudes, and hence the zonal winds through the thermal wind equation) Poker Flat (65°N), Saskatoon (52°N) and Christchurch (44°S) (Figures 2, 3, 6) also have poleward flow in the winter mesosphere, and equatorward above (GROVES, 1980). These may be portions of two cells, below and above the mesopause, respectively; the return flow could be in the stratosphere for the former (MEEK and MANSON, 1985), and the poleward flow would have to be above ~110 km for the latter. Notice the different contour shapes at 52°N and 44°S illustrating hemispheric differences. Durham also shows the summer equatorward flow (Figure 4) but overall its contour shapes differ significantly from Groves (Figures 7, 13) and neighbouring North American contours. For the low latitudes: at Atlanta (Figure 8) the phase of the changes is retarded by ~2 months; Kyoto (Figure 9) has more features in common with Durham and Saskatoon; and in the Southern Hemisphere, Adelaide and Townsville (Figures 10, 11) are quite similar to Christchurch. Our data differ considerably from Groves' compilation, and multiple meridional cells may be required to organize the data: longitudinal variations are evident.

Finally we show meridional height-latitude cross sections as for the zonal wind, but compare here with Groves' data (Figures 16, 17). For July, the general agreement is quite good, apart from the fact already noted, i.e., the NH summer equatorward flow is weaker and more restricted in height than Groves. December's patterns (Figure 17) illustrate the lack of hemispheric symmetry, as the SH summer flow is more like Groves. The contours of the NH winter flow are quite different from Groves, although overall there is poleward flow within thermosphere in both cross sections.

CONCLUSION

The radar zonal wind cross sections differ considerably from CIRA 1972, especially regarding winter variability and heights of reversals. There is good evidence that winds from 43-52 deg in the Northern Hemisphere vary quite significantly with latitude and longitude, being near CIRA'S 45-50 deg in some cases and CIRA's 35 deg in others, and that winds ~35°N may demonstrate mid-latitude (~35 CIRA 1972) or tropical characteristics (20 deg CIRA 1972). In the Southern Hemisphere 35 deg is similar to CIRA 1972 at 35 deg or even 45 deg and is more midlatitude in behaviour. The winds from near 20 deg show a mixture of midlatitude and tropical characteristics. The meridional cross sections evidence considerable seasonal and latitudinal variability, the main feature being a summer equatorward (~10 ms⁻¹) mesospheric flow. However, this does not dominate the year as in Groves' compilation. In other months at midlatitudes there is considerable poleward flow in the mesosphere. It is possible that the elimination of tidal components, which is crucial for these weak winds was not complete in the earlier data.

Overall, and based on other data from the various locations, the conclusions reached here about the zonal flows are probably valid. However, given the weakness of the meridional flow, the shapes of the contours for some of these cross sections are less certain -- given the probable importance of gravity wave momentum deposition for the zonal flow, this process will certainly also contribute to variability in the meridional flow. Nevertheless, the main differences from Groves' data are expected to remain.



REFERENCES

- Aso, T., and R. A. Vincent (1982), Some direct comparisons of mesospheric winds observed at Kyoto and Adelaide, *J. Atmos. Terr. Phys.*, **44**, 267.
- Balsley, B. B., and A. C. Riddle (1984), Monthly mean values of the mesospheric wind field over Poker Flat, Alaska, *J. Atmos. Sci.*, in press.
- Carter, D. A., and B. B. Balsley (1982), The summer wind field between 80 and 93 km observed by the MST radar at Poker Flat, Alaska (65°N), *J. Atmos. Sci.*, **39**, 2905.
- Clark, R. R. (1983), Upper atmosphere wind observations of winds and tides with the UNH meteor radar system at Durham 43°N (1977, 1978, and 1979), *J. Atmos. Terr. Phys.*, **45**, 621.
- Dolas, P. M., and R. G. Roper (1981), Prevailing wind in the meteor zone (80-100 km) over Atlanta and its association with midwinter stratospheric warming, *J. Atmos. Sci.*, **38**, 182.
- Elford, W. G. (1976), Prevailing winds in lower thermosphere, *Nature Lond.*, **261**, 123.
- Groves, G. V. (1969), Wind models from 60 to 130 km altitude for different months and latitudes, *J. Brit. Interplanet. Soc.*, **22**, 285.
- Groves, G. V. (1980), Seasonal and diurnal variations of middle atmosphere winds, *Phil Trans. R. Soc. Lond.*, **A296**, 19.

- Bolton, J. R. (1982), The role of gravity wave induced drag and diffusion in the momentum budget of the mesosphere, J. Atmos. Sci., **39**, 791.
- Lindzen, R. S. (1981), Turbulence and stress owing to gravity wave and tidal breakdown, J. Geophys. Res., **86**, 9707.
- Manson, A. H., C. E. Meek, and J. B. Gregory (1981a), Winds and waves (10 min - 30 days) in the mesosphere and lower thermosphere at Saskatoon (52°N, 107°W, L = 4.3) during the year, October 1979 to July 1980, J. Geophys. Res., **8**, 9615.
- Manson, A. H., C. E. Meek and J. B. Gregory (1981b), Long period oscillations in the mesospheric and lower thermospheric winds (60-110 km) at Saskatoon (52°N, 107°W, L = 4.3), J. Geomag. Geoelectr., **33**, 613.
- Manson, A. H., C. E. Meek, M. Massebeuf, J. L. Fellous, W. G. Elford, R. A. Vincent, R. L. Craig, R. G. Roper, S. Avery, B. B. Balsley, G. J. Fraser, M. J. Smith, R. R. Clark, S. Kato, T. Tsuda, and A. Ebel (1985), Mean winds of the upper middle atmosphere (69-110 km): a global model from radar systems (M.F., meteor, VHF). Rep. #4, Dynamics Group, Institute of Space and Atmospheric Studies, Univ. Saskatchewan, Saskatoon, Canada S7N 0W0.
- Manson, A. H., C. E. Meek, J. L. Fellous, and M. Massebeuf (1983), Wind oscillations (6 h - 6 d) in the upper middle atmosphere at Monpazier (France, 45°N, 1°E) and Saskatoon (Canada, 52°N, 107°W) in 1979-1980, Rep. #6, Dynamics Group, Institute of Space and Atmospheric Studies, Univ. Saskatchewan, Canada S7N 0W0.
- Massebeuf, M., R. Bernard, J. L. Fellous, and M. Glass (1979), The mean zonal circulation in the meteor zone above Carcay (France) and Kiruna (Sweden), J. Atmos. Terr. Phys., **41**, 647.
- Meek, C. E., and A. H. Manson (1984), Comparisons between Primrose Lake (54°N, 110°W) ROCOB winds (20-60 km) and Saskatoon (52°N, 107°W) MF radar winds (60-110 km): 1978-1983, Rep. #1, Dynamics Group, Institute of Space and Atmospheric Studies, Univ. Saskatchewan, Saskatoon, Canada, S7N 0W0.
- Meek, C. E., and A. H. Manson (1985), Combination of Primrose Lake (54°N, 110°W) ROCOB winds (20-60 km) and Saskatoon (52°N, 107°W) M.F. radar winds (60-110 km); 1978-1983, J. Atmos. Terr. Phys., **47**, 477-487.
- Nastrom, G. D., B. B. Balsley, and D. A. Carter (1982), Mean meridional winds in the mid and high latitude summer mesosphere, Geophys. Res. Lett., **9**, 139.
- Salby, M., and R. G. Roper (1980), Long-period oscillations in the meteor region, J. Atmos. Sci., **37**, 237.
- Smith, M. J. (1981), Upper atmosphere circulation and wave motion, Ph.D. Thesis, Univ. Canterbury, Christchurch, New Zealand.
- Vincent, R. A., and T. J. Stubbs (1979), A study of motions in the winter mesosphere using the partial reflection technique, Planet. Space Sci., **2**, 441.

Appendix to 3.2.1: Monthly mean tabulations, with standard deviations,
of the zonal and meridional winds discussed in Section
3.1.2

Saskatoon (52°N, 107°W) Mean Meridional Wind (m/s) 1979-1982

km	JAN	FEB	MAR	APR	MAY	JUN	JUL	AUG	SEP	OCT	NOV	DEC
111	-9	-4	-1	1	5	6	5	3	2	-2	-10	-2
108	-10	-6	-5	1	6	5	7	2	2	-3	-9	-4
105	-15	-11	-5	1	6	6	6	2	1	-5	-10	-7
102	-9	-6	-6	1	4	5	6	3	1	-4	-8	-9
99	-12	-6	-4	-1	2	2	6	3	2	-5	-7	-7
96	-9	-4	-3	-2	-1	-3	1	2	1	-3	-4	-5
93.5	-8	-3	-1	-1	-3	-6	-5	-1	2	-2	-2	-4
90.5	-4	-1	0	-1	-4	-9	-10	-2	2	-2	-1	-4
88	-2	1	2	-1	-2	-8	-8	-2	1	1	0	-3
85	1	3	3	-1	2	-3	-6	0	1	3	1	-1
82	4	6	6	0	4	0	1	3	3	6	2	3
79	8	8	7	2	2	2	1	1	1	9	1	3
76	6	9	10	3	2	1	0	1	1	9	-1	3
73	5	9	9	3	2	2	2	3	2	7	-4	3
70	3	7	7	3	3	3	3	4	3	6	-4	3
67	5	6	5	2	3	3	2	3	3	4	-5	4
64	4	5	3	3	3	2	2	3	3	3	-5	5
61	3	5	2	3	3	4	3	4	4	2	-6	5

N.B. -100 daily means per monthly mean (-200 values per daily mean above
80 km, -100 values below 80 km).

Saskatoon Meridional Standard Deviation (m/s)

km	JAN	FEB	MAR	APR	MAY	JUN	JUL	AUG	SEP	OCT	NOV	DEC
111	5	7	3	5	5	5	5	5	5	2	4	9
108	3	7	4	3	6	3	3	6	3	4	5	9
105	4	11	2	4	6	4	5	7	4	3	4	9
102	6	6	3	3	4	5	4	5	4	2	3	6
99	4	5	2	2	4	4	2	3	3	3	3	3
96	4	6	3	1	4	3	3	3	2	3	3	3
93.5	3	5	5	1	3	5	2	2	2	5	4	4
90.5	6	4	4	2	4	3	4	3	3	3	4	6
88	9	4	4	2	3	2	2	2	2	3	4	7
85	10	5	5	2	2	3	8	3	2	3	5	5
82	9	5	5	3	2	2	3	5	5	2	4	4
79	9	6	5	1	2	2	4	5	3	4	6	8
76	6	8	4	2	1	1	2	3	1	5	4	8
73	6	8	5	2	1	2	1	2	1	5	5	10
70	5	7	5	4	1	1	2	1	3	6	6	8
67	3	9	5	2	1	0	2	2	2	5	7	10
64	6	9	4	2	2	1	3	2	2	5	7	9
61	7	10	3	2	2	2	3	4	2	5	8	9

Saskatoon (52°N, 107°W) Mean Zonal Wind (m/s) 1979-1982

km	JAN	FEB	MAR	APR	MAY	JUN	JUL	AUG	SEP	OCT	NOV	DEC
111	-2	-6	-1	3	4	6	11	12	1	0	0	-3
108	0	-3	-1	1	5	10	13	17	0	1	0	-5
105	-1	4	-2	-1	5	13	14	17	-1	2	2	1
102	4	5	1	-1	4	13	15	17	2	2	5	5
99	7	7	2	-5	3	13	13	18	4	2	5	7
96	8	8	3	-8	-2	11	15	17	5	4	5	11
93.5	10	12	2	-11	-11	3	10	14	9	4	9	15
90.5	15	15	6	-9	-19	-6	1	11	11	7	14	18
88	20	19	11	-10	-27	-20	-20	-2	12	11	20	23
85	22	23	18	-7	-33	-39	-37	-19	9	17	25	25
82	26	27	21	-5	-34	-46	-51	-33	6	27	32	30
79	29	29	25	-3	-33	-49	-55	-37	3	32	35	31
76	26	29	26	-5	-31	-49	-58	-40	2	36	36	30
73	26	30	28	-2	-28	-44	-54	-38	2	38	37	38
70	28	31	29	-1	-26	-42	-51	-38	3	39	37	42
67	33	32	31	5	-22	-39	-48	-35	5	42	40	44
64	37	34	33	8	-19	-36	-45	-32	6	44	41	45
61	39	34	31	10	-15	-28	-35	-22	8	43	40	46

N.B. -100 daily means per monthly mean (-200 values per daily mean above 80 km, -100 values below 80 km).

Saskatoon Zonal Standard Deviation (m/s)

km	JAN	FEB	MAR	APR	MAY	JUN	JUL	AUG	SEP	OCT	NOV	DEC
111	3	9	5	4	7	6	5	6	4	4	7	6
108	4	5	4	4	7	4	5	5	3	3	5	8
105	5	12	7	6	8	5	10	8	4	7	7	6
102	6	7	6	7	8	6	8	6	3	4	4	5
99	5	7	7	5	8	6	8	9	3	4	4	5
96	6	6	7	5	10	7	5	7	3	4	4	6
93.5	6	7	6	5	13	10	4	7	5	4	4	6
90.5	8	7	5	6	13	8	4	3	4	5	4	2
88	9	6	8	6	11	6	7	6	4	5	4	3
85	8	7	13	5	6	8	7	8	5	9	6	6
82	11	8	15	4	5	7	6	8	7	11	6	9
79	12	9	15	4	5	5	4	8	9	12	6	12
76	10	14	9	6	4	5	4	3	4	7	7	12
73	10	15	12	7	3	2	4	3	2	6	8	6
70	9	17	12	10	3	2	3	3	2	6	9	10
67	9	19	15	7	3	3	4	3	3	6	11	11
64	10	20	16	8	4	3	4	4	4	7	11	13
61	10	20	15	9	5	5	3	4	3	6	10	10

Kyoto (35°N, 136°E) Mean Meridional Winds May 1983 - May 1984

km	JAN	FEB	MAR	APR	MAY	JUN	JUL	AUG	SEP	OCT	NOV	DEC
106	1	-1	1	/	/	14	/	/	-5	0	-5	-2
102	5	-2	-1	2	4	-2	-12	-8	6	-1	2	0
98	2	-3	-4	1	-3	-1	-4	4	-3	-3	-2	3
94	-4	-1	-3	-3	-5	-4	-2	-4	-1	-3	-1	1
90	-3	4	-1	-5	-4	-8	-6	-11	-6	-3	-1	-2
86	-3	-4	3	-4	-4	-6	-9	-11	-5	0	0	-1
82	-8	-1	-1	-1	-1	-3	-6	-8	3	1	3	-1

Mean Zonal Winds

km	JAN	FEB	MAR	APR	MAY	JUN	JUL	AUG	SEP	OCT	NOV	DEC
106	-1	-1	1	/	5	/	/	-6	-4	0	-2	-3
102	-3	-1	3	-5	3	4	14	9	0	2	-3	-3
98	2	3	2	-2	6	10	17	13	5	2	1	-1
94	5	1	-1	-3	8	11	19	19	4	1	1	1
90	7	2	2	-2	6	12	18	19	6	3	-1	0
86	7	4	0	3	2	5	14	12	6	1	2	3
82	7	2	0	-2	1	3	5	12	6	3	2	3

Atlanta (34°, 84°W) Mean Meridional Wind (m/s) 1974/5, 1976/7

km	JAN	FEB	MAR	APR	MAY	JUN	JUL	AUG	SEP	OCT	NOV	DEC
100	-2	3	1	-1	-6	-2	-4	-9	-3	2	1	5
96	5	6	3	-3	-2	0	0	0	-3	6	5	8
92	11	7	0	-2	4	0	-2	-10	-5	2	7	9
88	13	8	-1	0	8	0	0	-7	-5	-3	8	9
84	12	8	-3	1	8	-1	2	-2	-3	-2	8	8
80	4	8	-3	-2	2	-2	3	7	3	10	8	5

Mean Zonal Wind (m/s)

km	JAN	FEB	MAR	APR	MAY	JUN	JUL	AUG	SEP	OCT	NOV	DEC
100	13	34	18	26	16	13	14	24	8	8	-2	2
96	8	28	26	25	16	12	18	22	6	12	4	4
92	3	22	22	19	17	15	20	14	3	7	1	3
88	2	17	14	12	18	18	19	9	0	-1	-5	1
84	2	12	6	10	18	18	15	6	-3	-5	-5	-2
80	7	8	7	18	14	11	10	12	-5	2	4	-5

Atlanta Meridional Standard Deviation (m/s)

km	JAN	FEB	MAR	APR	MAY	JUN	JUL	AUG	SEP	OCT	NOV	DEC
100	11	8	19	12	10	6	4	8	7	4	19	13
96	11	11	15	10	5	10	5	9	6	8	12	15
92	12	8	10	9	5	8	6	10	2	10	9	13
88	13	5	6	8	11	4	6	13	4	11	9	11
84	12	7	9	10	13	9	6	13	6	15	8	10
80	7	8	10	14	7	11	4	8	5	23	10	11

Zonal Standard Deviation (m/s)

km	JAN	FEB	MAR	APR	MAY	JUN	JUL	AUG	SEP	OCT	NOV	DEC
100	30	19	12	24	14	14	15	14	8	6	30	18
96	20	19	10	28	12	14	13	14	5	13	27	15
92	15	18	6	28	10	11	10	16	6	12	20	13
88	15	17	4	25	12	8	7	16	10	9	17	19
84	15	17	5	23	11	9	6	16	11	8	20	16
80	16	13	7	23	7	9	7	14	11	10	25	13

Christchurch (44°S, 173°E) Mean Meridional Wind (m/s) June 1978 - Feb 1980

km	JAN	FEB	MAR	APR	MAY	JUN	JUL	AUG	SEP	OCT	NOV	DEC
102.5	-11	-13	11	19	2	7	14	10	10	-11	-12	-12
100	-9	-13	10	17	-1	1	11	6	5	-2	-11	-9
97.5	-3	-10	8	12	-1	-2	9	1	5	-3	-7	-5
95	-4	-8	4	5	-4	-7	3	1	4	-1	-3	-4
92.5	-1	-6	1	2	-9	-9	-1	-1	2	0	1	-3
90	-2	-6	-3	0	-6	-8	-3	-4	0	2	2	0
87.5	2	-7	-5	-3	-5	-8	-4	-6	-3	1	4	5
85	6	-9	-9	-4	-4	-6	-7	-7	-2	1	6	11
82.5	11	-7	-17	-7	-8	-8	-10	-8	-4	1	11	19
80	10	-3	-16	-16	-11	-10	-16	-6	-6	-4	5	20
77.5	4	2		-13	-13	-21	-18	-12	-8	-7	8	13
75	9	3		-13	-9	-18	-21	-9	-11	-6	1	11
72.5	9	4		-20	-13	-15	-20	-12	-13	-8	1	8
70	9	4		-15	-19	-7	-21	-11	-15	-8	-1	7
67.5	4	2		-14	-16	-6	-22	-11	-14	-9	0	4
65	6	3		-13	-13	2	-20	-14	-11	-9	0	7

N.B. 1000-2000 values >80 km; 200-400 values <80 km: sd ~7 m/s at 90 km, increasing to 10 m/s at 80 km.

Christchurch (44°S, 173°E) Mean Zonal Winds (m/s) June 1978 - Feb 1980

km	JAN	FEB	MAR	APR	MAY	JUN	JUL	AUG	SEP	OCT	NOV	DEC
102.5	32	21	-17	-8	-1	-3	-4	-6	-15	15	30	30
100	33	25	-5	-10	6	-5	-8	-7	-7	9	31	33
97.5	26	22	-7	-7	8	1	-6	-3	-6	8	20	23
95	18	18	2	-6	6	6	-4	-2	-5	2	3	18
92.5	15	15	2	-1	9	10	4	0	-4	-1	6	7
90	18	15	6	-1	6	10	3	4	-3	-6	4	10
87.5	12	20	8	4	9	11	6	9	3	-6	2	10
85	0	21	19	11	14	13	11	13	9	-10	-7	4
82.5	-23	13	26	20	21	20	17	20	20	-10	-14	-24
80	-37	1	28	33	33	23	29	26	33	-4	-18	-43
77.5	-56	-11		24	44	42	39	34	36	2	-28	-56
75	-68	-12		38	45	40	44	34	38	0	-23	-62
72.5	-71	-23		43	55	54	46	41	37	3	-25	-68
70	-70	-32		47	56	41	43	40	35	4	-26	-65
67.5	-63	-32		50	57	77	49	38	31	7	-26	-58
65	-46	-29		51	66	84	56	35	27	10	-21	-47

N.B. 1000-2000 values >80 km; 200-400 values <80 km: sd -7 m/s at 90 km, increasing to 10 m/s at 80 km.

Adelaide NS Mean 1978-1983 (35°S, 138°E)

HT	JAN	FEB	MAR	APR	MAY	JUN	JUL	AUG	SEP	OCT	NOV	DEC
100												
98	5	2	8	-13	-7	2	5	7	2	6	3	0
96	5	1	10	-8	-4	0	6	6	3	5	6	1
94	6	2	4	-7	-2	-2	-4	1	0	4	5	2
92	7	2	-1	-8	-3	-3	-6	1	-4	1	6	2
90	7	1	-8	0	-6	-5	-6	-3	-4	-2	6	4
88	8	-1	-11	-3	-9	-7	-5	-1	-4	-6	5	8
86	9	-3	-9	0	-11	-9	-4	-2	-6	-8	6	11
84	7	-6	-9	5	-12	-10	-7	-5	-7	-11	4	11
82	4	-8	-10	10	-8	-8	-12	-3	-2	-19	1	9
80	4	-9	-8	18	-9	-6	-10	-5	-7	-16	1	6
78	5	-5	-3	15	-3		-17	-9	-11	-19	2	6
76	1	-1	-5	8	-10		-1	-5	-12	-16	2	6
74	-2	0	-1	8	-8		1	-5	-12	-14	3	5
72	-3	2	-6	1	-6		-3	1	-13	-11	3	2
70	-2	-1	-6	-4	3		-2	2	-10	-6	-2	-2

Adelaide NS Standard Deviation 1978-1983

HT	JAN	FEB	MAR	APR	MAY	JUN	JUL	AUG	SEP	OCT	NOV	DEC
100												
98	8	6	1		4		1	2	9	4	4	10
96	6	6	8		5		5	2	10	6	3	12
94	5	4	4		3		2	7	5	8	5	10
92	7	5	3		4		2	5	4	6	7	9
90	6	5	1		0		9	3	4	5	9	6
88	2	4	2		4		3	1	6	5	9	6
86	2	6	6		6		4	4	5	5	12	4
84	6	4	8		8		4	5	7	7	9	2
82	9	3	6		13		8	9	5	4	8	3
80	7	5	1		20		6	12	10	3	5	1
78	8	1	0		20		3	9	10	8	2	2
76	3	7	8		14		16	5	10	7	3	5
74	5	14			16		12	8	9	3	5	6
72	2	13			14		10	3	11	5	4	5
70	2	8			8			5		5	4	0

Adelaide EW Mean 1978-1983 (35°S, 138°E)

HT	JAN	FEB	MAR	APR	MAY	JUN	JUL	AUG	SEP	OCT	NOV	DEC
100												
98	23	17	15	2	7	4	-6	1	-10	-11	23	34
96	25	17	18	1	9	4	0	6	-2	-11	21	32
94	24	17	11	0	14	2	1	9	0	-13	19	28
92	23	20	15	8	19	4	10	13	5	-15	11	24
90	20	20	17	17	22	5	13	13	7	-14	10	20
88	13	16	16	20	25	10	11	16	10	-10	3	13
86	7	14	17	26	30	16	14	21	11	-8	-1	7
84	-2	12	20	29	36	25	19	24	13	-9	-7	0
82	-13	2	16	35	43	35	30	29	13	-3	-14	-9
80	-24	-1	14	36	49	46	39	36	29	6	-21	-24
78	-35	-13	16	36	50		44	41	36	5	-31	-36
76	-40	-18	17	43	55		49	39	37	9	-38	-46
74	-45	-23	19	50	55		62	48	35	6	-37	-50
72	-48	-27	20	51	51		57	57	28	7	-34	-55
70	-53	-30	20	43	43		69	58	21	7	-30	-60

Adelaide EW Standard Deviation 1978-1983

HT	JAN	FEB	MAR	APR	MAY	JUN	JUL	AUG	SEP	OCT	NOV	DEC
100												
98	8	5	7		3		3	11	8	10	9	8
96	7	6	13		4		6	9	7	8	7	5
94	6	6	1		6		4	9	5	8	5	3
92	7	1	6		6		2	8	6	2	4	4
90	12	2	9		6		7	7	9	3	5	7
88	8	4	8		4		6	4	13	2	6	8
86	8	4	11		7		7	3	9	2	6	8
84	8	4	11		10		4	2	8	1	6	9
82	9	3	6		11		8	6	14	6	4	12
80	7	7	6		13		13	5	0	5	5	11
78	6	13	2		15		6	8	12	6	12	4
76	5	6	1		21		15	15	9	4	2	6
74	7	8			14		13	13	7	4	2	7
72	9	5			2		17	15	19	0	1	10
70	9	7			10			18		6	2	8

Townsville NS Mean 1978-1980 (20°S, 147°E)

HT	JAN	FEB	MAR	APR	MAY	JUN	JUL	AUG	SEP	OCT	NOV	DEC
100												
98	12		14		0	0	0	12	9	11	20	
96	13		9		-3	-8	-3	10	7	11	22	
94	13		5		-8	-15	-7	5	4	10	22	
92	12		2		-11	-17	-15	-15	2	6	17	
90	10		-3		-9	-14	-16	-16	-1	6	13	
88	7		-5		-6	-11	-15	-15	-1	2	6	
86	3		-5		-4	-3	-16	-16	-3	-3	-5	
84	-2		0		0	-10	-11	-11	-5	-8	-19	
82	-4		3		9	-9	-3	-3	-7	-9	-31	
80	-3		5		0	2	5	5	-8	-10	-31	
78	0		10		-4	1	15	15	-10	-6	-3	
76			11		-7	-2	12	12	-12	-10	5	
74			5		-6	-4	6	6	-9	-7	4	
72			-6		-1	-10	4	4	-7	-5	0	
70			4		2	-5	3	3	-6	12	-1	

Townsville EW Mean 1978-1980

HT	JAN	FEB	MAR	APR	MAY	JUN	JUL	AUG	SEP	OCT	NOV	DEC
100												
98	15		15		0	-5	-1	-4	-1	0	14	
96	15		10		7	1	0	-2	-2	-6	9	
94	15		0		10	6	5	0	-3	-12	7	
92	14		-5		16	12	6	2	-6	-15	8	
90	11		-9		20	17	10	5	-7	-16	3	
88	11		-12		27	22	17	8	-6	-15	0	
86	9		-14		32	29	23	11	-8	-12	-3	
84	2		-14		34	41	28	7	-7	-12	-2	
82	-4		-17		33	47	34	24	-18	-17	-5	
80	-11		-17		30	43	36	23	-18	-22	-21	
78	-5		-10		26	25	39	25	-15	-19	-32	
76			-1		31	24	36	29	-9	-14	-30	
74			5		31	23	28	27	-2	-12	-34	
72			8		37	26	25	23	3	-4	-38	
70			7		40	25	21	22	9	2	-37	

3.2.1 PLANETARY AND GRAVITY WAVES IN THE MESOSPHERE AND LOWER THERMOSPHERE

R. A. Vincent

Department of Physics, University of Adelaide
South Australia 5001

N86-12832

INTRODUCTION

Rocket and ground-based studies of the mesosphere and lower thermosphere show that waves play an important role in the dynamics of their region. The waves manifest themselves in wind, temperature, density, pressure, ionization and airglow fluctuations in the 80-120 km height range. Rockets have enabled the density and temperature structure to be measured with excellent height resolution, while long-term studies of wind motions using MST, partial reflection and meteor radars and, more recently, lidar investigations of temperature and density, have enabled the temporal behaviour of the waves to be better understood.

Figure 1 shows a composite of power spectra of wind motions measured near the mesopause at widely separated locations and illustrates how wave energy is distributed as a function of frequency. The spectra show three distinct parts, viz. (i) a long period section corresponding to periods longer than 24 h, (ii) a section between 12 and 24 h period where the spectra are dominated by narrow peaks associated with the semidiurnal and diurnal tides (see FORBES, this volume) and (iii) a section at periods less than 12 h where the spectral density decreases monotonically (except for the 8 h tidal peak). The long period section is associated with transient planetary scale waves while the short period motions are caused by gravity waves.

PLANETARY WAVES

The narrow spectral peak located near 48 h in the Adelaide data in Figure 1 is a manifestation of the quasi-two-day wave. This is one of a series of travelling global scale waves which have been discovered by long-term wind measurements made by ground-based radars. Spectral analyses of long data sets suggest that the wave energy tends to maximize in local summer (SMITH, 1981; MANSON et al., 1982; VINCENT, 1984b). A range of wave periods has been identified but the most commonly reported periods fall into three well-defined intervals which are 10-20 days, 4 to 7 days and 1.9 to 2.2 days. These are often referred to as the "16-day", "5-day" and "2-day" oscillations, respectively, although precise determination of the periods involved is often not possible. Comparative studies made at different longitudes suggest the waves are westward travelling with the best determinations of wave number being made for the 2- and 5-day waves. The inadequate length of many data sets have necessarily restricted studies of the "16-day" wave, although as continuous radar observations become available, this situation will improve. Table 1 summarizes some of the features of those waves which have been extensively reported, but it should be noted that waves of other periods (e.g., 1.6 to 1.7 days) have been found (CEVOLANI et al., 1983; SALBY and ROPER, 1980).

It is usually assumed that these oscillations are caused by Rossby gravity normal modes forced in the lower atmosphere. These modes are evanescent in the vertical except that in certain height ranges with westward winds (easterlies) and equatorward temperature gradients the waves can be locally propagating. SALBY (1984) has recently reviewed the characteristics of normal modes.

Each mode has a well-defined structure with respect to latitude and longitude, but in practice it has not always been possible to make a positive

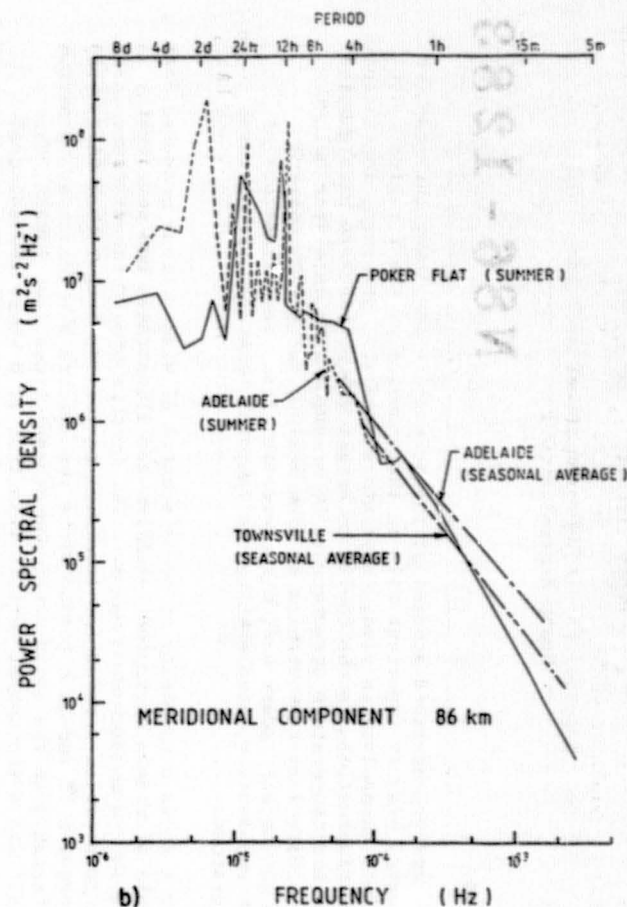
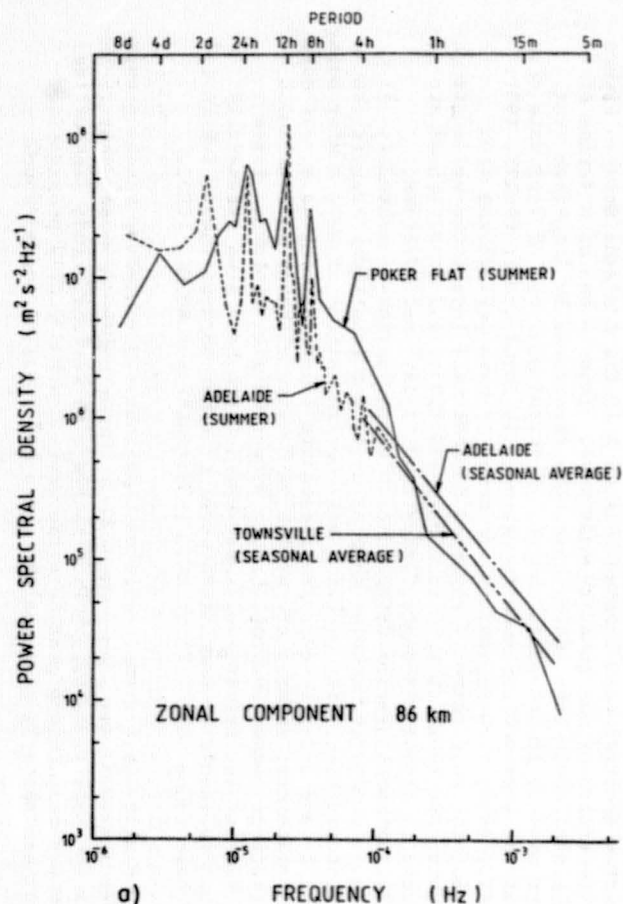


Figure 1. Power spectra of the meridional and zonal wind components observed at Poker Flat (65°S , 138°E) and Townsville (19°S , 147°E). The Poker Flat data is after CARTER and BALSLEY (1982).

Table 1. Characteristics of transient planetary waves

Period(days)	Amplitude(ms ⁻¹)	Vertical wavelength(km)	Zonal wave number
10-20	5-10	> 100	1(?)
4-7	5-30	25 to > 100	1
1.9-2.2	10-50	50 to > 100	3

identification from observations in the 80-120 km region because of inadequate geographic coverage. However, an association between 5-day wind oscillations in the mesosphere and a westward travelling wave number one wave in the stratosphere has been found (HIROTA et al., 1983). Satellite radiance studies show evidence for both 5-day and 2-day waves with temperature amplitudes tending to maximize in the lower mesosphere (RODGERS, 1976; RODGERS and PRATA, 1981) with values of about 0.5-0.8 K.

The most extensively studied oscillation is the "2-day" wave and the seasonal and spatial behaviour is now well established. The wave is usually observed in the summer hemisphere reaching maximum amplitudes at about 900 km in July/August in the Northern Hemisphere (MULLER and NELSON, 1978; RODGERS and PRATA, 1981) and in January in the Southern Hemisphere (CRAIG and ELFORD, 1981). Both radar wind measurements and satellite observations show that the wave amplitudes are maximum in the Southern Hemisphere (VINCENT, 1984b; RODGERS and PRATA, 1981). This is illustrated in Figure 2 which shows the mean meridional and zonal wind amplitudes plotted as a function of latitude; it is evident that the maximum response is in the meridional component at southern low-to-mid-latitudes. A hemispheric difference in wave period has also been noted (VINCENT, 1984b) with Northern Hemisphere observations giving periods near 51 h (MULLER and NELSON, 1978; CRAIG et al., 1983) while periods nearer 48 h are reported for the Southern Hemisphere (CRAIG and ELFORD, 1981; CRAIG et al., 1980).

Evidence for travelling planetary waves has also been found in radio soundings of the ionosphere and these often show clear correlations with wave activity in the stratosphere. This is clear evidence for the coupling of wave energy between the stratosphere and ionosphere (BROWN and WILLIAMS, 1971; CAVALIERI et al., 1974; FRASER, 1977). Eastward, as well as westward, travelling waves have been observed.

GRAVITY WAVES

Wave Amplitudes. Figure 1 shows that at a given location, the gravity wave amplitudes are the same for both the zonal (u') and meridional (v') wind components which show that the perturbation wave amplitudes are on the average isotropic. The spectra show that the energy density (proportional to $\overline{v'^2} = \overline{u'^2} + \overline{v'^2}$) follows a power relationship f^{-k} as a function of frequency, f . The exponent k , lies in the range 1.5 to 2.0 (CARTER and BALSLEY, 1982; VINCENT, 1984a) but may change with latitude and season (FREZAL et al., 1981). Averaged over the period range between 12 h and the Vaisala-Brunt period (about 5 min) the rms amplitudes are about 15-20 ms⁻¹ in each component (VINCENT, 1984a) although if the spectrum is assumed to extend out to the inertial frequency (the theoretical lowest frequency for gravity waves) then the rms amplitudes are about 25 ms⁻¹.

Vertical velocity motions are not as easy to measure as the horizontal components. However, measurements made over a range of latitudes with

QUASI 2-DAY WAVE AMPLITUDE / ms^{-1}
IN LOCAL SUMMER AT 95 km

56°N Obninsk	43°N Durham	19°S Townsville
53°N Sheffield (Sh)	34°N Atlanta (A)	35°S Adelaide
52°N Saskatoon (Sa)	34°N Kyoto (K)	43°S Christchurch
47°N Garchy	2°N Megadishu	67°S Molodezhnaya
45°N Budrio		

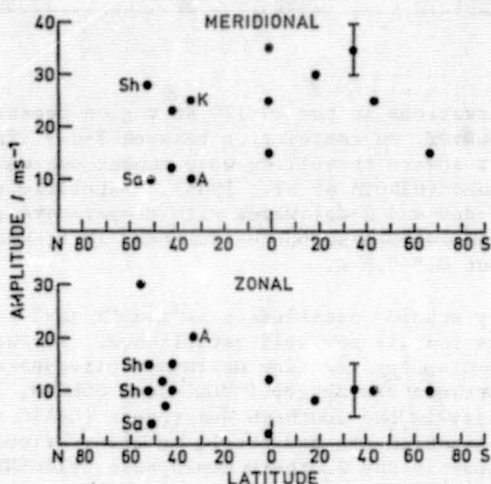


Figure 2. Amplitudes of 2-wave as a function latitude, after VINCENT (1984b).

vertically pointing narrow beam radars give rms amplitudes of the order $1\text{--}2 \text{ ms}^{-1}$ (VINCENT, 1984b; FREZAL et al., 1981; WOODMAN and GUILLEN, 1974). Vertical oscillations near the buoyancy frequency are particularly evident (period $\sim 5\text{--}15$ min).

Temperature and density fluctuations induced by gravity waves have been extensively studied by rockets (THEON et al., 1967; PHILBRICK et al., 1985; PHILBRICK, 1981) and recently by lidars (CHANIN and HAUCHECORNE, 1981). Figure 3 shows vertical profiles of temperature and density. Amplitudes are of the order of 0.5 to 0.1 in fractional density, and these values are consistent with those inferred from the gravity wave motions (VINCENT, 1984a). The figure indicates the very wide range of temperature variations which can be observed at high latitudes with the greatest wave activity occurring in winter (HEATH et al.). Amplitudes as large as 30 K are reached. At midlatitudes the temperature fluctuations are about 10 K.

Seasonal and geographical variations in wave activity are not well known in the 80–120 km height region. What observations are available indicate an annual variation at high latitudes (Figure 3), with maximum amplitudes occurring in winter, and a smaller variation at mid-to-low latitudes with a semiannual variation occurring in the tropics (VINCENT, 1984b; MANSON et al., 1981; FREZAL et al., 1981; THEON et al., 1967; BALSLEY et al., 1983). These observations are in general accord with studies of wave activity in the stratosphere (HIROTA, 1984).

It is emphasized that the amplitudes quoted above are long-term averages. On a time scale of a few hours or so there can be quite significant changes in

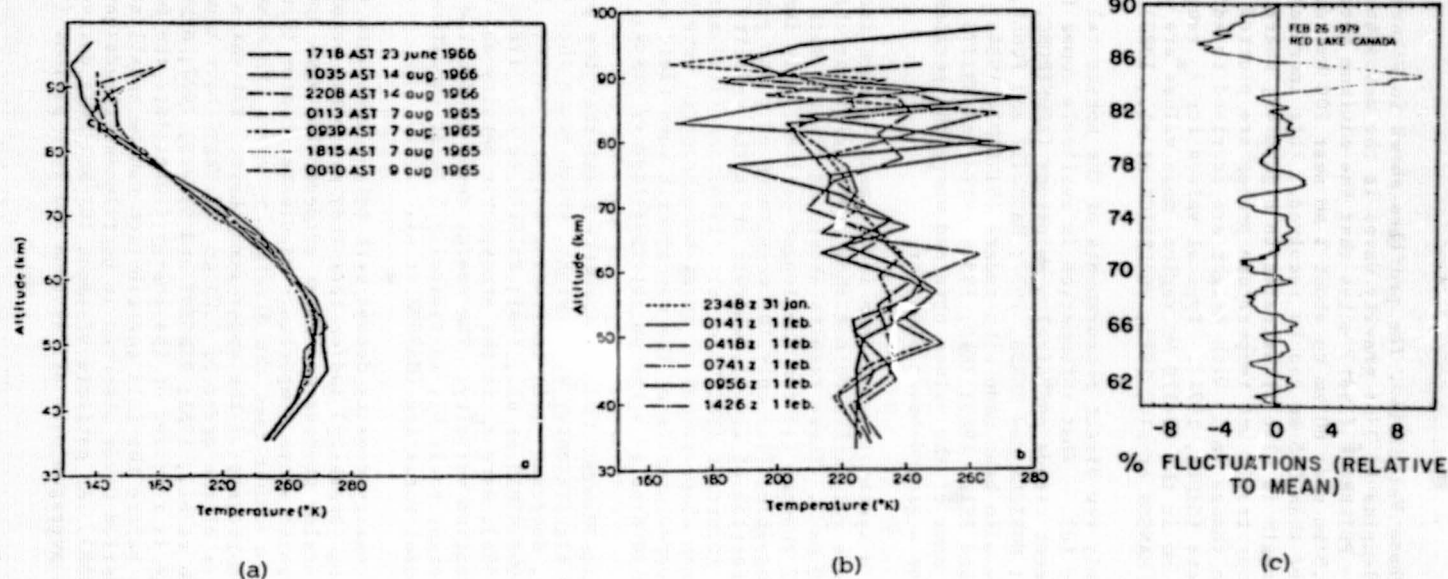


Figure 3. Rocket measurements of temperature in summer (a) and winter (b) at Barrow, Alaska (71°N), after HEATH et al., (c) Vertical profile of neutral density fluctuations (PHILBRICK, 1981).

wave amplitude in the mesosphere (PHILBRICK et al., 1983; VINCENT and REID, 1983).

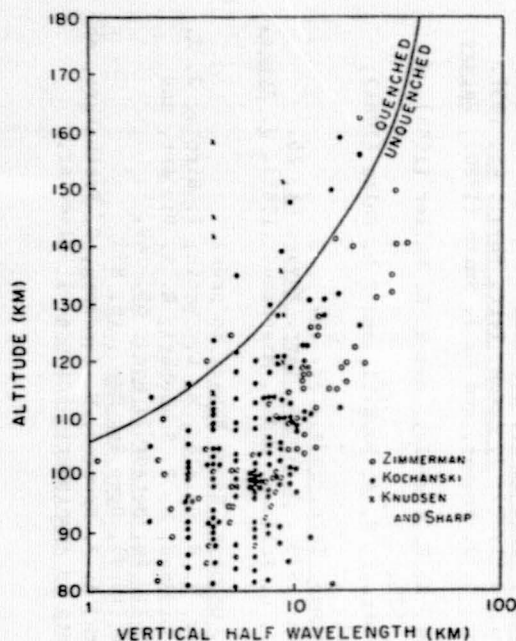
Wavelengths and Phase Velocities. The profiles shown in Figure 3 indicate that the vertical wavelengths (λ_z) of gravity waves in the mesosphere are greater than a few km. PHILBRICK (1981) notes that the minimum vertical scale increases from about 1.5 km near 60 km to about 3 km near 100 km despite the fact that scales smaller than 0.5 km can be resolved. This increase in the minimum vertical wavelength is also illustrated in Figure 4a, where values scaled from rocket vapour trails and temperature probes are plotted as a function of height; the change in λ_z with height are ascribed to eddy and molecular damping effects (HINES, 1974). Typical values for λ_z range from about 3 km to about 40 km in the 80-120 km region; mean values $\bar{\lambda}_z$ are about 10 to 12 km (VINCENT, 1984a; MANSON et al., 1982; PHILBRICK et al., 1983).

There are relatively few direct measurements of the horizontal wavelength (λ_h) and phase velocity (c). What information is available comes from photographs of noctilucent clouds and airglow emissions (ARMSTRONG, 1982; FREUND and JACKA, 1979; MOREELS and HERSE, 1977; HAURWITZ and FOGLE, 1969). Indirect estimates have also been made with radars (VINCENT, 1984a; COUNTRYMAN et al., 1981; VINCENT and REID, 1983; REID, 1984; SMITH and FRITTS, 1983). Figures 4a and 4b show some of the values obtained where the periods and phase velocities are given for a ground-based observer.

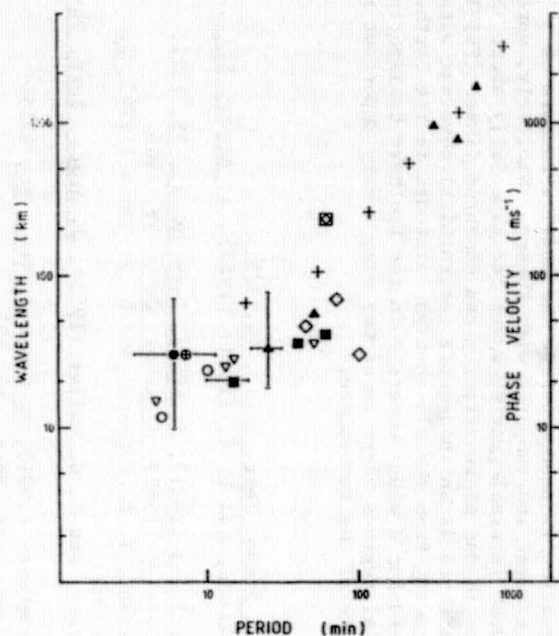
There seems to be a systematic increase in the mean λ_h with increasing period, whereas the phase velocities do not show any significant change but lie within the range 10-100 ms^{-1} . These results should be treated with some caution for a number of reasons (i) for the longer periods, only indirect estimates are so far possible, (ii) only the magnitudes of c are plotted, irrespective of the direction of travel, whereas it is the velocity relative to the mean flow which is important (FRITTS et al., 1984) and (iii) most values of λ_h and c are derived from observations of quasi-monochromatic wave motions, but these may not be representative of the mesospheric wave field as a whole which often appears to consist of a random superposition of waves.

Energy and Momentum Fluxes. It is frequently found that the gravity waves amplitudes do not grow significantly with height, which means that the wave energy, given by $\rho_0 \bar{v}^2$, decreases with increasing height (VINCENT, 1984a; MANSON et al., 1981; COUNTRYMAN et al., 1981; BALSLEY et al., 1983; VINCENT and STUBBS, 1977; HINES, 1965). Here ρ_0 is the atmospheric density and \bar{v}^2 is the mean square perturbation velocity. The energy decay is for the form $\exp(-z/h_0)$ where the height scale h_0 is typically 5 to 12 km although there may be some seasonal variation (MANSON et al., 1981).

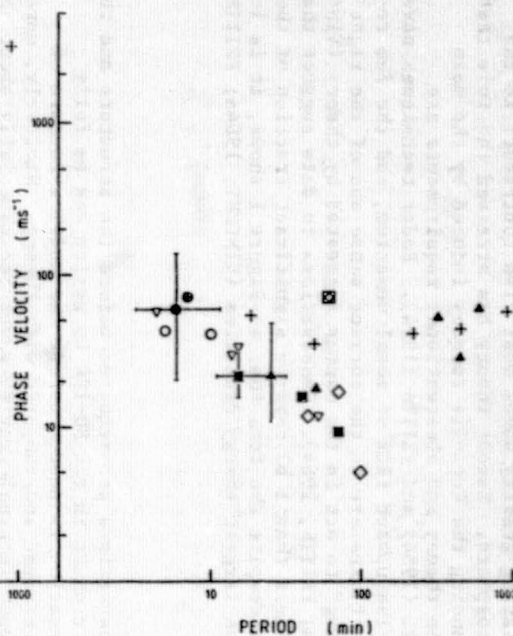
The fact that the energy density decays with height indicates either that the waves are saturating (breaking) and/or that they are being externally damped by eddy and molecular processes. Clear evidence for wave breaking may be seen in Figure 3b, which shows temperature gradients greater than the adiabatic lapse rate. In either case the dissipating waves are contributing to the energy and momentum budgets of the upper atmosphere. Estimates of the energy dissipation rates of the order of 0.01 to 0.2 W kg^{-1} have been given (VINCENT, 1984a; MANSON et al., 1981; VINCENT and STUBBS, 1977; HINES, 1965). However, more knowledge is required of the energy fluxes into the mesosphere and lower thermosphere before the full contribution can be established. An analysis of 50-60 km period waves observed in noctilucent clouds gave fluxes $\sim 7 \cdot 10^{-4} \text{ W m}^{-2}$ (HINES, 1968). An estimate of about 10^{-2} W m^{-2} was derived for radar measurements averaged over all seasons and wave periods (VINCENT, 1984b).



(a)



(b)



(c)

Figure 4. (a) Vertical wavelengths observed in small scale wind structure, the curve shows the theoretical minimum λ_z (after HINES, 1974). (b) Plot of gravity wave horizontal wavelength and phase velocity. (c) As a function of period. Key: \circ (FREUND and JACKA, 1979); ∇ (HAURWITZ and FOGLE, 1969); \diamond (MOREELS and HERSE, 1977); $+$ VINCENT (1984a); \blacksquare (REID, 1984); \bullet (VINCENT, 1972); \blacktriangle SMITH and FRITTS, 1983); \oplus (COUNTRYMAN et al., 1981); \boxtimes (ARMSTRONG, 1982).

ORIGINAL PAGE IS
OF POOR QUALITY

Dissipating and saturating gravity waves must also contribute to the momentum budget of the mesosphere. Recent theory has stressed the role that gravity waves play in balancing the Coriolis torques induced by the mean meridional circulation; the theory and observational requirements are summarized by FRITTS et al. (1984) and FRITTS (1984). Radar techniques have been developed to measure the upward flux of zonal momentum, and the few results to date suggest that fluxes are in the correct sense and of the right magnitude for the wave "drag" to act in the manner suggested by theory (VINCENT and REID, 1983; REID, 1984; FRITTS, 1984). Observations to date suggest that quite short period waves (less than 1 h) carry a significant fraction of the energy and momentum fluxes despite the fact that as Figure 1 shows, it is long period waves which have the largest energy densities (VINCENT, 1984a; FRITTS, 1984).

DISCUSSION

Considerably more observations are required before the structure and the roles played by atmospheric waves in the 80-100 km region can be fully elucidated. Further information is needed before the model structure of planetary waves can be determined and compared with theory. Similarly, more information is required about internal gravity waves and especially about the zonal components of wavelength and phase velocity and momentum fluxes (FRITTS et al., 1984). At present there is an inadequate geographical coverage with many of the observations coming from the mid-to-high latitudes in the Northern Hemisphere. There is a need for a wider coverage in the Southern Hemisphere and especially in equatorial regions where waves may play a very important role in determining the mean state of the atmosphere.

REFERENCES

- Armstrong, E. B. (1982), J. Atmos. Terr. Phys., **44**, 325.
 Balsley, B. B., W. L. Ecklund, and D. C. Fritts (1983), J. Atmos. Sci., **40**, 2451.
 Brown, G. M., and D. C. Williams (1971), J. Atmos. Terr. Phys., **33**, 1321.
 Carter, D. A., and B. B. Balsley (1982), J. Atmos. Sci., **39**, 2905.
 Cavalieri, D. J., R. J. Deland, T. A. Potemra, and R. F. Gavin (1974), J. Atmos. Terr. Phys., **36**, 561.
 Cevolani, G., S. P. Kingsley, and H. G. Muller (1983), J. Atmos. Terr. Phys., **45**, 275.
 Chanin, M. L., and A. Hauchecorne (1981), J. Geophys. Res., **86**, 9715.
 Clark, R. R. (1983), J. Atmos. Terr. Phys., **45**, 621.
 Craig, R. L., and W. G. Elford (1981), J. Atmos. Terr. Phys., **43**, 1051.
 Craig, R. L., R. A. Vincent, G. J. Fraser, and M. J. Smith (1980), Nature, **287**, 339.
 Craig, R. L., R. A. Vincent, S. P. Kingsley, and H. G. Muller (1983), J. Atmos. Terr. Phys., **45**, 529.
 Countryman, I. D., P. K. Rastogi, S. A. Bowhill, and P. M. Dolas (1981), Handbook for MAP, **2**, 301.
 Fraser, G. J. (1977), J. Atmos. Terr. Phys., **39**, 12.
 Freund, J. T., and F. Jacka (1979), J. Atmos. Terr. Phys., **41**, 25.
 Frezal, M. E., M. Glass, J. L. Fellous, and M. Massebeuf (1981), J. Atmos. Terr. Phys., **43**, 543.
 Fritts, D. C. (1984), Rev. Geophys. Space Phys., in press.
 Fritts, D. C., M. A. Geller, B. B. Balsley, M. L. Chanin, I. Hirota, J. R. Holton, S. Kato, R. S. Lindzen, M. R. Schoeberl, R. A. Vincent, and R. F. Woodman (1984), Bull. Am. Meteorol. Soc., **65**, 149.
 Haurwitz, B., and B. Fogle (1969), Deep Sea Res., **16**, 85.
 Heath, D. F., E. Hilsenrath, A. J. Krueger, W. Nordberg, C. Prabhakara, and J. S. Theon, Developments in Atmospheric Science, **1**, Elsevier, Amsterdam.

- Hines, C. O. (1965), J. Geophys. Res., **70**, 177.
- Hines, C. O. (1968), J. Atmos. Sci., **25**, 937.
- Hines, C. O. (1974), The Upper Atmosphere in Motion, 433, Am. Geophys. Union, Washington, D. C.
- Hirota, I. (1984), Dynamics of the Middle Atmosphere, 65, D. Reidel, Tokyo.
- Hirota, I., Y. Mackawa, S. Fukao, K. Fukuyama, M. P. Saltzer, J. L. Fellous, T. Tsuda, and S. Kato (1983), J. Geophys. Res., **88**, 6835.
- Manson, A. H., C. E. Meek, and J. B. Gregory (1981), J. Geophys. Res., **86**, 9615.
- Manson, A. H., C. E. Meek, J. B. Gregory, and D. K. Chakrabarty (1982), Planet. Space Sci., **30**, 1283.
- Massebeuf, M., R. Bernard, S. L. Fellous, and M. Glass (1981), J. Atmos. Terr. Phys., **43**, 535.
- Moreels, G., and H. Herse (1977), Planet. Space Sci., **25**, 265.
- Muller, H. G., and L. Nelson (1978), J. Atmos. Terr. Phys., **40**, 761.
- Philbrick, C. R. (1981), Handbook for MAP, **2**, 333.
- Philbrick, C. R., K. U. Grossman, R. Hennig, G. Lange, D. Krankowsky, D. Offermann, F. J. Schmidlin, and U. von Zahn (1983), Adv. Space Res., **2**, 121.
- Reid, I. M. (1984), Radar Studies of Atmospheric Gravity Waves, Ph.D. Thesis, University of Adelaide, Australia.
- Rodgers, C. D. (1976), J. Atmos. Sci., **33**, 710.
- Rodgers, C. D., and A. J. Prata (1981), J. Geophys. Res., **86**, 9661.
- Salby, M. L. (1984), Rev. Geophys. Space Phys., **22**, 209.
- Salby, M. L., and R. G. Roper (1980), J. Atmos. Sci., **38**, 1827.
- Smith, M. I. (1981), Upper Atmospheric Circulation and Wave Motion, Ph.D. Thesis, University of Canterbury, NZ.
- Smith, S. A., and D. C. Fritts (1983), Proc. 21st Conf. Radar Meteorology, Edmonton, Canada, 104.
- Theon, J. S., I. N. Nordberg, C. B. Katchen, and J. J. Horvath (1967), J. Atmos. Sci., **24**, 428.
- Vincent, R. A. (1972), J. Atmos. Terr. Phys., **34**, 1881.
- Vincent, R. A. (1984a), J. Atmos. Terr. Phys., **46**, 119.
- Vincent, R. A. (1984b), J. Atmos. Terr. Phys., in press.
- Vincent, R. A., and I. M. Reid (1983), J. Atmos. Sci., **40**, 1321.
- Vincent, R. A., and T. J. Stubbs (1977), Planet. Space Sci., **25**, 441.
- Woodman, R. F., and A. Guillen (1974), J. Atmos. Sci., **3**, 493.

3.2.2 ATMOSPHERIC TIDES BETWEEN 80 km AND 120 km

Jeffrey M. Forbes

Department of Electrical, Computer, and Systems Engineering
Boston University
Boston, MA 02167

ABSTRACT

The structure and variability of tides in the 80-120 km height region are reviewed. Particularly emphasized are seasonal-latitudinal variations in the vertical structure of diurnal and semidiurnal winds between 70-110 km as measured by meteor and partial reflection drift radars, and tidal temperatures determined by incoherent scatter radars between 100 and 140 km. Variations in tidal structures with longitude, from day to day, and during equinoctial transition periods are also addressed. A brief summary of the current status of atmospheric tidal modelling is provided.

INTRODUCTION

There are two classifications into which this chapter categorizes tidal observations. The first involves measurements which characterize "average" tidal structures over the period of a month or more, while the second pertains to measurements which delineate variations or deviations from "average" structures over periods from a few days to a month. The data are further subdivided according to the ease with which a particular experimental method determines a specific meteorological variable; that is, winds between roughly 80 km and 100 km in the case of meteor and partial reflection drift radars, and temperatures between 100 and 140 km by incoherent scatter radars. The present review explicitly includes only the more recent observational results and analyses; earlier works may be found in the references cited herein.

AVERAGE TIDAL STRUCTURES

Winds Between 70 km and 110 km. The near-continuous wind data covering the 70-110 km height range over Saskatoon, Canada (52°N, 107°W) (MANSON et al., 1981a) are ideal for examining month-to-month and seasonal variations of tides. (Similar studies for previous years at Saskatoon appear in STENING et al., 1978; MANSON et al., 1979, 1984b) Semidiurnal and diurnal tidal winds from winter/summer of 1979/1980 are illustrated in Figure 1. The December-February semidiurnal profiles consistently exhibit a vertical wavelength of order 50 km, with the westerly and northerly velocities in near quadrature. Amplitudes increase from about 10 msec⁻¹ at 70 km to 35 msec⁻¹ at 110 km. During spring equinox there is a transition to typical summer behavior, characterized by velocities of order 5-20 msec⁻¹ and a longer vertical wavelength (>80 km). The diurnal tide exhibits similar features; namely, a near evanescent behavior between April and October and distinctively shorter vertical wavelengths (~60 km) during the winter months. Amplitudes generally range from 10 to 20 msec⁻¹ from 70 to 110 km, except during January and February when amplitudes attain values of 30 msec⁻¹ at upper levels. The diurnal tide exhibits more variability, however, as indicated (on Figure 1) by the fewer number of days for which a reliable diurnal harmonic was able to be extracted from the fit.

The above seasonal characteristics are generally well established at midlatitude stations. Based on seasonal behaviors reported at Garchy (47°N, 3°E), Urbana (40°N, 88°W), Adelaide (35°S, 139°E), and Atlanta (34°N, 84°W), AHMED and ROPER (1983) find the following picture of the seasonal-latitudinal structure of semidiurnal tides in the meteor wind region: in summer, presence

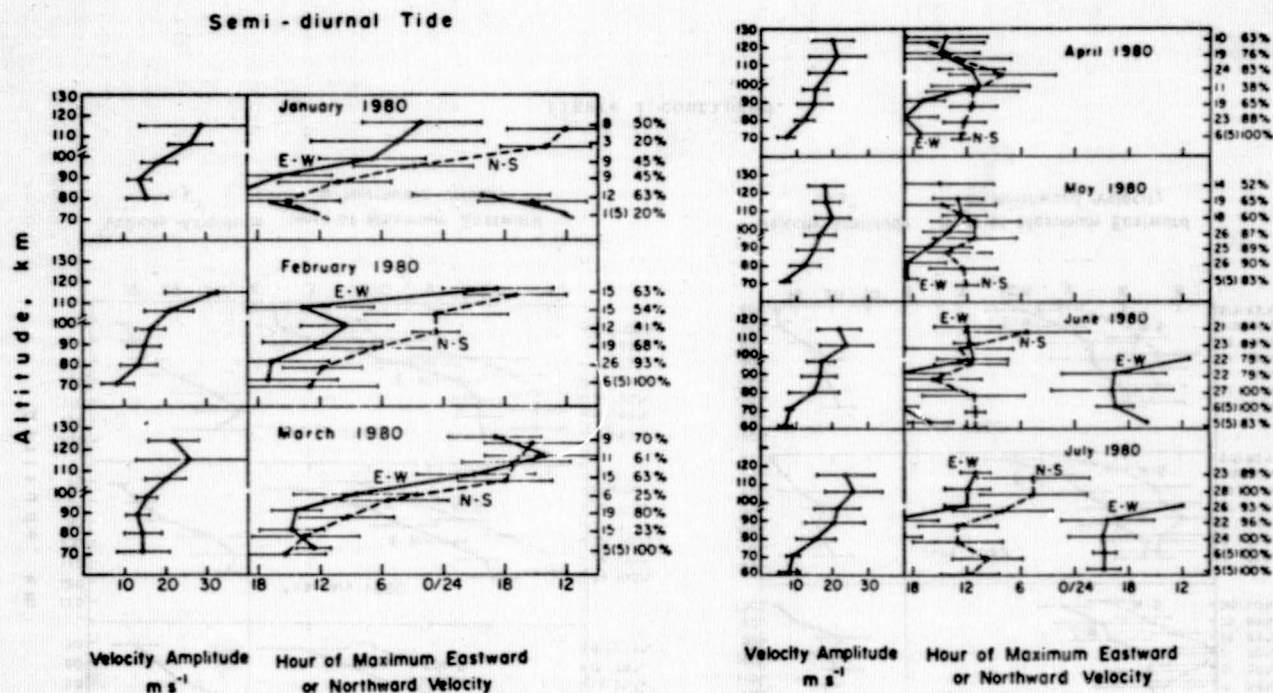


Figure 1. Means and standard deviations of semidiurnal and diurnal tidal winds observed at Saskatoon during 1979-1980.

ORIGINAL PAGE IS
OF POOR QUALITY

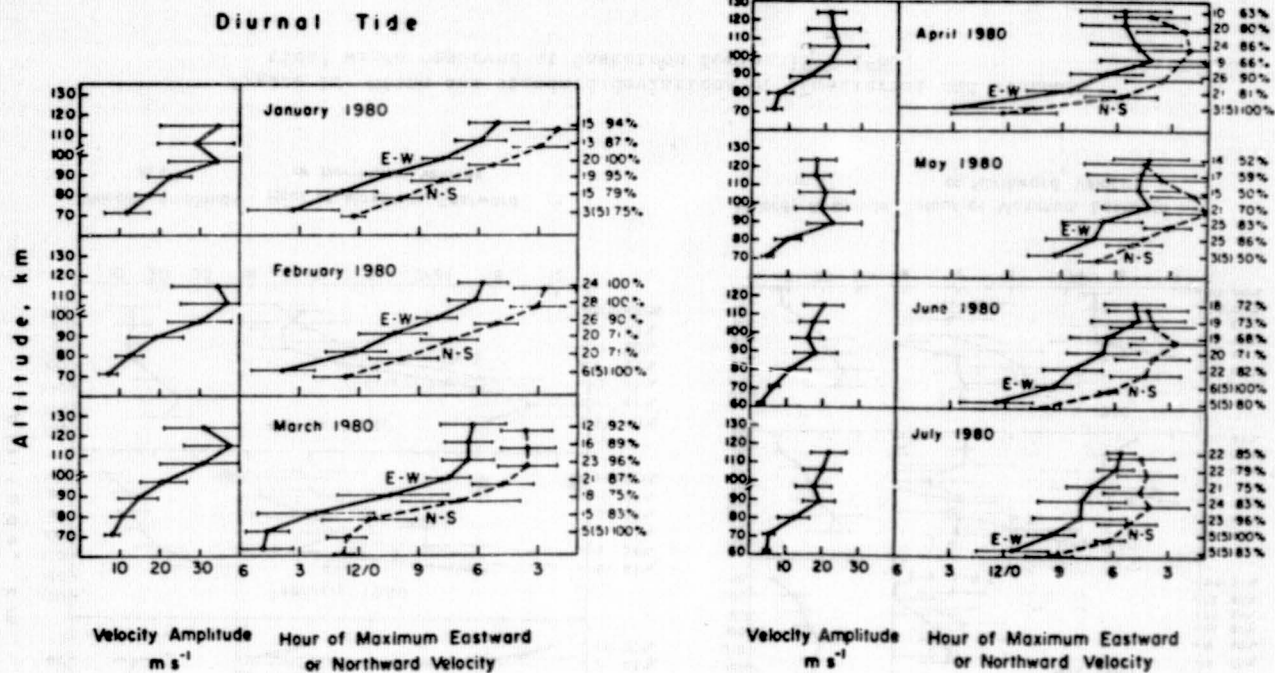


Figure 1 continued.

of long-wavelength ($\lambda \geq 120$ km) structures suggest predominance of the (2,2) and perhaps (2,3) modes. This behavior extends through autumn at all stations, except at Urbana where the observed wavelength is of order 42 km (ENGE and AVERY, 1979). In a recent study of the summer wind field at Poker Flat, Alaska (65°N), CARTER and BALSLEY (1982) find semidiurnal vertical wavelengths of roughly 30 km. This is not necessarily inconsistent with the observed long vertical wavelengths at lower latitudes as indicated by the theoretical models discussed later in this paper. During winter, shorter vertical wavelengths generally prevail: Poker Flat (~15 km), Saskatoon (~60 km), Garchy (~35 km), Urbana (~74 km), Atlanta (~63 km), suggesting presence of the (2,4) and (2,5) modes. It is curious that while the meridional component measured at Atlanta is characterized by $\lambda_z \sim 63$ km, λ is of order 120 km in the zonal component. The difficulty of ascribing a single mode to observations at a given station is clearly an issue. AHMED and ROPER (1983) further note that evidence exists for even shorter wavelengths during spring: Atlanta (~34 km), and Urbana (~54 km). Irregular phase structures are observed at Garchy during spring. The shift from typically short (~30-60 km) winter/spring wavelengths to long (≥ 100 km) summertime wavelengths appears to occur over a rather short (~2 weeks) spring transition period. The general shift from long wavelength behavior in summer to shorter characteristic wavelengths during winter is also substantiated by a more recent study (TSUDA et al., 1983) of data at the Kyoto, Japan (35°N, 136°E) meteor radar. Early seasonal studies covering several years of meteor wind data include those by MULLER (1966) for three stations in Great Britain and ELFORD (1973) at Adelaide, South Australia. AHMED and ROPER (1983) find it difficult to specify a characteristic seasonal-latitudinal behavior for the diurnal tide. Generally, the diurnal tide is evanescent at high latitudes (Poker Flat, Saskatoon) and propagating with short vertical wavelengths (≤ 30 km) at low latitudes (Arecibo, Townsville, Jicamarca). At midlatitudes (Garchy, Urbana, Atlanta, Adelaide) a variety of vertical structures can occur depending on phase interference between the evanescent and propagating components (FORBES, 1982a), making it difficult to define a "typical" structure.

Geographically symmetric radars at Kyoto (36°N) and Adelaide (36°S) delineate strongly asymmetric tidal behavior about the equator in both diurnal and semidiurnal components between 80 and 100 km altitude (ASO et al., 1979). Height profiles for the average tidal amplitudes and phases observed at Kyoto, Adelaide, as well as Townsville (19°S) for the period 14-29 March 1979, are illustrated in Figure 2. (Structures are also given on a day-by-day basis by these authors, illustrating strikingly similar characteristics to the mean values in Figure 2.) The diurnal amplitudes at Adelaide and Townsville are twice as large (~20-35 msec⁻¹) as at Kyoto, and clearly reflect a peak in the amplitude profile near 95 km and downward phase progression with height ($\lambda_z \sim 35$ km), whereas the Kyoto structures are much more evanescent in nature. Further, the westerly and northerly velocities are in quadrature at Adelaide, but in antiphase at Kyoto. Theoretically one might anticipate that the observed differences could be accounted for by:

1. Asymmetric forcing due to insolation absorption by O₃ or H₂O, either in the migrating trapped and propagating components, or possibly in non-migrating modes; or
2. Latitudinal "distortion" of the (1,1) mode due to asymmetries in background zonal winds (LINDZEN, 1972).

The semidiurnal amplitudes observed at these stations, often less than 10 msec⁻¹, are substantially less than the observed diurnal variations. It is more difficult to say anything definitive about the semidiurnal phases except that they all exhibit substantial latitude asymmetries. It is easier to see the origin of latitudinal asymmetries in the semidiurnal tide than the diurnal tide due to the greater degree of mode coupling due to background zonal winds, and the greater sensitivity of the thermal excitation on solar zenith angle.

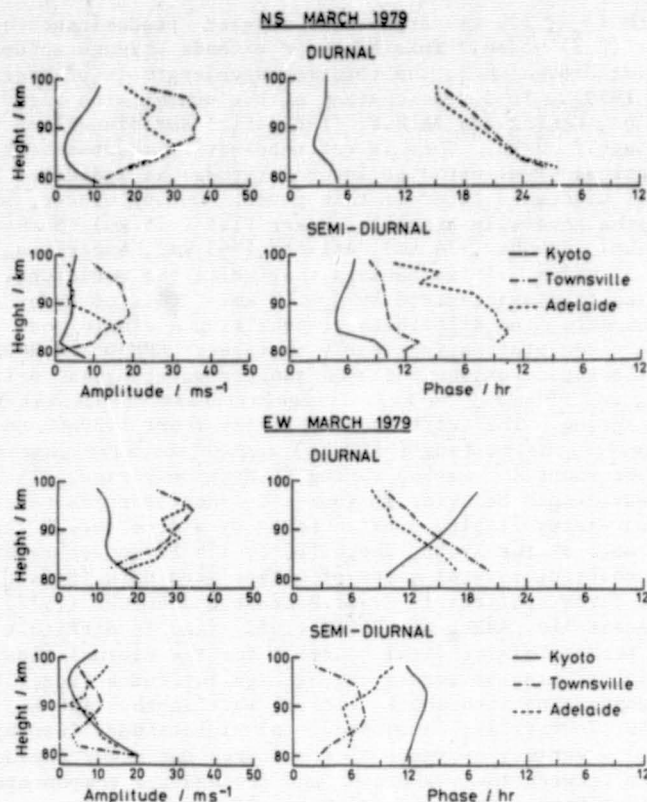


Figure 2. Height profiles of average tidal amplitudes and phases of winds observed at Adelaide, Townsville, and Kyoto for March 1979. (from ASO and VINCENT, 1982).

Evidence of asymmetric semidiurnal tidal components during equinox has been reported previously in the 100–130 km height region (LINDZEN, 1976). ASO and VINCENT (1982) find similar asymmetries during periods in September 1979 and January 1980. Other observations independently reported at Kyoto, Adelaide, and Townsville facilities during the past few years include those reported by ASO et al. (1979, 1980), VINCENT and BALL (1977, 1981), and VINCENT and STUBBS (1977).

TEMPERATURES BETWEEN 100 KM AND 130 KM

Daytime temperature determinations from 151 days of incoherent scatter radar measurements at Millstone Hill (42°N) from 1970 to 1975 are analyzed by WAND (1983) to characterize the semidiurnal temperature oscillation in the lower thermosphere (100–130 km). The annual mean semidiurnal oscillation has a maximum amplitude of 27 K at 115 km and a vertical wavelength of 47 km. Variations associated with season are large, for example, 17 K in amplitude and 1.2 h in phase at 115 km when referred to the annual mean semidiurnal vector. Generally, the altitude of maximum is lowest at the solstices and the longest vertical wavelength occurs in winter. (Note that this seasonal variation in vertical wavelength is opposite that observed in the semidiurnal winds between 80 and 100 km.) Wand notes that semidiurnal temperature measurements from Saint Santin show good agreement with the Millstone Hill

results in winter but some significant amplitude and phase differences are apparent in other seasons.

Between 1972 and 1975 approximately 30 days of simultaneous measurements of E-region neutral temperatures were made at the Arecibo (18°N) and Millstone Hill (42°N) observatories. Many of these results are reported by SALAH and WAND (1974), SALAH et al. (1975), SALAH (1974), and WAND (1976). For the present paper, 25 days of the better quality data with good seasonal coverage have been selected for examination. Seasonal averages of the semidiurnal temperatures measured at Arecibo and Millstone Hill are compared in Figure 3. The Millstone Hill amplitude profile is characterized by a peak near 110–115 km which varies in amplitude from 45 K (summer, equinox) to 60 K (winter). The Arecibo temperatures generally do not exhibit a well-defined peak. Both stations exhibit a downward phase progression with characteristic vertical scales of 30–45 km. Further, the Millstone Hill phases lead those at Arecibo by about 4 hours in summer and lag the Arecibo phases by 4–6 hours during winter. These amplitude and phase characteristics have led to the speculation that the observations reflect the strong presence of (2,4) and 2,5) semidiurnal tidal modes propagating upwards from below 100 km (LINDZEN, 1976).

THE VARIABILITY OF TIDES

Having established gross features of the vertical, latitudinal, and seasonal structures of tides in the upper mesosphere, attention has recently turned toward investigating the variability of tides on shorter time scales. For instance, details of the equinoctial transition of semidiurnal tidal structures (from typical winter to summer characteristics as described previously) has been examined by MANSON et al. (1981a) at Saskatoon. Their

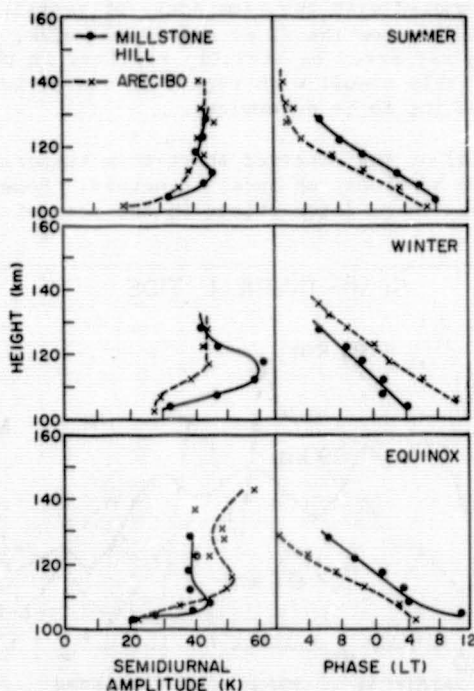


Figure 3. Seasonal averages of semidiurnal temperatures derived from 25 simultaneous daytime experiments at Arecibo and Millstone Hill.

data for the 1981 spring transition are illustrated in Figure 4. The transition from vertical wavelengths typical of March (~ 35 –40 km) to April (≥ 80 km) occurs over a period less than two weeks. The semidiurnal phase near 90 km typically experiences a phase shift from 0600 h to 0300 h over a similar time scale. This can be compared to a total phase shift (over about a month) from about 0800 h and 0300 h from typical winter to summer conditions at Saskatoon. The fall transition occurs over a period at least twice as long as the spring transition. An examination of mean temperature and flow characteristics during the Spring 1981 period indicated that the background atmosphere transition is a much slower process extending into May before completion occurs (MANSON et al., 1981a). This would suggest that seasonal tidal characteristics may be more strongly associated with variations in the thermotidal forcing than coupling effects due to asymmetric mean meridional temperature gradients and zonal winds (see also discussion on theoretical models).

A significant degree of tidal variability over time scales on the order of days has also been established, as clearly illustrated in the band-pass filtered Garchy data in Figure 5 (GLASS et al., 1978). BERNARD (1981) suggests that if the intrinsic time to set up stationarity around the earth for a particular mode is greater than a characteristic time scale associated with the variability, then transient effects would exert some influence over the observed "tidal" behavior. One might then ask to what extent we can discuss the existence of a "mode" and ascribe to it a characteristic horizontal and vertical structure. The horizontal group velocity (V_{gh}) of a tidal mode can be approximated by that of an equivalent gravity wave^{gh} at the latitude where the vertical group velocity (V_{gz}) of the gravity wave is identical to that of the tide (RICHMOND, 1975; SPIZZICHINO, 1969). A characteristic propagation time (τ_H) around the earth can then be computed for pertinent tidal modes in the earth's atmosphere and compared with the time scale of variability. Values of τ_H can be as great as ten days for the (2,6) and (1,1) modes, and hence the condition of stationarity may never be strictly realized in practice. However, the exact implications of this result with regard to distortions of the normal shape of these "modes" remains to be determined.

The dominant source(s) of the observed short-term temporal variability is basically unknown, and may be global or local in nature. Some possibilities include instability and nonlinear interactions in the case of the diurnal

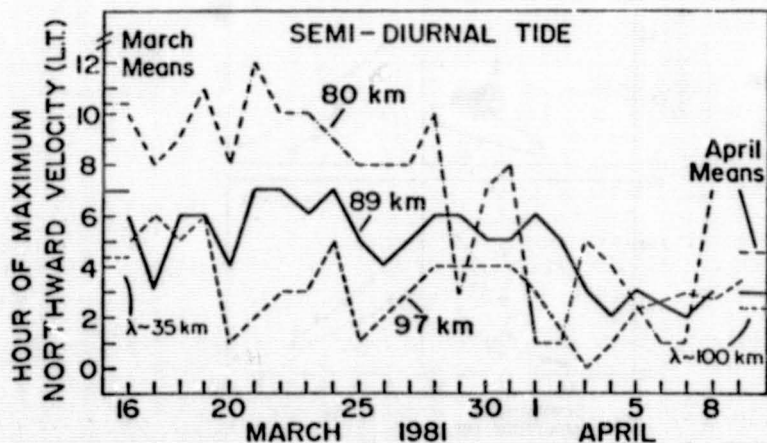


Figure 4. Spring transition of semidiurnal phase at Saskatoon for 1981. (from MANSON et al., 1981a).

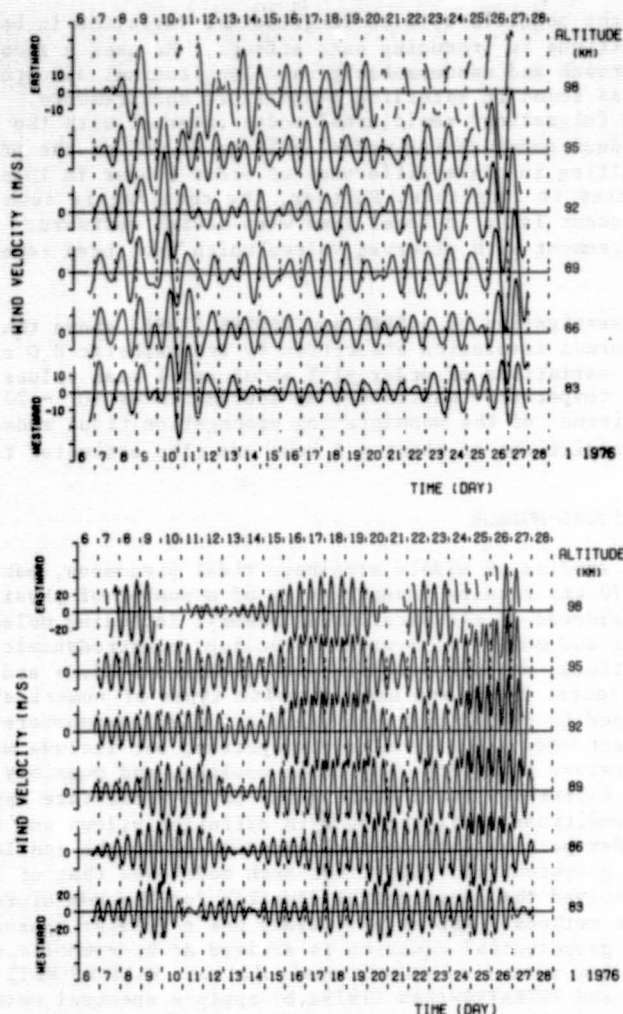


Figure 5. Band-pass filtered westerly velocities from the Garchy radar measurements at the diurnal frequency (top), and semi-diurnal frequency (bottom). (from GLASS et al., 1978).

propagating tide, variations in thermotidal heating (i.e., O_3 and H_2O concentrations) or background wind and temperature structure, or the tidal modulation of gravity wave momentum deposition into the mean flow (WALTERSCHEID, 1981). The mechanism most plausible to this author is simply that relatively slight changes in the phases of individual modes can result in interference patterns, which cause the day-to-day changes in the total tidal variation to be fairly significant. Such interference effects are discussed extensively by TSUDA et al. (1983).

Relatively few data comparisons have been performed to ascertain the presence of nonmigrating tides, which would give rise to longitudinal differences in tidal structure. Evidence of longitudinal differences in phase up to 1.5 h is reported by GLASS et al. (1975). Since his excitation model reveals little evidence of longitudinal variations in ozone heating, BERNARD

(1981) examines the possible role of longitudinal variation in background atmospheric conditions in producing such effects. He uses a second-order perturbation approach and assumes background longitudinal structure of wave numbers 1 and 2 as found in satellite temperature measurements. Bernard finds that the primary (migrating) semidiurnal modes interact with the background structure to produce nonmigrating modes as large as 50% of the primary tidal amplitudes, resulting in phase difference of order 1 hour in local time over 67°-120° differences in longitude. Further, the coupling is such that the time of maximum will occur later in local time when moving westward. Both of these trends are in agreement with observed values which have been reported (GLASS et al., 1975).

A recent investigation by FORBES and GROVES (1984) shows that longitude variations in diurnal insolation absorption by tropospheric H_2O can account for longitudinal variations of order $\pm 15\%$ about zonal mean values in the diurnal wind and temperature amplitudes at low latitudes ($0^\circ - 20^\circ$) between 80 and 100 km, by virtue of the nonmigrating propagation tidal modes which are excited. Phase variations of about ± 1 hour are also estimated to occur.

STATUS OF THEORETICAL MODELS

Theoretical studies of middle atmosphere tidal phenomena, particularly at upper levels (> 70 km) require investigation of a number of physical processes beyond those considered in classical tidal theory, including molecular and eddy diffusion of heat and momentum, Newtonian cooling, electrodynamic forces, composition variations, and interactions with background winds and meridional temperature gradients. There are basically two types of numerical models which have been developed in recent years to simulate middle atmosphere tides. The first genre neglect eddy and molecular dissipation, but include mean winds and meridional temperature gradients, Newtonian cooling, and possibly a Rayleigh friction term to filter out small-scale noise or to facilitate application of upper boundary conditions. Dispensing with diffusion allows one to derive a single second order partial differential equation in height and latitude for the perturbation geopotential. The first such model was that of LINDZEN and HONG (1974) who solved the geopotential equation for the semidiurnal tide using finite difference methods. ASO et al. (1982) use a similar approach, except that the lengthy geopotential equation is arrived at by symbolic computer software rather than manual algebraic manipulation. WALTERSCHEID et al. (1980) and WALTERSCHEID and VENKATESWARAN (1979a,b) apply a spectral method of tackling the same problem so that "coupling" between modes can be more explicitly studied. The latter two studies, while still restricted to the semidiurnal tide, utilize more detailed specifications of the background atmosphere and thermal excitation than does the LINDZEN and HONG (1974) study.

At the next hierarchical level of modelling pertaining to middle atmosphere tides, FORBES (1982a,b) includes eddy and molecular diffusion of momentum and heat so as to properly address the structural modification of tides in the 80 - 120 km region and their penetration into the upper thermosphere. This requires numerical solution of the four coupled partial differential equations in the 3 velocity components and temperature, as opposed to a single equation for the geopotential as in the above studies. Forbes provides explicit simulations from the surface to 400 km for the solar diurnal, solar semidiurnal, and lunar semidiurnal tides due to realistic thermal and gravitational forcing, as well as normalized thermospheric extensions of solar semidiurnal modes above 80 km of use in the fitting, extrapolation, and interpolation of observations data (FORBES and HAGAN, 1982).

An important issue that has been addressed by the above studies concerns the relative importance of tidal mode excitation due to (direct) thermal or

(indirect) mode coupling processes. The (2,4) mode appears to receive about equal contributions from direct thermal forcing and mode coupling via the (2,2) mean wind interaction which tend to add in phase. On the other hand, for the (2,3) mode the effect of mode coupling is to interfere with the directly forced component and to substantially reduce the (2,3) response above the level of ozone heating. In the case of (2,5) excitation appears to arise almost exclusively due to direct thermal forcing (mode coupling is weak). Difficulties in modelling and interpreting observations of semidiurnal tides in the 80 - 100 km region are expected due to the joint presence of the (2,2), (2,3), (2,4) and (2,5) modes; that is, even slight ($\sim 1-2$ hours) relative phase shifts among these components can lead to considerable changes in the total semidiurnal variation from day to day and with respect to latitude and height. The specific tidal structure in this region is sensitive to the thermal excitation, background mean wind distribution, and other atmospheric properties that the above models have only attempted to parameterize in a very "average" sense.

ACKNOWLEDGEMENT

Preparation of this work was supported under NSF Grant ATM-8113078.

REFERENCES

- Ahmed, M. I., and R. G. Roper (1983), The diurnal and semidiurnal oscillations in meteor winds over Atlanta, J. Atmos. Terr. Phys., **45**, 181.
- Aso, T., T. Naoyama, and S. Kato (1982), Numerical simulation of semidiurnal atmospheric tides, J. Geophys. Res., **86**, 388.
- Aso, T., T. Tsuda, and S. Kato (1979), Meteor radar observations at Kyoto University, J. Atmos. Terr. Phys., **41**, 517.
- Aso, T., T. Tsuda, Y. Takashima, R. Ito, and S. Kato (1980), Observations of lower ionospheric wind by the Kyoto meteor radar, J. Geophys. Res., **85**, 177.
- Aso, T., and R. A. Vincent (1982), Some direct comparisons of mesospheric winds observed at Kyoto and Adelaide, J. Atmos. Terr. Phys., **44**, 267.
- Bernard, R. (1981), Variability of the semidiurnal tide in the upper mesosphere, J. Atmos. Terr. Phys., **43**, 663.
- Carter, D. A., and B. B. Balsley (1982), The summer wind field between 80 and 93 km observed by the MST radar at Poker Flat, Alaska (65N), J. Atmos. Sci., **39**, 2905.
- Elford, W. G. (1973), a 6-year synoptic study of winds between 80 and 100 km from meteor trail drifts, IAGA Rep. to Comm. VIII.
- Eng, P. K., and S. K. Avery (1979), Day-to-day variation of atmospheric tides as observed by meteor radar, Aeron. Rep. No. 87, Aeron. Lab., Dep. Elec. Eng., Univ. Ill., Urbana.
- Forbes, J. M. (1982a), Atmospheric Tides 1. Model description and results for the solar diurnal component, J. Geophys. Res., **87**, 5222.
- Forbes, J. M. (1982b), Atmospheric Tides 2. The solar and lunar semidiurnal components, J. Geophys. Res., **87**, 5241.
- Forbes, J. M. (1984), Diurnal propagating tides in the low-latitude middle atmosphere, J. Atmos. Terr. Phys., submitted.
- Forbes, J. M., and M. E. Hagan (1982), Thermospheric extensions of the classical expansion functions for semidiurnal tides, J. Geophys. Res., **87**, 5253.
- Glass, M., R. Bernard, J. L. Fellous, and M. Massebeuf (1978), The French meteor radar facility, J. Atmos. Terr. Phys., **40**, 923.
- Glass, M., J. L. Fellous, M. Massebeuf, A. Spizzichino, I. A. Lysenko, Yu. I. Portnyagin (1975), Comparison and interpretation of the results of simultaneous wind measurements in the lower thermosphere at Carchy (France) and Obninsk (USSR) by meteor radar technique, J. Atmos. Terr. Phys., **3**, 1077.

- Lindzen, R. S. (1972), Equatorial planetary waves in shear: Part II, J. Atmos. Sci., 29, 1452.
- Lindzen, R. S. (1976), A modal decomposition of the semidiurnal tide in the lower thermosphere, J. Geophys. Res., 81, 2923.
- Lindzen, R. S., and S.-S. Hong (1974), Effects of mean winds and meridional temperature gradients on solar and lunar semidiurnal tides in the atmosphere, J. Atmos. Sci., 31, 142.
- Manson, A. H., J. B. Gregory, and C. E. Meek (1981b), Atmospheric waves (10 min-30 days) in the mesosphere and thermosphere at Saskatoon (52°N, 107°W), October 1978 - September 1979, Planet. Space Sci., 29, 615.
- Manson, A. H., C. E. Meek, and J. B. Gregory (1981a), Winds and waves (10 min-30 days) in the mesosphere and lower thermosphere at Saskatoon (52°N, 107°W, L=4.4) during the year October 1979 to July 1980, J. Geophys. Res., 86, 9615.
- Manson, A. H., C. E. Meek, and R. J. Stening (1979), The role of atmospheric waves (1.5h-10days) in the dynamics of the mesosphere and lower thermosphere at Saskatoon (52°N, 107°W) during four seasons of 1976, J. Atmos. Terr. Phys., 41, 325.
- Muller, H. G. (1966), Atmospheric tides in the meteor zone, Planet. Space Sci., 14, 1253.
- Richmond, A. D., (1975), Energy relations of atmospheric tides and their significance to approximate methods of solutions for tides with dissipative forces, J. Atmos. Sci., 32, 980.
- Salah, J. E. (1974), Daily oscillations of the midlatitude thermosphere studied by incoherent scatter at Millstone Hill, J. Atmos. Terr. Phys., 36, 1891.
- Salah, J. E., and R. H. Wand (1974), Tides in the temperature of the lower thermosphere at midlatitudes, J. Geophys. Res., 79, 4295.
- Salah, J. E., R. H. Wand, and J. V. Evans (1975), Tidal effects in the E-region from incoherent scatter radar observations, Radio Sci., 10, 347.
- Spizzichino, A. (1969), Etude des Interactions entre les Differentes Composantes du vent dans la Haute Atmosphere, Ann. Geophys., 25, 755.
- Stening, R. J., C. E. Meek, A. H. Manson, and D. G. Stephenson (1978), Winds and wave motions to 100 km at midlatitudes. VI. Tidal, gravity, and planetary waves, 1976, J. Atmos. Sci., 35, 2194.
- Tsuda, T., T. Aso, and F. Kato (1983), Seasonal variation of solar atmospheric tides at meteor heights (1983), J. Geomag. Geoelectr., 35, 65.
- Vincent, R. A., and S. Ball (1977), Tides and gravity waves in the mesosphere and mid- and low-latitudes, J. Atmos. Terr. Phys., 39, 965.
- Vincent, R. A., and S. Ball (1981), Mesospheric winds at low and mid-latitudes in the Southern Hemisphere, J. Geophys. Res., 86, 9159.
- Vincent, R. A., and T. J. Stubbs (1977), A study of motions in the winter mesosphere using the partial reflection drift technique, Planet. Space Sci., 25, 441.
- Walterscheid, R. L. (1981), Inertio-gravity wave induced accelerations of mean flows having an imposed periodic component: Implications for tidal observations in the meteor region, J. Geophys. Res., 86, 9698.
- Walterscheid, R. L., J. G. DeVore, and S. V. Venkateswaran (1980), Influence of mean zonal motion and meridional temperature gradients on the solar semidiurnal atmospheric tide: A revised spectral study with improved heating rates, J. Atmos. Sci., 37, 455.
- Walterscheid, R. L., and S. V. Venkateswaran (1979a), Influence of mean zonal motion and meridional temperature gradients on solar semidiurnal atmospheric tide: A spectral study, Part 1, Theory, J. Atmos. Sci., 36, 1623.
- Walterscheid, R. L., and S. V. Venkateswaran (1979b), Influence of mean zonal motion and meridional temperature gradients on solar semidiurnal atmospheric tide: A spectral study, Part 2., Numerical results, J. Atmos. Sci., 36, 1636.

- Wand, R. H. (1976), Semidiurnal tide in the E-region from incoherent scatter measurements at Arecibo (1976), Radio Sci., **11**, 641.
- Wand, R. H. (1983), Lower thermospheric structure from Millstone Hill incoherent scatter radar measurements, 2, Semidiurnal temperature component, J. Geophys. Res., **88**, 7211.

3.2.3. TURBULENCE IN THE ALTITUDE REGION 80-120 KM

W. K. Hocking

Department of Physics, University of Adelaide
Adelaide, South Australia 5001

ABSTRACT

Measurements of turbulent energy dissipation rates and eddy diffusion coefficients have been collated, and mean height profiles of fundamental turbulence parameters in the region 80-120 km are presented.

INTRODUCTION

It is generally agreed that there is significant turbulence in the region 80-120 km, although there is still some debate as to its temporal and spatial morphology. The main sources of turbulence are probably gravity waves and tides, and these generate turbulence by processes such as nonlinear breaking, shear instabilities, convective overturning and critical-level interactions. (e.g. LINDZEN, 1981; TEITELBAUM and SIDI, 1976; SIDI and TEITELBAUM 1978; HODGES 1969; JONES and HOUGHTON, 1971). Observations of turbulence have often shown turbulence to appear in horizontal laminae of thicknesses of a few kilometres or less, interspersed with nonturbulent regions (e.g. BLAMONT and BARAT, 1967; LLOYD et al., 1972; ROTTGER et al., 1979), and it appears that turbulence is both spatially and temporally intermittent. Turbulence appears to occur in patches (e.g., ANANDARAO et al., 1978). ZIMMERMAN and MURPHY (1977) have presented data to suggest that turbulence occurs from 20% and 80% of the time in the height region 80-100 km. Generally though, turbulence is important up to an altitude of between 95 and 110 km, whereupon the atmospheric viscosity becomes so large that it quickly damps any tendency to turbulence. This transition region is called the "turbopause".

Turbulence is characterized by two important features, which will form the basis of its quantization in this article. Firstly, turbulence causes diffusion, and secondly, it heats its environment. In laminar flow, the rate of diffusion of momentum is represented by the viscosity ν , and the rate of transfer of temperature is represented by the thermal diffusivity k_t . For the case of turbulence, similar equations apply to those of laminar flow, but ν is replaced by the "turbulent eddy viscosity" K_m (also called the momentum diffusion coefficient), and k_t is replaced by the parameter K_t . The ratio K_m/K_t is a constant, written as "Pr", the Prandtl number. In air, $Pr \approx 0.7$, so K_m and K_t are very similar, and often both are loosely denoted as "K". The rate of diffusion of minor constituents is controlled by K_t . In much of this paper, we will be looking only at small scales (less than ~ 5 km). The vertical eddy diffusion coefficient obtained at these scales is also the vertical diffusion coefficient over all scales, since vertical eddies of sizes greater than about 1 to 5 km are highly suppressed. This diffusion coefficient is often denoted K_{zz} , to indicate vertical diffusion. Horizontal diffusion occurs at much larger scales, (often denoted K_{xx} , K_{yy}) and is much faster than vertical diffusion. However, only K_{zz} will be dealt with in this work. For further discussion of K_{xx} , K_{yy} , the reader is referred to EBEL (1980).

For the molecular case for a gas, the viscosity and thermal diffusivity are proportional to the product of the molecular mean free path and the mean molecular speed. It is usual to regard K_m and K_t as a similar product of a typical scale and typical velocity, and for approximate calculations it is common to write

$$K_m \sim L_B v_L \quad (1)$$

where L_B is a "typical" scale, and v_L is the eddy velocity associated with this scale. More will be said of these "typical scales" later.

A general feature of three-dimensional turbulence is the energy transfer direction. Some large-scale feature such as a wind shear or temperature instability becomes unstable, and generates smaller scale cyclic motions. These motions generate smaller rotational random motions, and these new ones generate others. Eventually extremely small scales are reached, at which the small-scale shears are so large that molecular viscous forces become important and the energy is deposited as heat in the atmosphere. The rate at which heat is deposited will be denoted by " ϵ " here. Actually, energy is not only lost from turbulence at the smallest scales. It is lost at all scales, but most of the heat loss is at the smaller scales. Some energy can also be lost at larger scales by the weak radiation of buoyancy waves and also by modification of the temperature profile. These processes will not be parameterized here, but it is important to note that they do occur (e.g., JUSTUS 1967a; LLOYD et al. 1972; WEINSTOCK, 1978a).

2. KOLMOGOROFF THEORY

Many of the measurements of K and ϵ presented in this paper were deduced under the assumption that the turbulence being observed obeyed the classical Kolmogoroff theory of inertial-range turbulence (KOLMOGOROFF, 1941; TATARSKI, 1961). Many authors who used this theory commented on the possible inappropriateness of it to the lower thermosphere, but due to lack of alternative theories were forced to use it.

Indeed, it would not be surprising if the Kolmogoroff theory did not apply to the lower thermosphere. For example, the upper part of the region generally has a very stable temperature profile, something like that of the stratosphere, so buoyancy forces could well be important in producing anisotropic turbulence. However, high resolution measurements in the stratosphere (BARAT, 1982) have shown that in any turbulent layer, there is some part of the spatial spectrum which obeys the $k^{-5/3}$ spectrum predicted by Kolmogoroff, and the smallest and largest scales which obey this relation also agree nicely with theory.

A more serious difficulty for the thermosphere is the separation of the smallest and largest scales, or, equivalently, the value of the Reynolds' number. For Kolmogoroff's theory to apply, it is necessary that the Reynolds' number be very large (BATCHELOR, 1953). The Reynolds' number for the atmosphere is defined as

$$R_e \sim \frac{L_B v_L}{\nu} \quad , \quad (\sim K/\nu \text{ from (1)}) \quad (2)$$

in analogy with flow in pipes, where L is a typical "outer scale", and v_L is the velocity associated with scale L_B . In the troposphere, $\nu \sim 10^{-5} \text{ m}^2 \text{ s}^{-1}$, $L_B \sim 100 \text{ m} - 1 \text{ km}$ and $v_L \sim 1-10 \text{ ms}^{-1}$. Hence $R_e \sim 10^7 - 10^9$, which is satisfactorily large. However, in the lower thermosphere $\nu \sim 1 \text{ m}^2 \text{ s}^{-1}$, (e.g., see Figure 3a) whilst L_B and v_L are similar to the tropospheric values. Hence R_e is $< 10^2 - 10^4$, and values of 100 or so may not be large enough to maintain an inertial subrange.

Nevertheless, the little experimental data available suggests that the turbulence at least tries to tend to a $k^{-5/3}$ structure (e.g., ZIMMERMAN et

al., 1971; BOOKER and COHEN, 1956) at least in conditions of weak to moderate wind shear. For stronger wind shears, other theories (e.g., TCHEN, 1954) have occasionally been invoked.

The region 80-120 km is a difficult region to study. It is too low for insitu satellite measurements, too high for balloons, and too high for satellite remote sensing with adequate vertical resolution. Measurements of ϵ and K must be made by somewhat indirect means, and are therefore difficult. Given the apparent tendency for the atmosphere to at least try and approach an "inertial" spectrum, it will be assumed in this article that the Kolmogoroff theory may be approximately applied; this may mean some systematic errors in some of the profiles presented, but certainly the profiles should be applicable to accuracies of, at worst, a factor of 3, if not better.

It is freely admitted that the Kolmogoroff theory may not be an exact description of thermospheric turbulence.

3. RELATIONS BETWEEN K , ϵ AND THE SCALES OF TURBULENCE

The inertial range theory of Kolmogoroff applies between two scales, L_B and ℓ_0 . The first (larger) is called the outer scale of turbulence, the second the inner scale. Within this range, viscosity has negligible effect. However, at scales less than ℓ_0 , energy dissipation due to viscous forces becomes important. The so-called "Kolmogoroff microscale", η , is a scale well within this range of viscous dissipation, and is defined by

$$\eta = (\nu^3/\epsilon)^{1/4}. \quad (3)$$

It can be shown that $\ell_0 \approx 7.2\eta$ (e.g., HILL and CLIFFORD, 1978). It can also be shown that the outer scale is a function of ϵ , and is given by

$$L_B \approx c_1 \epsilon^{1/2} \omega_B^{-3/2} \quad (4)$$

(e.g., WEINSTOCK, 1978b). Here, ω_B is the Brunt-Vaisala angular frequency. Weinstock suggested that $c_1 \approx 2\pi/0.62$.

Finally K and ϵ can be shown to be related by the expression

$$K \approx c_2 \epsilon / \omega_B^2 \quad (5)$$

and various authors have suggested values for c_2 . WEINSTOCK (1978b) suggested that $c_2 \approx 0.8$, whilst LILLY et al. (1974) suggested $c_2 \approx 0.33$. CHANDRA (1980) took $c_2 = 0.6$. It appears that c_2 lies between 0.2 and 1.0.

Both (4) and (5) only apply in conditions of static stability, when ω_B^2 is positive. If turbulence is generated by convective processes, then (5) is clearly not valid.

The three equations (3), (4) and (5) together with the expression $\ell_0 \approx 7.2\eta$ form the main relation to be used in this article. However, it is also useful to note that

$$L_B/\eta \approx (R_e)^{3/4}, \quad (6)$$

where R_e is the Reynolds' number (see (2)). Thus the separation of the inner and outer scales is a very simple function of R_e .

4. THE TURBOPAUSE

The molecular kinematic viscosity ν increases exponentially with increasing height in the atmosphere, and at some height it becomes greater than the eddy viscosity K . The height at which $K \approx \nu$ (or equivalently, the Reynolds' number $R = 1$) is the turbopause. When this occurs, it may be seen from (6) that $L_B \approx \eta$. Hence, near the turbopause there can be no inertial range of turbulence whatsoever. The scales at which turbulence generation could occur are comparable to those at which viscous forces are important, and any mechanism which attempts to induce turbulence is very quickly damped.

The height of the turbopause varies because ϵ varies. At the turbopause $\nu = K$, so that $\epsilon \sim \nu \omega_B^2$. Larger values of ϵ allow larger ν values, pushing the turbopause height up.

The turbopause was first observed experimentally with rocket vapour trail measurements. The trails appeared turbulent up to the turbopause, and then quite suddenly became laminar above the height. The reason for the rapid change lies largely in the exponential increase in ν with height. When a vapour trail forms, it first diffuses by molecular processes, until a time $t_\eta \sim (\frac{\nu}{\epsilon})^{1/2}$ after release. Then the trail begins to appear turbulent. The kinematic viscosity increases exponentially with height, and near the turbopause, this transition time may typically increase from less than a minute to greater than 2 minutes in less than about 5-6 kms. Thus the trail appears laminar for a considerable time at the higher heights. This, coupled with higher damping which turbulence experiences due to the larger viscosity, results in the appearance of a rapid transition to laminar flow in the vapour trails. However, careful observation has shown that there can be evidence of turbulence up to latitudes as high as ~ 130 km (e.g. REES et al., 1972). Nevertheless, the turbopause does truly represent a level above which turbulence plays only a minor role. The height of the turbopause as a function of latitude and season would be useful to parameterize, but due to insufficient data no attempt has been made to do this in this paper.

5. METHODS OF DETERMINATION OF ϵ AND K

Determinations of ϵ and K values can be broadly classified into two types:

- (i) measurements of small scale motions (< 5 km) by direct observation, and
- (ii) large scale studies of the balance of heat and inert chemical species in the atmosphere.

The first method usually (though not always) results in direct measurements of ϵ , whilst the second results in direct measurements of K . It is usually in the first method that it is necessary to assume that the Kolmogoroff spectrum applies. This is not necessary in the second, but the second method suffers from other weaknesses which will be discussed later.

6. DIRECT DETERMINATIONS OF ϵ .

Most direct measurements of ϵ in the height range 80-120km have been made either by rocket measurements or radar, with one or two measurements by airglow techniques.

(a) Rocket Techniques

Most measurements of ϵ via rocket techniques have involved release of chemoluminescent compounds from a rocket, and then watching these evolve with time. This is a technique initiated by the work of Blamont (e.g., BLAMONT, 1963). These releases have either taken the form of explosions which produced

luminescent clouds, or "slow burns" which released the reactive components slowly as the rocket progressed, resulting in a long trail of luminescence. High resolution photographs of these clouds or trails were then recorded for several minutes after the release. Because of the need to photograph the clouds, these experiments have been restricted to nighttime and twilight periods. The mean drift of the cloud gave the wind velocity, and the growth of the cloud gave information concerning the turbulence. Generally, the trails grew first in a laminar way, with the trails "radius" r (see shortly for more concerning the definition of r) increasing approximately in the manner

$$(r-r_0)^2 \propto t, \quad (7)$$

$t=0$ being the time at which molecular diffusion begins, and r_0 the radius at time $t=0$. Then, after a characteristic time $\tau_\eta \sim (\frac{\nu}{\epsilon})^{1/2}$, turbulence sets in, and the trail expands more rapidly. Theory suggests that the relation

$$r^2 \propto \beta \epsilon t^3 \quad (8)$$

should be obeyed (e.g., BATCHELOR, 1950). The constant β is known from theory, so one method by which ϵ can be obtained is by examining the expansion of the trail according to (8) and thus finding ϵ .

There are problems with this method. One such problem occurs in defining zero time; the trails and clouds expand initially by nondiffusive mechanisms, such as heat gradients and explosive motions (e.g. ZIMMERMAN, 1968). Problems also exist in defining the trail "radius". The most rigorous definition of r would be to use the trail autocorrelation half width, but this was often difficult to find and was not always used.

REES et al. (1972) did not utilize (8) but rather examined the trail expansion to find the time τ_η when the trail expansion changed from (7) to (8). They then found ϵ via the relation $\epsilon = \nu \tau_\eta^{-2}$. Nevertheless, there are uncertainties in taking this as an equality.

JUSTUS (1967a) did not use either of these methods, but used a more precise formulation which required detailed knowledge of all three components of velocity and their spatial gradients. It is not clear whether adequate accuracy and resolution of these velocity components were actually attained.

ZIMMERMAN and MURPHY (1977) obtained both winds by cloud releases and temperature profiles by grenade experiments, and thus tried to calculate the Richardson number as a function of altitude. However, in connection with this data, it should be noted that grenade experiments cannot achieve a resolution of better than about 1-5 km and this may be too poor to really give good estimates of the Richardson number. Tropospheric observations of relations between Richardson number, wind speed, and turbulence intensity were applied to estimate the mean square eddy velocity, $\langle w^2 \rangle$. Then the relation

$$\epsilon \sim \frac{1}{3.4} \langle w^2 \rangle_B \quad (9)$$

was used to estimate ϵ . Some later work by WEINSTOCK (1981) suggested that the relation should more appropriately be

$$\epsilon = 0.4 \langle w^2 \rangle_B \quad (10)$$

and all the values of ZIMMERMAN and MURPHY (1977) have been corrected to suit (10) in this text.

ZIMMERMAN and ROSENBERG (1972) used HINES' (1961) theory of the relation between viscosity and the minimum vertical wavelength of gravity waves to help

extract turbulence parameters, and another method used involved calculations of structure functions from high resolution winds (ROPER, 1966).

It has at times been claimed that rocket measurements of turbulence are unreliable, because the rocket, or even the chemical release itself, could induce the turbulence (e.g. LAYZER and BEDINGER, 1969). This does not appear to be the case, since rocket results show good agreement with remote sensing measurements such as radar observations, which do not suffer from this possibility, but the possibility that the rocket could produce the turbulence must nevertheless be considered.

(b) Radar Techniques

The main two radar techniques involve (i) observations of meteor trails and (ii) medium frequency observations of radar fading times. The former method was originally implemented in detail by ELFORD and ROPER (1967) (based on earlier work done at Jodrell Bank, e.g. GREENHOW and NEUFELD, 1959) and involves firstly measurement of velocities transverse to the meteor trail alignment, and thence formation of the structure function

$$D_{tt}^2 = \langle |v_t(\underline{x}) - v_t(\underline{x} + \underline{r})|^2 \rangle,$$

v_t being the velocity perpendicular to \underline{r} .

According to theory,

$$D_{tt}^2 = 4/3 C_v^2 \epsilon^{2/3} r^{2/3}$$

in the inertial range, and recent measurements give $C_v^2 = 2.0$ (e.g. KAIMAL et al., 1972). However, Elford and Roper assumed that

$$D_{tt}^2 = 4.82 \epsilon^{2/3} r^{2/3}.$$

For this paper, values presented by ELFORD and ROPER (1967) have been corrected to satisfy the former formula. McAVANEY (1970) also applied this method, and ϵ values obtained have been similarly adjusted. More recently FELLOUS and FREZAL (1981) have also applied a similar meteor method.

When a backscatter radar with a narrow beam is used, it is possible to measure the mean square fluctuating velocity of the scatters by utilizing the spectral width of the received signal. Both HOCKING (1983a,b) and MANSON et al. (1980, 1981) have applied this technique, and have used a formula similar to (10) to obtain ϵ . It is important to remove other contaminating effects such as "beam-broadening" when applying this method, and these authors did this. However, MANSON et al. (1980, 1981) used a very wide polar diagram, and as pointed out by HOCKING (1983a,b), this can lead to contamination from larger scale horizontal fluctuating motions (e.g. gravity waves), particularly in conditions of weak turbulence. Thus the values recorded by MANSON et al. (1980, 1981) are at best upper limits on ϵ , and must be treated with caution. In this paper, the results of MANSON et al., and HOCKING (1983a,b) have been adjusted so that (10) is obeyed.

One final way by which energy dissipation rates can be obtained is to examine the decay of gravity wave energy with height, and this has been done by VINCENT and STUBBS (1977), MANSON et al. (1980), VINCENT and BALL (1981) and VINCENT (1984).

7. TYPICAL ENERGY DISSIPATION RATES

All techniques discussed above have some form of possible errors, be they

resolution problems, contamination by gravity waves or uncertainty as to the values of certain constants. Nevertheless, most methods are moderately sound in principle, and all results obtained by such methods are shown in Figure 1, together with plots of the means and medians (where possible) for the three latitude bands 0° - 20° , 21° - 50° and 51° - 90° . The means were taken at 1 km intervals, whilst medians refer to 3 km bands. The horizontal lines represent one standard deviation for the mean. Originally, the data were also divided into three seasons: summer, winter, and equinox. At 21° - 50° , ϵ appeared to be largely independent of season, and below 20° there was insufficient data to consider each season separately. Thus the three seasons for these latitude belts have been merged. If there was any trend for 21° - 50° , it was that summer values were greater than winter which were greater than equinox at 85-90 km, but the total variation was less than a factor of 3. This is a different seasonal trend to that found by ELFORD and ROPER (1967), and it is felt that there is too little data to place any emphasis on it. It is possible that the seasonal trend found by ELFORD and ROPER (1967) was unique to that year of observation. McAVANEY (1970), using a very similar measurement technique, found no seasonal trend, although ROPER (1977) claims to have produced a seasonal variation when the data were re-analysed in a different way to that used by McAvaney.

Notice that medians have been plotted for the band 21° - 50° , since there was sufficient data to do this. The mean may not be the best way to describe the data, as one large value of ϵ can seriously affect the mean. The straight edges surrounding the medians represent the lines below which 16% and 84% of the data lie, respectively (i.e., 66% of the data lay within the outlined region). Notice that at times ϵ values as large as 1.2 Wkg^{-1} have been observed, but generally ϵ is of the order of 0.1 Wkg^{-1} . Above ~ 95 km the means and medians agree fairly well, but below this height there are some discrepancies. The median is probably a better measure of typical ϵ at these heights.

In the 51° - 90° region, all the data are due to ZIMMERMAN and MURPHY (1977) for two stations at 60°N and 70°N and MANSON et al. (1980, 1981). The two extreme left profiles in Figure 1 are those due to ZIMMERMAN and MURPHY (1977) for summer. These values get very low in value, although it should be noted that below 80 km (at 75-80 km), Zimmerman and Murphy's values rose somewhat to values of the order of 0.1 Wkg^{-1} . Hence, all we can say is that the typical values at 80 km are $\sim .005 - .01 \text{ Wkg}^{-1}$ in summer.

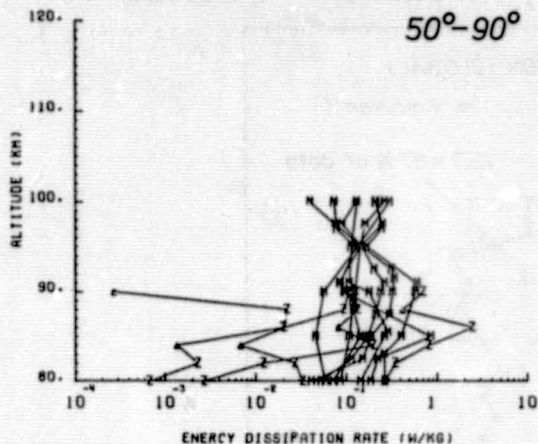
The values due to MANSON et al. (1980, 1981) for summer were $\geq 0.1 \text{ Wkg}^{-1}$. If the values due to Zimmerman and Murphy are taken as a reference, then it appears that the Manson values may be contaminated by horizontal gravity wave motion as discussed by HOCKING (1983a,b). Thus they have been ignored in forming the summer means. However, during winter, turbulence is much stronger according to Zimmerman and Murphy, so the values due to MANSON et al. (1980, 1981) are therefore probably more reliable, and have been included. It appears that there are larger seasonal fluctuations at high latitudes.

It should also be noted that the "means" above ~ 100 km are almost certainly an overestimate. Much of the time this region is above the turbopause, and so is laminar, but only ϵ values corresponding to turbulent conditions have been included in these means. Thus the profile above ~ 100 km is only representative of occasions when the turbopause is high.

Figure 2 shows the median values of ϵ for all data collectively, together with 16% and 84% percentiles. The broken arrows on Figure 1 (20° - 50°) and Figure 2 are meant to indicate that often the turbopause exists at heights as low as 95-100 km, and often ϵ profiles actually follow the broken lines rather than continuing up to ~ 115 km. The diagonal line in Figure 2 represents the line $\epsilon = v_{\text{TB}}^2$. Any ϵ values to the left of this curve are meaningless, as

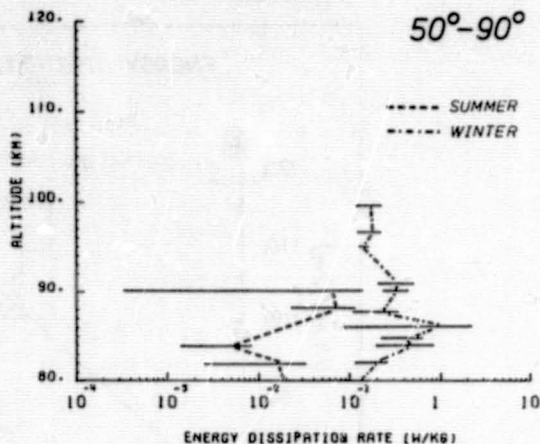
ORIGINAL PROFILES

50°-90°



MEANS

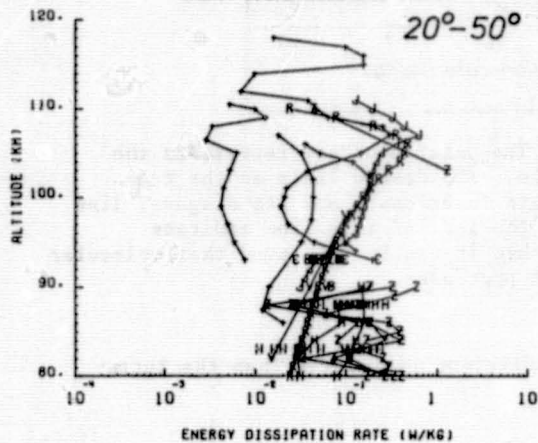
50°-90°



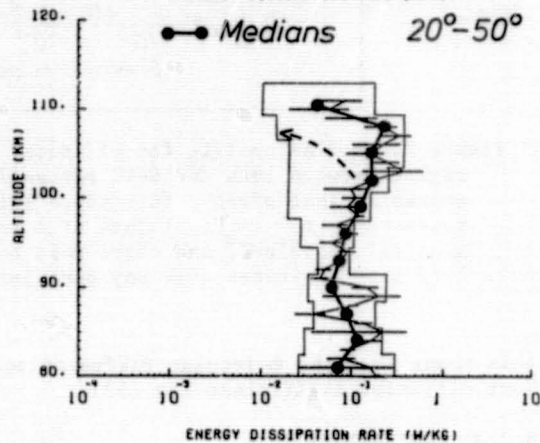
ENERGY DISSIPATION RATE (W/KG)

ENERGY DISSIPATION RATE (W/KG)

20°-50°



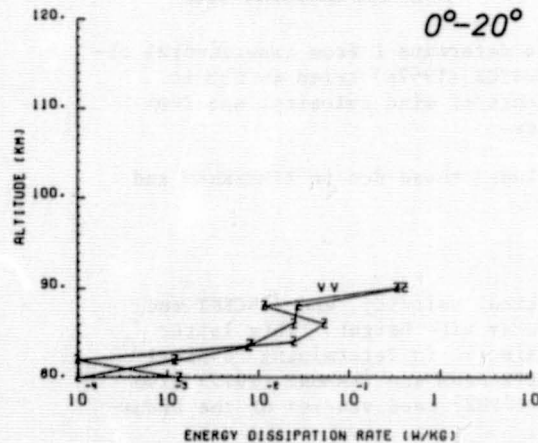
Medians 20°-50°



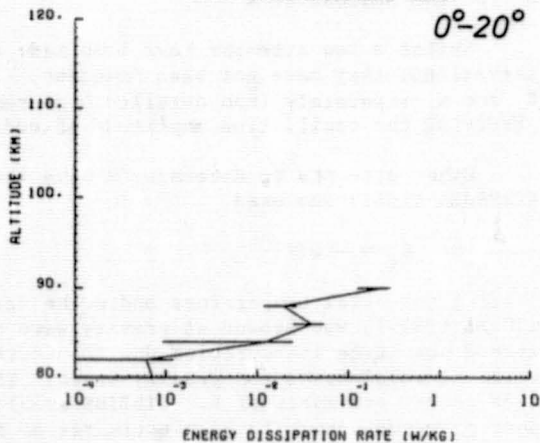
ENERGY DISSIPATION RATE (W/KG)

ENERGY DISSIPATION RATE (W/KG)

0°-20°



0°-20°



ENERGY DISSIPATION RATE (W/KG)

ENERGY DISSIPATION RATE (W/KG)

Figure 1. Energy dissipation rates for latitude bands 0-20°, 20-50° and 50-90°. On the left are shown all profiles as extracted from the relevant references, and on the right are the means ($\bar{x} \pm \sigma/\sqrt{n}$) and the medians (heavier lines). Symbols used: Z is used for all profiles involving Zimmerman, M for profiles involving Manson, H for HOCKING (1983b), R for ROPER (1966), J for JUSTUS (1967), + for LLOYD et al. (1972) and REES et al. (1972), V for profiles involving Vincent, B for Blamont and C for McAvaney.

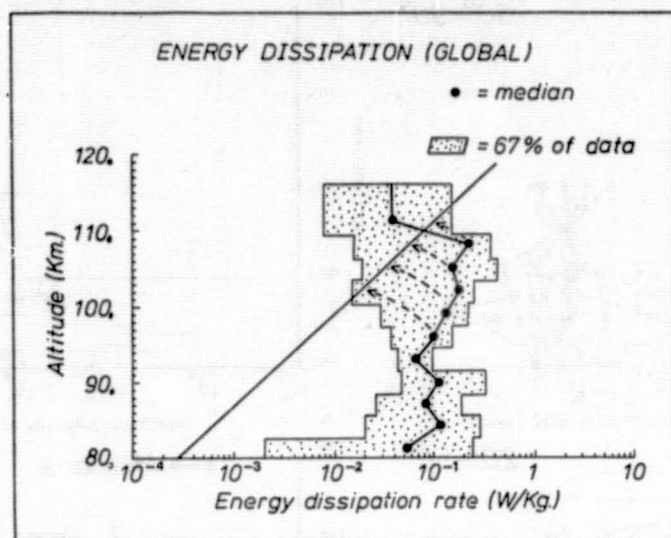


Figure 2. Median profile for all data. The outer boundary represents the region between 16th and 84th percentile. The dashed lines at the top emphasize that often a turbopause exists lower down, and the diagonal line represents $\epsilon \approx v\omega^2$. Values of ϵ to the left of this line indicate meaningless values^B, and where this occurs it can be concluded that molecular diffusion dominates over any turbulent processes.

this means that the molecular diffusion coefficient is greater than the turbulent diffusion coefficient (by (5)).

8. DETERMINATIONS OF K

Whilst a few attempts have been made to determine K from experimental observations, they have not been frequent. JUSTUS (1967a) tried to obtain K_m and K_t separately from detailed measurements of wind velocity, and from observing the oscillation amplitude of eddies.

Other attempts to determine K have included those due to ZIMMERMAN and KENESHEA (1981) who used

$$K_t = - \overline{w\theta} / \frac{d\theta}{dz},$$

θ being potential temperature and w the vertical velocity, and VINCENT and STUBBS (1977), who looked at gravity wave decay with height. This latter method has large inaccuracies due to uncertainties in determining "typical" vertical wavelengths for gravity waves. TEITELBAUM and BLAMONT (1977) also made rocket estimates of K. GIBBINS et al. (1982) used studies of the transport of water vapour to give estimates of K.

Some early estimates of K assumed that turbulent diffusion was identical to molecular diffusion in all aspects, and did not appreciate that turbulent diffusion obeys (8) for scales smaller than the largest scales of turbulence. These estimates have not been included.

More commonly, estimates of K have been made from global temperature and density profile considerations. JOHNSON and WILKINS (1965) noted that the

temperature gradient at 85-110 km is not as steep as it should be if only molecular diffusion acted. They concluded that turbulence must be acting to transfer the heat down from the regions where photodissociation (and therefore heating) take place, to the lower regions. From this concept they were then able to obtain approximate estimates of the expected eddy diffusion coefficient.

In a somewhat similar vein, COLEGROVE et al. (1965) noted that observed ratios of the concentration of O_2 to that of O at 120 km were higher than might be expected. They postulated that eddy diffusion could mix the O down from 120 km to ~ 90 km, where the mean free path is less, and so allow greater O_2 concentrations in the 90-120 km region. These authors also made estimates of K .

These two techniques form the basis of many subsequent estimates of K . Successive authors have included temporal variations (e.g., SHIMAZAKI, 1971; KENESHEA and ZIMMERMAN, 1970) and have looked at latitudinal and seasonal variation (e.g., HESSTVEDT 1968; JOHNSON and GOTTLEIB 1970; BLUM and SCHUCHARDT 1978a). KENESHEA and ZIMMERMAN (1970) pointed out that some of the earlier papers had assumed that turbulence existed above the turbopause and therefore were somewhat in error.

An interesting question arises from this work on energy and oxygen balance. Turbulence produces both heating and diffusion, and it is not at all obvious which process dominates. HUNTEN (1974) and JOHNSON (1975) pointed out that the rates of diffusion and heating are very similar. The question arises as to which is most effective -- is diffusion more effective, so that turbulence actually diffuses the heat gradients due to solar effects faster than it causes heating itself (and thus cooling the mesosphere), or is it more efficient at depositing heat, thus heating the mesosphere? It turns out that the answer to this question lies in the value of the constant c_2 in (5).

The reason for the dependence on c_2 can be seen by examining the Richardson number R_i . This is given by

$$R_i = \frac{\omega_B^2}{\langle (\frac{dV}{dz})^2 \rangle} = \frac{\omega_B^2}{(\epsilon/K_m)},$$

since $\epsilon \approx K_m \langle (\frac{dV}{dz})^2 \rangle$. (JUSTUS, 1967a)

Here, V is the horizontal velocity.

Thus $K_m = c_2 \epsilon / \omega_B^2$, where $c_2 = \bar{R}_i$ is the mean R_i of all turbulent patches. Hunten showed that the rate of transfer of heat through the mesosphere was $F = nH\rho\omega_B^2 K$, (where $n = 7/2$, H = scale height, ρ = density), whilst the rate of heating over one scale height was

$$P = \frac{1}{\bar{R}_i} H\rho\omega_B^2 K. \quad \text{Thus } P/F = (\bar{R}_i)^{-1}.$$

Clearly heating dominates if $\bar{R}_i < 0.28$, and diffusion if $\bar{R}_i > 0.28$. Hunten claimed that for turbulence to occur, R_i must be less than 0.25 so heating should dominate, whilst JOHNSON (1975) claimed that whilst R_i must be less than 0.25 to initiate turbulence, turbulence may then persist for values of R_i as high as 1.0. Thus Hunten claimed $\bar{R}_i \approx 0.2 - 0.25$, whilst Johnson claimed \bar{R}_i is nearer 1.0. The estimates suggested earlier (equation (5)) would imply diffusion dominates.

CHANDRA (1980) has presented a more rigorous treatment of estimation of eddy diffusivities which more properly considers the role of c_2 , and assumed $c_2 = 0.6$. EBEL (1980) has attempted a detailed model to estimate K from theoretical considerations alone, and from considering atmospheric dynamics. GORDIETS et al. (1982) have concluded that the question of whether turbulence heats or cools the atmosphere depends on the height gradient of K , and claim that it heats below about 105 km and cools above.

One problem with these theoretical estimates of K is that they do not consider the effects of vertical winds. For example, atomic oxygen from 120 km could be brought down to 90 km by vertical winds at one location, and lifted back up by vertical winds at another. The possibility of such "cells" of circulation has not been included in any of these analyses. Thus, in principle, all prior estimates are upper limits of K .

The relation (5) offers a means of converting the ϵ profile of Figures 1 and 2 to K profiles, but a possible problem arises because the lower thermosphere is not always turbulent. This being so, it may be that whilst the relation (5) controls diffusion across a turbulent patch, it may not control diffusion across the whole region 80-120 km. Rather, the rate of diffusion might depend partly on the temporal and spatial frequency of occurrence of turbulent patches in a manner similar to that proposed by DEWAN (1981) and WOODMAN et al. (1981) for the stratosphere. This is a point which needs further examination in the future, but for the present the relation (5) will be utilized.

In Figure 3a all the relevant K profiles due to all the mentioned authors have been presented. These include both theoretical and experimental ones. The approximate molecular viscosity has also been marked, and turbulent viscosities have been stopped when they encounter this region. In Figure 3b, the shaded region represents broadly the range of values in Figure 3a. The solid lines represent K values deduced by applying (5) to the medians of Figure 2. The Brunt-Vaisala periods were taken from GOSSARD and HOOKER (1975). The profile to the right assumes $K = \epsilon/\omega_B^2$, and that to the left assumes $K = 0.5\epsilon/\omega_B^2$ (equation 5). It is noteworthy that these K profiles derived from experimental estimates of ϵ agree so well with theoretical values of K deduced by heating and chemical considerations, which is a good check on the independent procedures used to derive K and ϵ . It also supplies some support for (5) and although it does not help to significantly resolve the value of c_2 , it does at least appear to suggest a value of C_2 of between .5 and 1.0.

9. SEASONAL AND LATITUDINAL VARIATIONS

BLUM and SCHUCHARDT (1978b) and KOROLEV and KOLENIK (1979) have used measurements of the ratio of the densities of O_2 to O at 120 km to estimate K as a function of season. Both get similar profiles and in particular both find a maximum in K in summer at mid to high latitudes. EBEL (1980) on the other hand, has attempted an entirely theoretical approach, and obtained a maximum in K during winter at $\sim 30-40^\circ$ latitude. Thus although attempts have been made to obtain seasonal and latitudinal variations, these are at too early a stage to be included in this book.

10. SCALES OF TURBULENCE

Based on the profiles derived earlier, it is possible to estimate ℓ_O and L_B at these altitudes. At 80 km, $\ell_O \sim 10-20$ m, whilst at 90 km, $\ell_O \sim 20-40$ m. The outer scale L_B is everywhere about 400-2000 m. Between these scales, turbulence should be largely isotropic -- at larger scales significant anisotropy may set in. These ranges are also consistent with experimental observations of ℓ_O (e.g., BOOKER and COHEN, 1956; ROPER 1977). (It should be noted that Booker and Cohen produced unrealistic estimates of ϵ , but neverthe-

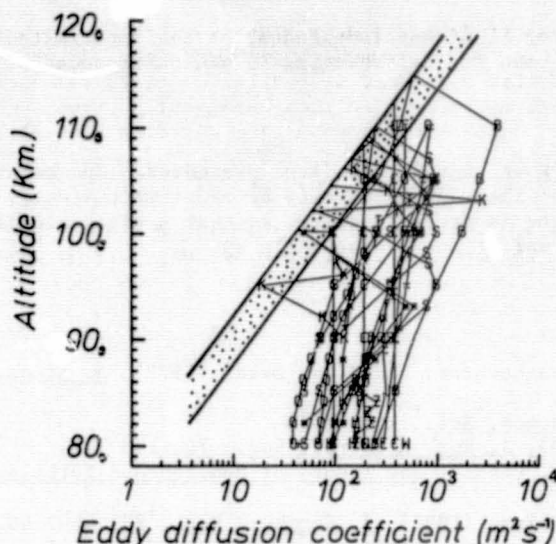


Figure 3a. Collective of all eddy diffusion coefficient profiles from all relevant references. No distinction has been made concerning latitude and season. The dotted region represents $K \approx \nu$, ν being molecular viscosity. Symbols used are: K for KENESHEA et al. (1979) and KENESHEA and ZIMMERMAN (1970), and J for JOHNSON and WILKINS (1965), C for papers involving Colgrove, O for JOHNSON and GOTTLIEB (1979), S for SHIMAZAKI (1972), H for HESSTVEDT (1968), W for WOFSY and McELROY (1973), T for TEITELBAUM and BLAMONT (1979), E for EBEL (1980), * for CHANDRA (1980), Z for ZIMMERMAN and KENESHEA (1981), + for GIBBINS et al. (1982), B for BLUM and SCHUCHARDT (1978), S for JUSTUS (1967a).

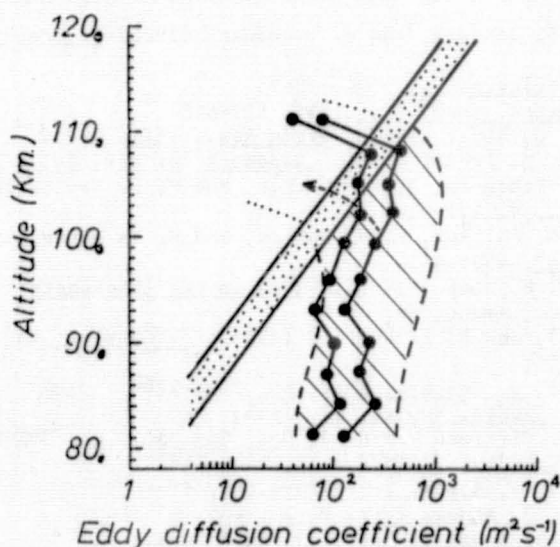


Figure 3b. Envelope of profiles from Figure 3a, together with ϵ/ω^2 (right) and $0.5\epsilon/\omega^2$ profiles (equation 5) deduced from the median curve in Figure 2. Note that the two curves deduced from ϵ both agree with the K profiles, so although this does not solve the problem of better defining C_2 in equation (5), it does appear to support that equation.

less their determination ϵ_0 of ϵ was independent of their estimates of ϵ and the method which they used for determining ϵ_0 was quite sound).

CONCLUSION

Curves of ϵ , and K vs. height have been presented. One point which has clearly emerged is that there is a scarcity of experimental data, and more effort in this direction is strongly urged, so that a clear global and seasonal picture of turbulence variations can be built up.

REFERENCES

- Anandarao, B. G., R. Raghavarao, and J. N. Desai (1978), J. Atmos. Terr. Phys., **40**, 157-163.
- Barat, J. (1982), J. Atmos. Sci., 2553-2564
- Batchelor, G. K. (1950), J. Roy. Meteorol. Soc., **76**, 133-146.
- Batchelor, G. K. Press. (1953), The Theory of Homogeneous Turbulence, Cambridge Univ.
- Battaner, E., and A. Molina (1980), J. Geophys. Res., **85**, 6803-6810.
- Blamont, J. E., and C. de Jager (1961), Ann. Geophys., **17**, 134-143.
- Blamont, J. (1963), Planet. Space Sci., **10**, 89-101.
- Blamont, J. E., and J. Barat (1964) in Aurora and Airglow, edited by B. M. McCormac, 156-159, Reinhold Pub. Co.
- Blum, P., K. G. H. Schuchardt, and U. von Zahn (1978), J. Atmos. Terr. Phys., **40**, 1131-1135.
- Blum, P. W., and K. G. A. Schuchardt (1978), J. Atmos. Terr. Phys., **40**, 1137-1142.
- Booker, H. G., and R. Cohen (1956), J. Geophys. Res., **61**, 707-733.
- Chandra, S. (1980), Planet. Space Sci., **28**, 585-593.
- Colegrove, F. D., W. B. Hanson, and F. S. Johnson (1965), J. Geophys. Res., **70**, 4931-4941.
- Colegrove, F. D., F. S. Johnson, and W. B. Hanson (1966) J. Geophys. Res., **71**, 2227-2236.
- Dewan, E. M. (1981), Science, **211**, 1041-1042.
- Ebel, A. (1980), J. Atmos. Terr. Phys., **42**, 617-628.
- Elford, W. G., and R. G. Roper (1967), Space Res., **VIII**, 42-54.
- Fellous, J. L., and M. E. Frezal (1981), Handbook for MAP, Vol. 2 323-332.
- Gibbons, O. T., P. R. Schwartz, D. L. Thacher, and R. M. Bevilacqua (1982), Geophys. Res. Lett., **9**, 131-134.
- Gordiets, B. F., Yu. N. Kulikov, M. N. Markov, and M. Ya Marov (1982), J. Geophys. Res., **87**, 4504-4514.
- Gossard, E. D., and W. H. Hooke (1975), Waves in the Atmosphere, Elsevier Scientific Publ. Co., Amsterdam.
- Greenhow, J. S. (1959), and E. L. Neufeld (1959), J. Geophys. Res., **64**, 2129-2153.
- Greenhow, J. S. (1959), J. Geophys. Res., **64**, 2208-2209.
- Hesstvedt, E. (1968), Geofys. Publik, **27**, 1-35.
- Hill, R. J., and S. F. Clifford (1978) J. Opt. Soc. Am., **68**, 892-899.
- Hines, C. O. (1960), Canadian J. Phys., **38**, 1441-1481.
- Hocking, W. K. (1983a), J. Atmos. Terr. Phys., **45**, 89-102.
- Hocking, W. K. (1983), J. Atmos. Terr. Phys., **45**, 103-114.
- Hodges, R. R. (1967), J. Geophys. Res., **72**, 3455-3458.
- Hunten, D. M. (1974), J. Geophys. Res., **79**, 2533-2534.
- Johnson, F. S. (1975), J. Atmos. Sci., **32**, 1658-1662.
- Johnson, F. S., and E. M. Wilkins (1965), J. Geophys. Res., **70**, 1281-1284.
- Johnson, F. S., and B. Gottlieb (1970), Planet. Space Sci., **18**, 1707-1718.
- Jones, W. L., and D. D. Houghton (1971), J. Atmos. Sci., **28**, 604-608.
- Justus, C. G. (1966), J. Geophys. Res., **71**, 3767-3773.

- Justus, C. G. (1967), J. Geophys. Res., 72, 1035-1039.
- Justus, C. G. (1967), J. Geophys. Res., 72, 1933-1940.
- Justus, C. G. (1968), J. Geophys. Res., 73, 455-458.
- Justus, C. G. (1969), J. Atmos. Sci., 26, 1137-1141.
- Kaimal, J. C., J. C. Wyngaard, Y. Izumi, and O. R. Cote (1972), Q. J. Roy Meteorol. Soc., 98, 563-589.
- Kellogg, W. W. (1964), Space Science Rev., 3, 275-316.
- Keneshea, T. J., and S. P. Zimmerman (1970), J. Atmos. Sci., 27, 831-849.
- Keneshea, T. J., S. P. Zimmerman, and C. R. Philbrick (1979), Planet. Space Sci., 27, 385-401.
- Kochanski, A. J. (1964), J. Geophys. Res., 69, 3651-3662.
- Kolmogoroff, A. N. (1941), Doklady Akad. Nauk USSR, 32, 16, (German translation in "Sammelband zur Statistischen Theorie der Turbulenz", Akademie-Verlag, Berlin (1958 p. 77)).
- Korolev, S. S., and A. G. Kolenik (1979), Geomag. Aeron., 19, 47-50.
- Layzer, D., and J. F. Bedinger (1969), Planet. Space Sci., 17, 1891-1911.
- Lilly, D. K., D. E. Waco, and S. I. Aldefang (1974), J. Appl. Meteorol., 13, 488-493.
- Lindzen, R. S. (1981), J. Geophys. Res., 86, 9707-9714.
- Lloyd, K. G., C. H. Low, B. J. McAvaney, D. Rees, and R. G. Roper (1971), Planet. Space Sci., 20, 761-769.
- Manson, A. H., and C. E. Meek (1980), J. Atmos. Terr. Phys., 42, 103-113.
- Manson, A. H., C. E. Meek, and J. B. Gregory (1981), J. Atmos. Terr. Phys., 43, 35-44.
- Massie, S. T. (1980), J. Geophys. Res., 85, 2155-2164.
- McAvaney, B. J. (1970), Small scale wind structure in the upper atmosphere Ph.D Thesis, University of Adelaide.
- Noel, T. M. (1963), J. Geophys. Res., 68, 2862-2863.
- Rees, D., R. G. Roper, K. W. Lloyd, and C. H. Low (1972), Phil. Trans. Roy. (Lond), A271, 631-666.
- Roper, R. G. (1966), J. Geophys. Res., 71, 4427-4428.
- Roper, R. G. (1977), Turbulence in the Lower Thermosphere, in The Upper Atmosphere and Magnetosphere, Studies in Geophysics, 129, 117 National Research Council, USA.
- Rosenberg, N. W., D. Golmb, S. P. Zimmerman, W. K. Vickery, and J. S. Theon (1973), Space Res. XIII, 435-439
- Rottger, J., P. K. Rastogi, and R. F. Woodman (1979), Geophys. Res. Lett., 6, 617-620.
- Shimazaki, T. (1971), J. Atmos. Terr. Phys., 33, 1383-1401.
- Sidi, C., and H. Teitelbaum (1978), J. Atmos. Terr. Phys., 40, 529-540.
- Tatarski, V. (1961), Wave Propagation in a Aturbulent Medium (translated from Russian by Silverman), McGraw-Hill, N. Y.
- Tchen, C. M. (1954), Phys. Rev., 93, 4-14.
- Teitelbaum, H. (1966), Space. Res., VI, 425-437.
- Teitelbaum, H., and J. E. Blamont (1977), Planet. Space Sci., 25, 723-734.
- Teitelbaum, H., and C. Sidi (1976), J. Atmos. Terr. Phys., 38, 413-421.
- Vincent, R. A., and S. M. Ball (1981), J. Geophys. Res., 86, 9159-9169.
- Vincent, R. A., and T. J. Stubbs (1977), Planet. Space Sci., 25, 442-455.
- Vincent, R. A. (1984), J. Atmos. Terr. Phys., 46, 119-128.
- Von Zahn, V., and T. Herwig (1977), Proc. NATO Advanced Study Institute, Spatind, Norway, April 12-22, edited by B. Grandal, and J. A. Holtet, Reidel Publ. Co.
- Weinstock, J. (1978), J. Atmos. Sci., 35, 1022-1027.
- Weinstock, J. (1978), J. Atmos. Sci., 35, 634-649.
- Weinstock, J. (1981), J. Atmos. Sci., 38, 880-883.
- Wofsy, S. C., and M. B. McElroy (1973), J. Geophys. Res., 78, 2619-2624.
- Woodman, R. F., P. K. Rastogi, and T. Sato (1981), MAP Handbook, Vol. 2, 363-369.
- Zimmerman, S. P. (1966), Space Res., VI, 425-437.
- Zimmerman, S. P. (1966), J. Geophys. Res., 71, 2439-2444.

- Zimmerman, S. P. (1968), J. Geophys. Res., 463-454.
- Zimmerman, S. P. (1973), J. Geophys. Res., 78, 3927-3938.
- Zimmerman, S. P., and K. S. W. Champion (1963), J. Geophys. Res., 68, 3049-3056.
- Zimmerman, S. P., and T. J. Keneshea (1981), MAP Handbook, Vol. 2, 311-322.
- Zimmerman, S. P., and E. A. Murphy (1977), in Proc. NATO Advanced Study Institute, Spatind, Norway, April 12-22, edited by B. Grandal, and J. A. Hostet, Reidel Publ. Co.
- Zimmerman, S. P., G. P. Pereira, E. A. Murphy, and J. Theon (1973), Space Res., XIII, 209-215.
- Zimmerman, S. P., and N. N. Rosenberg (1972), Space Res., XIII, 623-628.
- Zimmerman, S. P., and C. A. Trowbridge (1973), Space Res., XVIII, 203-208.
- Zimmerman, S. P., C. A. Trowbridge, and I. L. Kofsky (1971), Space Res., XI, 907-914.

4.1 CONTRIBUTION TO THE CIRA MODEL FROM GROUND-BASED LIDAR

M. L. Chanin, A. Hauchecorne, N. Smires

Service d'Aeronomie du CNRS
B. P. 3 - Verrieres le Buisson, France

INTRODUCTION

A new technique, the Rayleigh-Lidar Sounding, has been developed recently to probe the Middle Atmosphere and has demonstrated its ability to provide density and temperature profiles in the height range 30-90 km. It has been limited until now to ground-based observations, but it could be used in the future from a space-borne platform. The set of data, as it exists to-day, has been obtained from a unique midlatitude site, the Observatory of Haute-Provence (O.H.P. 44°N, 6°E) and consequently only local information has been obtained with that technique. Even with this limiting factor, it is thought to be a useful complement to a global model, mainly because of its spatial and temporal resolutions, usually not available from global data. Such resolutions give an insight into the atmospheric variability as a function of height and time, for time-scale ranging from minutes to years.

BRIEF DESCRIPTION OF THE METHOD

A description of the Rayleigh-Lidar technique and of the instrument is available in the published literature (HAUCHECORNE and CHANIN, 1980, 1982, 1983; CHANIN and HAUCHECORNE, 1981; BOURG-HECKLY et al., 1982; CHANIN et al., 1983) and its more complete and recent description is published in a previous issue of MAP Handbook (CHANIN and HAUCHECORNE, 1984). The purpose of this brief recall is to ensure that the data will be interpreted and used correctly as a contribution to the new model.

Nature of Measured Parameters. When a monochromatic laser beam is sent into the atmosphere, two processes can provide a backscattered signal: the Rayleigh scattering by atmospheric molecules and the Mie scattering by atmospheric aerosols. Above a level ranging from 30 to 35 km, the Mie contribution (scattering ratio $\ll 1,01$). Then the backscattered signal from a given height-range, $Z \pm \Delta Z$, is proportional to the density $\rho(Z)$. A profile of the atmospheric density can be obtained by a time analysis of the echo (with a proportionality constant to be determined). The temperature can be deduced in absolute value from the density profile by using a model value of the pressure at the top of the profile and assuming that the atmosphere is in hydrostatic equilibrium and obeys the perfect gas law. Because of the required fitting with the model at the top of the profile, the range of the temperature profile is reduced by 10 km compared to the density profile.

The main quantity preventing measurement of density in absolute value is the transmission of the atmosphere, which is known to vary widely with a short time constant; to obtain a density profile it requires a calibration at 30 km with another density measurement (radiosondes for example) which was not performed on a regular basis. Due to the fact that the temperature is obtained in absolute value from this technique, all the data mentioned in this contribution will be temperature data.

Altitude Range of the Lidar Sounding. As mentioned before, the lowest height where the backscattered signal can be interpreted directly in terms of density (and then temperature) is fixed by the upper level of the aerosol

layer. This level is usually below 30 km at midlatitudes with the exception of post-volcanic eruption periods. For the years 1981 to 1984 corresponding to the data presented here, such eruptions were quite frequent and care was taken to delete data at the levels where aerosols had been detected. The major disturbance came in 1982 from the El Chichon eruption, but as the aerosols content was monitored by lidar from the same site, it provided a double check to delimit the height range to be used.

The upper limit of the measurement is given by the signal-to-noise ratio, thus explaining the great care taken to reduce the sky-background which is the main contribution to noise. After a succession of improvements through the years, the range was pushed up from 70 km in 1981 to 90 km and occasionally to 95 km. In this altitude range (30-90 km) several tests using double wavelength measurements have been performed to ensure that the contribution of Mie scattering could be neglected. With a still increased sensitivity, one may be able in the future to detect the eventual presence of aerosols of meteoritic origin around 90-100 km, but, as for today, their abundance has never been measured by lidar and is then too small to disturb the measurements.

Resolutions. The lowest possible limit of the height resolution is fixed by the laser pulse duration; in our case 1.5 meter for the laser pulse duration of 10 nsec. Practically, the height resolution is given by the width of the time gate of the photon counting analysis; in the earlier measurements it was fixed at 4 μ s giving then $\Delta Z = 600$ m and it has been recently reduced to 2 μ s in order to obtain a height resolution of 300 m. For much of the data treatment performed in this analysis, such height resolution was smoothed to 2.4 or 3.0 km by use of a running average. The temporal resolution, theoretically limited by the laser repetition rate (here 10 Hz), is actually defined by the integration time necessary to reach a satisfactory accuracy. In order to reduce the size of the recorded data set, the time resolution has been limited to 5 of 5 minutes. For the lower height range (30-50 km) such an integration time of 5 minutes provides enough accuracy to study short time-scale fluctuations. But for the data used in this study the integration time was ranging between 2 and several hours.

Accuracy. The accuracy of the measurements depends on the number of received photons and then on both the time and height resolutions. For the values of those parameters used in this analysis ($\Delta z = 2.4$ km $\Delta t = 2$ H) the typical accuracy would be 0.1, 1 and 10% for the density measured at 35, 65 and 85 km and 0.3, 1 and 10 K for the temperature at 35, 50 and 80 km.

DESCRIPTION OF THE AVAILABLE SET OF DATA AND DATA PROCESSING

The first lidar data from which temperature profile have been deduced date from the year 1977 (HAUCHECORNE and CHANIN, 1980); at that time they were obtained as a by-product of the lidar sounding of sodium and lithium at the mesopause level. Those data were never obtained on a regular basis and their accuracy was lower by far than the present one. Consequently, even though those data can be useful for looking at long-term variations, they have not been used in this work. In June 1980 a new lidar station devoted to Rayleigh scattering measurements was set up at the O.H.P. and was put into service on a routine basis in January 1981. This survey has been going on since that date, with only 2 interruptions of more than a month duration to bring some necessary improvements to the equipment. A noticeable gain in accuracy and range was the consequence of those successive interventions, but the set of data obtained between January 1981 and June 1984 presents a good enough homogeneity to be used as a whole on this study. (The date of June 1st 1984 to end the series of data presented here was chosen because of the presentation of these

results at the COSPAR meeting in June 1984. For a definitive contribution to the CIRA Model in 1985 or 1986 the data set will be completed, as the collection of data has not been interrupted.) These three years and a half of data represent a total number of nights of measurements of 324, namely 67 for 1981, 107 for 1982, 104 for 1983 and 46 for the first 5 months of 1984.

On a regular basis, and when the meteorological conditions are favorable, the lidar operates for 3 consecutive hours during the first part of the night. For this study, most of the temperature data correspond to a 3 hour average. But for 10 cases, the data were obtained for longer periods, between 6 and 13 hours, with the purpose of studying diurnal and semidiurnal tides; in those cases the profile used in this study correspond to the profile averaged over the whole sequence. The reason for using time-averaged profiles was to reduce most of the fluctuations due to gravity waves. It should be mentioned that an instantaneous profile -- as the temperature or density rocket profile -- is more likely to be influenced by short time-scale fluctuations, as there is no way then to distinguish between short- and long-period waves. In addition, a smoothing function was applied to the lidar vertical profiles in order to suppress the vertical structures of small wavelengths still present after time averaging. The vertical resolution in this study has been reduced to 2.4 km or 3.0 km for that purpose.

From the set of individual profiles covering all the periods described earlier, the seasonal variation of the temperature is obtained using a 45-day half-width Blackman filter to suppress the short-period fluctuations and is then averaged over the 4 years, 1981 to 1984.

The variance of the temperature as a function of time is calculated as the square of the deviation of each individual profile from the averaged temperature. The variance is then smoothed by using the same Blackman filter as for the temperature and averaged over the 4 years of data.

RESULTS OF THE ANALYSIS OF THE PERIOD 1981-1984

Diurnal Variation. Long sequences of data have been recorded especially with the aim to study the diurnal and semidiurnal tides. In half of the cases a regular cooling of the atmosphere is observed with a minimum value at the end of the night; the cooling rate is about 1 K/hour in the stratosphere and up to 3 K/hour in the mesosphere; in the other cases, the amplitude of the gravity waves and/or of the semidiurnal tide being of the same order of magnitude or even larger than the diurnal variation hide completely this cooling effect (amplitudes of the temperature fluctuations as large as 10 to 30 K increasing from 30 to 70 km are not unusual).

A large enough statistics is not yet available to conclude and, at this stage, it looks unjustified to apply a systematic correction to the temperature values as a function of the time of day. The error due to the diurnal variation in this study is limited by the small dispersion of the data with time, as the measurements are usually performed in the early part of the night.

Day-to-Day Variance. A large variability is observed from one day to the next, mainly during the winter (from October to April) when the westerly winds allow the propagation of planetary waves. As the study of the interaction of planetary waves with the general circulation has been one of our main scientific objectives since 1981 (HAUCHECORNE and CHANIN, 1982, 1983), the lidar was due to operate very frequently during wintertime -- each night when the meteorological conditions were satisfactory -- while in summertime, where the variability was observed to be low, the number of observations was willingly

ORIGINAL PAGE IS OF POOR QUALITY

reduced to a few nights a week. From the large number of winter data, the variability of the wintertime temperature has been studied with a time resolution which is usually not available from rocket data (up to 19 nights of data during December 1982).

The height section of the standard deviation (square root of the variance) is shown on Figure 1. These results confirm what had been observed for 3 consecutive winters and indicate the presence of two relatively well-defined maxima of standard deviation centered around January: one at 35-40 km with a maximum of amplitude of 12 K, one at 65-70 km with an amplitude as high as 18 K. During the summer the variability is observed to be very low in the stratosphere (≤ 5 K) but stays quite large in the upper mesosphere near 75 km.

This notion of variance of geophysical quantity has not yet been introduced in the model as it is not available on a global basis. We feel that such results, even limited to a specific site, could be useful to estimate the expected deviation from the mean value as given by the model.

Seasonal Variation. The seasonal variation of the smoothed temperature (Figure 2) show a very similar behaviour for the successive years. A maximum of temperature is observed at the stratopause level around May-June and a minimum around December-January. At this level of the stratopause (45-50 km) the amplitude of the yearly variation is around 20 K. A regular feature also observed in the 3 consecutive winters corresponds to a small warming in the mid-mesosphere around November and is followed by a minimum temperature in January.

The strong similarity between the seasonal variations observed for the data set available, should indicate that the average map covering the whole period (Figure 2) could be used as representative of the seasonal variation for this site and for this part of the solar cycle.

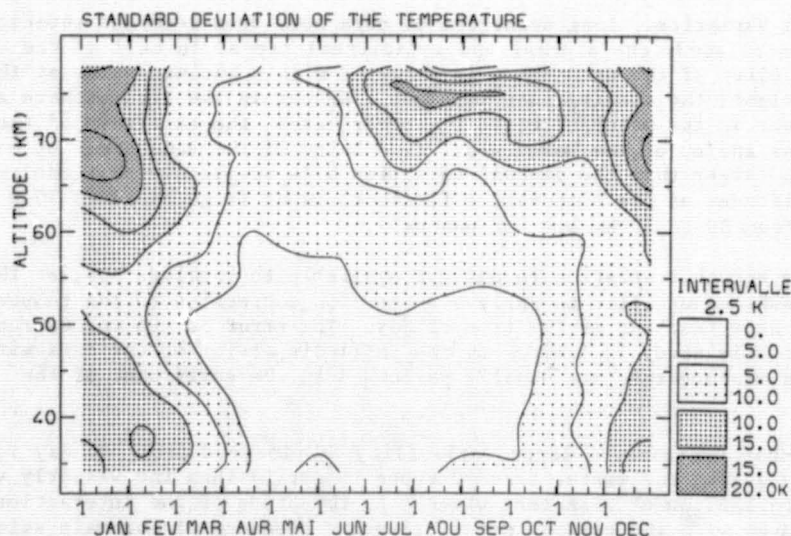


Figure 1. Height section of the temperature standard deviation calculated from the individual daily profile deviation from the 45-day running average for the period 1981-1984.

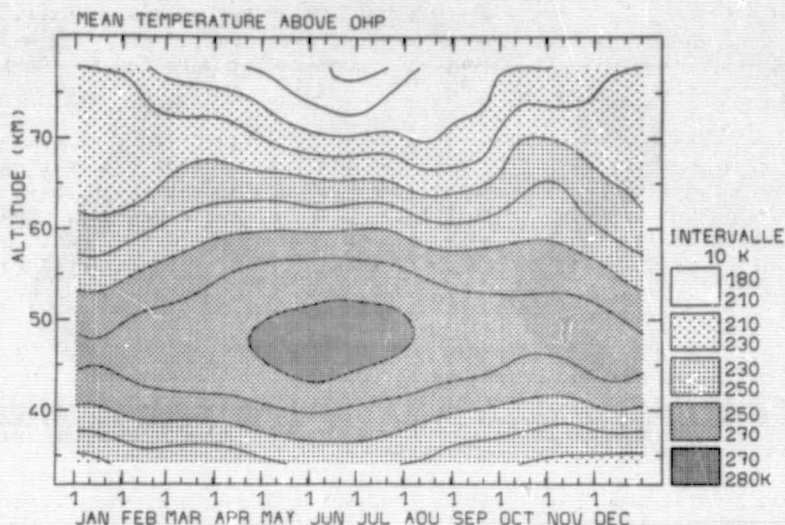


Figure 2. Height section of the mean temperature averaged over 4 years from 1981 to 1984.

These results are also presented in Figure 3 and Table 1 as a series of monthly averaged temperature profiles with an indication of the standard deviation corresponding to the day-to-day variability.

Year-to-Year Variability. As the data are only covering a four-year period, the data set is too small to calculate the year-to-year variance; however, the monthly profiles averaged for each of these years provides an indication on the yearly variability. For this purpose, a winter and a summer set of profiles are given in Figure 4. A large variability is observed as expected in winter as well in the mesosphere and in the stratosphere. The amplitudes of variation observed in February in the stratosphere are of the same order of magnitude as the day-to-day variability (> 20 K). In the summer months for the 3 years of data, the variability is larger than the day-to-day standard deviation and reaches a value close to 10 K at all heights.

Deviation From the Model. It is of interest to see how the local mean temperature deviates from the zonal mean as given by the model. The comparison was performed with the CIRA 1972 model by using a linear interpolation between the 40° N and 50° N models. Figure 5 presents the deviation from CIRA 72 for the mean temperature observed during the years 1981-1984. Differences as large as 20 K are observed in the mesosphere: the stratosphere at 44° N, 6° E, seems to be on the average warmer during winter and cooler during summer than indicated by the global model, while the situation is opposite for the lower mesosphere (50-65 km). The largest difference is observed in the upper mesosphere ≥ 65 km mainly at the beginning of the winter where a small warming is always observed around the October-November period.

The comparison with the revised model, which is of interest in this study, will be performed when the new revised model is available.

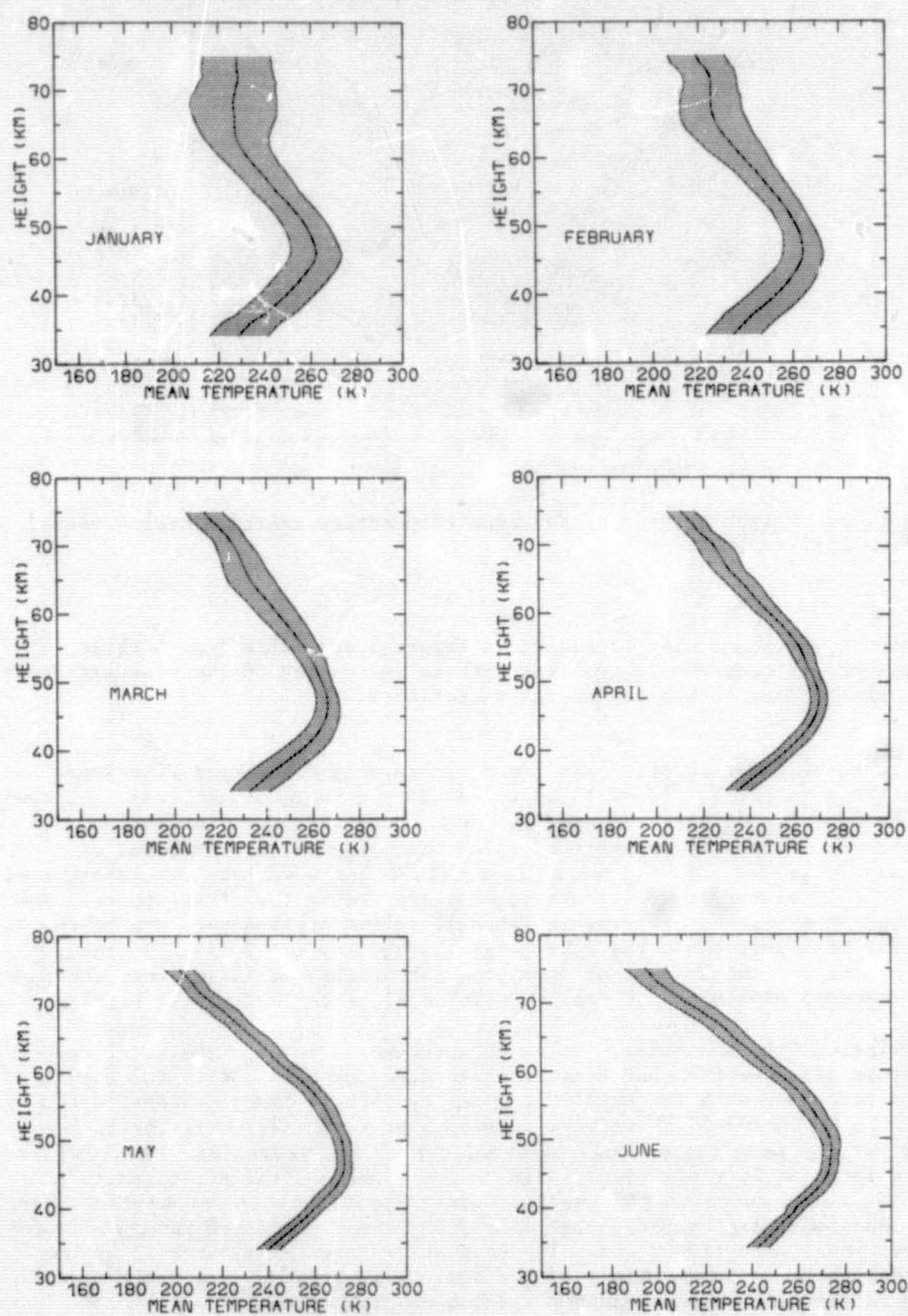


Figure 3. Monthly averaged temperature profiles for the period 1981-1984.

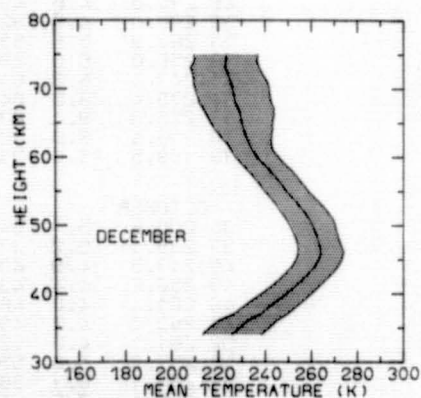
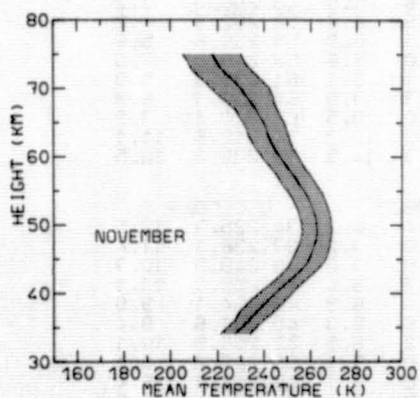
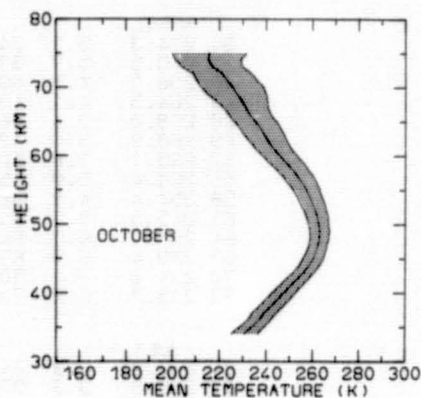
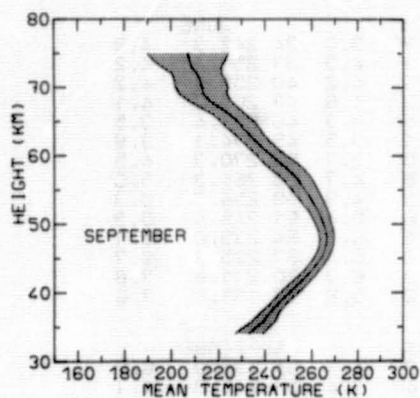
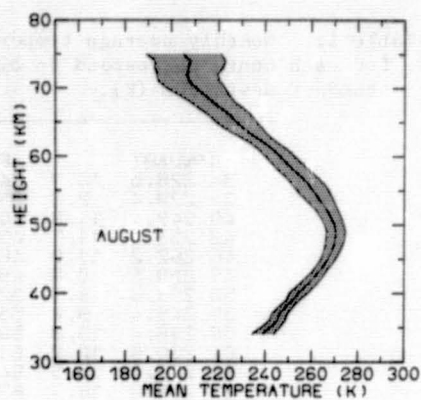
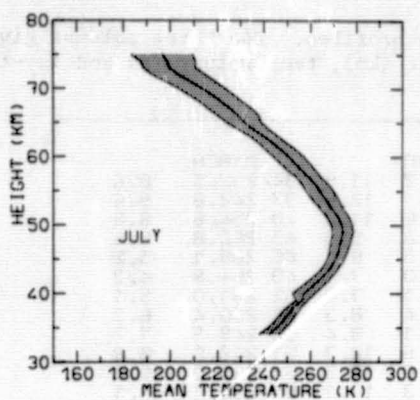


Figure 3 continued.

Table 1. Monthly average temperature profiles. The three columns given for each month correspond to altitude (km), temperature (K) and day-to-day standard deviation (K).

JANUARY			FEBRUARY			MARCH		
34	228.5	12.7	34	234.2	11.8	34	232.5	8.6
37	239.4	12.2	37	243.1	12.6	37	242.8	9.8
40	249.4	11.8	40	253.6	11.8	40	254.6	8.8
43	257.3	11.7	43	260.8	9.8	43	262.8	6.6
46	262.2	11.0	46	264.5	8.5	46	266.1	5.2
49	259.5	9.8	49	263.0	7.1	49	264.8	4.3
52	253.6	9.5	52	258.1	7.0	52	261.0	5.1
55	245.4	9.8	55	251.4	8.3	55	256.4	6.3
58	238.4	10.8	58	244.1	9.4	58	249.7	7.7
61	230.8	12.2	61	235.9	12.3	61	242.6	8.8
64	227.3	15.5	64	228.8	13.9	64	235.0	10.0
67	226.9	18.7	67	225.3	13.1	67	230.1	9.1
70	227.5	17.4	70	225.0	11.6	70	225.9	7.8
73	228.2	15.3	73	223.0	11.8	73	218.6	8.6
APRIL			MAY			JUNE		
34	234.3	5.3	34	239.7	5.0	34	242.3	4.9
37	245.5	5.7	37	250.1	4.5	37	251.4	4.2
40	256.0	4.5	40	259.7	4.2	40	259.3	4.2
43	264.5	4.1	43	268.3	4.6	43	269.3	4.1
46	269.0	3.4	46	272.5	3.3	46	273.4	3.5
49	268.9	3.5	49	272.1	3.5	49	274.1	3.8
52	265.1	3.8	52	268.5	3.7	52	270.3	4.5
55	261.4	5.0	55	263.8	4.7	55	264.3	5.0
58	254.4	4.9	58	256.3	4.9	58	256.7	5.3
61	245.5	5.7	61	245.6	5.4	61	245.4	5.9
64	237.7	6.7	64	237.1	6.0	64	235.0	6.1
67	229.4	6.9	67	227.2	5.4	67	225.3	6.7
70	224.2	7.1	70	216.3	6.9	70	211.8	7.8
73	215.7	6.2	73	207.2	5.8	73	199.6	7.6
JULY			AUGUST			SEPTEMBER		
34	242.2	4.3	34	238.9	4.7	34	233.0	6.0
37	250.5	3.3	37	246.4	3.4	37	241.9	4.1
40	257.1	4.7	40	254.4	4.0	40	250.5	3.8
43	266.8	3.7	43	262.9	3.0	43	259.3	3.2
46	272.0	3.9	46	268.7	3.4	46	265.3	3.0
49	274.0	4.5	49	270.6	4.0	49	266.0	3.2
52	270.0	4.9	52	266.9	4.6	52	262.5	4.2
55	263.9	5.9	55	260.5	6.9	55	256.8	5.6
58	256.0	6.0	58	252.0	6.6	58	249.5	7.0
61	247.1	6.3	61	243.1	6.1	61	239.3	5.9
64	235.4	6.5	64	230.7	7.9	64	230.7	6.9
67	225.3	9.4	67	221.0	9.5	67	220.4	7.9
70	213.1	9.6	70	210.2	12.3	70	212.9	11.1
73	199.5	11.0	73	207.3	14.5	73	208.6	12.5
OCTOBER			NOVEMBER			DECEMBER		
34	230.6	5.7	34	227.4	6.3	34	225.7	12.5
37	239.1	5.2	37	236.0	7.2	37	238.1	11.4
40	247.5	4.9	40	244.9	7.0	40	249.3	10.7
43	256.2	4.4	43	254.7	6.4	43	259.0	10.1
46	261.4	4.0	46	260.4	6.9	46	264.1	9.8
49	263.0	4.2	49	262.6	6.3	49	261.6	9.4
52	261.1	4.8	52	261.2	6.5	52	256.9	10.1
55	257.3	5.6	55	257.0	7.1	55	249.2	9.4
58	251.1	6.7	58	251.0	7.1	58	242.1	9.4
61	243.1	7.6	61	244.8	7.8	61	234.4	8.9
64	237.4	8.7	64	241.0	8.5	64	230.9	12.2
67	231.2	9.4	67	236.3	9.1	67	228.7	15.1
70	225.5	13.2	70	229.8	12.4	70	226.0	15.8
73	216.9	12.7	73	221.0	12.3	73	222.9	14.6

ORIGINAL PAGE IS
OF POOR QUALITY

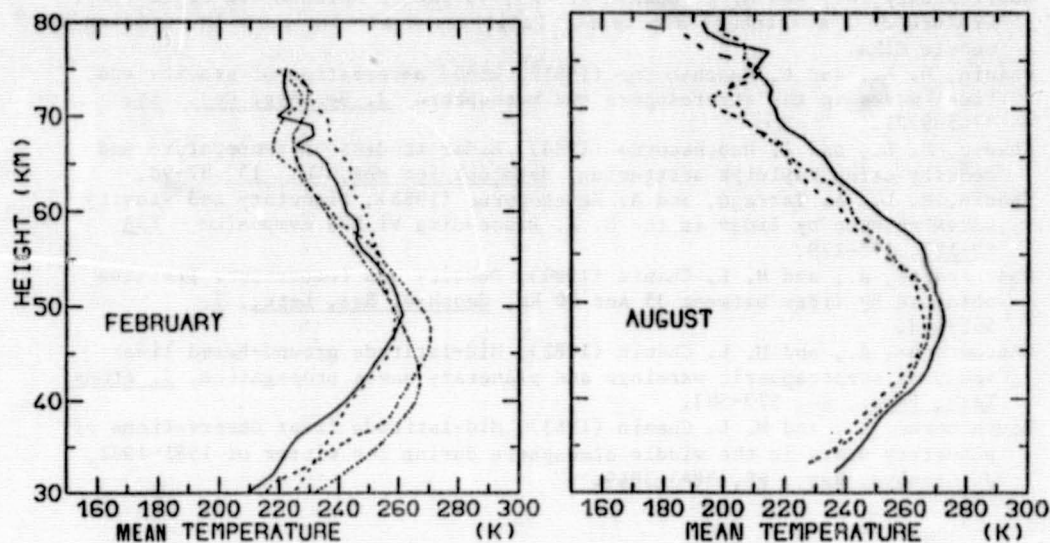


Figure 4. Monthly average temperature profiles February and August for the different years 1981 (—) 1982 (---) 1983 (.....) 1984(— · — · —).

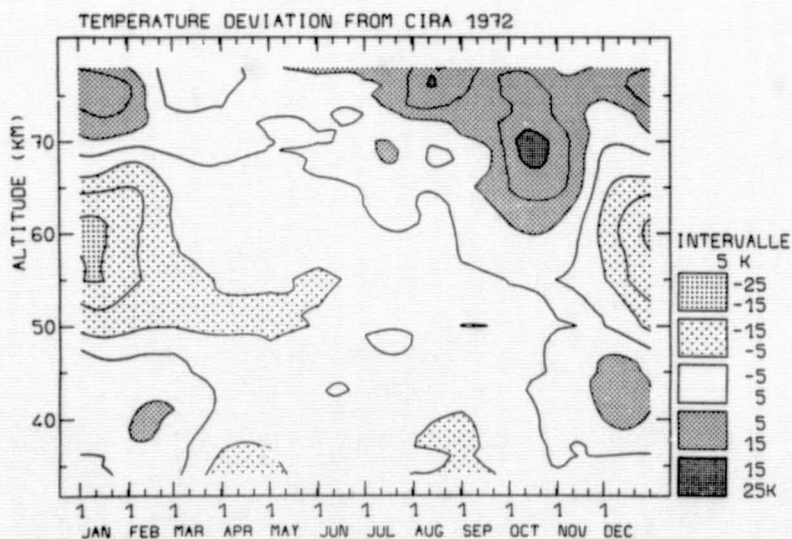


Figure 5. Deviation of the mean average temperature 1981-1984 from the CIRA 1972 model.

REFERENCES

- Bourg-Heckly, G., and M. L. Chanin (1982), Variation saisonniere de la temperature de l'atmosphere a moyenne latitude. Contribution a la revision du modele CIRA.
- Chanin, M. L., and A. Hauchecorne (1981), Lidar observation of gravity and tidal waves in the stratosphere and mesosphere, J. Geophys. Res., **86**, 9715-9721.
- Chanin, M. L., and A. Hauchecorne (1984), Lidar studies of temperature and density using Rayleigh scattering, Handbook for MAP, Vol. 13, 87-98.
- Chanin, M. L., A. Tarrago, and A. Hauchecorne (1983), Planetary and gravity waves as seen by lidar in the M. A. Proceeding VI ESA Symposium - ESA SP-183, 175-179.
- Hauchecorne, A., and M. L. Chanin (1980), Density and temperature profiles obtained by lidar between 35 and 70 km, Geophys. Res. Lett., **7**, 565-568.
- Hauchecorne, A., and M. L. Chanin (1982), Mid-latitude ground-based lidar study of stratospheric warmings and planetary waves propagation, J. Atmos. Terr. Phys., **44**, 577-583.
- Hauchecorne, A., and M. L. Chanin (1983), Mid-latitude lidar observations of planetary waves in the middle atmosphere during the winter of 1981-1982, J. Geophys. Res., **88**, 3843-3849.

4.2 THE MST RADAR TECHNIQUE

Ben B. Balsley

N86-12836Aeronomy Laboratory, National Oceanic and Atmospheric
Administration, Boulder, Colorado 80303

The past ten years have witnessed the development of a new radar technique to examine the structure and dynamics of the atmosphere between roughly 1-100 km on a continuous basis. The technique is known as the MST (for Mesosphere-Stratosphere-Troposphere) technique and is usable in all weather conditions, being unaffected by precipitation or cloud cover. MST radars make use of scattering from small-scale structure in the atmospheric refractive index, with scales of the order of one-half the radar wavelength. Pertinent scale sizes for middle atmospheric studies typically range between a fraction of a meter and a few meters. The structure itself arises primarily from atmospheric turbulence.

The relative ubiquity of turbulence enables continuous data to be gathered at heights below about 35 km, provided that the radar is sufficiently sensitive. Stipulations to this general statement require: 1) that the spatial resolution of the radar is coarse enough (> 150 m) to ensure that turbulent layers are present within each height interval, and 2) that the radar operating wavelength is sufficiently long to ensure that the pertinent half-wavelength of the scatterers lies in the inertial subrange (if the operating radar wavelength is too short, the half-wavelength structure will be damped out by viscosity in the higher heights).

While it is possible in principle to obtain echoes from atmospheric turbulence above about 35 km, the weaker turbulence at these heights due to a decreasing atmospheric density makes it exceedingly difficult to obtain useful data.

Above about 50 km, however, the presence of free electrons in the atmosphere enhances the radar cross section of the turbulent fluctuations and makes them again observable to a radar of reasonable sensitivity. The atmospheric density is still sufficient to ensure that the free electron motions are controlled completely by the dynamics of the neutral atmosphere. Thus, up to at least 90-100 km it is possible to use these electron-enhanced radar echoes to obtain useful data on neutral motions in the mesosphere and lower thermosphere. Above this height, however, the electron "gas" begins to move independently of the neutral background, so that the radar echoes carry little information on the neutral dynamics.

In the mesosphere-lower thermosphere, turbulent echoes are only observable during daylight (i.e., only when there is sufficient ionization and associated ionization gradients). However, it is possible to supplement the daytime echoes with echoes arising from ionized meteor trails that occur both during day and night. Thus MST meteor echoes are essential to preserve the diurnal continuity of the echo occurrence in the upper mesosphere-lower thermosphere.

In the ten years since the MST technique was first introduced by WOODMAN and GUILLEN (1974), there has been a remarkable increase in the number of radar systems that operate -- at least partially -- in the MST mode. As of this writing, at least 14 existing radars are dedicated to full-time MST studies, seven more systems are operating partially in this mode, and some 77 other systems have been either proposed or are under construction throughout the world. Most of these systems, however, are capable of observing only in the

troposphere and lower stratosphere. The concept of a network of both the less-sensitive (ST) systems and the more-sensitive (MST) systems has been proposed to provide continuous temporal and reasonable spectral coverage of the radar-measurable atmospheric parameters, i.e., winds, waves, turbulence, and atmospheric stability. Such a network of single "point" measurements would be highly complementary to existing satellite data base, which supplies gross features of the geotropic wind field and other parameters on a global scale.

The fundamental parameters measured by MST/ST radars are echo strength, Doppler shift, and Doppler width. Middle atmospheric variables deducible from a continuous measurement of these parameters include mean winds, planetary waves, tides, gravity waves, turbulence structure, and atmospheric stability.

The MST technique is also capable of measuring the vertical wind. High time resolution vertical wind measurements contain a great deal of information on gravity-wave activity, while the long-term mean value potentially is very useful in studying the large-scale circulation pattern. Vertical winds have heretofore been inferred from horizontal wind convergence and continuity arguments. Knowledge of the vertical wind field is of considerable importance in understanding troposphere-stratosphere exchange processes, large scale circulation patterns (e.g., the Hadley and Walker circulations), and wave transport phenomena.

Given the measurement capabilities outlined above, the MST technique appears to have a bright future of middle atmospheric dynamics studies in the coming years. Many preliminary studies designed to examine the limitations and full capabilities of the technique have been undertaken by many experimental groups throughout the world, and the results are very promising. Pertinent review papers, and some specific studies not yet included in the reviews, are listed at the end of this article. The results of more extensive investigations into all of the potential research areas listed below should make major inroads into our understanding of the dynamics of the middle atmosphere.

A partial list of the general areas of study amenable to the MST technique includes:

- 1) The effect of small-scale motions (gravity waves, turbulence, and convection) on the large-scale circulation of the atmosphere. The influence of small-scale motions on the general circulation is known to be appreciable, particularly in the upper mesosphere. Simple models that predict middle-atmospheric temperature structure and zonal mean flow are incapable of reproducing either the measured temperature profiles or the zonal mean flow. In order to produce reasonable results from these models, it is necessary to incorporate dissipation and momentum deposition by upward-traveling gravity waves (and, to a lesser extent, planetary waves and tides).
- 2) A determination of the mean zonal and meridional wind components in the mesosphere and lower thermosphere. The global circulation at these heights is only poorly known, particularly at low latitudes where the Coriolis parameter is either weak or non-existent.
- 3) The delineation of the horizontal wavelengths, phase velocity distributions, and vertical momentum fluxes of middle-atmospheric gravity waves, and a determination of their tropospheric origins. This appears to be a tractable problem using existing MST technology, provided that there are sufficient numbers of radars located at selected geographic locations.
- 4) A study of turbulence in the free atmosphere and its relationship to gravity-wave and tidal breakdown. Estimates of turbulence intensity and turbulent

diffusion appear to be possible using high spatial resolution radars with narrow antenna beams to study the space-time structure of atmospheric turbulence layers. Also, it is possible to examine the idea that the spectral distribution of atmospheric fluctuations may be due to a two-dimensional turbulent cascade process.

5) The morphology of atmospheric tides and other large-scale phenomena.

Atmospheric tidal processes are currently being studied using a variety of techniques. Data from MST radars, particularly if meteor-echoes are included at the higher heights to improve the continuity of the data base, will provide additional high-quality information for these studies.

6) A determination of the dynamic properties of the near-equatorial ionosphere.

The equatorial atmosphere within a few degrees of the equator is virtually devoid of Coriolis forcing. As a result, a separate class of relatively long period waves (Kelvin waves and mixed-Rossby gravity waves) can exist in the region. The dynamics of the equatorial atmosphere is thought to be strongly controlled by the evolution and breakdown of these waves. The high-time resolution afforded by continuous observations using a near-equatorial network of MST/ST radars should be extremely beneficial in studying the evolution of these waves.

7) The average kinetic energy distribution in the atmosphere. Knowledge of the power spectral density of the atmospheric fluctuations from a few minutes to many hours is available using existing MST data. Combining this kind of data with the mean atmospheric density enables an estimate to be made of the atmospheric kinetic energy $1/2 \rho v^2$ where ρ is the density and v^2 is the mean square value of the wind field over a specified range of frequencies. Vertical profiles of the atmospheric kinetic energy will be very useful in studies of energy dissipation rates and wave propagation processes (i.e., propagation, reflection, or absorption of planetary waves, tides, gravity waves, etc.).

8) Investigation of a possible relationship between solar activity and the mesospheric wind field. A number of existing studies using a variety of techniques (including the MST technique) point to a tenuous but promising relationship between solar activity and mesospheric wind fluctuations. Continuous, high-time resolution MST data will be very useful in such studies.

It is important to point out that, in addition to the MST technique, there are a number of other remote sounding techniques which measure some of the same atmospheric parameters. Both meteor radar systems and partial reflection drifts (PRD) systems have measured mesospheric and lower-thermospheric motions for many years, although their spatial and/or temporal resolution is somewhat more restrictive. Furthermore, horizontal winds, temperature, and humidity are typically measured up to around 30 km by a vast network of meteorological balloons over the entire globe. In addition to these methods, the temperature measuring capability of ground-based lidar systems appears to hold great promise for studying gravity wave propagation in the middle atmosphere, particularly when used in conjunction with radar wind measurements. Both satellite techniques and in situ measurement by rockets and special purpose balloons add new dimensions to the studies. Clearly, the overall picture of the atmospheric motions and energy exchange processes can only be garnered by cooperative, concerted efforts using all available techniques.

REFERENCES

- Avery, S. K., A. C. Riddle, and B. B. Balsley (1983), The Poker Flat, Alaska, MST radar as a meteor radar, Radio Sci., 18, 1021-1027.
- Balsley, B. B., W. L. Ecklund, and D. C. Fritts (1983), VHF echoes from the high-latitude mesosphere and lower thermosphere: Observations and interpretations, J. Atmos. Sci., 40, 2451-2466.
- Balsley, B. B., and K. S. Gage (1980), The MST radar technique: Potential for middle atmospheric studies, Pageoph 118, 452-493.
- Balsley, B. B., and R. Garell, The kinetic energy density in the troposphere, stratosphere and mesosphere: A preliminary study using the Poker Flat MST radar in Alaska, submitted to J. Geophys. Res.
- Carter, D. A., B. B. Balsley, W. L. Ecklund, M. Crochet, A. C. Riddle, and R. Garell (1984), Tropospheric gravity waves observed by three closely spaced ST radars, Handbook for MAP, Vol. 14.
- Fritts, D. C., M. A. Geller, B. B. Balsley, M. L. Chanin, I. Hirota, J. R. Holton, S. Kato, R. S. Lindzen, M. R. Schoeberl, R. A. Vincent, and R. F. Woodman (1984), Research status and recommendations from the Alaska workshop on gravity waves and turbulence in the middle atmosphere, Fairbanks, Alaska, 18-22 July 1983, Bull. Am. Meteorol. Soc., 65, 149-158.
- Gage, K. S., and B. B. Balsley, MST radar studies of wind and turbulence in the middle atmosphere, submitted to J. Atmos. Terr. Sci.
- Johnson, R., J. Luhmann, and B. B. Balsley, Neutral winds at the auroral zone mesopause: Geomagnetic effect?, submitted to J. Geophys. Res.
- Handbook for MAP, Vol. 9, edited by S. A. Bowhill and Belva Edwards, Dec. 1983.
- Rottger, J. (1980), Structure and dynamics of the stratosphere and mesosphere revealed by VHF radar investigations, Pageoph., 118, 494-527.
- Rottger, J. (1984), The MST radar technique, Handbook for MAP, Vol. 13, 187-232.
- Woodman, R. F., and A. Guillen (1974), Radar observations of winds and turbulence in the stratosphere and mesosphere, J. Atmos. Sci., 31, 493-505.